february 1958

the
institute
of
radio
engineers

Proceedings of the IRE

in this issue

MICROWAVE TECHNIQUES BEFORE 1900
GHOST MODES IN WAVEGUIDES
CRYSTAL FILTER DESIGN
8MM KLYSTRON POWER AMPLIFIER
FM DEMODULATOR REQUIREMENTS
HIGH-POWER TRAVELING-WAVE TUBE
INDEX TO IRE DEFINITIONS OF TERMS
RADAR CROSS-SECTION OF A MAN
IRE STANDARDS ON TV LUMINANCE
VARIABLE RESISTANCE NETWORKS
TRANSACTIONS ABSTRACTS
ABSTRACTS AND REFERENCES

A.D. 1896. JUNE 2, No. 12,039.
MARCONI'S COMPLETE SPECIFICATION.
(5th Edition)

Pre-1900 Microwave Antenna: Page 405

FILTERS
FOR EVERY APPLICATION

TELEMETERING FILTERS

UTC manufactures a wide variety of band pass filters for multi-channel telemetering. Illustrated are a group of filters supplied for 400 cycle to 40 KC service. Miniaturized units have been made for many applications. For example a group of 4 cubic inch units which provide 50 channels between 4 KC and 100 KC.

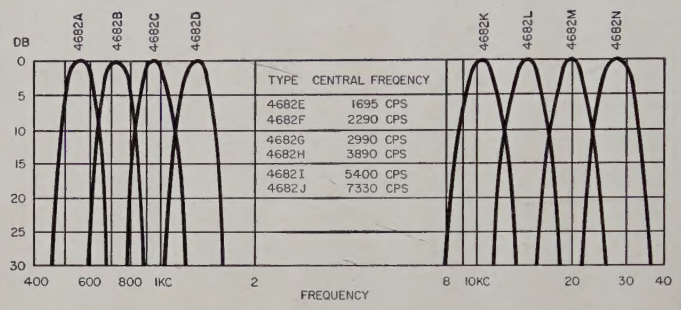

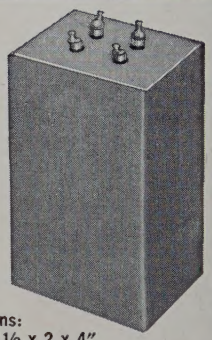

Dimensions:
(4682A) 1½ x 2 x 4"

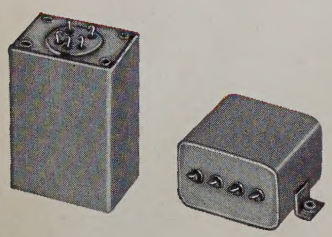

Dimensions:
(3834) 1¼ x 1¾ x 2-3/16".
(2000, 1) 1¼ x 1¾ x 1⅝".

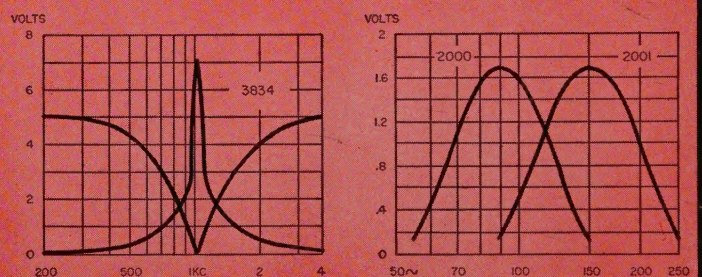

AIRCRAFT FILTERS

UTC has produced the bulk of filt used in aircraft equipment for o a decade. The curve at the left that of a miniaturized (1020 cycl range filter providing high atten tion between voice and range f quencies.

Curves at the right are that of miniaturized 90 and 150 cycle filt for glide path systems.

CARRIER FILTERS

A wide variety of carrier filters are available for specific applications. This type of tone channel filter can be supplied in a varied range of band widths and attenuations. The curves shown are typical units.

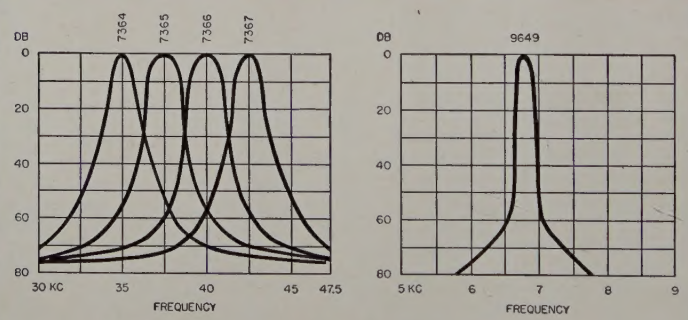

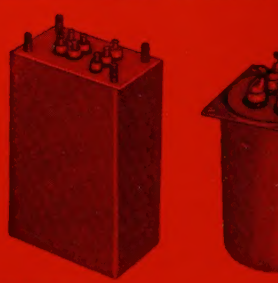

Dimensions:
(7364 series) 1⅝ x 1⅝ x 2¼".
(8649) 1½ x 2 x 4".

DISCRIMINATORS

These high Q discriminators provide exceptional amplification and linearity. Typical characteristics available are illustrated by the low and higher frequency curves shown.

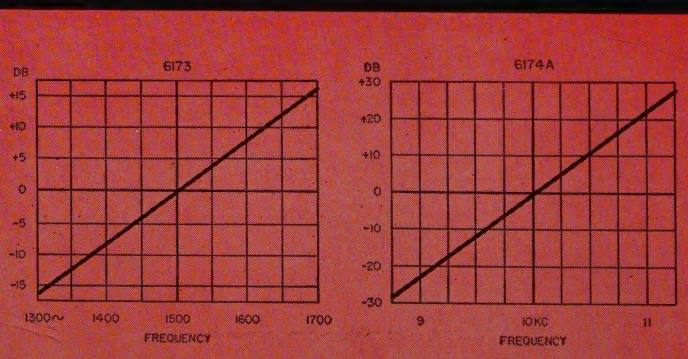

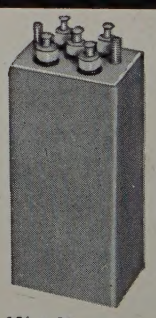

Dimensions:
(6173) 1-1/16 x 1⅜ x 3".
(6174A) 1 x 1¼ x 2¼".

For full data on stock UTC transformers, reactors, filters, and high Q coils, write for Catalog A.

UNITED TRANSFORMER C

150 Varick Street, New York 13, N. Y. EXPORT DIVISION: 13 E. 40th St., New York 16, N. Y. CABLES: "A
Pacific Mfg. Division: 4008 W. Jefferson Blvd., Los Angeles 16, Calif.

SOLA CONSTANT VOLTAGE TRANSFORMER + **HIGH CAPACITANCE FILTER SECTION** + **GERMANIUM RECTIFIER**

DC SOLAVOLT, *shown partly disassembled here, has major components identified. It is designed for relay-rack mounting on a standard, 19" frame or for bench use. Removable handles, for convenience when portability for bench use is desired, are available as accessory equipment.*

Unique combination of components in adjustable "DC Solavolt" regulated power supply reduces conventional size, weight, and cost

Compact size, low weight, high efficiency, and moderate price distinguish the new "DC Solavolt" from conventionally-designed, regulated, adjustable dc power supplies. These outstanding advantages have been secured by using a unique assembly of components (shown above) that occupy only 7" of height and 12¼" of depth on a standard, 19" relay rack frame.

Along with design simplicity, the "DC Solavolt" provides laboratory standards of performance:

OUTPUT VOLTAGE REGULATED WITHIN ±1% at full load with supply voltage variations up to ±15%. (Regulation within ±1.5% at 50% load and lowest voltage setting.)

RIPPLE VOLTAGE HELD WITHIN 0.10% (rms) at full load and nominal input voltage.

An important feature of this adjustable dc power supply is its ability to handle transient or "pulse" loads of up to twice the full load rating of the supply. The "DC Solavolt" has no tubes to replace, requires no "compensating" or "zero" adjustments, and needs no maintenance.

Six stock models provide outputs *adjustable in voltage ranges between 5 and 400 volts and load currents up to 7 amperes.* Your local electronic distributor now has the "DC Solavolt" in stock. He will be happy to give you further, technical information.

SOLA *Constant Voltage* **DC POWER SUPPLIES**

Write for Bulletin DC-245
SOLA ELECTRIC CO.
4633 W. 16th Street
Chicago 50, Illinois

WHO IS BORG?

George W. Borg, who founded this corporation, is the "Mr. Clutch" who started with Borg & Beck. He then helped organize the Borg-Warner Corporation of which he became president. Later he served as chairman of the board until he resigned to devote his full attention to The George W. Borg Corporation.

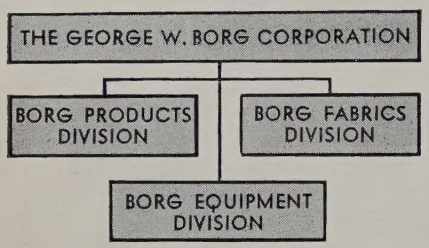

The George W. Borg Corporation is comprised of three divisions

- **Borg Products Division**
  Manufactures automotive clocks.
- **Borg Fabrics Division**
  Manufactures deep-pile fabrics best known of this line is the fashionable "Borgana" fabric.
- **Borg Equipment Division**
  Manufactures Micropots (precision potentiometers), Microdials (precision turn-counting dials), instrument motors, frequency standards, aircraft navigational instruments and components for systems.

HOW BORG EQUIPMENT DIVISION CAN HELP YOU . . .

Borg's background of experience will save you time and money by helping you solve design and production problems of electronic components. Whether you are faced with a special problem or interested in a standard component, call Borg Equipment Division for an economically sound solution. Write today for catalog BED-A56.

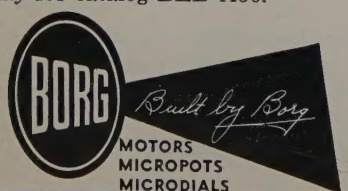

BORG EQUIPMENT DIVISION
THE GEORGE W. BORG CORPORATION
JANESVILLE, WISCONSIN

IRE People

At the annual meeting of the New York Chapter of the Armed Forces Communications and Electronics Association, **G. W. Bailey** (A'38–SM'46–F'56) was re-elected a director. The Association is an organization endeavoring to maintain and improve the cooperation between the armed forces and industry in the design, production, maintenance and operation of communication, electronic and photographic equipment.

Mr. Bailey, Executive Secretary of the IRE and National Convention Chairman since 1948, is chairman of the IRE Armed Forces Liaison Committee.

❖

M. V. Kiebert (A'31–M'38–SM'43), formerly director of electronics for the Miami Shipbuilding Corp., has joined Datalab, a division of Consolidated Electrodynamics Corporation, as proposals coordinator.

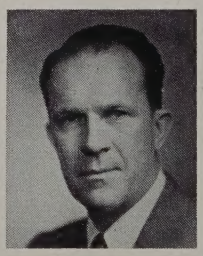
M. V. KIEBERT

A former Navy commander, Mr. Kiebert was head of the Special Weapons Branch of the government's Bureau of Aeronautics during World War II. In this capacity, he was responsible for all of the bureau's electronic activities in guided missiles.

Since 1947, in addition to his position with Miami Shipbuilding Corp., Kiebert has been director of research and development for TeleDynamics, Inc.; director, Special Products Research Lab., Bendix Aviation Corp.; chief engineer, Tuner Division of P. R. Mallory Co.; assistant to the chief engineer, Convair Guided Missiles Division, General Dynamics Corp.; and director of research and electronics, Applied Research, Inc.

A graduate of the University of Idaho with a B.S. degree in electrical engineering, Mr. Kiebert is a registered professional engineer in the District of Columbia.

He is a past national chairman of the IRE's Professional Group on Telemetry and Remote Control, and a charter member of the organization's Professional Group on Military Electronics. He is at present a member of the IRE's Administrative Communications Group.

Other affiliations include the Institute of Aeronautical Sciences, American Institute of Electrical Engineers, Franklin Institute, American Rocket Society, American Ordance Association, Audio Engineering Society, Society of Motion Picture and Television Engineers; and National Pilots Association.

The appointment of **S. R. Hennies** (S'44–A'49–M'52) as manager of applications engineering for Granger Associates has been announced by J. V. N. Granger, president of the Palo Alto firm specializing in electronic systems.

Since joining Granger last spring Mr. Hennies has been a senior member of the engineering staff. His widened responsibilities place him in charge of coordinating customer requirements with the development and application of the firm's electronic devices.

Mr. Hennies has B.S. and M.S. degrees in electrical engineering from the University of California. Wartime duty as a radar maintenance officer in the U. S. Navy gave him special training at Bowdoin College in Maine, Massachusetts Institute of Technology and Bell Telephone Laboratories in New York.

His first industrial connection was with Northrop Aircraft Co. at Hawthorne, Calif., which he joined as a radio systems engineer in 1948 and left in 1951 as assistant leader of the Telecommunications Group in charge of aircraft antenna and missile radio control systems development.

From 1951 through 1956 Mr. Hennies was with Varian Associates, Palo Alto. His first assignment with Varian was as a microwave tube design engineer specializing in reflex klystrons. Later, as an applications engineer, he was concerned with the utilization of klystrons in radar and microwave relay systems. He has had further experience with equipments employing traveling wave tubes and backward wave oscillators.

Mr. Hennies is an associate member of Sigma Xi.

❖

Establishment of the Space Technology Laboratories as an autonomous operating division of The Ramo-Wooldridge Corporation was announced recently by D. E. Wooldridge, President.

The new division is an outgrowth and extension of the former Guided Missile Research Division, a unit of the company responsible for the technical direction and systems engineering for the Air Force Ballistic Missile Program, and the ATLAS, TITAN and THOR missiles.

Space Technology Laboratories will have its own completely separate personnel, facilities and services, according to Dr. Wooldridge. Transfer to the laboratories of certain additional research facilities, technical and administrative supporting services previously provided on a company-wide basis, is also planned. In addition, transfer of several top R-W scientists and technical experts to the enlarged labo-

(Continued on page 16A)

Why Gamble?

THERE'S A BORG MICROPOT® TO MEET YOUR EXACT SPECIFICATIONS!

BORG MICROPOTS... the Ultimate in Multi-Turn Precision Potentiometers

Borg offers a complete line of high-precision, linear potentiometers called MICROPOTS. Precision is Borg's business . . . that's why MICROPOTS offer so many exclusive advantages. Superior design and production methods make Borg MICROPOTS available in any quantity. Write today for the name of your nearest Borg Jobber or "Tech-Rep."

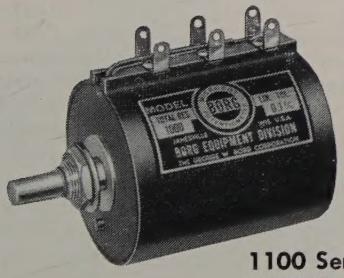

1100 Series MICROPOTS

A precision MICROPOT that offers your products a price advantage in today's competitive markets. Lug or lead type terminals. Accurate . . . dependable . . . long lived.

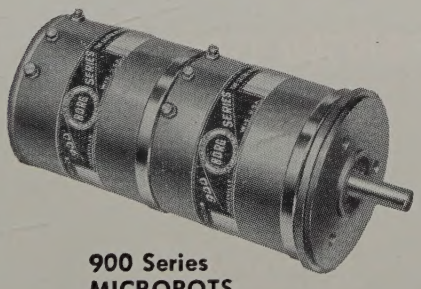

900 Series MICROPOTS

Standard ten-turn and three-turn models to fit most special design needs. Extremely accurate and dependable under adverse environmental conditions including severe vibration and shock.

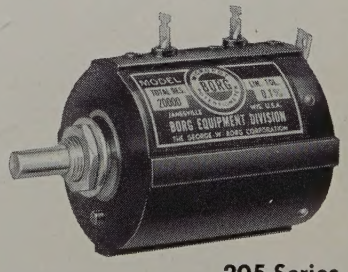

205 Series MICROPOTS

A quality MICROPOT. Designed for both military and commercial applications. Proven in many different mobile and stationary types of electronic circuitry.

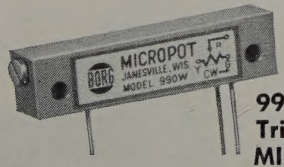

990 Series Trimming MICROPOTS

Small in size, lightweight, rugged and dependable. Three types of terminals . . . printed circuit, solder lugs or insulated wire leads.

WRITE FOR COMPLETE ENGINEERING DATA • CATALOG BED-A56

BORG EQUIPMENT DIVISION
THE GEORGE W. BORG CORPORATION
JANESVILLE, WISCONSIN

ELECTRONIC—MECHANICAL BORG EQUIPMENT

Built by Borg

MOTORS
MICROPOTS
MICRODIALS

Frequency JK PRODUCTS Management

Ultra-Stable, Shock-Mounted Glasline Crystals

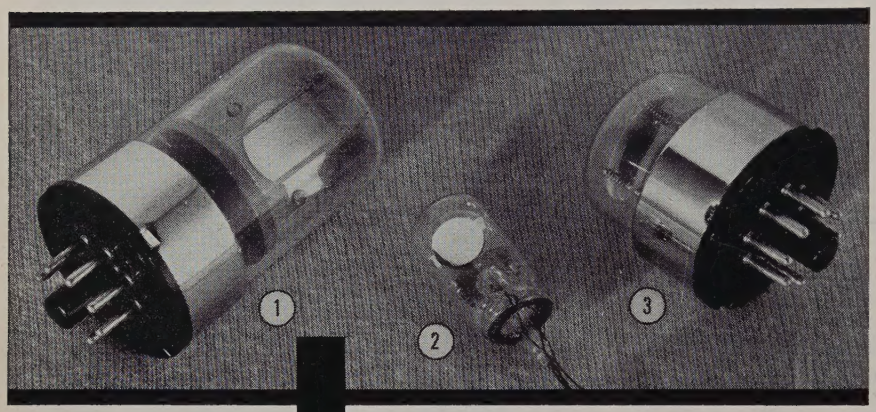

1. G-12A-1000 kc
2. G-6AS-5 mc
3. G-12AS-1000 kc

G-6AS and G-12AS meet stability demands of 1 PPB/day. Frequency tolerance ± 1 PPM. Secular stability 1 PPB/day. Shock—1 PPB at 20G impact. Write for data sheets.

THE JAMES KNIGHTS COMPANY—Sandwich, Ill.

OF COURSE—ONE SOURCE

from base laminates to completed

PRINTED CIRCUITS

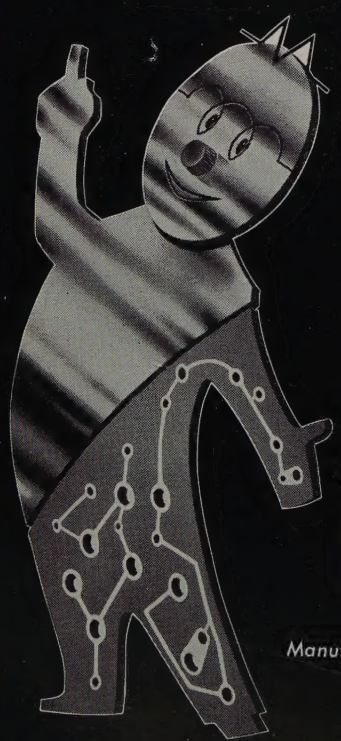

Only Norplex offers one-source manufacturing of both base laminates and printed circuits. You get top advantages in service, cost, quality on all circuitry . . . 1 or 2 side, selective soldering, flush for switching applications. Write today, or send print.

Over 5,000,000 Norplex printed circuits in use!

Norplex

Northern Plastics Corp.

Manufacturers and fabricators of industrial laminates for electrical, mechanical application.

Sales offices in principal cities.

2nd and Market Streets, La Crosse **2** *Wis.*

IRE People

(Continued from page 14A)

ratories organization will shortly be announced.

Simon Ramo (A'38–SM'44–F'50) will relinquish his duties as Executive Vice-President and Secretary of the Corporation to devote full time as President of the Space Technology Laboratories. Dr. Ramo will remain as a Board member of the parent Ramo-Wooldridge Corporation.

❖

A. W. Coven (SM'56) has been appointed head of the newly-formed Radio Navigation Branch of the Radio Division, Naval Research Laboratory. This branch will be the principal support for research and development of radio navigation in the Navy.

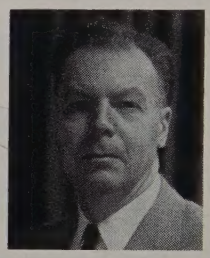

A. W. Coven

A graduate of the College of Wooster, Wooster, Ohio, Dr. Coven received the degrees of Master of Science from Washington University, St. Louis, Mo. and Doctor of Philosophy from the University of Chicago. He has served as an Associate Professor of Physics and Chairman of the Division of Natural Sciences at Kent State University, Kent, Ohio. During World War II, Dr. Coven taught physics at the U. S. Naval Academy. Since joining the Radio Division of NRL in 1946, he has served as an official of several scientific committees and has published numerous papers in the field of physics.

Dr. Coven is a Fellow of the American Association for the Advancement of Science, and a member of the American Physical Society. He holds honorary membership in Sigma Xi and Sigma Pi Sigma. In addition, he is an officer in the Naval Reserve.

❖

Elected as President of Interstate Electronics Corporation was **P. H. Reedy** (S'35–A'39–SM'55), who formerly served as Executive Vice-President.

❖

The Kahn Research Laboratories, Inc., Freeport, N. Y., announces the appointment of **L. O. Goldstone** (M'51–SM'55). He will be primarily concerned with problems of network design and synthesis, as well as the specialized circuitry of compatible single-sideband and other techniques for improving spectrum economy of voice communications.

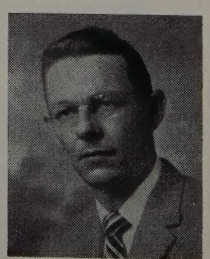

L. O. Goldstone

Dr. Goldstone received his B.E.E. degree from Clarkson

(Continued on page 20A)

650A — highly stable, wide band; 10 cps to 10 MC. For audio, supersonic, video, rf measurements. Output 15 mw/3 volts. Frequency response flat ±1 db. $490.00.

200AB — for audio tests, 20 cps to 40 KC. Output 1 watt/24.5 volts. Simple to use, compact, rugged. $130.00.

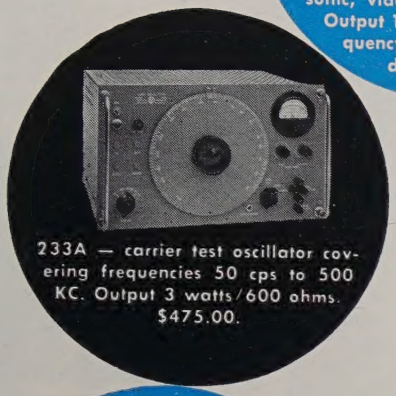

233A — carrier test oscillator covering frequencies 50 cps to 500 KC. Output 3 watts/600 ohms. $475.00.

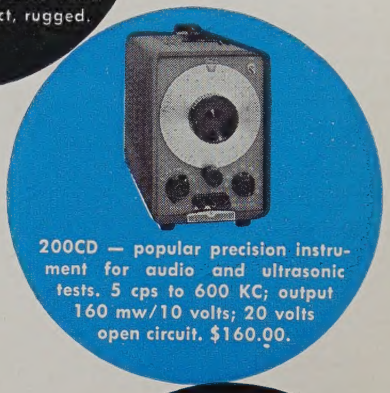

200CD — popular precision instrument for audio and ultrasonic tests. 5 cps to 600 KC; output 160 mw/10 volts; 20 volts open circuit. $160.00.

11

additional

-hp- quality oscillators

- outstanding value
- complete coverage
  0.008 cps to 10 MC
- stable RC circuit pioneered by -hp-
- each instrument designed to do a specific job best

206A — very low distortion; for high quality, high accuracy audio tests. Covers 20 cps to 20 KC; output +15 dbm. $565.00.

200J — extreme accuracy for interpolation and frequency measurements. Covers 6 cps to 6 KC, output 160 mw/10 volts; 20 volts open circuit. $275.00.

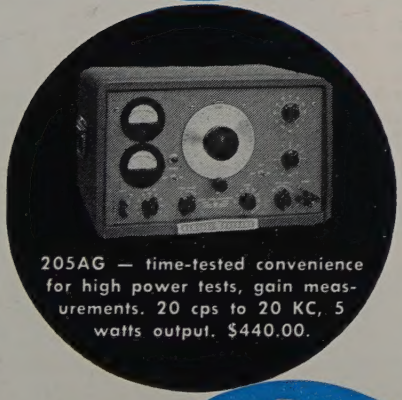

205AG — time-tested convenience for high power tests, gain measurements. 20 cps to 20 KC, 5 watts output. $440.00.

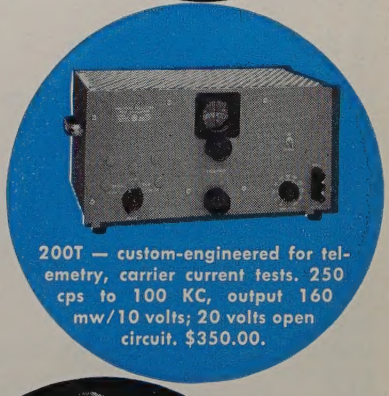

200T — custom-engineered for telemetry, carrier current tests. 250 cps to 100 KC, output 160 mw/10 volts; 20 volts open circuit. $350.00.

HEWLETT-PACKARD COMPANY
4170D Page Mill Rd., Palo Alto, Calif. ,U.S.A.
Cable "HEWPACK" • DAvenport 5-4451
Field engineers in all principal areas

World's most complete line of fast, accurate, easy to use oscillators!

202C — replaces famous 202B for low frequency measurements 1 cps to 100 KC. Output 160 mw/10 volts; 20 volts open circuit. $300.00.

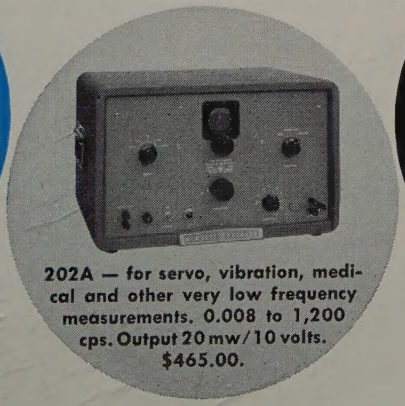

202A — for servo, vibration, medical and other very low frequency measurements. 0.008 to 1,200 cps. Output 20 mw/10 volts. $465.00.

201C — specifically designed for high quality audio tests. Covers 20 cps to 20 KC. Output 3 watts/42.5 volts. $225.00.

4170

AMATEURS find ROHN TOWERS *BEST* because

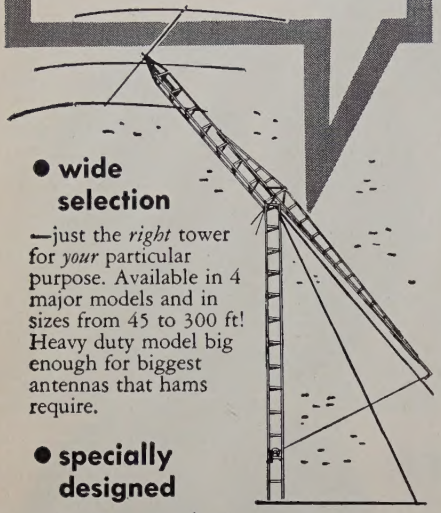

● wide selection

—just the *right* tower for *your* particular purpose. Available in 4 major models and in sizes from 45 to 300 ft! Heavy duty model big enough for biggest antennas that hams require.

● specially designed

—amateurs rave about the special "Fold-Over" Rohn Towers! No need to work "off the ground" on your antenna—merely fold completely over and then crank right back up. Thousands of hams acclaim that this is the *best* tower ever designed for them!

● hot dipped galvanized

—permanent, no-maintenance finish—stays bright and new.

● superior construction

—these towers rated to handle the equivalent of about any load you require —made by precision machines—fully tested—easily shipped and installed. Thousands in use coast-to-coast.

● Designed and manufactured by largest exclusive manufacturer of TV Communications towers. Get the *full facts*—then you'll buy ROHN!

FREE!! FREE!!
Send coupon or postcard for FREE catalog and prices.

MAIL COUPON TODAY

ROHN *Manufacturing Co.*
116 Limestone, Bellevue
Peoria, Illinois

Gentlemen: Please send FREE catalog on amateur towers and accessories.

NAME _____

ADDRESS _____

CITY _____ STATE _____

Satisfaction Guaranteed

IRE People

(Continued from page 16A)

College in 1947 and his M.E.E. and D.E.E. degrees from the Polytechnic Institute of Brooklyn in 1950 and 1957, respectively. From 1947 to 1954 he was instructor and then assistant professor in the electrical engineering department of the Polytechnic Institute of Brooklyn. Returning in 1957, he was again appointed assistant professor and is presently serving in that capacity.

From 1954 to 1957 he was a research associate at the Microwave Research Institute and was engaged in research on propagation in unconventional wave guides with applications to travelling wave antennas. He served in the U. S. Army Corps of Engineers from 1943 to 1946.

Dr. Goldstone is a member of Eta Kappa Nu and Sigma Xi.

❖

Emerick Toth (SM'48–F'58) has been named the new head of the Radio Techniques Branch, Radio Division, Naval Research Laboratory. He succeeds Mr. T. McL. Davis, who recently retired.

A graduate of Newark College of Engineering, Mr. Toth's background of experience includes positions with the Bakelite Corp., Kolster Radio Labs., Bell Telephone Labs., Wired Radio Inc., De Forest Radio Co., Sylvania Corp., Pilot Radio Corp. and Bendix Radio Corp. He joined the Radio Division of the Naval Research Laboratory in 1938.

A member of the Scientific Research Society of America and Union Radio Scientifique Internationale, Mr. Toth is the author of numerous scientific papers and a lecturer on radio reception techniques. He has more than twenty patents and about the same number of patent applications pending.

❖

Retirement from the General Electric Company of one of the world's leading pioneers in the broad field of electronics has been announced recently.

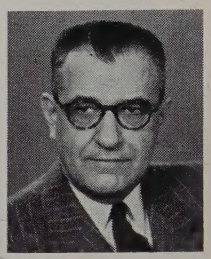

W. R. G. BAKER

W. R. G. Baker (A'19–F'28) a Vice-President since 1941, left the Company on his 65th birthday under provisions of its pension plan.

Simultaneously, Chancellor W. P. Tolley of Syracuse University announced that Dr. Baker has been appointed Vice-President for Research.

In his new position, Dr. Baker will be responsible for directing the University's contract research program. He had served previously as chairman of the Syracuse Research Institute's Board of Governors, and

(Continued on page 24A)

TELEPHONE AND TELEGRAPH EQUIPMENT

Radio Engineering Products is currently producing a number of types of equipment, electrically and mechanically interchangeable with standard Bell System apparatus.

CARRIER-TELEPHONE EQUIPMENT

C5 Carrier-Telephone Terminal (J68756). A kit for adding a fourth toll-grade channel to existing C systems is available. • C1 Carrier-Telephone Repeater (J68757) • 121A C Carrier Line Filter • H Carrier Line Filter (X66217C).

CARRIER-TELEGRAPH EQUIPMENT

40C1 Carrier-Telegraph Channel Terminal (J70047C) • 140A1 Carrier Supply (J70036A1, etc.) • 40AC1 Carrier-Telegraph Terminal.

VOICE-FREQUENCY EQUIPMENT

V1 Telephone Repeater (J68368F) • Power Supply (J68638A1) • V1 Amplifiers (J68635E2 and J68635A2) • V3 Amplifier (J68649A) • V-F Ringers (J68602, etc.) • Four Wire Terminating Set (J68625G1) • 1C Volume Limiter (J68736C).

D-C TELEGRAPH EQUIPMENT

16B1 Telegraph Repeater (J70037B) • 10E1 Telegraph Repeater (J70021A) • 128B2 Teletypewriter Subscriber Set (J70027A).

TEST EQUIPMENT

2A Tcll Test Unit (X63699A) • 12B, 13A, 30A (J64030A) and 32A (J64032A) Transmission Measuring Sets • 111A2 Relay Test Panel (J66118E) • 118C2 Telegraph Transmission Measuring Set (J70069K) • 163A2 Test Unit (J70045B) • 163C1 Test Unit (J70045D).

COMPONENTS AND ACCESSORIES

255A and 209FG Polar Relays • Repeating and Retard Coils, several types • 184, 185, 230A and 230B Jack Mountings.

RADIO ENGINEERING PRODUCTS
1080 UNIVERSITY ST., MONTREAL 3, CANADA
TELEPHONE
UNiversity 6-6887
CABLES
RADENPRO, MONTREAL

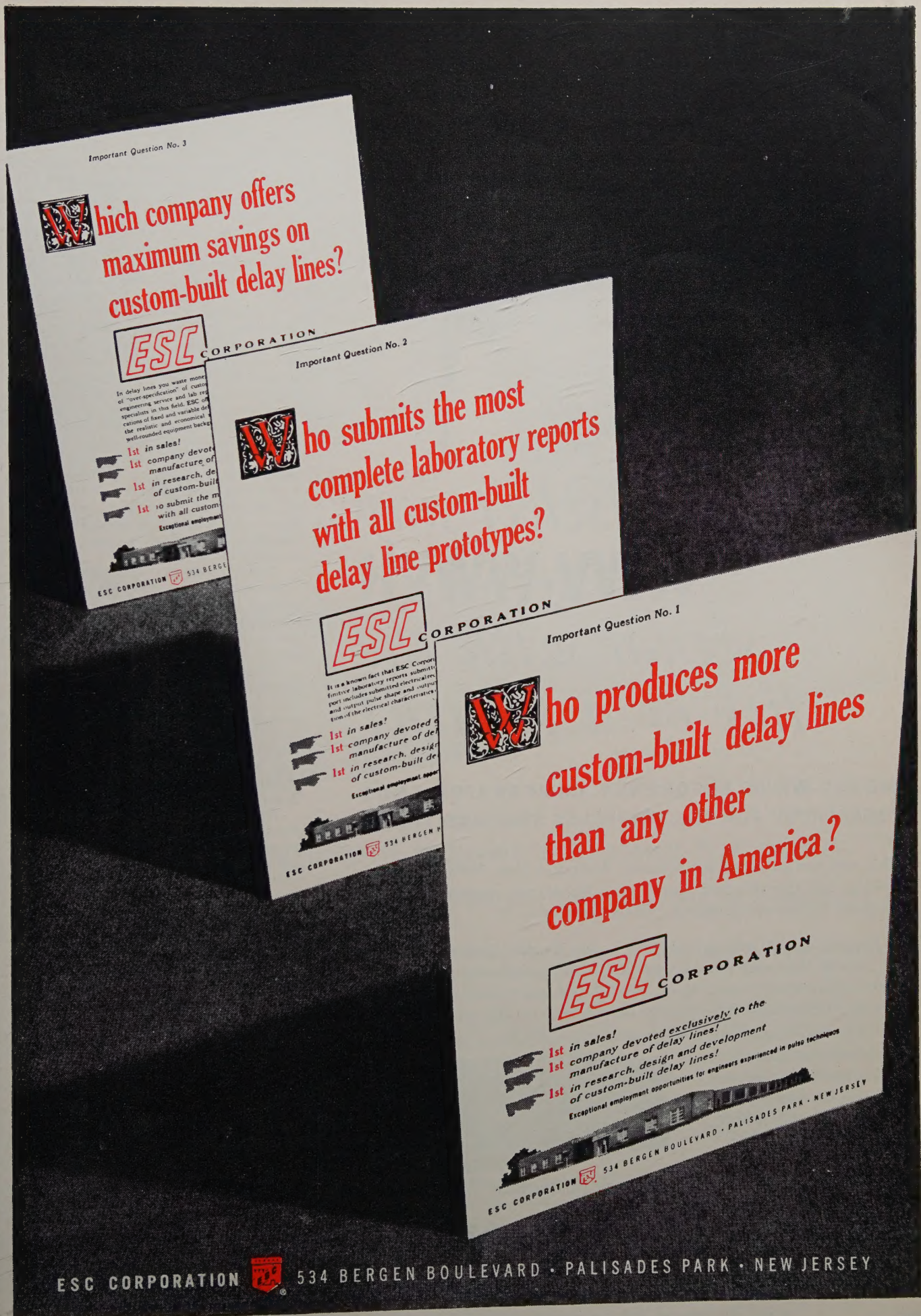
Important Question No. 3
Which company offers maximum savings on custom-built delay lines?
ESC CORPORATION
1st in sales!
1st company devoted exclusively to the manufacture of delay lines!
1st in research, design and development of custom-built delay lines!
Exceptional employment opportunities for engineers experienced in pulse techniques
ESC CORPORATION 534 BERGEN BOULEVARD · PALISADES PARK · NEW JERSEY
Important Question No. 2
Who submits the most complete laboratory reports with all custom-built delay line prototypes?
ESC CORPORATION
Important Question No. 1
Who produces more custom-built delay lines than any other company in America?
ESC CORPORATION
1st in sales!
1st company devoted exclusively to the manufacture of delay lines!
1st in research, design and development of custom-built delay lines!
Exceptional employment opportunities for engineers experienced in pulse techniques
ESC CORPORATION 534 BERGEN BOULEVARD · PALISADES PARK · NEW JERSEY
ESC CORPORATION 534 BERGEN BOULEVARD · PALISADES PARK · NEW JERSEY

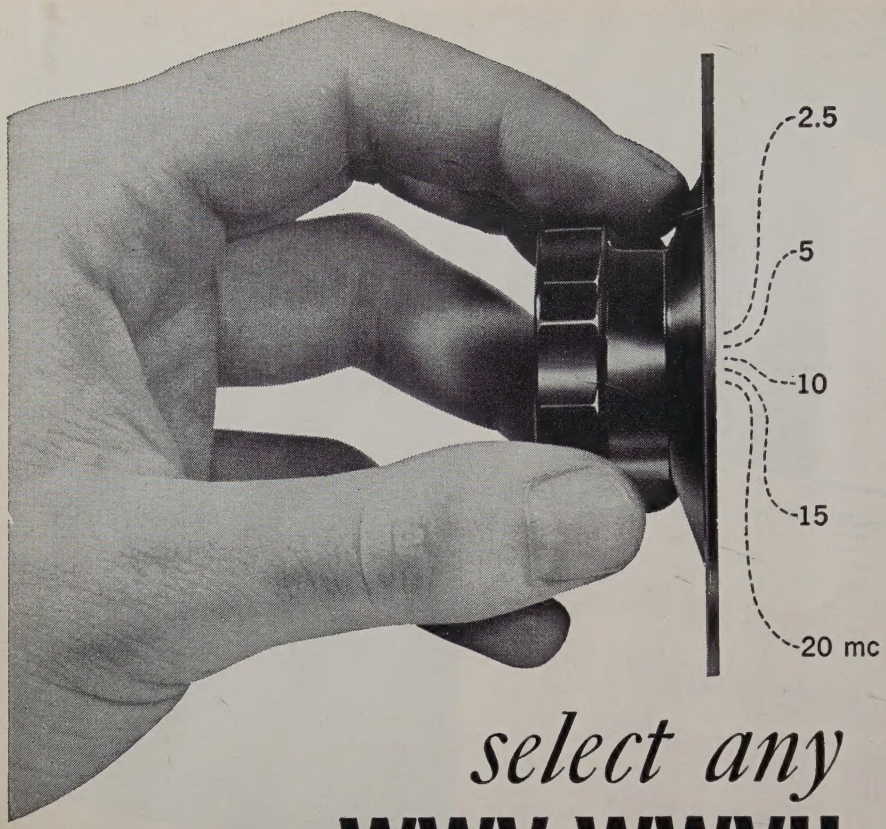

select any
WWV-WWVH
signal with the click of a switch!

MODEL WWVC FREQUENCY COMPARATOR ENDS "SEARCHING" FOR THE STRONGEST STANDARD SIGNAL

This new tool can save you valuable calibration time. With it you can quickly find the strongest signal available at any moment from the National Bureau of Standards – *without searching.*

A five-position dial switches precisely to any standard frequency – 2.5, 5, 10, 15 or 20 MC – each crystal controlled. Built-in oscilloscope and speaker make measurements easy. Model WWVC includes comparator function selector, Collins plug-in filter for high selectivity, automatic gain and volume controls, and adjustable threshold control which eliminates noise and other modulation in tick position. Calibrate any frequency *accurately* and *quickly* with the Model WWVC. Write for Bulletin C-1.

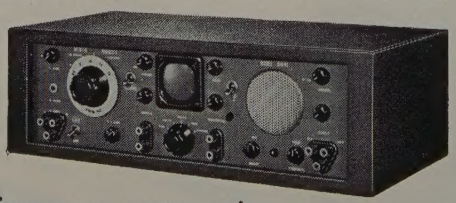

MODEL WWVC *standard frequency comparator*

SPECIFIC PRODUCTS

p. o. box 425; 21051 Costanso, Woodland Hills, California

IRE People

(Continued from page 20A)

helped the university to establish its Research Corporation.

Dr. Baker is leaving the Company after more than 34 years of service. For 15 of these years, 1941–1956, he directed the Company's electronics businesses as general manager of its Electronics Division. During this period General Electric electronic equipment sales grew to exceed the sales volume of the entire company in 1939.

During this period the company also established its Electronics Park research and manufacturing plant on a 200-acre site adjacent to the New York State Thruway seven miles northwest of Syracuse. The Park served until 1956 as the headquarters for all General Electric electronics business and Dr. Baker has maintained his headquarters here for the past ten years.

The Division's sixteen separate businesses and five electronics laboratories were reorganized into three electronics divisions—defense, industrial, and components—in June, 1956 when Dr. Baker was made a consultant to the company's executive office.

During his General Electric career, Dr. Baker worked for and was honored by the nation's leading professional and business associations for his technical and administrative contributions to the electronics industry.

He served as IRE president in 1947, Director since 1946 and Treasurer since 1951; is currently serving a second term as president of the Electronic Industries Association (formerly the Radio-Electronics Television Manufacturers' Association), and has received the highest awards granted by these groups, their Medals of Honor.

He also has the Army's Medal of Freedom citation. This was awarded in 1953 for advice and guidance to the Chief of Staff and to the Secretary of the Army, on the problems of utilization of electronic devices to the maximum extent in modern warfare.

In March, 1958 he will receive the Founders' Award of the Institute of Radio Engineers. The award is bestowed on special occasions only to outstanding administrative leaders in the radio and electronics fields. Dr. Baker will be the fourth person to get the award since the IRE was founded in 1912.

Among his best-known contributions to the electronics industry were the organization and direction of two national television system committees which recommended engineering standards to the Federal Communications Commission, paving the way for commercial monochrome telecasting in 1941 and color TV in 1953.

The second NTSC was awarded an "Emmy" by the Academy of Television Arts and Sciences for distinguished contributions to the television industry.

The General Electric pioneer television station at Schenectady uses Dr. Baker's

(Continued on page 28A)

NEWS ABOUT SILICON DEVICES

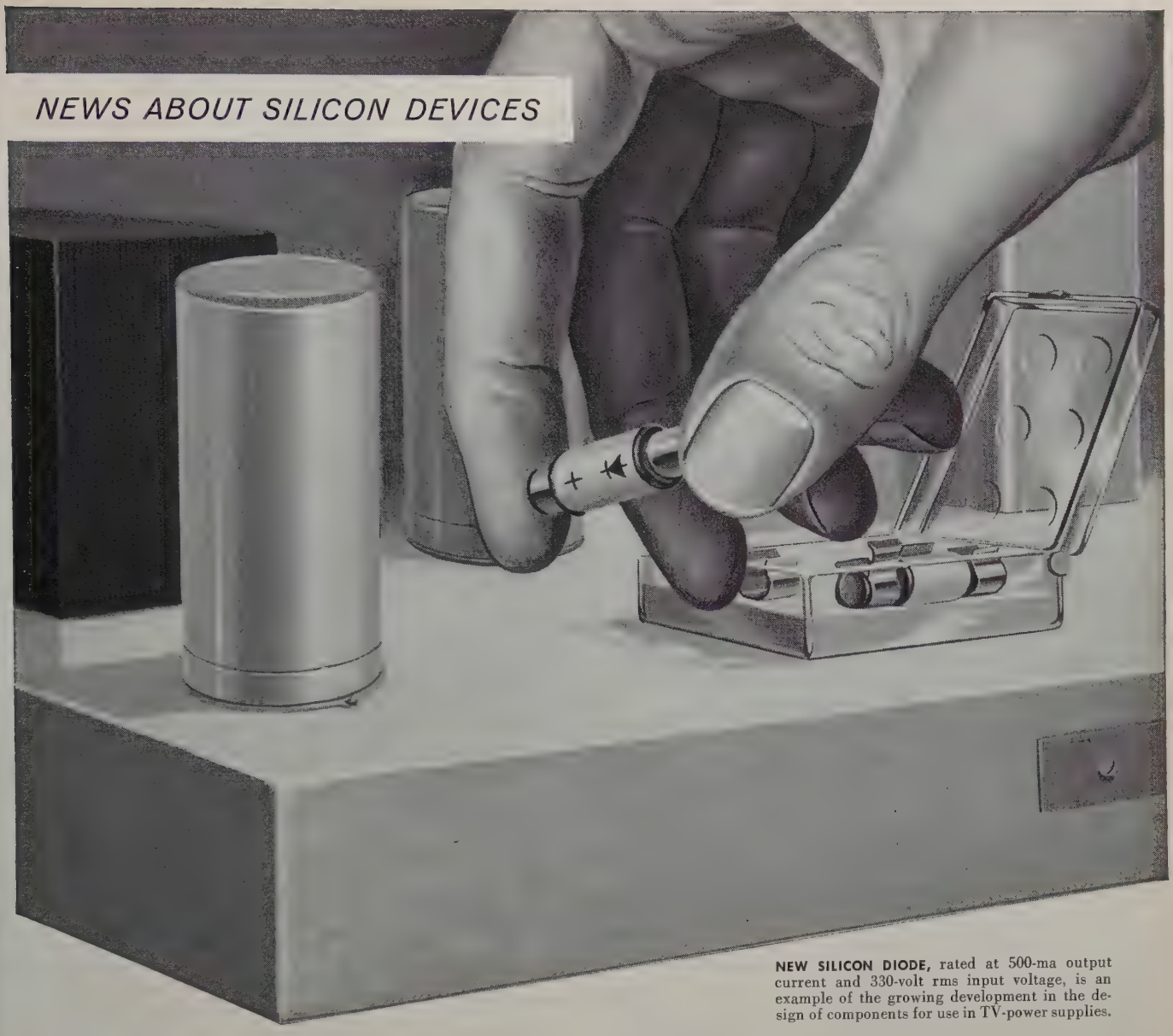

NEW SILICON DIODE, rated at 500-ma output current and 330-volt rms input voltage, is an example of the growing development in the design of components for use in TV-power supplies.

Now... more efficient power supplies for radio-TV made possible with Du Pont Hyperpure Silicon

Actual test results as reported by various manufacturers indicate important advantages of silicon diodes and rectifiers. One TV manufacturer, for example, operated samples of silicon rectifiers under load continuously for 5,000 hours—with no noticeable drop in output voltage. Another manufacturer reports no voltage change after 500 hours in 95% humidity.

Silicon-equipped sets are relatively free of a decline in B+ voltage. Silicon diodes are up to 99% efficient in units operated at 60 cps—reverse leakage is as low as a few microamperes. Both rectifiers and transistors of silicon have temperature ratings far higher than those of other semiconducting materials . . . can operate continuously at −65° to 200°C.

Note to device manufacturers: You can produce silicon transistors, rectifiers and diodes of the highest quality with Du Pont Hyperpure Silicon. It's now available in three grades for maximum efficiency and ease of use . . . having a purity range of 3 to 11 atoms of boron per billion. Technical information is available on crystal growing from Du Pont . . . pioneer producer of semiconductor-grade silicon.

NEW BOOKLET ON DU PONT HYPERPURE SILICON
You'll find our new, illustrated booklet about Hyperpure Silicon helpful and interesting—it describes the manufacture, properties and uses of Du Pont Hyperpure Silicon. For your copy write to: E. I. du Pont de Nemours & Co. (Inc.), Silicon N-2496-PI-2, Wilmington 98, Dela. (This offer is limited to U. S. and Canada.)

PIGMENTS DEPARTMENT

DU PONT
REG. U. S. PAT. OFF.

BETTER THINGS FOR BETTER LIVING
...THROUGH CHEMISTRY

Electrical Indicating Instruments by
SENSITIVE RESEARCH

Laboratory Standard and Reference Standard Portable and Panel Instruments that have earned Sensitive Research the reputation of *"Those Standards People."* All instruments have individually calibrated, hand drawn mirrored scales. Available with the now world famous SRIC *Diamond Pivot* and *Shock Mounted Jewel.* Write for Catalog 70.

The Diamond Pivot

Self-Checking Volt-Amp-Milliammeters.

Model THACH. AC-DC. 19 Ranges. Accuracy .2% to 4 KC.

Model BS. DC. 25 Ranges. 12" Vernier Scale. Accuracy .05%.

Edgewise Panel Type. AC or DC. 7" Scale. Accuracy .25%.

Waterproof! Ruggedized Polyranger. Accuracy .5%.

Single and Polyphase Wattmeters. Accuracies to .1%.

Model U88. AC-DC. 88 Ranges. Accuracy .5%.

- Ammeters
- Microammeters
- Milliammeters
- Voltmeters
- Millivoltmeters
- Kilovoltmeters
- Wattmeters
- Electrostatics
- GM and GMRP Meters
- Current Product Instruments
- Differential Galvanometers
- Corrosion Instruments
- Magnetic Test Sets
- AC and DC Test Sets
- Ratiometers
- Frequency Meters
- Fluxmeters

SENSITIVE RESEARCH INSTRUMENT CORPORATION

NEW ROCHELLE, N. Y. ELECTRICAL INSTRUMENTS OF PRECISION SINCE 1927

Symbol of Quality

IRE People

(Continued from page 24A)

initials, WRGB, to identify the station, in recognition of his contributions not only to the company's television developments but to the entire industry.

❖

The appointment of **R. L. Snyder** (M'46–SM'53) as manager of the semiconductor plant of Sylvania Electric Products Inc., in Woburn, Mass., was announced recently.

Prior to his new assignment, Mr. Snyder has held various supervisory positions within the company's Radio Tube Division. He joined Sylvania as an industrial engineer at Emporium, Pa., in 1946. Before that, he was an industrial engineer with Philco Corp. in Philadelphia.

A native of Timblin, Pa., Mr. Snyder graduated from Pennsylvania State University where he received a Bachelor of Science degree in industrial engineering in 1940. He has also done graduate work at Temple University.

During World War II, Mr. Snyder was an officer in the U. S. Army Signal Corps. He served both at the Signal Corps Engineering Laboratories at Ft. Monmouth, N. J. and in the Pacific Theatre.

❖

Buford Smith, Jr. (A'51–SM'52) has been promoted to Chief Engineer of Raytheon Manufacturing Company, Missile Systems Division, in Bristol, Tenn. Raytheon holds prime contracts with full systems responsibility for the Navy's air-to-air Sparrow III and the Army's ground-to-air Hawk Missiles.

B. Smith, Jr.

Before joining Raytheon, Mr. Smith was Supervisor of Missile Systems Section at the Naval Industrial Reserve Aircraft Plant in Bristol.

Mr. Smith received his B.S. degree in electrical engineering at the University of Tennessee in 1943, and his M.S. in electrical engineering at the University of Illinois 1949.

From 1951 to 1953 Mr. Smith was Assistant Professor in electrical engineering at the University of Akron. During this period he was a part-time consultant on radar research for Goodyear Aircraft Corporation. Prior to this he was an instructor at the University of Illinois.

Mr. Smith is a member of Tau Beta Pi, Eta Kappa Nu, and the American Society for Engineering Education. In 1949 he was a member of the Publication Committee of the National Electronics Conference. He was Secretary-Treasurer of the IRE Akron Section in 52–53.

(Continued on page 30A)

On April 7, 45 B.C., during the reign of Cleopatra, Memamadun Ptolemy (pronounced me-mama-done-toll-me), radar operator, fell asleep at just the time chosen by some unfriendly neighbors to make a border raid.

Memamadun (he was the only survivor) was brought before Cleopatra.

"Can you give me any reason why I shouldn't throw you to my pet crocodile Julius for letting such a terrible thing happen?" she asked.

Memamadun stifled a yawn.

"Even if I'd been awake, our radar wouldn't have prevented the attack," he said. "Our radar won't work."

"Why not?" the queen asked, stroking Julius' head.

"It can't," Ptolemy ptold her. "For one thing, Bomac tubes haven't been invented yet."*

"That's right, too!" Cleopatra said. "Case dismissed."

No. 2 of a series . . . **BOMAC LOOKS AT RADAR THROUGH THE AGES**

* *Bomac makes the finest microwave tubes and components this side of the Nile*

Bomac LABORATORIES, INC.
Salem Road, Beverly, Massachusetts

Leaders in the design, development and manufacture of TR, ATR, Pre-TR tubes; shutters;

Offices in major cities—Chicago • Kansas City • Los Angeles • Dallas • Dayton • Washington • Seattle • San Francisco • Toronto • **Export:** Maurice I. Parisier, 1860 Broadway, New York City

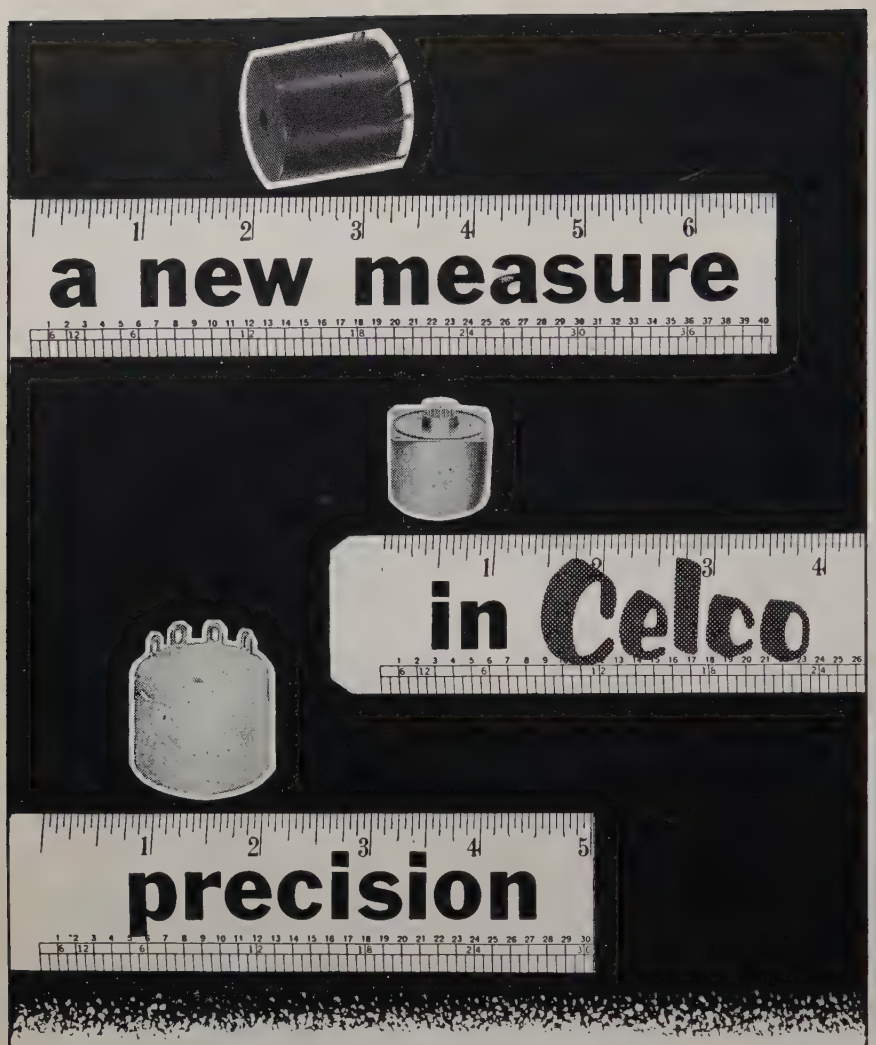

TOROIDAL COMPONENTS

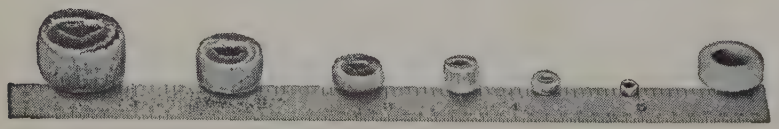

Whether it's a complex 10 winding magnetic amplifier or a simple choke . at Celco each toroid is precision-made. New core materials are used in Toroidal magnetic amplifiers, reactors and transformers to achieve maximum performance.

At Celco, the proper matching of cores, winding, handling, impregnation, encapsulation and electrical history of the final assembly is carefully controlled to maintain the original design characteristics.

Our years of design, development, and production know-how are available for application to your specific **TOROIDAL** problems.

* *For immediate attention, call* **DAvis 7-1123** *— or write today.*

Celco

Constantine Engineering Laboratories Co.

MAHWAH, NEW JERSEY

IRE People

(Continued from page 28A)

Mr. Smith has also been employed by Westinghouse Corporation and Aluminum Company of America.

❖

The scope of Sperry Gyroscope Company's commitments to the military for highly-classified electronic countermeasures, or electronic "jamming," equipment is indicated by a recent announcement of top-level appointments to the company's newly-created Countermeasures organization.

J. M. Lester (A'41–SM'47) has been named engineering manager, and **R. C. Lyons** (A'47–M'55) appointed sales manager.

Others named to Countermeasures, an organization within the company's Air Armament Division, included **K. H. Barney** (S'48–A'50–M'55–SM'57), engineering section head, systems integration; **R. V. Gould** (S'40–A'42–SM'48), engineering section head, microwave equipment; **G. K. Slaughter** (SM'52), engineering department head, electronic equipment; **J. N. Caswell** (A'42–SM'54) engineering department head, electronic equipment; and **C. E. Brockner** (A'43–SM'50), engineering department head for advanced development.

❖

J. S. Smith (S'17–A'49–SM'54) has been elected Treasurer of All-Tronics, Inc., Westbury, N. Y.

Dr. Smith, current chairman of the IRE New York Section, leaves the position of Director of Defense Engineering of the Control Instrument Company. He was previously Director of the Analog Computer Laboratory of New York University.

Don't miss the 1958 RADIO ENGINEERING SHOW!
March 24-27, 1958
New York Coliseum

Complete program and list of exhibitors in next month's issue.

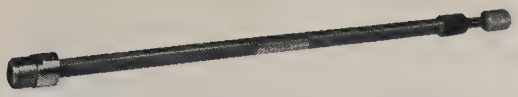

MODEL 372 SLIDING COAXIAL TERMINATIONS

This equipment, available only from Narda, provides the most convenient means for evaluating the residual VSWR of coaxial slotted lines. VSWR of the element is 1.05 or less; covers range from 2000 to 12,400 mc.

N Connector, male or female $110 **C Connector, male or female $116**

MODEL 371 FIXED COAXIAL TERMINATION

This Narda coaxial termination is the first and only to cover the entire frequency range from S to X band. Same range and element VSWR as above.

N Connector, male or female $55 **C Connector, male or female $58**

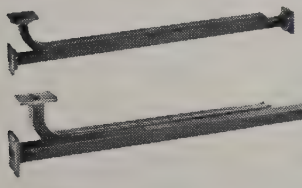

3, 6, 10 and 20 DB

40 DB HIGH POWER

HIGH DIRECTIVITY COUPLERS

The 40 db High Power Coupler is another exclusive Narda product. Similar to standard types, except that coupling irises are in the narrow wall, it may be used at full rated power of the waveguide size. Nominal coupling value is 40 db; directivity 40 db. Directivity for 3, 6, 10 and 20 db couplers is also 40 db. Standard cover flanges on primary line; low VSWR termination and standard cover flange on secondary. All bands covering frequencies from 2600 to 18,000 mc.

STANDARD REFLECTIONS

Narda offers five values of reflections for each of six different waveguide sizes . . . the most complete choice we know of! Provides calibrated reflections or VSWR's for use in standardizing reflectometers or calibrating slotted line impedance meters.

SPECIFICATIONS

Reflection Coefficient	0.00	0.05	0.10	0.15	0.20
Accuracy	0.002	0.0025	0.0035	0.0045	0.007
VSWR Equivalent	1.00	1.105	1.222	1.353	1.50

Models for 2.60 to 18.0 kmc, from $125 to $300

Microwave engineers—

Where can you use these exclusive features offered by narda?

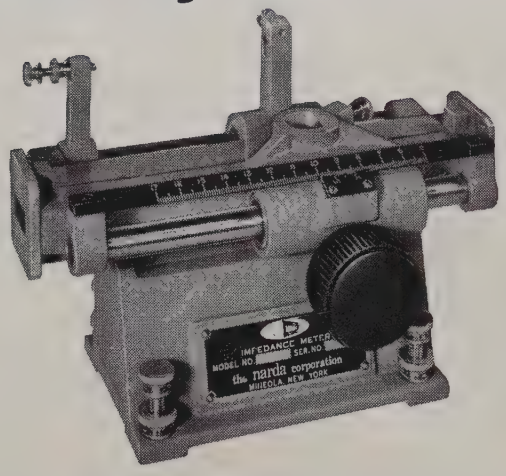

Waveguide and Coaxial IMPEDANCE METERS

Exclusively in Narda Waveguide and Coaxial Impedance Meters, the carriage mounting and drive mechanism are integral with the precisely machined transmission line casting. This insures permanent accuracy and freedom from slope errors—no more tedious adjustment or possibility of misalignment.

Other features include angle-mounted scale and vernier for optimum visibility; readily removable supporting pedestal; and smooth carriage travel action. Waveguide models, accurate for VSWR's of 1.01, are available for complete coverage from 2600 to 18,000 mc; N or C Connector coaxial models, from 1500 to 12,400 mc.

WAVEGUIDE IMPEDANCE METERS

Frequency (kmc)	Narda Model	Residual VSWR	Price
2.6 — 3.95	224	1.01	$425
3.95— 5.85	223		350
5.3 — 8.2	222		325
7.05—10.0	221		270
8.2 —12.4	220		250
12.4 —18.0	219		270

COAXIAL IMPEDANCE METERS

Frequency (kmc)	Connectors (One Male, One Female)	Narda Model	Price
1.5 to 12.4	Series N	231	$360
1.5 to 12.4	Series C	232	390

Complete Coaxial and Waveguide Instrumentation for Microwaves and UHF—including:

DIRECTIONAL COUPLERS	TUNERS	ATTENUATORS
TERMINATIONS	ECHO BOXES	STANDARD REFLECTIONS
FREQUENCY METERS	SLOTTED LINES	BOLOMETERS
HORNS	BENDS	THERMISTORS

the narda microwave corporation

160 HERRICKS ROAD, MINEOLA, N.Y. • PIONEER 6-4650

MAIL COUPON TODAY FOR FREE CATALOG AND NAME OF NEAREST REPRESENTATIVE

The Narda Microwave Corporation
160 Herricks Road
Mineola, N. Y.
Dept. PI-1

NAME_____

COMPANY_____

ADDRESS_____

CITY_____ ZONE____ STATE_____

NEWS and NEW PRODUCTS

FEBRUARY 1958

Power Supply For Transistor Circuitry

Dressen-Barnes Corp., 250 North Vinedo Ave., Pasadena, Calif., has designed a closely regulated dc power supply which offers the highest current capacity of 4 newly-designed units for powering transistor circuits. Output is 0 to 60 volts dc, continuously variable, at 3 amperes maximum. No derating of output current, or of regulation and ripple specifications, is necessary from 1 to 60 volts dc.

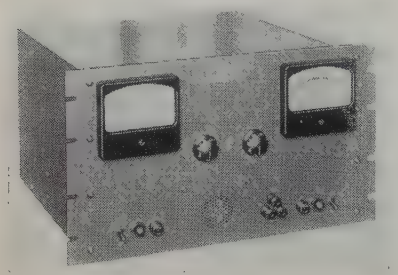

Regulation for 60 volt/3 amperes load is 20 mv change, no load to full load. For line voltage change of 105 to 125 volts ac (at 60 volt/3 ampere output), regulation is 20 mv change in output voltage. Ripple and internal noise are below 1.5 mv rms. Unit is designed for very low output impedance and fast recovery time. 1 per cent meters are supplied.

Designated as Model .6-3MB, instrument is built to fit in a standard 19 inch relay rack. Bulletin 1031 sent on request.

Magnetic Amplifier

Announcement of their new magnetic amplifier regulated 3 kva tubeless ac line voltage regulator has recently been made by **Perkin Engineering Corp.,** 345 Kansas St., El Segundo, Calif. Designated Model No. MIR-3000, this tubeless unit contains no moving parts or vibrating contacts, and

regulates the rms value. The input voltage range over which the unit operates within specifications is 95–135 volts, and the output voltage is 115 volts nominal adjustable from 110–120 volts. The regulation accuracy is ±0.50 per cent for any combination of line and load changes and the frequency range is 0.7 lagging to 0.9 leading. Maximum load is 3.0 kva and response time is 0.1 to 0.2 second.

Prompt delivery is now being offered. For further literature and specification sheets, please write to the firm on your company letterhead.

These manufacturers have invited PROCEEDINGS readers to write for literature and further technical information. Please mention your affiliation.

VHF Transceiver

Dare, Inc., Troy, Ohio, recently announced three new communication and navigation componenets which meet CAA-TSO requirements.

The new DTR-360A, a 260-channel VHF communications transceiver conforms to the requirements of TSO C37 and C38. Transmitter section of the unit provides a full 15 watts of output power on any channel from 118.0 to 135.95 mc. The double conversion receiver has a sensitivity of 2 microvolts or better on every channel. With a choice of control heads Single Channel Simplex, Double Channel Simplex or any cross channel Duplex operation can be provided. A unique circuit requires 10 conductors and a ground for connecting control head to transceiver. 38 crystals are required for 180 channel operation and 58 for 360 channel operation. Weight of the transceiver is 23.31 pounds.

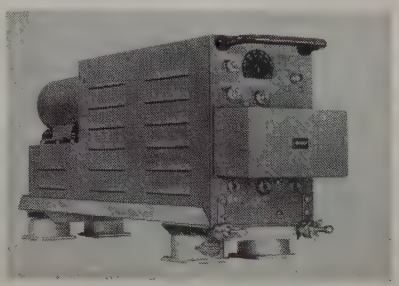

Two new communications antennas, the Dare DBA-1 and DBA-1-CP are available for use with the DTR-360A or other communications systems operating in the 118.0 to 140.0 mc region. Both models provide a Voltage Standing Wave Ratio of better than 1.5 to 1 over the entire band. The DBA-1-CP has a special long-life, two-coat plastic finish which is unaffected by the most severe weather. This same coating has been used on ship bottoms, showing no wear after two years service in salt water.

Plug-In Electronic Circuits

A completely new line of Plug-In Electronic circuits has just been announced by **Dayton Electronic Products Co.,** (DEPCO) 320 Vermont Ave., Dayton 4, Ohio. Designed to meet a wide variety of applications the P.I.E. (for Plug-In Electronics) units are being made in four standard series.

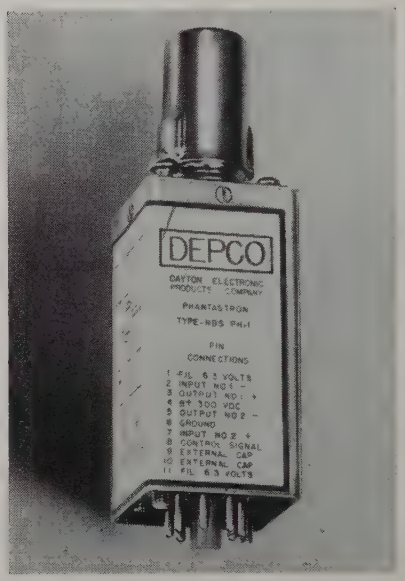

The NBS series comprises circuits recommended for use in Navy electronic equipment by the National Bureau of Standards. The instrument series includes Gate Circuits, Multivibrators, dc amplifiers and other instrument circuits with high degree of precision. The transistor series features miniaturized plug-in modules in a variety of circuit applications. The general purpose series includes a wide variety of voltage and power amplifiers plus control, regulating, and computing circuits.

All new plug-in units are designed on a basic size module to simplify physical design problems. Square, rather than round, physical shape provides better utilization of space, plus more efficient dissipation of heat. All cases are stainless steel (in smaller sizes) or aluminum (in larger plug-ins). Transistors series employ brass cases. Captive screws permit firm attachment to the unit in which the plug-in is incorporated yet prevent accidental loss of screws when the plug-in is removed. Each unit features a permament schematic on the outside of the case. Tubes used in vacuum tube circuits are premium types, and all plugs are standard.

Individual specification sheets on each plug-in are available giving application and descriptive data, plus schematic and full specifications.

(Continued on page 84A)

Use your IRE DIRECTORY! It's valuable!

TRANSFORMERS INCORPORATED has consistently designed and manufactured precision transformers that solved the transformer problems of its customers. What are YOUR problems?

PRECISION TRANSFORMER PROBLEMS?

SIZE AND WEIGHT

ACCURACY

RELIABILITY

Because of advances in transformer design calculation methods and technique, Transformers, Incorporated can accurately establish the size and weight of the required transformer from your performance specifications, without the expensive and time consuming construction and testing of prototypes. These same advances in transformer design engineering have enabled Transformers, Incorporated to produce the smallest and lightest precision transformers available. This is particularly important in this era of miniaturization, peculiar space envelopes, and rigid weight requirements.

Transformers, Incorporated designs and manufactures transformers with a measured voltage ratio accuracy of up to five parts per million (0.0005%) at room temperatures and under no-load condition, with comparable accuracies at other temperatures and loads. These accuracies can be maintained in all production quantities from one to one thousand—or any other quantity that you may require. The ability of Transformers, Incorporated to maintain specified accuracies has been consistently proven by samples submitted to the U. S. Bureau of Standards Testing Laboratory.

Each and every transformer is individually inspected and electrically tested, and samples are subjected to the required environmental tests, to ensure the highest degree of reliability. These methods far exceed the usual sampling techniques of most quality control systems, and enable Transformers, Incorporated to guarantee that every precision transformer will meet or exceed customer specifications.

Relieve your engineering department of the arduous task of designing precision transformers. Phone ENDICOTT, NEW YORK 8-3311, collect. Ask for Tres Park. There's no obligation.

Partial List of SATISFIED CUSTOMERS: Ballantine Laboratories • Bell Aircraft • Boeing Airplane Company • Curtiss-Wright • Daystrom Instrument • Dumont Laboratories • General Electric • Hughes Aircraft • IBM • Kollsman Instrument • Link Aviation • Leeds & Northrup Massachusetts Institute of Technology • Melpar, Inc. • Norden-Ketay • Raytheon • Sperry-Gyroscope • Sylvania . . . and others.

TRANSFORMERS, INCORPORATED

200 Stage Road, Vestal, N.Y.

why design your own

COAXIAL CRYSTAL MIXERS

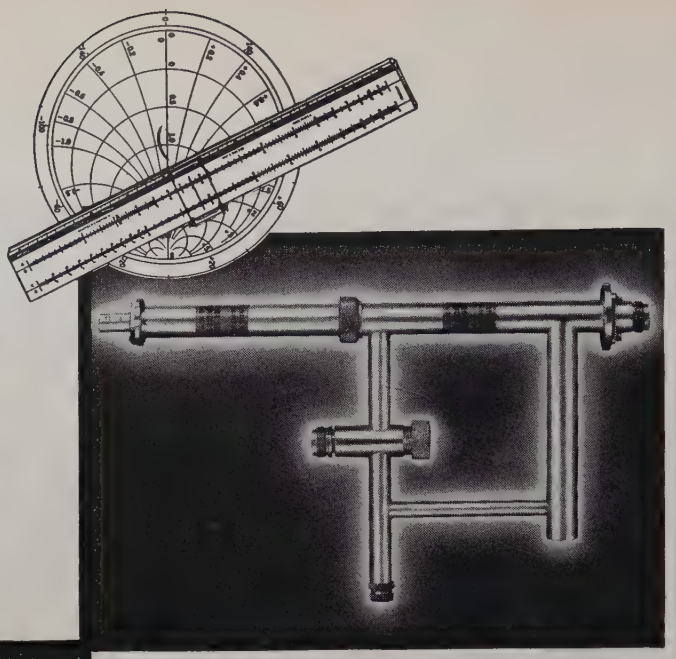

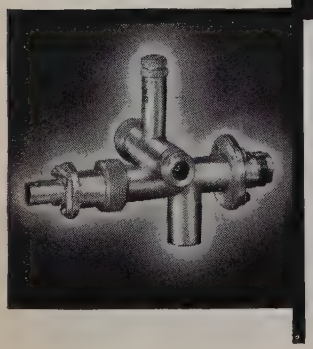

...you can buy them from stock!

Save time... reduce costs... avoid design headaches. Empire Devices offers a wide variety of standard broad band, fixed tuned coaxial crystal mixers to meet your needs. Specialized manufacturing facilities and techniques result in economy, and a high degree of quality control by competent engineers assures uniformity in manufacture. Immediate delivery in many instances.

Select one of 8 models in the CM-107 Series, covering the entire frequency range from 225 to 5600 mc. Input VSWR of any crystal mixer in the line is better than 2:1, without adjustments, for all frequencies within its rated range. Local oscillator input requires 10 milliwatts, has a VSWR of 2:1 or better with any injector adjustment. A choice of input connectors is available. Standard models can be modified for special purposes!

For complete engineering data, ask for our free catalog

NEW YORK—DIgby 9-1240 • SYRACUSE—GRanlt 4-7409 • PHILADELPHIA—SHerwood 7-9080 • BOSTON—TWinbrook 4-1955 • WASHINGTON, D. C.—DEcatur 2-8000 • ATLANTA—CEdar 7-7801 • DETROIT—BRoadway 3-2900 • CLEVELAND—EVergreen 2-4114 • PITTSBURGH—ATlantic 1-9248 • ST. LOUIS—EVergreen 5-7728 • DAYTON—FUlton 8794 • CHICAGO—ESterbrook 9-2700 • DENVER—MAin 3-0343 • FORT WORTH—WAlnut 6-4414 • ALBUQUERQUE—ALbuquerque 5-9632 • LOS ANGELES—REpublic 2-8103 • PALO ALTO—DAvenport 3-4455 • PORTLAND—CApitol 7-3830 • CANADA: STITTSVILLE, ONT.—HAzeldean 56 • EXPORT: NEW YORK—MUrray Hill 2-3760

edp

EMPIRE DEVICES

PRODUCTS CORPORATION

AMSTERDAM, NEW YORK

Telephone: Victor 2-8400

manufacturers of

FIELD INTENSITY METERS • DISTORTION ANALYZERS • IMPULSE GENERATORS • COAXIAL ATTENUATORS • CRYSTAL MIXERS

Industrial Engineering Notes*

EIA Activities

A "new record in production and dollar volume" was achieved by the electronics industry in 1957 and "further increases are expected in 1958," Executive Vice-President J. D. Secrest said at a sponsored U. S. Chamber of Commerce Symposium. Factory sales of electronic products rose "from $5.9 billion to more than $7 billion this year" and another "increase of 8 to 10 per cent is expected next year," Mr. Secrest said as he took part in the annual "Business Forecast Symposium" of the U. S. Chamber of Commerce. Military procurement led the electronic increase in 1957, he said, "rising from $2.7 billion to nearly $3.5 billion." Greater emphasis on missile output and a higher defense budget "are certain to boost this figure in 1958," Mr. Secrest said. Research expenditures also will rise, he noted. "It is significant that between 1950 and 1957 home entertainment products dropped from 58 per cent to 21 per cent of electronic factory sales, while the military share rose from 20 per cent to about 50 per cent. Uncle Sam is now by far the industry's biggest customer," he said. Mr. Secrest noted that industrial electronic progress is over-shadowed by military uses, but "offers the greatest promise for the future. Already," he said, "it is running a close second to the home entertainment business and may well surpass it next year." Industrial uses of electronics continued to increase in 1957, he said. Factory sales increased from $950 million to $1.3 billion, and further growth is indicated in this market in 1958, he said. "Only TV receiver production declined during the past year, but greater stability and balanced inventories improved the profit position of most companies. Retail sales declined less than factory output. Manufacturers believe both production and sales will rise in 1958," Mr. Secrest said. Noting that radio set output continued its climb "to near post-war peaks, rising 9 per cent above 1956," every indication points to a continuing trend upward in 1958, he said. "Phonograph sales rose 16 per cent in 1957 and are expected to pass the 5-million-a-year mark in 1958," he said. "Component manufacturers' sales were above those of 1956 largely because of the rising replacement market which gained another $50 million to reach $900 million for the year. Transistor sales reached 27 million—more than double the 1956 figure." In conclusion, Mr. Secrest said, "Closed circuit television made rapid advances in 1957 both in educational and industrial uses and made its debut as an entertainment medium in the home. While the future of the latter is problematical, there seems little doubt that wired TV is proving a valuable tool in the classroom and in many industrial processes."

(Continued on page 70A)

* The data on which these NOTES are based were selected by permission from *Industry Reports*, issues of November 25, and December 2, 19 and 16, published by the Electronic Industries Association whose helpfulness is gratefully acknowledged.

YOU CAN DEPEND ON

DALOHM Ω ®

MINIATURE POWER PRECISION

RESISTORS

HI-TEMPERATURE
– 65° C to + 275° C

HI-PRECISION
± 0.05% to ± 3%

HI-WATTAGE
10 to 250 WATTS

HI-RESISTANCE
0.1 Ohm to 100K Ohms

Dipped in MOLTEN SOLDER . . . yet retains 100% reliability!

Most requirements for DALOHM RH and PH wire wound resistors will not be as severe as the molten solder dip shown above. But, here are the tough parameters RH and PH types will meet.

- Operating temperature range: –65° C. to 275° C.
- Precision tolerance range: ± 0.05%, ± 0.1%, ± 0.25%, ± 0.5%, ± 1% and ± 3%.
- Powered at 10, 25, 50, 100 and 250 watts.
- Resistance range from 0.1 Ω to 100,000 Ω.
- Surpasses requirements of MIL-R-18546B
- Temperature coefficient: 0.00002/degree C.
- Complete protection from vibration, moisture and salt spray.
- Insulation breakdown: 1000 V AC or DC.

DALOHM RH and PH resistors are advanced design wire wound precision power resistors for applications under severe operating conditions, coupled with tight space requirements. These miniature powerhouse resistors offer complete protection from mechanical shock, vibration, moisture and salt spray.

DALOHM four point "ruggedized" construction provides 100% reliability with: 1. Precision wire wound resistor element. 2. All welded construction from terminal to terminal. 3. Suspension in special shock absorbing compound. 4. Insertion and sealing in radiator finned, anodized aluminum housing for maximum heat dissipation on panel mounting.

Careful advanced production techniques, backed by years of experience, and total progressive inspection assure reliability in all DALOHM resistors.

RH-10

10 watts, derating to 0 at 275° C.; .5 Ω to 30K Ω; ± 0.05% to ± 3%; Max. Working voltage; 500 volts.

TYPICAL RH-25 DERATING CURVE

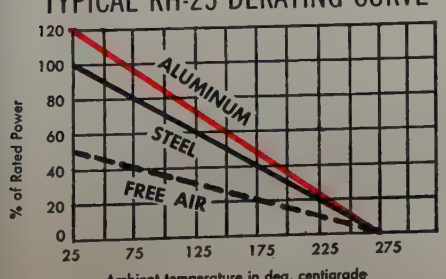

RH-25

25 watts, derating to 0 at 265° C.; .1 Ω to 15K Ω; ± 0.05% to ± 3%; Max. Working Voltage: 800

RH-50

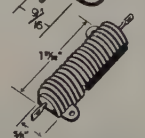

50 watts, derating to 0 at 265° C.; .3 Ω to 100K Ω; ± 0.05% to ± 3%; Max. working voltage: 1000 V DC or AC

RH-250

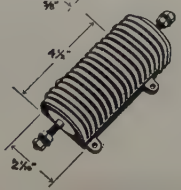

250 watts, derating to 0 at 265° C.; .3 Ω to 35K Ω; ± 0.05% to ± 3%; Max. working voltage: 1000 V DC or AC

PH TYPE

New hole mounted power resistor in shock absorbing compound and in black anodized aluminum radiator finned housing.

PH-25

25 watts, derating to 0 at 265° C.; .1 Ω to 60K Ω; ± 0.05% to ± 3%; Max. working voltage: 800 V DC or AC

PH-100

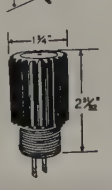

100 watts, derating to 0 at 275° C.; .5 Ω to 35K Ω; ± 0.05% to ± 3%; Max. working voltage: 1000 V DC or AC.

JUST ASK US

DALOHM line includes a complete selection of precision wire wound, power and precision deposited carbon resistors. Also trimmer potentiometers, precision wire wound and deposited carbon; and collet fitting knobs. Write for free catalog.

If none of DALOHM standard line meets your need, our engineering department is ready to help solve your problem in the realm of development, engineering, design and production. Just outline your specific situation.

DALE PRODUCTS, INC.
1302 28th Ave.
Columbus, Nebr., U.S.A.

For Fast, Accurate Matching of Resistors, Capacitors, Inductors

SIE® **E-2 COMPARISON BRIDGE**

1 ohm to 5 megohms, 500 mmfd to 2,000 mfd, 3 millihenrys to 10,000 henrys.

- Five meter ranges: 1%, 2.5%, 5% 10% and 25% difference readings at full scale.
- Accurate within 0.1% on 1% scale.
- Component differences of 1 part in 10,000 can be detected.
- Can be used with decade box for precise component measurements.

$185.00

SIE — ONE OF THE DRESSER INDUSTRIES

SOUTHWESTERN INDUSTRIAL ELECTRONICS COMPANY

2831 Post Oak Road • P. O. Box 13058 • Houston 19, Texas

WELWYN

Hermetically Sealed Deposited Carbon Resistors

High stability resistors bonded into glazed and vitrified ceramic shells for complete protection against ambient humidity changes.

Silicone oil filled—acts as efficient convective medium for improved heat dissipation. Also serves as infallible quality control for detecting seal leakage defects.

As part of quality control, each resistor is subjected to sustained pre-load test at 1½ times rated wattage. Insures against catastrophic failures under normal operating conditions.

Designed to meet military specifications. MIL-R-10509 (current issue)

for complete data, write to: Dept. CU-2

WELWYN INTERNATIONAL, INC.

3355 Edgecliff Terrace, Cleveland 11, Ohio

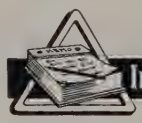

Industrial Engineering Notes

(Continued from page 68A)

GOVERNMENT

In General Information Bulletin—G' issued Dec. 3, the FCC has documented its provisions for single sideband radiotelephony. The Commission said it is: "Actively continuing its efforts to encourage wider use of single sideband transmission methods for radiotelephone transmissions on frequencies below 25 mc. The principal advantages of single sideband transmission are the savings in spectrum space occupied by the signals, the low power required for satisfactory communication, improved intelligibility and lesser interfering effects, as compared with amplitude modulation (double sideband) transmission." Copies of the bulletin can be had by writing to the FCC, New Post Office Building, Washington 25, D. C.

MARKETING

Television output in October totaled 661,994 compared with 832,631 TVs made in September and 820,781 television receivers made in October, 1956. The number of TVs produced with UHF tuners totaled 83,372 in October against the 87,040 made in September and 131,243 pro-

(Continued on page 72A)

MICROWAVE AND SPECIAL TUBE NEWS from SYLVANIA

MINIATURE COUNTER TUBES...

New 100 KC counter tube, type 7155, is introduced by Sylvania for smaller, lighter counting devices

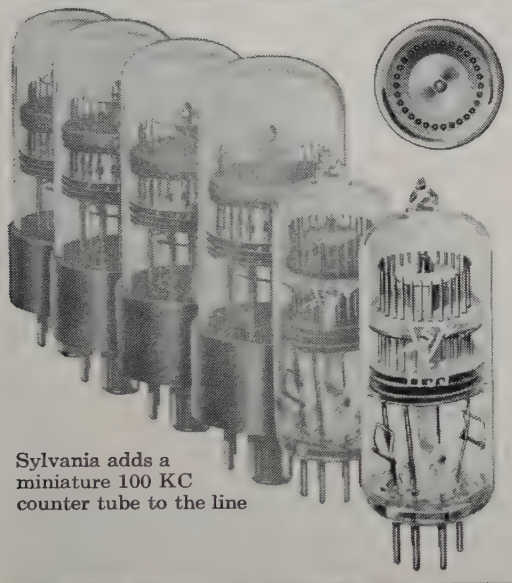

Sylvania adds a miniature 100 KC counter tube to the line

High-speed counter tube with three output cathodes in a T 5½ envelope is now available from Sylvania. The new tube, type 7155, is of particular value in equipment design where size and weight are important factors. This latest addition to the counter tube line follows by less than a year Sylvania's development of the first 100 KC counter tube.

Type 7155 operates with the reliability, accuracy and simple circuitry typical of all Sylvania counter tubes. As with the other high-speed tubes in the line, types 6909 and 6910, the new counter tube can be used singly or cascaded in multiple stage counting for laboratory or industrial applications.

RATINGS (Absolute Values)

Total Anode Current	0.7 Ma 1.2 Ma	Min. Max.
Voltage Between Electrodes (Other than Anode)	140 Volts	Max.
Supply Voltage (Anode to Cathode)	425 Volts	Min.
Input Frequency	100,000 P.P.A.	Max.

COAXIAL TR TUBES...

Sylvania develops new TR construction—a coaxial tube for low frequencies

New coaxial TR tube saves space and weight at low frequencies

TR tubes in coaxial construction for low frequency radar and countermeasure equipment are now in production at Sylvania. Typical of the new tubes available is the TR860, a 9-inch diameter type designed for very high power. It utilizes one of the largest ceramic-to-metal seals in existence.

The new coaxial construction is based on four years of research and development work by Sylvania. One of its major advantages over conventional rectangular TR's at low frequencies is the great saving in space and weight it makes possible. In addition, the new coaxial tubes are much more rugged than conventional types because of smaller window and seal areas.

NEW MICROWAVE CRYSTAL DIODES...

Double-ended construction adds new convenience to S and X band crystal diodes

Sylvania's new dual duty microwave crystal diodes utilize detachable spring-grip base

New Sylvania microwave crystal diodes in the S and X bands can now serve as either forward or reverse diodes. A detachable spring-grip base can be slipped on either end for forward or reverse use.

The dual diodes eliminate the need to specify reverse types and simplify ordering and stocking.

Designations for the new double-ended diodes are 1N416B, C, D and E for 1N21 types and 1N415B, C, D and E for the 1N23 series.

SYLVANIA ELECTRIC PRODUCTS INC.
1740 Broadway, New York 19, N.Y.
In Canada: Sylvania Electric (Canada) Ltd.
Shell Tower Building, Montreal

SYLVANIA

LIGHTING • TELEVISION • RADIO • ELECTRONICS • PHOTOGRAPHY • ATOMIC ENERGY • CHEMISTRY-METALLURGY

FREED TELEMETERING COMPONENTS

FOR IMMEDIATE DELIVERY FROM STOCK

BAND PASS FILTERS					DISCRIMINATORS				
Catalog No. $Z_0 = 500\Omega$	Catalog No. $Z_0 = 2,500\Omega$	3DB Bandwidth per cent of F_0 ± 9¾	± 19½	Center Frequency F_0 (KC)	Per cent Deviation of F_0 8½	15.	Per cent Linearity 0.5	1.0	Catalog No.
FBP-10	FBP-34	√		.4	√		√		DST-10
FBP-11	FBP-35	√		.56	√		√		DST-11
FBP-12	FBP-36	√		.73	√		√		DST-12
FBP-13	FBP-37	√		.96	√		√		DST-13
FBP-14	FBP-38	√		1.3	√		√		DST-14
FBP-15	FBP-39	√		1.7	√		√		DST-15
FBP-16	FBP-40	√		2.3	√		√		DST-16
FBP-17	FBP-41	√		3.0	√		√		DST-17
FBP-18	FBP-42	√		3.9	√		√		DST-18
FBP-19	FBP-43	√		5.4	√		√		DST-19
FBP-20	FBP-44	√		7.35	√		√		DST-20
FBP-21	FBP-45	√		10.5	√		√		DST-21
FBP-22	FBP-46	√		12.3	√		√		DST-22
FBP-23	FBP-47	√		14.5	√		√		DST-23
FBP-24	FBP-48	√		22.0	√		√		DST-24
FBP-25	FBP-49		√	22.0		√		√	DST-29
FBP-26	FBP-50	√		30.0	√		√		DST-25
FBP-27	FBP-51		√	30.0		√		√	DST-30
FBP-28	FBP-52	√		40.0	√		√		DST-26
FBP-29	FBP-53		√	40.0		√		√	DST-31
FBP-30	FBP-54	√		52.5	√		√		DST-27
FBP-31	FBP-55		√	52.5		√		√	DST-32
FBP-32	FBP-56	√		70.0	√		√		DST-28
FBP-33	FBP-57		√	70.0		√		√	DST-33

DISCRIMINATOR LOW PASS FILTERS

Catalog No.	Center Frequency F_0 (cps)	Catalog No.	Center Frequency F_0 (cps)	Catalog No.	Center Frequency F_0 (cps)	Attenuation
OUTPUT						
LPO-10	6	LPO-19	81	LPO-28	790	.2 DB to 0.5 F_0; 7 DB to 1 F_0; 20 DB to 2 F_0; 30 DB from 2.5 F_0
LPO-11	8	LPO-20	110	LPO-29	900	
LPO-12	11	LPO-21	160	LPO-30	1,050	
LPO-13	14	LPO-22	185	LPO-31	1,200	
LPO-14	20	LPO-23	220	LPO-32	1,600	
LPO-15	25	LPO-24	330	LPO-33	2,100	
LPO-16	35	LPO-25	450	LPO-34	7,200	
LPO-17	45	LPO-26	600	LPO-35	10,000	
LPO-18	60	LPO-27	660			
Characteristic impedance of all—330Ω						
INPUT						
LPI-10	400	LPI-17	3,000	LPI-23	14,500	.05 DB at 9¾% F_0; 30 DB at third; 50 DB at fifth Harmonics
LPI-11	560	LPI-18	3,900	LPI-24	22,000	
LPI-12	730	LPI-19	5,400	LPI-25	30,000	
LPI-13	960	LPI-20	7,350	LPI-26	40,000	
LPI-14	1,300	LPI-21	10,500	LPI-27	52,500	
LPI-15	1,700	LPI-22	12,300	LPI-28	70,000	
LPI-16	2,300					
Characteristic impedance of LPI-10 thru 23—30,000Ω of LPI-24 thru 28—5,100Ω						

Write for detailed information on these and other components for military and commercial applications. Send for NEW 48 page TRANSFORMER CATALOG. Also ask for complete LABORATORY TEST INSTRUMENT CATALOG.

FREED TRANSFORMER CO., INC.
1720 WEIRFIELD ST.
BROOKLYN (RIDGEWOOD) 27, N.Y.

Industrial Engineering Notes

(Continued from page 70A)

duced in October, 1956. Cumulative television production during the first 10 months of 1957 amounted to 5,251,158 receivers compared with 6,080,052 produced during the like 10-months period during 1956. . . . **Radio receiver production in October totaled 1,569,180 including 522,746 automobile receivers, compared with 1,610,748 radios produced in September, which included 446,419 auto sets, and 1,348,864 radios including 547,818 auto receivers produced in October, 1956.** Cumulative radio output during the first 10 months of 1957 totaled 11,945,534 including 4,362,091 automobile receivers, compared with 10,884,760 receivers made during the corresponding 10 months of 1956, which included 3,607,911 auto sets. . . . **Factory sales of transistors in October increased over the number sold in September and showed a continued, heavy cumulative gain over the corresponding period of 1956.** Factory sales of transistors in October totaled 3,544,000 units with a dollar value of $7,075,000. Cumulative sales of these semiconductor devices during the first 10 months of 1957 totaled 22,386,300 units valued at $56,131,000 compared with 9,403,000 transistors sold during the like months of 1956 with a dollar value of $27,102,000.

Military Electronics

R. M. Page, the man who built the first pulse radar system in the U. S., has been appointed Director of Research Laboratory, the Navy has announced. Dr. Page's duties will include the direction and coordination of the laboratory's overall research program, which includes research in fourteen fields of the physical sciences. Dr. Page's previous position was that of Associate Director of Research for Electronics at NRL. . . . **The electronic "brain" of guided missiles, aircraft, ammunition and many other electronic items can be greatly reduced in size through a new "printed circuit" method of making transistors developed by Army research scientists, the Army said.** Now, it said, the transistors, too, can be made as an integral part of the printed circuit. Technically, the new transistor method starts with a tiny wafer of the metal germanium. Photosensitive film provides precise positioning masks on a ceramic plate for the pin-point electrodes of the transistor. The electrodes are formed by vapor deposit. The present step, called micro-miniaturization, used transistors at first, and now cuts the size of transistors to about 1/20 inch wide and 1/100 inch high.

Use your IRE DIRECTORY! It's valuable!

Specialists in the Unusual
SIGMUND COHN
MOUNT VERNON, N.Y.
Electroplated
WIRES
for many different applications
Continuous electroplating methods permit coating of many metals on to wire (or ribbon) in specified thicknesses of plate . . . This very flexible operation makes it possible to designate a desirable base or precious metal with a coating of another metal for its own particular characteristics. In our laboratory Tungsten wire as small as .00015" has been electroplated with Gold. . . . New combinations of plating on wire are being developed by our research staff from time to time. Your inquiry is invited.
Write for List of Products
Consult us, without obligation, about your specific wire problems.
SINCE 1910
SIGMUND COHN MFG. CO., INC.
121 SO. COLUMBUS AVE., MOUNT VERNON, N. Y.

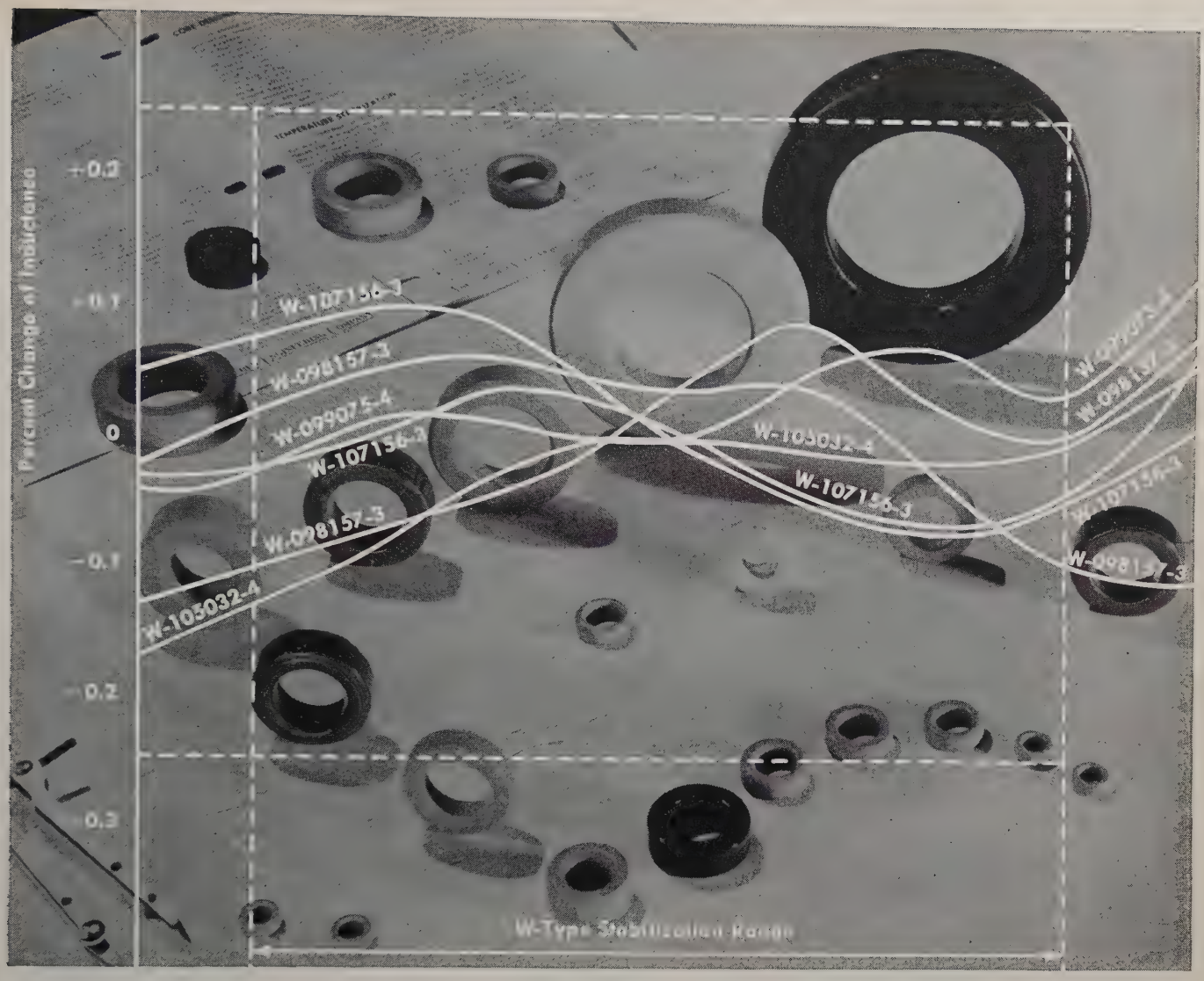

ARNOLD offers you the widest selection of Temperature Stabilized MO-PERMALLOY POWDER CORES

Arnold Molybdenum Permalloy powder cores are available with the temperature coefficient of inductance controlled within certain limits over specific temperature ranges. Most core sizes and permeability combinations can be supplied in at least one of the four different types of temperature stabilization available.

For example, most of the popular core sizes are manufactured in the new type of wide range—"W"—stabilized cores whose temperature coefficient of inductance does not exceed 0.5% over the temperature range covered by the MIL-T-27 specification of −55° C to +85° C.

This type of guaranteed maximum change of inductance with temperature, as well as the constancy of permeability with time and flux level, are of particular importance to apparatus and circuit engineers. Many precision military and industrial applications demand the uniform performance and the excellent physical properties found only in Arnold Mo-Permalloy powder cores.

For design flexibility they are furnished in a full range of sizes, up to 5.218" O.D., in four standard permeabilities: 125, 60, 26 and 14. You will find them dependable and easy to use. You will find most sizes and types in stock *now* for immediate shipment.

● Let us furnish your requirements for temperature stabilized Mo-Permalloy powder cores, or any magnetic materials you need, from the most complete line in the industry.

WSW 6999

For more information write for Bulletin PC-104B

Lists complete line of Mo-Permalloy Powder cores . . . available in 23 sizes from 0.500" O.D. to 5.218" O.D. Furnished also with various types of temperature stability from Type "A" unstabilized to Type "W" stabilized over the temperature range of −65° F to +185° F.

ADDRESS DEPT. P-82

THE ARNOLD ENGINEERING COMPANY

Main Office & Plant: Marengo, Illinois

Repath Pacific Division Plant: 641 East 61st Street, Los Angeles, Calif.

District Sales Offices:

Boston: 49 Waltham St., Lexington *Los Angeles:* 3450 Wilshire Blvd.

New York: 350 Fifth Ave. *Washington, D.C.:* 1001-15th St., N.W.

we don't make
a "SPECIAL"
of sealing out
SMOG,
SMOKE
and SWEAT

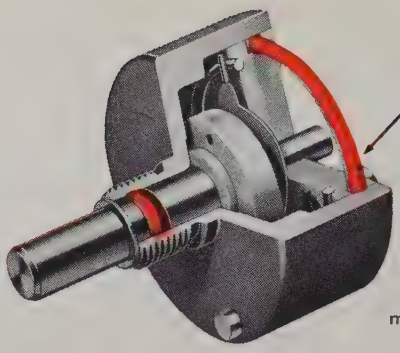

PRM-123 Precision Potentiometer
Rotary type, linear, single turn, 1¾" dia., bushing mounted, sleeve bearing.

This particular little precision pot of ours meets Government specs, competitive specs and specs that haven't been written yet, but we feel none of that lifetime performance is worth anything to you unless it's *sealed in*—against smog, smoke and sweat for the life of the pot. So we seal all our pots as *standard,* and don't charge you extra, to safeguard the dependability we've built *into* the pot.

General Controls maintains forty-two factory branch offices in key cities, staffed with sales engineers who know the story on why this PRM-123 is a better pot for you. They are in the phone book. Give them a call.

GENERAL CONTROLS
ELECTRONICS DIVISION
Glendale, California • Skokie, Illinois • Guelph, Ontario, Canada
Factory Branch Offices in 42 principal cities

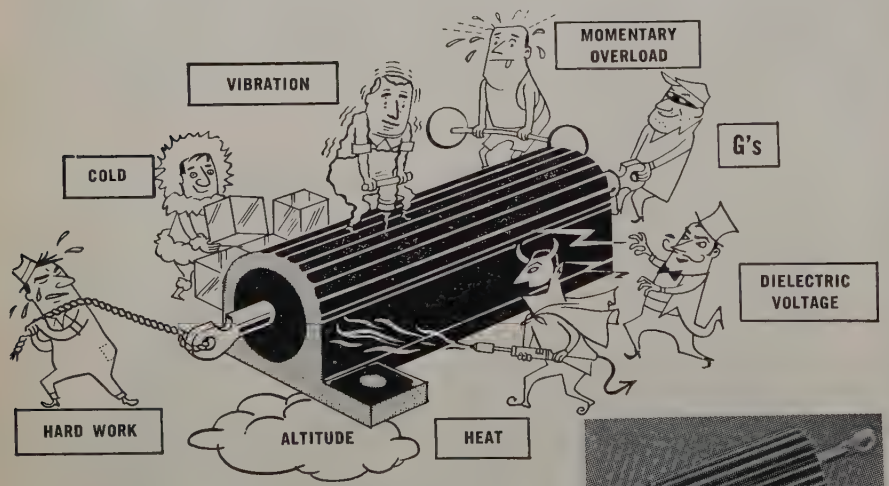

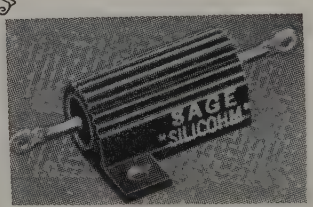

SAGE pioneered the metal-clad, chassis-mounted resistor. Truly miniature for the job it does, the Type "M" is establishing a reputation for dependable, trouble-free performance—a tribute to SAGE engineering skill and manufacturing "know-how."

We invite your inquiry regarding heat-sink applications . . . Write for complete specifications.

NEW SAGE "Silicohm"
TYPE "M", METAL-CLAD
RESISTORS
Available in 25 and 50 watts up to 60,000 ohms. Meet MIL-R-18546 requirements.

SAGE ELECTRONICS CORPORATION
300 North Goodman St., Rochester 7, N. Y.

News-New Products

These manufacturers have invited PROCEEDINGS readers to write for literature and further technical information. Please mention your IRE affiliation.

(Continued from page 34A)

Antennas-Accessories And Towers Catalog

Communications Products Co., Inc., Marlboro, N.J., recently published a new 40 page catalog completely describing their line of 2-way mobile radio antennas, accessories and towers.

In addition to listing and illustrating 45 items, accurate field strength patterns are given; a type and size for any service may be found here.

Jackson Moves To Larger Quarters

Jackson Electronic and Mfg. Co., manufacturer of custom electronic controls and specialized test equipment, has increased its floor space and added considerably to its manufacturing facilities in a move to new quarters at 695 Johnston Street, Akron, Ohio.

Jackson has been primarily engaged in developing and building special test units for use in aircraft production and maintenance, as well as electronic control equipment for the radar, communications and missile fields. The increased space provided by the new location will be used for expanding production in these fields.

Gas-Tetrode Thyratron

Electron Tube Div., Radio Corp. of America, 415 S. Fifth St., Harrison, N. J., announces the 5727, a "premium" gas-tetrode thyratron of the 7-pin miniature type. It is designed especially for use in relay, grid-controlled rectifier, and pulse-modulator circuits of military and industrial electronic equipment where dependable performance under shock and vibration is a fundamental consideration.

(Continued on page 86A)

You get MORE out of your oscilloscope investment..... when you choose a Tektronix Oscilloscope with the Plug-in Feature

Here's why: When you purchase your oscilloscope you can select one or more plug-in units, depending on your exact needs for the immediate future. Then, when an unexpected requirement develops – for instance, extremely-low-level work – you can purchase the appropriate plug-in unit at modest cost . . . in this case a Type 53/54E at only $165. With the present total of eleven available plug-in units, you are still able to enter any of several other highly-specialized application areas with the same oscilloscope, for just the cost of the appropriate plug-in unit.

Your Tektronix Field Engineer or Representative will be happy to supply you with complete specifications on these oscilloscopes and plug-in units, and arrange a demonstration in your particular application.

CHARACTERISTICS OF TYPE 53/54 PLUG-IN PREAMPLIFIERS

Plug-In Unit	Risetime of Combination —plugged into Type 541-545	Risetime of Combination —plugged into Type 531 535-536	Risetime of Combination —plugged into Type 532	Passband of Combination —plugged into Type 541-545	Passband of Combination —plugged into Type 531 535-536	Passband of Combination —plugged into Type 532	Calibrated Deflection Factor	Input Capacitance	Price
Type 53/54A Wide-Band DC	0.018 μsec	0.035 μsec	0.07 μsec	dc to 20 mc	dc to 10 mc	dc to 5 mc	0.05 v/cm to 20 v/cm	47 μμf	$ 85
Type 53/54B Wide-Band High-Gain	0.03 μsec	0.04 μsec	0.07 μsec	2 c to 12 mc	2 c to 9 mc	2 c to 5 mc	5 mv/cm to 0.05 v/cm	47 μμf	$125
	0.018 μsec	0.035 μsec	0.07 μsec	dc or 2 c to 20 mc	dc or 2 c to 10 mc	dc or 2 c to 5 mc	0.05 v/cm to 20 v/cm		
Type 53/54C Dual-Trace DC	0.015 μsec	0.035 μsec	0.07 μsec	dc to 24 mc	dc to 10 mc	dc to 5 mc	0.05 v/cm to 20 v/cm	20 μμf	$275
Type 53/54D High-Gain DC Differential	0.18 μsec	0.18 μsec	0.18 μsec	dc to 2 mc	dc to 2 mc	dc to 2 mc	1 mv/cm to 50 v/cm	47 μμf	$145
Type 53/54E Low-Level AC Differential	6 μsec	6 μsec	6 μsec	0.06 cycles to 60 kc	0.06 cycles to 60 kc	0.06 cycles to 60 kc	50 μv/cm to 10 mv/cm	Approximately 50 μμf	$165
Type 53/54G Wide-Band DC Differential	0.018 μsec	0.035 μsec	0.07 μsec	dc to 20 mc	dc to 10 mc	dc to 5 mc	0.05 v/cm to 20 v/cm	47 μμf	$175
Type 53/54H DC Coupled High-Gain Wide-Band	0.023 μsec	0.037 μsec	0.07 μsec	dc to 15 mc	dc to 9.5 mc	dc to 5 mc	0.005 v/cm to 20 v/cm	47 μμf	$175
Type 53/54K Fast-Rise DC	0.012 μsec	0.031 μsec	0.07 μsec	dc to 30 mc	dc to 11 mc	dc to 5 mc	0.05 v/cm to 20 v/cm	20 μμf	$125
Type 53/54L Fast-Rise High-Gain	0.015 μsec	0.035 μsec	0.07 μsec	3 c to 24 mc	3 c to 10 mc	3 c to 5 mc	5 mv/cm to 2 v/cm	20 μμf	$185
	0.012 μsec	0.031 μsec	0.07 μsec	dc or 3 c to 30 mc	dc or 3 c to 11 mc	dc or 3 c to 5 mc	0.05 v/cm to 20 v/cm		

Tektronix, Inc.

P. O. Box 831 • Portland 7, Oregon

Phone CYpress 2-2611 • TWX-PD 311

Cable: TEKTRONIX

Type 53/54T Time-Base Plug-In Unit

The Type 53/54T generates sweep voltages to drive the horizontal-deflection system of the Type 536 Oscilloscope. 22 calibrated sweep rates from 0.2 μsec/div to 2 sec/div are selected with a single control. 5x magnifier increases calibrated sweep rate to 0.04 μsec/div. Triggering is fully automatic or manual with amplitude-level selection and preset or manual stability control. Unblanking is dc-coupled. Price—$225.

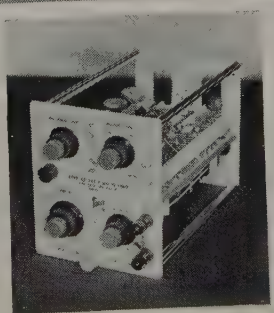

Type 53/54R Transistor Testing Plug-In Unit

The Type 53/54R Plug-In Unit contains a signal source and collector and bias supplies for accurately measuring delay, rise, storage, and fall times of transistors. A mercury switch operating at a repetition rate of 120 c/sec supplies the testing signal. Like all other Type 53/54 Plug-In Units, the Type 53/54R is interchangeable among all Tektronix Oscilloscopes with the plug-in feature. Scheduled for regular production in April, 1958.

Precision Potentiometers by RATTRAY

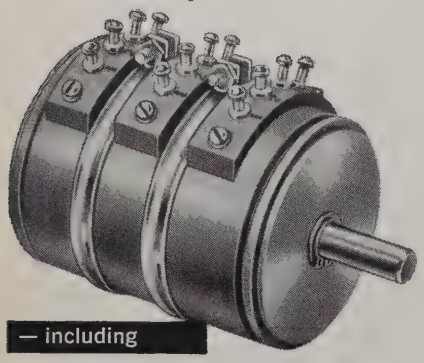

— including

- MINIATURE TYPES
- SUB-MINIATURES
- MULTI-GANG UNITS
- STANDARD TYPES

— featuring

- HIGH ACCURACY
- LOW TORQUE
- EXCELLENT RESOLUTION
- LOW NOISE

Rattray experience-engineered precision potentiometers are supplied in types that meet most electronic applications. Complete research and development facilities, and unique winding techniques, make it possible to produce custom designs to the most critical military and commercial specifications. All-metal construction of mounting and aligning surfaces provides precise mechanical interchangeability. Precise electrical performance is obtained by detailed quality checks throughout production. Special winding machines assure high resolution and function accuracy.

New Handbook Available—
28 pages of engineering data on Rattray precision potentiometers with helpful technical information for designers and engineers.

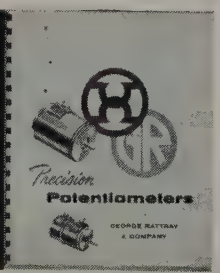

Call or write Rattray now for catalog or quotations on your potentiometer applications.

GEORGE RATTRAY & COMPANY
A Division of Hardwick, Hindle, Inc.
116-08 MYRTLE AVENUE
RICHMOND HILL 18, N. Y.

News-New Products

(Continued from page 84A)

Developed from the popular type 2D21, the 5727 offers important advantages in dependability and ability to resist shock and vibration—advantages achieved by structural refinements, stringent production controls, rigorous tests for shorts and leakage, and quality control of critical characteristics both initially and during life. These factors all contribute to the long and dependable performance of the 5727. Bulletin available.

AMF Names Childs

Samuel J. Childs has been appointed group executive of **American Machine & Foundry Company's Defense Products Group,** it was announced by Morehead Patterson, chairman and president. He replaces Tad Stanwick, who resigned.

AMF's Defense Products Groups, with headquarters in Alexandria, Virginia, comprises six divisions and a subsidiary, all working largely on major defense contracts.

(Continued on page 88A)

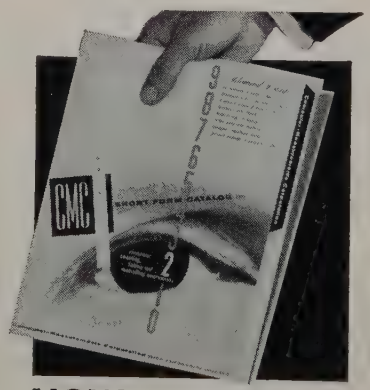

NOW Available . . .
Computer-Measurements' *SHORT FORM CATALOG*
Containing Condensed Information on:

Frequency and Period Counters
Decade Counting Units
Preset Decade Counting Units
Frequency Deviation Meters
Time-Function Translators
Digital Printers
Preset Controllers
Totalizing Counters
Time Interval Meters
Universal Counter-Timers

write for your copy today

Computer-Measurements Corporation
5528 Vineland, Dept. 86B North Hollywood, Calif.

THYRITE® VARISTORS CUT SURGE VOLTAGE

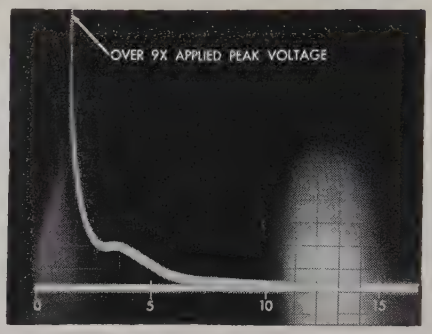

FROM 9 TO 3 TIMES APPLIED PEAK VOLTAGE

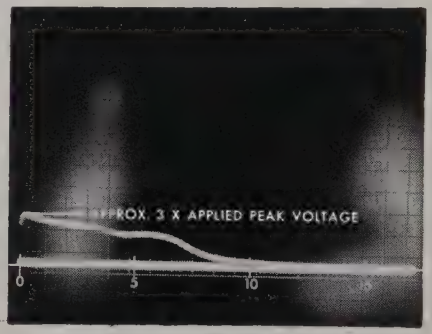

ON 115-V CIRCUITS

Sudden interruption in inductive current causes surge overvoltage, arcing, and high-frequency oscillation. Oscillograms (above) show how effectively G-E Thyrite varistors can limit these effects.

Without a Thyrite varistor (Fig. 1) in the 115-V circuit, surge voltage is 9 times applied peak voltage. With it (Fig. 2), surge voltage is limited to 3 times peak voltage.

With little current drain, they reduce surge voltage and arcing by offering low resistance at peak current . . . discharge circuit energy faster by offering higher resistances instantaneously as current decays.

G-E Thyrite varistors are available for components rated from 6 volts to 4000 volts.

For more information, or Thyrite varistor test kits, write: *Magnetic Materials Section, General Electric Company, 7808 N. Neff Avenue, Edmore, Michigan.*

THYRITE VARISTOR KITS

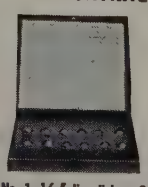

Kit No. 1: ½" dia. disks—2 each of 6 ratings (6V to 115V—.1w); color coded with connecting leads. Price: $5.00.

Kit No. 2: ¼" dia. rods—2 each of 5 ratings (115V to 4000V—.25w); color coded with connecting leads. Price: $5.00.

Progress Is Our Most Important Product

GENERAL ELECTRIC

"Thyrite" is a trademark of General Electric Company

APPROVAL DATA

STODDART & MILITARY TYPE	FREQUENCY	MIL-I-16910 (Ships)	MIL-I-6181	S.A.E.	A.S.A.	C.I.S.P.R.
NM-40A (AN/URM-41)	30cps-15Kc	CLASS '1'	Not Req'd	Not Req'd	Not Req'd	Not Req'd
NM-10A (AN/URM-6B)	14Kc-250Kc	CLASS '1'	Not Req'd	Not Req'd	C63.2 (Proposed)	Not Req'd
NM-20B (AN/PRM-1A)	150Kc-25Mc	CLASS '1'	CLASS '1' *CATEGORY 'A'	Not Req'd	C63.2 (Proposed)	**
NM-30A (AN/URM-47)	20Mc-400Mc	CLASS '1'	CLASS '1' *CATEGORY 'A'	APPROVED	C63.3 (Proposed)	**
NM-50A (AN/URM-17)	375Mc-1000Mc	CLASS '1'	CLASS '1' *CATEGORY 'A'	Not Req'd	C63.3 (Proposed)	Not Req'd

*MIL-I-6181C (Proposed)
**Can be supplied to C.I.S.P.R. Recommendations
S.A.E. (Society of Automotive Engineers)
A.S.A. (American Standards Association)
C.I.S.P.R. (Comite International Special des Perturbations Radioelectriques) (International Special Committee on Radio Interference)

STODDART'S **5** self-contained Radio Interference Measuring Equipments, each designed for its specific frequency range, provide:
5 instruments, which can be used by—
5 engineers, to measure over—
5 different frequency ranges, at—
5 different locations, at—
1 time.

FEATURES:

- Each equipment performs Quasi-Peak, Peak, and Average (Field Intensity) measurement functions.
- Approved for use by all Departments of the U. S. Department of Defense.
- Commercial and military equipments are identical.
- Precision laboratory equipment with rugged all-weather design for field use.
- **Immediate delivery from stock.**

—Serving 33 countries in radio interference control—

STODDART

AIRCRAFT RADIO CO., INC.

6644 Santa Monica Blvd., Hollywood 38, California HOllywood 4-9294

LAPP INSULATION FOR WATER-COOLED SYSTEMS

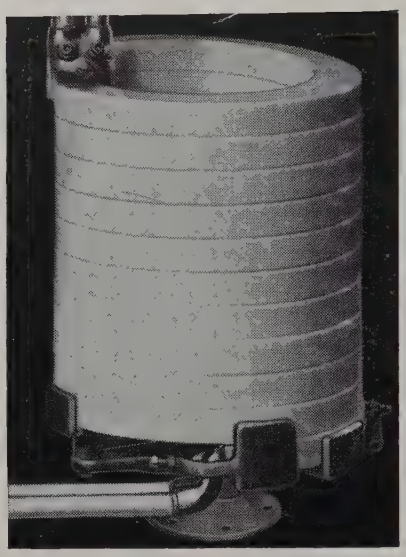

For carrying cooling water which must undergo a change in potential, use of Lapp porcelain eliminates trouble arising from water contamination and conductivity, sludging and electrolytic attack of fittings. Permanent cleanness and high resistance of cooling water is assured with the completely vitrified, non-absorbent Lapp porcelain.

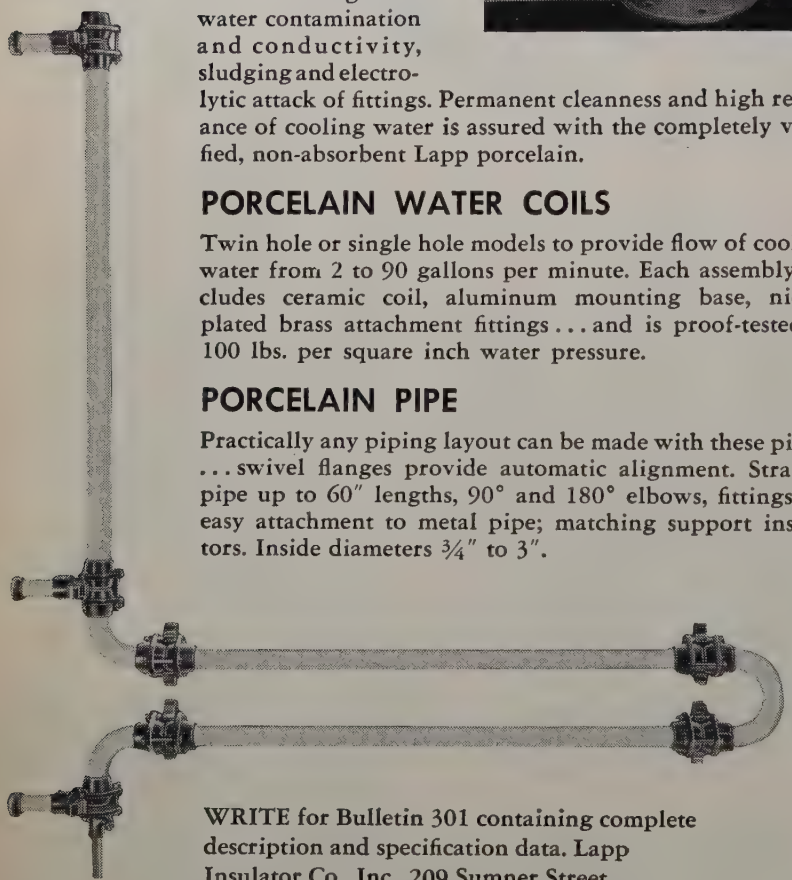

PORCELAIN WATER COILS

Twin hole or single hole models to provide flow of cooling water from 2 to 90 gallons per minute. Each assembly includes ceramic coil, aluminum mounting base, nickel plated brass attachment fittings . . . and is proof-tested to 100 lbs. per square inch water pressure.

PORCELAIN PIPE

Practically any piping layout can be made with these pieces . . . swivel flanges provide automatic alignment. Straight pipe up to 60″ lengths, 90° and 180° elbows, fittings for easy attachment to metal pipe; matching support insulators. Inside diameters ¾″ to 3″.

WRITE for Bulletin 301 containing complete description and specification data. Lapp Insulator Co., Inc., 209 Sumner Street, Le Roy, New York.

Lapp

News-New Products

These manufacturers have invited PROCEEDINGS readers to write for literature and further technical information. Please mention your IRE affiliation.

(Continued from page 86A)

Childs comes to AMF from Weston Electrical Products where he was vice president and general manager. He also served as president of the Daystrom Furniture Company and was formerly president and co-owner of Bennett Manufacturing Co. and Friend Manufacturing Co.

Childs was graduated from Stevens Institute of Technology in 1936 with an M.E. degree. He is a member of the American Ordnance Association and American Management Association.

High-Vacuum Pumping Station

A high performance high-vacuum pumping station combining mobility with versatility and modern design is now available from **Veeco Vacuum Corp.**, 86 Denton Ave., New Hyde Park, L. I., N.Y.

Known as the VS-9, the fully equipped unit provides industry and research laboratories with multi-purpose high-vacuum station incorporating these features: very fast pumpdown; extremely high vacuum—with bakeout, better than 10^{-8} mm Hg; high speed air-cooled diffusion pump with an 85 liter per second capacity, with no water connection needed; specially designed low-loss cold trap which will operate from 8 to 10 hours on one filling; full valving, including roughing line; ultra-stable Veeco-designed RG-3 ion gauge circuit, and the Veeco RG-75 non-burnout ion gauge. The RG-3 Circuit has a measured drift of less than 2 per cent of full scale per day, and permits readings down to 2×10^{-9} mm Hg.

A leak detector can be connected to the auxiliary leak-test line, so that an object can be leak-tested while it is being evacuated. Special atmosphere can also be introduced into the evacuated object through this line.

(Continued on page 90A)

Use your IRE DIRECTORY! It's valuable!

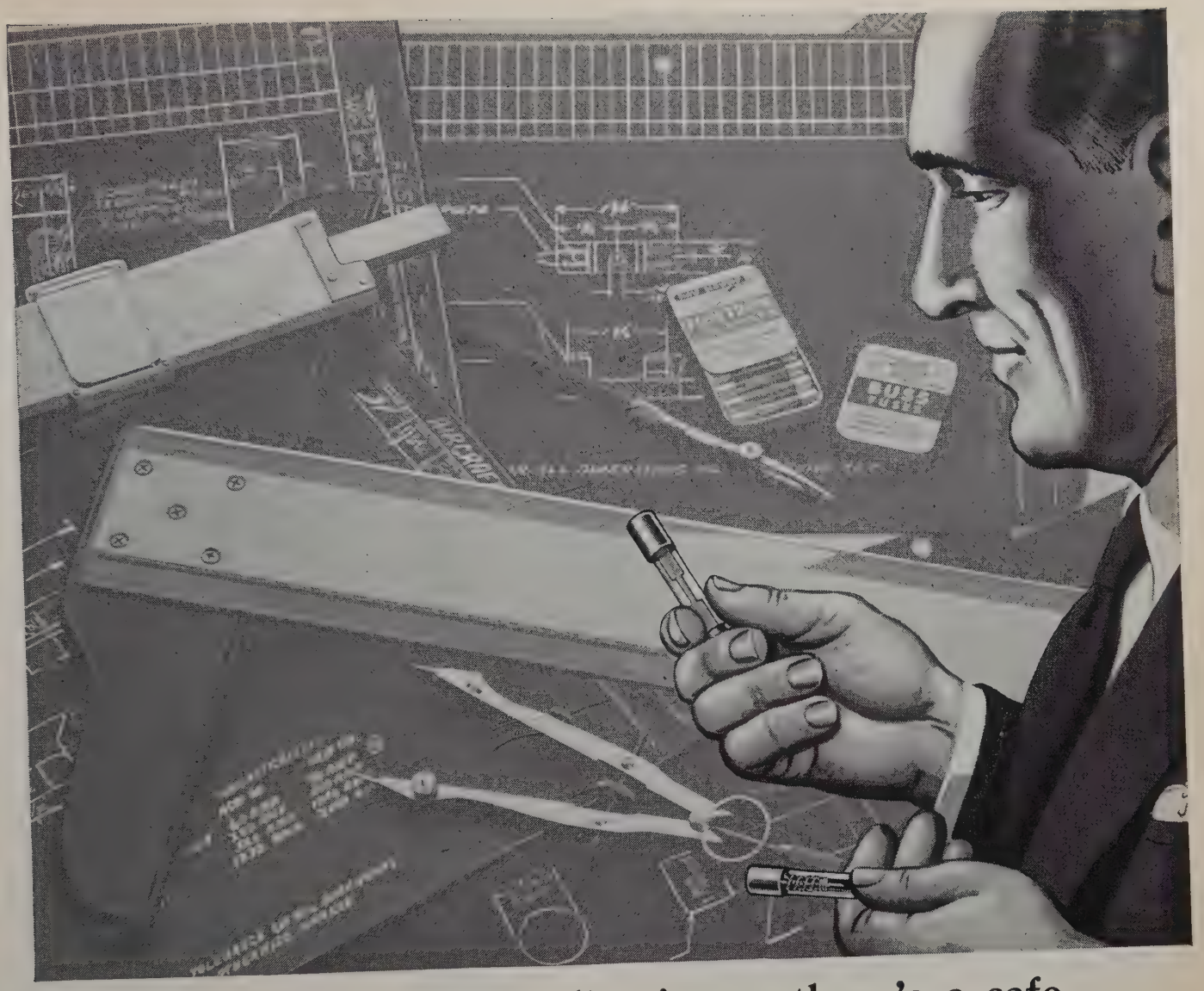

For every fuse application — there's a safe and dependable BUSS fuse . .

You'll save time and trouble by specifying only BUSS fuses!

You can select a fuse that meets your exact circuit protection requirement from the complete BUSS fuse line. There are fuses in all sizes and types for the protection of television, radio, instruments, controls, avionics and other electronic and electrical equipment. A companion line of fuse clips, blocks and holders is most complete.

Relying on BUSS as your one source for fuses saves you time, trouble and simplifies record keeping.

Specifying BUSS fuses helps safeguard good name of your product

Faulty fuses can cause trouble by failing to protect — or by blowing needlessly. Users of your product would then be faced with unnecessary repair bills or needless shutdowns. Such an experience could jolt the users confidence in your product.

By specifying BUSS fuses, you are sure of dependable electrical protection under all service conditions. Every BUSS fuse is tested in a sensitive electronic device that automatically rejects any fuse not correctly calibrated, properly constructed and right in all physical dimensions.

Should you have a special problem in Electrical protection . . . The BUSS fuse engineers are at your service — and in many cases can save you engineering time by helping you choose the right fuse for the job. Whenever possible, the fuse selected will be available in local wholesalers' stocks so that your device can be serviced easily.

Before your final design is crystalized, be sure to get the latest information on BUSS and FUSETRON Small Dimension fuses and fuseholders . . . Write for bulletin SFB. Bussmann Mfg. Division McGraw-Edison Co., University at Jefferson, St. Louis 7, Mo.

FUSETRON
TRUSTWORTHY NAMES IN ELECTRICAL PROTECTION
BUSS

MAKERS OF A COMPLETE LINE OF FUSES FOR HOME, FARM, COMMERCIAL, ELECTRONIC, AUTOMOTIVE AND INDUSTRIAL USE.

BUSS fuses are made to protect — not to blow, needlessly

AMPERITE PREFERRED

by design engineers—because they're
MOST COMPACT • SIMPLEST • MOST ECONOMICAL
HERMETICALLY SEALED

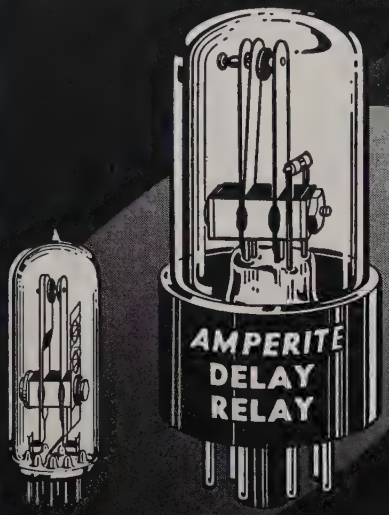

Thermostatic DELAY RELAYS

2 to 180 Seconds

Actuated by a heater, they operate on A.C., D.C., or Pulsating Current.

Hermetically sealed. Not affected by altitude, moisture, or climate changes.

SPST only—normally open or closed.

Compensated for ambient temperature changes from —55° to +70° C. Heaters consume approximately 2 W. and may be operated continuously. The units are **rugged, explosion-proof, long-lived,** and—**inexpensive!**

TYPES: Standard Radio Octal, and 9-Pin Miniature . . . **List Price, $4.00.** Standard Delays

Also—**Amperite Differential Relays:** Used for automatic overload, under-voltage or under-current protection.

PROBLEM? Send for Bulletin No. TR-81

BALLAST REGULATORS

Amperite Regulators are designed to keep the current in a circuit **automatically regulated** at a definite value (for example, 0.5 amp.) . . . For currents of 60 ma. to 5 amps. Operate on A.C., D.C., or Pulsating Current.

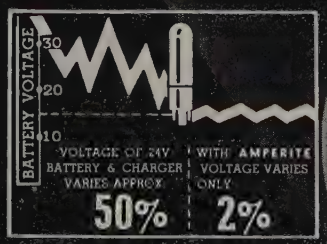

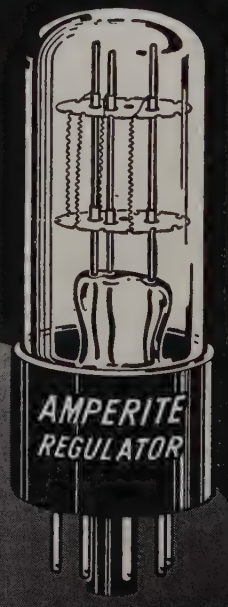

Hermetically sealed, they are not affected by changes in altitude, ambient temperature (—55° to +90° C.), or humidity . . . Rugged, light, compact, most inexpensive . . . **List Price, $3.00.**

Write for 4-page Technical Bulletin No. AB-51

AMPERITE CO. Inc., 561 Broadway, New York 12, N. Y.
Telephone: CAnal 6-1446
In Canada: Atlas Radio Corp., Ltd., 50 Wingold Ave., Toronto 10

News-New Products

These manufacturers have invited PROCEEDINGS readers to write for literature and further technical information. Please mention your IRE affiliation.

(Continued from page 88A)

Technology Instrument Elects Searle & Packard

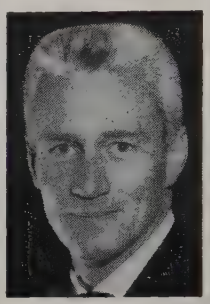

PACKARD

SEARLE

Technology Instrument Corp., 535 Main St., Acton, Mass., announces the election of Raymond W. Searle, Weston, Mass., as president and treasurer, and Lucius E. Packard, Framingham, Mass., as new board chairman to replace William H. Long, Concord, Mass., who has resigned from the company. Searle and Packard founded the electronics manufacturing firm in 1946, successfully pioneering design and mass production of precision wire-wound potentiometers.

All Transistor Null Detector

Freed Transformer Co., Inc., 1720 Wierfield St., Brooklyn, N.Y., is now making delivery on its new battery operated, portable Model 2050 all transistor null detector. This Model 2050, when used in conjunction with other battery operated equipment, allows complete isolation from

the power lines. This feature, plus battery operation, provide a lower noise level which makes it useful in all types of ac bridge measurements. Other features include economical operation; high sensitivity throughout battery life; maintenance—free service; simplified operations—no

(Continued on page 92A)

Whatever the *horsepower*

there is a right wire for it

—And there is one dependable source—with over 50 years experience—to meet your every need. Specialized new wires are engineered for every phase of the industry—and Belden quality assures lowest over-all cost on your production line.

if it's worth engineers' time
it's worth engineered wire

Belden
WIREMAKER FOR INDUSTRY
SINCE 1902
CHICAGO

ONE SOURCE
ONE QUALITY

10-I

Magnet Wire • Lead Wire • Power Supply Cords, Cord Sets and Portable Cord • Aircraft Wires
Welding Cable • Electrical Household Cords • Electronic Wires • Automotive Wire and Cable

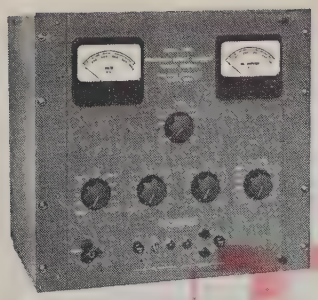

Model 301C

1.02 to 1012 VOLT RANGE
PRECISION D. C. POWER SUPPLY
CHOPPER STABILIZED

OUTPUT VOLTAGE—1.02 to 1012 volts DC.
OUTPUT CURRENT—0 to 400 milliamperes.
OUTPUT POLARITY—Either side may be grounded or both may be floated.
REGULATION VS. LINE—.005% or 1 millivolt for 10% line voltage change.
REGULATION VS. LOAD—.005% or 1 millivolt for 200 milliampere load change.
STABILITY—.005% per hour, .01% per day.
REFERENCE ELEMENT—Eppley standard cell.
RIPPLE—Less than 2 millivolts RMS.
VOLTAGE RESOLUTION—.5 millivolt for any output voltage.
CALIBRATION ACCURACY—±.1% or 2 millivolts.
SIZE AND WEIGHT—19"W x 17½"H x 15"D—120 lbs.
PRICE—$995.00 f.o.b. Seattle.

MODELS	405	407	403 M	406
OUTPUT VOLTAGE	600 to 3100 volts DC	0 to 555 VDC; 0 to —250 VDC; 0 to —25VDC; 2 6.3VAC@5A	500 to 1600 volts	0 to 530VDC; 0 to —225; 0 to —22.5DC 6.3VAC @ 3A.
OUTPUT CURRENT	0 to 15maDC	0 to 300ma	0 to 1ma	0 to 100ma
OUTPUT POLARITY	pos. or neg.	pos., neg., or floating	pos. or neg.	pos., neg., or floating
REGULATION VS. LINE	.01% max. for 20% line change	.01% for line change from 105 to 130 volts	.03% max. from 100 to 130 volts	.01% for line change from 105 to 130 volts
REGULATION VS. LOAD	.01% max. for 2ma change	.01% from 0 to 300ma	.03% no load to full load	.01% for load change from 0 to 100ma
STABILITY	.005% per hour	.01% per hour	.02% per hour	.01% per hour
RESOLUTION	10mv at any output voltage	2mv over entire range	100 mv at any output voltage	2mv over entire range
CALIBRATION ACCURACY	Better than .5%	Better than .5%	2%	
RIPPLE	Less than 5mv RMS	1mv or less	5mv max.	1mv or less
SIZE AND WEIGHT	19"W x 10½"H x 14"D—46 lbs.	Cab. 9¾"W x 13"H x 14"D—32lbs; Rack 19"W x 8¾"H x 16¾"D—32 lbs.	19"W x 7"H x 13"D—22 lbs.	Cab. 13"H x 9¾"W x 14"D—32lbs; Rack 8¾"H x 19"W x 16¾"D—30 lbs.
PRICE	$595.00	Cab. $335; Rack, $355	$209.00	Cab., $260; Rack, $280

MODELS	400EDA	402M	404M	400CEM
OUTPUT VOLTAGE	500 to 5100 volts DC	500 to 1600 volts	500 to 2000 volts DC	500 to 1600 volts
OUTPUT CURRENT	0 to 1ma	0 to 100ma	0 to 5ma at 500 to 1500 volts; 0 to 2ma at 1500 to 2000 volts	0 to 1 ma
OUTPUT POLARITY	pos. or neg.	pos. or neg.	pos. or neg.	pos. or neg.
REGULATION VS. LINE	.01% max. from 100 to 130 volts	.03% max. from 100 to 130 volts	.01% max from 100 to 130 volts	.01% max. from 100 to 130 volts
REGULATION VS. LOAD	.01% max. no load to full load	.03% no load to full load	.03% no load to full load	.01% max. no load to full load
STABILITY	.005% per hour	.01% per hour	.005% per hour	.005% per hour
RESOLUTION	100 mv at any output voltage	100mv at any output voltage	100mv at any output voltage	100mv at any output voltage
CALIBRATION ACCURACY	1%	1%	Better than 1%	Better than 1%
RIPPLE	5mv max.	5mv max.	Less than 5mv RMS	Less than 5mv RMS
SIZE AND WEIGHT	19"W x 10½"H x 14"D—42 lbs.	19"W x 7"H x 13"D—22 lbs.	19"W Rack x 7"H x 13"D—27 lbs.	19"W Rack x 7"H x 13"D—27 lbs.
PRICE	$595.00	$265.00	$435.00	$395.00

JOHN FLUKE MANUFACTURING CO., INC.
1111 W. NICKERSON STREET, SEATTLE 99, WASHINGTON

News-New Products

These manufacturers have invited PROCEEDINGS readers to write for literature and further technical information. Please mention your IRE affiliation.

(Continued from page 90A)

warm up, no zero setting; and built-in Harmonic filters.

Specifications include: Sensitivity: (with 400 or 1000 cps filter), In "Linear" position—200 μv for full-scale 80 μv for 30 per cent deflection, In "Null" position—2000 μv for full-scale 100 μv for 30 per cent deflection.

Input Impedance: Approximately 1 Megohm (resistive) at 1000 cps. Frequency Range; 40 cps to 20 kc. ±1 db. In "Direct" position: 20 cps to 50 kc+5 db. Filters: 400 and 1000 cps, greater than 22 db rejection of 2nd harmonics. Power Supply: 5.2 volts (4 mercury cells). Battery Life: At least 1800 hours. Size: 6×8×3½ inches. Weight: 3½ pounds with batteries.

Dipped Mica Capacitors

Meeting electrical and environmental test requirements of MIL-C-5A and RETMA RS-153, Type ADM dipped-mica capacitors as manufactured by **Aerovox Corp.**, New Bedford, Mass., are designed for all printed-wiring and general purpose applications.

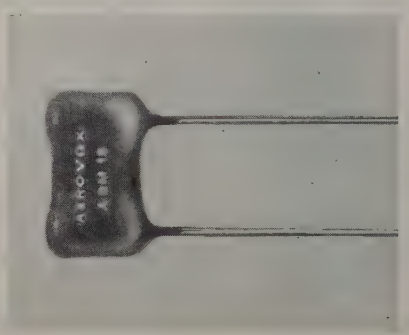

Aerovox Type ADM units feature extremely small size, extended operating temperature range of −55°C to 125°C, narrow temperature coefficient and excellent long-life characteristics. Exclusive dipped plastic casing enables use of these units in all types of electronic equipment. For full technical details write: Applications Engineering Department.

Transistor Performance Chart

Bendix Aviation Corp., Red Bank Div., has printed a new transistor chart which provides information in a convenient form about typical performance and ratings of many Bendix transistors. These charts are available on request. Your inquiries will be expedited if they are addressed as follows; Dr. R. R. Meijer, Marketing Manager, Semiconductor Products, Red Bank Div., Bendix Aviation Corp., Long Branch, N.J.

(Continued on page 102A)

BOARD OF DIRECTORS, 1958

*D. G. Fink, *President*
C. E. Granqvist, *Vice-President*
*W. R. G. Baker, *Treasurer*
*Haraden Pratt, *Secretary*
*J. D. Ryder, *Editor*
A. V. Loughren,
Senior Past-President
*J. T. Henderson
Junior Past President

1958

A. N. Goldsmith
H. R. Hegbar (R4)
E. W. Herold
K. V. Newton (R6)
A. B. Oxley (R8)
F. A. Polkinghorn (R2)
D. B. Sinclair
*Ernst Weber
J. R. Whinnery

1958–1959

R. I. Cole (R3)
G. A. Fowler (R7)
*R. L. McFarlan (R1)
D. E. Noble
E. H. Schulz (R5)
Samuel Seely

1958–1960

G. S. Brown
W. H. Doherty
**Members of Executive Committee*

George W. Bailey,
Executive Secretary

Evelyn Benson, *Assistant to the Executive Secretary*
John B. Buckley, *Chief Accountant*
Laurence G. Cumming,
Technical Secretary
Emily Sirjane, *Office Manager*

EDITORIAL DEPARTMENT

Alfred N. Goldsmith,
Editor Emeritus
J. D. Ryder, *Editor*
E. K. Gannett,
Managing Editor
Henene Frischauer,
Associate Editor

ADVERTISING DEPARTMENT

William C. Copp,
Advertising Manager
Lillian Petranek,
Assistant Advertising Manager

EDITORIAL BOARD

J. D. Ryder, *Chairman*
Ferdinand Hamburger, Jr.
Vice-Chairman
E. K. Gannett
Keith Henney
E. W. Herold
T. A. Hunter
G. K. Teal
W. N. Tuttle

Authors are requested to submit three copies of manuscripts and illustrations to the Editorial Department, Institute of Radio Engineers, 1 East 79 St., New York 21, N. Y.

Responsibility for the contents of papers published in the PROCEEDINGS OF THE IRE rests upon the authors. Statements made in papers are not binding on the IRE for its members.

MEMBER AUDIT BUREAU OF CIRCULATIONS

Change of address (with 15 days advance notice) and letters regarding subscriptions and payments should be mailed to the Secretary of the IRE, 1 East 79 Street, New York 21, N. Y.

All rights of publication, including foreign language translations are reserved by the IRE. Abstracts of papers with mention of their source may be printed. Requests for republication should be addressed to The Institute

PROCEEDINGS OF THE IRE®

Published Monthly by

The Institute of Radio Engineers, Inc.

VOLUME 46 — *February, 1958* — NUMBER 2

CONTENTS

Scanning the Issue 402
Poles and Zeros 403
Carl E. Granqvist, Vice-President, 1958 404
Microwave Antenna and Waveguide Techniques Before 1900 ..... *John F. Ramsay* 405
Ghost Modes in Imperfect Waveguides ..... *E. T. Jaynes* 416
High-Frequency Crystal Filter Design Techniques and Applications ..... *David I. Kosowsky* 419
Experimental 8-MM Klystron Power Amplifiers ..... *T. J. Bridges and H. J. Curnow* 430
FM Demodulator Time-Constant Requirements for Interference Rejection ..... *Elie J. Baghdady* 432
A High-Power Periodically Focused Traveling-Wave Tube ..... *O. T. Purl, J. R. Anderson, and G. R. Brewer* 441
Index to IRE Standards on Definitions of Terms, 1942–1957 449
Measurement of the Radar Cross Section of a Man ..... *F. V. Schultz, R. C. Burgener, and S. King* 476
IRE Standards on Television: Measurement of Luminance Signal Levels, 1958 482
Theory of Networks of Linearly Variable Resistances ..... *Harold Levenstein* 486

Correspondence:
A Parametric Electron Beam Amplifier ..... *T. J. Bridges* 494
On the Earth Geometry—A Theorem ..... *Kurt Toman* 495
Behavior of Noise Figure in Junction Transistors ..... *W. N. Coffey* 495
Electrolytic Tank Design of Electron Guns with Curved Electron Trajectories ..... *E. J. Cook* 497
Space-Charge-Balanced Hollow Beam with Uniform Charge Distribution ..... *M. Chodorow and C. Susskind* 497
Design of Three-Resonator Dissipative Band-Pass Filters Having Minimum Insertion Loss ..... *M. Dishal, B. Sellers, J. J. Taub, and B. F. Bogner* 498
Space-Frequency Equivalence ..... *W. E. Kock and J. L. Stone* 499
Thermal Properties of Tungsten vs Copper for Electron Tube Delay Lines ..... *Roy A. Paananen* 500
Microwave Magnetic Field in Dielectric-Loaded Coaxial Line ..... *B. J. Duncan, L. Swern, and K. Tomiyasu* 500
Carrier Mobilities at Low Injection Levels ..... *J. A. Hoerni* 502
Hyperbolic Analogs ..... *Melbourne J. Hellstrom* 502

Contributors 503

IRE News and Radio Notes:
Calendar of Coming Events 505
Obituaries 507
Professional Group News 507
1958 Transistor & Solid State Circuits Conference 508

Books:
"Microwave Measurements," by E. L. Ginzton ..... *Reviewed by A. B. Giordano* 508
"Analytical Design of Linear Feedback Controls," by G. C. Newton, Jr., L. A. Gould, and J. F. Kaiser ..... *Reviewed by A. M. Hopkin* 508
"Nomograms of Complex Hyperbolic Functions," 2nd ed., by Jorgen Rybner ..... *Reviewed by Martin Katzin* 509
"Solid State Physics, Vol. IV," ed. by F. Seitz and D. Turnbull ..... *Reviewed by L. T. DeVore* 509

Scanning the TRANSACTIONS 510
Abstracts of IRE TRANSACTIONS 512
Abstracts and References 516

ADVERTISING SECTION

Meetings with Exhibits 6A
IRE People 14A
News—New Products 34A
Membership 38A
Section Meetings 58A
Industrial Engineering Notes 68A
Professional Group Meetings 74A
Positions Open 118A
Positions Wanted 130A
Advertising Index 141A

THE COVER—This reproduction of Marconi's patent specification for a 25-centimeter wavelength transmitter reveals that parabolic reflector antennas were in use as early as 1896. This is but one of a surprisingly large number of microwave antenna and waveguide techniques that were developed by early radio experimenters in the decade prior to 1900. An interesting history of these early microwave developments is presented in a paper starting on page 405 of this issue.

Copyright © 1958, by the Institute of Radio Engineers, Inc.

Scanning the Issue

Scanning the Transactions (p. 510)—A new monthly feature of the PROCEEDINGS starts in this issue which will endeavor to provide readers with an informative sample of new developments drawn from current issues of the TRANSACTIONS and other IRE publications.

Microwave Antenna and Waveguide Techniques Before 1900 (Ramsey, p. 405)—Our modern microwave technology is built largely on discoveries and developments made between 1930 and 1940. We associate with this period the beginning of the microwave era. Nevertheless, the earliest radio experimenters, in the period from Hertz's initial demonstration of radio waves in 1888 to the turn of the century, did a surprising amount of work in the microwave portion of the spectrum before it was abandoned for the then more practical and useful lower frequencies. This historical review of these many early developments in the microwave art, at wavelengths as short as 5 millimeters and high peak powers, will come as an eye-opener to most readers.

Ghost Modes in Imperfect Waveguides (Jaynes, p. 416)—This paper calls attention to the fact that imperfections in a waveguide, such as that caused by placing a dielectric in it, can cause so-called ghost modes in the immediate vicinity of the imperfection which can give rise to unexpected and troublesome resonance effects, especially in high-power applications. These spurious resonances may in fact arise just outside the pass band of any periodic structure that has a localized imperfection. Indeed, they are analogous to certain phenomena that have been observed in imperfect crystals of solid-state materials. While this phenomenon probably has no practical applications, it does improve our understanding of an effect which can in some cases cause an operational breakdown in a wide variety of wave propagating systems.

High-Frequency Crystal Filter Design Techniques and Applications (Kosowsky, p. 419)—This paper gives what is probably the first description of the use of crystals in filters at frequencies well above one megacycle. High-frequency crystal filters are now becoming commercially available in the 5 to 40 mc range which exhibit performance characteristics previously attainable only at lower frequencies, with Q's ranging from 50,000 to as high as 1,000,000 and bandwidths from one cycle to several hundred kilocycles per second. These high-frequency filters will find a substantial number of uses in single sideband, AM and FM equipment. For example, FM receivers can now be designed with only a single frequency conversion and a high-frequency IF, instead of multiple frequency conversions and a lower IF, without impairing adjacent channel selectivity and with a resultant reduction of circuits. The discussion of crystal filter design techniques presented here will be of major interest to a large number of communication equipment designers, while the easily followed presentation and the many interesting applications cited will appeal to all readers.

Experimental 8-mm Klystron Power Amplifiers (Bridges and Curnow, p. 430—By extending the emission capabilities of oxide cathodes to 1.5 a/sq. cm it has proven possible to produce 75 watts of cw power at 8 millimeter wavelengths. This represents a six-fold increase over previous efforts and the highest power yet reported at these high frequencies.

FM Demodulator Time-Constant Requirements for Interference Rejection (Baghdady, p. 432)—An investigation has been made of the demands imposed on FM receiver circuits in order that they may operate satisfactorily in the presence of a high level interfering signal. It is found that these demands require that ideally the time constants of the limiter and discriminator circuits must be short enough to cope with the sharp amplitude and frequency changes that are characteristic of a disturbed signal. These ideal requirements may conflict, however, with other fundamental requirements. Some simple schemes are discussed which minimize the conflict and greatly enhance the capture performance of a FM receiver.

A High-Power Periodically Focused Traveling-Wave Tube (Purl, *et al.*, p. 441)—Periodically placed magnets have been widely used in beam focusing systems in order to reduce the weight and power requirements of low-power traveling-wave tubes to more practical values. However, as the power of tubes increases so do the problems of focusing the higher density beams. This paper describes a periodically focused tube that operates from 2 to 4 kmc at the kilowatt level. The achievement of such relatively high powers and wide bandwidths by means of this type of focusing is a significant step forward in making high power twt's a practical component in systems.

Index to IRE Standards on Definitions of Terms, 1942–1957 (p. 449)—The entire technical language of the radio engineer, from "A and R Display" to "Zoning," culled from some three dozen IRE Standards on the subject, is brought together in this one alphabetical list. Approximately 3500 terms, representing 15 years of work on the part of IRE technical committees, are listed with a reference to the Standard and the PROCEEDINGS page where the definition of each term may be found. This will be an invaluable aid to the future work of individuals and committees in this field, and stands as imposing evidence of the extent to which a still young profession has advanced.

Measurement of the Radar Cross-Section of a Man (Schultz, *et al.*, p. 476)—This is the first disclosure of quantitative measurements of how good a radar target a man is. CW Doppler measurements were performed at five frequencies ranging from 410 mc to 9375 mc, using both vertical and horizontal polarization from various angles. It was found that the side view of a man presented the smallest radar target and the back view the greatest, and that the difference between polarizations was greatest at the lowest frequency, with horizontal polarization giving the smaller value. While the authors do not go into the applications of these experiments, it is obvious that the data will be of value in the design of military equipment for the detection of the movement of small patrols.

IRE Standards on Television: Measurement of Luminance Signal Levels (p. 482)—This Standard specifies the method by which operating personnel of a television transmitter may measure the relative levels of monochrome signals or of the luminance portion of color signals by means of an oscilloscope. It is a revision of a 1950 IRE Standard covering monochrome signal levels which, because it came before the adoption of color television signal standards in the U. S., was inadequate for color signal measurements.

Theory of Networks of Linearly Variable Resistances (Levenstein, p. 486)—The design of analog devices frequently calls for the use of potentiometers whose output voltage must vary in some special nonlinear manner as the shaft is rotated. A variety of ingenious and intricate circuits have been devised to meet these requirements, designed, of necessity, by empirical methods. The guesswork that goes into the empirical approach does not, however, result in the best possible design. In this paper, the author proposes that a network consisting simply of fixed resistances and linear rheostats driven by a common shaft be used instead of nonlinear elements, and shows that such networks are very amenable to good design techniques. Moreover, he shows that these networks can be described in a mathematical form that is analogous to that of fixed RL networks. This leads to the development of a general theory of variable resistance networks that permits them to be analyzed by the more highly developed techniques of fixed RL network theory.

Poles and Zeros

Standards Story. In this issue appears an index to all IRE Standards Definitions of Terms, indicating where you can find the terms defined in standard form. This should prove useful to the membership because in the past 15 years of intense IRE activity, these definitions have become scattered throughout nearly three dozen Standards publications. You may be surprised to note that the list approximates 3500 special words or definitions required to describe conditions or things in our profession. Thirty years ago there were only 277 such terms on the books. If one assumes a continued growth of terminology at this rate for the *next* thirty years, we would have 37,000 definitions. However, one can cast considerable doubt on such prediction by noting that a typical modern abridged American dictionary contains only about 60,000 words. In fact, it might be better to bet on Madison Avenue as a source of fifty per cent of our words in the next thirty years. It is also possible to conclude that at some point one has enough words available to adequately describe his activities, and then there will be those who will say we already have too many words, or at least we use them much too often.

It is interesting to note the many cases where technical words have grown out of something which started as typical American slang. To mention a few are monkey chatter, grass, blip, back porch, wow, and flutter. This seems to indicate a healthy down-to-earth view of our daily work, and it is to be hoped that electronics can continue to keep its feet on the ground.

The Standards Committee is certainly to be congratulated on the completion of an excellent job.

Nothing New! Immersed as we are in an industry producing things for tomorrow, it always comes as a rude shock to find that we are not nearly as modern as we had thought. Such a shock, or at least a mild thrill should come from the reading of the paper by John F. Ramsay in this issue entitled, "Microwave Antenna and Wave Guide Techniques Before 1900." To one who had the general impression that Barrow, Chu, Southworth, and a few other more or less modern investigators had discovered how to pour electromagnetic energy down the drain, this paper is deflationary. When one discovers that, prior to 1900 and Marconi, our predecessors were working in microwaves with wavelengths as short as 5 millimeters and peak powers of 70 kilowatts, one is even more hammered down in size.

When Marconi ultimately showed that the longer wavelengths seemed more suited for communication to great distances, the investigations into the microwaves of that date were dropped. We then had to wait many years for the amateurs to show the efficacy of the short waves, for radar to require development of the centimeter waves and microwave plumbing. Now we have come more than full circle to a realization that many valuable properties of the long waves have been overlooked.

A somewhat similar situation developed in the early 1920's. With the crowded radio broadcast spectrum of the time, investigators were looking into the possibilities of frequency modulation to reduce bandwidth. Carson published a paper which showed this was not possible, but which everyone interpreted as saying that frequency modulation had no value. Again, numerous years passed until Armstrong showed that there was value to the use of frequency modulation if we looked in exactly the opposite direction in which we had been looking in the early 1920's.

Apparently a scientific investigator is as easily bent as a twig in the wind.

Students and High Schools. One eminent engineering educator defines a vacuum tube as "something full of nothing out of which you get lots you do not expect." This might well be broadened to a definition for the whole field of electronics. Certainly the IRE STUDENT QUARTERLY, in its thorough and surprising manner, has come up with a result which was not fully expected.

While we hear much about the poor quality of our high school science educations, we actually seem to lack proof. This past fall our sister publication polled the junior and senior electrical engineering students asking their reactions towards their own high school preparations for engineering college. Many interesting comments were obtained, some of which were published in the December issue of the QUARTERLY (advertisement), but the most surprising result was that, in general, the students, about to become electronic engineers, are fairly well-satisfied with the job the high schools did on them.

To an educator interested in best utilizing the brains and intellectual man power of this country this raises a disquieting question. Are our high schools really that good, or does this mean that a student having a poor high school preparation stands no reasonable chance of reaching the junior or senior year of a modern electrical engineering curriculum? Having in the last several years talked to some hundreds of aspiring engineers who were not making it, we have a disquieting feeling that the latter conclusion may be correct. In any case, with Sputniks overhead, we have heard surprisingly little from the secondary school front as to what they are going to do about our need for better science and mathematics. As one educator has said, it is now time to start *learning* in our high schools and grade schools.—J. D. R.

C. E. Granqvist

VICE-PRESIDENT, 1958

Carl Eric Granqvist was born on March 2, 1910 in Ljungby, Sweden. He has the Master of Art degree in electrical engineering from the Royal University of Technology in Stockholm.

Mr. Granqvist holds over twenty-five patents in the field of radio air navigation systems and devices. He has written several textbooks on radio and descriptive booklets on the aga talking beacon and the aga vhf direction finder.

As Chief Engineer of Svenska Aktiebolaget Gasaccumulator, Stockholm-Lidingo, Sweden, he was in charge of design, research and development in the electronic laboratory of that company. His present title is Director of that laboratory.

Mr. Granqvist belongs to the Swedish society, Svenska Teknologforeningen. He has also served as adviser on the Swedish Electric Committee and member of Standard Committee NK 50. He became an IRE Associate Member in 1946, and a Fellow in 1955.

Microwave Antenna and Waveguide Techniques Before 1900*

JOHN F. RAMSAY†, ASSOCIATE MEMBER, IRE

Summary—Between the years 1888, when Hertz first launched electromagnetic radiation in the radio spectrum, and 1900, when Marconi was successfully establishing communication by radio, the scientific investigators of the time turned their attention to microwaves. Later, when it was found that the longer waves were more suited to long-distance communication, interest in the microwaves waned. Between 1888 and 1900, however, microwave devices and techniques had a rich development anticipating much of present-day practice. This paper reviews the antennas and waveguides of the period, with some reference to the associated microwave techniques then developed.

Apart from Hertz's dipole, with or without a plane reflector, the principal microwave antennas evolved were the cylindrical parabola, the dielectric lens, the waveguide cavity radiator, the radiating iris, and the electromagnetic horn.

Among the waveguides produced were the round, square, and rectangular forms, the open end being used as a radiator. The experimental development of these hollow pipe radiators appears to have anticipated Rayleigh's theoretical paper on waveguides by a number of years, Lodge discovering the mode property experimentally in 1894.

Many of the associated microwave components were of the "free-space" or quasi-optical type, rather than of the constrained or bounded type as common today, since the investigators between Hertz and Marconi were interested profoundly in the representation of optical phenomena at microwave frequencies. Hertz himself was the founder of "microwave optics," a classical subject being revived today.

Thus, we find the Hertzians making and using polarized mirrors, "cutoff" metal-plate gratings, quarter-wave and half-wave plates, artificial dielectrics, microwave absorbers, prisms of wax, ice, or liquid filled, or of artificial dielectric, totally reflecting prisms, lenses of sulphur, ebonite, wax, pitch, and so on, a wealth of microwave components only partly exploited today.

In the field of systems, measuring arrangements preponderated and included microwave spectrometers, interferometers, diffraction gratings plane or curved, transmission test sets, recorders, polarimeters. With the polarimeter, Bose established microwave analog physics, with macroscopic models of molecules subjected to microwave radiation. Otherwise, representations of optical phenomena were made with the enormous scale advantage arising from the use of microwaves. The properties of dielectrics, particularly anomalous dispersion, were studied and measured extensively.

All of this microwave work was carried out using spark discharge generators, often of considerable peak power, and with surprising accuracy. For detection, many devices were investigated, the most popular being the semiconducting coherer and the gaseous discharge tube.

Introduction

In 1888, Hertz launched decimeter-wave radiation from a parabolic mirror antenna fed by a dipole. The dipole was excited by spark discharges produced by an induction coil. The radiation was received on a similar parabolic mirror antenna and the dipole was transmission line fed to a spark gap detector behind the mirror. The wavelength was 66 cm.

With this simple microwave apparatus Hertz conducted a series of experiments of great importance. First, he established action at a distance. Second, he showed the action was communicated to a distance by a wave motion exactly analogous to the known wave motion characterizing visible light. Third, he substantiated experimentally the theoretical predictions of James Clerk-Maxwell that the waves known to account for optical phenomena were electromagnetic, by the completeness of his experimental demonstrations and his accompanying theoretical analysis.

Hertz showed that his "electric waves" traveled in straight lines (although he surmised that diffraction would take place too). Shadows could be produced by obstacles. Different substances, whether solid, liquid, or gaseous, transmitted or absorbed the waves by different amounts. The waves could be reflected from walls or conducting metallic sheets. Standing waves were obtained which allowed the wavelength to be obtained. The shift of the pattern occasioned by the interposing of a dielectric obstacle allowed the properties of dielectrics to be investigated.

With oblique incidence on a conducting sheet, Hertz found the angle of reflection was equal to the angle of incidence. Using an opaque prism in the path of the radiation, the refracted waves were found to follow the optical law of refraction. The main features of geometrical optics were established.

The standing-wave experiments and the reinforcing action of a reflector behind a dipole radiator emphasized the wave nature of the radiation, being simple illustrations of interference. Just as Young had provided the first means of determining the wavelength of visible light by an interference experiment, so Hertz determined the first radio wavelength using the same principle.

In his experiments, Hertz observed from the start that the microwave radiation was strongly polarized. He pursued this feature making it both an experimental technique and an elucidation of the Maxwellian character of the waves. A new component that appeared, unknown to optics, was the grid of parallel wires, where the wire spacing was a small fraction of the wavelength. In one striking experiment, the transmitter and receiver antennas were cross-polarized and a grid introduced in the path with its wires at 45°. A response was obtained on the receiver previously inactive. "Clearly," wrote

* Original manuscript received by the IRE, September 9, 1957.
† Canadian Marconi Co., Montreal, Quebec, Canada; formerly with Marconi's Wireless Telegraph Co., Ltd., Chelmsford, Essex, England.

Hertz, "the screen resolves the advancing oscillation into two components and transmits only that component which is perpendicular to the direction of its wires. This component is inclined at 45° to the focal line of the second mirror, and may thus, after being again resolved by the mirror, act upon the secondary conductor. The phenomenon is exactly analogous to the brightening of the dark field of two crossed Nicols by the interposition of a crystalline plate in a suitable position."[1]

Hertz was fully aware that he had discovered radio-frequency optics, where the phenomenology of optics could be represented by microwaves. "It is a fascinating idea," he wrote, "that the processes in air which we have been investigating represent to us on a million-fold larger scale the same processes which go on in the neighborhood of a Fresnel mirror or between the glass plates used for exhibiting Newton's rings."[1]

It is important to notice that directive antennas played a major part in Hertz's system, providing him with a laboratory microwave link. In the path of the beam he introduced components and devices of a quasi-optical (the adjective proposed by Lodge) character which contributed to the realization of a microwave optical system as known today.

The success of Hertz's experiments attracted universal attention. Maxwell's theory was correct; light was an electromagnetic phenomenon. The scientific world, to whom electromagnetism was then the major interest, immediately took up the study of Hertz's waves and their optical implications. A school of investigators known as "the followers of Hertz," or as we may say now "the Hertzians," repeated Hertz's experiments and analytical investigations and extended the field of the work considerably. It was at this time that the divorce of optics from electromagnetism began to appear, contrary to what was expected. The electrically-minded investigators took greater interest in the generators and receivers and regarded the optical representations as well established and less important. On the other hand, physicists imbued with the long history of classical optics found in the new technique a fresh interest and the possibility of experimental verification of much that previously had been theoretical conjectures only. Of the latter group, Righi of Bologna was the most outstanding; his book, "L'Ottica delle Oscillazioni Elettriche," is a treatise on microwave optics.[2]

The young Marconi, inspired by Righi's work, conceived the idea of modulating the generator so that intelligence could be transmitted on the radio-frequency optical link. In an era of wire and cable telegraphy this was a major practical application of Hertz's apparatus, and of other components, notably the Branly-Lodge coherer detector developed by the Hertzians. Using two Hertz-type parabolic reflectors separated by a range of four miles on Salisbury Plain in England in 1897, Marconi proved to the British Post Office that his system of "wireless" telegraphy on a wavelength of 25 cm was completely successful. Marconi's consummate engineering skill dwarfed Hertz's scientific virtuosity. Today, the name Marconi is a household word; Hertz is still a textbook reference.

As time went on the followers of Hertz split. The electrically-minded joined the many followers of the youthful Marconi, the optically-minded reducing to a small minority. Other contemporary scientific advances, notably the discovery of X rays and electrons, tended to remove the scientific interest from microwave optics. Until 1900, it hardly existed as a subject. When the followers of Marconi found that longer wavelengths were more suited for communication to longer distances and that unexplained vagaries in communication at these longer wavelengths existed, microwaves vanished from wireless telegraphy, and the new problems of the longer wave radio also attracted the scientists.

With the return to microwaves in our own time, it is amazing to find the extent of the development between Hertz and Marconi. This paper illustrates the development with special reference to the directive antennas that were produced. One important nonoptical type was the hollow pipe waveguide radiator. Since antenna techniques are partly optical and partly electrical, the quasi-optical components of the Hertzians are described also.

Parabolic Cylinder Antennas of Hertz, Righi, and Marconi

The optical properties of a parabolic reflector were well known to the Hertzians. A source at the focus would provide a "parallel" beam. Hence when Hertz found a dipole "source," he wrote, "As soon as I had succeeded in proving that the action of an electric oscillation spreads out as a wave into space, I planned experiments with the object of concentrating this action and making it perceptible at greater distances by putting the primary conductor (*i.e.*, *dipole*) in the focal line of a large concave parabolic mirror."[1] It is interesting to note that Hertz's need for an antenna was the same as Marconi's, *viz.*, to make the effects "perceptible at greater distances." Antenna gain was appreciated at a very early stage in radio!

Hertz's reflector was made of sheet zinc mounted on a timber frame (Fig. 1). The horizontal aperture was 1.2 m and the vertical aperture 2 m. The focal length was only 12.5 cm, the parabola extending forward of the focal plane to make the over-all depth of the mirror 70 cm. Since the wavelength was 66 cm, it will be appreciated that this was a very small antenna when measured in wavelengths. A most optimistic estimate of the 3-db beamwidth in the horizontal plane would be 35°;

[1] H. Hertz, "Electric Waves," Macmillan and Co., Ltd., London, Eng.; 1893.
[2] A Righi, "L'Ottica delle Oscillazioni Elettriche," N. Zanichelli, Bologna, Italy; 1897.

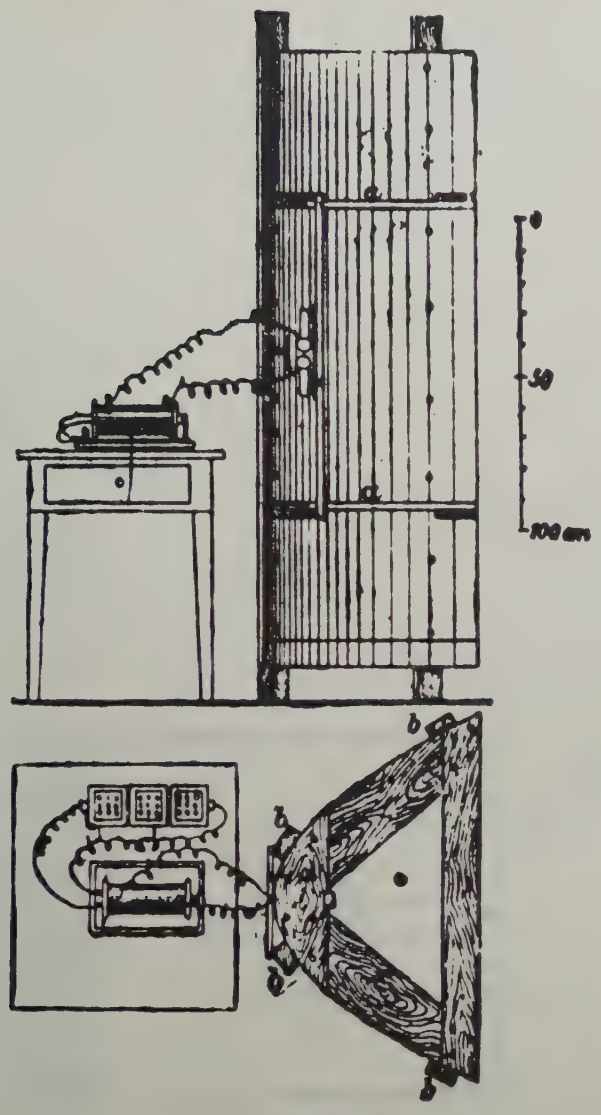

(a)

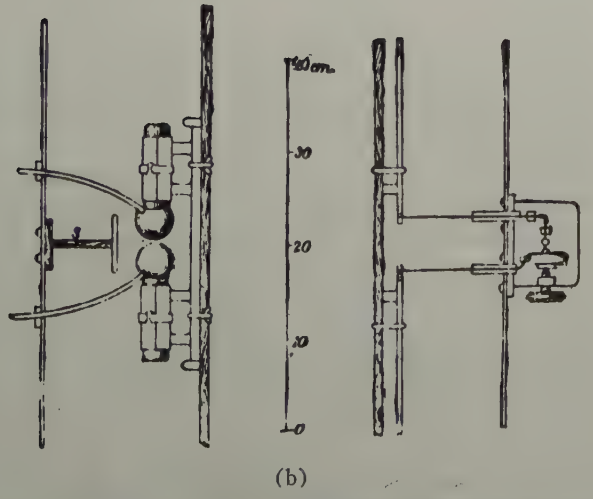

(b)

Fig. 1—(a) Hertz's parabolic reflector antenna for radiating on a wavelength of 66 cm (1888). (b) Hertz's sketches of his dipole feed arrangements for 1) transmitting and 2) receiving. (*Courtesy of Macmillan and Co., Ltd., and St. Martin's Press, Inc.*).

the beamwidth in the vertical plane would be around 80°. Such beamwidths resemble those used nowadays on "feeds" for parabolic antennas. It is surprising that Hertz was able to do so much fundamental work with these broad beams. He was often troubled by unwanted reflections from room surroundings, no doubt brought about by the use of the broad-beam antennas.

Righi, on the other hand, wishing to approach more closely to optics, worked on 3 cm and 10 cm (the *X* and *S* bands of today) with smaller parabolic cylinder reflectors.[2] Measured in wavelengths, however, the antennas were larger than those of Hertz, and very much sharper beams must have resulted. In one of Righi's illustrations he shows a parabolic cylinder used in, presumably, an *X*-band spectrometer. He did perform, however, many quasi-optical experiments in general, and must have used the parabolic cylinder antennas extensively, as in the Hertzian standing-wave experiment of Fig. 2.

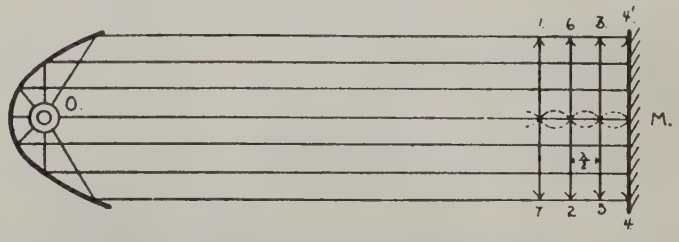

Interference by reflection from a single mirror, M. 1, 2, 3, etc., represent wave fronts differing in phase by a half period, 1 to 4 being direct and 4′ to 7 reflected and reversed in sign. The planes in which two opposite wave fronts, 4–4′, 5–3, 2–6, etc., meet are interference stripe, separated by a half wavelength, λ/2. (Poincaré.)

Fig. 2—Standing waves in free space produced by a reflecting surface. (Poincaré's drawing of Hertz's experiment.) (*Courtesy of Constable and Co., Ltd.*)

Marconi adopted the cylindrical parabola in his early 25-cm experiments, as his first patent of 1896 shows (Fig. 3).

Instead of a single spark gap, a multiple gap due to Righi was used in the focal line. Marconi had observed the need for sizeable apertures as he stated that the aperture of the antenna should be more than two wavelengths.[3]

Trouton of Dublin made copies of Hertz's apparatus, including the antennas, and repeated the optical experiments, extending the polarization analysis, and investigating the propagation into water filling a large tank made of paraffin wax.[4]

Bose of Calcutta, in 1897, was using a reflector in the form of a portion of a circular cylinder for microwave optical investigations at a wavelength of 5 mm.[5]

[3] G. Marconi, British Patent Specification No. 12039. Her Majesty's Stationery Office, June 2, 1896.

[4] F. J. Trouton, "Repetition of Hertz's experiments and determination of the vibration of light," *Nature*, vol. 39, pp. 391–393; February 21, 1889.

[5] J. C. Bose, "Collected Physical Papers," Longmans, Green and Co., New York, N. Y.; 1927.

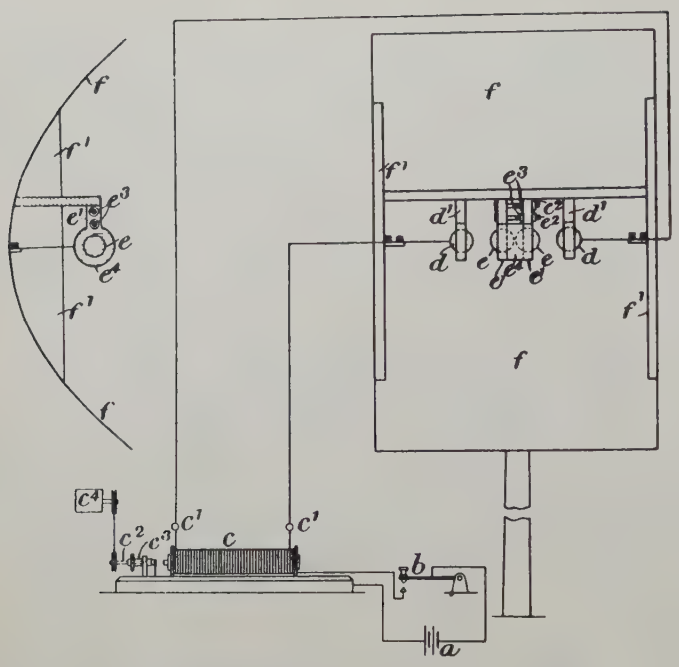

Fig. 3—Marconi's parabolic reflector antenna for transmitting information at a wavelength of 25 cm (1896). (Reproduced from Brit. Pat. Spec. No. 12039, June 2, 1896.)

The popularity of the parabolic cylinder in the 90's was no doubt due to the ease with which it could be constructed. Today in an age of improved constructional techniques, the doubly-curved paraboloidal reflector takes first place and the parallel beams the Hertzians expected but rarely obtained are now possible.

Microwave Lenses of Lodge, Righi, Bose, and Fleming

It was natural in the early microwave optics for the investigators to consider lenses. Hertz had established refraction through a prism of pitch at radio frequencies. Lodge, who knew Hertz personally, and had translated his papers for *Nature*, in 1889 collaborated with Howard in building a cylindrical lens of pitch.[6]

Lodge's lens was 1 m square, with a focal length of 51 cm, and a thickness at the center of 21 cm. The weight was 336 pounds. As the wavelength was found to be 101 cm, this lens antenna was a very small one, measured in wavelengths. Since it was only about one wavelength square, the 3-db beamwidth would be 50° at the best. Lodge found difficulty in distinguishing any definite signs of a focus. This is not surprising, since the focal spot (or Airy disk of optics) would be nearly as large as the lens. The device was in reality a diffracting obstacle, and thus could give some antenna gain. Lodge found the received signal on a Hertzian link was increased using the "lens." Later, in 1894, he used a 9-inch-diameter glass lens on (probably) 4000 mc, where he was able to demonstrate a positive focusing action.

[6] O. J. Lodge and J. L. Howard, "On the concentration of electric radiation by lenses," *Nature*, vol. 40, p. 94; May 23, 1889.

In Italy, Righi[2] made microwave lenses of paraffin and of sulphur. These lenses were 32 cm in diameter with a focal length of 50 cm. The thickness at the center was 7 cm. He claimed to have good results. As he used wavelengths down to 3 cm, it is highly likely that his results were superior to those of Lodge due to the increased aperture in wavelengths. The optical effects would be more marked.

Bose contributed to microwave lenses in a major way in originating techniques.[5] He used 5 mm as wavelength for systematic measurements. First, using a spectrometer and the principle of total internal reflection he measured the refractive index of sulphur finding a value of 1.734.[7] Second, he was able to calculate the profiling of a sulphur lens. Third, he put the lens at the end of a tube, *i.e.*, devised a "shielded-lens" antenna (Fig. 4). Fourth, in order to avoid unwanted reflections from the inside of the tube, he made extensive investigations of materials for coating the tube, *i.e.*, looked for a suitable "microwave absorber." He found blotting paper dipped in electrolyte to be the most satisfactory absorber.

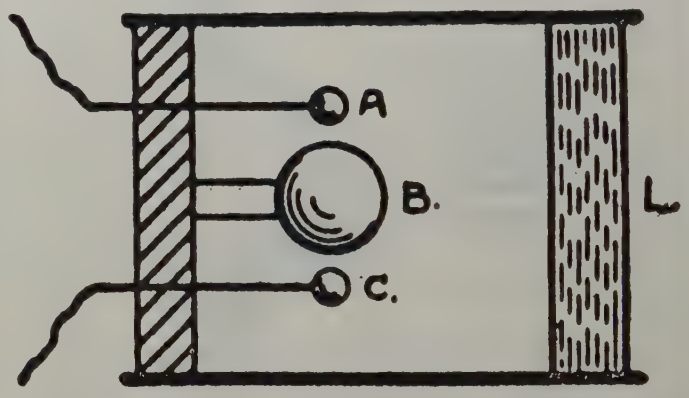

Bose's oscillator. The platinum sphere *B*, which is insulated, is the seat of the oscillations. The spheres *A* and *C* are connected to the induction coil. *L* is a cylindrical lens for concentrating the radiation. (Bose's caption.)

Fig. 4—Shielded lens antenna of Bose for radiating on wavelengths between 5 mm and 2.5 cm (1897). (*Courtesy of Longmans, Green and Co.*)

The diameter of Bose's lens was only about 1 inch so that, like many of the Hertzians, he used a relatively broad beam.

Fleming (later inventor of the thermionic diode) used a cylindrical lens of paraffin wax to demonstrate microwave optical effects.[8] As the aperture was only about 1 λ at a wavelength of 20 cm the lens action was, like Lodge's large lens, indistinct. Fleming did indeed express surprise that he succeeded in obtaining quasi-optical results at all, with such small components.

Of all the experimenters, it would appear that Righi alone succeeded in building microwave lenses of ade-

[7] J. C. Bose, "The refraction of electric waves," *Nature*, Sci. Amer. Suppl.; December 3, 1898.

[8] J. A. Fleming, "The Principles of Electric Wave Telegraphy and Telephony," Longmans, Green and Co., New York, N. Y.; 1906.

quate enough aperture to give convincing performance.

Although artificial dielectrics were devised by the followers of Hertz, and an artificial dielectric prism was actually investigated, it would appear that no one ever considered building a lens of artificial dielectric.

Hollow Pipe Radiators of Lodge, Bose, and Fleming

The first hollow pipe or "waveguide" radiators were demonstrated at the Royal Institution in London on Friday, June 1, 1894, by Lodge in the course of his memorial lecture on "The Work of Hertz and Some of His Successors."[9]

Lodge's waveguide radiator (Fig. 5) consisted of a short length of copper tube closed at one end and open at the other. A spark gap was mounted in the tube and the leads to the induction coil were taken out through small holes in the closed end of the copper tube. Microwave radiation generated by the spark discharge was launched down the tube, and proceeded to free space from the open end. A broad radio-frequency transmitting beam was thereby obtained.

For receiving, a similar tube was used, closed at one end, a glass tube containing coarse iron filings, *i.e.*, a "coherer,"[10] replacing the spark gap of the transmitter.

Lodge called his antennas "copper hats." Referring to the mounting of the coherer tube, he said:

"Sometimes the tube is put lengthways in the hat instead of crossways, which makes it less sensitive, and has also the advantage of doing away with polarizing, or rather analyzing, power of a crossway tube."[9]

It is evident that Lodge had discovered the mode property of propagation in a hollow tube: this was to be explained later by Lord Rayleigh in 1897.[11] With the "crossway" disposition the coherer would be responsive to the TE_{11} mode and therefore polarization sensitive. With the coherer lying along the axis of the tube it would be sensitive to the TM_{01} mode, which has circular symmetry. The radiation pattern (for reception) for the latter mode has a null on axis. Lodge mentioned that he mounted his copper hat "with its mouth turned well askew to the source," a factor contributing to TM_{01} detection at the expense of TE_{11} detection.

In order to reduce the transmitter power radiated, the copper hat was "stopped down by a diaphragm plate with holes in it of varying size" clamped to it. By this artifice Lodge had secured a waveguide cavity subject to different amounts of radiation damping. Here too were some of the first radiating irises, used as attenuators. No doubt some narrowing of the spark spectrum

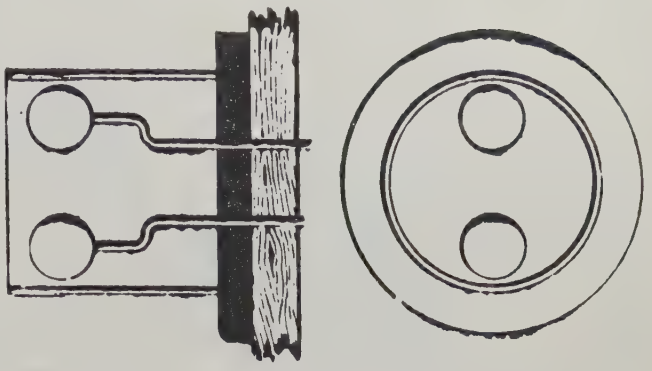

Dr. Lodge's hollow cylindrical radiator, arranged horizontally against the outside of a metal-lined box. Emitting three-inch waves. (Lodge's caption.)

(a)

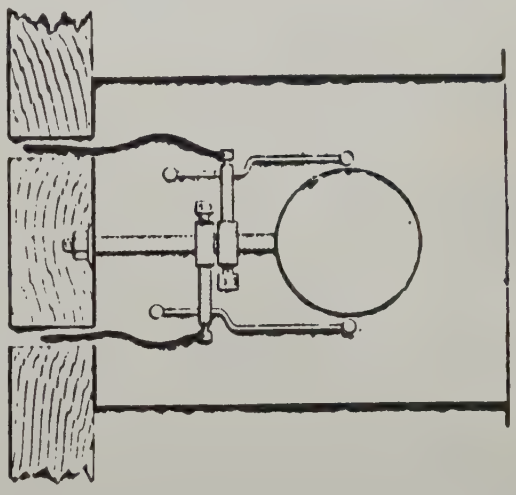

Spherical radiator for emitting a horizontal beam, arranged inside a copper hat, fixed against the outside of a metal-lined box. The wires pass into the box through glass tubes not shown. (Lodge's caption.)

(b)

Fig. 5—Hollow pipe waveguide radiators of Lodge for transmitting on centimeter wavelengths (1894). For reception a "coherer" replaced the spark gap in the tube. (*"The Electrician" Printing and Publishing Co., Ltd.*)

was also obtained by their use. In all cases, it appears a TE_{11} mode was radiated from the transmitter.

Lodge used wavelengths of $7\frac{1}{2}$ cm and about 20 cm. He at one time made an estimate of 70-kw peak power as obtainable from an induction coil: this is a surprising figure. There is no doubt that power availability was not a major difficulty with the followers of Hertz. Given very good screening of the coil and all leads, microwave power was obtainable. This screening requirement may account for the appearance of waveguides.

Lodge's laboratory equipment for demonstrating microwave phenomena, using waveguide radiators for transmission and reception, is shown in Fig. 6. Note the prism of paraffin and the polarizing grid, two of Hertz's components on a much smaller scale.

Bose,[5] in India, between 1895 and 1897, used hollow tubes of either circular or square section as waveguides

[9] O. J. Lodge, "Signalling through Space without Wires," "The Electrician" Printing and Publishing Co., Ltd.; London, Eng., 1898.

[10] O. J. Lodge, "The history of the coherer principle," *Electrician;* November 12, 1897.

[11] Lord Rayleigh, "On the passage of electric waves through tubes, or the vibrations of dielectric cylinders," *Phil. Mag.*, vol. 43, pp. 125–132; February, 1897.

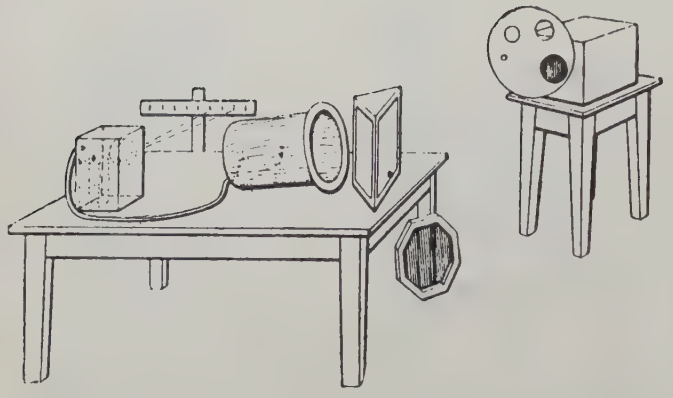

General arrangement of experiments with the copper "hat," showing metal box on a stool, inside which the radiators were fixed; the copper hat containing the coherer, with the metal box containing battery and galvanometer coil connected to it by a compo pipe conveying the wires; a paraffin prism; and a polarizing grid. (Lodge.)

Fig. 6—Microwave equipment of 1894. Lodge's drawing of his quasi-optical bench using waveguide antennas at a wavelength of about 20 cm (June 1, 1894). (*"The Electrician" Printing and Publishing Co., Ltd.*)

and waveguide radiators on wavelengths between 5 mm and 2.5 cm. Sometimes a small lens was fitted to the radiating end of the tube as has been described (Fig. 4). At Bose's lowest frequencies, his tubes would behave as slightly oversize waveguides, as the width was around 1 inch. At 5 mm, however, the tube would act more as a shield, liable to produce higher order modes, whence Bose's search for absorbent material. His adoption of hollow tubes was probably based on the use of metal tubes in telescopes and microscopes.

Fleming[8] gave lecture demonstrations on the optical features of Hertzian waves, following very closely Lodge's celebrated Royal Institution lecture of 1894. However, it is exceedingly interesting for us to find that he had replaced Lodge's round tube radiators by rectangular boxes, resembling the rectangular waveguide of the present day. Fleming used a wavelength of about 20 cm.

An inspection of the diagrams (Fig. 7) of Fleming's equipment indicates 1) that the polarization is parallel to the broad face instead of the narrow face as in a dominant-mode waveguide and 2) that the rectangular tubes would act more as cut-off attenuators than as waveguides. As, however, the spectrum of the spark would have many higher frequency components, it is likely that the boxes radiated significant power. Fleming's comment that the excellence of the quasi-optical demonstrations was surprising, having regard to the orders of magnitude in his system, may be explained, in fact, by his having very much shorter waves present.

Lodge, Bose, and Fleming must all have unconsciously used the high-pass filter property of waveguides, for the noisy sparks would be likely to have an enormous low-frequency spectral content. All three resorted to, and emphasized the need for screening the transmitting equipment.

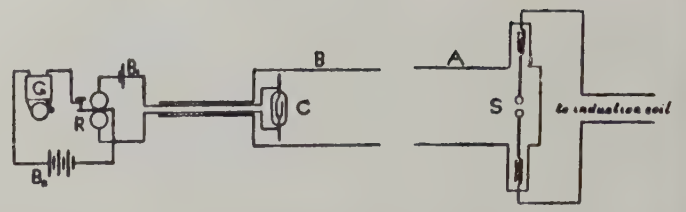

Apparatus for producing and detecting electric waves. *S*, spark balls in metal box, *A*, with open mouth; *C*, coherer in metal box; *B*, with open mouth; *R*, relay; *G*, electric bell; B_1, relay battery; B_2, electric bell battery.

(a)

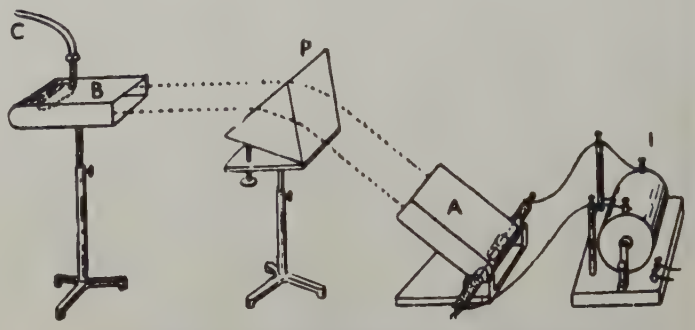

Refraction of an electric beam by a paraffin prism.

(b)

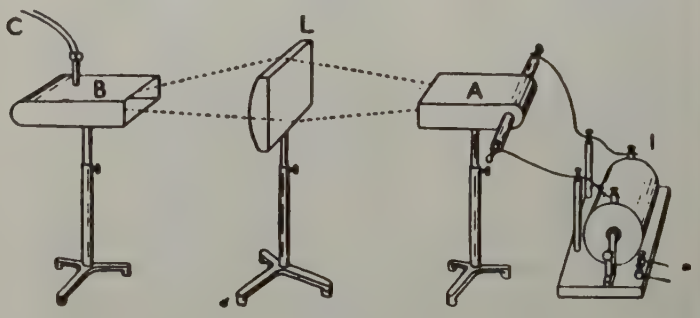

Convergence of an electric beam by a paraffin lens.

(c)

Fig. 7—Microwave-optical equipment and experiments of Fleming showing rectangular waveguide antennas used at a wavelength of 20 cm (1900). (Captions by Fleming.) (*Courtesy of Longmans, Green and Co.*)

The fact that they discovered the radiation could be led out of the transmitter box by a hollow tube represented a major step, as we now know, on the evolution of microwave transmission technique.

In radiating to free space from the open end of a hollow pipe, Lodge, Bose, and Fleming found a directive radiator unknown to optics or to Hertz. Bose was to make the next significant step.

The Electromagnetic Horn Antenna of Bose

In 1897, Bose gave a lecture at the Royal Institution in London on the quasi-optical researches he had been carrying out with "electric waves" at a wavelength of 5 mm.[5] For demonstration purposes he had

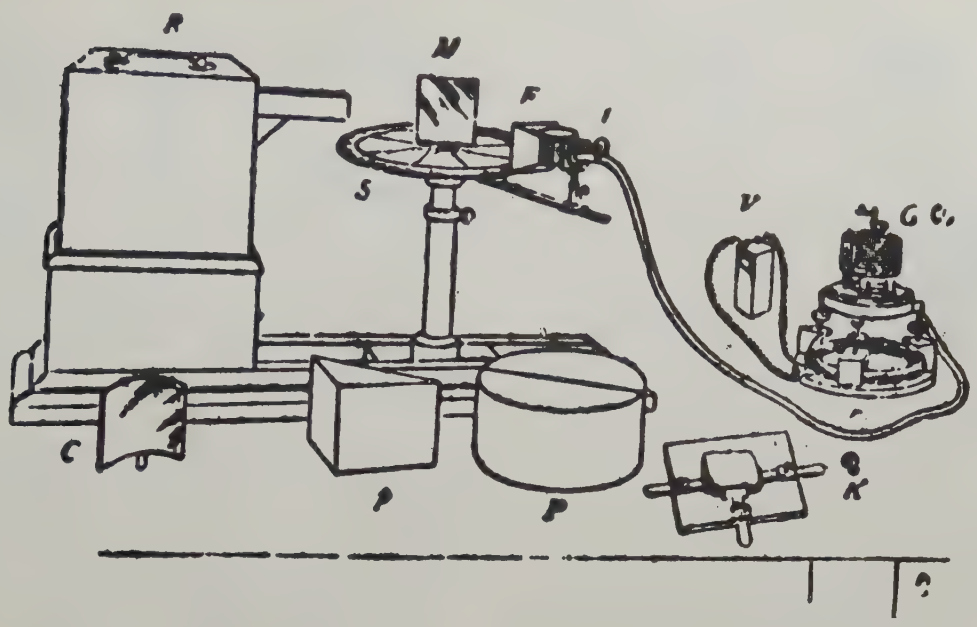

Arrangement of the apparatus. *R*, radiator; *S*, spectrometer-circle; *M*, plane mirror; *C*, cylindrical mirror; *p*, totally reflecting prism; *P*, semicylinders; *K*, crystal-holder; *F*, collecting funnel attached to the spiral spring receiver; *t*, tangent screw, by which the receiver is rotated; *V*, voltaic cell; *r*, circular rheostat; *G*, galvanometer. (Bose's caption.)

Fig. 8—Electromagnetic horn receiving antenna on microwave spectrometer used for quasi-optical demonstrations by Bose (1897). Transmitting antenna is square waveguide radiator. Wavelengths 5 mm–2.5 cm. (*Courtesy of Longmans, Green and Co.*)

brought from India a microwave spectrometer complete with screened transmitter and a receiver that rotated around the spectrometer table. Numerous quasi-optical components were also associated with this equipment for use in the demonstrations. A diagram of the equipment still exists (Fig. 8).

An inspection of Bose's receiver arrangements shows that the receiving antenna was a pyramidal electromagnetic horn, as we now call it. Bose termed his antenna a "collecting funnel," a colloquial but more vivid description. To this funnel a semiconducting detector of a multiplicity of touching spiral springs developed by Bose was connected (Fig. 9).[12]

Bose had already used waveguiding tubes—one is shown on his transmitter—so that it is natural he would conjecture that by increasing the cross section, a receiving aperture would collect more energy. This aperture could be attached to a smaller tube by tapering it down to fit, *i.e.*, by a hollow truncated pyramid construction, whence his pyramidal funnel. Thus, Bose made the first flared waveguide or small electromagnetic horn. As with so many of the components developed by the followers of Hertz, the horn was used for investigations in microwave optics as is evident in Fig. 8.

Polarization Techniques Before 1900

Hertz initiated techniques on microwaves based on the polarization properties of electromagnetic waves. He showed that his dipole transmitter and loop receiver were linearly polarized and that the linear polarizations were substantially unaffected on reflection from plane or parabolic mirrors. He made exact studies of the polarizations in the near fields of primary and secondary radiators. His principal invention, however, was the screen or grating, a grid of parallel wires, which he described as follows:

"I next had made an octagonal frame, 2 meters high and 2 meters broad; across this were stretched copper wires 1 mm thick, the wires being parallel to each other and 3 cm apart."[1]

At a wavelength of 66 cm as used by Hertz, this screen would reflect 96 per cent of the incident power in a plane wave normally incident and polarized linearly parallel to the wires.

If however, the incident wave were polarized at right angles to the wires, most of its power would be transmitted *through* the screen. Such a device might have been called a "transflector," transmitting when the polarization was perpendicular and reflecting when the polarization was parallel to the wires.

Hertz discovered the sensitivity inherent in a "cross-polarized" link, where the transmitter and receiver polarizations are perpendicular. As referred to in the Introduction, he showed that such an arrangement resembled the crossed Nicols of optics, and in fact constituted a microwave polarimeter.

This attracted the attention of Bose who built microwave polarimeters on 5-mm wavelength with crossed gratings at the transmitter and receiver (see

[12] J. C. Bose, "On a complete apparatus for the study of the properties of electric waves," *Elec. Eng. London;* October 2, 1896.

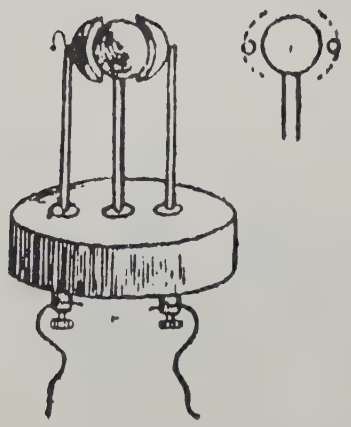

The radiator.

(a)

The spiral-spring receiver.

(b)

Fig. 9—(a) Spark gap arrangements for generating wavelengths down to 5 mm (Bose, 1895). Material: platinum. (b) Bose's microwave, "semi-conducting" detector consisting of rows of horizontal spiral steel springs under adjustable pressure and a small polarizing voltage (1895). (*Courtesy of Longmans, Green and Co.*)

Figs. 10–12).[13] Bose's gratings, however, were not always grids of wires but sometimes consisted of parallel strips of metal (Fig. 12) as in the cut-off metal-plate grating of today. He produced these initially in a particularly simple way by interleaving the pages of a Bradshaw railway timetable with sheets of tinfoil. (Similar virtuosity was shown by Marconi on a later occasion when he inserted parallel wires into corrugated cardboard to make a Hertzian grating.)[14] Bose had found that the leakage through a cut-off grating, as we term it, was much less than that occurring with a wire grid.

With the polarimeter, Bose investigated the properties of many natural substances and artificial devices. In the class of natural substances he studied crystals of many kinds, and vegetable fibers, in addition to strained

[13] J. C. Bose, "On a new electro-polariscope," *Electrician;* December 27, 1895.

[14] Described to the author by E. L. Payne, Marconi's Wireless Telegraph Co., Ltd., Baddow Res. Labs., Chelmsford, Essex, Eng.

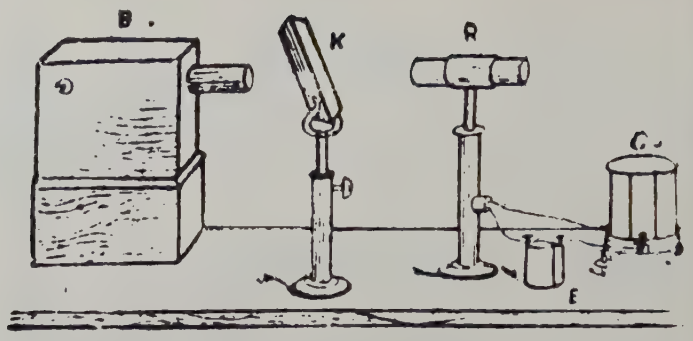

Polarization apparatus. *B*, metallic box enclosing the Ruhmkorff coil and radiator; *K*, the crystal to be examined; *E*, voltaic cell; *G*, the galvanometer; *R*, tube enclosing sensitive receiver. (Bose.)

Fig. 10—Microwave optical bench of Bose showing hollow-pipe waveguide antennas and polarization analyzer, *R* (1895). (*Courtesy of Longmans, Green and Co.*)

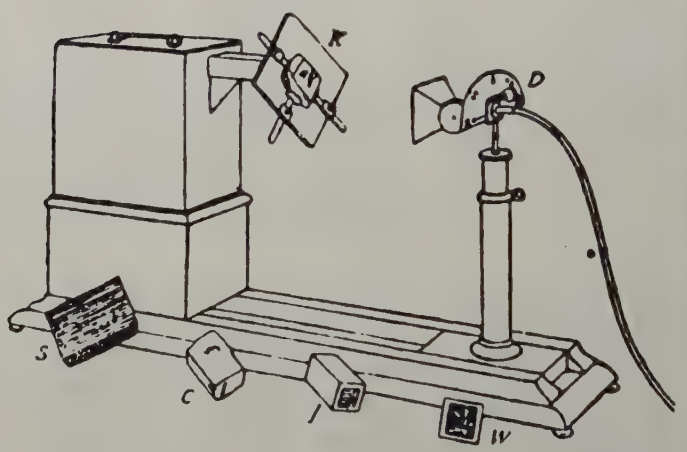

Polarization apparatus. *K*, crystal-holder; *S*, a piece of stratified rock; *C*, a crystal; *J*, jute polarizer; *W*, wire-grating polarizer; *D*, vertical graduated disk by which the rotation is measured. (Bose.)

Fig. 11—Microwave optical bench for polarization analysis. Note electromagnetic horn receiving antenna, square waveguide transmitting antenna, and Hertzian grids (Bose, 1897). (*Courtesy of Longmans, Green and Co.*)

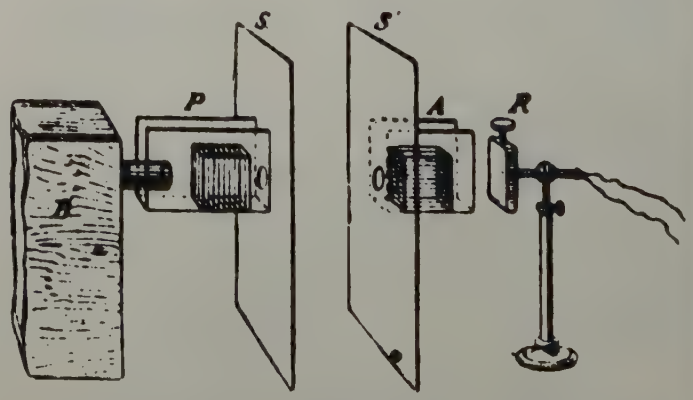

Polarization apparatus. *B*, the radiating box; *P*, the polarizer; *A*, the analyzer; *S*, *S'*, the screens; *R*, the receiver.

Fig. 12—"Cut-off waveguide" polarized mirrors as used in a polarimeter by Bose. (*Proc. Roy. Soc.*, vol. 63, p. 148; 1898.)

dielectrics as found in stratified rocks and fossils. Artificial polarizers of different forms he constructed from wires or jute fibers (Fig. 10).

One of the most remarkable applications of the microwave polarimeter developed by Bose was his use of it for analog physics.[15] Knowing that certain sugar solutions were optically active in producing polarization rotations, he conjectured that the mechanism resided in the molecule. He therefore made macroscopic or model molecules of twisted jute fibers, some with a right-hand twist, others with a left-hand twist (Fig. 13).

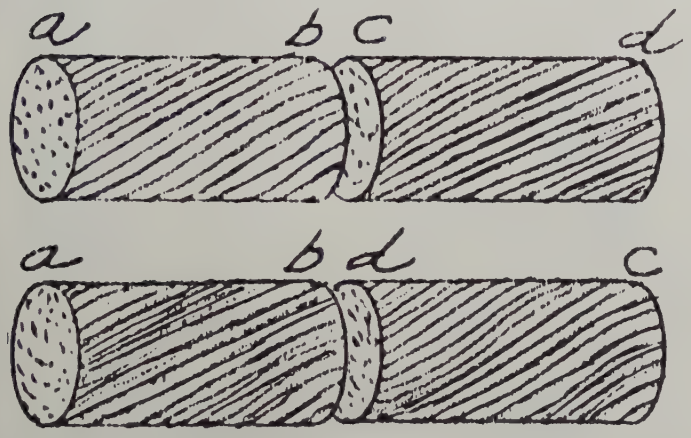

Fig. 13—Model "molecules" of twisted jute as used by Bose in 1898. (*Courtesy of Longmans, Green and Co.*)

Examined in a millimeter wave polarimeter these "molecules" gave either right or left-hand polarization twists, and jointly, no twist. Here, according to Bose, was an analog of the sugar rotations. The significant feature of this microwave technique was in its providing a macroscopic representation of the submicroscopic. Recently, in 1955, quasi-crystallographic reflections have been obtained from model crystal structures of macroscopic "atoms" when irradiated by millimeter waves.[16] The basic technique is, however, reminiscent of Bose's early experiments in microwave modeling.

Circular and elliptical polarizations of microwaves were familiar and well-understood phenomena to the followers of Hertz, the majority of whom had a trained optical background. Righi and Bose both observed the polarized structure of wood, Righi actually constructing a wooden quarter-wave plate or circular polarizer.[2] The radio half-wave plate also had its origin at this time.

Zehnder in Germany in 1894 used Hertzian grids to produce circular or elliptic polarization.[17] Lodge's description is so clear as to merit reproduction: "He takes a couple of plane polarizing grids and places them parallel to each other at a little distance apart with their wires crossed. If the two grids are close together they will act like wire-gauze, reflecting any kind of polarized radiation equally; but if the warp and woof are an eighth-wavelength apart, and the plane of the incident radiation is at 45° to the wires, the reflected radiation will be circularly polarized. A change in the circumstances will, of course, make it elliptical. Such a pair of grids acts, in fact, like a Babinet's Compensator."[9] The modern form of the arrangement consists usually of one grid spaced one-eighth wavelength from a metal sheet reflector.[18]

Garbasso and Aschkinass, by breaking up the wires of a Hertzian grid into uniform short lengths, *i.e.*, dipoles, showed that a dispersive, or frequency-sensitive, polarized mirror then existed.[19] The tuned reflector of a modern television receiving antenna is a simple case of this phenomenon. Marconi, in the first experiments in scatter communication in 1932, used parabolic mirrors of tuned elements constituting the reflectors.[20]

The optical problem to the Hertzians was to reproduce a dispersive Newtonian prism on microwaves. Such a prism was constructed from layers of dispersive dipoles by Garbasso and Aschkinass in 1894; this prism was the first component of "artificial dielectric" as we now term such a structure. The layers consisted of tinfoil strips fixed to glass plates. The wavelength was 7.5 cm (4000 mc).

It is evident that the study of the polarization properties of microwaves in microwave optics led to considerable advances in the art before 1900.

Dielectrics in the Hertzian Epoch

Hertz's great achievement in experimentally confirming Maxwell's electromagnetic theory of light by generating, controlling, and detecting microwave radiation, arose as a by-product of a general research into the properties of dielectrics or insulators.[1]

In the years following, extensive investigations of dielectrics were carried out by the followers of Hertz. Hertz's own dielectric researches were the basis of much of the work. He developed standing-wave measurements and evolved the nodal shift technique. He was interested in secondary reradiation from dielectric masses, not ignoring the polarization characteristics. He achieved the first dielectric constant determination by refraction, using the celebrated prism of pitch. His

[15] J. C. Bose, "On the rotation of plane of polarisation of electric waves by a twisted structure," *Proc. Roy. Soc.*, vol. 63, p. 146; 1898.
[16] J. F. Ramsay and S. C. Snook, "Microwave model crystallography," *Electronic and Radio Engr.*, pp. 165–169; May, 1957.
[17] Zehnder, *Ber naturforsch. Ges. zu Freiburg i. B.*, Bd. 9, Heft 2; June 21, 1894.
[18] J. F. Ramsay, "Circular polarization for cw radar," *Marconi Rev.*, vol. 15, pp. 71–89; 2nd Quarter, 1952.
[19] Garbasso and Aschkinass, "Brechnung und Dispersion electrischer Strahlen," *Ann. der Phys.*, vol. 53, p. 534, 1894.
[20] G. Marconi, "Radio communication by means of very short electric waves," reprint, IRE Trans., vol. AP-5, pp. 90–99; January, 1957.

work is notable both for the number of substances he investigated, and in some cases for the size of the experimental samples. A list of the substances gives some idea of the thoroughness of his approach (Fig. 14).

Solids	Liquids	Gases
Metals	Water	Air
Paraffin	Sulphuric Acid	Hydrogen
Shellac	Alcohol	Carbonic Acid
Resin	Ether	Coal Gas
Ebonite	Hydrochloric Acid	Chlorine
India-Rubber	Nitric Acid	Nitrous Oxide
Glass	Ammonia (Soln)	Bromine Vapor
Porcelain	Paraffin	Iodine Vapor
Earthenware	Benzole	
Wood	Petrol	
Pasteboard	Carbon Disulphide	
Paper	Ammonium Sulphide	
Ivory	Fuchsine	
Horn	Potassium Permanganate	
Hides	Nitrate of Mercury	
Feathers	Sodium Hyposulphite	
Agate	Potassium Bromide	
Mica	Potassium Iodide	
Copper Sulphate	Iron Salts	
Crystals	Copper Salts	
Topaz	Sal-Ammoniac	
Amethyst	Zinc Sulphate	
Crystallized Sugar	Common Salt	
Alum	Potassium Sulphate	
Calc-Spar	Sodium Sulphate	
Rock-Salt	Magnesium Sulphate	
Gypsum		
Rock-Crystal		
Smoke Glass		
Quartz		

Fig. 14—List of substances investigated by Hertz. (*Courtesy of Macmillan and Co., Ltd., and St. Martin's Press, Inc.*)

Some of his experimental samples may be quoted.[1] His first material being paper, and the wavelength in the meter band, he "piled up books in the form of a parallelopiped 1.5 meter long, 0.5 m broad, and 1 m high." He also had cast "800 kgm of unmixed asphalt" in a block of similar size. Another block was of artificial pitch. A sulphur sample consisted of "a massive block 70 cm long, 20 cm broad and 35 cm high." As a dielectric cylinder Hertz made use of "a sandstone pillar in the building." For one liquid dielectric he used "an oak trough with 45 liters of pure paraffin."

These investigations were highly stimulating to his successors, the majority of whom used shorter waves—and smaller samples. The low-loss characteristics of paraffin and paraffin wax were known to most of the Hertzians. The liquid form was popular around the spark gap where its dielectric constant allowed greater power to be obtained. The solid form was used for components, *e.g.*, lenses and prisms, and as an insulating support. Sulphur and ebonite were used for the same purposes.

The dielectric properties of water were examined on different frequencies, both as liquid[21] and ice.[8] Alcohol, castor oil, olive oil, xylol, and petrol were also measured at microwave frequencies.[22]

Anomalous dispersion was of great interest to the followers of Hertz who, realizing the truth of the electromagnetic theory, saw a solution to the optical uncertainties. Trouton in Dublin, for example, in 1889 asked, "Would the interspersing of bodies of nearly the same period in Hertz's pitch prism alter the angle of refraction?

If so, then anomalous dispersion may yet be successfully demonstrated."[4] Today we know that he was correct and experiment has confirmed his conjecture. Trouton may be regarded as the father of artificial dielectrics; his dipole-loaded medium was the first suggestion made in this field. To the modern it is interesting to find Trouton suggested as well that the particles need not be identical. As we have seen earlier, Garbasso and Aschkinass carried out the experiment with identical dipoles in 1894.

Trouton was also aware of the need for microwave photographs and suggested molecular dissociation and ac electrolytes as possible techniques. This problem is still unsolved today.

With the current modern interest in ferrites, germanium, and powdered artificial dielectrics at microwaves, it is relevant to mention that Birkeland in 1894 made up synthetic dielectrics from paraffin and metal filings or powders.[23] His "ferro-paraffin" consisted of iron filings or chemically obtained iron powder mixed with powdered quartz in paraffin. Birkeland desired "to demonstrate in magnetic cylinders stationary magnetic waves analogous to the electric stationary waves along metallic wires." He was unsuccessful due to losses which even then were a feature of artificial dielectrics. Birkeland did observe the detuning effect in a resonant circuit of a ferro-paraffin rod, and the excessive skin depth of the current in the rod. Control experiments were also carried out with brass filings and with zinc filings in paraffin.

Bose developed lossy artificial media in his search for a microwave absorber; the blotting paper soaked in electrolyte proved the best.[5]

It is doubtful if the Faraday rotation of the plane of polarization was ever investigated by the Hertzians. It is likely however that Lodge realized that polarization rotation by a magnetic field was possible with Hertzian waves, judging from some of his experiments and papers.

Among the classical optical phenomena that were reinvestigated on centimeter and millimeter waves were total internal reflection and the evanescent field at the interface,[5] Brewster angle,[4] the quarter-wave and half-wave thickness feature of dielectric slabs,[2] polarization

[21] A. D. Cole, "Measurement of short electrical waves and their transmission through water cells," *Phys. Rev.*, vol. 7; November, 1898.

[22] E. Branly, "The transmission of Hertz waves through liquids," *Compt. Rend*, October 30, 1899.

[23] M. Birkeland, "On magnetisation produced by Hertzian currents; a magnetic dielectric," *Compt. Rend.*, June 11, 1894.

rotations,[5] double refraction,[24] and selective absorption.[5]

For these measurements and other applications, instrumentation covered microwave spectrometers,[5] interferometers,[25] diffraction gratings,[26] polarimeters,[5] all used with incoherent spark generators and (usually) coherer detectors. A notable interferometer built by Hull under the direction of Prof. A. A. Michelson at Chicago University in 1897 operated on 9.12-cm wavelength and could measure wavelength and index of refraction with an accuracy of better than 1 per cent. Fig. 15 illustrates Righi's interference experiment with Fresnel mirrors as drawn by Poincaré.[27] The wavelength was probably in X band.

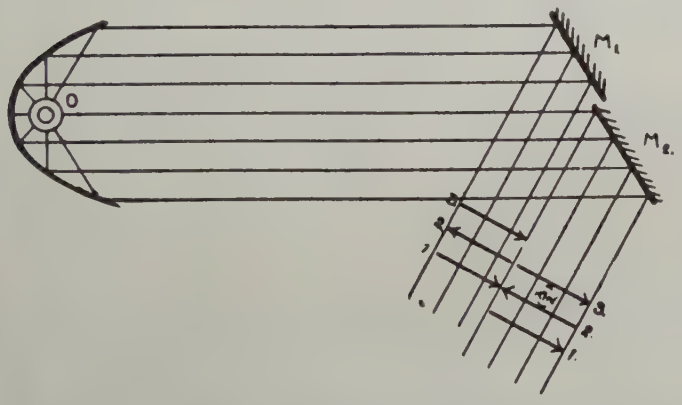

Interference between two parallel rays in the same direction. The two reflected rays have the same phase difference at all points, and the degree of interference depends upon the distance between the mirrors M_1 and M_2.

Fig. 15—Fresnel mirror experiment modelled on 3 cm by Righi (description by Poincaré). (*Courtesy of Constable and Co., Ltd.*)

Conclusion

The above historical investigation was not written just because it provided interesting history, and to the author at least, fresh light on origins, but because in a strange way it presented a parallel with the microwave situation today.

Today, millimeter waves research is in a similar position to that existing in the 1890's. It does not know where it is going. Any objectives it seems to have are scientific, as it was with the Hertzians. Generation of the waves presents formidable difficulties, detectors are almost as crude as those of the early experimentalists. The only positive application that may appear now is hollow-pipe waveguide communications. Radar and wireless communications are beset by propagation difficulties.

Yet, every time a region of the spectrum is developed a major practical application arises. World communications arose from the so-called short-wave region, television appeared in the very-high frequency band, radar and tropospheric scatter communications exploited the centimeter waveband. "What next?" is a natural question.

It will be observed that the major practical advances tended to arise from the development of the optical features of radio waves—beam radio, line-of-sight tv, high resolution radar, scatter communications, these descriptions are optical. The closer radio techniques approach the optical, the more likely they are to yield fruitful developments. Radio astronomy is the latest example.

Therefore, the work of the Hertzians, masters of microwave optics, then points the direction in which the new microwave radio must go.

If the signposts are correct the undeveloped millimeter waveband should see a major everyday application of radio optics.

Otherwise, the millimeter waveband remains an ideal region of the spectrum for modeling devices and phenomena from other regions of the spectrum. Antennas, for example, which are too large, can be modeled as conveniently as atoms which are too small. Particularly all wave phenomena can be reproduced with a convenience not realizable in other regions of the spectrum. Optics textbooks may yet require another chapter, one on "Microwave Optics."

Acknowledgment

The author wishes to thank the Engineer-in-Chief of Marconi's Wireless Telegraph Company Limited for permission to publish this paper. To Canadian Marconi Company special thanks are due for assistance in preparing the material for publication. Acknowledgment is also made to Dr. A. A. Oliner, Polytechnic Institute of Brooklyn, for suggesting and arranging IRE-URSI presentation of this historical review on May 23, 1957.

[24] P. Lebededev, "Double refraction of electric rays," *Electrician;* November 15, 1895.
[25] G. F. Hull, "On the use of the interferometer in the study of electric waves," *Phys. Rev.*, vol. 5, p. 231; October, 1897.
[26] J. C. Bose, "On the determination of the wavelength of electric radiation by a diffraction grating," *Proc. Roy. Soc.*, vol. 60; 1897.
[27] H. Poincaré and F. K. Vreeland, "Maxwell's Theory and Wireless Telegraphy," Constable and Co., Ltd., London, Eng.; 1905.

Ghost Modes in Imperfect Waveguides*

E. T. JAYNES†, SENIOR MEMBER, IRE

Summary—Attention is called to the existence of microwave resonances which have the unusual property that they are nonradiating, and thus have high Q, in spite of the fact that the fields are not enclosed completely by metallic walls. These "ghost modes" represent fields which are derived from those of the usual waveguide modes, but are "trapped" in the vicinity of imperfections in the waveguide. Their resonant frequency is slightly lower than the corresponding cutoff frequency. If one attempts to use a waveguide in its lowest mode, over a range of frequencies which includes the ghosts of higher modes, complicated resonance effects may be observed which can cause trouble in some types of microwave circuits. The same phenomenon exists in any structure which has pass bands and rejection bands, such as periodic structures or crystals.

Introduction

THE phenomenon described herein explains certain curious and troublesome effects observed in waveguides operating close to the cutoff frequency of a propagation mode, and it may have applications for waveguide filters. In addition, it has a certain educational value because of a mathematical analogy with the phenomenon of localized bound states due to imperfections in crystals.

Ghost Modes Due to a Dielectric

To illustrate the simplest case, and one which can be analyzed completely, consider the structure of Fig. 1. A dielectric disk of thickness d, dielectric constant ϵ, is placed in a cylindrical waveguide of radius a. Let the center of the disk be the origin of a cylindrical coordinate system $(r\theta z)$. A possible electromagnetic field is one whose transverse structure is that of the TM_{01} mode, derived from the field component

$$E_z = \begin{cases} BJ_0(k_1 r)\exp\left[-(k_1^2 - k^2)^{1/2} z\right], & z > \dfrac{d}{2} \\ AJ_0(k_1 r)\cos\left[(\epsilon k^2 - k_1^2)^{1/2} z\right], & |z| < \dfrac{d}{2} \\ BJ_0(k_1 r)\exp\left[+(k_1^2 - k^2)^{1/2} z\right], & z < -\dfrac{d}{2} \end{cases} \cdot \quad (1)$$

In (1),

$$k_1 = \frac{2.405}{a} = \frac{\omega_c}{c}, \qquad k = \frac{\omega}{c},$$

where ω_c and ω are, respectively, the TM_{01} cutoff frequency and an operating frequency to be determined presently. Matching solutions across the dielectric-air interfaces, we obtain the condition

$$\tan\left[(\epsilon k^2 - k_1^2)^{1/2}\frac{d}{2}\right] = \epsilon\left[\frac{k_1^2 - k^2}{\epsilon k^2 - k_1^2}\right]^{1/2}. \quad (2)$$

For any $\epsilon > 1$, (2) has at least one solution for k with $k < k_1$. If $(\epsilon - 1)^{1/2} k_1 d < 2\pi$, only one such solution exists. We consider, in particular, the case where ϵ is appreciably greater than unity and $k_1 d \ll 1$. Then k as determined from (2) is very close to k_1, and it will be a good approximation to set

$$(\epsilon k^2 - k_1^2)^{1/2} d \simeq (\epsilon - 1)^{1/2} k_1 d \ll 1,$$

so that (2) reduces to the following formula for ω:

$$\omega^2 \simeq \omega_c^2\left[1 - \left(\frac{\epsilon - 1}{\epsilon}\frac{k_1 d}{2}\right)^2\right]. \quad (3)$$

The field derived from (1) thus represents a resonant mode with resonant frequency slightly below the cutoff frequency of the TM_{01} mode, in which the fields are localized to the vicinity of the dielectric disk. The electric field configuration is sketched in Fig. 1. The longitudinal extension of this ghost mode is described by the "$1/e$ distance"

$$x_0 = \frac{1}{(k_1^2 - k^2)^{1/2}} = \frac{\lambda_c}{2\pi(1 - \omega^2/\omega_c^2)^{1/2}} \quad (4)$$

where $\lambda_c = 2\pi/k_1 = 2.6a$ is the TM_{01} cutoff wavelength. Numerical values of (x_0/λ_c) are indicated in Fig. 2. It is seen that the ghost is surprisingly well localized; for example, in the case $\omega = 0.99\,\omega_c$, x_0 is less than 1.5 pipe diameters. If the waveguide extends a distance three or four times x_0 on either side of the dielectric disk, this ghost will be essentially nonradiating and will have a very high Q, limited only by losses in the waveguide walls and the dielectric.

Suppose this waveguide were being operated in the TE_{11} propagating mode, at frequencies near the TM_{01} cutoff frequency. This is a rather common condition in practice, since the TM_{01} cutoff frequency is only about 30 per cent higher than that of the TE_{11} mode. In a perfect waveguide the fact that we were close to the TM_{01} propagating range would not cause any trouble. However, the disk represents an "imperfection" in what would otherwise be a smooth waveguide. The slightest asymmetry in structure near the disk, or the slightest inhomogeneity in dielectric constant of the disk, can couple the ghost to the TE_{11} mode and cause a large absorption of energy at the frequency given by (3). The field of the ghost can attain a magnitude several hundred times that of the propagating TE_{11} mode, so that

* Original manuscript received by the IRE, September 6, 1957.
† Microwave Laboratory, Stanford University, Stanford, Calif.

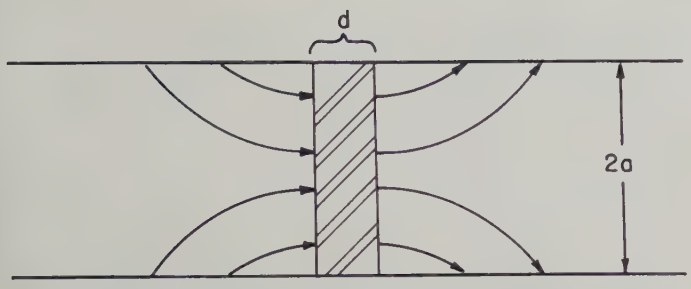

Fig. 1—TM_{01} ghost mode due to a dielectric disk.

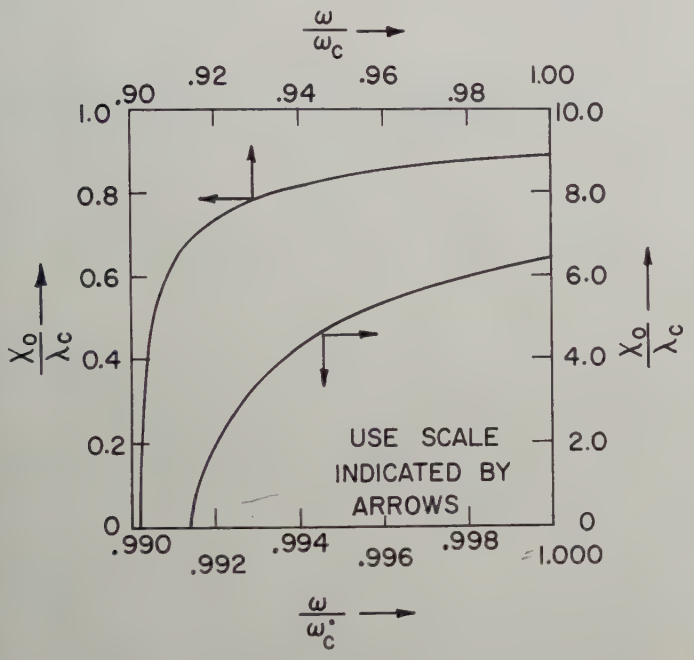

Fig. 2—"(1/e) distance" of ghost modes as a function of frequency.

in a high-power device a ghost can cause breakdown. It was, in fact, the persistent failure of ceramic windows in the output waveguides of high-powered klystrons feeding the Stanford linear electron accelerator (carrying about 20 megw at 3 kmc), which led to the recognition of ghost modes. Spurious resonances in certain ferrite devices may also be traceable to this cause.

What was said for the TM_{01} mode evidently applies in general for the structure of Fig. 1; every propagation mode of the waveguide is accompanied by a ghost with the same transverse field pattern, localized to the vicinity of the disk, with a resonant frequency slightly below the corresponding cutoff frequency.

General Ghost Modes

The presence of a dielectric is not necessary for existence of ghosts; *any* localized imperfection in a waveguide will cause them to appear. Consider first a perfect, infinitely long waveguide with zero loss, excited in one of the propagation mode patterns at exactly its cutoff frequency. It is thus a large resonant cavity with resonant frequency ω_c. Let the electric and magnetic fields in the vicinity of any point P on the waveguide wall be E, H. Now if $\epsilon_0 E^2 > \mu_0 H^2$, push the wall in slightly at P, while

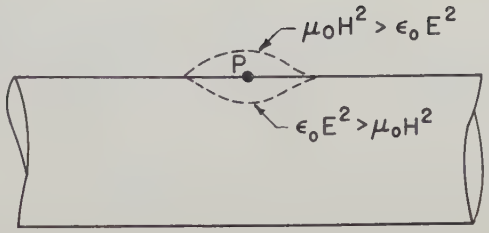

Fig. 3—Wall perturbations which create ghost modes.

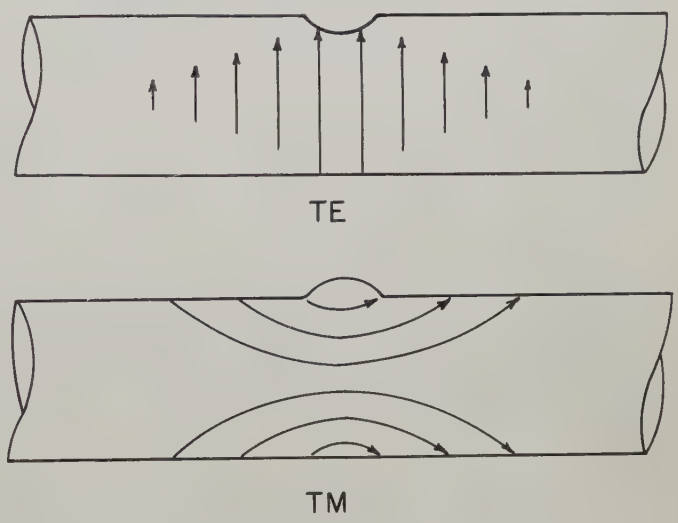

Fig. 4—Electric field lines of TE and TM ghost modes due to wall imperfections.

if $\mu_0 H^2 > \epsilon_0 E^2$, pull out a small "blister" as in Fig. 3. According to the Slater perturbation formula [1], the resonant frequency of the cavity is always lowered by this change. But at any lower frequency than ω_c the fields will be attenuated exponentially as we move away from the imperfection; thus a ghost has been created, trapped to the vicinity of the imperfection, with a resonant frequency slightly lower than ω_c. Two examples are given in Fig. 4, in which only the electric field lines are sketched.

The Q of a ghost mode due to a small imperfection as in Fig. 4 is given to order of magnitude by

$$Q \simeq \frac{a}{\delta} = \frac{\text{waveguide radius}}{\text{skin depth}}, \tag{5}$$

from which it is seen that values in excess of 10^4 are easily attained. For the ghost of any mode other than the lowest one, there also will be a "loaded Q" involving the strength of coupling to propagating modes.

Crude estimates of the frequency and longitudinal extension of these ghosts, obtained from (4) and the Slater perturbation formula, are

$$\omega^2 \simeq \omega_c^2 \left[1 - \left(\frac{\pi \alpha \delta V}{A \lambda_c} \right)^2 \right], \tag{6}$$

$$x_0 \simeq \frac{A \lambda_c^2}{2\pi^2 \alpha \delta V}. \tag{7}$$

Here A is the cross-sectional area of the waveguide, δV is the volume added or removed by the imperfection, and α a dimensionless quantity of the order of magnitude unity, given by

$$\alpha = \frac{|\mu_0 H^2 - \epsilon_0 E^2|}{<\mu_0 H^2 + \epsilon_0 E^2>_{Av}} \tag{8}$$

where the fields in the numerator are values near the imperfection, while the denominator is an average over a waveguide cross section passing through the imperfection [2].

From these formulas several general conclusions may be drawn. If the imperfection is so small that

$$\delta V < \frac{A\lambda_c}{100}, \tag{9}$$

then one may expect the ghost to be separated from the cutoff frequency by less than the bandwidth ω_c/Q, so that it does not appear as a well-resolved resonance, but only a slight broadening of the cutoff region. If, on the other hand,

$$\delta V > \frac{A\lambda_c}{100}, \tag{10}$$

the ghost will generally appear as a distinct resonance. The longitudinal extension x_0 of any well-resolved ghost will, from Fig. 2, never be more than a few times λ_c. The δV required by (10) is so large that the usual mechanical imperfections due to machining errors, inadvertent hammer blows, etc., do not cause separation of ghosts from the waveguide modes. However, installation of almost any kind of apparatus inside a waveguide will cause them to appear, as may the presence of any twist or bend.

Periodic Structures

What was said above for waveguides applies equally well to any periodic structure, such as those used in linear accelerators, traveling-wave tubes, or, in fact, any lumped-constant filter composed of a cascade of identical networks. By reasoning exactly like that in the preceding section, one can show that any localized imperfection in such a structure will cause a bound resonance to appear, with resonant frequency just outside the pass band of the structure. In this case, it may lie either above or below the pass band. Once again, the imperfection has to be quite large in order to cause separation of a well-resolved resonance, so that reasonable care in construction is sufficient to avoid troubles due to these ghosts.

There is an interesting, and pedagogically useful, analogy with certain well-known features of solid-state theory. Here a crystal represents a three-dimensional periodic structure, and solutions of the Schrödinger equation, in one-electron approximation, show an almost perfect mathematical analogy with those in the corresponding electrical problem [3]. In particular, the conduction bands of the crystal correspond to pass bands of the filter, and any localized imperfection in the crystal (such as a vacancy, interstitial atom, or impurity atom), results in at least one localized bound state, with an energy just above or just below the edge of a conduction band. In this way one can understand the creation of donor or acceptor impurity levels involved in n-type and p-type conductivity in semiconductors [4].

Further work on ghost modes, by M. Forrer and the writer, is being prepared for publication. Experimental results, universal curves for predicting the occurrence of ghosts, and discussion of their possible use in waveguide filters and mode convertors will be included.

Bibliography

[1] Slater, J. C. *Microwave Electronics*, New York: D. Van Nostrand Company, Inc., 1950, p. 81.
[2] The derivation of (6) and (7) is a bit tricky, since a small change in δV alters the "length" x_0 of the cavity. One must apply the Slater formula only to infinitesimal changes in δV, and integrate to obtain their cumulative effect. For this reason the frequency shift involves $(\delta V)^2$ rather than (δV), as one might at first expect.
[3] Brillouin, L. *Wave Propagation in Periodic Structures*, New York: McGraw-Hill Book Company, Inc., 1946.
[4] Kittel, C. *Introduction to Solid-State Physics*. New York: John Wiley & Sons, Inc., 1953, Ch. 14.

High-Frequency Crystal Filter Design Techniques and Applications*

DAVID I. KOSOWSKY†, MEMBER, IRE

Summary—**High-frequency crystal filters which operate to 40 mc are now being commercially produced. These filters, with bandwidths ranging from one cycle to several hundred kilocycles per second, have been made possible by new design techniques and simplified circuitry.**

Eliminating the need for multiple frequency conversion, the small rugged filters are already beginning to find wide use in many AM, SSB, and fm receivers as well as single-sideband generators.

Crystal filters are normally composed of from two to eight quartz resonators in a lattice or bridge network. The filter components are characterized by high Q and stability under extreme environmental conditions. Normal values of Q for crystal filter components in the 1 to 40 mc range are from 50,000 to 200,000; in certain filters, element Q's exceed 1,000,000.

Introduction

WITH more and more radio communication messages crowding the radio-frequency spectrum, allotment of frequency bands to various radio and radar needs has become a serious problem. New systems have been developed to aid in the economical utilization of existing frequency space. These include schemes such as single-sideband and narrow-band frequency modulation. To be successful, each of these systems must operate within a narrow, well-defined band of frequencies. As a result, filter selectivity requirements have become increasingly stringent.

At frequencies greater than a few megacycles, equipment designers up to now have been forced to resort to systems of multiple-frequency conversion in order to obtain required equipment performance. Conventional types of filters may not perform suitably for single frequency conversion. The multiple conversion process brings about increased circuit complexity, with corresponding loss in efficiency and reliability.

The high-frequency crystal filter offers a solution to the frequency conversion problem as well as other general design problems in the higher frequency ranges.

Compact filter units employing miniature quartz crystal resonators in the 5- to 40-mc range exhibit filter performance which has previously been possible only at significantly lower frequencies. The result is that multiple frequency conversions may be eliminated. Equipment simplification and size reduction can be effected, along with improved performance and reliability.

One primary reason why crystal filters perform so well at high frequencies is the inherent high Q of the resonators. In a band-pass filter, high selectivity and low dissipation or insertion loss require that the Q's of the critical filter components be much greater than the ratio of center frequency to bandwidth.[1] Quartz crystal resonators used in filter networks have Q's that range from 10,000 to 200,000 in general. Filters have been produced with crystal Q's in excess of 1,000,000. By comparison, the Q's normally attainable in conventional inductances may range from 50 to 200. Nickel alloy resonators commonly employed in "mechanical" filters have Q's ranging from 2000 to 10,000.[2] The advantages of using crystal resonators in filter networks have been known for over 30 years,[3] but not until recently have high-frequency filter units with controlled characteristics been made commercially available.

Quartz Crystal Resonators

Of the hundreds of crystals that exhibit the piezoelectric effect, only the quartz crystal has been employed to any significant extent in oscillators and filters. Among other qualities, quartz crystals possess an extremely high order of stability over wide temperature variations during long time periods. In the presence of severe shock and vibration, the quartz crystal designed for filter applications does not exhibit microphonic behavior. These qualities are necessary to achieve good narrow-band filtering devices at high frequencies.

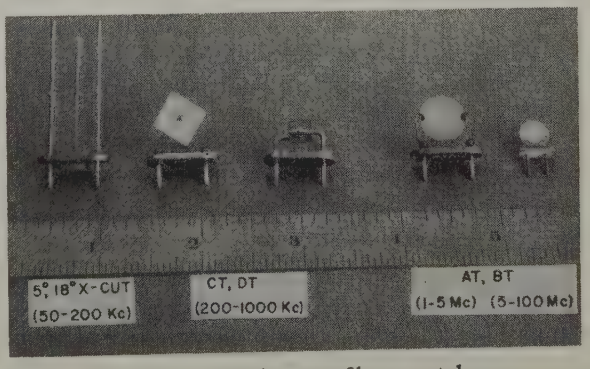

Fig. 1—Typical quartz filter crystals.

Typical quartz filter crystal resonators are shown in Fig. 1. Any plate cut from a piece of natural quartz has a number of resonant frequencies. The frequencies of resonance depend on the crystal dimensions, the vibra-

* Original manuscript received by the IRE, September 6, 1957; revised manuscript received, October 30, 1957.

† Hycon Eastern, Inc., Cambridge, Mass.

[1] E. A. Guillemin, "The effect of incidental dissipation in filters," *Electronics*, vol. 19, pp. 130–135; October, 1946.

[2] J. C. Hathaway and D. F. Babcock, "Survey of mechanical filters and their applications," PROC. IRE, vol. 45, pp. 5–16; January, 1957.

[3] W. G. Cady, "The piezo-electric resonator," PROC. IRE, vol. 10, pp. 83–114; April, 1922.

tional mode involved, and the orientation of the cut. The AT-cut crystal, which operates in a thickness shear vibrational mode, is particularly attractive because of its extremely small size at frequencies above 5 or 6 mc. Also, the AT-cut component possesses an excellent temperature coefficient. Over the temperature range of $-55°C$ to $+85°C$ the resonant frequency of a typical AT crystal will shift less than ± 0.005 per cent of its nominal value.

Equivalent Circuit

In the vicinity of a resonant frequency, a crystal resonator may be represented by an equivalent electrical circuit[4] of the type shown in Fig. 2(a). The inductance L_1 and capacitance C_1 represent the effective mass and stiffness of the crystal, respectively. C_0 is the static capacitance and includes stray-wiring and holder capacitance. The resistance R_1 represents the frictional loss of the vibrating crystal. The crystal Q is defined as the ratio of the reactance of L_1 at the resonant frequency to the resistance R_1. Because of the extremely large value of Q, the crystal may be considered a purely reactive network for most filter applications.

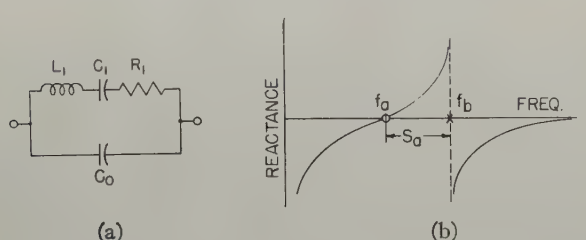

Fig. 2—Crystal resonator equivalent circuit.

The reactance curve corresponding to the lossless equivalent circuit is shown in Fig. 2(b). The resonant frequency or "zero" of the crystal unit (f_a) and the antiresonant frequency or "pole" (f_b) are related to one another by the ratio of capacitances of the crystal defined by

$$r \equiv \frac{C_0}{C_1} . \tag{1}$$

The relationship is easily seen to be:

$$f_b^2 = f_a^2\left(1 + \frac{1}{r}\right). \tag{2}$$

Because of the coupling that exists between the electrical and mechanical stresses within the crystal, there will always be a fixed ratio of capacitances for any crystal cut.[5] The lowest ratio found for quartz is 115, but because of stray-wiring and holder capacitance the minimum ratio for practical quartz cuts is approximately 125. At frequencies above one megacycle, the coupling factor associated with the AT-cut crystal increases the minimum value of r to approximately 250 From (2), the zero-pole spacing [S_a in Fig. 2(b)] can be approximated by

$$S_a = f_b - f_a \doteq \frac{f_a}{2r} . \tag{3}$$

S_a is, therefore, a very small percentage of the crystal resonant frequency, being at most 0.4 per cent of f_a at low frequencies, and 0.2 per cent of f_a at high frequencies

A quartz crystal may have a number of vibrational modes in the vicinity of the desired response. However, by properly dimensioning the resonator and the electrodes which supply electrical excitation, it has been possible to produce crystals with essentially single-resonance characteristics at frequencies as high as 40 mc. Through the proper utilization of from 4 to 8 such resonators, filters are produced in which the level of undesirable or spurious responses is from 80 to 100 db below the mean pass band level.

Dimensioning a crystal resonator to suppress undesirable modes of vibration and to produce a given temperature coefficient generally limits the equivalent electrical parameters to a narrow range of values. This limitation, together with the existence of a fixed ratio of capacitances for the crystal resonator, places both theoretical and practical restrictions on the maximum bandwidth attainable with a given crystal filter configuration. Such restrictions apply even when inductances or resonant circuits are arranged in series or parallel with the crystal resonator in order to modify the resonator critical-frequency or zero-pole configuration.

These bandwidth restrictions make it desirable to utilize a design procedure which will rapidly and accurately indicate the range of filter characteristics obtainable with a given crystal resonator. A synthesis procedure developed for this purpose follows.

Crystal Filter Circuitry

Almost all crystal filters of any significance produced in the past twenty years have been based on the symmetrical-lattice or bridge networks developed by Mason.[6] The symmetrical lattice, which is the most general form of symmetrical network, provides analytical flexibility. In addition, practical considerations peculiar to crystal filter realization often make it necessary to employ this configuration.

Several examples of crystal lattice filter circuits are illustrated in Fig. 3. Attenuation characteristics of these filters depend completely upon the arrangement of critical frequencies or zeros and poles of the series (A) and shunt (B) arms of the lattice. Fig. 3(a) and 3(b) illustrates the crystal-capacitor lattices normally designated as narrow-band filters. The bandwidth of these filters is limited directly by the zero-pole spacings

[4] K. S. Van Dyke, "The piezo-electric resonator and its equivalent network," Proc. IRE, vol. 16, pp. 742–764; June, 1928.

[5] R. A. Heising, "Quartz Crystals for Electrical Circuits," D. Van Nostrand Co., Inc., New York, N. Y., ch. 1; 1946.

[6] W. P. Mason, "Electric wave filters employing quartz crystals as elements," *Bell Sys. Tech. J.*, vol. 13, pp. 405–452; July, 1934.

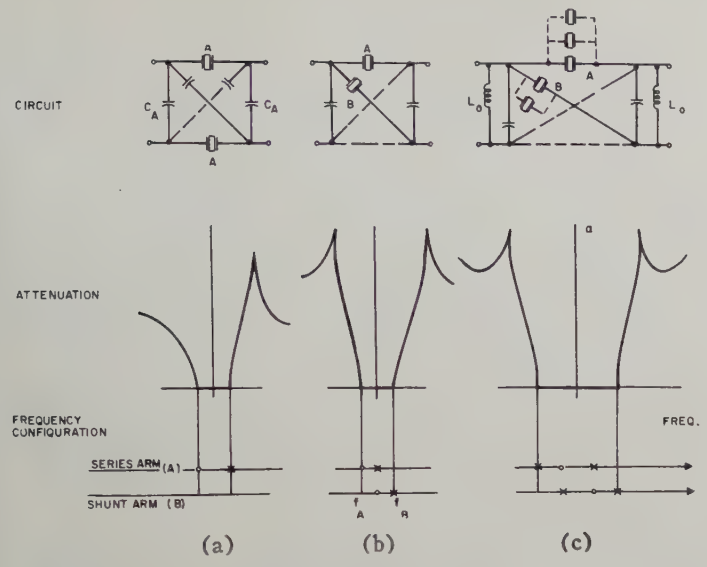

Fig. 3—Crystal lattice filter configurations.

of the associated crystals and therefore, by the ratio of capacitances (r). The ratio of capacitances must include the effects of external capacitance C_A, which may be considered to be in parallel with both series and shunt lattice arms, and will, therefore, increase the normal static capacitance C_0. From (3) it may be seen that the upper bandwidth limit of the narrow-band crystal filter is only a few tenths of one per cent of the filter center frequency. The lower percentage bandwidth limit, which is set by crystal dissipation and frequency tolerances, may be as small as 0.01 per cent.[7]

In order to obtain wider filter bandwidths, inductances may be placed in series or in parallel with the lattice network as shown in Fig. 3(c). The inductance L_0 may be considered to resonate in the vicinity of the center frequency with all or part of the crystal effective shunt capacitance (C_0+C_A). A number of the resultant critical frequencies of the series and shunt lattice arms may be so arranged as to provide a narrow pass band region. The remaining poles and zeros, far removed in frequency from the filter pass band, have negligible effect on the over-all characteristic.[8] The width of the pass band formed in this manner is not limited directly by the crystal ratio of capacitances. This type of filter, which will be called an intermediate-band crystal filter, may have somewhat wider bandwidths than the crystal-capacitor filter. It is highly significant that the inductances associated with the intermediate-band crystal filter need not have extremely high Q's. In general, inductor Q's in the order of 40–60 will be sufficient to permit bandwidths up to 2 or 3 times the bandwidth of the crystal-capacitor filter, with negligible increase in filter dissipation.

The wide-band crystal filter is obtained when all the critical frequencies resulting from an inductance-crystal combination are contained within the filter bandwidth limits, as shown in Fig. 3(c). The bandwidth range for this filter type is approximately 1.5 per cent to 10 per cent of the filter center frequency. The upper limit, which is somewhat smaller at high frequencies, is set by the crystal ratio of capacitances, while the lower limit is fixed[7] by the Q's realizable for L_0. The dissipation present in the external inductances may be associated directly with the filter terminating impedances, producing no effect on the network attenuation characteristics other than a constant insertion loss.

The dissipation, or midband insertion loss, introduced by the filter network is only 1 or 2 db for most narrow- and intermediate-band filters. For wide-band filters, the corresponding loss depends upon filter bandwidth and external inductance Q. For a 5 per cent filter bandwidth and a Q of 100, the filter loss is approximately 6 db.

The simple filters shown in Fig. 3 form the basic building blocks for more complicated filter networks. Greater attenuation and selectivity may be obtained either by cascading sections of the type shown, or by placing several crystals in parallel in any lattice arm as shown in Fig. 3(c) (connections shown dotted).

Unbalanced Networks

Until recently, the most significant application of crystal filters has been to low-frequency filters for carrier telephone systems. These filters, designed for use with balanced transmission lines, employ crystal resonators with divided electrodes[9] to obtain performance equivalent to the lattice networks shown in Fig. 3.

For vacuum tube or transistor circuitry, and at frequencies above several hundred kilocycles, it is desirable to utilize an unbalanced equivalent of the symmetrical lattice network. One of the most useful lattice equivalents is the "hybrid" network shown in Fig. 4(a).[10] The "hybrid" transformer has closely-balanced, tightly-coupled, secondary windings, and a primary winding which is uniformly coupled to the secondaries. Crystals 2A and 2B have twice the impedance of crystals A and B, respectively ($2L_1$, $C_1/2$, $C_0/2$). The inductance L_a may be resonated by parallel capacitance, or it may be used as one of the inductances L_0 shown in Fig. 3(c).

Fig. 4(b) and 4(c) illustrates two methods of cascading hybrid-type filter networks to achieve greater attenuation and selectivity. Hybrid leakage reactance has been neglected in these circuits. Any combination of Fig. 4(a)–4(c) may be employed to provide still better performance. Alternatively, crystals placed in parallel

[7] D. I. Kosowsky, "Synthesis and Realization of Crystal Filters," Mass. Inst. Tech., Cambridge, Mass., Res. Lab. of Electronics, Tech. Rep. No. 298, pp. 38–42; June 1, 1955.

[8] See, for example, Fig. 10. The frequencies f_1 and f_2 may be closely spaced and form part of a filter pass band, while f_3 may be far removed from the pass band region.

[9] C. E. Lane, "Crystal channel filters for the cable carrier system," *Bell Sys. Tech. J.*, vol. 17, pp. 125–136; January, 1938.

[10] W. P. Mason, "Resistance-compensated band-pass crystal filters for unbalanced circuits," *Bell Sys. Tech. J.*, vol. 16, pp. 423–436; October, 1937.

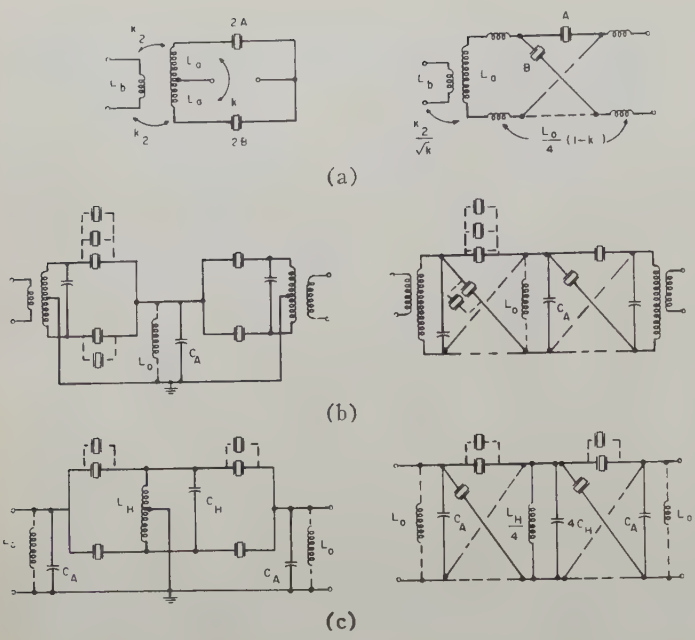

Fig. 4—"Hybrid" filter networks.

(shown dotted) in any lattice arm will accomplish the same result.

The inductances L_0 may be added to convert the network from the crystal-capacitor lattice [Fig. 3(b)] to the intermediate band or wide-band lattice [Fig. 3(c)]. In addition, the parallel circuit L_0–C_A in Fig. 4(c), provides a convenient means for altering the nominal impedance level of the filter. The desired impedance transformation is easily accomplished by "tapping" L_0 or C_A for the appropriate impedance level.

Utilizing the hybrid filter networks illustrated in Fig. 4, crystal filters have been produced throughout the frequency range of 10 kc to 40 mc, with bandwidths ranging from one cycle per second to several hundred kilocycles per second. The corresponding range of percentage bandwidths is 0.01 per cent to 7 per cent of center frequency.

Synthesis Procedure

Design of the lattice-type crystal filter network may be accomplished by utilizing classical image-parameter synthesis techniques[6,11,12] or by considering the total insertion loss of a given filter network.[13] However, as mentioned previously, the values of the equivalent electrical parameters of the crystal resonator are not completely within the control of the filter designer. A design procedure which rapidly indicates whether a given set of filter specifications can be realized is therefore highly desirable.

Since the crystal filter is normally restricted to bandwidths which are a very small percentage of the center frequency, and because of the nature of the equations involved in the image parameter synthesis of these filters, it has been possible to develop a procedure which permits the design of even the more complicated crystal filters utilizing only simple calculations and graphical aids. This procedure is based on a normalization or approximation technique which provides solutions with accuracies that are normally well within the tolerances placed on the filter components. A complete description of the synthesis procedure is given in another report[7] and is outlined below.

As shown in Fig. 3, the pass band region of a crystal lattice filter extends from the lowest critical frequency of the series arm reactance to the highest critical frequency of the shunt arm reactance. These two frequencies, f_A and f_B, are called the cutoff frequencies. The remaining critical frequencies of the series arm coincide with those of the shunt arm to produce a continuous pass band. For a given filter, the attenuation characteristic has a number of "infinite peaks" (bridge nulls) which can be no greater than one plus the number of "coincident" frequencies in the pass band.

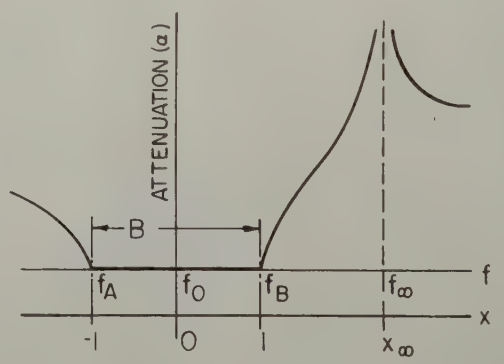

Fig. 5—"Normalized" basic section.

The simplest band-pass crystal filter [Fig. 3(a) and Fig. 5] will be referred to as the "basic" section. The characteristic of the basic section has, at most, one attenuation peak. The position of this attenuation peak may lie anywhere outside the filter pass band.

The attenuation characteristic of a filter having n infinite peaks and a bandwidth B, is equal to the sum of the characteristics of n basic sections, wherein each section has a bandwith B and an attenuation peak corresponding to one of the n peaks of the composite filter. The degree of complexity of a crystal filter necessary to meet a given set of specifications may, therefore, be determined through the addition of basic section characteristics.

Image attenuation of the basic section is a function of the filter cut-off frequencies, f_A and f_B, and of the frequency of infinite attenuation f_∞:

$$\alpha = \ln\left(\frac{1+p}{1-p}\right) = \text{attenuation loss} \qquad (4)$$

[11] D. Indjoudjian and P. Andrieux, "Les Filtres a Cristaux Piezoelectriques," Gauthier-Villars, Paris, France; 1953.
[12] E. A. Guillemin, "Communications Networks," John Wiley & Sons, Inc., New York, N. Y., vol. 2, ch. 10; 1935.
[13] W. Herzog, "Siebschaltungen mit Schwingkristallen," Dieterich'sche Verlagsbuchhandling, Wiesbaden, Germany; 1949.

where

$$p^2 = \left(\frac{f_\infty^2 - f_B^2}{f_\infty^2 - f_A^2}\right)\left(\frac{f^2 - f_A^2}{f^2 - f_B^2}\right). \tag{5}$$

Although (5) permits the calculation of all possible attenuation characteristics obtainable with the basic section, a complete set of characteristics would be necessary for each choice of filter relative bandwidth (ratio of bandwidth to center frequency). It is possible, however, to derive an approximation for p that is independent of bandwidth and center frequency and yet introduces negligible error in practice. Referring to Fig. 5, a normalization variable defined by

$$x \equiv \frac{f - f_0}{B/2} \tag{6}$$

where

$$B \equiv f_B - f_A; \qquad f_0 \equiv \frac{f_A + f_B}{2} \tag{7}$$

is substituted into (5), resulting in

$$p^2 = \left[\frac{x_\infty - 1}{x_\infty + 1}\right]\left[\frac{x+1}{x-1}\right] \cdot \left[\frac{1 + \frac{B_r}{4}(x_\infty + 1)}{1 + \frac{B_r}{4}(x_\infty - 1)}\right]\left[\frac{1 + \frac{B_r}{4}(x-1)}{1 + \frac{B_r}{4}(x+1)}\right] \tag{8}$$

where

$$B_r = B/f_0 \text{ (relative bandwidth)} \tag{9}$$

and

$$x_\infty \equiv \frac{f_\infty - f_0}{B/2}.$$

Consideration of the values of B_r and x_∞ normally encountered in crystal filter design, leads to the conclusion that (8) may be closely approximated by

$$p^2 \doteq p_0^2 = \left(\frac{x_\infty - 1}{x_\infty + 1}\right)\left(\frac{x+1}{x-1}\right). \tag{10}$$

Normalized Characteristics

The normalized attenuation characteristic is a function only of the variable x and the position of the attenuation peak (x_∞). Since (10) contains neither f_0 nor B, the normalized attenuation expression will hold regardless of filter center frequency or filter bandwidth.

Reference to (8) indicates that (10) is an excellent approximation in cases of very small percentage bandwidths and small values of x_∞. The set of normalized basic section characteristics shown in Fig. 6 illustrates the fact that even for the largest possible value of x_∞ and for extremely wide bandwidths (for the crystal

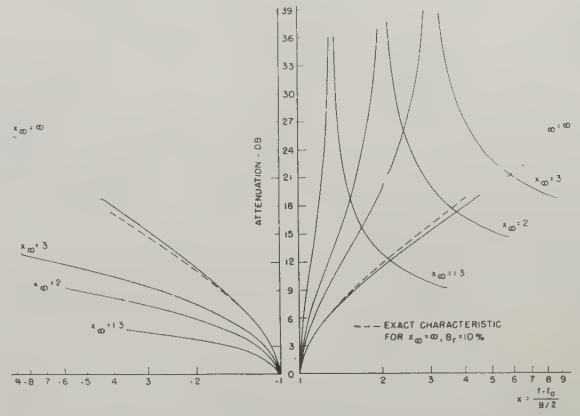

Fig. 6—"Normalized" basic section attenuation characteristics.

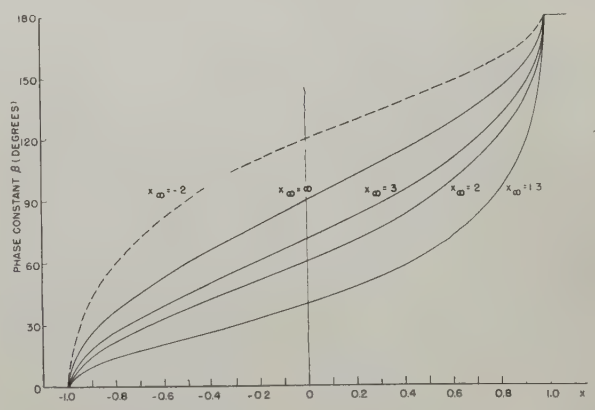

Fig. 7—Phase characteristics of basic section.

filter), the error involved in the normalization procedure is of no practical significance.

The attenuation α of a symmetrical network expresses the loss introduced by the network when it is terminated in its image or characteristic impedance. In practice the terminal impedances of a filter are generally fixed resistances. Image attenuation loss only approximately describes the performance of the filter. Filter termination effects, commonly called reflection and interaction losses, are of greatest importance in the filter pass band region. In this region, the attenuation loss is zero and the filter loss is primarily the result of mismatch.

To describe completely the filter transmission characteristic or insertion loss, it is necessary to determine the corresponding image impedance and phase characteristics. Fortunately, the same normalization technique may be applied to these characteristics to provide the complete insertion loss of any crystal filter.

The expression for a basic section normalized phase characteristic is given by

$$\beta_0 = 2 \tan^{-1} jp_0 \tag{11}$$

where

$$\beta_0 = \text{normalized image phase constant.}$$

A set of phase characteristics is shown in Fig. 7. The composite phase constant for a number of cascaded

basic sections is the sum of the phase constants for the individual sections at any value of x.

The image impedance characteristics of the crystal filters described above may be classified into three types depending on the nature of the cutoff frequencies f_A and f_B. In normalized form the three types are as follows:

Type I: Zero at f_A and pole at f_B

$$Z_{01} = R_{01}\left(\frac{1+x}{1-x}\right)^{1/2} \tag{12}$$

Type II: Zero at f_A and f_B

$$Z_{02} = R_{02}(1-x^2)^{1/2} \tag{13}$$

Type III: Pole at f_A and f_B

$$Z_{03} = R_{03}(1-x^2)^{-1/2} \tag{14}$$

where R_{01}, R_{02}, and R_{03} are resistances whose values depend on both the relative bandwidth of the filter and the equivalent circuit parameters of the crystal resonators. Eqs. (12) and (13) are plotted in Fig. 8.

In the filter pass band region ($-1<x<+1$), the image impedance is resistive (solid line). In the attenuating region, the image impedance is reactive and the corresponding magnitude is shown by the dotted line. The Type I image impedance is characteristic of the narrow-band filter [Fig. 3(a), 3(b)], while the Type II and Type III may result when external inductances are employed in wide-band or intermediate-band filters [Fig. 3(c)].

Utilizing the data of Figs. 6–8, it is possible to construct the total insertion loss characteristic corresponding to any number of basic sections (*i.e.*, any degree of filter complexity). As an example, Fig. 9 illustrates the composite transmission characteristics of a filter consisting of 6 basic sections (peaks at $x_\infty = \pm 1.3, \pm 1.6, \infty, \infty$). These values have been chosen to provide a maximum filter attenuation of 60 db. The shape factor (ratio of 60-db bandwidth to 6-db bandwidth) is approximately 1.3:1. A Type II image impedance characteristic is assumed, and the filter is resistively terminated.

A filter of this type might be employed in a telephone carrier channel system in the vicinity of 100 kc, or in an intermediate-frequency amplifier at 10 to 15 mc where extremely high selectivity is preferred to high final attenuation. For applications requiring final attenuations of 80 to 100 db, the attenuation peaks may be placed farther from the pass band. (See Fig. 13.)

Fig. 9 illustrates the degree of approximation to "flat" pass band and linear phase characteristics which may be obtained with the crystal filter. These factors, combined with linear voltage characteristics, result in low signal distortion and contribute to good transient performance.

To complete the design of a given crystal filter, it is necessary to determine the values of the equivalent parameters of the crystal resonators from the filter insertion loss characteristic. This is accomplished first by

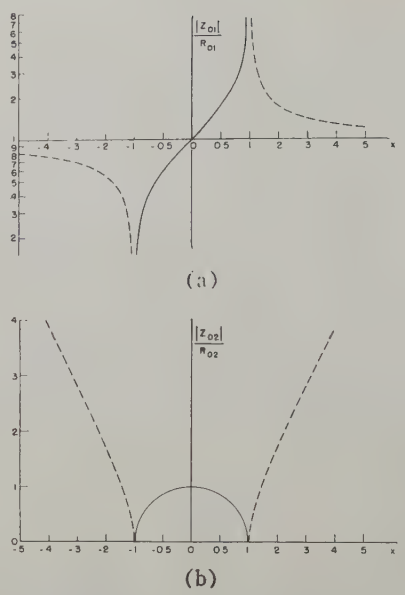

Fig. 8—Image impedance characteristics of band-pass filters. (a) Type I, (b) Type II.

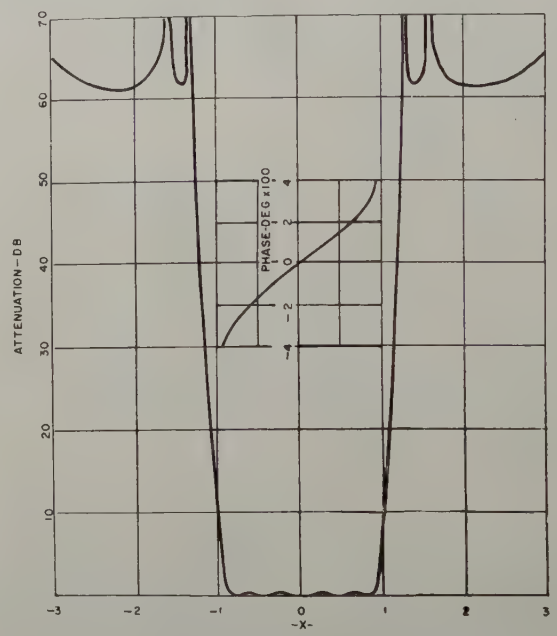

Fig. 9—Six-section transmission characteristics.

determining the locations of the pass band critical frequencies (see Fig. 3) from the attenuation peak positions, and then by calculating the element values of the filter reactances from these critical frequency configurations. It is interesting to note that even this portion of the synthesis procedure may be normalized so that the relative values of the filter elements may be determined for any given configuration without specifying filter frequency or bandwidth.

Fig. 10 illustrates the use of the normalization procedure to determine element values from zero-pole configurations. The configuration shown might represent one arm of the lattice network of Fig. 3(c). The zero and pole frequencies (f_1, f_2, f_3) can be derived from the attenuation frequencies of the filter utilizing conventional

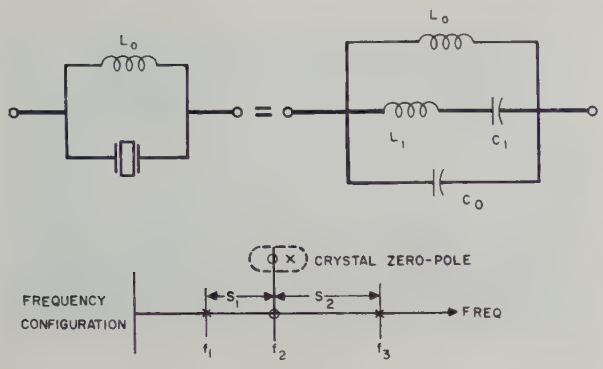

Fig. 10—Lattice-arm reactance.

synthesis techniques. On the other hand, the normalization procedure yields S_1 and S_2 directly (as functions of the filter bandwidth B).

Since f_2 is also the crystal resonant frequency, the realizability of the crystal resonator is uniquely determined by the required ratio of capacitances ($r = C_0/C_1$). If C_0 is chosen to determine the filter image impedance, or if C_1 is fixed by an available crystal unit, then the remaining element values may be determined from the ratio of capacitances and the frequency of resonance of L_0 and C_0 called f_α. That is,

$$f_\alpha \equiv \frac{1}{2\pi(L_0C_0)^{1/2}} . \tag{15}$$

A comparison of the exact and normalized (approximate) values of f_α and r, for the network of Fig. 10 is given in (16) and (17).

Exact	Approximate	
$f_\alpha = \dfrac{f_1 f_3}{f_2}$	$f_\alpha \doteq f_2 + (S_2 - S_1)$	(16)
$r = \dfrac{f_2^2}{(f_1^2 + f_3^2) - (f_\alpha^2 + f_2^2)}$	$r \doteq \dfrac{f_2^2}{4S_1S_2}$.	(17)

Approximations such as (16) and (17) may be written for an entire filter configuration. By the proper combination of these equations, conditions of filter realizability as well as the values of all network parameters may be described in terms of filter performance characteristics. Once equations are derived for a given filter configuration, complete filter design is accomplished by simply substituting the values of center frequency, bandwidth, and impedance level. Simple manipulation of these equations provides additional important information, such as the effects parameter variations have on the filter transmission characteristic. As a result, the normalization procedure is useful not only in filter synthesis, but also in practical considerations connected with filter realization, such as the specification of tolerances and the development of alignment techniques.

Applications and Typical Characteristics

Without useful application, the design of high-frequency crystal filters would be to little avail. Some of the more immediately apparent applications are explored in the following paragraphs.

Bandwidth ranges from one or two cycles to several hundred kilocycles per second represent the present-day boundaries of crystal filter technique. These ranges include the majority of channel or information bands allocated to communications and navigation equipments. The ability to produce a given bandwidth at substantially higher frequencies, together with the excellent selectivity, stability, and loss characteristics of the high-frequency crystal filter, has already resulted in many interesting applications.

Crystal filters are widely applied to intermediate frequency filtering applications in AM, SSB, and fm receivers, as well as single-sideband generators. For mobile versions of these systems, filters from 10 to 30 mc are particularly attractive, offering the advantages of small size ($\frac{1}{2}$–2 cubic inches) and freedom from microphonic behavior.

Crystal filters are employed in data handling systems utilizing pulse techniques, where uniform time delay and smooth transient response characteristics are significant. Other important applications in which the crystal filter is utilized to select a band of frequencies or an entire bank of frequency bands include fixed-channel receivers at frequencies as high as 40 mc, carrier telephone systems, telemetering systems, Doppler radar, fire control and missile systems, and spectrum analysis.

Single-Conversion Receivers

A single-conversion crystal-filter receiver, as shown in Fig. 11, offers the advantage of a high-frequency first IF (*i.e.*, good image rejection), combined with high adjacent channel selectivity (heretofore achieved only through multiple frequency conversion). At the same time, the elimination of multiple conversions reduces cross modulation and receiver desensitization due to mixer overload, and locally generated spurious signals.

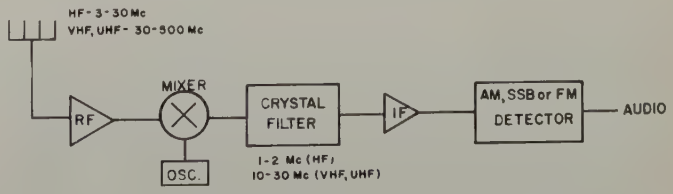

Fig. 11—Single-conversion crystal-filter receiver.

Since the frequency selection characteristics of the entire receiver are determined primarily by the crystal filter unit, it is possible to alter the receiver bandwidth and selectivity characteristics by simply changing the filter. Crystal filters designed for single conversion receivers have been produced with bandwidths ranging from 250 cps (for hf-cw telegraphy) to 50 kc (for vhf-fm or uhf-AM).

Fig. 12 illustrates the attenuation characteristics of two filters designed for single-conversion hf communica-

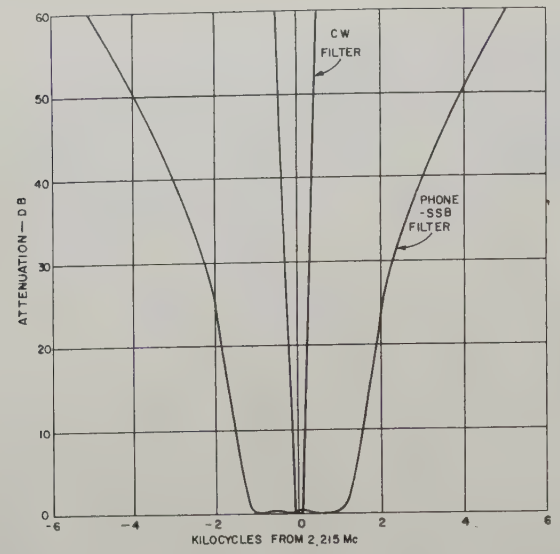

Fig. 12—Crystal filters for single conversion hf receivers.

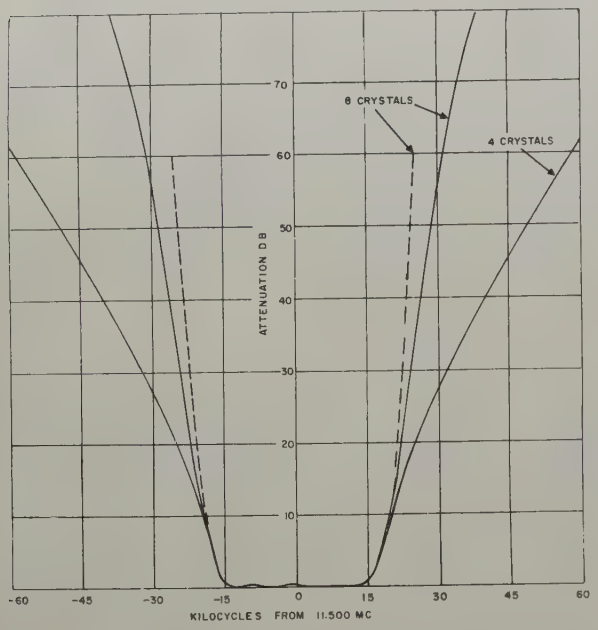

Fig. 13—Crystal filters for vhf fm receivers.

tion receivers.[14] The narrow filter has a 6-db bandwidth of 250 cps and is intended for cw telegraphy. The wider filter has a 6-db bandwidth of 2800 cps for phone-SSB reception. In both cases, the center frequency is 2.215 mc, and the shape factor (ratio of bandwidth at 60-db attenuation to bandwidth at 6-db attenuation) is slightly greater than 3:1. Pass band response variation or "ripple" is less than $\pm\frac{1}{2}$ db, while the insertion loss is less than 3 db. Each filter utilizes four crystal resonators in a hybrid configuration (Fig. 4) and is equivalent to two cascaded narrow-band lattices [Fig. 3(b)].

For vhf-fm applications, an intermediate frequency in the 10- to 15-mc range is normally chosen. Fig. 13

[14] "A selective IF amplifier for phone and cw," in "Radio Amateur's Handbook," American Radio Relay League, Inc., 34th ed., pp. 137–140; 1957.

Fig. 14—Hybrid-type crystal filters.

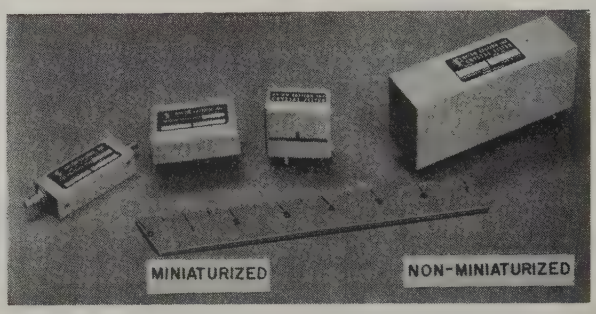

Fig. 15—High-frequency crystal filter mounting cases.

shows the attenuation characteristics of filters at 11.5 mc designed for mobile fm receivers. A comparison is made between a four-crystal filter (shape factor approximately 3.5:1) and an eight-crystal filter (shape factor approximately 1.7:1). The eight-crystal device may be made considerably more selective (*i.e.*, smaller shape factor), at the sacrifice of the final or "ultimate" attenuation reached by the filter. For example, the dotted characteristic in Fig. 13 (shape factor approximately 1.3:1) may be obtained by permitting the filter to return to an attenuation slightly greater than 60 db (see Fig. 9). The solid eight-crystal characteristic reaches an attenuation well over 80 db and represents a good compromise between final attenuation and shape factor for this application. The 6-db bandwidth for the filters shown in Fig. 13 is approximately 35 kc. For the new split-channel fm operation, filters with identical characteristics have been produced with bandwidths of 15 kc.

The filters illustrated in Fig. 13 are intermediate-band lattice networks produced in hybrid configuration. Fig. 14 shows one component arrangement for a four- and an eight-crystal filter of this type. The miniature crystal units, which occupy a volume of only 0.035 cubic inch and weigh about 1/25 of an ounce, are extremely rugged and will withstand vibration frequencies as high as 2000 cps and shock accelerations greater than 30 g.

The small size of crystal units and associated components at frequencies greater than 10 mc, makes possible extremely compact filters. Several packaging arrangements of these filters are shown in Fig. 15. The smallest of the miniaturized units ($\frac{1}{2}$ cubic inch) will accommodate a four-crystal filter. The other units may contain

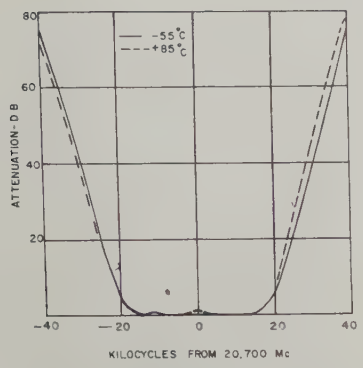

Fig. 16—Temperature performance of crystal filter.

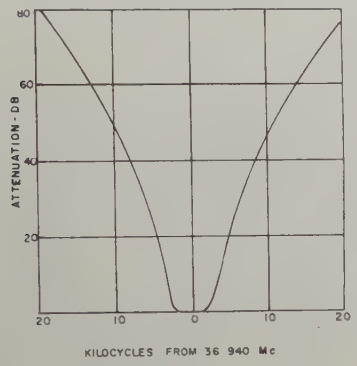

Fig. 17—Harmonic resonator filter.

up to 5 or 6 crystals, to yield characteristics lying between the 4- and 8-crystal selectivities illustrated in Fig. 13. The remaining package is nonminiaturized and accommodates the 8-crystal filter illustrated in Fig. 14.

Since the crystal filter supplies most of the selectivity of the receiver, the need for multiple-tuned interstage transformers in the IF amplifier is eliminated. Instead, the amplifier interstage networks become simple single-tuned circuits designed for maximum gain (high Q, high L/C ratio). Furthermore, as previously mentioned, the impedance level of the crystal filter may be varied over wide limits through the use of single-tuned terminating circuits.

Therefore, one filter may be employed at a high impedance level to obtain maximum gain with vacuum tube circuitry; or it may be used at lower impedance levels to obtain maximum power transfer with transistor circuitry. In either case, the same filter is used.

Fig. 16 illustrates the attenuation characteristic of a crystal filter designed for vhf-uhf AM and fm reception. The 6-db bandwidth is approximately 40 kc and the shape factor is approximately 1.7:1. The filter characteristics at −55°C and +85°C are illustrated. Even at frequencies as high as 20 mc, the extremely high stability of the crystal resonator makes possible the realization of filters which operate over wide temperature ranges with negligible degradation of performance.

At frequencies greater than approximately 30 mc, it becomes difficult to produce crystal resonators which operate in fundamental vibrational modes. At these elevated frequencies, it is common to employ crystal

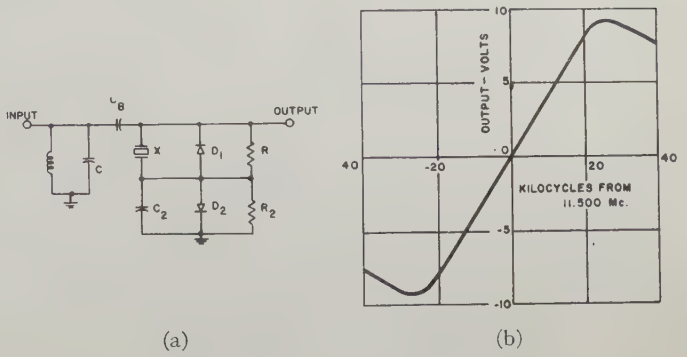

Fig. 18—Crystal discriminator.

resonators at 3rd, 5th, or 7th harmonics of their fundamental response. However, the ratio of capacitances of a harmonic resonator increases as the square of the order of the harmonic, making it difficult to obtain useful filter characteristics with such crystals. Fig. 17 shows the characteristic of a 4-crystal hybrid filter utilizing 3rd-overtone AT quartz resonators. The bandwidth of this filter is only 6 kc (0.016 per cent of center frequency).

Crystal Discriminator

In order to utilize the single conversion technique in fm receivers, it is necessary that fm detection be performed at the first IF. Since the first intermediate frequency may be too high to permit the realization of a conventional type of fm detector or discriminator, a crystal discriminator has been developed which possesses a stability comparable to that of the high-frequency crystal filter and which operates at the filter frequency. This device may be applied not only to fm receivers but also to automatic frequency control systems and frequency modulation generators.

The basic circuit diagram of the crystal discriminator is illustrated in Fig. 18(a). The voltage developed across the resonant circuit L_1–C_1 is transferred through bypass capacitor C_B, to the series crystal-capacitor circuit, X–C_2. The voltage developed across each element in this series combination is rectified by the diodes, D_1–D_2. The difference between these voltages is developed across the combination R_1–R_2, and has the form shown in Fig. 18(b). The discriminator in Fig. 18(b) is designed for use in conjunction with the filters of Fig. 13. The discriminator has a center frequency of 11.5 mc and a peak-to-peak bandwidth of approximately 50 kc. When driven from a conventional pentode limiter, which operates at a peak rf input voltage of 2 volts, the discriminator output voltage is approximately 16 volts peak-to-peak.

Single-Sideband Generators

In the generation of single-sideband signals by filtering techniques, the signal quality is largely dependent upon the ability of a filter to pass, with negligible distortion, one sideband of an amplitude modulated signal, and simultaneously to effectively eliminate the other

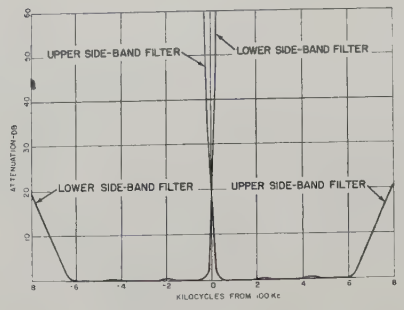

Fig. 19–Single-sideband crystal filters.

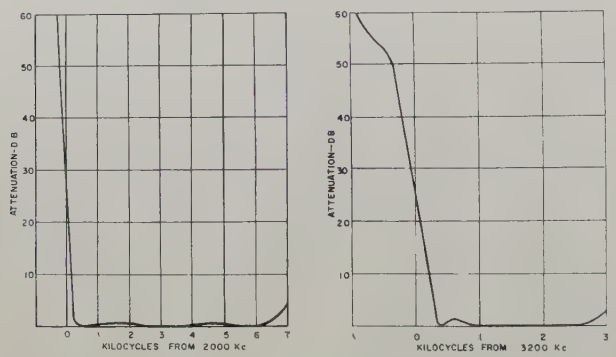

(a) (b)

Fig. 20—High-frequency SSB crystal filters.

sideband. Fig. 19 shows the attenuation characteristics of two filters designed for single-sideband generation at a frequency of 100 kc. Each filter has a bandwidth (at 2 db) of over 6 kc, and an attenuation slope which rises from 2 db to 60 db in less than 600 cps. If either filter were produced with the same steep attenuation characteristic on both sides of its pass band, the filter would have an equivalent shape factor of less than 1.2:1.

The single-sideband signal which is generated at the filter frequency is modulated onto a high frequency carrier through processes of frequency mixing or conversion, similar to those employed in the communications receiver. As was true in the receiver case, one or more frequency conversions may be eliminated by increasing the frequency of the filtering operation. To accomplish this end, crystal filters for SSB generation have been produced at frequencies as high as 16 mc.[15]

Fig. 20 (a) shows the attenuation characteristic of a single-sideband filter nearly identical with the upper-sideband filter in Fig. 19, except for a center frequency of 2 mc. The 2-mc SSB crystal filter is an intermediate-band hybrid filter.

For SSB-voice operation in the hf bands, requiring audio frequencies of 300 to 3000 cps, the attenuation characteristic shown in Fig. 20(b) is generally sufficient. This filter utilizes only 4 crystal resonators in a simple narrow-band hybrid configuration.

[15] W. E. Morrow, Jr., C. L. Mark, B. E. Nichols, and J. Leonhard, "Single-sideband techniques in uhf long-range communications," PROC. IRE, vol. 44, pp. 1854–1873; December, 1956.

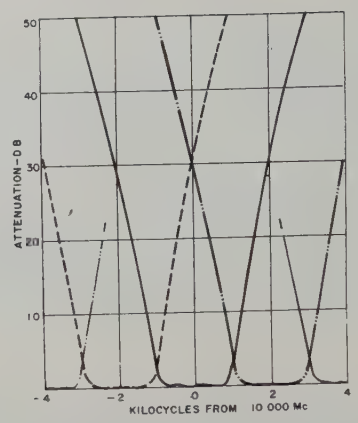

Fig. 21—"Comb" filter set.

Fixed-Channel Receivers

It is often desired to construct a receiver which operates on a fixed channel or small number of channels at some frequency below 30 mc. By producing a crystal filter at the given channel frequency and with the required bandwidth, a tuned radio frequency (trf) receiver may be constructed. This is equivalent to removing the rf, mixer, and oscillator stages from the crystal-filter receiver. (See Fig. 11.) For fixed-channel operation, the trf receiver, in addition to its simplicity, provides the maximum possible protection against adjacent channel interference. Any communications receiver may be converted to a fixed-channel receiver by inserting a crystal filter between the antenna and the first rf stage. In the presence of strong adjacent-channel interference in the hf bands, this technique materially reduces interference caused by intermodulation and desensitization.[16]

Frequency Multiplexing

Perhaps the best-known application of crystal filters is to frequency multiplexing systems, and more particularly to carrier-telephone systems.[9] Filters for this application are generally wide-band lattice filters with bandwidths of 4 kc, spaced 4 kc apart, in the range of 60–108 kc. The shape factor required is approximately 1.5:1. As illustrated in Fig. 9 and Fig. 13, it is possible to produce high-frequency as well as low-frequency crystal filters with this type of characteristic.

The close tolerances which can be maintained on the shape of a crystal filter characteristic make this device particularly well suited for frequency channelizing or "comb" filter applications. Fig. 21 illustrates part of a bank of closely-spaced filters. Each filter has a bandwidth of 2 kc in the vicinity of 10 mc, utilizes 4 crystal resonators, and occupies a volume of approximately 1 cubic inch. Filter comb sets of this type have been produced at frequencies as low as 100 kc and as high as 28 mc, for application to Doppler radar and fire control and to spectrum analysis.

[16] F. Raymond, "Reduction of Interference in the HF Range (2–32 MC) Through the Use of Bandpass Crystal Filter (Hycon Type 44)," Rome Air Dev. Center, Air Res. and Dev. Command, Tech. Memo, RADC-TM-56-33; 1957.

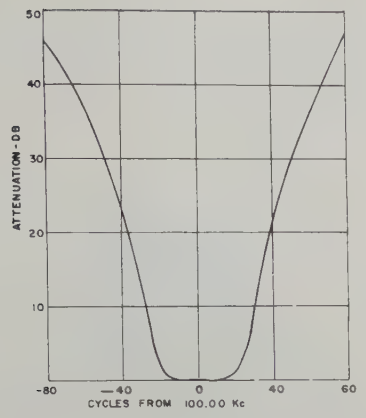

Fig. 22—Narrow-band filter for spectrum analysis.

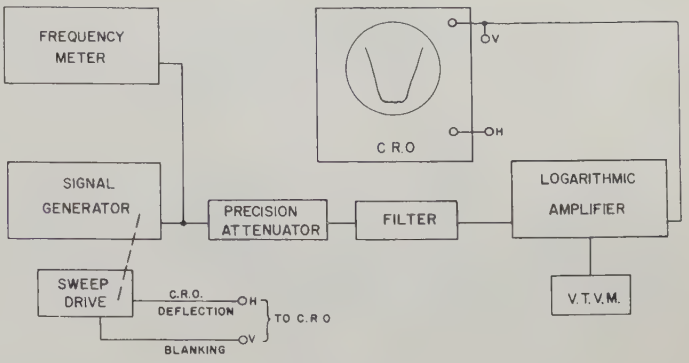

Fig. 23—Block diagram of crystal filter test facility.

In some types of spectrum analysis equipments, a single filter is made to cover an entire band of frequencies by employing the superheterodyne principle. Narrow-band crystal filters have been produced for this application with bandwidths as small as 1 cps (at a center frequency of 10 kc). Fig. 22 shows the attenuation characteristic of a 4-crystal hybrid filter at 100 kc. The bandwidth of this filter is approximately 50 cps and it has been employed in spectrum analysis equipment, in SSB equipment for carrier selection, and in channelizing equipment for pilot selection.

Measurement of Filter Characteristics

Fig. 23 is a block diagram of the test facility which is employed for the alignment and measurement of crystal filters in the range of 10 kc to 50 mc. Basically, the filter test facility provides means of accurate frequency and attenuation-level measurements while simultaneously presenting to the operator a visual display of the entire attenuation characteristic. The attenuation display is obtained with a mechanically-swept signal generator and a logarithmic amplifier. The test circuit compresses a voltage variation of 80 db into a signal suitable for presentation on any dc oscilloscope or X-Y plotter. A single amplifier, using several sets of plug-in inductors, covers the entire range of 10 kc to 50 mc.

The precision attenuator is operated at its proper impedance level at all times, providing accurate attenuation-level settings. The frequency meter provides accurate frequency measurement when the sweep is stopped at some chosen attenuation point. The dc output of the logarithmic amplifier is derived from an automatic gain control (agc) circuit which provides feedback around a 3-stage amplifier.

Because the crystal filter is a relatively narrow-band device compared to a conventional low-Q tuned circuit, it is a simple matter to tailor the frequency characteristics of the logarithmic amplifier to have negligible effect on the attenuation characteristics of the filter. A blanking voltage, derived from the sweep drive, eliminates the effect of backlash in the drive by preventing the retrace of the filter characteristic when the direction of sweep is reversed.

Before a filter is inserted into the test facility, the output of the logarithmic amplifier is observed over the entire frequency band of interest and at a number of attenuation levels. The resulting oscilloscope display, which should be a series of evenly spaced horizontal lines, is used to check the level of the signal generator output and the flatness of the logarithmic amplifier characteristic over the frequency and attenuation ranges used in testing the crystal filter.

Conclusion

Further progress in the development of quartz resonators may make possible the extension of crystal filter ranges to frequencies approaching 100 mc. Filter bandwidths in the order of 1 to 5 mc may be achieved, permitting the application of crystal filters to wide-band systems such as pulsed radar.

High-frequency crystal filters are beginning to play an important role in the battle to expand the number of usable channels of communication in our limited frequency spectrum. The device provides a new standard of stability and selectivity. Crystal filter units are now being produced in quantity to operate at frequencies where full advantage may be derived from their unique characteristics.

Experimental 8-MM Klystron Power Amplifiers*

T. J. BRIDGES†, MEMBER, IRE, AND H. J. CURNOW‡

Summary—Experimental klystron amplifiers, which were used to investigate the cw power obtainable at a wavelength of 8 mm, are described. Working at 5000 volts with a beam current of 0.2 a, these tubes produced an output power of 75 watts cw. Operation was limited by the maximum current density of 1.5 a/cm² which could be drawn from sprayed-oxide cathodes.

Introduction

A RECENT paper[1] described a klystron oscillator of the floating-drift-tube type with a cw output of 12 watts in the 8-mm wavelength band, and a life in excess of 1000 hours. It was considered that the major limitation to the output power was the cathode emission which could be obtained. At the time the only cathode available was the standard oxide-coated type and even employing special techniques, such as a 700°C bake out, the maximum emission density which could be drawn with useful life was 0.6 a/cm². However, cathodes with superior emission capabilities are now becoming available. If these were combined with the techniques referred to, a substantial increase in the output power might be possible.

To investigate this possibility, work has been carried out on klystron power amplifiers at 8-mm wavelength. The object was to discover whether the output could be increased significantly before overheating or other limitations became prohibitive. Conventional sprayed-oxide cathodes were used in these experiments since they were readily available and it was found that current densities up to 1.5 a/cm² could be drawn from them for short periods. The same electron gun as in the oscillators was used and the dc input power was increased by raising the applied voltage. As the efficiency of a klystron increases with the applied voltage and the dc input power is proportional to the 5/2 power of the voltage, it was expected that the output power would increase very rapidly as the voltage was raised. Because a floating-drift-tube oscillator is limited to a number of discrete, narrow bands of operating voltage, the tubes were constructed so that they could be used either as amplifiers or as oscillators with a phase-shifting network in the feedback loop. They were then capable of working over a wide, continuous range of voltage, and thus of dc input power.

Description of the Tubes

The general arrangement of the tubes used in the experiments is shown in Fig. 1, while details of the resonant cavities may be seen in Fig. 2. The cavities were of the doubly re-entrant type, and the gap dimensions were such that at an operating voltage of 5000 volts the gap transit angle was 2 radians and the normalized tunnel diameter 2.8 radians. The ends of the cavity cones had different diameters to avoid multipactor effects and to shield the thin cone tips from beam interception.

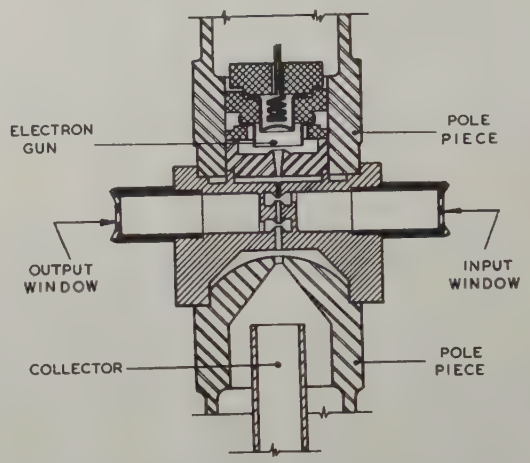

Fig. 1—General arrangement of 8-mm klystron amplifier.

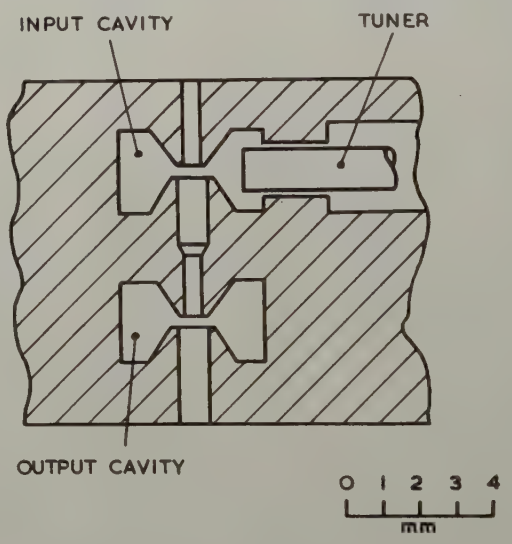

Fig. 2—Details of the resonant cavities.

The drift length between the cavities was 0.15 inch, which was about 0.16 of the effective plasma wavelength for the electron beam used. A value less than the optimum 0.25-plasma wavelength was chosen in order to reduce the length over which the focusing magnetic field had to be maintained.

The method of construction of the tubes was similar to that of the oscillators.[1] There were of course, some extra features made necessary by the different cavity arrangement. With separate cavities some means had to

* Original manuscript received by the IRE, September 18, 1957.
† Bell Telephone Labs., Inc., Murray Hill, N. J.
‡ Services Electronics Res. Lab., Baldock, Hertfordshire, Eng.
[1] R. L. Bell and M. Hillier, "An 8-mm klystron power oscillator," PROC. IRE, vol. 44, pp. 1155–1159; September, 1956.

be provided of aligning them to the same resonant frequency. The cavities were approximately tuned by adjusting the lengths of the gaps during construction. Final adjustment was made during operation by tuning the input cavity. The resonant frequency of this could be varied over a 1 per cent range by means of a fine-tuning device, which consisted of a 1-mm-diameter copper wire, shown in Fig. 2, protruding through a hole in the wall of the cavity and supported by a flexible diaphragm (not shown). Each of the cavities was coupled to a separate waveguide, the coupling being arranged to be a nominal match in the absence of the electron beam. For ease of construction the waveguides inside the tubes were circular (TE_{11} mode) and simple glass windows were used. Specially designed transitions at the windows enabled a good match to be obtained directly to standard rectangular waveguide. The windows of high-melting-point aluminosilicate glass could pass a mean power of 50 watts before forced cooling became necessary.

The electron optical system was identical with that used in the oscillators, apart from the length of the tunnel. The gun had a perveance of about 0.5×10^{-6} a/volt$^{3/2}$, and the current density multiplication was 100 times. A transmission efficiency of 75–80 per cent was obtained through a 0.023-inch diameter tunnel, 0.3 inch in length. The increased magnetic field required for focussing at elevated voltages was obtained with an electromagnet.

Experimental Results

It was found that in tubes which had been baked out at 700°C, ordinary sprayed-oxide cathodes could be used at emission densities up to 1.5 a/cm^2. The exact conditions needed to achieve this performance were not determined, and the results varied from one cathode to another. When this emission density could be obtained it was possible to operate a tube quite consistently at 5000 volts and a beam current of 0.2 a for periods of a few hours. These conditions corresponded to a power density in the beam of 500 kw/cm^2.

The construction of the tubes was such that the gun could easily be replaced and satisfactory operation at 5000 volts was eventually achieved with each of four structures, with identical cavity arrangements. The low-signal gain under these conditions was 8 db. As this was so small there was no signal source available which could be used to drive the tubes to their full output. They were accordingly operated as oscillators, with an external waveguide feedback loop (see Fig. 3). The attenuation of the loop was set at about 4.5 db by the inclusion of a ring hybrid and by the loss in the waveguide components. The output power was measured with a calorimeter through a directional coupler. The phase of the feedback was adjusted with a phase shifter for optimum output. Matching stubs (not shown) were used to compensate for the mismatch caused by the presence of the electron beam across the gaps.

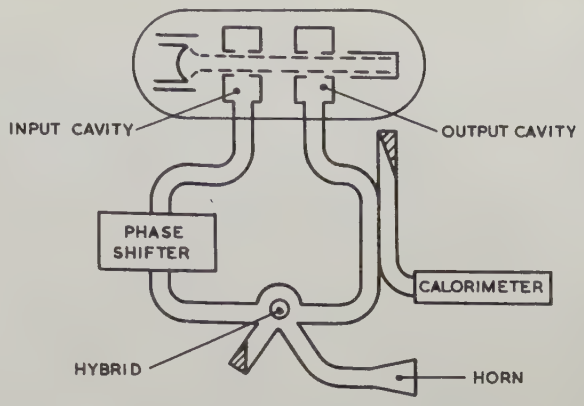

Fig. 3—Feedback loop.

Operating under the conditions described the average output power of the four tubes was 75 watts cw, corresponding to an efficiency of 7.5 per cent.

The limit to the current which could be drawn from a cathode was set by a deterioration in the transmission efficiency, causing unacceptably high dissipation on the rf structure. This was revealed by detuning the cavities, rather than by catastrophic heating effects. With better cathodes higher emission densities should be obtained before this defocusing effect occurs and the input power could then be raised even further.

Comparison with Theory

In order to determine whether the output obtained was a fair test of the potentialities of the tubes, a comparison was made with a theoretical estimate of the power to be expected. The efficiency can be expressed in terms of the low-signal gain, the bunching angle, and the maximum rf current which can be induced in the electron stream. The low-signal gain depends on various parameters of the tube from which it can be calculated; it can also be measured directly. The maximum rf current which can be induced in an electron stream has been calculated from the theory of the bunching process. The simple theory of Webster[2] predicts that this will have an amplitude 1.16 times the beam current. A more elaborate analysis[3] suggests that the value should be rather less than this, but for the values of the parameters for these tubes the efficiency so calculated is only slightly less.

In order to work out what low-signal gain might be expected, it was necessary to know the values of the cavity resonant conductance, and the effective gap-coupling and gap-loading coefficients. These were obtained from perturbation measurements on a scaled-up model of the cavity, and from Q-factor measurements on the actual cavities. From the perturbation measurements the ratio R/Q for the cavity was found to be 120.

[2] D. L. Webster, "Cathode ray bunching," *J. Appl. Phys.*, vol. 10, pp. 501–508; July, 1939.
[3] M. Chodorow, E. L. Ginzton, and E. J. Nalos, "Debunching of electron beams constrained by strong magnetic fields," Proc. IRE, vol. 41, pp. 999–1003; August, 1953.

Q-factor measurements on the cavities used in the tubes showed that the loaded Q was 750. The cold-loaded conductance was therefore 1.11×10^{-5} mhos. The gap-coupling and gap-loading coefficients were also calculated from the shape of the gap field given by the perturbation measurements. This was preferred to calculations based on assumed field shapes, as the gap dimensions were rather larger than those for which the common assumptions are valid. The values obtained were a mean-square coupling coefficient of 0.3 and a gap-loading conductance of 0.75×10^{-5} mhos. Allowing for the effects of space-charge debunching and the mismatch introduced by the gap-loading, the low-signal gain was calculated to be 11.2 db. The experimentally observed value (8 db) was less than this. The most probable cause for this departure from theory lies in the nature of the electron stream, which certainly was not the uniform beam filling the drift tube assumed in the calculations. The effect of a smaller beam diameter would be to reduce the coupling coefficient and to increase the effect of space-charge debunching. If the observed value of the gain is used, together with the assumption of a maximum rf current 1.16 times the beam current, then the expected efficiency is 7.8 per cent, in good agreement with the observed value. Thus it may be concluded that the observed output was that which could be expected from the tubes, and no large advantage was being lost through the lack of a powerful driving source.

Conclusion

The work carried out on these klystrons has shown that it is possible to obtain cw powers of at least 75 watts in the 8-mm wavelength band. A necessary condition for this is that the cathode must be capable of giving an emission density of 1.5 a/cm^2 in an electron gun with a density multiplication of 100 times. Although the power density in the beam was 500 kw/cm^2, the limit was not set by thermal considerations, but by cathode performance.

The actual tubes used in this investigation would be of little practical use as the life was short and the gain low. In order to produce a useful tube giving this order of output power, it would be necessary to incorporate a cathode of improved performance and to increase the gain by adding extra cavities. Neither of these operations should present any major difficulties.

Acknowledgment

This paper is published by permission of the British Admiralty.

FM Demodulator Time-Constant Requirements for Interference Rejection*

ELIE J. BAGHDADY†, MEMBER, IRE

Summary—**Under conditions of high-level interference fm receiver performance is often impaired because of improper low-frequency time constants in the limiter and discriminator circuits. The computation of the upper bounds on the permissible values of these time constants is illustrated. Severe restrictions are indicated which often conflict with other fundamental requirements. The computational results of this paper demonstrate that these severe restrictions can be alleviated by means of simple schemes that will greatly enhance the capture performance of the fm receiver.**

I. Introduction

A BASIC requirement in fm receiver design for suppressing multipath and cochannel disturbances is the use of the proper time constants in the low-frequency parts of the limiter and discriminator circuits. The presence of an undesired signal, which is weaker than the desired one, within the linear pass band of the receiver causes the resultant signal delivered to the first limiter to exhibit severe AM and fm disturbances under conditions of high-level interference. For proper amplitude-limiting operation, the limiter circuit must be capable of following the sharp changes in the envelope of the resultant impressed signal, which may recur at a rate (in cps) equivalent to the bandwidth of the IF amplifier. In the discriminator the output circuit across which the rectified voltage is taken must be capable of following the detected instantaneous-frequency disturbance pattern. This performance is necessary in order to avert diagonal clipping and leave the variational control of the operation of the rectifying diodes entirely in the hands of the envelope of the signal delivered by the fm-to-AM-conversion section of the discriminator. Here, also, the sharp changes in the detected fm disturbance waveform may recur at a maximum rate (in cps) of one IF bandwidth. In order to insure proper

* Original manuscript received by the IRE, May 16, 1957; revised manuscript received, November 8, 1957. This work was supported in part by the U. S. Army (Signal Corps), the U. S. Air Force (Office of Sci. Res., Air Res. and Devel. Command), and the U. S. Navy (Office of Naval Res.).

† Dept. Elec. Eng. and Res. Lab. Electronics, Mass. Inst. Tech., Cambridge, Mass.

operation, it is necessary, therefore, to determine the upper bounds on the time constant of the output circuit.

After discussing briefly the properties of the disturbances caused by the interference, and of the effect of narrow-band limiting upon the fm disturbance, we shall demonstrate how certain well-known principles can be applied to the determination of the upper bounds on the limiter and discriminator time constants. These upper bounds will be quite stringent if the requirements of high-capture performance are to be met, particularly because they may conflict with other fundamental requirements. To alleviate these restrictions, the disturbances must be suppressed (or minimized) before they reach the appropriate low-frequency circuits. It is believed that, more often than not, the impairment of proper performance of most available fm receivers can be traced to improper time constants in the limiters, or discriminators—particularly in the discriminators. The present study should suggest some remedies for these difficulties.

II. Disturbances Caused by High-Level Interference

Consider the situation in which two carriers of constant relative amplitudes 1 and a ($a<1$) and of frequencies p and $p+r$ rad/second ($r \ll p$) are passed simultaneously by the IF amplifier of an fm receiver. The AM and fm disturbances caused by the superposition of two such carriers have been extensively discussed in published work.[1,2] The aspects of these disturbances that are of interest in the present discussion will now be summarized.

The signals are assumed to be unmodulated in amplitude and frequency or, at worst, to have frequency modulations that are so slow, relative to the frequency difference r, that the signal frequencies are not appreciably changed during a period of $2\pi/r$ seconds. It will become evident presently that the severity of the interference increases with the increase in the frequency difference r, and is greatest, therefore, when r assumes its largest possible value of one IF bandwidth (assuming, for simplicity, that this bandwidth is well defined). Thus, the assumption that r is much higher than the highest modulating frequency (if any) corresponds to the situation in which the interference causes the most troublesome amplitude and frequency disturbances. This is the situation of greatest interest in the determination of the design requirements on the limiter and discriminator circuits to insure their proper operation under all possible conditions of two-signal interference.

At the input of the first amplitude limiter the resultant signal will be

$$\begin{aligned} e_{if}(t) &= \cos pt + a \cos (p+r)t \\ &= A(t) \cos [pt + \theta(t)] \end{aligned} \tag{1}$$

if time is counted from the instant at which the two signal phasors are in phase. In this expression

$$A(t) = \sqrt{1 + 2a \cos rt + a^2} \tag{2}$$

and

$$\theta(t) = \tan^{-1} \frac{a \sin rt}{1 + a \cos rt} . \tag{3}$$

The instantaneous frequency of the resultant signal is $\omega_i(t) = p + d\theta/dt$. The presence of the weaker signal within the IF pass band causes the fm demodulator (limiter-discriminator combination) to see a resultant signal whose instantaneous frequency differs from the frequency of the stronger signal by $d\theta/dt$. Therefore, $d\theta/dt$ is the fm disturbance, while $A(t)$ contains the AM disturbance. Plots of $A(t)$ and of $d\theta/dt$ are shown in Fig. 1 and Fig. 2 (next page).

It is important to observe that the average value of $d\theta/dt$ over a period of $2\pi/r$ seconds is zero. In essence, the most important step toward achieving satisfactory capture of the stronger signal is to make the instantaneous-frequency deviation of the resultant signal from the desired frequency p average out to zero over one period of the frequency difference r, at every point in the receiver before the fm-to-AM conversion and detection process.[3,4] The outcome of this process must then be a detected disturbance waveform that is superimposed upon the output voltage which corresponds to the frequency p and contributes a zero average deviation from this desired voltage. If r is beyond the audible range, then the preceding requirements are necessary and sufficient, since no disturbance will be passed by the de-emphasis and audio filters. If, however, r is audible, then these requirements (though necessary) will not insure complete rejection of the interference but the disturbance that gets through can be greatly reduced, if not effectively eliminated.

Two important schemes for improving the capture performance of an fm receiver will be briefly described. For the simpler scheme,[3,4] it has been shown that limiters with bandwidths of the order of the IF bandwidth will introduce significant reductions in the effectiveness of high-level interference. The reductions result from the fact that the filter sluggishness to the violent fm disturbance can cause deformation of this disturbance into milder waveforms that maintain a zero average over a frequency-difference cycle. An extremely effective scheme for suppressing the disturbance of the weaker of two fm signals can be achieved, therefore, by cascading

[1] M. S. Corrington, "Frequency-modulation distortion caused by multipath transmission," Proc. IRE, vol. 33, pp. 878–891; December, 1945.

[2] M. S. Corrington, "Frequency-modulation distortion caused by common- and adjacent-channel interference," *RCA Rev.*, vol. 7, pp. 522–560; December, 1946.

[3] E. J. Baghdady, "Frequency-modulation interference rejection with narrow-band limiters," Proc. IRE, vol. 43, pp. 51–61; January, 1955.

[4] E. J. Baghdady, "Interference Rejection in FM Receivers," Res. Lab. Electronics, M.I.T., Cambridge, Mass., Tech. Rep. 252; September 24, 1956.

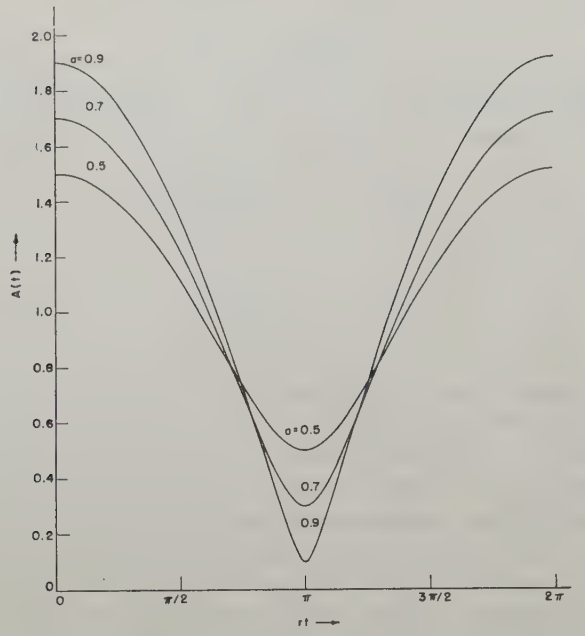

Fig. 1—Instantaneous envelope variations of the resultant of two sinusoids of relative amplitudes 1 and a, whose frequencies differ by r rad/second.

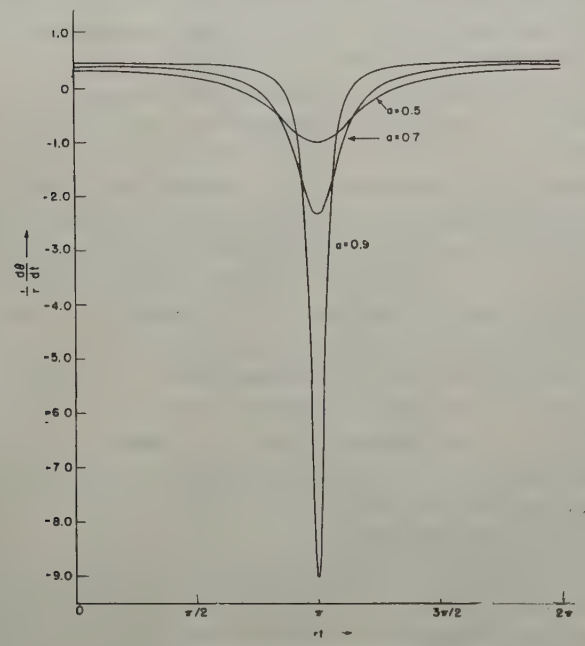

Fig. 2—Instantaneous-frequency disturbance caused by the superposition of two sinusoids of relative amplitudes 1 and a. The frequency of the stronger sinusoid is p rad/second; the frequency of the weaker sinusoid is $p+r$ rad/second.

several stages of amplitude limiting, each of which is followed by a band-pass filter of appropriate bandwidth. With such a scheme interference is effectively suppressed, by any desired amount, ahead of the discriminator rather than after it, and requirements on the performance of a satisfactory discriminator are greatly relaxed. This has been demonstrated with conventional circuits.

The mechanism by which the cascading scheme suppresses interference is based on the fact that the first amplitude limiter spreads out the significant spectrum (which is necessary for the reproduction of the fm disturbance) over a frequency range that exceeds many times the bandwidth of the IF amplifier. The more severe the interference, the greater will be the spread of the spectrum through amplitude limiting; it will be of the order of 100 times the bandwidth of the IF amplifier if the signal strengths differ by 10 per cent of the amplitude of the stronger signal.

It follows that sizeable portions of the interference spectrum can be excluded without substantially affecting the spectrum that carries the message modulation by filtering after amplitude limiting. After one stage of limiting and filtering, a significant amount of interference will pass in a spectrum that cannot be eliminated without impairing the desired signal. Successive limiters will again spread out the interference spectrum which can be reduced further by additional filtering. As more limiter-filter units are added in cascade, more of the energy of the interference spectrum is drained off until the remaining energy is negligible. Beyond this point, the cascading of more stages of limiting and filtering is not economically justifiable.

The practical importance of the cascading scheme is enhanced significantly by the fact that the near elimination of the high-level interference (caused by undesired signals that are either delayed replicas of the desired signal, or are caused by other stations or by impulse radiation such as that from ignition systems) can be achieved with from 3 to 6 properly designed narrow-band limiters.

The greatest achievable reduction in the effective interference ratio in one stage of narrow-band limiting[5] can reduce a to $(1/2)a$, when $a>0.5$. The performance of one stage of ideal narrow-band limiting with only one IF bandwidth is indicated in Fig. 3. In this plot a_{out} is the output ratio of weaker-to-stronger signal amplitude (or interference ratio) and a_{in} is the corresponding input ratio. The analysis leading to this plot assumes that $r>1/2(\mathrm{BW})_{if}$, and the plot only applies when $a<0.84$. It turns out, however, that this performance can be improved by various methods. One relatively simple method (which has been tested in the laboratory) is to apply positive feedback through a bandwidth of the order of the IF bandwidth from the output of the limiter to its input.[6] Under the more serious conditions of interference, this scheme results in pronounced improvement in the capture performance of the receiver. The positive feedback will increase the amplitudes of both signal and interference at the input of the limiter, but it will add more to the stronger signal than to the weaker signal. In this way, the predominance of the stronger signal is improved at the input of the limiter, and further improvement is effected by narrow-band limiting

[5] E. J. Baghdady, "Theory of stronger-signal capture in fm reception," (submitted for publication); March 15, 1957.
[6] E. J. Baghdady, "Theory of feedback around the limiter," 1957 IRE National Convention Record, Pt. 8, pp. 176–202.

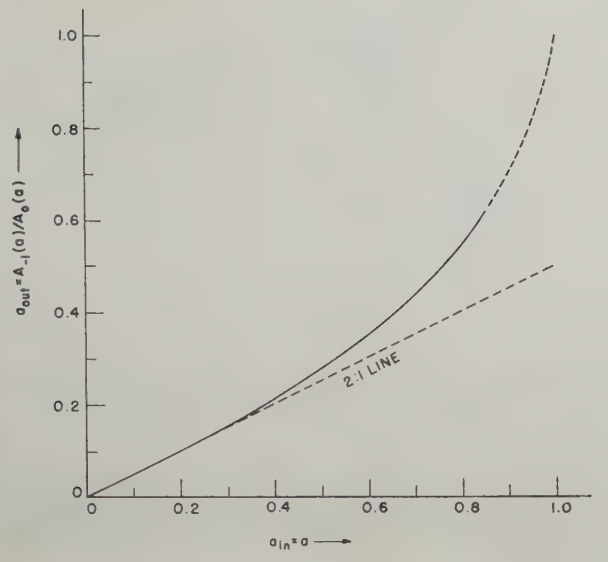

Fig. 3—Variation of the interference ratio at the output of one narrow-band limiter, whose bandwidth equals $(BW)_{if}$, with the interference ratio at the input, when the frequency difference $r=(BW)_{if}$.

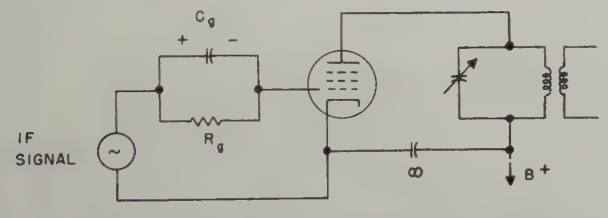

Fig. 4—Grid-circuit limiter for time-constant computation.

in the same limiter stage. The over-all improvement in one stage with band-limited positive feedback can be made equivalent to the improvement that would result from several stages that do not use feedback.

Positive feedback that causes a self-sustained oscillation in the absence of an input signal will not only cause pronounced improvement in capture performance, but it will also bring about effective interstation noise squelch, improved amplitude-limiting performance, and significant relaxation in the limiter time-constant requirements.

III. Limiter Time-Constant Requirements

Perhaps, the only important limiter circuit that presents a time-constant problem, at present, is the grid-bias pentode limiter circuit shown in Fig. 4. It will suffice, for our purposes, to recall[7] that the operation of this limiter depends upon the control by the instantaneous amplitude of the input signal of an automatic self-rectified grid bias. This, in turn, controls the conduction angle and the height of the plate-current pulses, increasing the height and decreasing the angle with increasing signal amplitude so that the net charge delivered by each pulse to the plate-tank capacitor is kept approximately constant.

[7] L. B. Arguimbau, "Vacuum-Tube Circuits," John Wiley & Sons, Inc., New York, N.Y.; 1948.

The mechanism of the operation in the grid circuit of the grid-bias limiter lends itself to a treatment that is very similar to the usual analysis of the simple diode peak detector. In our problem there are three time-constant considerations that must be taken into account if this circuit is to be used in a receiver designed to handle a specified interference ratio a.

1) The product R_gC_g must be sufficiently small to enable the circuit to follow the amplitude variations of a resultant two-carrier signal, and thus keep the dynamic self-bias under the exclusive control of these amplitude variations.

2) C_g must be sufficiently large to bypass R_g at radio frequencies and offer an impedance at radio frequencies which is much lower than the input impedance of the tube in order for the IF voltage to appear effectively between the grid and the cathode of the tube when the grid potential is on the negative swing. If ω_0 is the intermediate frequency and C_{in} is the input capacitance of the stage, the present requirements can be summarized as $C_gR_g \gg 1/\omega_0$ and $C_g \gg C_{in}$.

3) R_g must be sufficiently large for the development of the necessary bias on the grid for effective smoothing of the envelope of the input wave. If the grid-to-cathode conduction resistance is r_g, then we want $R_g \gg r_g$.

Requirement 1) can be translated into an explicit condition on R_gC_g. Let $A(t)$ denote the instantaneous amplitude of the resultant signal impressed at the input of the grid circuit. We recognize that the magnitude of the rate at which the capacitor tends to charge (or discharge) at any instant of time must be greater than (or, at worst, equal to) the magnitude of the rate at which $A(t)$ is increasing (or decreasing), in order for the self-rectified bias on the grid to follow the amplitude variations of the input signal. For example, if $A'(t)$ is positive, the charging rate at time t must be

$$\frac{A(t)}{R_gC_g} \geq A'(t).$$

Therefore the desired condition on the RC time constant of the grid circuit can be written

$$R_gC_g \leq \left|\frac{A(t)}{A'(t)}\right|.$$

The quantity on the right-hand side will vary with time. Therefore if the most unfavorable situation is to be met, the condition should read

$$R_gC_g \leq \left|\frac{A(t)}{A'(t)}\right|_{\min}. \tag{4}$$

Under two-signal interference conditions, $A(t)$ is given by (2). With substitution in condition (4) and evaluation of the indicated minimum, we obtain

$$R_gC_g \leq \frac{1-a^2}{ar}.$$

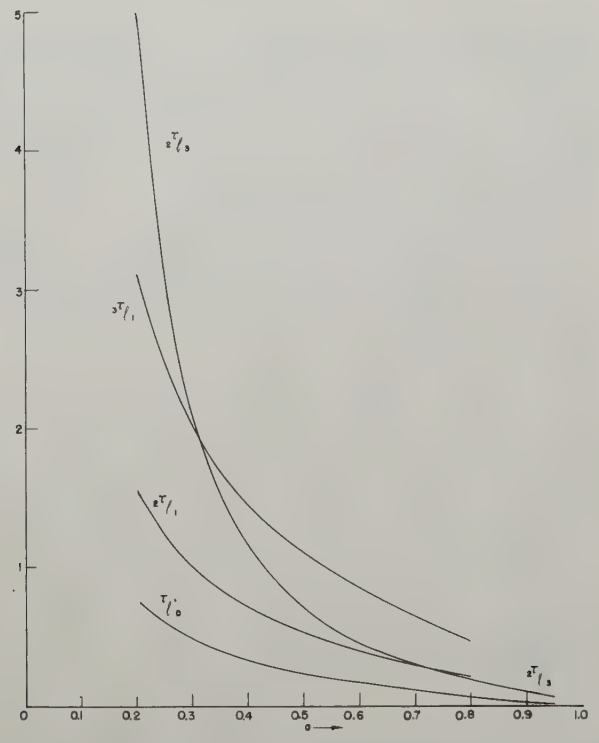

Fig. 5—Variation of the maximum permissible values of the grid-circuit time constant with the interference ratio a.

The frequency difference r can have a maximum value, $r_{max}=2\pi W_{if}$, where W_{if} denotes the IF bandwidth in cps. Therefore, under the worst interference conditions, we must have

$$\tau_{l0} = W_{if}R_gC_g \leq \frac{1-a^2}{2\pi a}. \tag{5}$$

The maximum permissible value of τ_{l0}, as given by the equality sign in (5), is shown in Fig. 5 plotted against a. Multiplication by a scale factor appropriate to the value of W_{if} will convert the normalized values of time constant to microseconds.

For conditions at the input of the second-limiter stage, which immediately follows the filter of the first limiter, the problem is greatly simplified if the filter is assumed to have idealized amplitude and phase characteristics. Thus, if we consider the filter in the plate circuit of the first grid-bias pentode limiter as an ideal filter, then the input signal of the next stage is described in terms of the worst configuration of sideband components that this filter will pass. The amplitude of the resultant of these components will not be constant since, in general, not all of the components with significant amplitudes at the output of the first limiter will be passed. The spectrum of the amplitude-limited resultant of the two input signals is given by

$$e(t) = \cos\left[pt + \theta(t)\right] = \sum_{n=-\infty}^{\infty} A_n(a)\cos(p-nr)t. \tag{6}$$

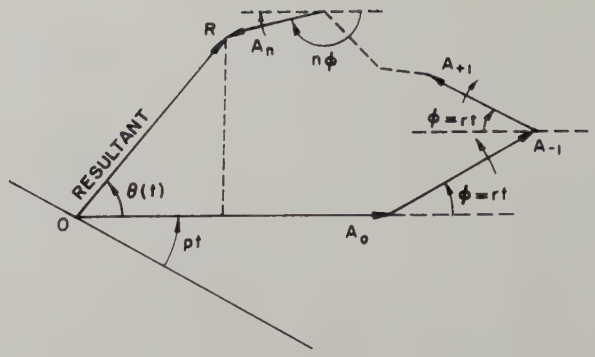

Fig. 6—Linear superposition of phasors representing the spectral components passed by the ideal-limiter filter.

This spectrum has been computed by Granlund,[8] who presented ten-place tables of $A_n(a)$. A detailed study of the properties of this spectrum has been undertaken by the author.[3,4]

If the bandwidth of the first-limiter filter is assumed to equal one IF bandwidth (as is permissible for all $a \leq 0.863$), then we know that the configuration A_0, A_{-1} will be the worst possible spectrum for all a's up to approximately 0.84, and thus, for all such cases, condition (5) is directly applicable with a replaced by A_{-1}/A_0. Fig. 3 is a plot of $A_{-1}/A_0=a_{out}$ against $a=a_{in}$. Since $(A_{-1}/A_0)<a$, it is recognized that the highest permissible value of the time constant R_gC_g is larger at the input of the second limiter than it was at the input of the first—a decided improvement in the design conditions. The extent to which improvement has been achieved is readily seen from the curve for ${}_2\tau_{l1}$, as shown in Fig. 5. Conditions at the input of the third-limiter stage are similarly computed if the second stage is assumed to be identical with the first one, and so on. Fig. 5 also shows a curve for ${}_3\tau_{l1}$ which applies to the time constant at the input of the third limiter.

When the ideal filter that follows the first limiter has three times the IF bandwidth, values of a up to 0.9807 can be considered. In the critical spectrum for this bandwidth the components whose amplitudes are given by $A_1(a)$, $A_0(a)$, $A_{-1}(a)$, and $A_{-2}(a)$ are passed. These have frequencies of $p-r$, p, $p+r$, and $p+2r$ rad/second.

With reference to Fig. 6, we note that if the idealized limiter filter passes a spectrum made up of M lower sideband components and N upper sideband components, then the square of the amplitude of the resultant signal is

$$A^2(t) = \left[\sum_{n=-N}^{M} A_n\cos n\phi\right]^2 + \left[\sum_{n=-N}^{M} A_n\sin n\phi\right]^2$$

where $\phi=rt$. When the first-limiter bandwidth is three times the IF bandwidth, the most unfavorable situation arises when $M=1$, $N=2$, and $r=2\pi W_{if}$. In this case, the value of ϕ that gives a minimum is a root of a fifth-degree equation in $\cos\phi$. The resultant maximum

[8] J. Granlund, "Interference in Frequency-Modulation Reception," Res. Lab. Electronics, M.I.T., Cambridge, Mass., Tech. Rep. 42; January 20, 1949.

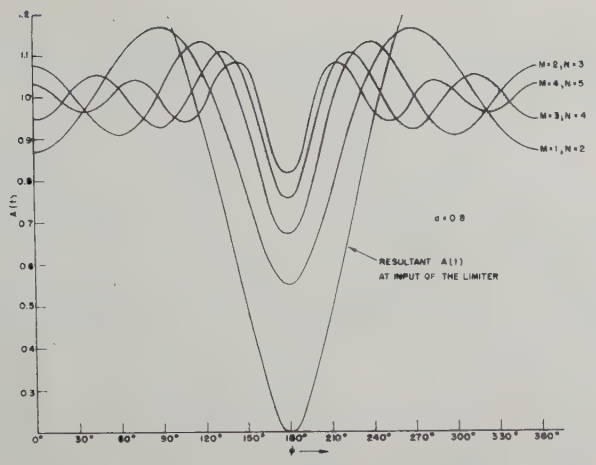

Fig. 7—Variations in the instantaneous amplitude of the resultant signal at the output of a narrow-band limiter compared with the corresponding variations at the input of the limiter.

permissible values of ${}_2\tau_{i3} \equiv W_{i1} R_g C_g$ (in the grid circuit of the second limiter when the first-limiter bandwidth is three times the IF bandwidth) are plotted in Fig. 5 for comparison with the other normalized time-constant curves.

With larger values of first-limiter bandwidth, the variations in the amplitude of the most troublesome signal delivered to the second limiter become less and less severe, and the upper bound on the permissible $R_g C_g$ product at the input of the second stage becomes higher and higher. The appearance of $A(t)$ for various spectral configurations is illustrated in Fig. 7.

We may now conclude that although the action of a narrow-band limiter upon the character of the resultant signal effects only a partial reduction in the severity of the amplitude variations of the signal (instead of a complete smoothing-out process), the partial abatement of the amplitude variation is sufficient, nevertheless, to show a significant increase in the upper bound on the permissible grid-circuit time constant. Eventually, with a sufficient number of cascaded narrow-band limiters, the resultant signal amplitude is smoothed out to an essentially constant value, and the upper bound on the RC product in the later stages is sufficiently high to be of no importance in the design of these stages. As for the first stage, the time-constant requirements are best relieved either by the application of regenerative feedback,[6] or by the use of a limiter whose operation does not depend upon a low-frequency time constant.

IV. Discriminator Time-Constant Requirements

The time-constant requirements of two commonly encountered discriminator low-frequency output circuits will be discussed in the order of their simplicity. The low-frequency output circuit of many discriminators can be reduced to the forms shown in Fig. 8 and Fig. 9. In Fig. 8, the detected voltage, which ideally is proportional to the instantaneous-frequency variations of the signal at the discriminator input, appears across

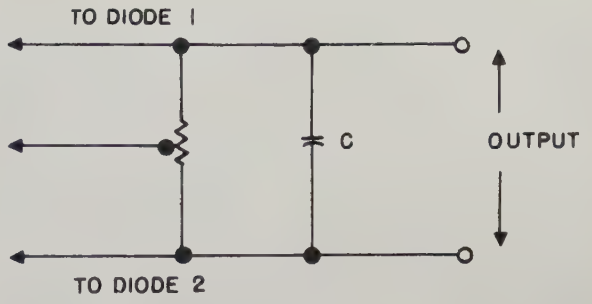

Fig. 8—Discriminator-output circuit for time-constant computation.

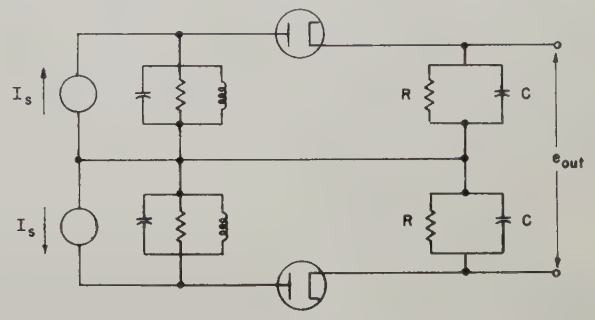

Fig. 9—Common form of balanced discriminator.

the equivalent RC combination. In some circuits this RC combination is a reduced form of a slightly more elaborate connection, in others C is the capacitor across which the output voltage of the discriminator is taken, and R either appears explicitly or consists essentially of a low equivalent output resistance that is associated with the rest of the discriminator circuit.

Let us first consider the situation in which the discriminator is either amplitude insensitive, and hence not preceded by any limiters, or amplitude sensitive but preceded by an "infinitely" wide-band ideal limiter. Assume that the discriminator has a linear over-all detection characteristic of unit slope over the whole range of the instantaneous-frequency variations of the input signal. Then, under the two-carrier interference conditions described in Section II, the voltage waveform that the output RC combination must handle is given by $E_0(p) + d\theta/dt$, where $E_0(p)$ is a direct-voltage level that is dictated by the frequency p of the stronger signal, and $\theta(t)$ is defined in (3). Since $d\theta/dt$ averages out to zero over $2\pi/r$ seconds, $E_0(p)$ is the only direct-voltage term that should appear at the output, inasmuch as the slow variation in this level will deliver the message of the stronger signal. If the frequency difference r lies outside the range of the desired message spectrum, subsequent de-emphasis and audio (or video) filtering will yield $E_0(p)$ with no distortion from the interference.

However, failure of the voltage across the capacitor to follow the voltage variations dictated by the instantaneous frequency of the signal at the discriminator input will cause the output low-frequency voltage to have an average value (over one frequency-difference cycle) that does not correspond to the value dictated by the frequency of the stronger signal. If the average value of

the output-capacitor voltage (over a period of $2\pi/r$ seconds) is to be maintained at the value dictated by the frequency p, the capacitor must, at every instant of time, tend to charge or discharge at a rate that is faster than (or, at worst, just as fast as) the rate at which the impressed waveform tends to change at that instant. Equivalently, the ratio of the instantaneous value of the capacitor voltage to the RC product must always exceed or, at worst, equal the time derivative of the impressed voltage evaluated at the same instant of time. This will enable the capacitor voltage to keep in step with the dictates of the instantaneous frequency of the resultant input signal, and thus ensure proper detector operation and lack of harmful diagonal clipping effects. Analogous with the problem of the limiter time constant, the restriction to be imposed on the RC product is, from condition (4),

$$RC \leq \left| \frac{e(t)}{e'(t)} \right|_{\min}, \qquad e'(t) \equiv \frac{d}{dt} e(t), \tag{7}$$

where $e(t)$ is the total capacitor voltage. Evidently, $e(t)$ cannot go to zero (unless $e'(t)$ vanishes simultaneously with it). Under the aforementioned conditions,

$$e(t) = E_0(p) + \frac{1}{2} r \left[1 - \frac{1 - a^2}{1 + 2a \cos rt + a^2} \right], \tag{8}$$

where we must require that

$$E_0(p) > \frac{ar}{1 - a}. \tag{9}$$

Since $E_0(p)$ is the voltage level that corresponds to the frequency p, and p is likely to lie on either side of the center frequency of the IF pass band, it is evident that condition (7) will define a nonzero upper bound on the RC product only if the discriminator output, as seen across the RC combination of Fig. 8, is not balanced to give zero voltage at the center frequency. Furthermore, values of $E_0(p)$ that do not satisfy condition (9) will cause $e(t)/e'(t)$ to have a zero minimum magnitude, and thus require that RC be zero. The equality sign is excluded in condition (9) for the same reason.

With $e(t)$ as given by (8), we can show that the ratio

$$-\frac{e(t)}{e'(t)} = \frac{[E_0(1+a^2)+a^2r+a(2E_0+r)\cos\phi][1+2a\cos\phi+a^2]}{ar^2(1-a^2)\sin\phi}$$

has a minimum magnitude at the negative real root of

$$\cos^3\phi - \left[\frac{5}{2} + \frac{E_0(1+a^4)+a^4r}{2a^2(2E_0+r)} \right] \cos\phi - \left[\frac{E_0(1+a^2)+a^2r}{a(2E_0+r)} + \frac{1+a^2}{2a} \right] = 0,$$

which has a magnitude smaller than unity. An analytical expression for the resultant upper bound on the RC product is available, but it is too cumbersome to be useful.

When the discriminator is preceded by one stage of narrow-band limiting whose bandwidth equals one IF bandwidth, the formulas of the preceding computation are directly applicable to the computation of the maximum permissible discriminator RC product. Here, since the most unfavorable conditions at the limiter-filter output arise only when A_0 and A_{-1} pass and $r = 2\pi W_{if}$, it is merely necessary to replace a in the formulas by (A_{-1}/A_0). A similar extension of the computation to the situation in which more than two limiters, each of which has a bandwidth of one $(BW)_{if}$, precede the discriminator is fairly evident.

It is of interest to observe that with a discriminator whose output across the RC combination shown in Fig. 8 is balanced, the upper bound on the RC product will be nonzero as long as the two signals lie symmetrically on opposite sides of the center frequency. For this situation, the upper bound is specified by

$$rCR \leq \frac{1 - a^2}{2a} \tag{10}$$

which is one half of the upper bound on the grid-circuit time constant of the limiter. Frequently, the capture ratio of a receiver is measured by simulating an interference situation in which the two (unmodulated) signals lie at opposite ends of the IF pass band. It is clear that, under this condition of measurement, a discriminator whose output is balanced about the intermediate frequency when it is observed across the RC combination of Fig. 8 will appear to meet the test if its RC product satisfies condition (10). Evidently, under the more general (but milder) interference conditions, it will fail.

In order to illustrate the manner in which the cascading of narrow-band limiters raises the upper bounds on the output-circuit time-constant requirements of the discriminator, we shall choose a discriminator whose characteristic goes through zero at a frequency that corresponds to a cutoff frequency of the IF amplifier. In view of condition (9), this situation is mainly of academic interest (unless the interference is effectively suppressed before it reaches the discriminator). The weaker of the two carriers will be assumed to fall at the frequency of balance. In the absence of narrow-band limiting, the voltage waveform impressed across the output capacitor is

$$e(t) = r \frac{1 + a \cos rt}{1 + 2a \cos rt + a^2}.$$

Consequently, the maximum permissible values of $\tau_{d0} = W_{if}RC$ are the values plotted in Fig. 10. If one narrow-band limiter whose bandwidth equals the IF bandwidth precedes the discriminator, the upper bounds are specified by the plotted values of ${}_1\tau_{d1}$. The curve marked

"$_2\tau_{d1}$" applies when two limiters, both of one IF bandwidth, precede the discriminator. Fig. 10 also presents a curve marked "$_1\tau_{d3}$," which applies when the discriminator is preceded by a limiter whose bandwidth equals $3(\mathrm{BW})_{if}$.

The plots of Fig. 10 show how the upper bound on the permissible time constant in the output circuit of the discriminator is raised when the discriminator is preceded by a process of narrow-band limiting. The effect produced by one narrow-band limiter will, clearly, be displayed by additional stages. After a sufficient number of stages has been cascaded, the upper bound on the maximum permissible time-constant values becomes sufficiently high, so that it exercises no important restraint on the design of the output circuit of the discriminator.

We shall now illustrate the computation of the maximum permissible time constant for the common type of discriminator circuit shown in Fig. 9. Alternative forms of this circuit (particularly, the one in which the AM-to-fm conversion is achieved through a double-tuned transformer, in which the top of the primary is connected to the center tap of the secondary) can be manipulated into the form of Fig. 9, and are, therefore, included in this treatment. The output voltage, e_{out}, is a superposition of the envelope of one tank-circuit response upon the other tank-circuit response with reversed polarity.

Assuming that the high-Q tank circuits have the same damping factor α, let one circuit be tuned to a frequency that is $b\alpha$ rad/second above the center frequency of operation ω_0 and the other tuned to $b\alpha$ rad/second below ω_0. Furthermore, let the instantaneous frequency of the excitation be deviated by $\alpha x(t)$ rad/second from the center frequency of operation. Then, if the conditions for a quasi-stationary analysis of the tuned-circuit responses are satisfied, and if the RC combination of each peak detector is able to follow the envelope of the corresponding tank-circuit response, the output voltage can be normalized into the form

$$e_{out} = [1 + (x + b)^2]^{-1/2} - [1 + (x - b)^2]^{-1/2}. \quad (11)$$

For optimum linearity,[9] b must be 1.225. Indeed, with this value of b,

$$e_{out} = kx(t), \qquad \text{for } -0.6 < x < 0.6.$$

The extent of this nearly perfect linearity is, therefore, 1.2α rad/second centered about $x=0$, while the peak-to-peak separation of the discriminator characteristic is 2.45 α rad/second.

Under conditions of two-signal interference, the instantaneous frequency of the amplitude-limited resultant of the two signals is

$$\omega_i(t) = \omega_{ave} - \frac{1}{2} r \frac{1 - a^2}{1 + 2a \cos rt + a^2},$$

[9] L. B. Arguimbau, "Discriminator linearity," *Electronics*, vol. 18, pp. 142–144; March, 1945.

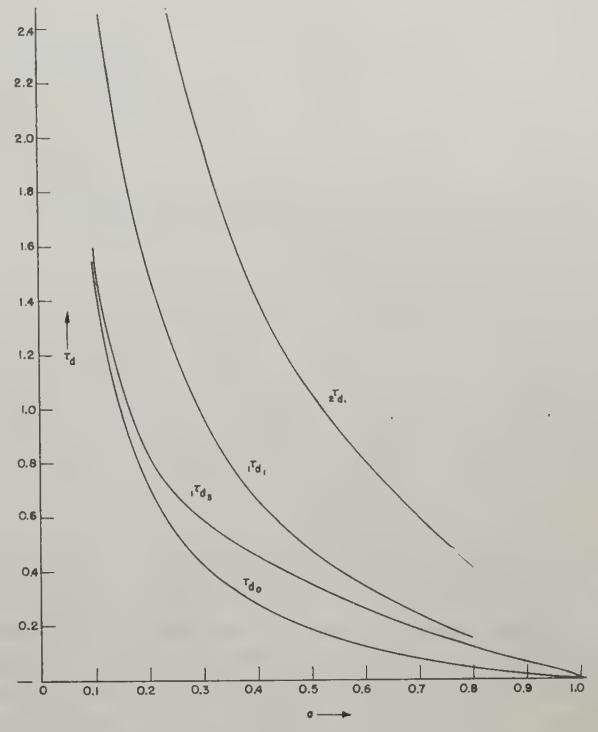

Fig. 10—Curves showing effect of cascading scheme upon the upper bounds on the time constant of Fig. 8, under the conditions of the illustrative example.

where $\omega_{ave} = p + \frac{1}{2}r$, the average of the two signal frequencies. Therefore

$$x(t) = x_{ave} - \frac{r}{2a} \frac{1 - a^2}{1 + 2a \cos rt + a^2}, \quad (12)$$

where $x_{ave} = 1/\alpha(\omega_{ave} - \omega_0)$. When the two signals are symmetrically disposed with respect to the center frequency, $x_{ave} = 0$ and

$$x(t) = -\frac{r}{2a} \frac{1 - a^2}{1 + 2a \cos rt + a^2}. \quad (13)$$

If r is given its maximum value of $(\mathrm{BW})_{if}$, (13) will represent the most troublesome instantaneous-frequency deviations from ω_0, measured in units of α rad/second.

Theory[10] shows that if

$$\frac{r}{2a} = \beta \frac{1 - a}{1 + a}, \quad (14)$$

then the conditions for quasi-stationary analysis, which justify use of (11), are satisfied if β is bounded by the values plotted in Fig. 11. Substitution in (13) leads to

$$x(t)_1 = \frac{-\beta(1 - a)^2}{1 + 2a \cos rt + a^2}. \quad (15)$$

The upper bound on the RC product can now be found by requiring that the RC combination follow the voltage waveform given by

[10] E. J. Baghdady, "Theory of Low-Distortion Transmission of FM Signals Through Linear Systems," Res. Lab. Electronics, M.I.T., Cambridge, Mass., Tech. Rep. 332; July 30, 1957. (To be published.)

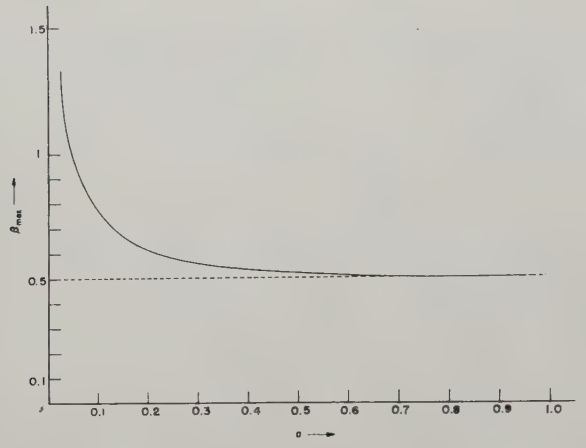

Fig. 11—The upper bounds on the value of β in (14).

$$e(t) = 1 + \{ [x(t) + 1.225]^2 \}^{-1/2} \qquad (16)$$

$x(t)$ being given by (15). In Fig. 12 we present the results of a computation in which use was made of the values of $\beta = \beta_{max}$ that are plotted in Fig. 11. For all values of $a \leq 0.84$, the plot of Fig. 3 can be used in conjunction with the plot of Fig. 3 to determine the maximum permissible values of $\tau = W_{if}RC$ when any specified number of narrow-band limiters, each of one IF bandwidth, are cascaded ahead of the discriminator. Multiplication by a scale factor appropriate to the value of W_{if} that is used will convert the dimensionless vertical scale in Fig. 12 into microseconds.

Finally, we would like to emphasize the fact that any interference suppression scheme which is used to minimize the fm disturbance before it reaches the discriminator circuit will, by virtue of its function, alleviate the low-frequency time-constant restrictions on the discriminator circuit. The results of this paper are readily adaptable to the computation of the time-constant requirements when an interference suppressor precedes the discriminator, once the manner in which the interference ratio is decreased by the suppressor has been determined.

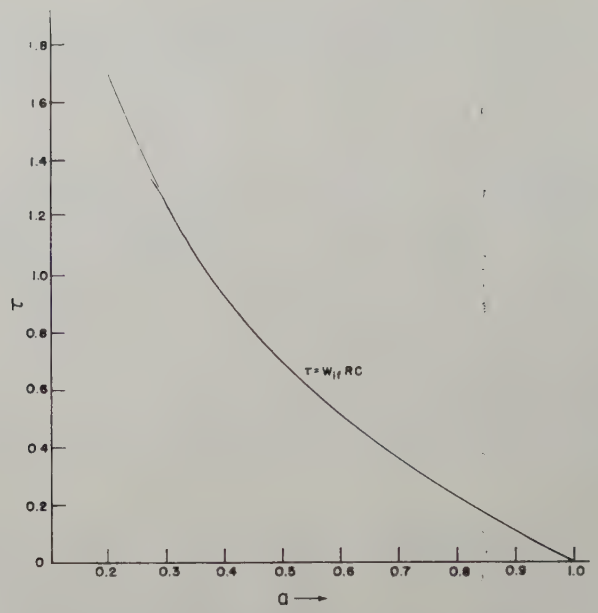

Fig. 12—Maximum permissible values of $\tau = W_{if}RC$ for each half of the balanced discriminator of Fig. 9.

A High-Power Periodically Focused Traveling-Wave Tube*

O. T. PURL†, ASSOCIATE MEMBER, IRE, J. R. ANDERSON†, MEMBER, IRE, AND G. R. BREWER†, SENIOR MEMBER, IRE

Summary—**The design considerations, construction, and performance of an *S*-band, pulsed, kilowatt-level traveling-wave tube, focused by means of periodic permanent magnets are described. The tube exhibits saturated power gain in excess of 30 db, with a bandwidth of approximately 2–4 kmc and weighs 17 pounds or less, complete with package.**

The results of studies on the electron beam defocusing effect of strong rf fields and on the effect of attenuator design on power build-up and saturation level are reported. Factors affecting the design of a high-power traveling-wave tube using periodic magnetic focusing are described in order to show the design constraints imposed by the periodic focusing system.

Introduction

A SERIOUS limitation to the extensive use of traveling-wave tubes in electronic systems has been the bulk and weight of the magnetic focusing system required to collimate the electron beam. This is particularly true for high-gain tubes, which frequently are too long to utilize uniform magnets efficiently. In the past few years, the use of periodic permanent magnets[1–4] for the beam-focusing system has allowed a considerable reduction to be made in the weight and power requirements for traveling-wave tubes. The use of periodic focusing, however, imposes some considerations and design limitations in addition to those for a tube focused with a uniform magnetic field. In many cases these limitations so influence the design as to make it almost imperative to consider the periodic focusing requirements from the outset.

The purpose of this paper is to present the results of work directed toward the design and development of a periodically focused *S*-band, kilowatt-level traveling-wave tube. Previous periodically focused tubes[1, 5–7] have made use of electron beams of considerably lower density than required in high-power tubes. As the power level is increased, in general, the beam current density and perveance is increased correspondingly, resulting in greater difficulty in obtaining the necessary field from existing magnet materials and in the formation and focusing of the beam. The aspects of the focusing problem peculiar to tubes of the kilowatt level or greater will be emphasized in this paper.

In the following sections, the design, construction, and electrical performance of this tube will be described in detail. In addition, the results of studies of the defocusing effect of the strong rf fields in the helix and of the rate of power build-up in the tube, as measured on a special traveling coupler, will be reported.

General Features and Performance

A photograph of the tube package is shown in Fig. 1, in which a pulsed kilowatt-level traveling-wave tube for operation in immersed flow, as described by Caldwell and Iversen,[8] is also shown for comparison. The present periodically focused tube represents a complete redesign, which incorporates coupled-helix matches, converging beam gun, external attenuator, and shrunk glass helix to provide compatibility with the periodic permanent-magnet focusing system. In addition, the power output has been increased from 1 to 2 kw in midband and the 3-db bandwidth has been extended to the range 2200–4000 mc.

A cross-sectional drawing of the complete tube package is shown in Fig. 2. In order to obtain maximum field amplitude, the magnet outer diameter is greater than the pole piece outer diameter. The pole pieces are aligned by means of nonmagnetic spacers and the couplers and tube are mounted concentrically with the pole piece inner diameter. The collector is connected directly to the case for good thermal conductivity and no additional cooling is required for the collector.

A typical gain-frequency curve for this tube is shown in Fig. 3, exhibiting 30 db or greater (peak power output > one kw) at one watt drive from 2200–4000 mc. The large signal gain curve is quite flat (± 0.5 db from 2500–3500 mc) in spite of operation at a low $\gamma a (\gamma a \approx 1)$. The broad-band operation is achieved by optimizing the beam voltage at the upper band edge. Operation very close to saturation also contributes to the flat gain char-

* Original manuscript received by the IRE, October 1, 1957.

† Electron Tube Lab., Hughes Aircraft Co., Culver City, Calif.

[1] J. T. Mendel, C. F. Quate, and W. H. Yocom, "Electron beam focusing with periodic permanent magnet fields," PROC. IRE, vol. 42, pp. 800–810; May, 1954.

[2] A. M. Clogston and H. Heffner, "Focusing of an electron beam by periodic fields," *J. Appl. Phys.*, vol. 25, pp. 436–447; April, 1954.

[3] K. K. N. Chang, "Beam focusing by periodic and complementary fields," PROC. IRE, vol. 43, pp. 62–71; January, 1955.

[4] G. R. Brewer, "On the focusing of high-current electron beams," *J. Appl. Phys.*, vol. 25, pp. 243–251; February, 1954.

[5] K. K. N. Chang, "Periodic magnetic field focusing for low-noise traveling-wave tubes," *RCA Rev.*, vol. 16, pp. 423–431; September, 1955.

[6] W. W. Siekanowicz and F. Sterzer, "A developmental wide-band, 100-watt, 20-db, *S*-band traveling-wave amplifier utilizing periodic permanent magnets," PROC. IRE, vol. 44, pp. 55–61; January, 1956.

[7] N. Nishio, T. Nemoto, and S. Yasuda, "A package type traveling-wave amplifier for 4000 mc band," *L'Onde Elec.*, vol. 37, pp. 147–152; February, 1957.

[8] J. J. Caldwell and A. H. Iversen, "The design and performance of a kilowatt traveling-wave amplifier for pulsed operation at 3000 mc/sec," paper presented at the PGED conference, Washington, D. C.; 1955.

ALUMINUM FOIL SOLENOID
TOTAL WEIGHT = 42 LBS
POWER REQUIRED = 1300 WATTS
PERIODIC MAGNET FOCUSING SYSTEM
TOTAL WEIGHT = 16 LBS.
0 1 2 3 4 5 6 7 8 9 10 11 12

Fig. 1—Comparison of periodic-magnet and immersed-flow focusing systems for a kilowatt-level traveling-wave tube.

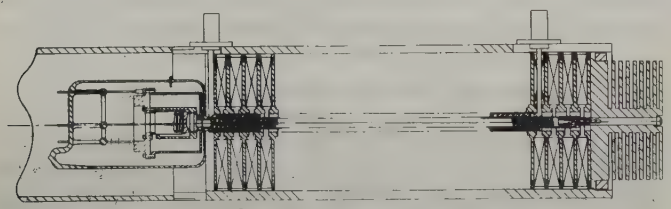

Fig. 2—Cross-sectional drawing of tube and package assembly.

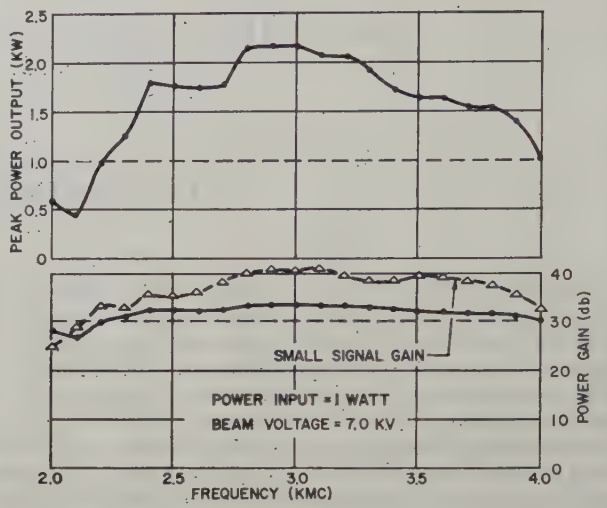

Fig. 3—Variation of power output and gain with one-watt drive power vs frequency. The small signal gain is shown also for comparison. These characteristics can be altered significantly by optimizing the attenuator to emphasize the performance feature (power output, stability, etc.) desired.

acteristic. By peaking the power output at midband, 2 kw can be obtained over several hundred megacycles. The tube has operated satisfactorily at duty cycle values up to 0.006; typical values are 5-μsec pulse length, 1000 prf, and the maximum pulse length at which the tube has been operated is 16 μsec. A tube has been life tested for greater than 500 hours at 0.005 duty cycle without appreciable change in performance. It is believed that this duty cycle limit can be increased by a considerable factor by making use of more effective heat dissipation techniques; and since a tungsten-impregnated "L" cathode is used ($T_k \approx 1100$°C Br), the exhaustion of emission material should not occur until after a life of several times 500 hours.

Fig. 4 shows the power output as a function of power input for several frequencies. The saturation gain is 5–7 db down from that in the small signal region. This value, along with the entire shape of the curve, can be altered significantly by using different types of attenuators, as will be shown later.

The variation of power output with beam voltage is shown in Fig. 5 for both small and large signal conditions. It is seen that the optimum beam voltage is approximately 7 kv. This optimum voltage in a periodically focused tube results from a compromise between the beam transmission characteristic of the magnet system and the characteristics of the tube and is therefore more difficult to interpret than in the case of a less voltage-sensitive focusing system such as a uniform magnetic field.

A reproducible efficiency value of 20 per cent has been observed on various experimental tubes, and values as high as 30 per cent with an attenuator optimized for maximum power output. A slight increase in power output has been observed when using a uniform focusing field (from a solenoid), but this increase occurred at elevated beam voltages so that no increase in efficiency resulted. Fig. 6 shows comparative data taken with the same tube in a periodic focusing system and uniform magnetic field. The difference in the curves can be attributed to the different matches used. The gain in the uniform field will be slightly higher at a higher beam voltage.

The tube is short-circuit stable to the extent that no spurious output can be observed at a level 60 db or more down from the normal signal level. Two tubes have been operated in cascade (without intermediate matching or loss device) to give a gain of over 60 db (from one milliwatt to over a kilowatt) with the total weight of both tubes and focusing systems of 34 pounds.

Beam Formation and Focusing

The electron gun is a converging beam type (perveance 2.2×10^{-6}), and was designed according to the method outlined by Brewer.[9] The role of the gun in successful periodic focusing should not be underestimated. It is the authors' experience that if the beam is not properly formed and injected into the periodic focusing field, no amount of magnetic field adjustment further down the tube will undo the damage. Consequently, a considerable amount of care was spent to assure correct

[9] G. R. Brewer, "Formation of high density electron beams," *J. Appl. Phys.*, vol. 28, pp. 7–15; January, 1957.

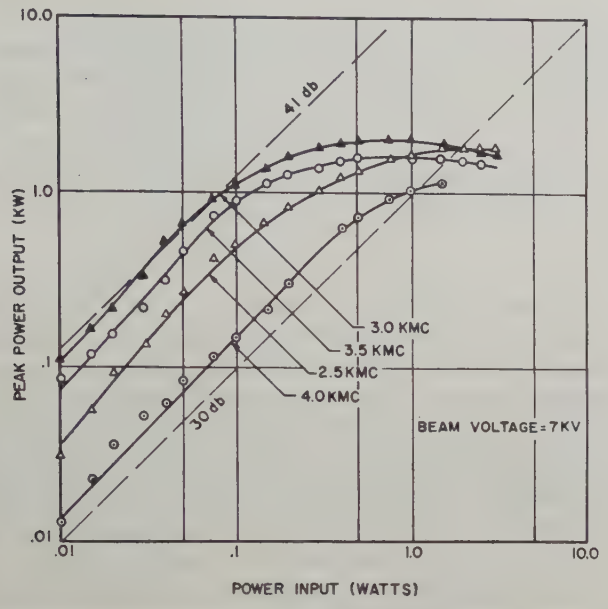

Fig. 4—Power output vs power input characteristics for several frequencies.

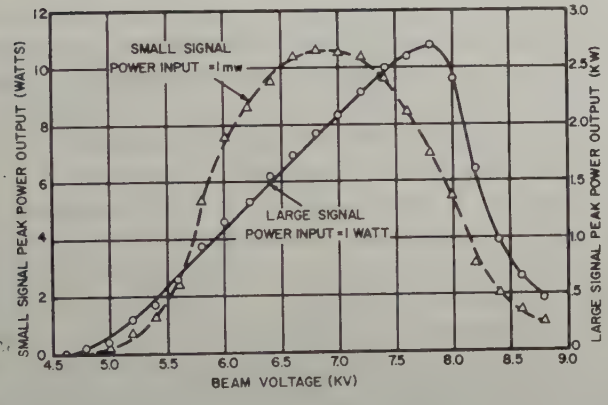
SMALL SIGNAL
POWER INPUT = 1 mw
LARGE SIGNAL
POWER INPUT = 1 WATT
SMALL SIGNAL PEAK POWER OUTPUT (WATTS)
LARGE SIGNAL PEAK POWER OUTPUT (KW)
BEAM VOLTAGE (KV)

Fig. 5—Variation of output power (or gain) with beam voltage with periodic focusing and under small-signal and large-signal conditions. The equivalent curves observed in a uniform magnetic field were somewhat less peaked, and the small signal curve extended from about 6 to 9.5 kv. The beam transmission characteristic of the periodic system results in the sharp drop-off at higher voltages in these curves.

alignment of the gun parts and to shield the cathode from the stray leakage field (less than 1 per cent of the peak field has been measured at the cathode position). Entrance conditions can be designed by determining an electron trajectory from knowledge of leakage field vs axial length and matching this to the gun focusing characteristic. The use of periodic magnets, arranged with alternate polarity so that the external fields tend to cancel, results in best utilization of the magnetic material and thus corresponding compactness and light weight.

Two important focusing criteria must be satisfied for proper collimation of a periodically focused beam. First, the peak amplitude of the periodic field must be within a narrow range of values centered around that given by (1); second, the period of the field must be adjusted so that operation occurs in a "stable" region of flow.

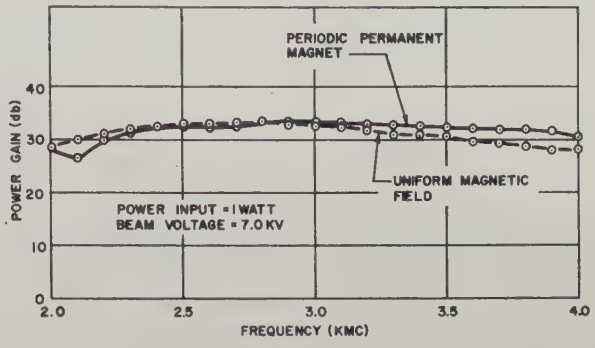

Fig. 6—Comparison of power gain for tube focused in a uniform magnetic field (Brillouin flow) and in a periodic magnetic system. Some of the difference in gain observed is due to different helix couplers used in the two tests. It is seen that the periodic focusing certainly does not degrade the tube performance.

The criterion for the amplitude of the field for minimum beam ripple is[1]

$$B_0 = 925 \frac{\sqrt{PV}}{d} \tag{1}$$

where P = beam perveance in micropervs., V = beam voltage in volts, d = beam diameter in inches, and B_0 = peak amplitude of axial magnetic flux density in Gauss. Typical values for the tube are $P = 2.2 \times 10^{-6}$ μpervs, $V = 7 \times 10^3$ volts, $d = 0.100$ inch, giving required $B_0 = 1150$ Gauss. This equation expresses the condition for balance, on the average, between the outward space-charge and centrifugal forces of the beam and the inward confining force of the magnetic focusing field.

It will be illuminating to express the required field value in terms of the operating parameters of the tube. In a given design the desired power output is usually specified and an estimate of the efficiency can be made so that one can write the tube output power in terms of the beam voltage:

$$P_{out} = \text{eff } V_0 I_0 = \text{eff } V_0^{5/2} P \tag{2}$$

and

$$B_0 \sim \left[\frac{P_{out}}{\text{eff} \times V_0^{5/2} d} \right]^{1/2}. \tag{3}$$

It is seen from (3) that the desired field is proportional to the square root of the power output, so that as higher power tubes are required with reasonable beam voltages, the required field strength increases. There is an upper bound to the value B_0 that can be obtained in practice, arising from the maximum value of the coercive force, H_c, available in present-day magnetic materials and by the geometry of the tube and magnetic circuit.

Chang[10] has computed the magnetic field that can be obtained from a set of periodic ring magnets. If we take

[10] K. K. N. Chang, "Optimum design of periodic magnet structures for electron beam focusing," *RCA Rev.*, vol. 16, pp. 65–81; March, 1955.

an approximate form of his result, assuming the shim thickness is small, the peak axial flux density, B_0, can be written

$$B_0 \approx \frac{2H_m}{I_0\left(\frac{2\pi R_1}{L}\right)}. \quad (3a)$$

The notation follows that of Chang. I_0 is the zero-order modified Bessel function of the first kind.

In order to make the demagnetizing force H_m as large as possible, the ratio of magnet-to-gap area is made very large so that the operating value H_m is very nearly equal to H_c, the coercive force. However, one soon reaches a region of diminishing returns by increasing the magnet outer diameter; then one must resort to other means to increase B_0. With the assumption that $H_m = H_c$, (3) may be written

$$B_0 \approx \frac{2H_c}{I_0\left(2\pi \frac{R_1/d}{L/d}\right)} \quad (4)$$

where R_1 = pole piece inner radius, d = beam diameter, and L = magnet period.

The maximum magnetic field that can be obtained from a given magnet depends on the coercive force of the material and also upon the R_1/L ratio. The pole piece diameter is restricted in most cases by the tube envelope or at least by the beam diameter. The period, L, is limited by the second consideration mentioned above; *i.e.*, by instability regions or "stop bands," expressed by the criterion[1]

$$P\left(\frac{L}{d}\right)^2 < 4.36 \times 10^{-4} \quad (5)$$

which is the mathematical expression of the theoretical condition beyond which the periodic magnet system is no longer an effective focusing system. In practice it seems necessary to remain below about 70 per cent of this value. Since there is often only a small range of variation for the ratio L/d, (4) indicates that it is important in most cases to reduce the ratio of pole piece inner diameter to beam diameter, $2R_1/d$, in order to utilize a given size magnet efficiently. This means that one must design the tube either with the pole piece extending through the vacuum envelope or reduce to a minimum value the radial space occupied by those tube parts between the beam and pole piece. For this reason the envelope diameter was reduced from 0.400 for the immersed-flow version to 0.250 for this tube.

The magnetic field had a period of 0.660 inch, with a peak axial value of 1200 Gauss, obtained with 3-inch od Indox magnets. The uniformity of the peaks can be maintained to within ±2 per cent by using annealed Armco iron pole pieces and selected magnets. It was found that any discontinuity in the initial part of the magnetic circuit, such as slots for couplers, etc., caused considerable decrease (10 to 15 per cent) in beam transmission, so that the input coupler is inserted between the tube envelope and first pole piece. A small-diameter coaxial line is used on the input coupler to decrease the distance from the anode to the first pole piece. A slot in the magnet for the output coupler does not cause any noticeable difficulties. Beam transmission to the collector of more than 90 per cent has been attained.

RF Defocusing

The beam defocusing due to the action of the intense rf electric fields is more serious in a periodically focused than in a uniform-field-focused tube and the 90-per cent beam transmission observed under zero drive conditions may drop to 75 per cent with 2 kw of output power as the beam is defocused to the point of striking the helix. This defocusing can be a serious limitation on the average power capabilities of the tube. There are two reasons for the increased sensitivity of a periodically focused beam to rf fields. First, the periodic field counterbalances the space-charge field only on the average over a period, not at every point along the beam, so that radial rf fields existing in the region of zero magnetic field will have a relatively larger effect; and second, in the process of rf interaction, the axial velocity of some of the electrons is reduced to a value for which the periodic focusing is not longer effective; *i.e.*, to a velocity which corresponds to a stop band for the periodic system.

The dependence of "rf defocusing" on power level is shown in Fig. 7, where the change in helix current expressed as a percentage of the total beam current is plotted as a function of power output for different values of the focusing field period. The increase in helix current can be plotted vs L^2 and is shown in Fig. 8 to be roughly proportional to this quantity. Since the position of the stop band depends on L^2, this linear dependence would indicate that the presence of the stop band is undoubtedly a large contributor to the defocusing of the beam. For large periods, the defocusing is quite marked but by reducing the period, the helix current can be reduced considerably to compare reasonably well with the uniform field, as shown in Fig. 9. It is possible, as shown by the lower curve, to reduce the defocusing to a very small value by using a large uniform field over the entire circuit. It has also been shown that an increased field in the output region alone will suffice and that the amount of magnetic flux threading the cathode greatly influences the rf defocusing.[11]

The comparison of the rf defocusing in periodic and uniform fields is complicated by the fact that the power levels along the tube length in the two cases are different for the same applied parameters such as beam voltage, power input, etc. However, the gross behavior is clearly indicated by these curves. The rf defocusing also depends on the beam voltage as shown in Fig. 10. Lower voltage operation at the same power level results in

[11] G. R. Brewer and O. T. Purl, "Electron beam defocusing due to high intensity rf fields," paper presented at the Conference on Electron Tube Research, Boulder, Colo.; 1956.

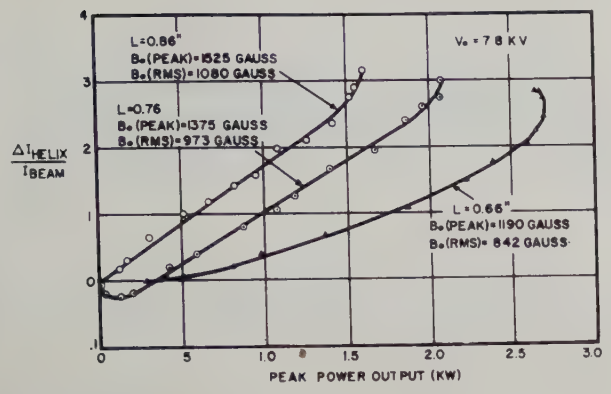

Fig. 7—Dependence of electron beam defocusing due to rf fields on power output for three values of magnet period. It is seen that the "rf defocusing" becomes greater with increase in magnet period. It is also noted that under some conditions the rf fields can focus the beam; this effect has been observed also for certain values of magnetic cathode flux with a uniform field system. (See Brewer and Purl.[11])

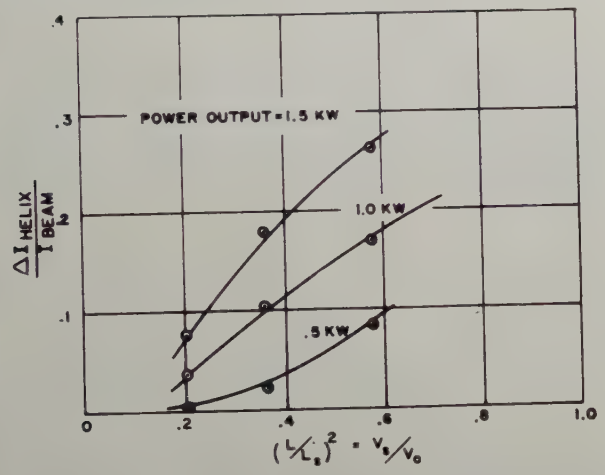

Fig. 8—Dependence of rf defocusing effect on magnet period. The abscissa scale is the square of the magnet period (data from Fig. 7) divided by the stop band period for the magnetic field used; it is also equal to the ratio of the stop band voltage to beam voltage. It is seen that the defocusing effect is roughly proportional to this quantity and that the curves appear to intersect the abscissa around 0.1.

more electrons reaching the stop-band region and becoming defocused to the helix. It is clear from the curves shown that the rf defocusing can be minimized to a great extent by operating with a smaller-period structure and at a higher beam voltage than normal. It may be worth while in certain instances to depart from maximum power output slightly by reducing the period and increasing the beam voltage in order to increase materially the possible duty cycle.

Although it is in general undesirable to collect a large percentage of the beam on the helix, the response of the beam focusing to rf fields can be utilized to provide a sensitive microwave detector tube.[12] If small duty cycle operation is permissible, the rf defocusing can be maximized and the rectified helix current will provide the detected signal. The magnitude of this effect is shown by a

[12] J. T. Mendel, "Microwave detector," Proc. IRE, vol. 44, pp. 503–508; April, 1956.

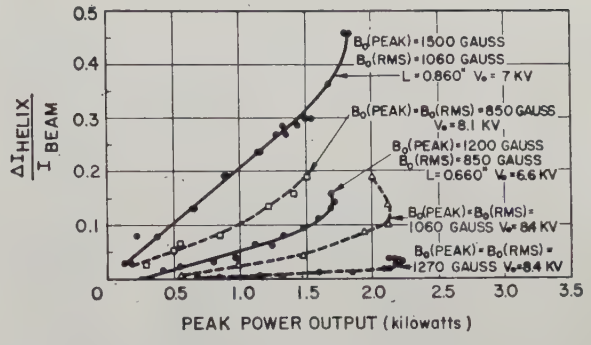

Fig. 9—Dependence of electron beam defocusing due to rf fields on power output for two values of magnet period and three values of uniform field strength. The beam voltages were adjusted for maximum power output in each case. Although the beam voltage variation slightly obscures the comparison, it is seen that periodic magnetic focusing results in considerably greater rf defocusing than use of a uniform magnetic field.

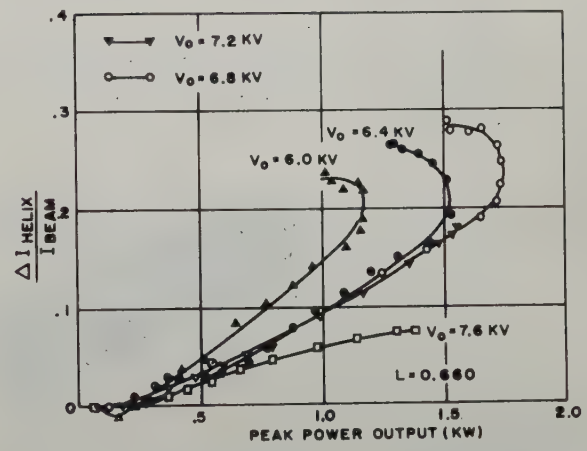

Fig. 10—Dependence of electron beam defocusing due to rf fields on power output for various values of beam voltage. As the beam voltage is reduced, the ratio V_s/V_0 becomes greater, resulting in larger rf defocusing, as shown in Fig. 8.

curve of helix current as a function of power input (Fig. 11). It is noted that the characteristic is relatively linear over a range of values of input power greater than ten to one.

Components

The principal mechanical features of the tube are shown in Fig. 12, which is an exploded view of the tube, matches, and attenuator.

The match for a 50-Ω coax line to the slow-wave circuit is accomplished by using coupled helix transducers. No vacuum seal is required, and the outer helix unit can be made to occupy less than 0.050 inch of radial space. The vswr can be held to less than 2 to 1 over the 2–4 kmc band, and the insertion loss per coupler is less than 1 db at midband. The outer helix is moulded in Teflon for rigidity, and the perpendicular entry has been used for the coax connection. A termination is applied to both ends of the inner helix, but none is necessary on the outer helix. The helix structure is mounted in a precision-ground glass tube which is shrunk around the helix under vacuum to increase the heat dissipating

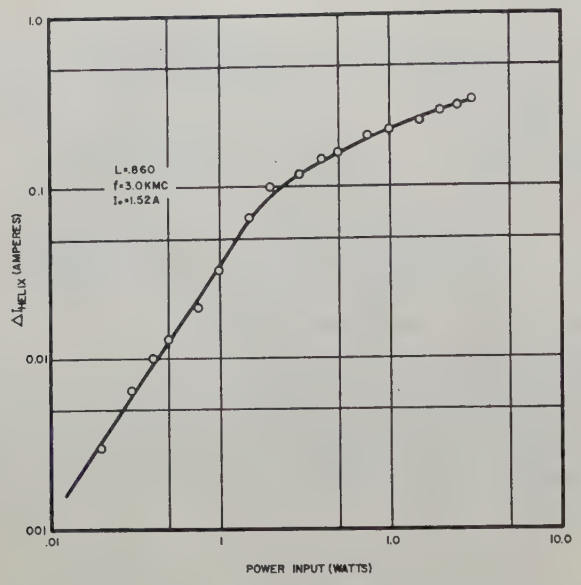

Fig. 11—Change in helix current due to rf defocusing vs input power. It is noted that the characteristic is linear up to $I_h = 0.10$ ampere so that when used as a detector, an output voltage linear up to 5 volts could be obtained with a 50-Ω load.

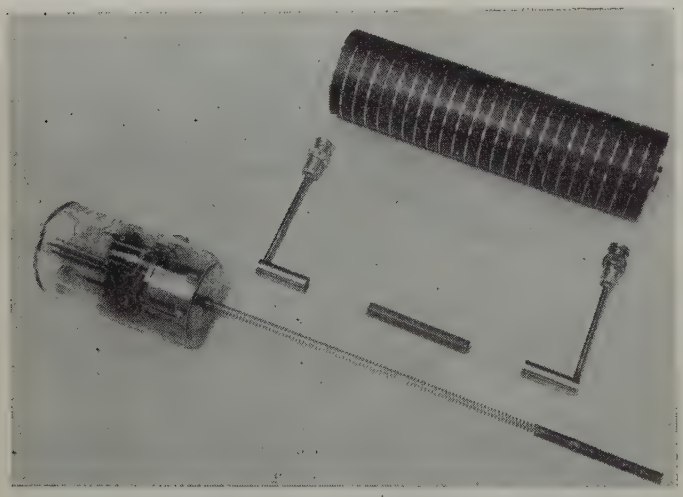

Fig. 12—Photograph of tube, coupled-helix matches, coupled-helix attenuator, and periodic-magnet stack.

quality of the circuit. Such a structure can dissipate about 9 watts per inch safely without forced air cooling. The amount of dielectric loading (DLF = 0.8) was measured by probing the field with a moving single-turn coil mounted on a carriage. The increase in loading after shrinking was found to be of the order of 2 per cent.

Several types of attenuators have been tested; *e.g.*, lossy wall attenuators of Aquadag, lossy ceramic, Teledeltos paper, and other lossy plastic materials, and coupled helix attenuators with distributed loss. The cold transmission loss as a function of frequency is shown in Fig. 13 for both types. The Teledeltos paper is molded in a layer of Teflon to keep it moisture free. The 400°C temperature, required to cure the Teflon, does not deteriorate the lossy paper. This type of attenuator has been found to be more consistent from tube to tube than spraying or painting Aquadag or other commercially available lossy materials and is capable of dissipating 12 watts of average power without any apparent damage.

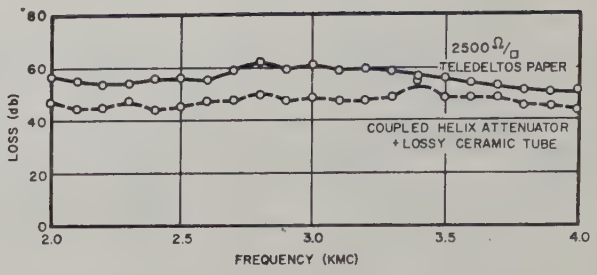

Fig. 13—Loss obtained with Teledeltos paper attenuator as compared to that with a coupled-helix plus lossy-ceramic attenuator.

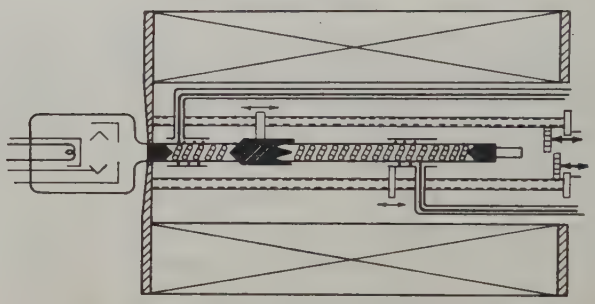

Fig. 14—Schematic drawing of movable coupler device. The input coupled-helix match is fixed in position and the attenuator and output coupled-helix match are movable independently or ganged together. The tube was operated in a uniform magnetic field for these tests.

A coupled helix attenuator has also been developed for this tube, consisting of a quadrifilar Kanthal wire helix moulded in Teflon in conjunction with a carbon impregnated ceramic tubing to provide additional loss. The saturation power output has consistently been 2–3 db lower than that with the lossy wall variety.[13]

The lossy wall attenuator has three sections—a slightly tapered input, a constant resistance center section, and a long tapered output section.

It was desirable for the tube to be short-circuit stable. For a high gain tube this imposes a stringent condition (vswr ≈ 1.04) on the match looking into the attenuator from the output. A gradual taper of the lossy material in this transition region is therefore essential and this gradual transition also apparently improves the "saturation characteristic."[14]

A program is under way to incorporate a grid in the gun which would decrease greatly the size of modulator required for the tube.

Movable Coupler Device

In order to study further the effect of the attenuator on the tube behavior, a device was built using coupled helix matches, which allows movement of both the at-

[13] N. Rynn, "Analysis of coupled structure traveling-wave tubes," IRE Trans., vol. ED-4, pp. 172–177; April, 1957.

[14] J. J. Caldwell, "High-power traveling-wave tube gain and saturation characteristics as a function of attenuator configuration and resistivity," IRE Trans., vol. ED-4, pp. 28–32; December, 1953.

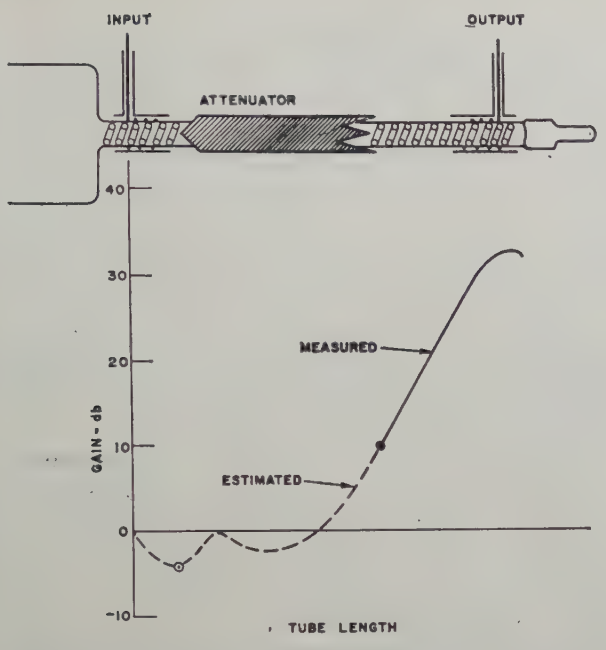

Fig. 15—Illustration of the power build-up along the tube, as determined from movable coupler measurements. The dotted parts of the curve are estimated and are therefore less accurate.

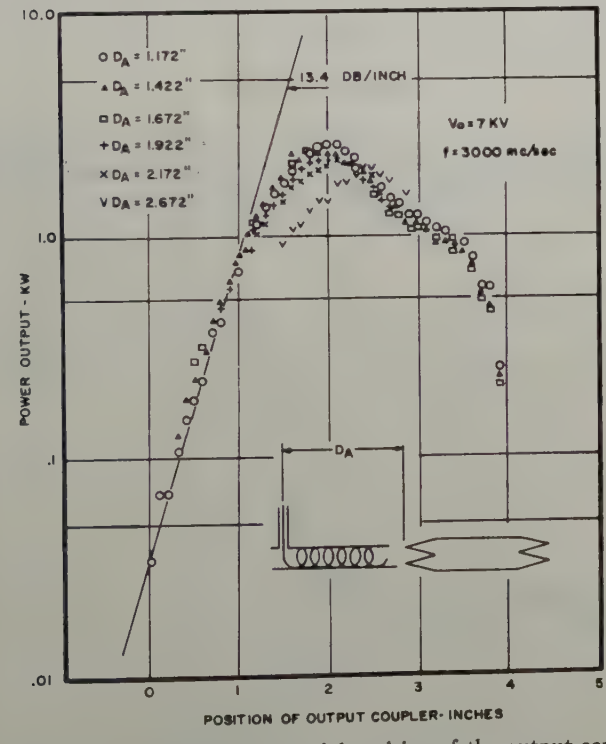

Fig. 16—Tube power output vs axial position of the output coupler for various positions of the attenuator. The zero coupler position was located at the extreme output end of the attenuator when the input end of the attenuator was $D_A = 1.172$ inches from the center line of the input coaxial line. It is seen that the power build-up after the attenuator was almost independent of attenuator position and the saturation level was highest for the attenuator in the closest position to the input.

tenuator and output match during tube operation. In contrast to probing the field, this device actually changes the electrical length of the tube during operation. A uniform field was used for focusing in these tests

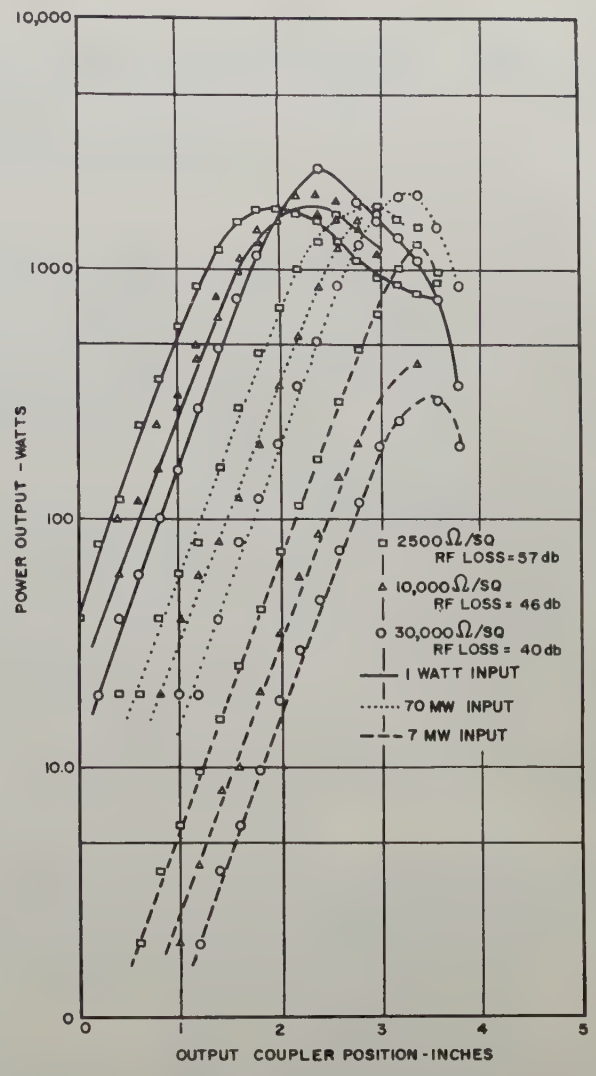

Fig. 17—Tube power output vs axial position of the output coupler for several values of attenuator resistivity and drive power levels. The attenuator was made of Teledeltos paper. $D_A = 1.172$ inches.

and the following results were observed. A schematic diagram of the apparatus is shown in Fig. 14 and an illustration of the power build-up vs position along the helix is shown in Fig. 15, as determined from these measurements. First, the position of the attenuator is not critical, as shown by the curves of Fig. 16, but for best performance should be located close to the input. The length of the input coupler is equal to 0.22 CN, which is close to the optimum Pierce value.[15] Second, the change in power build-up as a function of the Ω/square surface resistivity of the attenuator is shown in Fig. 17. Note that although the saturated output is higher with the higher Ω/square attenuator, a longer tube length is required to reach saturation.

The rate of power build-up can be measured rather accurately in the lossless region and is noted to be 5.6 db/λ_g. From a knowledge of b and c, x_1 can be computed using this experimentally obtained value of gain per

[15] J. R. Pierce, "Traveling-Wave Tubes," D. Van Nostrand Co., Inc., New York, N. Y., p. 140; 1950.

wavelength. The resulting value obtained using $C=0.145$ and $b=1.0$, $N=11.9$ is $x_1=0.805$. The value of x_1 obtained by small-signal theory[16] using the above values and $QC=0.2$ gives $x_1=0.79$ to 0.80, which is within the accuracy of the curves used. The gain profile along the tube length, shown in Fig. 15, is based on the best data available from this device.

The values of the parameters $C=0.145$, $QC=0.2$, and $\gamma r_0=0.56$ are quite close to those measured by Cutler[17] to yield the optimum efficiency; from his work efficiencies of 30 per cent and greater can be expected. Efficiencies of 30 per cent have been observed, but it has been found difficult to optimize the attenuator design to achieve both maximum efficiency and maximum stability (*i.e.*, short-circuit stability).

By adjusting the attenuator it is possible to optimize the tube design to meet a variety of requirements involving the gain, power output, stability, and duty cycle. For example, if the tube is not required to operate into a bad mismatch, the attenuation can be reduced with a corresponding increase in power output and efficiency. Conversely, if a lower power and efficiency can be tolerated, the gain can be made flatter over a wider band by designing the attenuator to cause premature saturation of the tube in the midband region.

[16] C. K. Birdsall and G. R. Brewer, "Traveling-wave tube characteristics for finite values of C," IRE TRANS., vol. ED-1, pp. 1–11; August, 1954. These computations in turn were based on the small-signal theory of Pierce, *op. cit.*

[17] C. C. Cutler, "The nature of power saturation in traveling-wave tubes," *Bell Sys. Tech. J.*, vol. 35, pp. 841–876; July, 1956.

Conclusion

It has been shown that a relatively high-power electron beam for use in a broad-band (essentially 2:1) traveling-wave tube can be periodically focused. Such periodic focusing does not degrade the performance of the tube but in fact can result in a tube with more diversified operating characteristics. A total of about 25 of these tubes have been built and tested, with good reproducibility of the operating characteristics. RF defocusing becomes an important factor to consider in high-power periodically focused tubes, but the effect can be reduced by proper attention to the period of the magnetic circuit and the operating voltage.

The attenuator position is not critical, but should be located near the input of the tube for maximum saturated power output. The Ω/square value used in a lossy wall attenuator can markedly affect the saturation output, and values near 2500 Ω/square seem reasonably good. A wide variety of tube requirements can be met by changing the periodic magnet circuit, the attenuator configuration, or both. It is apparent that further extensions of periodic focusing into regions of higher power will come about by either incorporating part of the magnetic circuit inside the vacuum envelope or by obtaining magnetic materials of higher coercive force.

Acknowledgment

The assistance of T. Gorman, W. Perkins, T. Leonard, L. Toy, and B. Kesterson in the assembling and processing of these tubes is gratefully acknowledged.

Index to IRE Standards on Definitions of Terms 1942-1957*

(58 IRE 20.S1)

Introduction

This index covers all Standards on Definitions of Terms issued by the IRE from 1942 through July, 1957, that are still in force. It brings together in one alphabetical list approximately 3500 technical terms defined in those Standards, indicating the IRE code number of the Standard and the issue and page number of the PROCEEDINGS OF THE IRE where the definition may be found. Standards issued prior to 1949, which were published as separate reports instead of in the PROCEEDINGS, are identified by the word "separate" in the index.

In some instances the same term has been defined in more than one Standard. If the Standards are in the same field, only the last published definition is referenced in the index; if they are in different fields, all definitions are referenced.

A list of the Standards covered in the index and their IRE code numbers is given below. Reprints may be ordered at the indicated prices from IRE headquarters. Reprints of this index are also available as indicated in the footnote below.*

The IRE is greatly indebted to Chester H. Page, Vice-Chairman and Definitions Coordinator of the Standards Committee, for the substantial task of compiling this index.

Standards Covered by Index

Standard No.	*Title and Where Published*	*Reprint Price*
48 IRE 2, 11, 15.S1	Standards on Antennas, Modulation Systems, and Transmitters: Definitions of Terms, 1948 (Separate Report)	$0.75
53 IRE 2.S1	Standards on Antennas and Waveguides: Definitions of Terms, 1953 (December, 1953, PROC. IRE)	$0.75
55 IRE 2.S1	Standards on Antennas and Waveguides: Definitions for Waveguide Components, 1955 (September, 1953, PROC. IRE)	$0.25
54 IRE 3.S1	Standards on Audio Techniques: Definitions of Terms, 1954 (July, 1954, PROC. IRE)	$0.50
50 IRE 4.S1	Standards on Circuits: Definitions of Terms in Network Topology, 1950 (January, 1951, PROC. IRE)	$0.50
53 IRE 4.S1	Standards on Circuits: Definitions of Terms in the Field of Linear Varying Parameter and Nonlinear Circuits, 1953 (March, 1954, PROC. IRE)	$0.25
51 IRE 6.S1	Standards on Electroacoustics: Definitions of Terms, 1951 (May, 1951, PROC. IRE)	$1.00
50 IRE 7.S1	Standards on Electron Tubes: Definitions of Terms, 1950 (April, 1950, PROC. IRE)	†
54 IRE 7.S1	Standards on Electron Devices: Definitions of Terms Related to Phototubes, 1954 (August, 1954, PROC. IRE)	$0.25
54 IRE 7.S2	Standards on Electron Devices: Definitions of Semiconductor Terms, 1954 (October, 1954, PROC. IRE)	$0.50
56 IRE 7.S3	Standards on Electron Tubes: TR and ATR Tube Definitions, 1956 (August, 1956, PROC. IRE)	$0.50
57 IRE 7.S2	Standards on Electron Tubes: Definitions of Terms, 1957 (July, 1957, PROC. IRE)	$1.00
50 IRE 8.S1	Standards on Electronic Computers: Definitions of Terms, 1950 (March, 1951, PROC. IRE)	†
56 IRE 8.S1	Standards on Electronic Computers: Definitions of Terms, 1956 (September, 1956, PROC. IRE)	$0.60
42 IRE 9.S1	Standards on Facsimile: Definitions of Terms, 1942 (Separate Report)	†
56 IRE 9.S1	Standards on Facsimile: Definitions of Terms, 1956 (June, 1956, PROC. IRE)	$0.60
55 IRE 10.S1	Standards on Industrial Electronics: Definitions of Industrial Electronics Terms, 1955 (September, 1955, PROC. IRE)	$0.50
53 IRE 11.S1	Standards on Modulation Systems: Definitions of Terms, 1953 (May, 1953, PROC. IRE)	$0.50
54 IRE 12.S1	Standards on Radio Aids to Navigation: Definitions of Terms, 1954 (February, 1955, PROC. IRE)	$1.00
52 IRE 17.S1	Standards on Receivers: Definitions of Terms, 1952 (December, 1952, PROC. IRE)	$0.60
51 IRE 20.S1	Standards on Pulses: Definitions of Terms —Part I, 1951 (June, 1951, PROC. IRE)	$0.50
51 IRE 20.S2	Standards on Transducers: Definitions of Terms, 1951 (August, 1951, PROC. IRE)	$0.50
52 IRE 20.S1	Standards on Pulses: Definitions of Terms —Part II, 1952 (May, 1952, PROC. IRE)	$0.50
55 IRE 22.S1	Standards on Television: Definitions of Color Terms, 1955 (June, 1955, PROC. IRE)	$0.60
55 IRE 23.S1	Standards on Television: Definitions of Television Signal Measurement Terms, 1955 (May, 1955, PROC. IRE)	$1.00
45 IRE 24.S1	Standards on Radio Wave Propagation: Definitions of Terms Relating to Guided Waves, 1945 (Separate Report)	$0.20
50 IRE 24.S1	Standards on Wave Propagation: Definitions of Terms, 1950 (November, 1950, PROC. IRE)	$0.60
55 IRE 26.S2	Standards on Terminology for Feedback Control Systems, 1955 (January, 1956, PROC. IRE)	$0.50

† Out of print.

* Reprints of this index may be purchased while available from the Institute of Radio Engineers, 1 East 79 Street, New York 21, N.Y., at $1.00 per copy. A 20 per cent discount will be allowed for 100 or more copies mailed to one address.

PUBLISHED IRE DEFINITIONS

	Standard	Proceedings Vol Page Mo
A		
A and R Display	54 IRE 12.S1	43 192 Feb
Absolute Delay	54 IRE 12.S1	43 192 Feb
Absorption	50 IRE 24.S1	38 1265 Nov
Absorption Loss	51 IRE 6.S1	39 510 May
Absorption Modulation	48 IRE 2,11,15.S1	Separate
Accelerating Electrode	57 IRE 7.S2	45 986 Jul
Acceleration	51 IRE 6.S1	39 510 May
Access Time	56 IRE 8.S1	44 1167 Sep
Accessible Terminal	50 IRE 4.S1	39 27 Jan
Acceptor	54 IRE 7.S2	42 1506 Oct
Accumulator	56 IRE 8.S1	44 1167 Sep
Accuracy	56 IRE 8.S1	44 1167 Sep
AC Erasing Head	51 IRE 6.S1	39 510 May
AC Magnetic Biasing	51 IRE 6.S1	39 510 May
Acetate Disks	51 IRE 6.S1	39 510 May
Achromatic Locus	55 IRE 22.S1	43 742 Jne
Acoustic	51 IRE 6.S1	39 510 May
Acoustic Compliance	51 IRE 6.S1	39 510 May
Acoustic Dispersion	51 IRE 6.S1	39 510 May
Acoustic Generator	51 IRE 6.S1	39 510 May
Acoustic Horn	51 IRE 6.S1	39 510 May
Acoustic Impedance	51 IRE 6.S1	39 510 May
Acoustic Interferometer	51 IRE 6.S1	39 510 May
Acoustic Mass	51 IRE 6.S1	39 510 May
Acoustic Pickup	51 IRE 6.S1	39 510 May
Acoustic Radiating Element	51 IRE 6.S1	39 510 May
Acoustic Radiometer	51 IRE 6.S1	39 510 May
Acoustic Reactance	51 IRE 6.S1	39 510 May
Acoustic Refraction	51 IRE 6.S1	39 510 May
Acoustic Resistance	51 IRE 6.S1	39 510 May
Acoustic Scattering	51 IRE 6.S1	39 510 May
Acoustic Stiffness	51 IRE 6.S1	39 510 May
Acoustic Transmission System	51 IRE 6.S1	39 511 May
Acoustical	51 IRE 6.S1	39 511 May
Acoustical Ohm	51 IRE 6.S1	39 511 May
Acoustical Reciprocity Theorem	51 IRE 6.S1	39 511 May
Acoustical Units	51 IRE 6.S1	39 511 May
Acoustics	51 IRE 6.S1	39 511 May
Active Transducer	51 IRE 20.S2	39 898 Aug
Active Transducer (Audio)	54 IRE 3.S1	42 1110 Jul
Actuating Transfer Function	55 IRE 26.S2	44 108 Jan
ADF	54 IRE 12.S1	43 192 Feb
A-Display	54 IRE 12.S1	43 192 Feb
Adcock Antenna	48 IRE 2,11,15.S1	Separate
Adder	56 IRE 8.S1	44 1167 Sep
Adder, Algebraic	50 IRE 8.S1	39 272 Mar
Address	56 IRE 8.S1	44 1167 Sep
Address Part	56 IRE 8.S1	44 1167 Sep
Adjacent-Channel Attenuation	52 IRE 17.S1	40 1682 Dec
Adjacent-Channel Interference	52 IRE 17.S1	40 1682 Dec
Admittance	57 IRE 7.S2	45 986 Jul
Advance Ball	51 IRE 6.S1	39 511 May
Aeolight	51 IRE 6.S1	39 511 May
Aerophare	54 IRE 12.S1	43 192 Feb
AI Radar	54 IRE 12.S1	43 192 Feb
Aided Tracking	54 IRE 12.S1	43 192 Feb
Air Conduction	51 IRE 6.S1	39 511 May
Airport Surface Detection Equipment (ASDE)	54 IRE 12.S1	43 209 Feb
Air-Position Indicator (API)	54 IRE 12.S1	43 207 Feb
Air Speed	54 IRE 12.S1	43 192 Feb
Airborne Radar	49 IRE 12.S1	37 1366 Dec
Airport Surveillance Radar	54 IRE 12.S1	43 192 Feb
Alford Loop	54 IRE 12.S1	43 192 Feb
Algebraic Adder	50 IRE 8.S1	39 272 Mar
Alternator Transmitter	48 IRE 2,11,15.S1	Separate
Altimetric Flare-Out	54 IRE 12.S1	43 192 Feb
Altitude	49 IRE 12.S1	37 1367 Dec
AM to FS Converter	56 IRE 9.S1	44 776 Jne
Ambient Temperature	48 IRE 2,11,15.S1	Separate
Ambiguity	54 IRE 12.S1	43 192 Feb
Amplification	54 IRE 3.S1	42 1110 Jul
Amplification Factor	57 IRE 7.S2	45 986 Jul
Amplifier	57 IRE 7.S2	45 986 Jul
Amplifier	48 IRE 2,11,15.S1	Separate
Amplifier Torque	50 IRE 8.S1	39 272 Mar
Amplitude Balance Control	54 IRE 12.S1	43 192 Feb
Amplitude Discriminator	54 IRE 12.S1	43 192 Feb
Amplitude Distortion	53 IRE 4.S1	42 554 Mar
Amplitude Distortion (old usage)	48 IRE 2,11,15.S1	Separate
Amplitude-Frequency Distortion	53 IRE 4.S1	42 554 Mar
Amplitude vs Frequency Response Characteristic	48 IRE 2,11,15.S1	Separate
Amplitude-Modulated Transmitter	48 IRE 2,11,15.S2	Separate
Amplitude-Modulated Noise Level	48 IRE 2,11,15.S1	Separate
Amplitude Modulation	53 IRE 11.S1	41 612 May
Amplitude Modulation	52 IRE 17.S1	40 1682 Dec
Amplitude Response (Camera Tubes)	57 IRE 7.S2	45 986 Jul
Amplitude Response Characteristic	57 IRE 7.S2	45 986 Jul
A-N Radio Range	54 IRE 12.S1	43 207 Feb
Analog	56 IRE 8.S1	44 1167 Sep
Analog Computer	56 IRE 8.S1	44 1167 Sep
And-Circuit	56 IRE 8.S1	44 1167 Sep
And-Gate	56 IRE 8.S1	44 1167 Sep
Angle	57 IRE 7.S2	45 986 Sep
Angle, Maximum-Deflection	57 IRE 7.S2	45 986 Jul
Angle Modulation	53 IRE 11.S1	41 612 May
Angle of Elevation	49 IRE 12.S1	37 1367 Dec
Angle or Phase of a Sine Wave	53 IRE 11.S1	41 612 May
Angular Deviation Loss	51 IRE 6.S1	39 511 May
Angular Deviation Sensitivity	54 IRE 12.S1	43 192 Feb
Angular Frequency	50 IRE 24.S1	38 1265 Nov
Angular Resolution	54 IRE 12.S1	43 192 Feb
Angular Width	54 IRE 12.S1	43 193 Feb
Anode (Electron Tubes)	57 IRE 7.S2	45 986 Jul
Anode Breakdown Voltage	57 IRE 7.S2	45 986 Jul
Anode Current	57 IRE 7.S2	45 986 Jul
Anode Strap (Magnetrons)	57 IRE 7.S2	45 986 Jul
Anode Voltage	57 IRE 7.S2	45 986 Jul
Anode Voltage Drop	57 IRE 7.S2	45 986 Jul
Antenna	52 IRE 17.S1	40 1682 Dec
Antenna Array	48 IRE 2,11,15.S1	Separate
Antenna Cross Talk	48 IRE 2,11,15.S1	Separate
Antenna Effect	54 IRE 12.S1	43 193 Feb
Antenna Resistance	48 IRE 2,11,15.S1	Separate
Anti-Clutter Circuits	54 IRE 12.S1	43 193 Feb
Anti-TR Switch	54 IRE 12.S1	43 193 Feb
Antinoise Microphone	51 IRE 6.S1	39 511 May
Aperture	48 IRE 2,11,15.S1	Separate
Aperture Illumination	48 IRE 2,11,15.S1	Separate
Applicator (Electrodes)	55 IRE 10.S1	43 1070 Sep
Applicator Impedance	55 IRE 10.S1	43 1070 Sep

	Standard	Proceedings Vol Page Mo
Applied Shock	51 IRE 6.S1	39 511 May
Approach Navigation	54 IRE 12.S1	43 193 Feb
Approach Path	54 IRE 12.S1	43 193 Feb
Arc	57 IRE 7.S2	45 986 Jul
Arc-Back	57 IRE 7.S2	45 986 Jul
Arc Converter	48 IRE 2,11,15.S1	Separate
Arc-Drop Loss (Gas Tubes)	57 IRE 7.S2	45 986 Jul
Arc-Drop Voltage	57 IRE 7.S2	45 986 Jul
Arc Loss	57 IRE 7.S2	45 986 Jul
Arc-Through	57 IRE 7.S2	45 986 Jul
Arithmetic Element	56 IRE 8.S1	44 1167 Sep
Arithmetic Organ	50 IRE 8.S1	39 272 Mar
Arithmetic Unit	56 IRE 8.S1	44 1167 Sep
Articulation and Intelligibility	51 IRE 6.S1	39 511 May
Arm	50 IRE 4.S1	39 27 Jan
Artificial Antenna	48 IRE 2,11,15.S1	Separate
Artificial Ear	51 IRE 6.S1	39 512 May
Artificial Line	53 IRE 2.S1	41 1722 Dec
Artificial Load	48 IRE 2,11,15.S1	Separate
Artificial Voice	51 IRE 6.S1	39 512 May
ASR	54 IRE 12.S1	43 193 Feb
A-Scan	54 IRE 12.S1	43 193 Feb
A-Scope	54 IRE 12.S1	43 193 Feb
"A" Station	54 IRE 12.S1	43 193 Feb
Aspect Ratio	52 IRE 17.S1	40 1682 Dec
Astigmatism	57 IRE 7.S2	45 986 Jul
ATR (Anti-Transmit-Receive) Tube	57 IRE 7.S2	45 986 Jul
Atmospheric Duct	50 IRE 24.S1	38 1265 Nov
Atmospheric Radio Waves	50 IRE 24.S1	38 1265 Nov
Attenuation (of Radio Waves)	50 IRE 24.S1	38 1265 Nov
Attenuation (General)	54 IRE 3.S1	42 1110 Jul
Attenuation (Waveguide)	53 IRE 2.S1	41 1722 Dec
Attenuation Band	53 IRE 2.S1	41 1722 Dec
Attenuation Constant	53 IRE 2.S1	41 1722 Dec
Attenuation Equalizer	42 IRE 9.S1	Separate
Attenuation-Frequency Distortion	42 IRE 9.S1	Separate
Attenuation Ratio	50 IRE 24.S1	38 1265 Nov
Attenuator Tube	57 IRE 7.S2	45 986 Jul
Attenuator, Waveguide	55 IRE 2.S1	43 1073 Sep
Audio Frequency	51 IRE 6.S1	39 512 May
Audio Frequency	48 IRE 2,11,15.S1	Separate
Audio Frequency	52 IRE 17.S1	40 1682 Dec
Audio-Frequency Harmonic Distortion	48 IRE 2,11,15.S1	Separate
Audio-Frequency Peak Limiter	48 IRE 2,11,15.S1	Separate
Audiogram	51 IRE 6.S1	37 512 May
Audiometer	51 IRE 6.S1	39 512 May
Auditory Sensation Area	51 IRE 6.S1	39 512 May
Aural Harmonic	51 IRE 6.S1	39 512 May
Aural Radio Range	54 IRE 12.S1	43 193 Feb
Aural Transmitter	48 IRE 2,11,15.S1	Separate
Auto-Radar Plot	49 IRE 12.S1	37 1367 Dec
Automatic Chart-Line Follower	54 IRE 12.S1	43 193 Feb
Automatic Check	56 IRE 8.S1	44 1167 Sep
Automatic Direction Finder	54 IRE 12.S1	43 193 Feb
Automatic Frequency Control	48 IRE 2,11,15.S1	Separate
Automatic Gain Control	52 IRE 17.S1	40 1682 Dec
Automatic Gain Control Instantaneous	54 IRE 12.S1	43 193 Feb
Automatic Grid Bias	48 IRE 2,11,15.S1	Separate
Automatic Pilot (Autopilot)	54 IRE 12.S1	43 193 Feb
Automatic Track-Follower	54 IRE 12.S1	43 193 Feb
Automatic Tracking	54 IRE 12.S1	43 193 Feb
Autopilot Coupler	54 IRE 12.S1	43 193 Feb
Autoradar Plot	54 IRE 12.S1	43 193 Feb
Autoregulation Induction Heater	55 IRE 10.S1	43 1070 Sep
Available Conversion Gain	57 IRE 7.S2	45 986 Jul
Available Conversion Power Gain	51 IRE 20.S2	39 899 Aug
Available Harmonic	51 IRE 6.S1	39 512 May
Available Line	56 IRE 9.S1	44 776 Jne
Available Power	51 IRE 20.S2	39 899 Aug
Available Power	57 IRE 7.S2	45 986 Jul
Available Power (of a Linear Source of Electric Energy)	54 IRE 3.S1	42 1110 Jul
Available Power Efficiency	51 IRE 6.S1	39 512 May
Available-Power Gain	57 IRE 7.S2	45 986 Jul
Available-Power Gain	51 IRE 20.S2	39 899 Aug
Available-Power Gain Maximum	57 IRE 7.S2	45 987 Jul
Available Power Response	51 IRE 6.S1	39 512 May
Avalanche	57 IRE 7.S1	45 987 Jul
Average Absolute Pulse Amplitude	51 IRE 20.S1	39 625 Jne
Average Electrode Current	57 IRE 7.S2	45 987 Jul
Average Power Output (of a Transmitter)	48 IRE 2,11,15.S1	Separate
Average Pulse Amplitude	51 IRE 20.S1	39 625 Jne
Axial Ratio	53 IRE 2.S1	41 1722 Dec
Azimuth	54 IRE 12.S1	43 193 Feb
Azimuth Marker	54 IRE 12.S1	43 193 Feb
Azimuth Stabilized PPI	54 IRE 12.S1	43 193 Feb
B		
Babble	48 IRE 2,11,15.S1	Separate
BABS (Blind Approach Beacon System)	54 IRE 12.S1	43 208 Feb
Backed Stamper	51 IRE 6.S1	39 513 May
Background Noise (in Recording)	51 IRE 6.S1	39 513 May
Background Noise (in Receivers)	52 IRE 17.S1	40 1682 Dec
Background Noise (in Transmitters)	48 IRE 2,11,15.S1	Separate
Background Returns	54 IRE 12.S1	43 193 Feb
Backplate	57 IRE 7.S2	45 987 Jul
Back Porch	55 IRE 23.S1	43 620 May
Back Scatter	54 IRE 12.S1	43 193 Feb
Back-Scattering Coefficient	48 IRE 2,11,15.S1	Separate
Back-Shunt Keying	48 IRE 2,11,15.S1	Separate
Backward Wave	57 IRE 7.S2	45 987 Jul
Back Wave	48 IRE 2,11,15.S1	Separate
B-Display	54 IRE 12.S1	43 193 Feb
B-Scope	49 IRE 12.S1	37 1367 Dec
"B" Station	54 IRE 12.S1	43 194 Feb
Baffle	51 IRE 6.S1	39 513 May
Balanced Amplifier	48 IRE 2,11,15.S1	Separate
Balanced Currents	53 IRE 2.S1	41 1722 Dec
Balanced Line	53 IRE 2.S1	41 1722 Dec
Balanced Line System	53 IRE 2.S1	41 1722 Dec
Balanced Modulator	48 IRE 2,11,15.S1	Separate
Balanced Oscillator	48 IRE 2,11,15.S1	Separate
Balanced Termination	53 IRE 2.S1	41 1722 Dec
Background Counts	57 IRE 7.S2	45 987 Jul
Balanced Voltages	53 IRE 2.S1	41 1722 Dec
Band (in Electronic Computers)	56 IRE 8.S1	44 1167 Sep
Band-Pass Tube	57 IRE 7.S2	45 987 Jul
Band Pressure Level	51 IRE 6.S1	39 513 May
Bandwidth	52 IRE 17.S1	40 1682 Dec
Bandwidth, Facsimile	56 IRE 9.S1	44 776 Jne
Bandwidth of an Antenna	48 IRE 2,11,15.S1	Separate
Bar Generator	52 IRE 17.S1	40 1682 Dec
Barrier	54 IRE 7.S2	42 1506 Oct
Barkhausen-Kurz Oscillator	48 IRE 2,11,15.S1	Separate
Base (of Number System)	56 IRE 8.S1	44 1167 Sep
Baseband	56 IRE 9.S1	44 777 Jne
Baseline	54 IRE 12.S1	43 193 Feb

	Standard	PROCEEDINGS Vol Page Mo
Base Electrode	54 IRE 7.S2	42 1506 Oct
Base Region	54 IRE 7.S2	42 1506 Oct
Basic Frequency	51 IRE 6.S1	39 513 May
Basic Repetition Rate	54 IRE 12.S1	43 193 Feb
Baud	53 IRE 11.S1	41 612 May
Beam Alignment	57 IRE 7.S2	45 987 Jul
Beam Bending	57 IRE 7.S2	45 987 Jul
Beam-Deflection Tube	57 IRE 7.S2	45 987 Jul
Beam-Indexing Color Tube	57 IRE 7.S2	45 987 Jul
Beam Modulation Percentage	57 IRE 7.S2	45 987 Jul
Beam Power Tube	57 IRE 7.S2	45 987 Jul
Bearing	54 IRE 12.S1	43 193 Feb
Beating	52 IRE 17.S1	40 1682 Dec
Beat Note	52 IRE 17.S1	40 1682 Dec
Bel	48 IRE 2,11,15.S1	Separate
Bend	54 IRE 12.S1	43 193 Feb
Bend, Waveguide	55 IRE 2.S1	43 1073 Sep
Benito	54 IRE 12.S1	43 208 Feb
Bias Telegraph Distortion	48 IRE 2,11,15.S1	Separate
Biconical Antenna	48 IRE 2,11,15.S1	Separate
Bidirectional Microphone	51 IRE 6.S1	39 513 May
Bidirectional Pulse	52 IRE 20.S1	40 553 May
Bidirectional Pulses	48 IRE 2,11,15.S1	Separate
Bidirectional Pulse Train	52 IRE 20.S1	40 553 May
Bilateral-Area Track	51 IRE 6.S1	39 513 May
Bilateral Transducer	51 IRE 20.S2	39 898 Aug
Binary	56 IRE 8.S1	44 1167 Sep
Binary Cell	56 IRE 8.S1	44 1167 Sep
Binary-Coded-Decimal System	56 IRE 8.S1	44 1167 Sep
Binary Digit	50 IRE 8.S1	39 272 Mar
Binary Number System	56 IRE 8.S1	44 1167 Sep
Binary Point	56 IRE 8.S1	44 1167 Sep
Binder	51 IRE 6.S1	39 513 May
Bit	56 IRE 8.S1	44 1167 Sep
Black and White	55 IRE 22.S1	43 743 Jne
Black Compression	55 IRE 23.S1	43 620 May
Black Level	55 IRE 23.S1	43 620 May
Black Peak	55 IRE 23.S1	43 620 May
Black Recording	56 IRE 9.S1	44 777 Jne
Black Signal	56 IRE 9.S1	44 777 Jne
Black Transmission	56 IRE 9.S1	44 777 Jne
Blanked Picture Signal	55 IRE 23.S1	43 620 May
Blanking Level	55 IRE 23.S1	43 620 May
Blanking Signal	55 IRE 23.S1	43 620 May
Blemish	57 IRE 7.S2	45 987 Jul
Blind Speed	54 IRE 12.S1	43 193 Feb
Blinking	54 IRE 12.S1	43 193 Feb
Blip (PIP)	54 IRE 12.S1	43 194 Feb
Block	56 IRE 8.S1	44 1167 Sep
Blocked Impedance	51 IRE 6.S1	39 513 May
Blocking Oscillator	48 IRE 2,11,15.S1	Separate
Blooming	54 IRE 12.S1	43 194 Feb
Bone Conduction	51 IRE 6.S1	39 513 May
Bootstrap Circuit	48 IRE 2,11,15.S1	Separate
Boresighting	54 IRE 12.S1	43 194 Feb
Borrow	56 IRE 8.S1	44 1167 Sep
Boundary	54 IRE 7.S2	42 1506 Oct
Boundary Marker	54 IRE 12.S1	43 208 Feb
Branch (in Circuits)	50 IRE 4.S1	39 27 Jan
Branch (in Computing)	56 IRE 8.S1	44 1167 Sep
Branch Point	50 IRE 4.S1	39 27 Jan
Breakdown	57 IRE 7.S2	45 987 Jul
Breakdown Transfer Characteristic	57 IRE 7.S2	45 987 Jul
Breakdown Voltage	57 IRE 7.S2	45 987 Jul

	Standard	PROCEEDINGS Vol Page Mo
Break-in-Keying	48 IRE 2,11,15.S1	Separate
Break Point	56 IRE 8.S1	44 1167 Sep
Bridge Rectifier	48 IRE 2,11,15.S1	Separate
Bridged-T Network	50 IRE 4.S1	39 27 Jan
Bridging	54 IRE 3.S1	42 1110 Jul
Bridging Gain	54 IRE 3.S1	42 1110 Jul
Bridging Loss	54 IRE 3.S1	42 1110 Jul
Brightness	55 IRE 22.S1	43 743 Jne
Brightness Signal	55 IRE 22.S1	43 743 Jne
Broad-Band Tube	57 IRE 7.S2	45 987 Jul
Broadside Array	48 IRE 2,11,15.S1	Separate
Buffer (in computors)	56 IRE 8.S1	44 1167 Sep
Buffer Amplifier	48 IRE 2,11,15.S1	Separate
Bunching	57 IRE 7.S2	45 987 Jul
Bunching Angle	57 IRE 7.S2	45 987 Jul
Bunching Optimum	57 IRE 7.S2	45 987 Jul
Bunching Parameter	57 IRE 7.S2	45 987 Jul
Burnishing Surface	51 IRE 6.S1	39 513 May
Bus (in Electronic Computers)	56 IRE 8.S1	44 1167 Sep
Butt Joint	55 IRE 2.S1	43 1073 Sep
C		
Cable	53 IRE 2.S1	41 1722 Dec
CCA	54 IRE 12.S1	43 194 Feb
C-Display	54 IRE 12.S1	43 197 Feb
Cake Wax	51 IRE 6.S1	39 513 May
Calibration Markers	54 IRE 12.S1	43 194 Feb
Camera Tube	57 IRE 7.S2	45 987 Jul
Cancellation Ratio	54 IRE 12.S1	43 194 Feb
Cancelled Video	54 IRE 12.S1	43 194 Feb
Candle	55 IRE 22.S1	43 743 Jne
Candlepower	55 IRE 22.S1	43 743 Jne
Capacitance	57 IRE 7.S2	45 987 Jul
Capacitor Pickup	51 IRE 6.S1	39 513 May
Carbon Microphone	51 IRE 6.S1	39 513 May
Carbon Pressure Recording	56 IRE 9.S1	44 777 Jne
Carrier (in Modulation)	53 IRE 11.S1	41 612 May
Carrier (in Semiconductor)	54 IRE 7.S2	42 1506 Oct
Carrier-Amplitude Regulation	48 IRE 2,11,15.S1	Separate
Carrier Beat	56 IRE 9.S1	44 777 Jne
Carrier-Controlled Approach	54 IRE 12.S1	43 194 Feb
Carrier Frequency	53 IRE 11.S1	41 612 May
Carrier-Frequency Pulse	52 IRE 20.S1	40 553 May
Carrier-Frequency Range	48 IRE 2,11,15.S1	Separate
Carrier-Frequency Stability	48 IRE 2,11,15.S1	Separate
Carrier Noise Level	48 IRE 2,11,15.S1	Separate
Carrier Suppression	48 IRE 2,11,15.S1	Separate
Carrier-to-Noise Ratio	53 IRE 11.S1	41 612 May
Carrier Wave	42 IRE 9.S1	Separate
Carry	56 IRE 8.S1	44 1167 Sep
Cascade (in Circuits)	50 IRE 4.S1	38 27 Jan
Cascaded Carry	56 IRE 8.S1	44 1168 Sep
C-Scope	49 IRE 12.S1	37 1367 Dec
Cathode	57 IRE 7.S2	45 987 Jul
Cathode Coating Impedance	57 IRE 7.S2	45 988 Jul
Cathode Current	57 IRE 7.S2	45 988 Jul
Cathode Follower	48 IRE 2,11,15.S1	Separate
Cathode Glow	57 IRE 7.S2	45 988 Jul
Cathode Heating Time	57 IRE 7.S2	45 988 Jul
Cathode Interface (Layer) Capacitance	57 IRE 7.S2	45 988 Jul
Cathode Interface (Layer) Impedance	57 IRE 7.S2	45 988 Jul
Cathode Interface (Layer) Resistance	57 IRE 7.S2	45 988 Jul
Cathode Luminous Sensitivity	54 IRE 7.S1	42 1277 Aug

	Standard	Proceedings Vol Page Mo
Cathode Modulation	48 IRE 2,11,15.S1	Separate
Cathode Preheating Time	57 IRE 7.S2	45 988 Jul
Cathode Pulse Modulation	48 IRE 2,11,15.S1	Separate
Cathode-Ray Tube	57 IRE 7.S2	45 988 Jul
Cathode Spot	57 IRE 7.S2	45 988 Jul
Cavitation	51 IRE 6.S1	39 513 May
Cavity Resonator	55 IRE 2.S1	43 1073 Sep
Cavity Resonator Frequency Meter	55 IRE 2.S1	43 1073 Sep
Cell (in Computers)	56 IRE 8.S1	44 1168 Sep
Cell, Binary	50 IRE 8.S1	39 272 Mar
Cell-Type Tube	57 IRE 7.S2	45 988 Jul
Cent (in Acoustics)	51 IRE 6.S1	39 513 May
Center Frequency	48 IRE 2,11,15.S1	Separate
Center Line	54 IRE 12.S1	43 194 Feb
Chain	54 IRE 12.S1	43 194 Feb
Challenge	54 IRE 12.S1	43 194 Feb
Challenger	54 IRE 12.S1	43 194 Feb
Channel (in Computers)	56 IRE 8.S1	44 1168 Sep
Channel, Melting	55 IRE 10.S1	43 1070 Sep
Channel, Radio	52 IRE 17.S1	40 1682 Dec
Channeling	42 IRE 9.S1	Separate
Character (in Computers)	56 IRE 8.S1	44 1168 Sep
Characteristic	57 IRE 7.S2	45 988 Jul
Characteristic Impedance	53 IRE 2.S1	41 1722 Dec
Characteristic Telegraph Distortion	48 IRE 2,11,15.S1	Separate
Characteristic Wave Impedance	53 IRE 2.S1	41 1723 Dec
Charge (Induction Heating)	55 IRE 10.S1	43 1070 Sep
Charge-Storage Tube	57 IRE 7.S2	45 988 Jul
Chart-Comparison Unit	54 IRE 12.S1	43 194 Feb
Check	56 IRE 8.S1	44 1168 Sep
Check, Automatic	56 IRE 8.S1	44 1168 Sep
Check Digits	56 IRE 8.S1	44 1168 Sep
Check, Forbidden-Combination	56 IRE 8.S1	44 1168 Sep
Check Point	54 IRE 12.S1	43 194 Feb
Check Problem	56 IRE 8.S1	44 1168 Sep
Check, Programmed	56 IRE 8.S1	44 1168 Sep
Check Routine	56 IRE 8.S1	44 1168 Sep
Check, Selection	56 IRE 8.S1	44 1168 Sep
Check, Transfer	56 IRE 8.S1	44 1168 Sep
Cheese Antenna	48 IRE 2,11,15.S1	Separate
Chip	51 IRE 6.S1	39 513 May
Choke Joint	55 IRE 2.S1	43 1074 Sep
Chroma	55 IRE 22.S1	43 743 Jne
Chromaticity	55 IRE 22.S1	43 743 Jne
Chromaticity Co-ordinate	55 IRE 22.S1	43 743 Jne
Chromaticity Diagram	55 IRE 22.S1	43 743 Jne
Chromaticity Flicker	55 IRE 22.S1	43 743 Jne
Chrominance	55 IRE 22.S1	43 743 Jne
Chrominance Components	55 IRE 22.S1	43 743 Jne
Chrominance Demodulator	55 IRE 22.S1	43 743 Jne
Chrominance Modulator	55 IRE 22.S1	43 744 Jne
Chrominance Primary	55 IRE 22.S1	43 744 Jne
Chrominance Signal	55 IRE 22.S1	43 744 Jne
Chrominance Subcarrier	55 IRE 22.S1	43 744 Jne
CIE	55 IRE 22.S1	43 744 Jne
Circuit	50 IRE 4.S1	38 27 Jan
Circuit Efficiency	57 IRE 7.S2	45 988 Jul
Circuit Gap Admittance	57 IRE 7.S2	45 988 Jul
Circular Electric Wave	53 IRE 2.S1	41 1727 Dec
Circular Magnetic Wave	53 IRE 2.S1	41 1727 Dec
Circular Scanning	48 IRE 2,11,15.S1	Separate
Circularly Polarized Wave	50 IRE 24.S1	38 1265 Nov
Circulating Register (or Memory)	56 IRE 8.S1	44 1168 Sep
Class-A Amplifier	57 IRE 7.S2	45 988 Jul
Class-AB Amplifier	57 IRE 7.S2	45 988 Jul
Class-A Modulator	48 IRE 2,11,15.S1	Separate
Class-A Push-Pull Sound Track	51 IRE 6.S1	39 513 May
Class-B Amplifier	57 IRE 7.S2	45 988 Jul
Class-B Modulator	48 IRE 2,11,15.S1	Separate
Class-B Push-Pull Sound Track	51 IRE 6.S1	39 514 May
Class-C Amplifier	57 IRE 7.S2	45 989 Jul
Clear	56 IRE 8.S1	44 1168 Sep
Clearance	54 IRE 12.S1	43 194 Feb
Clipper	48 IRE 2,11,15.S1	Separate
Clipper Limiter	48 IRE 2,11,15.S1	Separate
Clock	56 IRE 8.S1	44 1168 Sep
Close-Tailing Microphone	51 IRE 6.S1	39 514 May
Cloud Pulse	57 IRE 7.S2	45 989 Jul
Clutter	54 IRE 12.S1	43 194 Feb
Coarse Chrominance Primary	55 IRE 22.S1	43 744 Jne
Coaxial Antenna	48 IRE 2.11,15.S1	Separate
Coaxial Transmission Line	53 IRE 2.S1	41 1723 Dec
Co-Channel Interference	52 IRE 17.S1	40 1682 Dec
Code (in Computers)	56 IRE 8.S1	44 1168 Sep
Code Distinguishability	54 IRE 12.S1	43 194 Feb
Code, Instruction	50 IRE 8.S1	39 272 Mar
Coded Program	50 IRE 8.S1	39 272 Mar
Coder	49 IRE 12.S1	37 1367 Dec
Coder, Pulse-Duration	54 IRE 12.S1	43 194 Feb
Coding Delay	54 IRE 12.S1	43 194 Feb
Cohered Video	54 IRE 12.S1	43 194 Feb
Coherent Oscillator	54 IRE 12.S1	43 194 Feb
Coherent System	54 IRE 12.S1	43 194 Feb
COHO	54 IRE 12.S1	43 194 Feb
Cold Cathode	57 IRE 7.S2	45 989 Jul
Cold-Cathode Tube	57 IRE 7.S2	45 989 Jul
Collector	57 IRE 7.S2	45 989 Jul
Color	55 IRE 22.S1	43 744 Jne
Color Breakup	55 IRE 22.S1	43 744 Jne
Color Burst	55 IRE 22.S1	43 744 Jne
Color Carrier	55 IRE 22.S1	43 744 Jne
Color Cell	57 IRE 7.S2	45 989 Jul
Color Center	57 IRE 7.S2	45 989 Jul
Color Coder	55 IRE 22.S1	43 744 Jne
Color Contamination	55 IRE 22.S1	43 744 Jne
Color Co-ordinate Transformation	55 IRE 22.S1	43 744 Jne
Color Decoder	55 IRE 22.S1	43 744 Jne
Color-Difference Signal	55 IRE 22.S1	43 744 Jne
Color Encoder	55 IRE 22.S1	43 744 Jne
Color Flicker	55 IRE 22.S1	43 744 Jne
Color Field Corrector	57 IRE 7.S2	45 989 Jul
Color Fringing	55 IRE 22.S1	43 744 Jne
Color Match	55 IRE 22.S1	43 744 Jne
Color Mixture	55 IRE 22.S1	43 744 Jne
Color-Mixture Data	55 IRE 22.S1	43 745 Jne
Color Picture Signal	55 IRE 22.S1	43 745 Jne
Color Picture Tube	57 IRE 7.S2	45 989 Jul
Color Plane	57 IRE 7.S2	45 989 Jul
Color Purity Magnet	57 IRE 7.S2	45 989 Jul
Color-Selecting-Electrode System	57 IRE 7.S2	45 989 Jul
Color-Selecting-Electrode System Transmission	57 IRE 7.S2	45 989 Jul
Color Signal	55 IRE 22.S1	43 745 Jne
Color Temperature	55 IRE 22.S1	43 745 Jne
Color Transmission	55 IRE 22.S1	43 745 Jne
Color Triad	57 IRE 7.S2	45 989 Jul
Color Triangle	55 IRE 22.S1	43 745 Jne
Colorimetry	55 IRE 22.S1	43 745 Jne
Colpitts Oscillator	48 IRE 2,11,15.S1	Separate
Column	56 IRE 8.S1	44 1168 Sep

	Standard	Proceedings Vol Page Mo
Combination Microphone	51 IRE 6.S1	39 514 May
Command (in Computers)	56 IRE 8.S1	44 1168 Sep
Command (in Control Systems)	55 IRE 26.S2	44 109 Jan
Commutation Factor	57 IRE 7.S2	45 989 Jul
Companding	53 IRE 11.S1	41 612 May
Comparator	50 IRE 8.S1	39 272 Mar
Compass Bearing	49 IRE 12.S1	37 1367 Dec
Compass Course	49 IRE 12.S1	37 1367 Dec
Compass Heading	49 IRE 12.S1	37 1367 Dec
Compatibility	55 IRE 22.S1	43 745 Jne
Complement	56 IRE 8.S1	44 1168 Sep
Complementary Wavelength	55 IRE 22.S1	43 745 Jne
Complete Carry	56 IRE 8.S1	44 1168 Sep
Complex Target	54 IRE 12.S1	43 194 Feb
Complex Tone	51 IRE 8.S1	44 1168 Sep
Composite Color Signal	55 IRE 22.S1	43 745 Jne
Composite Color Sync	55 IRE 22.S1	43 745 Jne
Composite Controlling Voltage	57 IRE 7.S2	45 989 Jul
Composite Picture Signal	55 IRE 23.S1	43 620 May
Composite Pulse	54 IRE 12.S1	43 194 Feb
Compound Horn	48 IRE 2,11,15.S1	Separate
Compound Target	54 IRE 12.S1	43 194 Feb
Compression	53 IRE 11.S1	41 612 May
Compression (in Television)	55 IRE 23.S1	43 620 May
Compression Ratio	57 IRE 7.S2	45 989 Jul
Compressional Wave	51 IRE 6.S1	39 514 May
Computer	56 IRE 8.S1	44 1168 Sep
Condensed-Mercury Temperature	57 IRE 7.S2	45 989 Jul
Conditional Jump	56 IRE 8.S1	44 1168 Sep
Conditional Transfer of Control	56 IRE 8.S1	44 1169 Sep
Condor	54 IRE 12.S1	43 208 Feb
Conductance	57 IRE 7.S2	45 989 Jul
Conductance for Rectification	57 IRE 7.S2	45 989 Jul
Conduction Band	54 IRE 7.S2	42 1506 Oct
Conductivity	54 IRE 7.S2	42 1506 Oct
Conductivity Modulation	54 IRE 7.S2	42 1506 Oct
Conductivity, P-Type	54 IRE 7.S2	42 1506 Oct
Cone of Nulls	48 IRE 2,11,15.S1	Separate
Cone of Silence	54 IRE 12.S1	43 194 Feb
Conical Horn	51 IRE 6.S1	39 514 May
Conical Scanning	48 IRE 2,11,15.S1	Separate
Connected	50 IRE 4.S1	38 27 Jan
Connector Waveguide	55 IRE 2.S1	43 1074 Sep
Consol	54 IRE 12.S1	43 208 Feb
Consolan	54 IRE 12.S1	43 208 Feb
Constant Amplitude Recording	51 IRE 6.S1	39 514 May
Constant-Current Characteristic	57 IRE 7.S2	45 989 Jul
Constant-Current Modulation	48 IRE 2,11,15.S1	Separate
Constant-Delay Discriminator	54 IRE 12.S1	43 194 Feb
Constant Luminance Transmission	55 IRE 22.S1	43 745 Jne
Constant Velocity Recording	51 IRE 6.S1	39 514 May
Contact, High Recombination Rate	54 IRE 7.S2	42 1506 Oct
Contact, Majority Carrier	54 IRE 7.S2	42 1506 Oct
Contact Potential Difference	57 IRE 7.S2	45 989 Jul
Contact Rectifier	48 IRE 2,11,15.S1	Separate
Contactor, Load	55 IRE 10.S1	43 1070 Sep
Continuous-Duty Rating	48 IRE 2,11,15.S1	Separate
Continuous Waves or CW	48 IRE 2,11,15.S1	Separate
Control (in Computers)	56 IRE 8.S1	44 1169 Sep
Control Characteristic	57 IRE 7.S2	45 989 Jul
Control Circuits	50 IRE 8.S1	39 273 Mar
Control Electrode	57 IRE 7.S2	45 989 Jul
Control-Electrode Discharge Recovery Time	57 IRE 7.S2	45 989 Jul
Control Grid	57 IRE 7.S2	45 990 Jul
Control Ratio	57 IRE 7.S2	45 990 Jul
Control Track	51 IRE 6.S1	39 514 May
Controlled Carrier	48 IRE 2,11,15.S1	Separate
Convection Current	57 IRE 7.S2	45 990 Jul
Convection-Current Modulation	57 IRE 7.S2	45 990 Jul
Convergence	57 IRE 7.S2	45 990 Jul
Convergence, Dynamic	57 IRE 7.S2	45 990 Jul
Convergence Electrode	57 IRE 7.S2	45 990 Jul
Convergence Magnet	57 IRE 7.S2	45 990 Jul
Convergence Plane	57 IRE 7.S2	45 990 Jul
Convergence Surface	57 IRE 7.S2	45 990 Jul
Conversion Transconductance	57 IRE 7.S2	45 990 Jul
Conversion Transducer	57 IRE 7.S2	45 990 Jul
Conversion Voltage Gain	57 IRE 7.S2	45 990 Jul
Converter	51 IRE 20.S2	39 898 Aug
Converter, Facsimile	56 IRE 9.S1	44 777 Jne
Converter, Mercury Arc, Pool Cathode	55 IRE 10.S1	43 1070 Sep
Converter, Mercury Hydrogen Spark Gap	55 IRE 10.S1	43 1070 Sep
Converter Tube	57 IRE 7.S2	45 990 Jul
Converter, Quenched Spark Gap	55 IRE 10.S1	43 1070 Sep
Copy	56 IRE 8.S1	44 1169 Sep
Core	51 IRE 6.S1	39 514 May
Core Type Induction Heater or Furnace	55 IRE 10.S1	43 1070 Sep
Coreless Type Induction Heater or Furnace	55 IRE 10.S1	43 1070 Sep
Corner Reflector	54 IRE 12.S1	43 194 Feb
Corrected Compass Course	54 IRE 12.S1	43 194 Feb
Corrected Compass Heading	54 IRE 12.S1	43 195 Feb
Correction	56 IRE 8.S1	44 1169 Sep
Corrective Network (Shaping Network)	42 IRE 9.S1	Separate
Cosecant-Squared Pattern	54 IRE 12.S1	43 195 Feb
Count	57 IRE 7.S2	45 990 Jul
Count Down	54 IRE 12.S1	43 195 Feb
Counter	56 IRE 8.S1	44 1169 Sep
Counterpoise	48 IRE 2,11,15.S1	Separate
Counter Ring	56 IRE 8.S1	44 1169 Sep
Counter Tube Externally Quenched	57 IRE 7.S2	45 990 Jul
Counter Tube, Gas-Filled Radiation	57 IRE 7.S2	45 990 Jul
Counter Tube, Gas-Flow	57 IRE 7.S2	45 990 Jul
Counter Tube, Geiger-Mueller	57 IRE 7.S2	45 990 Jul
Counter-Tube, Proportional	57 IRE 7.S2	45 990 Jul
Counter Tube, Self-Quenched	57 IRE 7.S2	45 990 Jul
Counting Efficiency	57 IRE 7.S2	45 990 Jul
Counting-Rate-vs-Voltage Characteristic	57 IRE 7.S2	45 990 Jul
Coupler	54 IRE 12.S1	43 195 Feb
Coupling Aperture	55 IRE 2.S1	43 1074 Sep
Coupling (Induction Heating Usage)	55 IRE 10.S1	43 1070 Sep
Coupling Coefficient, Small Signal	57 IRE 7.S2	45 990 Jul
Coupling Loop	55 IRE 2.S1	43 1074 Sep
Coupling Probe	55 IRE 2.S1	43 1074 Sep
Course	54 IRE 12.S1	43 195 Feb
Course Error	54 IRE 12.S1	43 195 Feb
Course Error, Indicated	54 IRE 12.S1	43 195 Feb
Course Line	54 IRE 12.S1	43 195 Feb
Course Line Deviation	54 IRE 12.S1	43 195 Feb
Course (Line) Computer	49 IRE 12.S1	37 1367 Dec
Course (Line) Selector	49 IRE 12.S1	37 1367 Dec
Course Made Good	54 IRE 12.S1	43 195 Feb
Course Push (or Pull)	54 IRE 12.S1	43 195 Feb
Course Sensitivity	54 IRE 12.S1	43 195 Feb
Course Softening	54 IRE 12.S1	43 195 Feb
Course Width	54 IRE 12.S1	43 195 Feb

	Standard	Proceedings Vol	Page	Mo
Coverage Diagram	54 IRE 12.S1	43	195	Feb
Crab Angle	54 IRE 12.S1	43	195	Feb
Crest Factor of a Pulse	51 IRE 20.S1	39	625	Jne
Crest Factor of a Pulse Carrier	48 IRE 2,11,15.S1	Separate		
Critical Anode Voltage	57 IRE 7.S2	45	990	Jul
Critical Area	42 IRE 9.S1	Separate		
Critical Field	57 IRE 7.S2	45	990	Jul
Critical Frequency	50 IRE 24.S1	38	1265	Nov
Critical Grid Current	57 IRE 7.S2	45	990	Jul
Critical Grid Voltage	57 IRE 7.S2	45	990	Jul
Critical High-Power Level	57 IRE 7.S2	45	990	Jul
Critical Voltage	57 IRE 7.S2	45	990	Jul
Cross Talk	48 IRE 2,11,15.S1	Separate		
Cross Coupling	53 IRE 2.S1	41	1723	Dec
Cross-Modulation (General)	52 IRE 17.S1	40	1682	Dec
Cross-Modulation (in Transmitters)	48 IRE 2,11,15.S1	Separate		
Cross Neutralization	48 IRE 2,11,15.S1	Separate		
Cross Polarization	48 IRE 2,11,15.S1	Separate		
Cross Section	54 IRE 12.S1	43	195	Feb
Crossing Angle	54 IRE 12.S1	43	195	Feb
Crossover Characteristic Curve	54 IRE 12.S1	43	195	Feb
Crossover Frequency	51 IRE 6.S1	39	514	May
Crossover Region	54 IRE 12.S1	43	195	Feb
Crystal-Controlled Transmitter	48 IRE 2,11,15.S1	Separate		
Crystal Cutter	51 IRE 6.S1	39	514	May
Crystal Loudspeaker	51 IRE 6.S1	39	514	May
Crystal Microphone	51 IRE 6.S1	39	514	May
Crystal Oscillator	48 IRE 2,11,15.S1	Separate		
Crystal Pickup	51 IRE 6.S1	39	514	May
Crystal Pulling	54 IRE 7.S2	42	1506	Oct
Crystal-Stabilized Transmitter	48 IRE 2,11,15.S1	Separate		
Crystal-Video Receiver	54 IRE 12.S1	43	195	Feb
Curie Point	55 IRE 10.S1	43	1070	Sep
Current	57 IRE 7.S2	45	991	Jul
Current Amplification	54 IRE 3.S1	42	1110	Jul
Current Amplification	57 IRE 7.S2	45	991	Jul
Current Attenuation	54 IRE 3.S1	42	1110	Jul
Current Generator	57 IRE 7.S2	45	991	Jul
Cutoff Field	57 IRE 7.S2	45	991	Jul
Cutoff Frequency	53 IRE 2.S1	41	1723	Dec
Cutoff Voltage (Electron Tubes)	57 IRE 7.S2	45	991	Jul
Cutoff Voltage (Magnetrons)	57 IRE 7.S2	45	991	Jul
Cutoff Wavelength	53 IRE 2.S1	41	1723	Dec
Cut Paraboloidal Reflector	48 IRE 2,11,15.S1	Separate		
Cut-Set	40 IRE 4.S1	39	27	Jan
Cutter	51 IRE 6.S1	39	515	May
Cutting Stylus	51 IRE 6.S1	39	515	May
Cycle, Major	50 IRE 8.S1	39	273	Mar
Cycle, Minor	50 IRE 8.S1	39	273	Mar
Cyclic Shift	56 IRE 8.S1	44	1169	Sep
Cyclotron Frequency	57 IRE 7.S2	45	991	Jul
Cyclotron-Frequency Magnetron Oscillations	57 IRE 7.S2	45	991	Jul
Cylindrical Reflector	48 IRE 2,11,15.S1	Separate		
Cylindrical Wave	50 IRE 24.S1	38	1265	Nov

D

DBM	54 IRE 3.S1	42	1110	Jul
DC Electron-Stream Resistance	57 IRE 7.S2	45	991	Jul
DC Erasing Head	51 IRE 6.S1	39	515	May
DC Magnetic Biasing	51 IRE 6.S1	39	515	May
D-Display	54 IRE 12.S1	43	197	Feb
DDM	54 IRE 12.S1	43	196	Feb
DME (Distance Measuring Equipment)	54 IRE 12.S1	43	208	Feb
D Region	50 IRE 24.S1	38	1265	Nov
Damped Waves	48 IRE 2,11,15.S1	Separate		
Dark Current	57 IRE 7.S2	45	991	Jul
Dark Trace Tube	54 IRE 12.S1	43	195	Feb
Data, Handling Capacity	54 IRE 12.S1	43	195	Feb
Data Stabilization	54 IRE 12.S1	43	195	Feb
Dead Reckoning	54 IRE 12.S1	43	195	Feb
Dead Room	51 IRE 6.S1	39	515	May
Dead Time (in Navigation Aids)	54 IRE 12.S1	43	195	Feb
Dead Time (Radiation Counters)	57 IRE 7.S2	45	991	Jul
Decalescent Point (of a metal)	55 IRE 10.S1	43	1070	Sep
Decay (Charge-Storage Tubes)	57 IRE 7.S2	45	991	Jul
Decay (Characteristic)	57 IRE 7.S2	45	991	Jul
Decay Time (Charge-Storage Tubes)	57 IRE 7.S2	45	991	Jul
Decca	54 IRE 12.S1	43	208	Feb
Decelerating Electrode (Electron-Beam Tubes)	57 IRE 7.S2	45	991	Jul
Decibel	48 IRE 2,11,15.S1	Separate		
Decimal Number System	56 IRE 8.S1	44	1169	Sep
Decimal Point	56 IRE 8.S1	44	1169	Sep
Decineper	48 IRE 2,11,15.S1	Separate		
Decoder (in Computers)	56 IRE 8.S1	44	1169	Sep
Decoder (in Navigation Aids)	49 IRE 12.S1	37	1368	Dec
De-Emphasis	52 IRE 17.S1	40	1682	Dec
De-Emphasis	53 IRE 11.S1	41	612	May
De-Emphasis Network	48 IRE 2,11,15.S1	Separate		
Definition	56 IRE 9.S1	44	777	Jne
Deflecting Electrode	57 IRE 7.S2	45	991	Jul
Deflecting Yoke	50 IRE 7.S1	38	431	Apr
Deflection Center	57 IRE 7.S2	45	991	Jul
Deflection Factor	57 IRE 7.S2	45	991	Jul
Deflection Plane	57 IRE 7.S2	45	991	Jul
Deflection Sensitivity	57 IRE 7.S2	45	991	Jul
Deflection Yoke	57 IRE 7.S2	45	991	Jul
Deflection-Yoke Pull-Back	57 IRE 7.S2	45	991	Jul
Degeneration	48 IRE 2,11,15.S1	Separate		
Degrees of Freedom	50 IRE 4.S1	39	27	Jan
Deionization Time	57 IRE 7.S2	45	991	Jul
Delay Distortion	56 IRE 9.S1	44	777	Jne
Delay Distortion	53 IRE 4.S1	42	554	Mar
Delay Distortion	52 IRE 17.S1	40	1682	Dec
Delay Equalizer	56 IRE 9.S1	44	777	Jne
Delay Line	56 IRE 8.S1	44	1169	Sep
Delay-Line Memory	56 IRE 8.S1	44	1169	Sep
Delay-Line Register	50 IRE 8.S1	39	273	Mar
Delay-Line Storage	56 IRE 8.S1	44	1169	Sep
Delayed PPI	54 IRE 12.S1	43	196	Feb
Delta Network	50 IRE 4.S1	39	27	Jan
Demodulation	53 IRE 11.S1	41	613	May
Demodulation	52 IRE 17.S1	40	1682	Dec
Densitometer	51 IRE 6.S1	39	515	May
Density (in Facsimile)	56 IRE 9.S1	44	777	Jne
Depletion Layer	54 IRE 7.S2	42	1506	Oct
Depth of Heating	55 IRE 10.S1	43	1070	Sep
Depth of Modulation	54 IRE 12.S1	43	196	Feb
Depth of Penetration (Induction Heating Usage)	55 IRE 10.S1	43	1070	Sep
Depth of Velocity Modulation, Small Signal	57 IRE 7.S2	45	991	Jul
Desired Tract	54 IRE 12.S1	43	196	Feb
Destination	49 IRE 12.S1	37	1368	Dec
Detail	42 IRE 9.S1	Separate		
Detection	53 IRE 11.S1	41	613	May
Detector	52 IRE 17.S1	40	1682	Dec
Deviation Frequency	52 IRE 17.S1	40	1682	Dec

	Standard	PROCEEDINGS Vol	Page	Mo
Deviation from Pulse Flatness	54 IRE 12.S1	43	196	Feb
Deviation Distortion	52 IRE 17.S1	40	1682	Dec
Deviation Ratio	53 IRE 11.S1	41	613	May
Deviation Sensitivity (in FM)	52 IRE 17.S1	40	1682	Dec
Deviation Sensitivity (in Navigation Aids)	54 IRE 12.S1	43	196	Feb
Deviation Sensitivity Angular	54 IRE 12.S1	43	196	Feb
Diagnostic Routine	56 IRE 8.S1	44	1169	Sep
Dielectric Antenna	48 IRE 2,11,15.S1	Separate		
Dielectric Dissipation Factor	55 IRE 10.S1	43	1070	Sep
Dielectric Heating	55 IRE 10.S1	43	1070	Sep
Dielectric Phase Angle	55 IRE 10.S1	43	1070	Sep
Dielectric Power Factor	55 IRE 10.S1	43	1070	Sep
Dielectric Strength	55 IRE 10.S1	43	1070	Sep
Dielectric Waveguide	53 IRE 2.S1	41	1723	Dec
Difference Detector	54 IRE 12.S1	43	196	Feb
Difference in Depth of Modulation (DDM)	54 IRE 12.S1	43	196	Feb
Difference Limen	51 IRE 6.S1	39	515	May
Difference Transfer Function	55 IRE 26.S2	44	108	Jan
Differential Gain	55 IRE 23.S1	43	620	May
Differential Gain Control	54 IRE 12.S1	43	196	Feb
Differential Phase	55 IRE 23.S1	43	620	May
Differentiating Network	48 IRE 2,11,15.S1	Separate		
Differentiator	53 IRE 11.S1	41	613	May
Differentiator (in Electronic Computers)	56 IRE 8.S1	44	1169	Sep
Diffracted Wave	51 IRE 6.S1	39	515	May
Diffraction	51 IRE 6.S1	39	515	May
Diffuse Sound	51 IRE 6.S1	39	515	May
Diffuse Transmission Density	51 IRE 6.S1	39	515	May
Diffusion Constant	54 IRE 7.S2	42	1506	Oct
Diffusion Length	54 IRE 7.S2	42	1506	Oct
Digit	56 IRE 8.S1	44	1169	Sep
Digit, Binary	50 IRE 8.S1	39	273	Mar
Digit, Sign	50 IRE 8.S1	39	273	Mar
Digital Computer	56 IRE 8.S1	44	1169	Sep
Diode Characteristic	57 IRE 7.S2	45	992	Jul
Diode (Electron Tube)	57 IRE 7.S2	45	991	Jul
Diode, Semiconductor	54 IRE 7.S2	42	1506	Oct
Diplex Radio Transmission	48 IRE 2,11,15.S1	Separate		
Dipole Antenna	48 IRE 2,11,15.S1	Separate		
Direct-Coupled Attenuation	57 IRE 7.S2	45	992	Jul
Direct-Current Amplifier	48 IRE 2,11,15.S1	Separate		
Direct Grid Bias	57 IRE 7.S2	45	992	Jul
Direct Radiator Loudspeaker	51 IRE 6.S1	39	515	May
Direct Recording	56 IRE 9.S1	44	777	Jne
Direct Wave	50 IRE 24.S1	38	1265	Nov
Directed Reference Flight	54 IRE 12.S1	43	196	Feb
Direction	54 IRE 12.S1	43	196	Feb
Direction Finder (DF)	54 IRE 12.S1	43	196	Feb
Direction Finder Deviation	54 IRE 12.S1	43	196	Feb
Direction of Polarization	50 IRE 24.S1	38	1265	Nov
Direction of Propagation	53 IRE 2.S1	41	1723	Dec
Directional Antenna	48 IRE 2,11,15.S1	Separate		
Directional Coupler	55 IRE 2.S1	43	1074	Sep
Directional Gain	55 IRE 23.S1	43	620	May
Directional Homing	54 IRE 12.S1	43	196	Feb
Directional Microphone	51 IRE 6.S1	39	515	May
Directive Gain	48 IRE 2,11,15.S1	Separate		
Directivity	48 IRE 2,11,15.S1	Separate		
Directivity Factor	51 IRE 6.S1	39	515	May
Directivity Index	51 IRE 6.S1	39	515	May
Directivity Pattern	51 IRE 6.S1	39	515	May
Director	48 IRE 2,11,15.S1	Separate		

	Standard	PROCEEDINGS Vol	Page	Mo
Discharge	57 IRE 7.S2	45	992	Jul
Discrete Sentence Intelligibility	51 IRE 6.S1	39	515	May
Discrete Word Intelligibility	51 IRE 6.S1	39	516	May
Discriminator (General)	54 IRE 12.S1	43	196	Feb
Discriminator (Specific)	53 IRE 11.S1	41	613	May
Discriminator Constant Delay	54 IRE 12.S1	43	196	Feb
Discriminator, Pulse Duration	54 IRE 12.S1	43	196	Feb
Dish	54 IRE 12.S1	43	196	Feb
Disk Recorder	51 IRE 6.S1	39	516	May
Dispatcher	50 IRE 8.S1	39	273	Mar
Display	54 IRE 12.S1	43	196	Feb
Display Primaries	55 IRE 22.S1	43	745	Jne
Dissector Tube	57 IRE 7.S2	45	992	Jul
Dissymmetrical Transducer	51 IRE 20.S2	39	898	Aug
Distance Mark	54 IRE 12.S1	43	199	Feb
Distance Measuring Equipment	54 IRE 12.S1	43	208	Feb
Distance Resolution	54 IRE 12.S1	43	199	Feb
Distortion	53 IRE 4.S1	42	554	Mar
Distortion	52 IRE 17.S1	40	1682	Dec
Distortion Barrel	57 IRE 7.S2	45	992	Jul
Distortion, Keystone	57 IRE 7.S2	45	992	Jul
Distortion, Pincushion	57 IRE 7.S2	45	992	Jul
Distortion, S	57 IRE 7.S2	45	992	Jul
Distortion, Spiral	57 IRE 7.S2	45	992	Jul
Distributed Constant	53 IRE 2.S1	41	1723	Dec
Distribution Coefficients	55 IRE 22.S1	43	745	Jne
Disturbance	55 IRE 26.S2	44	109	Jan
Divergence Loss	51 IRE 6.S1	39	516	May
Dividing Network	51 IRE 6.S1	39	516	May
Doherty Amplifier	48 IRE 2,11,15.S1	Separate		
Domestic Induction Heater	55 IRE 10.S1	43	1070	Sep
Dominant Mode of Propagation	53 IRE 2.S1	41	1723	Dec
Dominant Wave	53 IRE 2.S1	41	1723	Dec
Dominant Wavelength	55 IRE 22.S1	43	745	Jne
Donor	54 IRE 7.S2	42	1506	Oct
Doping	54 IRE 7.S2	42	1506	Oct
Doping Compensation	54 IRE 7.S2	42	1506	Oct
Doppler Effect	51 IRE 6.S1	39	516	May
Doppler Shift	51 IRE 6.S1	39	516	May
Doppler System	54 IRE 12.S1	43	199	Feb
Doppler System, Pulsed	54 IRE 12.S1	43	199	Feb
Dot-Sequential	55 IRE 22.S1	53	745	Jne
Double-Length Number	56 IRE 8.S1	44	1169	Sep
Double Pole-Piece Magnetic Head	51 IRE 6.S1	39	516	May
Double-Precision Number	56 IRE 8.S1	44	1169	Sep
Double-Sideband Transmitter	48 IRE 2,11,15.S1	Separate		
Downward Modulation	52 IRE 17.S1	40	1682	Dec
Drift Angle	54 IRE 12.S1	43	199	Feb
Drift Correction Angle	54 IRE 12.S1	43	199	Feb
Drift Mobility	54 IRE 7.S2	42	1506	Oct
Drift Rate	57 IRE 7.S2	45	992	Jul
Drift Space	57 IRE 7.S2	45	992	Jul
Drive Pattern	56 IRE 9.S1	44	777	Jne
Drive Pin	51 IRE 6.S1	39	516	May
Drive-Pin Hole	51 IRE 6.S1	39	516	May
Driving-Point Admittance	57 IRE 7.S2	45	992	Jul
Driving Signals (in Television)	55 IRE 23.S1	43	620	May
Drum Speed	56 IRE 9.S1	44	777	Jne
Dual Frequency Induction Heater or Furnace	55 IRE 10.S1	43	1070	Sep
Dual Modulation	56 IRE 9.S1	44	777	Jne
Dual Networks	50 IRE 4.S1	39	27	Jan
Dubbing	51 IRE 6.S1	39	516	May
Dummy Antenna	52 IRE 17.S1	40	1682	Dec
Dummy Load	52 IRE 17.S1	40	1682	Dec

	Standard	Proceedings Vol	Page	Mo
Duplex Cavity	54 IRE 12.S1	43	199	Feb
Duplex Operation	48 IRE 2,11,15.S1	Separate		
Duplexing Assembly	54 IRE 12.S1	43	199	Feb
Duty Cycle	48 IRE 2,11,15.S1	Separate		
Duty Factor	48 IRE 2,11,15.S1	Separate		
Duty Ratio	54 IRE 12.S1	43	199	Feb
Dynamic Characteristic	57 IRE 7.S2	45	992	Jul
Dynamic Sequential Control	50 IRE 8.S1	39	273	Mar
Dynatron Oscillation	48 IRE 2,11,15.S1	Separate		
Dynatron Oscillator	48 IRE 2,11,15.S1	Separate		
Dynode	57 IRE 7.S2	45	992	Jul
Dynode Current	57 IRE 7.S2	45	992	Jul
Dynode Spots	57 IRE 7.S2	45	992	Jul
E				
E-Display	54 IRE 12.S1	43	199	Feb
E Layer	50 IRE 24.S1	38	1265	Nov
E-plane Bend	55 IRE 2.S1	43	1074	Sep
E-plane Tee Junction	55 IRE 2.S1	43	1074	Sep
E Region	50 IRE 24.S1	38	1265	Nov
E-H Tee	55 IRE 2.S1	43	1074	Sep
E-H Tuner	55 IRE 2.S1	43	1074	Sep
Earphone	51 IRE 6.S1	39	516	May
Earphone Coupler	51 IRE 6.S1	39	516	May
Eccentric Groove	51 IRE 6.S1	39	516	May
Eccentricity	51 IRE 6.S1	39	516	May
Echo (in Electroacoustics)	51 IRE 6.S1	39	516	May
Echo (in Facsimile)	56 IRE 9.S1	44	777	Jne
Echo (in Navigation Aids)	54 IRE 12.S1	43	199	Feb
Echo Box	54 IRE 12.S1	43	199	Feb
Echo, Second-Time Around	54 IRE 12.S1	43	199	Feb
Echo Suppressor	54 IRE 12.S1	43	199	Feb
Effective Acoustic Center	51 IRE 6.S1	39	516	May
Effective Area	48 IRE 2,11,15.S1	Separate		
Effective Band (in Facsimile)	56 IRE 9.S1	44	777	Jne
Effective Bandwidth	48 IRE 2,11,15.S1	Separate		
Effective Bunching Angle	57 IRE 7.S2	45	992	Jul
Effective Height	48 IRE 2,11,15.S1	Separate		
Effective Percentage Modulation	48 IRE 2,11,15.S1	Separate		
Effective Radius of the Earth	50 IRE 24.S1	38	1265	Nov
Effective Sound Pressure	51 IRE 6.S1	39	516	May
Efficiency	57 IRE 7.S2	45	992	Jul
Efficiency (Radiation Counter Tubes)	57 IRE 7.S2	45	992	Jul
Efficiency, Load Circuit	55 IRE 10.S1	43	1070	Sep
Efficiency, Over-all Electrical	55 IRE 10.S1	43	1070	Sep
Electra	54 IRE 12.S1	43	208	Feb
Electric Dipole	48 IRE 2,11,15.S1	Separate		
Electric Displacement Density	50 IRE 24.S1	38	1265	Nov
Electric Field	50 IRE 24.S1	38	1265	Nov
Electric Field Strength	50 IRE 24.S1	38	1265	Nov
Electric (Magnetic) Field Strength	52 IRE 17.S1	40	1682	Dec
Electric Field Vector	53 IRE 2.S1	41	1723	Dec
Electric Flux Density	50 IRE 24.S1	38	1265	Nov
Electric Transducer	51 IRE 20.S2	39	898	Aug
Electrical Distance	54 IRE 12.S1	43	199	Feb
Electrical Function Switch	50 IRE 8.S1	39	273	Mar
Electrical Length	53 IRE 2.S1	41	1723	Dec
Electrical Length	50 IRE 24.S1	38	1265	Nov
Electrical Noise	48 IRE 2,11,15.S1	Separate		
Electroacoustic Transducer	51 IRE 6.S1	39	516	May
Electroacoustic Transducer	51 IRE 20.S2	39	898	Aug
Electroacoustical Reciprocity Theorem	51 IRE 6.S1	39	516	May
Electrochemical Recording	56 IRE 9.S1	44	777	Jne
Electrode (Electron Tubes)	57 IRE 7.S2	45	992	Jul
Electrode (Semiconductor)	54 IRE 7.S2	42	1506	Oct
Electrode Admittance	57 IRE 7.S2	45	992	Jul
Electrode Capacitance	57 IRE 7.S2	45	993	Jul
Electrode Characteristic	57 IRE 7.S2	45	993	Jul
Electrode Conductance	57 IRE 7.S2	45	993	Jul
Electrode Current	57 IRE 7.S2	45	993	Jul
Electrode-Current Averaging Time	57 IRE 7.S2	45	993	Jul
Electrode Dark Current	57 IRE 7.S2	45	993	Jul
Electrode Dissipation	57 IRE 7.S2	45	993	Jul
Electrode Impedance	57 IRE 7.S2	45	993	Jul
Electrode Resistance	57 IRE 7.S2	45	993	Jul
Electrode Voltage	57 IRE 7.S2	45	993	Jul
Electrolytic Recording	56 IRE 9.S1	44	777	Jne
Electromagnetic Wave	50 IRE 24.S1	38	1265	Nov
Electromagnetic Wave	53 IRE 2.S1	41	1723	Dec
Electromechanical Recording	56 IRE 9.S1	44	777	Jne
Electromechanical Transducer	51 IRE 6.S1	39	517	May
Electromechanical Transducer	51 IRE 20.S2	39	898	Aug
Electrometer Tube	57 IRE 7.S2	45	993	Jul
Electron-Beam Tube	57 IRE 7.S2	45	993	Jul
Electron-Coupled Oscillator	48 IRE 2,11,15.S1	Separate		
Electron Device	57 IRE 7.S2	45	993	Jul
Electron Emission	57 IRE 7.S2	45	993	Jul
Electron Gun	57 IRE 7.S2	45	993	Jul
Electron-Gun Density Multiplication	57 IRE 7.S2	45	993	Jul
Electron Multiplier	57 IRE 7.S2	45	993	Jul
Electron-Stream Potential	57 IRE 7.S2	45	993	Jul
Electron-Stream Transmission Efficiency	56 IRE 7.S1	44	347	Mar
Electron Tube	57 IRE 7.S2	45	993	Jul
Electron-Wave Tube	57 IRE 7.S2	45	993	Jul
Electrons, Conduction	54 IRE 7.S2	42	1506	Oct
Electronic	57 IRE 7.S2	45	993	Jul
Electronic Efficiency	57 IRE 7.S2	45	993	Jul
Electronic Gap Admittance	57 IRE 7.S2	45	993	Jul
Electronic Keying	48 IRE 2,11,15.S1	Separate		
Electronic Line Scanning	56 IRE 9.S1	44	777	Jne
Electronic Microphone	51 IRE 6.S1	39	517	May
Electronic Raster Scanning	56 IRE 9.S1	44	777	Jne
Electronics	57 IRE 7.S2	45	993	Jul
Electrophonic Effect	51 IRE 6.S1	39	517	May
Electrostatic Actuator	51 IRE 6.S1	39	517	May
Electrostatic Focusing	57 IRE 7.S2	45	993	Jul
Electrostatic Loudspeaker	51 IRE 6.S1	39	517	May
Electrostatic Memory	50 IRE 8.S1	39	273	Mar
Electrostatic Memory Tube	50 IRE 8.S1	39	273	Mar
Electrostatic Microphone	51 IRE 6.S1	39	517	May
Electrostatic Recording	56 IRE 9.S1	44	777	Jne
Electrothermal Recording	56 IRE 9.S1	44	777	Jne
Element (of a Circuit)	50 IRE 4.S1	39	27	Jan
Element (Semiconductor)	54 IRE 7.S2	42	1506	Oct
Element (of a Tube)	57 IRE 7.S2	45	993	Jul
Elemental Area	56 IRE 9.S1	44	777	Jne
Elements of a Fix	54 IRE 12.S1	43	199	Feb
Elliptically Polarized Wave	53 IRE 2.S1	41	1723	Dec
Ellipticity	53 IRE 2.S1	41	1723	Dec
Elongation	42 IRE 9.S1	Separate		
Embossing Stylus	51 IRE 6.S1	39	517	May
Emission	57 IRE 7.S2	45	993	Jul
Emission Characteristic	57 IRE 7.S2	45	994	Jul
Emitter, Majority	54 IRE 7.S2	42	1506	Oct
Emitter, Minority	54 IRE 7.S2	42	1506	Oct
Enabling Pulse	54 IRE 12.S1	43	199	Feb
Encoder	56 IRE 8.S1	44	1169	Sep
End-Around Carry	56 IRE 8.S1	44	1169	Sep
End-Fire Array	48 IRE 2,11,15.S1	Separate		
End-of-Copy Signal	56 IRE 9.S1	44	778	Jne

	Standard	Proceedings Vol Page Mo
End Shield (Magnetrons)	57 IRE 7.S2	45 994 Jul
Energy Gap	54 IRE 7.S2	42 1506 Oct
Envelope Delay	56 IRE 9.S1	44 778 Jne
Envelope Delay	50 IRE 24.S1	38 1265 Nov
Envelope Delay Distortion	56 IRE 9.S1	44 778 Jne
Equal-Energy Source	55 IRE 22.S1	43 745 Jne
Equalizing Pulses	55 IRE 23.S1	43 620 May
Equally Tempered Scale	51 IRE 6.S1	39 517 May
Equation Solver	50 IRE 8.S1	39 273 Mar
Equiphase Surface	50 IRE 24.S1	38 1265 Nov
Equiphase Zone	54 IRE 12.S1	43 199 Feb
Equipotential Cathode	57 IRE 7.S2	45 994 Jul
Equisignal Localizer	54 IRE 12.S1	43 199 Feb
Equisignal Zone	49 IRE 12.S1	37 1368 Dec
Equivalent Conductance	57 IRE 7.S2	45 994 Jul
Equivalent Dark-Current Input	57 IRE 7.S2	45 994 Jul
Equivalent Diode	57 IRE 7.S2	45 994 Jul
Equivalent Noise Conductance	57 IRE 7.S2	45 994 Jul
Equivalent Noise Current	57 IRE 7.S2	45 994 Jul
Equivalent Noise Resistance	57 IRE 7.S2	45 994 Jul
Erase	57 IRE 7.S2	45 994 Jul
Erasing Head	51 IRE 6.S1	39 517 May
Erasing Speed (in Charge-Storage Tubes)	57 IRE 7.S2	45 994 Jul
Error	56 IRE 8.S1	44 1169 Sep
Error-Detecting Code	56 IRE 8.S1	44 1169 Sep
Error, Height	54 IRE 12.S1	43 199 Feb
Error, Instrumental	54 IRE 12.S1	43 199 Feb
Error, Round-Off	50 IRE 8.S1	39 273 Mar
Error, Sky	54 IRE 12.S1	43 199 Feb
Error, Truncation	50 IRE 8.S1	39 273 Mar
Eureka	54 IRE 12.S1	43 208 Feb
Excess-Three Code	56 IRE 8.S1	44 1169 Sep
Excitation (Drive)	48 IRE 2,11,15.S2	Separate
Excitation Purity	55 IRE 22.S1	43 745 Jne
Excited Field Loudspeaker	51 IRE 6.S1	39 517 May
Exciter	48 IRE 2,11,15.S1	Separate
Expansion	53 IRE 11.S1	41 613 May
Exponential Flare-Out	54 IRE 12.S1	43 199 Feb
Exponential Horn	51 IRE 6.S1	39 517 May
Exponential Transmission	53 IRE 2.S1	41 1723 Dec
External Termination	57 IRE 7.S2	45 994 Jul
Externally Quenched Counter Tube	57 IRE 7.S2	45 994 Jul
Extract	56 IRE 8.S1	44 1169 Sep
Extract Instruction	50 IRE 8.S1	39 273 Mar
Extraordinary-Wave Component	50 IRE 24.S1	38 1266 Nov
Extrinsic Properties	54 IRE 7.S2	42 1506 Oct

F

F-Display	54 IRE 12.S1	43 200 Feb
F Layer	50 IRE 24.S1	38 1266 Nov
F Region	50 IRE 24.S1	38 1266 Nov
FS to AM Converter	56 IRE 9.S1	44 778 Jne
FTC	54 IRE 12.S1	43 200 Feb
Facsimile (in Electrical Communications)	56 IRE 9.S1	44 778 Jne
Facsimile Receiver	42 IRE 9.S1	Separate
Facsimile Recorder	42 IRE 9.S1	Separate
Facsimile Signal (Picture Signal)	56 IRE 9.S1	44 778 Jne
Facsimile-Signal Level	56 IRE 9.S1	44 778 Jne
Facsimile System	56 IRE 9.S1	44 778 Jne
Facsimile Transient	56 IRE 9.S1	44 778 Jne
Facsimile Transmission	56 IRE 9.S1	44 778 Jne
Facsimile Transmitter	42 IRE 9.S1	Separate
Factor	57 IRE 7.S2	45 994 Jul
Fading	50 IRE 24.S1	38 1266 Nov
False Course	54 IRE 12.S1	43 199 Feb
Fan Beam	54 IRE 12.S1	43 200 Feb
Fan Marker	54 IRE 12.S1	43 208 Feb
Fanned-Beam Antenna	48 IRE 2,11,15.S1	Separate
Fast Groove	51 IRE 6.S1	39 517 May
Fast-Time-Constant Circuit	54 IRE 12.S1	43 200 Feb
Fault Electrode Current	57 IRE 7.S2	45 994 Jul
Feedback	48 IRE 2,11,15.S1	Separate
Feedback Control Loop	55 IRE 26.S2	44 108 Jan
Feedback Control System	55 IRE 26.S2	44 108 Jan
Feedback Control System Linear	56 IRE 26.S2	44 108 Jan
Feedback Control System Nonlinear	56 IRE 26.S2	44 109 Jan
Feedback Control System, Quasi-Linear	56 IRE 26.S2	44 109 Jan
Feedback Oscillator	48 IRE 2,11,15.S1	Separate
Feedback Path	56 IRE 26.S2	44 108 Jan
Feedback Regulator	56 IRE 26.S2	44 109 Jan
Feedback Transfer Function	56 IRE 26.S2	44 108 Jan
Fermi Level	54 IRE 7.S2	42 1506 Oct
Fidelity	52 IRE 17.S1	40 1682 Dec
Fidelity	48 IRE 2,11,15.S1	Separate
Field (in Television)	55 IRE 23.S1	43 620 May
Field Emission	57 IRE 7.S2	45 994 Jul
Field-Enhanced Photoelectric Emission	57 IRE 7.S2	45 994 Jul
Field-Enhanced Secondary Emission	57 IRE 7.S2	45 994 Jul
Field-Free Emission Current	57 IRE 7.S2	45 994 Jul
Field Frequency	55 IRE 23.S1	43 620 May
Field Sequential	55 IRE 22.S1	43 746 Jne
Field Strength, Electric or Magnetic	52 IRE 17.S1	40 1682 Dec
Field Strength Meter	55 IRE 10.S1	43 1070 Sep
Filament	57 IRE 7.S2	45 994 Jul
Filament Current	50 IRE 7.S1	38 433 Apr
Filament Voltage	50 IRE 7.S1	38 433 Apr
Filler	51 IRE 6.S1	39 517 May
Fine Chrominance Primary	55 IRE 22.S1	43 746 Jne
Fired Tube	57 IRE 7.S2	45 994 Jul
Firing Time, High-Level	57 IRE 7.S2	45 995 Jul
Fishbone Antenna	48 IRE 2,11,15.S1	Separate
Fix	54 IRE 12.S1	43 200 Feb
Fixed-Frequency Transmitter	48 IRE 2,11,15.S1	Separate
Fixed-Point System	56 IRE 8.S1	44 1169 Sep
Fixed Transmitter	48 IRE 2,11,15.S1	Separate
Flag Alarm	54 IRE 12.S1	43 200 Feb
Flare-Out	54 IRE 12.S1	43 200 Feb
Flat Leakage Power	57 IRE 7.S2	45 995 Jul
Flat Spot	54 IRE 12.S1	43 200 Feb
Flection-Point Emission Current	57 IRE 7.S2	45 995 Jul
Flicker	55 IRE 22.S1	43 746 Jne
Flight Path	54 IRE 12.S1	43 200 Feb
Flight Path Computer	54 IRE 12.S1	43 200 Feb
Flight Path Deviation	54 IRE 12.S1	43 200 Feb
Flight-Path-Deviation Indicator	54 IRE 12.S1	43 200 Feb
Flight-Path-Reference Flight	54 IRE 12.S1	43 200 Feb
Flight Track	54 IRE 12.S1	43 200 Feb
Flip-Flop	56 IRE 8.S1	44 1169 Sep
Floating-Point System	56 IRE 8.S1	44 1169 Sep
Flood Projection	56 IRE 9.S1	44 778 Jne
Flow Diagram (in Electronic Computers)	56 IRE 8.S1	44 1169 Sep
Flowed Wax	51 IRE 6.S1	39 517 May
Flutter	52 IRE 17.S1	40 1683 Dec
Flutter Echo	51 IRE 6.S1	39 517 May

	Standard	PROCEEDINGS Vol	Page	Mo
Flux Guide	55 IRE 10.S1	43	1070	Sep
Focusing	57 IRE 7.S2	45	995	Jul
Focusing and Switching Grille	57 IRE 7.S2	45	995	Jul
Focusing Coil or Focusing Magnet	57 IRE 7.S2	45	995	Jul
Focusing Dynamic	57 IRE 7.S2	45	995	Jul
Focusing Electrode	57 IRE 7.S2	45	995	Jul
Focusing Magnet or Coil	57 IRE 7.S2	45	995	Jul
Folded Dipole Antenna	48 IRE 2,11,15.S1	Separate		
Footcandle	55 IRE 22.S1	43	746	Jne
Footlambert	55 IRE 22.S1	43	746	Jne
Forbidden-Combination Check	56 IRE 8.S1	44	1169	Sep
Force Factor	56 IRE 6.S1	39	517	May
Fork Beat	56 IRE 9.S1	44	778	Jne
Forming	54 IRE 7.S2	42	1506	Oct
Fortuitous Telegraph Distortion	48 IRE 2,11,15.S1	Separate		
Forward Path	56 IRE 26.S2	44	108	Jan
Forward Transfer Function	56 IRE 26.S2	44	108	Jan
Forward Wave	57 IRE 7.S2	45	995	Jul
Four-Address Code	56 IRE 8.S1	44	1169	Sep
Four-Pole	50 IRE 4.S1	39	27	Jan
Frame (in Facsimile)	56 IRE 9.S1	44	778	Jne
Frame (in TV)	55 IRE 23.S1	43	620	May
Frame Frequency	55 IRE 23.S1	43	620	May
Framer	42 IRE 9.S1	Separate		
Framing	56 IRE 9.S1	44	778	Jne
Framing Signal	56 IRE 9.S1	44	778	Jne
Fraunhofer Region	48 IRE 2,11,15.S1	Separate		
Free Field	51 IRE 6.S1	39	517	May
Free-Field Current Response	51 IRE 6.S1	39	518	May
Free-Field Voltage	51 IRE 6.S1	39	518	May
Free Impedance	51 IRE 6.S1	39	518	May
Free Motional Impedance	51 IRE 6.S1	39	518	May
Free Oscillations	48 IRE 2,11,15.S1	Separate		
Free Progressive Wave	51 IRE 6.S1	39	518	May
Free-Running Frequency	52 IRE 17.S1	40	1683	Dec
Frequency Band	48 IRE 2,11,15.S1	Separate		
Frequency Band of Emission	48 IRE 2,11,15.S1	Separate		
Frequency Conversion Transducer	51 IRE 20.S2	39	898	Aug
Frequency Departure	48 IRE 2,11,15.S1	Separate		
Frequency Departure	52 IRE 17.S1	40	1683	Dec
Frequency Deviation	53 IRE 11.S1	41	613	May
Frequency Deviation	52 IRE 17.S1	40	1683	Dec
Frequency Distortion	53 IRE 4.S1	42	554	Mar
Frequency Divider	51 IRE 20.S2	39	898	Aug
Frequency-Division Multiplex	53 IRE 11.S1	41	613	May
Frequency Doubler	48 IRE 2,11,15.S1	Separate		
Frequency Interlace	55 IRE 22.S1	43	746	Jne
Frequency-Modulated Transmitter	48 IRE 2,11,15.S1	Separate		
Frequency Modulation	52 IRE 17.S1	40	1683	Dec
Frequency Modulation	53 IRE 11.S1	41	613	May
Frequency Multiplier	48 IRE 2,11,15.S1	Separate		
Frequency Multiplier	51 IRE 20.S2	39	898	Aug
Frequency Pulling	57 IRE 7.S2	45	995	Jul
Frequency Range (of a Device)	57 IRE 7.S2	45	995	Jul
Frequency Record	51 IRE 6.S1	39	518	May
Frequency-Response Equalization	51 IRE 6.S1	39	518	May
Frequency-Shift Keying or FSK	53 IRE 11.S1	41	613	May
Frequency Stabilization	48 IRE 2,11,15.S1	Separate		
Frequency Swing	53 IRE 11.S1	41	613	May
Frequency Tolerance of a Radio Transmitter	48 IRE 2,11,15.S1	Separate		
Frequency Tripler	48 IRE 2,11,15.S1	Separate		
Fresnel Region	48 IRE 2,11,15.S1	Separate		
Front Porch	55 IRE 23.S1	43	620	May
Front-to-Rear Ratio	48 IRE 2,11,15.S1	Separate		
Fruit Pulse	52 IRE 20.S1	40	553	May
Function Switch	50 IRE 8.S1	39	274	Mar
Function Switch, Many-One	50 IRE 8.S1	39	274	Mar
Function Switch, One-Many	50 IRE 8.S1	39	274	Mar
Function Unit	50 IRE 8.S1	39	274	Mar
Fundamental Component	53 IRE 4.S1	42	554	Mar
Fundamental Frequency	53 IRE 4.S1	42	554	Mar
Fundamental Tone	51 IRE 6.S1	39	518	May
G				
Gate	56 IRE 8.S1	44	1169	Sep
GCA (Ground-Controlled Approach)	54 IRE 12.S1	43	208	Feb
GCI (Ground-Controlled Interception)	54 IRE 12.S1	43	208	Feb
G-Display	54 IRE 12.S1	43	200	Feb
GEE	54 IRE 12.S1	43	208	Feb
GEE-H	54 IRE 12.S1	43	208	Feb
GPI (Ground Position Indicator)	54 IRE 12.S1	43	208	Feb
Gain (General)	54 IRE 3.S1	42	1110	Jul
Gain (Specific)	50 IRE 7.S1	38	433	Apr
Gain, Available Conversion	57 IRE 7.S2	45	995	Jul
Gain, Available-Power	57 IRE 7.S2	45	995	Jul
Gain, Available Power Maximum	57 IRE 7.S2	45	995	Jul
Gain-Control, Temporal	54 IRE 12.S1	43	200	Feb
Gain Conversion Voltage	57 IRE 7.S2	45	995	Jul
Gain, Insertion	57 IRE 7.S2	45	995	Jul
Gain, Insertion Voltage	57 IRE 7.S2	45	995	Jul
Gain of an Antenna	48 IRE 2,11,15.S1	Separate		
Gain Time Control	54 IRE 12.S1	43	200	Feb
Gain, Transducer	57 IRE 7.S2	45	995	Jul
Gain Turn Down	54 IRE 12.S1	43	200	Feb
Galvanometer	51 IRE 6.S1	39	518	May
Gamma (Film Recording)	51 IRE 6.S1	39	518	May
Gamma (Picture Tube)	57 IRE 7.S2	45	995	Jul
Gamma (TV)	55 IRE 22.S1	43	746	Jne
Gamma Correction	55 IRE 22.S1	43	746	Jne
Gap	57 IRE 7.S2	45	996	Jul
Gap Admittance, Circuit	57 IRE 7.S2	45	996	Jul
Gap Admittance, Electronic	57 IRE 7.S2	45	996	Jul
Gap Capacitance Effective	57 IRE 7.S2	45	996	Jul
Gap Coding	54 IRE 12.S1	43	200	Feb
Gap Length	51 IRE 6.S1	39	518	May
Gap Loading Multipactor	57 IRE 7.S2	45	996	Jul
Gap Loading Primary Transit-Angle	57 IRE 7.S2	45	996	Jul
Gap Loading, Secondary Electron	57 IRE 7.S2	45	996	Jul
Gas Amplification	57 IRE 7.S2	45	996	Jul
Gas Amplification Factor	57 IRE 7.S2	45	996	Jul
Gas (Ionization) Current	57 IRE 7.S2	45	996	Jul
Gas-Filled Radiation-Counter Tube	57 IRE 7.S2	45	996	Jul
Gas-Flow Counter Tube	57 IRE 7.S2	45	996	Jul
Gas Focusing	57 IRE 7.S2	45	996	Jul
Gas Ratio	57 IRE 7.S2	45	996	Jul
Gas Tube	57 IRE 7.S2	45	996	Jul
Gaseous Tube Generator	55 IRE 10.S1	43	1070	Sep
Gating	53 IRE 11.S1	41	613	May
Gear Pattern	56 IRE 9.S1	44	778	Jne
Geiger-Mueller Counter Tube	57 IRE 7.S2	45	996	Jul
Geiger-Mueller Region	57 IRE 7.S2	45	996	Jul
Geiger-Mueller Threshold	57 IRE 7.S2	45	996	Jul
Generation Rate	54 IRE 7.S2	42	1506	Oct
Generator	57 IRE 7.S2	45	996	Jul
Geodesic	54 IRE 12.S1	43	200	Feb
Geometrical Error	54 IRE 12.S1	43	200	Feb
Geometrical Factor	54 IRE 12.S1	43	200	Feb
Ghost Pulse	54 IRE 12.S1	43	200	Feb
Ghost Signals	54 IRE 12.S1	43	200	Feb

	Standard	PROCEEDINGS Vol	Page	Mo
Gill-Morrell Oscillator	48 IRE 2,11,15.S1	Separate		
Glide-Path	54 IRE 12.S1	43	200	Feb
Glide-Slope	54 IRE 12.S1	43	200	Feb
Glide-Slope Angle	54 IRE 12.S1	43	200	Feb
Glide-Slope Deviation	54 IRE 12.S1	43	200	Feb
Glide-Slope Facility	54 IRE 12.S1	43	200	Feb
Glide-Slope Sector	54 IRE 12.S1	43	200	Feb
Glow Discharge	57 IRE 7.S2	45	996	Jul
Glow-Discharge Cold-Cathode Tube	50 IRE 7.S1	38	434	Apr
Glow-Discharge Tube	57 IRE 7.S2	45	996	Jul
Glue Line Heating	55 IRE 10.S1	43	1070	Sep
Gradient Microphone	51 IRE 6.S1	39	518	May
Grain	51 IRE 6.S1	39	518	May
Graininess	51 IRE 6.S1	39	518	May
Grass	54 IRE 12.S1	43	200	Feb
Grating Reflector	48 IRE 2,11,15.S1	Separate		
Grid (of a Tube)	57 IRE 7.S2	45	996	Jul
Grid Bearing	49 IRE 12.S1	37	1368	Dec
Grid Bias	57 IRE 7.S2	45	996	Jul
Grid Characteristic	57 IRE 7.S2	45	996	Jul
Grid-Controlled Mercury-Arc Rectifier	48 IRE 2,11,15.S1	Separate		
Grid Course	49 IRE 12.S1	37	1368	Dec
Grid Current	57 IRE 7.S2	45	996	Jul
Grid-Drive Characteristic	57 IRE 7.S2	45	996	Jul
Grid Driving Power	57 IRE 7.S2	45	996	Jul
Grid Emission	57 IRE 7.S2	45	996	Jul
Grid Heading	49 IRE 12.S1	37	1368	Dec
Grid Modulation	48 IRE 2,11,15.S1	Separate		
Grid Neutralization	48 IRE 2,11,15.S1	Separate		
Grid North	49 IRE 12.S1	37	1368	Dec
Grid Pulse Modulation	48 IRE 2,11,15.S1	Separate		
Grid Voltage	57 IRE 7.S2	45	996	Jul
Groove	51 IRE 6.S1	39	518	May
Groove Angle	51 IRE 6.S1	39	518	May
Groove Shape	51 IRE 6.S1	39	518	May
Groove Speed	51 IRE 6.S1	39	518	May
Ground-Controlled Approach	49 IRE 12.S1	37	1368	Dec
Ground Clutter	54 IRE 12.S1	43	200	Feb
Ground Distance	54 IRE 12.S1	43	200	Feb
Ground Equalizer Inductors	48 IRE 2,11,15.S1	Separate		
Ground Noise	51 IRE 6.S1	39	519	May
Ground-Position Indicator	49 IRE 12.S1	37	1368	Dec
Ground Return (Radar)	54 IRE 12.S1	43	200	Feb
Ground Speed	54 IRE 12.S1	43	200	Feb
Ground Surveillance Radar	49 IRE 12.S1	37	1368	Dec
Ground System of an Antenna	48 IRE 2,11,15.S1	Separate		
Ground Wave	50 IRE 24.S1	38	1266	Nov
Grounded-Cathode Amplifier	48 IRE 2,11,15.S1	Separate		
Grounded-Grid Amplifier	48 IRE 2,11,15.S1	Separate		
Grounded-Plate Amplifier	48 IRE 2,11,15.S1	Separate		
Grouping (in Recording)	51 IRE 6.S1	39	519	May
Grouping (in Facsimile)	56 IRE 9.S1	44	778	Jne
Group Velocity	50 IRE 24.S1	38	1266	Nov
Guard Circle	51 IRE 6.S1	39	519	May
Guided Wave	50 IRE 24.S1	38	1266	Nov

H

H	54 IRE 12.S1	43	208	Feb
H and D Curve	51 IRE 6.S1	39	519	May
H-Display	54 IRE 12.S1	43	201	Feb
H Network	50 IRE 4.S1	39	27	Jan
H-plane Bend	55 IRE 2.S1	43	1074	Sep
H-plane Tee Junction	55 IRE 2.S1	43	1074	Sep
Half Adder	56 IRE 8.S1	44	1170	Sep
Half-Power Width of a Radiation Lobe	48 IRE 2,11,15.S1	Separate		
Halftone Characteristic	56 IRE 9.S1	44	778	Jne
Hall Constant	54 IRE 7.S2	42	1506	Oct
Harmonic	53 IRE 4.S1	42	554	Mar
Harmonic Conversion Transducer	51 IRE 20.S2	39	898	Aug
Harmonic Conversion Transducer	57 IRE 7.S2	45	996	Jul
Harmonic Distortion	53 IRE 4.S1	42	554	Mar
Harmonic Distortion	52 IRE 17.S1	40	1683	Dec
Harmonic Leakage Power	57 IRE 7.S2	45	996	Jul
Harmonic Series of Sounds	51 IRE 6.S1	39	519	May
Hartley Oscillator	48 IRE 2,11,15.S1	Separate		
Heading	54 IRE 12.S1	43	201	Feb
Hearing Loss	51 IRE 6.S1	39	519	May
Hearing Loss for Speech	51 IRE 6.S1	39	519	May
Heat Loss	53 IRE 2.S1	41	1723	Dec
Heater	57 IRE 7.S2	45	996	Jul
Heater Coil	55 IRE 10.S1	43	1070	Sep
Heater Current	50 IRE 7.S1	38	434	Apr
Heater Voltage	50 IRE 7.S1	38	434	Apr
Heater Warm-Up Time	57 IRE 7.S2	45	996	Jul
Heating Pattern	55 IRE 10.S1	43	1070	Sep
Heating Station	55 IRE 10.S1	43	1070	Sep
Heating Time	57 IRE 7.S2	45	997	Jul
Height Error	54 IRE 12.S1	43	201	Feb
Height Error, Ionospheric	54 IRE 12.S1	43	201	Feb
Height Markers (Radar)	54 IRE 12.S1	43	201	Feb
Heptode	57 IRE 7.S2	45	997	Jul
Heterodyne Conversion Transducer	57 IRE 7.S2	45	997	Jul
Heterodyne Conversion Transducer (Converter)	51 IRE 20.S2	39	898	Aug
Hexadecimal	56 IRE 8.S1	44	1170	Sep
Hexode	57 IRE 7.S2	45	997	Jul
High-Frequency Induction Heater or Furnace	55 IRE 10.S1	43	1070	Sep
High-Level Firing Time	57 IRE 7.S2	45	997	Jul
High-Level Modulation	48 IRE 2,11,15.S1	Separate		
High-Level Radio-Frequency Signal	57 IRE 7.S2	45	997	Jul
High-Level VSWR	57 IRE 7.S2	45	997	Jul
High-Speed Carry	56 IRE 8.S1	44	1170	Sep
High-Velocity Scanning	57 IRE 7.S2	45	997	Jul
Hold	57 IRE 7.S2	45	997	Jul
Holding Beam	50 IRE 8.S1	39	274	Mar
Hole	54 IRE 7.S2	42	1506	Oct
Homing	54 IRE 12.S1	43	201	Feb
Horizontal Ring Induction Furnace	55 IRE 10.S1	43	1071	Sep
Horizontally Polarized Wave	50 IRE 24.S1	38	1266	Nov
Horn Loudspeaker	51 IRE 6.S1	39	519	May
Horn Mouth	51 IRE 6.S1	39	519	May
Horn Radiator	48 IRE 2,11,15.S1	Separate		
Horn Throat	51 IRE 6.S1	39	519	May
Hot Cathode	57 IRE 7.S2	45	997	Jul
Hot-Cathode Tube	57 IRE 7.S2	45	997	Jul
Hot-Wire Microphone	51 IRE 6.S1	39	519	May
Hue	55 IRE 22.S1	43	746	Jne
Hum	52 IRE 17.S1	40	1683	Dec
Hum Modulation	52 IRE 17.S1	40	1683	Dec
Hybrid Electromagnetic Wave	53 IRE 2.S1	41	1727	Dec
Hybrid Junction	55 IRE 2.S1	43	1074	Sep
Hybrid Tee	55 IRE 2.S1	43	1074	Sep
Hydrophone	51 IRE 6.S1	39	519	May
Hyperbolic Flare-Out	54 IRE 12.S1	43	201	Feb
Hysteresis (of an Oscillation)	57 IRE 7.S2	45	997	Jul
Hysteresis (Radiation-Counter)	57 IRE 7.S2	45	997	Jul
Hysteresis Heater	55 IRE 10.S1	43	1071	Sep

	Standard	Proceedings Vol	Page	Mo
I				
ICI	55 IRE 22.S1	43	746	Jne
ICW	48 IRE 2,11,15.S1	Separate		
I-Display (also I-Scan or I-Scope)	54 IRE 12.S1	43	201	Feb
IF	52 IRE 17.S1	40	1683	Dec
ILS (Instrument-Landing-System)	54 IRE 12.S1	43	208	Feb
IR	54 IRE 12.S1	43	201	Feb
Iconoscope	57 IRE 7.S2	45	997	Jul
Ideal Noise Diode	57 IRE 7.S2	45	997	Jul
Ideal Transducer	51 IRE 20.S2	39	898	Aug
Ideal Transducer	54 IRE 3.S1	42	1110	Jul
Ideal Transformer	54 IRE 3.S1	42	1110	Jul
Identification	54 IRE 12.S1	43	201	Feb
Ignitor	57 IRE 7.S2	45	997	Jul
Ignitor Current	57 IRE 7.S2	45	997	Jul
Ignitor-Current Temperature Drift	57 IRE 7.S2	45	997	Jul
Ignitor Discharge	57 IRE 7.S2	45	997	Jul
Ignitor Electrode	57 IRE 7.S2	45	997	Jul
Ignitor Firing Time	57 IRE 7.S2	45	997	Jul
Ignitor Interaction	57 IRE 7.S2	45	997	Jul
Ignitor Leakage Resistance	57 IRE 7.S2	45	997	Jul
Ignitor Oscillation	57 IRE 7.S2	45	997	Jul
Ignitor Voltage Drop	57 IRE 7.S2	45	997	Jul
Illuminance	55 IRE 22.S1	43	746	Jne
Image Converter Tube	57 IRE 7.S2	45	997	Jul
Image Dissector Tube	57 IRE 7.S2	45	997	Jul
Image Frequency	52 IRE 17.S1	40	1683	Dec
Image Ionoscope	57 IRE 7.S2	45	997	Jul
Image Orthicon	57 IRE 7.S2	45	997	Jul
Image Ratio	52 IRE 17.S1	40	1683	Dec
Image Tube	57 IRE 7.S2	45	997	Jul
Impedance	57 IRE 7.S2	45	997	Jul
Impedance Compensator	42 IRE 9.S1	Separate		
Imperfection	54 IRE 7.S2	42	1506	Oct
Improvement Threshold	53 IRE 11.S1	41	613	May
Impulse Excitation	48 IRE 2,11,15.S1	Separate		
Impulse Noise	48 IRE 2,11,15.S1	Separate		
Impurity (Chemical)	54 IRE 7.S2	42	1506	Oct
Impurity, Acceptor	54 IRE 7.S2	42	1506	Oct
Impurity, Donor	54 IRE 7.S2	42	1507	Oct
Impurity, Stoichiometric	54 IRE 7.S2	42	1507	Oct
Incident Wave	50 IRE 24.S1	38	1266	Nov
Incident Wave	53 IRE 2.S1	41	1723	Dec
Incoherent Scattering	50 IRE 24.S1	38	1266	Nov
Index of Cooperation (in Facsimile)	56 IRE 9.S1	44	778	Jne
Indicated Course Error	54 IRE 12.S1	43	201	Feb
Indicator Tube	57 IRE 7.S2	45	997	Jul
Indirectly Heated Cathode	57 IRE 7.S2	45	997	Jul
Induced Current	55 IRE 10.S1	43	1071	Sep
Induction-Conduction Heater	55 IRE 10.S1	43	1071	Sep
Induction Heating	55 IRE 10.S1	43	1071	Sep
Induction Loudspeaker	51 IRE 6.S1	39	519	May
Induction Ring Heater	55 IRE 10.S1	43	1071	Sep
Inductive Neutralization	48 IRE 2,11,15.S1	Separate		
Inflection-Point Emission Current	57 IRE 7.S2	45	997	Jul
Infrasonic Frequency	51 IRE 6.S1	39	519	May
Inhibiting Input	56 IRE 8.S1	44	1170	Sep
Initial Ionizing Event	57 IRE 7.S2	45	998	Jul
Ink Vapor Recording	56 IRE 9.S1	44	778	Jne
Input Capacitance	57 IRE 7.S2	45	998	Jul
Input Equipment (in Computers)	50 IRE 8.S1	39	274	Mar
Input Gap	57 IRE 7.S2	45	998	Jul
Input Impedance	54 IRE 3.S1	42	1110	Jul
Input Impedance (of a Transmission Line)	53 IRE 2.S1	41	1723	Dec
Inscriber	50 IRE 8.S1	39	274	Mar
Insert Earphones	51 IRE 6.S1	39	519	May
Insertion Gain	54 IRE 3.S1	42	1110	Jul
Insertion Gain	51 IRE 20.S2	39	899	Aug
Insertion Gain	57 IRE 7.S2	45	998	Jul
Insertion Loss	57 IRE 7.S2	45	998	Jul
Insertion Loss (General)	51 IRE 20.S2	39	899	Aug
Insertion Loss (General)	54 IRE 3.S1	42	1111	Jul
Insertion Loss (Waveguide)	53 IRE 2.S1	41	1723	Dec
Insertion Power Gain	50 IRE 7.S1	38	434	Apr
Insertion Voltage Gain	57 IRE 7.S2	45	998	Jul
Instantaneous Automatic Gain Control	54 IRE 12.S1	43	201	Feb
Instantaneous Companding	53 IRE 11.S1	41	613	May
Instantaneous Frequency	53 IRE 11.S1	41	613	May
Instantaneous Power Output	48 IRE 2,11,15.S1	Separate		
Instantaneous Recording	51 IRE 6.S1	39	519	May
Instantaneous Sampling	53 IRE 11.S1	41	613	May
Instantaneous Sound Pressure	51 IRE 6.S1	39	519	May
Instruction	56 IRE 8.S1	44	1170	Sep
Instruction Code	56 IRE 8.S1	44	1170	Sep
Instrument Approach	54 IRE 12.S1	43	201	Feb
Instrument Approach System	54 IRE 12.S1	43	201	Feb
Instrument Landing System	54 IRE 12.S1	43	201	Feb
Instrumental Error (in Navigation)	54 IRE 12.S1	43	201	Feb
Integrating Network	53 IRE 11.S1	41	613	May
Integrator	56 IRE 8.S1	44	1170	Sep
Intelligence Bandwidth	48 IRE 2,11,15.S1	Separate		
Intensifier Electrode	57 IRE 7.S2	45	998	Jul
Intensity Level	51 IRE 6.S1	39	519	May
Intensity Modulation	54 IRE 12.S1	43	201	Feb
Interaction Circuit Phase Velocity	57 IRE 7.S2	45	998	Jul
Interaction Gap	57 IRE 7.S2	45	998	Jul
Interaction Impedance	57 IRE 7.S2	45	998	Jul
Interaction Space	57 IRE 7.S2	45	998	Jul
Intercarrier Sound	52 IRE 17.S1	40	1683	Dec
Interdigital Magnetron	57 IRE 7.S2	45	998	Jul
Interelectrode Capacitance	57 IRE 7.S2	45	998	Jul
Interelectrode Transadmittance	57 IRE 7.S2	45	998	Jul
Interelectrode Transconductance	57 IRE 7.S2	45	998	Jul
Interference (General)	52 IRE 17.S1	40	1683	Dec
Interference (Induction Heating)	55 IRE 10.S1	43	1071	Sep
Interference Guard Bands	48 IRE 2,11,15.S1	Separate		
Interlaced Scanning	55 IRE 23.S1	43	620	May
Intermediate Frequency	52 IRE 17.S1	40	1683	Dec
Intermediate-Frequency-Harmonic Interference	52 IRE 17.S1	40	1683	Dec
Intermediate-Frequency Interference Ratio	52 IRE 17.S1	40	1683	Dec
Intermediate-Frequency Response Ratio	52 IRE 17.S1	40	1683	Dec
Intermediate Subcarrier	53 IRE 11.S1	41	613	May
Intermittent-Duty Rating	48 IRE 2,11,15.S1	Separate		
Intermodulation	52 IRE 17.S1	40	1683	Dec
Internal Correction Voltage	57 IRE 7.S2	45	998	Jul
Interrogation	54 IRE 12.S1	43	201	Feb
Interrogator	54 IRE 12.S1	43	201	Feb
Interrogator-Responsor	54 IRE 12.S1	43	201	Feb
Interval	51 IRE 6.S1	39	519	May
Intrinsic Properties	54 IRE 7.S2	42	1507	Oct
Intrinsic Temperature Range	54 IRE 7.S2	42	1507	Oct
Inverse Electrode Current	57 IRE 7.S2	45	998	Jul
Inverse Limiter	53 IRE 11.S1	41	613	May
Ionic-Heated Cathode	57 IRE 7.S2	45	998	Jul
Ionic-Heated-Cathode Tube	57 IRE 7.S2	45	998	Jul
Ionization Current	57 IRE 7.S2	45	998	Jul

	Standard	Proceedings Vol	Page	Mo
Ionization Time	57 IRE 7.S2	45	998	Jul
Ionizing Event	57 IRE 7.S2	45	998	Jul
Ionosphere	50 IRE 24.S1	38	1266	Nov
Ionospheric Error	54 IRE 12.S1	43	201	Feb
Ionospheric Height Error	54 IRE 12.S1	43	201	Feb
Ionospheric Wave	50 IRE 24.S1	38	1266	Nov
Ion Spot	50 IRE 7.S1	38	434	Apr
Ion Spot (Camera Tube)	57 IRE 7.S2	45	998	Jul
Ion Spot (Picture Tube)	57 IRE 7.S2	45	998	Jul
Iris	55 IRE 2.S1	43	1074	Sep
J				
J Antenna	48 IRE 2,11,15.S1	Separate		
J-Display	54 IRE 12.S1	43	201	Feb
Jitter	54 IRE 12.S1	43	201	Feb
Jitter (in Facsimile)	56 IRE 9.S1	44	778	Jne
Johnson Noise	57 IRE 7.S2	45	998	Jul
Jump	56 IRE 8.S1	44	1170	Sep
Junction	54 IRE 7.S2	42	1507	Oct
Junction, Alloy	54 IRE 7.S2	42	1507	Oct
Junction, Collector	54 IRE 7.S2	42	1507	Oct
Junction, Diffused	54 IRE 7.S2	42	1507	Oct
Junction, Doped	54 IRE 7.S2	42	1507	Oct
Junction Emitter	54 IRE 7.S2	42	1507	Oct
Junction, Fused	54 IRE 7.S2	42	1507	Oct
Junction, Grown	54 IRE 7.S2	42	1507	Oct
Junction, *N-N*	54 IRE 7.S2	42	1507	Oct
Junction, *P-N*	54 IRE 7.S2	42	1507	Oct
Junction, *P-P*	54 IRE 7.S2	42	1507	Oct
Junction Point	50 IRE 4.S1	38	27	Jan
Junction, Rate-Grown	54 IRE 7.S2	42	1507	Oct
Just Scale	51 IRE 6.S1	39	519	May
K				
K-Display	54 IRE 12.S1	43	201	Feb
Keep-Alive	57 IRE 7.S2	45	998	Jul
Keep-Alive Circuit	54 IRE 12.S1	43	201	Feb
Kendall Effect	56 IRE 9.S1	44	778	Jne
Keyer	48 IRE 2,11,15.S1	Separate		
Keying	53 IRE 11.S1	41	613	May
Kink	54 IRE 12.S1	43	201	Feb
Knee of Transfer Characteristic	57 IRE 7.S2	45	998	Jul
L				
LANAC (Laminar Navigation, Anti-Collision)	54 IRE 12.S1	43	208	Feb
L-Display	54 IRE 12.S1	43	201	Feb
L Network	50 IRE 4.S1	38	27	Jan
LOP	54 IRE 12.S1	43	202	Feb
Lacquer Disks	51 IRE 6.S1	39	520	May
Lacquer Original	51 IRE 6.S1	39	520	May
Lacquer Recording	51 IRE 6.S1	39	520	May
Ladder Network	50 IRE 4.S1	38	28	Jan
Lag	57 IRE 7.S2	45	998	Jul
Lambert	55 IRE 22.S1	43	746	Jne
Laminated Record	51 IRE 6.S1	39	520	May
Landing, Poor	57 IRE 7.S2	45	998	Jul
Land	51 IRE 6.S1	39	520	May
Lane	54 IRE 12.S1	43	201	Feb
Language	56 IRE 8.S1	44	1170	Sep
Lapel Microphone	51 IRE 6.S1	39	520	May
Lateral Recording	51 IRE 6.S1	39	520	May
Lattice	54 IRE 12.S1	43	201	Feb
Lattice Network	50 IRE 4.S1	38	28	Jan
Lead-In Groove	51 IRE 6.S1	39	520	May
Lead-Out Groove	51 IRE 6.S1	39	520	May
Lead-Over Groove	51 IRE 6.S1	39	520	May
Leader Cable	54 IRE 12.S1	43	201	Feb
Leading Edge	55 IRE 23.S1	43	620	May
Leading Edge Pulse Time	51 IRE 20.S1	39	625	Jne
Leading Edge Pulse Time	55 IRE 23.S1	43	621	May
Leakage Power	57 IRE 7.S2	45	998	Jul
Leakage Radiation	48 IRE 2,11,15.S1	Separate		
Left-Handed Polarized Wave	50 IRE 24.S1	38	1266	Nov
Length of Scanning Line	42 IRE 9.S1	Separate		
Lens	48 IRE 2,11,15.S1	Separate		
Level (in Audio)	54 IRE 3.S1	42	1111	Jul
Level (in Charge-Storage Tubes)	57 IRE 7.S2	45	998	Jul
Level (in Television)	55 IRE 23.S1	43	621	May
Level Above Threshold	51 IRE 6.S1	39	520	May
Lifetime, Volume	54 IRE 7.S2	42	1507	Oct
Light	55 IRE 22.S1	43	746	Jne
Light-Beam Pickup	51 IRE 6.S1	39	520	May
Light Carrier Injection	56 IRE 9.S1	44	778	Jne
Light-Microsecond	54 IRE 12.S1	43	201	Feb
Light Modulation	42 IRE 9.S1	Separate		
Light Modulator	51 IRE 6.S1	39	520	May
Light Value	51 IRE 6.S1	39	520	May
Limited Signal	54 IRE 12.S1	43	201	Feb
Limited Stability	53 IRE 4.S1	42	555	Mar
Limiter	48 IRE 2,11,15.S1	Separate		
Limiter	52 IRE 17.S1	40	1683	Dec
Limiting	52 IRE 17.S1	40	1683	Dec
Line Frequency	55 IRE 23.S1	43	621	May
Line Hydrophone	51 IRE 6.S1	39	520	May
Line Microphone	51 IRE 6.S1	39	520	May
Line of Position	54 IRE 12.S1	43	202	Feb
Line or Trace	57 IRE 7.S2	45	998	Jul
Line Stretcher	55 IRE 2.S1	43	1074	Sep
Linear Array	48 IRE 2,11,15.S1	Separate		
Linear Power Amplifier	48 IRE 2,11,15.S1	Separate		
Linear Rectifier	48 IRE 2,11,15.S1	Separate		
Linear Transducer	51 IRE 20.S2	39	898	Aug
Linear Varying-Parameter Network	53 IRE 4.S1	42	555	Mar
Linearity Region	54 IRE 12.S1	43	202	Feb
Linearly Polarized Wave	50 IRE 24.S1	38	1266	Nov
Lin-Log Receiver	54 IRE 12.S1	43	202	Feb
Lip Microphone	51 IRE 6.S1	39	520	May
Live Room	51 IRE 6.S1	39	520	May
Load (General)	54 IRE 3.S1	42	1111	Jul
Load (Induction Heating)	55 IRE 10.S1	43	1071	Sep
Load (of a Tube)	57 IRE 7.S2	45	999	Jul
Load (Dynamic) Characteristic	57 IRE 7.S2	45	999	Jul
Load Circuit (Induction Heating)	55 IRE 10.S1	43	1071	Sep
Load Circuit (in Transmitters)	48 IRE 2,11,15.S1	Separate		
Load-Circuit Efficiency (Induction Heating)	55 IRE 10.S1	43	1071	Sep
Load-Circuit Efficiency	48 IRE 2,11,15.S1	Separate		
Load-Circuit Power Input (Transmitters)	48 IRE 2,11,15.S1	Separate		
Load Coil	55 IRE 10.S1	43	1071	Sep
Load Impedance	54 IRE 3.S1	42	1111	Jul
Load Impedance Diagram	57 IRE 7.S2	45	999	Jul
Load Leads	55 IRE 10.S1	43	1071	Sep
Load Matching	55 IRE 10.S1	43	1071	Sep
Load Matching Network	55 IRE 10.S1	43	1071	Sep
Load Matching Switch	55 IRE 10.S1	43	1071	Sep
Load Switch	55 IRE 10.S1	43	1071	Sep
Load Transfer Switch	55 IRE 10.S1	43	1071	Sep
Loaded Applicator Impedance	55 IRE 10.S1	43	1071	Sep
Loaded Impedance	51 IRE 6.S1	39	520	May
Loaded Q	57 IRE 7.S2	45	999	Jul
Lobe Switching	54 IRE 12.S1	43	202	Feb

	Standard	Proceedings Vol Page Mo
Local Control	48 IRE 2,11,15.S1	Separate
Local Oscillator	52 IRE 17.S1	40 1683 Dec
Local Oscillator Tube	57 IRE 7.S2	45 999 Jul
Localizer	54 IRE 12.S1	43 202 Feb
Localizer On-Course Line	54 IRE 12.S1	43 202 Feb
Localizer Sector	54 IRE 12.S1	43 202 Feb
Locked Groove	51 IRE 6.S1	39 520 May
Lodar	54 IRE 12.S1	43 208 Feb
Logic	56 IRE 8.S1	44 1170 Sep
Logical Design	56 IRE 8.S1	44 1170 Sep
Logical Diagram	56 IRE 8.S1	44 1170 Sep
Logical Element	56 IRE 8.S1	44 1170 Sep
Logical Operation	56 IRE 8.S1	44 1170 Sep
Logical Symbol	56 IRE 8.S1	44 1170 Sep
Long Distance	54 IRE 12.S1	43 202 Feb
Long-Range Navigation	49 IRE 12.S1	37 1369 Dec
Long-Wire Antenna	48 IRE 2,11,15.S1	Separate
Longitudinal Magnetization	51 IRE 6.S1	39 520 May
Loop	50 IRE 4.S1	38 28 Jan
Loop Actuating Signal	55 IRE 26.S2	44 108 Jan
Loop, Alford	54 IRE 12.S1	43 202 Feb
Loop Antenna	48 IRE 2,11,15.S1	Separate
Loop Difference Signal	55 IRE 26.S2	44 108 Jan
Loop Error	55 IRE 26.S2	44 109 Jan
Loop Error Signal	55 IRE 26.S2	44 108 Jan
Loop Feedback Signal	55 IRE 26.S2	44 108 Jan
Loop Input Signal	55 IRE 26.S2	44 108 Jan
Loop Output Signal	55 IRE 26.S2	44 108 Jan
Loop Return Signal	55 IRE 26.S2	44 108 Jan
Loop Transfer Function	55 IRE 26.S2	44 108 Jan
Loop Transfer Ratio	55 IRE 26.S2	44 108 Jan
Lorac	54 IRE 12.S1	43 208 Feb
Lorad (See Lodar)	54 IRE 12.S1	43 208 Feb
Loran	49 IRE 12.S1	37 1371 Dec
Loran Repetition Rate	54 IRE 12.S1	43 202 Feb
Lorhumb Line	54 IRE 12.S1	43 202 Feb
Loss	57 IRE 7.S2	45 999 Jul
Loss (Transmission Loss)	54 IRE 3.S1	42 1111 Jul
Loudness	51 IRE 6.S1	39 520 May
Loudness Contours	51 IRE 6.S1	39 520 May
Loudness Level	51 IRE 6.S1	39 520 May
Loudspeaker	52 IRE 17.S1	40 1683 Dec
Loudspeaker	51 IRE 6.S1	39 520 May
Loudspeaker System	51 IRE 6.S1	39 520 May
Loudspeaker Voice Coil	51 IRE 6.S1	39 520 May
Low Clearance Area	54 IRE 12.S1	43 202 Feb
Low Clearance Points	54 IRE 12.S1	43 202 Feb
Low-Frequency Induction Heater or Furnace	55 IRE 10.S1	43 1071 Sep
Low-Level Modulation	48 IRE 2,11,15.S1	Separate
Low-Level Radio-Frequency Signal	57 IRE 7.S2	45 999 Jul
Low-Velocity Scanning	57 IRE 7.S2	45 999 Jul
Lowest Useful High Frequency	50 IRE 24.S1	38 1266 Nov
Lumen	55 IRE 22.S1	43 746 Jne
Luminance	55 IRE 22.S1	43 746 Jne
Luminance Flicker	55 IRE 22.S1	43 746 Jne
Luminance Primary	55 IRE 22.S1	43 746 Jne
Luminance Signal	55 IRE 22.S1	43 746 Jne
Luminosity	55 IRE 22.S1	43 746 Jne
Luminosity Coefficients	55 IRE 22.S1	43 746 Jne
Luminous Efficiency	55 IRE 22.S1	43 746 Jne
Luminous Flux	55 IRE 22.S1	43 747 Jne
Luminous Intensity	55 IRE 22.S1	43 747 Jne
Luminous Sensitivity	54 IRE 7.S1	42 1277 Aug

	Standard	Proceedings Vol Page Mo
M		
Machine Check	56 IRE 8.S1	44 1170 Sep
Machine Language	56 IRE 8.S1	44 1170 Sep
Magic Tee	55 IRE 2.S1	43 1074 Sep
Magnetic Armature Loudspeaker	51 IRE 6.S1	39 521 May
Magnetic Bearing	49 IRE 12.S1	37 1369 Dec
Magnetic Biasing	51 IRE 6.S1	39 521 May
Magnetic Course	49 IRE 12.S1	37 1369 Dec
Magnetic Cutter	51 IRE 6.S1	39 521 May
Magnetic Deviation	49 IRE 12.S1	37 1369 Dec
Magnetic Field	50 IRE 24.S1	38 1266 Nov
Magnetic Focusing	57 IRE 7.S2	45 999 Jul
Magnetic Head	51 IRE 6.S1	39 521 May
Magnetic Heading	49 IRE 12.S1	37 1369 Dec
Magnetic Plated Wire	51 IRE 6.S1	39 521 May
Magnetic Powder-Coated Tape	51 IRE 6.S1	39 521 May
Magnetic Powder-Impregnated Tape	51 IRE 6.S1	39 521 May
Magnetic Printing	51 IRE 6.S1	39 521 May
Magnetic Recorder	51 IRE 6.S1	39 521 May
Magnetic Recording	56 IRE 9.S1	44 778 Jne
Magnetic Reproducing Head	51 IRE 6.S1	39 521 May
Magnetic Recording Head	51 IRE 6.S1	39 521 May
Magnetic Recording Medium	51 IRE 6.S1	39 521 May
Magnetic Recording Reproducer	51 IRE 6.S1	39 521 May
Magnetic Tape	51 IRE 6.S1	39 521 May
Magnetic Wire	51 IRE 6.S1	39 521 May
Magneto-Ionic Wave Component	50 IRE 24.S1	38 1266 Nov
Magnetostriction Loudspeaker	51 IRE 6.S1	39 521 May
Magnetostriction Microphone	51 IRE 6.S1	39 521 May
Magnetostriction Oscillator	48 IRE 2,11,15.S1	Separate
Magnetron	57 IRE 7.S2	45 999 Jul
Magnetron	55 IRE 10.S1	43 1071 Sep
Magnetron Oscillator	48 IRE 2,11,15.S1	Separate
Main Bang	52 IRE 20.S1	40 553 May
Main Gap	57 IRE 7.S2	45 999 Jul
Major Cycle	56 IRE 8.S1	44 1171 Sep
Major Lobe (Beam)	48 IRE 2,11,15.S1	Separate
Majority Carrier	54 IRE 7.S2	42 1507 Oct
Malfunction	56 IRE 8.S1	44 1171 Sep
Marginal Checking	56 IRE 8.S1	44 1171 Sep
Marginal Testing	56 IRE 8.S1	44 1171 Sep
Marker	49 IRE 12.S1	37 1369 Dec
Marking Wave (Keying Wave)	48 IRE 2,11,15.S1	Separate
Mask Microphone	51 IRE 6.S1	39 521 May
Masking	51 IRE 6.S1	39 521 May
Masking (Audio)	52 IRE 17.S1	40 1683 Dec
Masking Audiogram	51 IRE 6.S1	39 521 May
Master	51 IRE 6.S1	39 521 May
Master Clock	50 IRE 8.S1	39 274 Mar
Master Oscillator	48 IRE 2,11,15.S1	Separate
Master Routine	56 IRE 8.S1	44 1171 Sep
Master Station	54 IRE 12.S1	43 202 Feb
Matched Termination	53 IRE 2.S1	41 1723 Dec
Matched Transmission Line	53 IRE 2.S1	41 1723 Dec
Matched Waveguide	53 IRE 2.S1	41 1723 Dec
Matching	49 IRE 12.S1	37 1369 Dec
Mathematical Check	56 IRE 8.S1	44 1171 Sep
Matrix (TV)	55 IRE 22.S1	43 747 Jne
Matrix (in Computers)	56 IRE 8.S1	44 1171 Sep
Matrix Unit	55 IRE 22.S1	43 747 Jne
Maximum Available Power Gain	57 IRE 7.S2	45 999 Jul
Maximum-Deviation Sensitivity	52 IRE 17.S1	40 1683 Dec
Maximum Distance	54 IRE 12.S1	43 202 Feb

	Standard	PROCEEDINGS Vol Page Mo
Maximum Keying Frequency (Facsimile)	56 IRE 9.S1	44 778 Jne
Maximum Modulating Frequency (Facsimile)	56 IRE 9.S1	44 778 Jne
Maximum Output	52 IRE 17.S1	40 1683 Dec
Maximum Sensitivity	52 IRE 17.S1	40 1683 Dec
Maximum Sound Pressure	51 IRE 6.S1	39 521 May
Maximum System Deviation	52 IRE 17.S1	40 1683 Dec
Maximum Usable Frequency	50 IRE 24.S1	38 1266 Nov
Maximum Undistorted Output	52 IRE 17.S1	40 1684 Dec
MCW	48 IRE 2,11,15.S1	Separate
M-Display	54 IRE 12.S1	43 202 Feb
Mean Free Path	51 IRE 6.S1	39 521 May
Mean Pulse Time	51 IRE 20.S1	39 625 Jne
Mechanical Phonograph Recorder	51 IRE 6.S1	39 521 May
Mechanical Transmission System	51 IRE 6.S1	39 521 May
Meissner Oscillator	48 IRE 2,11,15.S1	Separate
Mel	51 IRE 6.S1	39 522 May
Melting Channel	55 IRE 10.S1	43 1071 Sep
Memory	56 IRE 8.S1	44 1171 Sep
Memory Capacity	50 IRE 8.S1	39 274 Mar
Memory Capacity	56 IRE 8.S1	44 1171 Sep
Memory Circulating	50 IRE 8.S1	39 274 Mar
Memory, Delay-Line	50 IRE 8.S1	39 274 Mar
Memory, Electrostatic	50 IRE 8.S1	39 274 Mar
Memory Tube	57 IRE 7.S2	45 999 Jul
Memory Tube, Electrostatic	50 IRE 8.S1	39 274 Mar
Mercury Arc Converter, Pool Cathode	55 IRE 10.S1	43 1071 Sep
Mercury Hydrogen Spark Gap Converter	55 IRE 10.S1	43 1071 Sep
Mercury Vapor Tube	57 IRE 7.S2	45 999 Jul
Mesh	50 IRE 4.S1	38 28 Jan
MEW (Microwave Early Warning)	54 IRE 12.S1	43 208 Feb
Microbar	51 IRE 6.S1	39 522 May
Microphone	51 IRE 6.S1	39 522 May
Microphone	52 IRE 17.S1	40 1684 Dec
Microphonism	57 IRE 7.S2	45 999 Jul
Middle Marker	54 IRE 12.S1	43 208 Feb
Minimum Distance	54 IRE 12.S1	43 202 Feb
Minimum Firing Power	57 IRE 7.S2	45 999 Jul
Minor Cycle	56 IRE 8.S1	44 1171 Sep
Minor Lobe	48 IRE 2,11,15.S1	Separate
Minority Carrier	54 IRE 7.S2	42 1507 Oct
Mistake	56 IRE 8.S1	44 1171 Sep
Mixed Highs	55 IRE 22.S1	43 747 Jne
Mixer	51 IRE 6.S1	38 522 May
Mixer Tube	57 IRE 7.S2	45 999 Jul
Mixing Point	55 IRE 26.S2	44 108 Jan
Mobile Transmitter	48 IRE 2,11,15.S1	Separate
Mobility	54 IRE 7.S2	42 1507 Oct
Mobility, Hall	54 IRE 7.S2	42 1507 Oct
Mode	57 IRE 7.S2	45 999 Jul
Mode Filter	55 IRE 2.S1	43 1074 Sep
Mode of an Oscillator	57 IRE 7.S2	45 999 Jul
Mode of Propagation	53 IRE 2.S1	41 1723 Dec
Mode Purity	57 IRE 7.S2	45 999 Jul
Mode of Resonance	53 IRE 2.S1	41 1723 Dec
Mode Separation	57 IRE 7.S2	45 999 Jul
Mode Transducer	53 IRE 2.S1	41 1723 Dec
Mode Transducer	51 IRE 20.S2	39 898 Aug
Mode Transformer	51 IRE 20.S2	39 898 Aug
Moder	49 IRE 12.S1	37 1369 Dec
Modes, Degenerate	57 IRE 7.S2	45 999 Jul
Modified Index of Refraction	50 IRE 24.S1	38 1266 Nov
Modulated Wave	48 IRE 2,11,15.S1	Separate
Modulating Electrode	50 IRE 7.S1	38 435 Apr
Modulating Signal	52 IRE 17.S1	40 1684 Dec
Modulating Wave	53 IRE 11.S1	41 613 May
Modulation	53 IRE 11.S1	41 613 May
Modulation	52 IRE 17.S1	40 1684 Dec
Modulation Capability	48 IRE 2,11,15.S1	Separate
Modulation Factor	53 IRE 11.S1	41 613 May
Modulation Factor	52 IRE 17.S1	40 1684 Dec
Modulation Index	53 IRE 11.S1	41 614 May
Modulation Noise	51 IRE 6.S1	39 522 May
Modulated Amplifier	48 IRE 2,11,15.S1	Separate
Modulator	53 IRE 11.S1	41 614 May
Moire	57 IRE 7.S2	45 999 Jul
Moire	55 IRE 22.S1	43 747 Jne
Mold	51 IRE 6.S1	39 522 May
Monochromatic	55 IRE 22.S1	43 747 Jne
Monochrome	55 IRE 22.S1	43 747 Jne
Monochrome Signal	55 IRE 22.S1	43 747 Jne
Monochrome Transmission	55 IRE 22.S1	43 747 Jne
Monoscope	57 IRE 7.S2	45 999 Jul
Monoscope	52 IRE 17.S1	40 1684 Dec
Motional Impedance	51 IRE 6.S1	39 522 May
Motor Effect	55 IRE 10.S1	43 1071 Sep
Motor Field Induction Heater	55 IRE 10.S1	43 1071 Sep
Mount	57 IRE 7.S2	45 999 Jul
Moving-Coil Loudspeaker	51 IRE 6.S1	39 522 May
Moving-Coil Microphone	51 IRE 6.S1	39 522 May
Moving-Coil Pickup	51 IRE 6.S1	39 522 May
Moving-Conductor Loudspeaker	51 IRE 6.S1	39 522 May
Moving-Conductor Microphone	51 IRE 6.S1	39 522 May
Moving Target Indicator (MTI)	54 IRE 12.S1	43 202 Feb
MTI	54 IRE 12.S1	43 202 Feb
MTI Subclutter Visibility	54 IRE 12.S1	43 202 Feb
MTI Target Visibility	54 IRE 12.S1	43 202 Feb
MTR (Multiple Track Range)	54 IRE 12.S1	43 208 Feb
Mu-(μ) Factor	57 IRE 7.S2	45 1000 Jul
Multicavity Magnetron	51 IRE 7.S2	45 1000 Jul
Multicellular Horn	51 IRE 6.S1	39 522 May
Multichannel Radio Transmitter	48 IRE 2,11,15.S1	Separate
Multielectrode Tube	57 IRE 7.S2	45 1000 Jul
Multifrequency Transmitter	48 IRE 2,11,15.S1	Separate
Multipath	56 IRE 9.S1	44 779 Jne
Multipath Transmission (Multipath)	56 IRE 9.S1	44 779 Jne
Multiple-Address	50 IRE 8.S1	39 274 Mar
Multiple-Address Code	56 IRE 8.S1	44 1171 Sep
Multiple Course	54 IRE 12.S1	43 202 Feb
Multiple Modulation	53 IRE 11.S1	41 614 May
Multiple Sound Track	51 IRE 6.S1	39 522 May
Multiple Spot Scanning	56 IRE 9.S1	44 779 Jne
Multiple Tube Counts	57 IRE 7.S2	45 1000 Jul
Multiple-Tuned Antenna	48 IRE 2,11,15.S1	Separate
Multiple-Unit Tube	57 IRE 7.S2	45 1000 Jul
Multiplex Radio Transmission	48 IRE 2,11,15.S1	Separate
Multiplication Point	56 IRE 26.S2	44 108 Jan
Multiplier	56 IRE 8.S1	44 1171 Sep
Multiplier Phototube	57 IRE 7.S2	45 1000 Jul
Multisegment Magnetron	57 IRE 7.S2	45 1000 Jul
Multitrack Recording System	51 IRE 6.S1	39 522 May
Multivibrator	48 IRE 2,11,15.S1	Separate
Musa Antenna	48 IRE 2,11,15.S1	Separate
Musical Echo	51 IRE 6.S1	39 522 May

N

Narrow-Band Axis	55 IRE 22.S1	43 747 Jne
Navaglobe	54 IRE 12.S1	43 209 Feb
Navar	54 IRE 12.S1	43 209 Feb

	Standard	Proceedings Vol	Page	Mo
Nava-Rho	54 IRE 12.S1	43	209	Feb
Navigation	54 IRE 12.S1	43	202	Feb
Navigation Co-ordinate	54 IRE 12.S1	43	202	Feb
Navigation Parameter	54 IRE 12.S1	43	202	Feb
N-Display	54 IRE 12.S1	43	202	Feb
Negative Feedback	48 IRE 2,11,15.S1	Separate		
Negative Modulation	42 IRE 9.S1	Separate		
Negative-Resistance Oscillator	48 IRE 2,11,15.S1	Separate		
Negative-Transconductance Oscillator	48 IRE 2,11,15.S1	Separate		
Neper	48 IRE 2,11,15.S1	Separate		
Network	50 IRE 4.S1	38	28	Jan
Neutralization	48 IRE 2,11,15.S1	Separate		
Neutralizing Indicator	48 IRE 2,11,15.S1	Separate		
Neutralizing Voltage	48 IRE 2,11,15.S1	Separate		
Night Effect	54 IRE 12.S1	43	202	Feb
Node	50 IRE 4.S1	38	28	Jan
Noise	56 IRE 9.S1	44	779	Jne
Noise	57 IRE 7.S2	45	1000	Jul
Noise-Current Generator	57 IRE 7.S2	45	1000	Jul
Noise Diode, Ideal	57 IRE 7.S2	45	1000	Jul
Noise Factor	57 IRE 7.S2	45	1000	Jul
Noise Factor	57 IRE 17.S1	40	1684	Dec
Noise Factor, Average	52 IRE 17.S1	40	1684	Dec
Noise Factor, Average	57 IRE 7.S2	45	1000	Jul
Noise Factor, Spot	52 IRE 17.S1	40	1684	Dec
Noise Factor, Spot	57 IRE 7.S2	45	1000	Jul
Noise Reduction	51 IRE 6.S1	39	522	May
Noise Temperature	52 IRE 17.S1	40	1684	Dec
Noise Temperature	57 IRE 7.S2	45	1000	Jul
Noise Temperature, Standard	57 IRE 7.S2	45	1000	Jul
Noise-Voltage Generator	57 IRE 7.S2	45	1001	Jul
Nominal Band	42 IRE 9.S1	Separate		
Nominal Line Width	56 IRE 9.S1	44	779	Jne
Nonlinear Distortion	53 IRE 4.S1	42	555	Mar
Nonlinear Distortion	52 IRE 17.S1	40	1684	Dec
Nonlinear Network	53 IRE 4.S1	42	555	Mar
Nonphysical Primary	55 IRE 22.S1	43	747	Jne
Nonplanar Network	50 IRE 4.S1	38	28	Jan
Normalized Admittance	53 IRE 2.S1	41	1723	Dec
Normalized Impedance	53 IRE 2.S1	41	1723	Dec
Normalized Plateau Slope	57 IRE 7.S2	45	1001	Jul
North-Stabilized PPI	54 IRE 12.S1	43	202	Feb
Notation, Positional	50 IRE 8.S1	39	274	Mar
Note	51 IRE 6.S1	39	522	May
N-Terminal Network	50 IRE 4.S1	38	28	Jan
N-Terminal Pair Network	50 IRE 4.S1	38	28	Jan
Nth Harmonic	53 IRE 4.S1	42	555	Mar
Nullity	50 IRE 4.S1	38	28	Jan
Number	56 IRE 8.S1	44	1171	Sep
Number, Double-Precision	50 IRE 8.S1	39	274	Mar
Number of Loops	57 IRE 7.S2	45	1001	Jul
Number System	56 IRE 8.S1	44	1171	Sep
Nutating Feed	54 IRE 12.S1	43	202	Feb
Nutation Field	54 IRE 12.S1	43	202	Feb
No. 1 Mold	51 IRE 6.S1	39	522	May
No. 2, No. 3, etc., Master	51 IRE 6.S1	39	522	May
O				
OBI (Omnibearing Selector)	54 IRE 12.S1	43	209	Feb
Oboe	54 IRE 12.S1	43	209	Feb
OBS (Omnibearing Selector)	54 IRE 12.S1	43	209	Feb
Octal	56 IRE 8.S1	44	1171	Sep
Octave	51 IRE 6.S1	39	522	May
Octave-Band Pressure Level	51 IRE 6.S1	39	522	May
Octode	57 IRE 7.S2	45	1001	Jul
Octonary	56 IRE 8.S1	44	1171	Sep
Off Center PPI	54 IRE 12.S1	43	202	Feb
Offset Angle	51 IRE 6.S1	39	523	May
Offset Course Computer	49 IRE 12.S1	37	1369	Dec
Offset Crossover Characteristic-Deprecated	54 IRE 12.S1	43	202	Feb
Ohmic Contact	54 IRE 7.S2	42	1507	Oct
Omnibearing	54 IRE 12.S1	43	202	Feb
Omnibearing Converter	49 IRE 12.S1	37	1369	Dec
Omnibearing-Distance Facility	54 IRE 12.S1	43	203	Feb
Omnibearing-Distance Navigation (OBD)	54 IRE 12.S1	43	203	Feb
Omnibearing Indicator	49 IRE 12.S1	37	1369	Dec
Omnibearing Selector	49 IRE 12.S1	37	1369	Dec
Omnidirectional Antenna	48 IRE 2,11,15.S1	Separate		
Omnidirectional Microphone	51 IRE 6.S1	39	523	May
Omnidirectional Range (Omnirange)	54 IRE 12.S1	43	203	Feb
Omnidistance	49 IRE 12.S1	37	1369	Dec
Omnirange	49 IRE 12.S1	37	1369	Dec
On-Course Curvature	54 IRE 12.S1	43	203	Feb
One-Address Code	56 IRE 8.S1	44	1171	Sep
Opacity	51 IRE 6.S1	39	523	May
Open Center PPI	54 IRE 12.S1	43	203	Feb
Operand	50 IRE 8.S1	39	274	Mar
Operating Characteristic	57 IRE 7.S2	45	1001	Jul
Operation	50 IRE 8.S1	39	274	Mar
Operation Code	56 IRE 8.S1	44	1171	Sep
Operation Part	56 IRE 8.S1	44	1171	Sep
Operation Time	57 IRE 7.S2	45	1001	Jul
Optical Pattern	51 IRE 6.S1	39	523	May
Optimum Bunching	57 IRE 7.S2	45	1001	Jul
Optimum Working Frequency	50 IRE 24.S1	38	1266	Nov
Or-Circuit	56 IRE 8.S1	44	1171	Sep
Order	56 IRE 8.S1	44	1171	Sep
Ordinary-Wave Component	50 IRE 24.S1	38	1266	Nov
Organ	50 IRE 8.S1	39	275	Mar
Or-Gate	56 IRE 8.S1	44	1171	Sep
Original Master	51 IRE 6.S1	39	523	May
Orthicon	57 IRE 7.S2	45	1001	Jul
Oscillator	48 IRE 2,11,15.S1	Separate		
Oscillator	52 IRE 17.S1	40	1684	Dec
Oscillator Starting Time, Pulsed	52 IRE 20.S1	40	553	May
Oscilloscope Tube	57 IRE 7.S2	45	1001	Jul
Outer Marker	54 IRE 12.S1	43	209	Feb
Output Capacitance	57 IRE 7.S2	45	1001	Jul
Output Equipment	50 IRE 8.S1	39	274	Mar
Output Gap	57 IRE 7.S2	45	1001	Jul
Output Impedance	54 IRE 3.S1	42	1111	Jul
Outscriber	50 IRE 8.S1	39	275	Mar
Over-All Electrical Efficiency	55 IRE 10.S1	43	1071	Sep
Overbunching	57 IRE 7.S2	45	1001	Jul
Overcutting	51 IRE 6.S1	39	523	May
Overflow	56 IRE 8.S1	44	1171	Sep
Over Interrogation Control	54 IRE 12.S1	43	203	Feb
Overlap X	56 IRE 9.S1	44	779	Jne
Overload Capacity	48 IRE 2,11,15.S1	Separate		
Overthrow (or Overshoot)	42 IRE 9.S1	Separate		
Overtone	51 IRE 6.S1	39	523	May
Overvoltage	57 IRE 7.S2	45	1001	Jul
O Wave	50 IRE 24.S1	38	1266	Nov
P				
Packaged Magnetron	57 IRE 7.S2	45	1001	Jul
Pad Electrode	55 IRE 10.S1	43	1072	Sep
PAR (Precision Approach Radar)	54 IRE 12.S1	43	209	Feb
Parabolic-Reflector Microphone	51 IRE 6.S1	39	523	May

	Standard	PROCEEDINGS Vol	Page	Mo
Paraboloidal Reflector	48 IRE 2,11,15.S1	Separate		
Parallel Arithmetic Unit	50 IRE 8.S1	39	275	Mar
Parallel Digital Computer	56 IRE 8.S1	44	1171	Sep
Parallel Elements	50 IRE 4.S1	39	28	Jan
Parallel (in Computers)	56 IRE 8.S1	44	1171	Sep
Parallel Transmission	50 IRE 8.S1	39	275	Mar
Parallel Two-Terminal Pair Networks	50 IRE 4.S1	39	28	Jan
Parasitic Element	48 IRE 2,11,15.S1	Separate		
Parasitic Oscillations	48 IRE 2,11,15.S1	Separate		
Parity Check	57 IRE 8.S1	44	1171	Sep
Partial	51 IRE 6.S1	39	523	May
Partial Carry	56 IRE 8.S1	44	1171	Sep
Partial Velocity	51 IRE 6.S1	39	523	May
Passive Transducer	51 IRE 20.S2	39	898	Aug
Passive Transducer	54 IRE 3.S1	42	1111	Jul
Path	54 IRE 12.S1	43	203	Feb
P-Display	54 IRE 12.S1	43	203	Feb
Peak Alternating Gap Voltage	57 IRE 7.S2	45	1001	Jul
Peak Cathode Current	57 IRE 7.S2	45	1001	Jul
Peak Electrode Current	57 IRE 7.S2	45	1001	Jul
Peak Forward Anode Voltage	57 IRE 7.S2	45	1001	Jul
Peak Inverse Anode Voltage	57 IRE 7.S2	45	1001	Jul
Peak Power Output	48 IRE 2,11,15.S1	Separate		
Peak Pulse Amplitude	56 IRE 23.S1	43	621	May
Peak Pulse Amplitude	51 IRE 20.S1	39	625	Jne
Peak Pulse Power	52 IRE 20.S1	40	553	May
Peak Pulse Power Carrier Frequency	52 IRE 20.S1	40	553	May
Peak-Signal Level	42 IRE 9.S1	Separate		
Peak Sound Pressure	51 IRE 6.S1	39	523	May
Pencil Beam	54 IRE 12.S1	43	203	Feb
Pencil-Beam Antenna	48 IRE 2,11,15.S1	Separate		
Penetration Frequency	50 IRE 24.S1	38	1267	Nov
Pentode	57 IRE 7.S2	45	1001	Jul
Per Cent Hearing	51 IRE 6.S1	39	523	May
Per Cent Hearing Loss	51 IRE 6.S1	39	523	May
Per Cent Ripple	48 IRE 2,11,15.S1	Separate		
Percentage Modulation	53 IRE 11.S1	41	614	May
Percentage Modulation	52 IRE 17.S1	40	1684	Dec
Percentage Modulation	48 IRE 2,11,15.S1	Separate		
Performance Chart	57 IRE 7.S2	45	1001	Jul
Periodic Electromagnetic Wave	50 IRE 24.S1	38	1267	Nov
Periodic Pulse Train	52 IRE 20.S1	40	553	May
Permanent Echo	54 IRE 12.S1	43	203	Feb
Permanent Magnet Loudspeaker	51 IRE 6.S1	39	523	May
Perpendicular Magnetization	51 IRE 6.S1	39	523	May
Persistence Characteristic	57 IRE 7.S2	45	1001	Jul
Persistence Characteristic (Camera Tubes)	57 IRE 7.S2	45	1001	Jul
Perveance	57 IRE 7.S2	45	1001	Jul
Phanton Target	54 IRE 12.S1	43	203	Feb
Phase Constant	53 IRE 2.S1	41	1724	Dec
Phase Delay	56 IRE 9.S1	44	779	Jne
Phase Deviation	53 IRE 11.S1	41	614	May
Phase Distortion	53 IRE 4.S1	42	555	Mar
Phase Distortion	56 IRE 9.S1	44	779	Jne
Phase-Frequency Distortion	53 IRE 4.S1	42	555	Mar
Phase-Frequency Distortion	56 IRE 9.S1	44	779	Jne
Phase-Frequency Response Characteristic	48 IRE 2,11,15.S1	Separate		
Phase Localizer	54 IRE 12.S1	43	203	Feb
Phase-Modulated Transmitter	48 IRE 2,11,15.S1	Separate		
Phase Modulation (PM)	53 IRE 11.S1	41	614	May
Phase Modulation	52 IRE 17.S1	40	1684	Dec
Phase-Propagation Ratio	**50 IRE 24.S1**	**38**	**1267**	**Nov**
Phase-Recovery Time	57 IRE 7.S2	45	1001	Jne
Phase-Shift Microphone	51 IRE 6.S1	39	523	May
Phase-Shift Oscillator	48 IRE 2,11,15.S1	Separate		
Phase Shifter Waveguide	55 IRE 2.S1	43	1074	Sep
Phase-Tuned Tube	57 IRE 7.S2	45	1001	Jul
Phaser	42 IRE 9.S1	Separate		
Phase Velocity	50 IRE 24.S1	38	1267	Nov
Phase Velocity	53 IRE 2.S1	41	1724	Dec
Phasing	56 IRE 9.S1	44	779	Jne
Phasing Line	42 IRE 9.S1	Separate		
Phasing Signal	56 IRE 9.S1	44	779	Jne
Phi (Φ) Polarization	48 IRE 2,11,15.S1	Separate		
Phon	51 IRE 6.S1	39	523	May
Phonograph Pickup	51 IRE 6.S1	39	524	May
Phosphor	50 IRE 7.S1	38	436	Apr
Photocathode	57 IRE 7.S2	45	1001	Jul
Photoelectric Emission	57 IRE 7.S2	45	1001	Jul
Photographic Emulsion	51 IRE 6.S1	39	524	May
Photographic Recording	42 IRE 9.S1	Separate		
Photographic Sound Recorder	51 IRE 6.S1	39	524	May
Photographic Sound Reproducer	51 IRE 6.S1	39	524	May
Photographic Transmission Density	51 IRE 6.S1	39	524	May
Photometry	55 IRE 22.S1	43	747	Jne
Photomultiplier	57 IRE 7.S2	45	1001	Jul
Photosensitive Recording	56 IRE 9.S1	44	779	Jne
Phototube	57 IRE 7.S2	45	1001	Jul
Photovaristor	54 IRE 7.S2	42	1507	Oct
(Pi) π-Mode	57 IRE 7.S2	45	1002	Jul
Pi Network	50 IRE 4.S1	39	28	Jan
Pickup	52 IRE 17.S1	40	1684	Dec
Pickup Arm	51 IRE 6.S1	39	524	May
Pickup Cartridge	51 IRE 6.S1	39	524	May
Pickup Spectral Characteristic	55 IRE 22.S1	43	747	Jne
Pickup Tube	57 IRE 7.S2	45	1001	Jul
Picture Black (or "Black")	42 IRE 9.S1	Separate		
Picture Frequencies	56 IRE 9.S1	44	779	Jne
Picture Inversion	56 IRE 9.S1	44	779	Jne
Picture Signal (Facsimile)	56 IRE 9.S1	44	779	Jne
Picture Signal (TV)	55 IRE 23.S1	43	621	May
Picture Tube	50 IRE 7.S1	38	436	Apr
Picture White (Facsimile)	42 IRE 9.S1	Separate		
Pierce Oscillator	48 IRE 2,11,15.S1	Separate		
Pill-Box Antenna	48 IRE 2,11,15.S1	Separate		
Pilotage	54 IRE 12.S1	43	203	Feb
Pinch Effect	55 IRE 10.S1	43	1072	Sep
PIP	54 IRE 12.S1	43	203	Feb
PIP Matching	54 IRE 12.S1	43	203	Feb
PIP-Matching Display	54 IRE 12.S1	43	199	Feb
Pistonphone	51 IRE 6.S1	39	524	May
Pitch	51 IRE 6.S1	39	524	May
Pitch Attitude	49 IRE 12.S1	37	1369	Dec
Place	56 IRE 8.S1	44	1171	Sep
Plan Position Indicator (PPI)	54 IRE 12.S1	43	203	Feb
Planar Network	50 IRE 4.S1	39	28	Jan
Planckian Locus	55 IRE 22.S1	43	747	Jne
Plane Earth Factor	50 IRE 24.S1	38	1267	Nov
Plane of Polarization	50 IRE 24.S1	38	1267	Nov
Plane Polarized Wave	50 IRE 24.S1	38	1267	Nov
Plane Wave	50 IRE 24.S1	38	1267	Nov
Plan Position Indicator	49 IRE 12.S1	37	1369	Dec
Plate	57 IRE 7.S2	45	1002	Jul
Plate Characteristic	57 IRE 7.S2	45	1002	Jul
Plate Current	57 IRE 7.S2	45	1002	Jul
Plate (Anode) Efficiency	48 IRE 2,11,15.S1	Separate		
Plate Keying	**48 IRE 2,11,15.S1**	**Separate**		

	Standard	Proceedings Vol	Page	Mo
Plate (Anode) Load Impedance	48 IRE 2,11,15.S1	Separate		
Plate (Anode) Modulation	48 IRE 2,11,15.S1	Separate		
Plate Neutralization	48 IRE 2,11,15.S1	Separate		
Plate (Anode) Power Input	48 IRE 2,11,15.S1	Separate		
Plate (Anode) Pulse Modulation	48 IRE 2,11,15.S1	Separate		
Plate Voltage	57 IRE 7.S2	45	1002	Jul
Plateau	57 IRE 7.S2	45	1002	Jul
Plateau Length	57 IRE 7.S2	45	1002	Jul
Plateau Slope Normalized	57 IRE 7.S2	45	1002	Jul
Plateau Slope Relative	57 IRE 7.S2	45	1002	Jul
Playback	51 IRE 6.S1	39	524	May
Plotting Board	50 IRE 8.S1	39	275	Mar
Plumbing	54 IRE 12.S1	43	203	Feb
Plunger, Waveguide	55 IRE 2.S1	43	1074	Sep
PM Erasing Head	51 IRE 6.S1	39	523	May
Pneumatic Loudspeaker	51 IRE 6.S1	39	524	May
Poid	51 IRE 6.S1	39	524	May
Point	56 IRE 8.S1	44	1171	Sep
Point, Binary	50 IRE 8.S1	39	275	Mar
Point Contact	54 IRE 7.S2	42	1507	Oct
Point, Decimal	50 IRE 8.S1	39	275	Mar
Point, Radix	50 IRE 8.S1	39	275	Mar
Polar Grid	49 IRE 12.S1	37	1369	Dec
Polarization Ellipse	53 IRE 2.S1	41	1724	Dec
Polarization Error	54 IRE 12.S1	43	203	Feb
Polarization Receiving Factor	53 IRE 2.S1	41	1724	Dec
Polarization Unit Vector	53 IRE 2.S1	41	1724	Dec
Polarity of Picture Signal	55 IRE 23.S1	43	621	May
Polyplexer	54 IRE 12.S1	43	203	Feb
Pool Cathode Mercury Arc Converter	55 IRE 10.S1	43	1072	Sep
POPI (Post Office Position Indicator)	54 IRE 12.S1	43	209	Feb
Port	57 IRE 7.S2	45	1002	Jul
Portable Transmitter	48 IRE 2,11,15.S1	Separate		
Porthole	57 IRE 7.S2	45	1002	Jul
Position	54 IRE 12.S1	43	203	Feb
Position of the Effective Short (Switching Tubes)	56 IRE 7.S3	44	1039	Aug
Positional Crosstalk	57 IRE 7.S2	45	1002	Jul
Positional Notation	56 IRE 8.S1	44	1172	Sep
Position of the Effective Short	57 IRE 7.S2	45	1002	Jul
Positive Feedback	48 IRE 2,11,15.S1	Separate		
Positive Modulation (Facsimile)	42 IRE 9.S1	Separate		
Post Acceleration	57 IRE 7.S2	45	1002	Jul
Post Waveguide	55 IRE 2.S1	43	1074	Sep
Power	57 IRE 7.S2	45	1002	Jul
Power Amplification	54 IRE 3.S1	42	1111	Jul
Power Attenuation	54 IRE 3.S1	42	1111	Jul
Power Carrier-Frequency, Peak Pulse	52 IRE 20.S1	40	553	May
Power Gain	57 IRE 7.S2	45	1002	Jul
Power Gain	54 IRE 3.S1	42	1111	Jul
Power Gain (of an Antenna)	48 IRE 2,11,15.S1	Separate		
Power Level	54 IRE 3.S1	42	1111	Jul
Power Loss	54 IRE 3.S1	42	1111	Jul
Power, Peak Pulse	52 IRE 20.S1	40	553	May
PPI	54 IRE 12.S1	43	203	Feb
Preamplifier	54 IRE 12.S1	43	203	Feb
Precision	56 IRE 8.S1	44	1172	Sep
Predissociation	57 IRE 7.S2	45	1002	Jul
Pre-Emphasis	51 IRE 6.S1	39	524	May
Pre-Emphasis	53 IRE 11.S1	41	614	May
Pre-Emphasis	52 IRE 17.S1	40	1685	Dec
Pre-Emphasis Network	48 IRE 2,11,15.S1	Separate		
Preform	51 IRE 6.S1	39	524	May
Preoscillation Current	57 IRE 7.S2	45	1002	Jul
Pressing	51 IRE 6.S1	39	524	May
Pressure Microphone	51 IRE 6.S1	39	524	May
Pressure Spectrum Level	51 IRE 6.S1	39	524	May
Pre-TR Tube	57 IRE 7.S2	45	1002	Jul
PRF (Pulse Repetition Frequency)	54 IRE 12.S1	43	203	Feb
Primaries	55 IRE 22.S1	43	747	Jne
Primary-Color Unit	57 IRE 7.S2	45	1002	Jul
Primary Flow	54 IRE 7.S2	42	1507	Oct
Primary Radar	54 IRE 12.S1	43	203	Feb
Prime	57 IRE 7.S2	45	1002	Jul
Priming Speed	57 IRE 7.S2	45	1002	Jul
Principal Axis	51 IRE 6.S1	39	525	May
Principal E Plane	48 IRE 2,11,15.S1	Separate		
Principal H Plane	48 IRE 2,11,15.S1	Separate		
Problem, Check	50 IRE 8.S1	39	275	Mar
Problem, Trouble Location	50 IRE 8.S1	39	275	Mar
Program	56 IRE 8.S1	44	1172	Sep
Program Level	54 IRE 3.S1	42	1111	Jul
Program Signal	54 IRE 3.S1	42	1111	Jul
Programmed Check	56 IRE 8.S1	44	1172	Sep
Propagation Constant	53 IRE 2.S1	41	1724	Dec
Propagation Constant	50 IRE 24.S1	38	1267	Nov
Propagation Factor	50 IRE 24.S1	38	1267	Nov
Propagation Ratio	50 IRE 24.S1	38	1267	Nov
Proportional Counter Tube	57 IRE 7.S2	45	1002	Jul
Proportional Region	57 IRE 7.S2	45	1002	Jul
Proximity Effect	55 IRE 10.S1	43	1072	Sep
Pulling Figure (of an Oscillator)	57 IRE 7.S2	45	1002	Jul
Pulse	55 IRE 23.S1	43	621	May
Pulse	51 IRE 20.S1	39	625	Jne
Pulse Amplitude	51 IRE 20.S1	39	625	Jne
Pulse Amplitude, Average	51 IRE 20.S1	39	625	Jne
Pulse Amplitude, Average Absolute	51 IRE 20.S1	39	625	Jne
Pulse-Amplitude Modulation	51 IRE 20.S1	39	625	Jne
Pulse Amplitude, Peak	51 IRE 20.S1	39	625	Jne
Pulse Amplitude, RMS	51 IRE 20.S1	39	625	Jne
Pulse Bandwidth	51 IRE 20.S1	39	625	Jne
Pulse, Bidirectional	52 IRE 20.S1	40	553	May
Pulse Carrier	51 IRE 20.S1	39	625	Jne
Pulse, Carrier-Frequency	52 IRE 20.S1	40	553	May
Pulse Code	52 IRE 20.S1	40	553	May
Pulse Code	53 IRE 11.S1	41	614	May
Pulse-Code Modulation	53 IRE 11.S1	41	614	May
Pulse-Code Modulation	52 IRE 20.S1	40	553	May
Pulse Coder	49 IRE 12.S1	37	1369	Dec
Pulse Decay Time	51 IRE 20.S1	39	625	Jne
Pulse Decay Time	55 IRE 23.S1	43	621	May
Pulse Delay, Receiver	52 IRE 20.S1	40	553	May
Pulse Delay, Transducer	52 IRE 20.S1	40	553	May
Pulse Delay, Transmitter	52 IRE 20.S1	40	553	May
Pulse-Demoder (Constant-Delay Discriminator)	54 IRE 12.S1	43	203	Feb
Pulse Droop	55 IRE 23.S1	43	621	May
Pulse Droop	52 IRE 20.S1	40	553	May
Pulse Duration	55 IRE 23.S1	42	621	May
Pulse Duration	51 IRE 20.S1	39	625	Jne
Pulse Duration Coder	54 IRE 12.S1	43	203	Feb
Pulse-Duration Discriminator	54 IRE 12.S1	43	203	Feb
Pulse-Duration Modulation	53 IRE 11.S1	41	614	May
Pulse-Duration Modulation	51 IRE 20.S1	39	625	Jne
Pulse Duty Factor	51 IRE 20.S1	39	626	Jne
Pulse Flatness, Deviation From	54 IRE 12.S1	43	203	Feb
Pulse Forming Line	54 IRE 12.S1	43	203	Feb
Pulse Frequency Modulation	52 IRE 20.S1	40	553	May
Pulse Frequency Modulation	53 IRE 11.S1	41	614	May

	Standard	Proceedings Vol	Page	Mo
Pulse Frequency Spectrum	51 IRE 20.S1	39	626	Jne
Pulse, Ghost	54 IRE 12.S1	43	203	Feb
Pulse Interleaving	51 IRE 20.S1	39	626	Jne
Pulse Interrogation	52 IRE 20.S1	40	553	May
Pulse Interval	51 IRE 20.S1	39	626	Jne
Pulse-Interval Modulation	51 IRE 20.S1	39	626	Jne
Pulse-Interval Modulation	53 IRE 11.S1	41	614	May
Pulse Jitter	52 IRE 20.S1	40	553	May
Pulse-Length Modulation	51 IRE 20.S1	39	626	Jne
Pulse Mode	52 IRE 20.S1	40	553	May
Pulse-Mode Multiplex	52 IRE 20.S1	40	553	May
Pulse Mode, Spurious	52 IRE 20.S1	40	553	May
Pulse-Moder	54 IRE 12.S1	43	203	Feb
Pulse Modulation	52 IRE 20.S1	40	553	May
Pulse Modulation	53 IRE 11.S1	41	614	May
Pulse Modulator	48 IRE 2,11,15.S1	Separate		
Pulse Multiplex	52 IRE 20.S1	40	553	May
Pulse Packet	54 IRE 12.S1	43	203	Feb
Pulse-Phase Modulation	52 IRE 20.S1	40	553	May
Pulse-Position Modulation	53 IRE 11.S1	41	614	May
Pulse-Position Modulation	51 IRE 20.S1	39	626	Jne
Pulse Power, Carrier-Frequency, Peak	52 IRE 20.S1	40	553	May
Pulse Power, Peak	52 IRE 20.S1	40	553	May
Pulse, Radio-Frequency	51 IRE 20.S1	39	626	Jne
Pulse Rate	54 IRE 12.S1	43	203	Feb
Pulse Regeneration	51 IRE 20.S1	39	626	Jne
Pulse Repeater (Transponder)	48 IRE 2,11,15.S1	Separate		
Pulse Repetition Frequency	54 IRE 12.S1	43	203	Feb
Pulse Repetition Frequency	51 IRE 20.S1	39	626	Jne
Pulse Repetition Period	51 IRE 20.S1	39	626	Jne
Pulse Repetition Rate	51 IRE 20.S1	39	626	Jne
Pulse Repetition Rate (PRF)	54 IRE 12.S1	43	203	Feb
Pulse Reply	52 IRE 20.S1	40	554	May
Pulse Rise Time	51 IRE 20.S1	39	626	Jne
Pulse Separation	52 IRE 20.S1	40	554	May
Pulse Shaper	52 IRE 20.S1	40	554	May
Pulse Shaping	52 IRE 20.S1	40	554	May
Pulse, Single-Polarity	52 IRE 20.S1	40	554	May
Pulse Spacing	51 IRE 20.S1	39	626	Jne
Pulse Spectrum	51 IRE 20.S1	39	626	Jne
Pulse Spike	51 IRE 20.S1	39	626	Jne
Pulse Spike Amplitude	52 IRE 20.S1	40	554	May
Pulse Tilt	55 IRE 23.S1	43	621	May
Pulse Tilt	52 IRE 20.S1	40	554	May
Pulse Time, Leading Edge	51 IRE 20.S1	39	626	Jne
Pulse Time, Mean	51 IRE 20.S1	39	626	Jne
Pulse-Time Modulation	53 IRE 11.S1	41	614	May
Pulse-Time Modulation	51 IRE 20.S1	39	626	Jne
Pulse Time, Trailing Edge	51 IRE 20.S1	39	626	Jne
Pulse Train	51 IRE 20.S1	39	626	Jne
Pulse Train, Bidirectional	52 IRE 20.S1	40	554	May
Pulse Train, Periodic	52 IRE 20.S1	40	554	May
Pulse-Train Spectrum	52 IRE 20.S1	40	554	May
Pulse Train, Undirectional	52 IRE 20.S1	40	554	May
Pulse Transmitter	48 IRE 2,11,15 S1	Separate		
Pulse Undirectional	51 IRE 20.S1	39	626	Jne
Pulse Valley	52 IRE 20.S1	40	554	May
Pulse Width	55 IRE 23.S1	43	621	May
Pulse Width	52 IRE 20.S1	40	554	May
Pulse-Width Modulation	51 IRE 20.S1	39	626	Jne
Pulsed Doppler System	54 IRE 12.S1	43	203	Feb
Pulsed Oscillator	48 IRE 2,11,15.S1	Separate		
Pulsed Oscillator	52 IRE 20.S1	40	554	May
Pulsed-Oscillator Starting Time	52 IRE 20.S1	40	554	May
Pulses Equalizing	52 IRE 20.S1	40	554	May
Purity	55 IRE 22.S1	43	747	Jne
Purple Boundary	55 IRE 22.S1	43	747	Jne
Push-Pull Currents (Balanced Currents)	53 IRE 2.S1	41	1724	Dec
Push-Pull Microphone	51 IRE 6.S1	39	525	May
Push-Pull Oscillator	48 IRE 2,11,15.S1	Separate		
Push-Pull Voltages	53 IRE 2.S1	41	1724	Dec
Pushing Figure (of an Oscillator)	57 IRE 7.S2	45	1002	Jul
Push-Push Circuit	48 IRE 2,11,15.S1	Separate		
Push-Push Currents	53 IRE 2.S1	41	1724	Dec
Push-Push Voltages	53 IRE 2.S1	41	1724	Dec
Pyramidal Horn	48 IRE 2,11,15.S1	Separate		
Pythagorean Scale	51 IRE 6.S1	39	525	May
Q				
Quadripole	50 IRE 4.S1	39	28	Jan
Quadrantal Error	49 IRE 12.S1	37	1369	Dec
Quantization	53 IRE 11.S1	41	614	May
Quantization Distortion	53 IRE 11.S1	41	614	May
Quantization Level	53 IRE 11.S1	41	614	May
Quantization Noise	53 IRE 11.S1	41	614	May
Quantized Pulse Modulation	53 IRE 11.S1	41	614	May
Quantum Efficiency	57 IRE 7.S2	45	1002	Jul
Quenched Spark Gap Converter	55 IRE 10.S1	43	1072	Sep
Quenching	57 IRE 7.S2	45	1002	Jul
Quieting Sensitivity	52 IRE 17.S1	40	1685	Dec
R				
Racon	54 IRE 12.S1	43	209	Feb
Radar	54 IRE 12.S1	43	203	Feb
Radar Equation	54 IRE 12.S1	43	203	Feb
Radar Performance Figure	54 IRE 12.S1	43	203	Feb
Radar Pilotage Equipment	54 IRE 12.S1	43	204	Feb
Radar Range Equation	54 IRE 12.S1	43	204	Feb
Radar Relay	54 IRE 12.S1	43	204	Feb
Radar Shadow	54 IRE 12.S1	43	204	Feb
Radar Transmitter	48 IRE 2,11,15.S1	Separate		
Radial	54 IRE 12.S1	43	204	Feb
Radial Time Base Display	54 IRE 12.S1	43	204	Feb
Radial Transmission Line	53 IRE 2.S1	41	1724	Dec
Radiance	55 IRE 22.S1	43	747	Jne
Radiant Flux	55 IRE 22.S1	43	747	Jne
Radiant Intensity	55 IRE 22.S1	43	747	Jne
Radiant Sensitivity (of a Photo-Tube)	54 IRE 7.S1	42	1277	Aug
Radiating Element	48 IRE 2,11,15.S1	Separate		
Radiation Counter	57 IRE 7.S2	45	1002	Jul
Radiation-Counter Tube	57 IRE 7.S2	45	1002	Jul
Radiation Efficiency	48 IRE 2,11,15.S1	Separate		
Radiation Intensity	48 IRE 2,11,15.S1	Separate		
Radiation Lobe	48 IRE 2,11,15.S1	Separate		
Radiation Loss	53 IRE 2.S1	41	1724	Dec
Radiation (Nuclear)	57 IRE 7.S2	45	1002	Jul
Radiation Pattern	48 IRE 2,11,15.S1	Separate		
Radiation Resistance	48 IRE 2,11,15.S1	Separate		
Radio-Autopilot Coupler	49 IRE 12.S1	37	1369	Dec
Radio Beacon	54 IRE 12.S1	43	204	Feb
Radio Broadcasting	48 IRE 2,11,15.S1	Separate		
Radio Channel	52 IRE 17.S1	40	1685	Dec
Radio Communication Circuit	48 IRE 2,11,15.S1	Separate		
Radio Direction Finding	54 IRE 12.S1	43	204	Feb
Radio Field Strength	50 IRE 24.S1	38	1267	Nov
Radio Frequency	50 IRE 24.S1	38	1267	Nov
Radio Frequency	52 IRE 17.S1	40	1685	Dec
Radio-Frequency Alternator	48 IRE 2,11,15.S1	Separate		
Radio-Frequency Converter	55 IRE 10.S1	43	1072	Sep

	Standard	Proceedings Vol	Page	Mo
Radio-Frequency Generator-Electron Tube Type	55 IRE 10.S1	43	1072	Sep
Radio-Frequency Pulse	51 IRE 20.S1	39	626	Jne
Radio-Frequency Signal, High Level	57 IRE 7.S2	45	1002	Jul
Radio-Frequency Signal, Low-Level	57 IRE 7.S2	45	1003	Jul
Radio Horizon	50 IRE 24.S1	38	1267	Nov
Radio Magnetic Indicator (RMI)	54 IRE 12.S1	43	204	Feb
Radio Navigation	49 IRE 12.S1	37	1370	Dec
Radio Proximity Fuze	48 IRE 2,11,15.S1	Separate		
Radio Range	54 IRE 12.S1	43	204	Feb
Radio Receiver	52 IRE 17.S1	40	1685	Dec
Radio Transmitter	48 IRE 2,11,15.S1	Separate		
Radio Wave Propagation	50 IRE 24.S1	38	1267	Nov
Radiolocation	54 IRE 12.S1	43	204	Feb
Radiophare	54 IRE 12.S1	43	204	Feb
Radiosonde	48 IRE 2,11,15.S1	Separate		
Radix	56 IRE 8.S1	44	1172	Sep
Radix Point	50 IRE 8.S1	39	276	Mar
Radome	48 IRE 2,11,15.S1	Separate		
Radux	54 IRE 12.S1	43	209	Feb
Rain Return	54 IRE 12.S1	43	204	Feb
Ramark	54 IRE 12.S1	43	209	Feb
Random Errors	54 IRE 12.S1	43	204	Feb
Random Noise	48 IRE 2,11,15.S1	Separate		
Range	54 IRE 12.S1	43	204	Feb
Range Mark	54 IRE 12.S1	43	204	Feb
Range Resolution	54 IRE 12.S1	43	204	Feb
Range, Visual-Aural	54 IRE 12.S1	43	204	Feb
Range, Visual Radio	54 IRE 12.S1	43	204	Feb
Rank	50 IRE 4.S1	39	28	Jan
Raster	57 IRE 7.S2	45	1003	Jul
Raster Burn	57 IRE 7.S2	45	1003	Jul
Rate of Decay	51 IRE 6.S1	39	525	May
Ratio	57 IRE 7.S2	45	1003	Jul
Raydist	54 IRE 12.S1	43	209	Feb
Rayleigh Disk	51 IRE 6.S1	39	525	May
R-C Oscillator	48 IRE 2,11,15.S1	Separate		
RDF-Radio Direction Finding	54 IRE 12.S1	43	204	Feb
Reactance Modulator	48 IRE 2,11,15.S1	Separate		
Read	56 IRE 8.S1	44	1172	Sep
Read (in Charge-Storage Tubes)	57 IRE 7.S2	45	1003	Jul
Read-Around Number	57 IRE 7.S2	45	1003	Jul
Read-Around Ratio	57 IRE 7.S2	45	1003	Jul
Read Number	57 IRE 7.S2	45	1003	Jul
Reading Speed	57 IRE 7.S2	45	1003	Jul
Ready-To-Receive Signal	56 IRE 9.S1	44	779	Jne
Rebecca	54 IRE 12.S1	43	209	Feb
Recalescent Point	55 IRE 10.S1	43	1072	Sep
Receiver, Facsimile	56 IRE 9.S1	44	779	Jne
Receiver Gating	54 IRE 12.S1	43	204	Feb
Receiver Primaries	55 IRE 22.S1	43	748	Jne
Receiver Pulse Delay	52 IRE 20.S1	40	554	May
Receiving Converter, Facsimile (FS to AM Converter)	56 IRE 9.S1	44	779	Jne
Reciprocal Transducer	51 IRE 20.S2	39	989	Aug
Recombination Rate, Surface	54 IRE 7.S2	42	1507	Oct
Recombination Rate, Volume	54 IRE 7.S2	42	1507	Oct
Recombination Velocity	54 IRE 7.S2	42	1507	Oct
Record Medium	56 IRE 9.S1	44	779	Jne
Record Sheet	56 IRE 9.S1	44	779	Jne
Recorded Spot	56 IRE 9.S1	44	779	Jne
Recorded Spot X Dimension	56 IRE 9.S1	44	779	Jne
Recorded Spot Y Dimension	56 IRE 9.S1	44	779	Jne
Recorder, Facsimile	56 IRE 9.S1	44	779	Jne
Recording Channel	51 IRE 6.S1	39	525	May
Recording (in Facsimile)	56 IRE 9.S1	44	779	Jne
Recording Loss	51 IRE 6.S1	39	525	May
Recording Spot (in Facsimile)	56 IRE 9.S1	44	779	Jne
Recording Stylus	51 IRE 6.S1	39	525	May
Recovery Time	57 IRE 7.S2	45	1003	Jul
Recovery Time (ATR Tubes)	56 IRE 7.S3	44	1039	Aug
Recovery Time (Gas Tubes)	57 IRE 7.S2	45	1003	Jul
Recovery Time (Geiger-Mueller Counters)	57 IRE 7.S2	45	1003	Jul
Recovery Time (TR and Pre-TR Tubes)	57 IRE 7.S2	45	1003	Jul
Rectangular Scanning	48 IRE 2,11,15.S1	Separate		
Rectification Factor	57 IRE 7.S2	45	1003	Jul
Rectifier	48 IRE 2,11,15.S1	Separate		
Rectilinear Scanning	42 IRE 9.S1	Separate		
Recurrence Rate	54 IRE 12.S1	43	204	Feb
Redistribution	57 IRE 7.S2	45	1003	Jul
Redundancy Check	56 IRE 8.S1	44	1172	Sep
Reference Black Leve	55 IRE 23.S1	43	621	May
Reference Direction	49 IRE 12.S1	37	1370	Dec
Reference Line	49 IRE 12.S1	37	1370	Dec
Reference Volume	54 IRE 3.S1	42	1111	Jul
Reference White	55 IRE 22.S1	43	748	Jne
Reference White Level	55 IRE 23.S1	43	621	May
Reflected Wave	53 IRE 2.S1	41	1724	Dec
Reflection Coefficient	53 IRE 2.S1	41	1724	Dec
Reflection Coefficient (of Transmission Medium)	53 IRE 2.S1	41	1724	Dec
Reflection Color-Tube	57 IRE 7.S2	45	1003	Jul
Reflection Error	54 IRE 12.S1	43	204	Feb
Reflection Loss	53 IRE 2.S1	41	1724	Dec
Reflector (Antenna)	48 IRE 2,11,15.S1	Separate		
Reflector (in Tubes)	57 IRE 7.S2	45	1003	Jul
Reflex Baffle	51 IRE 6.S1	39	525	May
Reflex Bunching	57 IRE 7.S2	45	1003	Jul
Refracted Wave	53 IRE 2.S1	41	1724	Dec
Refracted Wave	50 IRE 24.S1	38	1267	Nov
Refraction Error	54 IRE 12.S1	43	204	Feb
Refraction Loss	51 IRE 6.S1	39	525	May
Refractive Index	50 IRE 24.S1	38	1267	Nov
Refractive Modulus	50 IRE 24.S1	38	1267	Nov
Regeneration (in Charge-Storage Tubes)	57 IRE 7.S2	45	1003	Jul
Regeneration (in Computers)	56 IRE 8.S1	44	1172	Sep
Regeneration (in Transmitters)	48 IRE 2,11,15.S1	Separate		
Regenerative Repeater	53 IRE 11.S1	41	614	May
Region, Geiger-Mueller	57 IRE 7.S2	45	1003	Jul
Region of Limited Proportionality	57 IRE 7.S2	45	1003	Jul
Region, Proportional	57 IRE 7.S2	45	1003	Jul
Register	56 IRE 8.S1	44	1172	Sep
Register, Delay-Line	50 IRE 8.S1	39	276	Mar
Register Length	56 IRE 8.S1	44	1172	Sep
Register, Static	50 IRE 8.S1	39	276	Mar
Regulation (Gas Tubes)	57 IRE 7.S2	45	1003	Jul
Reignition	57 IRE 7.S2	45	1003	Jul
Rejection Band	53 IRE 2.S1	41	1724	Dec
Relative Bearing	54 IRE 12.S1	43	204	Feb
Relative Course	49 IRE 12.S1	37	1370	Dec
Relative Heading	49 IRE 12.S1	37	1370	Dec
Relative Luminosity	55 IRE 22.S1	43	748	Jne
Relative Plateau Slope	57 IRE 7.S2	45	1003	Jul
Relative Refractive Index	50 IRE 24.S1	38	1267	Nov
Relative Response	51 IRE 6.S1	39	525	May
Relative Velocity	51 IRE 6.S1	39	525	May
Relaxation Oscillator	48 IRE 2,11,15.S1	Separate		
Relay Radar	54 IRE 12.S1	43	204	Feb
Remote Control	48 IRE 2,11,15.S1	Separate		

	Standard	Proceedings Vol Page Mo
Repeatability	57 IRE 7.S2	45 1003 Jul
Repeller	57 IRE 7.S2	45 1004 Jul
Repetition Frequency	54 IRE 12.S1	43 204 Feb
Repetition Rate	54 IRE 12.S1	43 204 Feb
Repetition Rate, Basic	54 IRE 12.S1	43 204 Feb
Repetition Rate, Specific	54 IRE 12.S1	43 204 Feb
Reply	54 IRE 12.S1	43 204 Feb
Reply Efficiency, Transponder	54 IRE 12.S1	43 204 Feb
Reproducing Stylus	51 IRE 6.S1	39 525 May
Reproduction Speed	56 IRE 9.S1	44 779 Jne
Re-Recording	51 IRE 6.S1	39 525 May
Re-Recording System	51 IRE 6.S1	39 525 May
Reset	56 IRE 8.S1	44 1172 Sep
Residual Error	54 IRE 12.S1	43 204 Feb
Resistance	57 IRE 7.S2	45 1004 Jul
Resolution	49 IRE 12.S1	37 1370 Dec
Resolution	57 IRE 7.S2	45 1004 Jul
Resolution, Structural	57 IRE 7.S2	45 1004 Jul
Resolver	50 IRE 8.S1	39 276 Mar
Resolving Power	48 IRE 2,11,15.S1	Separate
Resolving Time	57 IRE 7.S2	45 1004 Jul
Resolving Time	54 IRE 12.S1	43 204 Feb
Resonant Gap	57 IRE 7.S2	45 1004 Jul
Resonant-Line Oscillator	48 IRE 2,11,15.S1	Separate
Resonant Modes in Cylindrical Cavities	45 IRE 24.S1	Separate
Resonant Window (Switching Tubes)	56 IRE 7.S3	44 1038 Aug
Resonator Mode	57 IRE 7.S2	45 1004 Jul
Resonator, Waveguide	55 IRE 2.S1	43 1074 Sep
Responder	54 IRE 12.S1	43 204 Feb
Responder Beacon	54 IRE 12.S1	43 204 Feb
Response	57 IRE 7.S2	45 1004 Jul
Retained Image	57 IRE 7.S2	45 1004 Jul
Retarding-Field (Position-Grid) Oscillator	48 IRE 2,11,15.S1	Separate
Retention Time, Maximum	57 IRE 7.S2	45 1004 Jul
Retrace Line	52 IRE 17.S1	40 1685 Dec
Return Loss	53 IRE 2.S1	41 1724 Dec
Return Transfer Function	55 IRE 26.S2	44 108 Jan
Reverberation	51 IRE 6.S1	39 525 May
Reverberation Chamber	51 IRE 6.S1	39 525 May
Reverberation Time	51 IRE 6.S1	39 525 May
Reverberation Time Meter	51 IRE 6.S1	39 525 May
Reverse Emission	57 IRE 7.S2	45 1004 Jul
Rewrite	56 IRE 8.S1	44 1172 Sep
Rho Theta	54 IRE 12.S1	43 204 Feb
Rhombic Antenna	48 IRE 2,11,15.S1	Separate
Ribbon Microphone	51 IRE 6.S1	39 525 May
Rieke Diagram	57 IRE 7.S2	45 1004 Jul
Right-Handed (Clockwise) Polarized Wave	50 IRE 24.S1	38 1267 Nov
Ring Around	54 IRE 12.S1	43 205 Feb
Ring Counter	56 IRE 8.S1	44 1172 Sep
Ring Head	51 IRE 6.S1	39 525 May
Ring Oscillator	48 IRE 2,11,15.S1	Separate
Ring Time	54 IRE 12.S1	43 205 Feb
Ringing (in Facsimile)	56 IRE 9.S1	44 780 Jne
Ringing (in Receivers)	52 IRE 17.S1	40 1685 Dec
Ripple	52 IRE 17.S1	40 1685 Dec
Ripple Voltage	48 IRE 2,11,15.S1	Separate
Rising-Sun Magnetron	57 IRE 7.S2	45 1004 Jul
RMI	54 IRE 12.S1	43 205 Feb
RMS (Effective) Pulse Amplitude	51 IRE 20.S1	39 626 Jne
Roll Out	50 IRE 8.S1	39 276 Mar
Root-Sum Square	52 IRE 17.S1	40 1685 Dec
Rotary Generator	55 IRE 10.S1	43 1072 Sep
Rotating Joint	55 IRE 2.S1	43 1074 Sep
Round-Off	50 IRE 8.S1	39 276 Mar
Round-Off Error	50 IRE 8.S1	39 276 Mar
Routine	56 IRE 8.S1	44 1172 Sep
RT Box	54 IRE 12.S1	43 205 Feb
Rumble	51 IRE 6.S1	39 525 May
Rumble, Turntable	52 IRE 17.S1	40 1685 Dec
S		
Sabin	51 IRE 6.S1	39 526 May
Sampling Gate	54 IRE 12.S1	43 205 Feb
Saturated Signal	54 IRE 12.S1	43 205 Feb
Saturating Signal	54 IRE 12.S1	43 205 Feb
Saturation	55 IRE 22.S1	43 748 Jne
SBA (Standard Beam Approach)	54 IRE 12.S1	43 209 Feb
Scale	51 IRE 6.S1	39 526 May
Scale Factor	50 IRE 8.S1	39 276 Mar
Scanner	56 IRE 9.S1	44 780 Jne
Scanning (Antenna)	48 IRE 2,11,15.S1	Separate
Scanning Antenna Mount	48 IRE 2,11,15.S1	Separate
Scanning, High-Velocity	57 IRE 7.S2	45 1004 Jul
Scanning (in Facsimile)	56 IRE 9.S1	44 780 Jne
Scanning (in Navigation Aids)	49 IRE 12.S1	37 1370 Dec
Scanning Line Frequency	56 IRE 9.S1	44 780 Jne
Scanning Line Length	56 IRE 9.S1	44 780 Jne
Scanning Loss	48 IRE 2,11,15.S1	Separate
Scanning Low-Velocity	57 IRE 7.S2	45 1004 Jul
Scanning Spot X Dimension	56 IRE 9.S1	44 780 Jne
Scanning Spot Y Dimension	56 IRE 9.S1	44 780 Jne
Scatterband	54 IRE 12.S1	43 205 Feb
Scattering Loss	51 IRE 6.S1	39 526 May
Schottky Emission	57 IRE 7.S2	45 1004 Jul
Scintillation	54 IRE 12.S1	43 205 Feb
Scope	54 IRE 12.S1	43 205 Feb
Scoring System	51 IRE 6.S1	39 526 May
Screen	57 IRE 7.S2	45 1004 Jul
Screen Grid	57 IRE 7.S2	45 1004 Jul
Screen-Grid Characteristic	57 IRE 7.S2	45 1004 Jul
Screen-Grid Current	57 IRE 7.S2	45 1004 Jul
Screen-Grid Modulation	48 IRE 2,11,15.S1	Separate
Sea Return	54 IRE 12.S1	43 205 Feb
Searchlighting	54 IRE 12.S1	43 205 Feb
Search Radar	54 IRE 12.S1	43 205 Feb
Secondary Emission	57 IRE 7.S2	45 1004 Jul
Secondary-Emission Ratio	57 IRE 7.S2	45 1004 Jul
Secondary Grid Emission	57 IRE 7.S2	45 1004 Jul
Secondary Radar	54 IRE 12.S1	43 205 Feb
Second-Channel Attenuation	52 IRE 17.S1	40 1685 Dec
Second-Channel Interference	52 IRE 17.S1	40 1685 Dec
Second-Time-Around Echo	54 IRE 12.S1	43 205 Feb
Sectionalized Vertical Antenna	48 IRE 2,11,15.S1	Separate
Sectoral Horn	48 IRE 2,11,15.S1	Separate
Sector Display	54 IRE 12.S1	43 205 Feb
Sector Scanning	48 IRE 2,11,15.S1	Separate
Selectance	52 IRE 17.S1	40 1685 Dec
Selection Check	56 IRE 8.S1	44 1172 Sep
Selective Fading	50 IRE 24.S1	38 1267 Nov
Selectivity	52 IRE 17.S1	40 1685 Dec
Selector Pulse	54 IRE 12.S1	43 205 Feb
Self-Checking Code	56 IRE 8.S1	44 1172 Sep
Self-instructed Carry	50 IRE 8.S1	39 276 Mar
Self-Pulse Modulation	48 IRE 2,11,15.S1	Separate
Self-Quenched Counter Tube	57 IRE 7.S2	45 1004 Jul
Semiconductor	54 IRE 7.S2	42 1507 Oct
Semiconductor, Compensated	54 IRE 7.S2	42 1507 Oct

	Standard	Proceedings Vol	Page	Mo
Semiconductor Device	54 IRE 7.S2	42	1507	Oct
Semiconductor Device, Multiple Unit	54 IRE 7.S2	42	1507	Oct
Semiconductor Device, Single Unit	54 IRE 7.S2	42	1507	Oct
Semiconductor, Extrinsic	54 IRE 7.S2	42	1507	Oct
Semiconductor, Intrinsic	54 IRE 7.S2	42	1507	Oct
Semiconductor, N-Type	54 IRE 7.S2	42	1507	Oct
Semiconductor P-Type	54 IRE 7.S2	42	1508	Oct
Semiremote Control	48 IRE 2,11,15.S1	Separate		
Semitone	51 IRE 6.S1	39	526	May
Semitransparent Photocathode	57 IRE 7.S2	45	1004	Jul
Sending End Impedance	53 IRE 2.S1	41	1724	Dec
Sense	54 IRE 12.S1	43	205	Feb
Sensing	54 IRE 12.S1	43	205	Feb
Sensitive Volume	57 IRE 7.S2	45	1004	Jul
Sensitivity	50 IRE 7.S1	38	436	Apr
Sensitivity	52 IRE 17.S1	40	1685	Dec
Sensitivity, Cathode Luminous	57 IRE 7.S2	45	1004	Jul
Sensitivity, Cathode Radiant	57 IRE 7.S2	45	1004	Jul
Sensitivity, Illumination	57 IRE 7.S2	45	1004	Jul
Sensitivity, Luminous	57 IRE 7.S2	45	1005	Jul
Sensitivity, Radiant	57 IRE 7.S2	45	1005	Jul
Sensitivity Time Control	54 IRE 12.S1	43	205	Feb
Sensitometry	51 IRE 6.S1	39	526	May
Sensor	54 IRE 12.S1	43	205	Feb
Separate Parts of a Network	50 IRE 4.S1	38	28	Jan
Separately Instructed Carry	50 IRE 8.S1	39	276	Mar
Serial	56 IRE 8.S1	44	1172	Sep
Serial Arithmetic Unit	50 IRE 8.S1	39	276	Mar
Serial Digital Computer	56 IRE 8.S1	44	1172	Sep
Serial Transmission	50 IRE 8.S1	39	276	Mar
Series Elements	50 IRE 4.S1	38	28	Jan
Series Fed Vertical Antenna	48 IRE 2,11,15.S1	Separate		
Series Tee Junction	55 IRE 2.S1	43	1074	Sep
Series Two-Terminal Pair Networks	50 IRE 4.S1	38	28	Jan
Service Area	54 IRE 12.S1	43	205	Feb
Service Band	48 IRE 2,11,15.S1	Separate		
Servomechanism	55 IRE 26.S2	44	109	Jan
Set	56 IRE 8.S1	44	1172	Sep
Setup	55 IRE 23.S1	43	621	May
Sexadecimal	56 IRE 8.S1	44	1172	Sep
Shading	57 IRE 7.S2	45	1005	Jul
Shadow Factor	50 IRE 24.S1	38	1267	Nov
Shadow Mask	57 IRE 7.S2	45	1005	Jul
Shaped-Beam Antenna (Phase-Shaped)	48 IRE 2,11,15.S1	Separate		
Shaping Network	42 IRE 9.S1	Separate		
Shaving	51 IRE 6.S1	39	526	May
Shear Wave	51 IRE 6.S1	39	526	May
Shield	55 IRE 10.S1	43	1072	Sep
Shield Grid	57 IRE 7.S2	45	1005	Jul
Shielded Pair	53 IRE 2.S1	41	1724	Dec
Shielded Transmission Line	53 IRE 2.S1	41	1724	Dec
Shift	56 IRE 8.S1	44	1172	Sep
Shift, Cyclic	50 IRE 8.S1	39	276	Mar
Shock Excitation	48 IRE 2,11,15.S1	Separate		
Shock Motion	51 IRE 6.S1	39	526	May
Shoran (Short Range Navigation)	54 IRE 12.S1	43	209	Feb
Short-Circuit Driving-Point Admittance	57 IRE 7.S2	45	1005	Jul
Short-Circuit Feedback Admittance	57 IRE 7.S2	45	1005	Jul
Short-Circuit Forward Admittance	57 IRE 7.S2	45	1005	Jul
Short-Circuit Input Admittance	57 IRE 7.S2	45	1005	Jul
Short-Circuit Input Capacitance	57 IRE 7.S2	45	1005	Jul
Short-Circuit Output Admittance	57 IRE 7.S2	45	1005	Jul
Short-Circuit Output Capacitance	57 IRE 7.S2	45	1005	Jul
Short-Circuit Transfer Admittance	57 IRE 7.S2	45	1005	Jul
Short-Circuit Transfer Capacitance	57 IRE 7.S2	45	1005	Jul
Short-Distance Navigation Aid	54 IRE 12.S1	43	205	Feb
Shot Noise, Full	57 IRE 7.S2	45	1005	Jul
Shot Noise, Reduced	57 IRE 7.S2	45	1005	Jul
Shot Noise Reduction Factor	57 IRE 7.S2	45	1005	Jul
Shunt-Fed Vertical Antenna	48 IRE 2,11,15.S1	Separate		
Shunt Tee Junction	55 IRE 2.S1	43	1074	Sep
Sidebands	53 IRE 11.S1	41	614	May
Sidebands	52 IRE 17.S1	40	1685	Dec
Sideband Attenuation	48 IRE 2,11,15.S1	Separate		
Side Frequency	53 IRE 11.S1	41	614	May
Side Thrust	51 IRE 6.S1	39	526	May
Sign Digit	56 IRE 8.S1	44	1173	Sep
Signal	54 IRE 3.S1	42	1111	Jul
Signal Contrast (in Facsimile)	56 IRE 9.S1	44	780	Jne
Signal Electrode	50 IRE 7.S1	38	437	Apr
Signal Electrode Capacitance	57 IRE 7.S2	45	1005	Jul
Signal Frequency Shift	56 IRE 9.S1	44	780	Jne
Signal Level	54 IRE 3.S1	42	1111	Jul
Signal Output Current	57 IRE 7.S2	45	1005	Jul
Signal-to-Noise Ratio	48 IRE 2,11,15.S1	Separate		
Signal-to-Noise Ratio	57 IRE 7.S2	45	1006	Jul
Signal-Wave Envelope	42 IRE 9.S1	Separate		
Significant Digits	50 IRE 8.S1	39	276	Mar
Simple Scanning	56 IRE 9.S1	44	780	Jne
Simple Sound Source	51 IRE 6.S1	39	526	May
Simple Target	54 IRE 12.S1	43	205	Feb
Simple Tone	51 IRE 6.S1	39	526	May
Simplex Operation of a Radio System	48 IRE 2,11,15.S1	Separate		
Simulation	50 IRE 8.S1	39	276	Mar
Simultaneous Lobing	54 IRE 12.S1	43	205	Feb
Sine Wave	48 IRE 2,11,15.S1	Separate		
Singing	48 IRE 2,11,15.S1	Separate		
Singing Point	48 IRE 2,11,15.S1	Separate		
Single-Address Code	50 IRE 8.S1	39	276	Mar
Single-Address Code	56 IRE 8.S1	44	1173	Sep
Single-Ended Amplifier	48 IRE 2,11,15.S1	Separate		
Single-Polarity Pulse	52 IRE 20.S1	40	554	May
Single Pole-Piece Magnetic Head	51 IRE 6.S1	39	526	May
Single-Sideband Modulation	53 IRE 11.S1	41	614	May
Single-Sideband Transmission	48 IRE 2,11,15.S1	Separate		
Single-Sideband Transmitter	48 IRE 2,11,15.S1	Separate		
Single-Tone Keying	53 IRE 11.S1	41	615	May
Single Track	51 IRE 6.S1	39	526	May
Sink (of an Oscillator)	57 IRE 7.S2	45	1006	Jul
Sinusoidal Electro-Magnetic Wave	50 IRE 24.S1	38	1267	Nov
Site Error	54 IRE 12.S1	43	205	Feb
Skew (in Facsimile)	56 IRE 9.S1	44	780	Jne
Skiatron	54 IRE 12.S1	43	205	Feb
Skin Depth	53 IRE 2.S1	41	1724	Dec
Sky Error	54 IRE 12.S1	43	205	Feb
Sky Wave	50 IRE 24.S1	38	1267	Nov
Sky-Wave Accuracy Pattern	54 IRE 12.S1	43	205	Feb
Sky-Wave Correction	54 IRE 12.S1	43	205	Feb
Sky-Wave Station-Error	54 IRE 12.S1	43	205	Feb
Slant Distance	54 IRE 12.S1	43	206	Feb
Slant Range	54 IRE 12.S1	43	206	Feb
Slave Station	54 IRE 12.S1	43	206	Feb
Slave Sweep	54 IRE 12.S1	43	206	Feb
Sleeve-Dipole Antenna	48 IRE 2,11,15.S1	Separate		
Sleeve Stub	48 IRE 2,11,15.S1	Separate		
Slope	54 IRE 12.S1	43	206	Feb
Slope Angle	54 IRE 12.S1	43	206	Feb

	Standard	PROCEEDINGS Vol Page Mo
Slope Deviation	49 IRE 12.S1	37 1370 Dec
Slot Antenna	48 IRE 2,11,15.S1	Separate
Slug Tuner	55 IRE 2.S1	43 1074 Sep
Slug Tuning	48 IRE 2,11,15.S1	Separate
Small-Signal Forward Transadmittance	57 IRE 7.S2	45 1006 Jul
Soft Spot	54 IRE 12.S1	43 206 Feb
Sonar	54 IRE 12.S1	43 206 Feb
Sone	51 IRE 6.S1	39 526 May
Sonne	54 IRE 12.S1	43 209 Feb
Sound	51 IRE 6.S1	39 526 May
Sound Absorption	51 IRE 6.S1	39 526 May
Sound Absorption Coefficient	51 IRE 6.S1	39 526 May
Sound Analyzer	51 IRE 6.S1	39 526 May
Sound Articulation	51 IRE 6.S1	39 526 May
Sound Energy	51 IRE 6.S1	39 526 May
Sound-Energy Density	51 IRE 6.S1	39 526 May
Sound-Energy Flux	51 IRE 6.S1	39 527 May
Sound Field	51 IRE 6.S1	39 527 May
Sound Intensity	51 IRE 6.S1	39 527 May
Sound Level	51 IRE 6.S1	39 527 May
Sound Level Meter	51 IRE 6.S1	39 527 May
Sound Power of a Source	51 IRE 6.S1	39 527 May
Sound Pressure Level	51 IRE 6.S1	39 527 May
Sound Probe	51 IRE 6.S1	39 528 May
Sound Recording System	51 IRE 6.S1	39 528 May
Sound Reflection Coefficient	51 IRE 6.S1	39 528 May
Sound Reproducing System	51 IRE 6.S1	39 528 May
Sound Track	51 IRE 6.S1	39 528 May
Sound Transmission Coefficient	51 IRE 6.S1	39 528 May
Source	54 IRE 3.S1	42 1112 Jul
Source Impedance	54 IRE 3.S1	42 1112 Jul
Space Charge	57 IRE 7.S2	45 1006 Jul
Space-Charge Debunching	57 IRE 7.S2	45 1006 Jul
Space-Charge Density	57 IRE 7.S2	45 1006 Jul
Space-Charge Grid	57 IRE 7.S2	45 1006 Jul
Space-Charge-Limited Current	57 IRE 7.S2	45 1006 Jul
Space-Charge Region	54 IRE 7.S2	42 1508 Oct
Space Pattern	55 IRE 23.S1	43 621 May
Spacing Wave (Back Wave)	48 IRE 2,11,15.S1	Separate
Spark-Gap Modulation	48 IRE 2,11,15.S1	Separate
Spark Transmitter	48 IRE 2,11,15.S1	Separate
Speaker	52 IRE 17.S1	40 1685 Dec
Specific Acoustic Impedance	51 IRE 6.S1	39 528 May
Specific Acoustic Reactance	51 IRE 6.S1	39 528 May
Specific Acoustic Resistance	51 IRE 6.S1	39 528 May
Specific Repetition Rate	54 IRE 12.S1	43 206 Feb
Spectral Characteristic	57 IRE 7.S2	45 1006 Jul
Spectral Characteristic	55 IRE 22.S1	43 748 Jne
Spectral Sensitivity Characteristic	57 IRE 7.S2	45 1006 Jul
Spectrum Locus	55 IRE 22.S1	43 748 Jne
Spherical-Earth Factor	50 IRE 24.S1	38 1267 Nov
Spherical Hyperbola	54 IRE 12.S1	43 206 Feb
Spherical Wave	50 IRE 24.S1	38 1267 Nov
Spike Leakage Energy	57 IRE 7.S2	45 1006 Jul
Spill	57 IRE 7.S2	45 1006 Jul
Spinner	54 IRE 12.S1	43 206 Feb
Spiral Scanning	48 IRE 2,11,15.S1	Separate
Split-Anode Magnetron	57 IRE 7.S2	45 1006 Jul
Split Hydrophone	51 IRE 6.S1	39 528 May
Split Projector	51 IRE 6.S1	39 528 May
Spot	50 IRE 7.S1	38 437 Apr
Spot Projection	56 IRE 9.S1	44 780 Jne
Spot Speed	56 IRE 9.S1	44 780 Jne
Spurious Pulse Mode	52 IRE 20.S1	40 554 May
Spurious Radiation	48 IRE 2,11,15.S1	Separate
Spurious Response Ratio	52 IRE 17.S1	40 1685 Dec
Spurious Tube Counts	57 IRE 7.S2	45 1006 Jul
Sputtering	51 IRE 6.S1	39 528 May
Square Wave	52 IRE 17.S1	40 1685 Dec
Square-Wave Response	57 IRE 7.S2	45 1006 Jul
Square-Wave Response Characteristic	57 IRE 7.S2	45 1006 Jul
Squeezable Waveguide	54 IRE 12.S1	43 206 Feb
Squeeze Track	51 IRE 6.S1	39 528 May
Squelch	52 IRE 17.S1	40 1685 Dec
Squint	54 IRE 12.S1	43 206 Feb
Squitter	54 IRE 12.S1	43 206 Feb
SRE (Surveillance Radar Element)	54 IRE 12.S1	43 209 Feb
Stabilization	54 IRE 12.S1	43 206 Feb
Stabilized Feedback	48 IRE 2,11,15.S1	Separate
Stabilized Flight	54 IRE 12.S1	43 206 Feb
Stable Element	54 IRE 12.S1	43 206 Feb
Stage Efficiency	48 IRE 2,11,15.S1	Separate
Stagger	56 IRE 9.S1	44 780 Jne
Stalo	54 IRE 12.S1	43 206 Feb
Stamper	51 IRE 6.S1	39 528 May
Standard Microphone	51 IRE 6.S1	39 528 May
Standard Observer	55 IRE 22.S1	43 748 Jne
Standard Pitch	51 IRE 6.S1	39 528 May
Standard Propagation	50 IRE 24.S1	38 1267 Nov
Standard Refraction	50 IRE 24.S1	38 1267 Nov
Standard Sea Water Conditions	51 IRE 6.S1	39 529 May
Standard Volume Indicator	54 IRE 3.S1	42 1112 Jul
Standing-on-Nines Carry	56 IRE 8.S1	44 1173 Sep
Standing Wave	50 IRE 24.S1	38 1268 Nov
Standing Wave	53 IRE 2.S1	41 1725 Dec
Standing-Wave Loss Factor	53 IRE 2.S1	41 1725 Dec
Standing-Wave Ratio	53 IRE 2.S1	41 1725 Dec
Star Chain	54 IRE 12.S1	43 206 Feb
Star Network	50 IRE 4.S1	38 28 Jan
Start Record Signal	56 IRE 9.S1	44 780 Jne
Start Signal	56 IRE 9.S1	44 780 Jne
Starter	57 IRE 7.S2	45 1006 Jul
Starter Breakdown Voltage	57 IRE 7.S2	45 1006 Jul
Starter Gap	57 IRE 7.S2	45 1006 Jul
Starter Voltage Drop	57 IRE 7.S2	45 1006 Jul
Starting Current of an Oscillator	57 IRE 7.S2	45 1006 Jul
Static Characteristic	57 IRE 7.S2	45 1006 Jul
Static Pressure	51 IRE 6.S1	39 529 May
Static Register	50 IRE 8.S1	39 276 Mar
Staticizer	56 IRE 8.S1	44 1173 Sep
STC	54 IRE 12.S1	43 206 Feb
Steady-State Oscillation	51 IRE 6.S1	39 529 May
Steerable Antenna	48 IRE 2,11,15.S1	Separate
Stereophonic Sound System	51 IRE 6.S1	39 529 May
Sticking Picture	57 IRE 7.S2	45 1006 Jul
Stirring Effect	55 IRE 10.S1	43 1072 Sep
Stop Record Signal	56 IRE 9.S1	44 780 Jne
Stop Signal	56 IRE 9.S1	44 780 Jne
Storage	56 IRE 8.S1	44 1173 Sep
Storage Capacity	56 IRE 8.S1	44 1173 Sep
Storage Element	57 IRE 7.S2	45 1006 Jul
Storage Time	57 IRE 7.S2	45 1006 Jul
Storage Tube	57 IRE 7.S2	45 1006 Jul
Storage Tube	50 IRE 8.S1	39 277 Mar
Store	56 IRE 8.S1	44 1173 Sep
Streaming	51 IRE 6.S1	39 529 May
Strength of a Sound Source	51 IRE 6.S1	39 529 May
Striation Technique	51 IRE 6.S1	39 529 May
Stroke Speed (Scanning or Recording Line Frequency)	56 IRE 9.S1	44 780 Jne

	Standard	PROCEEDINGS Vol	Page	Mo
Structurally Dual Networks	50 IRE 4.S1	38	28	Jan
Structurally Symmetrical Network	50 IRE 4.S1	38	28	Jan
Stub, Waveguide	55 IRE 2.S1	43	1074	Sep
Stylus Drag	51 IRE 6.S1	39	529	May
Stylus Force	51 IRE 6.S1	39	529	May
Subcarrier	53 IRE 11.S1	41	615	May
Subcarrier	56 IRE 9.S1	44	780	Jne
Subharmonic	48 IRE 2,11,15.S1	Separate		
Subject Copy	56 IRE 9.S1	44	780	Jne
Submerged Register Induction Furnace	55 IRE 10.S1	43	1072	Sep
Subprogram	50 IRE 8.S1	39	277	Mar
Subroutine	56 IRE 8.S1	44	1173	Sep
Summing Point	55 IRE 26.S2	44	108	Jan
Supersonics	51 IRE 6.S1	39	529	May
Suppressed Time Delay	54 IRE 12.S1	43	206	Feb
Suppressor Grid	57 IRE 7.S2	45	1006	Jul
Surface Duct	50 IRE 24.S1	38	1268	Nov
Surface Noise	51 IRE 6.S1	39	529	May
Surface of Position	54 IRE 12.S1	43	206	Feb
Surge Electrode Current	50 IRE 7.S1	38	437	Apr
Surveillance Radar Airport	54 IRE 12.S1	43	206	Feb
Syllabic Companding	53 IRE 11.S1	41	615	May
Syllable Articulation	51 IRE 6.S1	39	529	May
Symmetrical Network	50 IRE 4.S1	38	29	Jan
Symmetrical Transducer	51 IRE 20.S1	39	898	Aug
Sync Compression	55 IRE 23.S1	43	621	May
Sync Level	55 IRE 23.S1	43	621	May
Sync Signal (Synchronizing Signal)	55 IRE 23.S1	43	621	May
Synchronization Error	54 IRE 12.S1	43	206	Feb
Synchronizing (in Facsimile)	56 IRE 9.S1	44	780	Jne
Synchronizing (in Television)	55 IRE 23.S1	43	621	May
Synchronizing Signal	56 IRE 9.S1	44	780	Jne
Synchronous Gate	53 IRE 11.S1	41	615	May
Synchronous Voltage	57 IRE 7.S2	45	1006	Jul
Systematic Errors	54 IRE 12.S1	43	206	Feb
T				
Tailing (Hangover)	56 IRE 9.S1	44	780	Jne
Tailing (or Hangover)	42 IRE 9.S1	Separate		
Tandem	50 IRE 4.S1	38	29	Jan
Tangential Wave Path	50 IRE 24.S1	38	1268	Nov
Tank Circuit	48 IRE 2,11,15.S1	Separate		
Tapered Transmission Line	53 IRE 2.S1	41	1725	Dec
Taper, Waveguide	55 IRE 2.S1	43	1074	Sep
Tapered Waveguide	55 IRE 2.S1	43	1074	Sep
Target	54 IRE 12.S1	43	206	Feb
Target	57 IRE 7.S2	45	1006	Jul
Target Capacitance	57 IRE 7.S2	45	1007	Jul
Target Cutoff Voltage	57 IRE 7.S2	45	1007	Jul
Target Glint	54 IRE 12.S1	43	206	Feb
Target Voltage	57 IRE 7.S2	45	1007	Jul
Tee Junction	55 IRE 2.S1	43	1074	Sep
Telephone Receiver	51 IRE 6.S1	39	529	May
Telephone Transmitter	51 IRE 6.S1	39	530	May
Teleran	49 IRE 12.S1	37	1371	Dec
Teleran (Television and Radar Navigation System)	54 IRE 12.S1	43	209	Feb
Television Transmitter	48 IRE 2,11,15.S1	Separate		
$TE_{m,n}$ Wave in Circular Waveguide	53 IRE 2.S1	41	1728	Dec
$TE_{M,n}$ Wave in Rectangular Waveguide	53 IRE 2.S1	41	1727	Dec
$TE_{m,m,p}$ Resonant Mode in Cylindrical Cavity	53 IRE 2.S1	41	1728	Dec
Temperature	57 IRE 7.S2	45	1007	Jul
Temperature Coefficient of Voltage Drop	57 IRE 7.S2	45	1007	Jul
Temporal Gain Control	54 IRE 12.S1	43	206	Feb
Tenth-Power Width	48 IRE 2,11,15.S1	Separate		
Terminal	50 IRE 4.S1	38	29	Jan
Terminal Pair	50 IRE 4.S1	38	29	Jan
Ternary	56 IRE 8.S1	44	1173	Sep
Terrain Clearance Indicator	49 IRE 12.S1	37	1370	Dec
Terrain Echoes	54 IRE 12.S1	43	206	Feb
Terrain Error	54 IRE 12.S1	43	206	Feb
Terrestrial-Reference Flight	54 IRE 12.S1	43	206	Feb
Test Routine	56 IRE 8.S1	44	1173	Sep
Tetrode	57 IRE 7.S2	45	1007	Jul
Theta (θ) Polarization	48 IRE 2,11,15.S1	Separate		
Thermal Noise	57 IRE 7.S2	45	1007	Jul
Thermal Tuning Time	57 IRE 7.S2	45	1007	Jul
Thermal Tuning Time (Heating)	57 IRE 7.S2	45	1007	Jul
Thermal Tuning Time (Cooling)	57 IRE 7.S2	45	1007	Jul
Thermionic Cathode	57 IRE 7.S2	45	1007	Jul
Thermionic Emission	57 IRE 7.S2	45	1007	Jul
Thermionic Grid Emission	57 IRE 7.S2	45	1007	Jul
Thermionic Tube	57 IRE 7.S2	45	1007	Jul
Thermistor	54 IRE 7.S2	42	1508	Oct
Thermophone	51 IRE 6.S1	39	530	May
Three-Address Code	56 IRE 8.S1	44	1173	Sep
Threshold	51 IRE 6.S1	39	526	May
Threshold of Audibility	51 IRE 6.S1	39	530	May
Threshold of Feeling	51 IRE 6.S1	39	530	May
Threshold Signal	54 IRE 12.S1	43	206	Feb
Throat Microphone	51 IRE 6.S1	39	530	May
Through Path	55 IRE 26.S2	44	108	Jan
Through Transfer Function	55 IRE 26.S2	44	108	Jan
Thyratron	57 IRE 7.S2	45	1007	Jul
Tilt	49 IRE 12.S1	37	1370	Dec
Tilt Angle	54 IRE 12.S1	43	206	Feb
Tilt Error	54 IRE 12.S1	43	206	Feb
Timbre	51 IRE 6.S1	39	530	May
Time	57 IRE 7.S2	45	1007	Jul
Time Discriminator	54 IRE 12.S1	43	206	Feb
Time-Division Multiplex	53 IRE 11.S1	41	615	May
Time Gain Control	49 IRE 12.S1	37	1370	Dec
Time Gate	53 IRE 11.S1	41	615	May
Time Pattern	55 IRE 23.S1	43	622	May
Time-Varied Gain (TVG)	54 IRE 12.S1	43	207	Feb
Timer	54 IRE 12.S1	43	207	Feb
$TM_{m,n}$ Wave in Circular Waveguide	53 IRE 2.S1	41	1728	Dec
$TM_{M,n}$ Wave in Rectangular Waveguide	53 IRE 2.S1	41	1727	Dec
$TM_{m,n,p}$ Resonant Mode in Cylindrical Cavity	53 IRE 2.S1	41	1728	Dec
T-Network	50 IRE 4.S1	38	29	Jan
Toe and Shoulder	51 IRE 6.S1	39	530	May
To-From Indicator	54 IRE 12.S1	43	207	Feb
Tone	51 IRE 6.S1	39	530	May
Tone Localizer	54 IRE 12.S1	43	207	Feb
Top-Loaded Vertical Antenna	48 IRE 2,11,15.S1	Separate		
Torque Amplifier	50 IRE 8.S1	39	277	Mar
Total Telegraph Distortion	48 IRE 2,11,15.S1	Separate		
Totally Unbalanced Currents	53 IRE 2.S1	41	1725	Dec
TR Box	54 IRE 12.S1	43	207	Feb
TR Cavity	54 IRE 12.S1	43	207	Feb
TR Switch	54 IRE 12.S1	43	207	Feb
TR (Transmit Receive) Tube	57 IRE 7.S2	45	1007	Jul
Tracing Distortion	51 IRE 6.S1	39	530	May
Track (Computers)	56 IRE 8.S1	44	1173	Sep
Track (navigation)	54 IRE 12.S1	43	207	Feb
Track Homing	54 IRE 12.S1	43	207	Feb
Tracking (antenna)	48 IRE 2,11,15.S1	Separate		

	Standard	PROCEEDINGS Vol Page Mo
Tracking (Navigation)	49 IRE 12.S1	37 1370 Dec
Tracking (Receivers)	52 IRE 17.S1	40 1685 Dec
Tracking Error	51 IRE 6.S1	39 530 May
Trailing Edge	55 IRE 23.S1	43 622 May
Trailing Edge Pulse Time	51 IRE 20.S1	39 626 Jne
Transadmittance	57 IRE 7.S2	45 1007 Jul
Transadmittance Forward	57 IRE 7.S2	45 1007 Jul
Transmittance Compression Ratio	57 IRE 7.S2	45 1007 Jul
Transconductance	57 IRE 7.S2	45 1007 Jul
Transcriber	56 IRE 8.S1	44 1173 Sep
Transducer	54 IRE 3.S1	42 1112 Jul
Transducer	57 IRE 7.S2	45 1007 Jul
Transducer	51 IRE 20.S2	39 898 Aug
Transducer Equivalent Noise Pressure	51 IRE 6.S1	39 530 May
Transducer Gain	54 IRE 3.S1	42 1112 Jul
Transducer Gain	51 IRE 20.S2	39 899 Aug
Transducer Gain	57 IRE 7.S2	45 1008 Jul
Transducer Loss	54 IRE 3.S1	42 1112 Jul
Transducer Loss	51 IRE 20.S2	39 899 Aug
Transducer Pulse Delay	52 IRE 20.S1	40 554 May
Transfer	56 IRE 8.S1	44 1173 Sep
Transfer Admittance	42 IRE 9.S1	Separate
Transfer Admittance	57 IRE 7.S2	45 1008 Jul
Transfer Characteristic	57 IRE 7.S2	45 1008 Jul
Transfer Characteristic	52 IRE 17.S1	40 1685 Dec
Transfer Check	56 IRE 8.S1	44 1173 Sep
Transfer, Conditional	50 IRE 8.S1	39 277 Mar
Transfer Control	56 IRE 8.S1	44 1173 Sep
Transfer Current	57 IRE 7.S2	45 1008 Jul
Transfer Function	55 IRE 26.S2	44 108 Jan
Transfer Ratio	42 IRE 9.S1	Separate
Transfer Ratio	55 IRE 26.S2	44 108 Jan
Transfer, Unconditional	50 IRE 8.S1	39 277 Mar
Transformer Loss	54 IRE 3.S1	42 1112 Jul
Transformer, Waveguide	55 IRE 2.S1	43 1074 Sep
Transient Motion	51 IRE 6.S1	39 530 May
Transistor	54 IRE 7.S2	42 1508 Oct
Transistor, Conductivity Modulation	54 IRE 7.S2	42 1508 Oct
Transistor, Filamentary	54 IRE 7.S2	42 1508 Oct
Transistor, Junction	54 IRE 7.S2	42 1508 Oct
Transistor, Point-Contact	54 IRE 7.S2	42 1508 Oct
Transistor, Point-Junction	54 IRE 7.S2	42 1508 Oct
Transistor, Unipolar	54 IRE 7.S2	42 1508 Oct
Transit Angle	57 IRE 7.S2	45 1008 Jul
Transit-Time Mode	57 IRE 7.S2	45 1008 Jul
Transition Frequency	51 IRE 6.S1	39 530 May
Transition Loss (in Audio Systems and Components)	54 IRE 3.S1	42 1112 Jul
Transition Region	54 IRE 7.S2	42 1508 Oct
Transitron Oscillator	48 IRE 2,11,15.S1	Separate
Translation Loss	51 IRE 6.S1	39 530 May
Translator	56 IRE 8.S1	44 1173 Sep
Transmission	51 IRE 6.S1	39 530 May
Transmission Band	53 IRE 2.S1	41 1725 Dec
Transmission Coefficient	53 IRE 2.S1	41 1725 Dec
Transmission Gain	42 IRE 9.S1	Separate
Transmission Level	48 IRE 2,11,15.S1	Separate
Transmission Level	42 IRE 9.S1	Separate
Transmission Line	53 IRE 2.S1	41 1725 Dec
Transmission Loss	53 IRE 2.S1	41 1725 Dec
Transmission Loss (or "Loss")	42 IRE 9.S1	Separate
Transmission Primaries	55 IRE 22.S1	43 748 Jne
Transmitted Wave	53 IRE 2.S1	41 1725 Dec
Transmitted Wave	50 IRE 24.S1	38 1268 Nov
Transmitter, Facsimile	56 IRE 9.S1	44 780 Jne
Transmitter Pulse Delay	52 IRE 20.S1	40 554 May
Transmitting Converter, Facsimile (AM to FS Converter)	56 IRE 9.S1	44 780 Jne
Transmitting Current Response	51 IRE 6.S1	39 530 May
Transmitting Efficiency	51 IRE 6.S1	39 531 May
Transmitting Power Response	51 IRE 6.S1	39 531 May
Transmitting Voltage Response	51 IRE 6.S1	39 531 May
Trans-u Factor	57 IRE 7.S2	45 1008 Jul
Transponder	54 IRE 12.S1	43 207 Feb
Transponder Beacon	54 IRE 12.S1	43 207 Feb
Transponder Crossband	54 IRE 12.S1	43 207 Feb
Transponder Reply Efficiency	54 IRE 12.S1	43 207 Feb
Transportable Transmitter	48 IRE 2,11,15.S1	Separate
Transrectification Factor	57 IRE 7.S2	45 1008 Jul
Transverse-Beam Traveling-Wave Tube	57 IRE 7.S2	45 1008 Jul
Transverse Electric Wave	53 IRE 2.S1	41 1725 Dec
Transverse Electric Wave	50 IRE 24.S1	38 1268 Nov
Transverse Electromagnetic Wave	50 IRE 24.S1	38 1268 Nov
Transverse Electromagnetic Wave	53 IRE 2.S1	41 1725 Dec
Transverse-Field Traveling Wave Tube	57 IRE 7.S2	45 1008 Jul
Transverse Magnetic Wave	53 IRE 2.S1	41 1725 Dec
Transverse Magnetic Wave	50 IRE 24.S1	38 1268 Nov
Transverse Magnetization	51 IRE 6.S1	39 531 May
Traveling Plane Wave	53 IRE 2.S1	41 1725 Dec
Traveling Plane Wave	50 IRE 24.S1	38 1268 Nov
Traveling-Wave Magnetron	57 IRE 7.S2	45 1008 Jul
Traveling-Wave Magnetron Oscillations	57 IRE 7.S2	45 1008 Jul
Traveling-Wave Tube	57 IRE 7.S2	45 1008 Jul
Traveling-Wave Tube Interaction Circuit	57 IRE 7.S2	45 1008 Jul
Tree	50 IRE 4.S1	38 29 Jan
Triad	54 IRE 12.S1	43 207 Feb
Tricon	54 IRE 12.S1	43 209 Feb
Trigatron	54 IRE 12.S1	43 207 Feb
Trigger Level	54 IRE 12.S1	43 207 Feb
Triode	57 IRE 7.S2	45 1008 Jul
Triplet	54 IRE 12.S1	43 207 Feb
Tristimulus Values	55 IRE 22.S1	43 748 Jne
Troposphere	50 IRE 24.S1	38 1268 Nov
Tropospheric Wave	50 IRE 24.S1	38 1268 Nov
Trouble-Location Problem	50 IRE 8.S1	39 277 Mar
True Bearing	49 IRE 12.S1	37 1370 Dec
True Course	49 IRE 12.S1	37 1370 Dec
True Heading	49 IRE 12.S1	37 1370 Dec
True Homing	49 IRE 12.S1	37 1370 Dec
Truncation Error	50 IRE 8.S1	39 277 Mar
Tube	57 IRE 7.S2	45 1008 Jul
Tube	52 IRE 17.S1	40 1685 Dec
Tube Count	57 IRE 7.S2	45 1009 Jul
Tube Heating Time	57 IRE 7.S2	45 1009 Jul
Tube, Vacuum	52 IRE 17.S1	40 1685 Dec
Tube Voltage Drop	57 IRE 7.S2	45 1009 Jul
Tuned-Grid Oscillator	48 IRE 2,11,15.S1	Separate
Tuned-Grid Tuned-Plate Oscillator	48 IRE 2,11,15.S1	Separate
Tuned-Plate Oscillator	48 IRE 2,11,15.S1	Separate
Tuner, Waveguide	55 IRE 2.S1	43 1074 Sep
Tuning, Electronic	57 IRE 7.S2	45 1009 Jul
Tuning Probe	55 IRE 2.S1	43 1074 Sep
Tuning Range	57 IRE 7.S2	45 1009 Jul
Tuning Range, Electronic	57 IRE 7.S2	45 1009 Jul

	Standard	Proceedings Vol Page Mo
Tuning Rate Thermal	57 IRE 7.S2	45 1009 Jul
Tuning Sensitivity, Electronic	57 IRE 7.S2	45 1009 Jul
Tuning Sensitivity Thermal	57 IRE 7.S2	45 1009 Jul
Tuning Susceptance	57 IRE 7.S2	45 1009 Jul
Tuning Thermal	57 IRE 7.S2	45 1009 Jul
Tuning Time Constant, Thermal	57 IRE 7.S2	45 1009 Jul
Turntable Rumble	52 IRE 17.S1	40 1685 Dec
Turnstile Antenna	48 IRE 2,11,15.S1	Separate
TVG (Time-Varied Gain)	54 IRE 12.S1	43 207 Feb
Twist, Waveguide	55 IRE 2.S1	43 1074 Sep
Two-Source Frequency Keying	53 IRE 11.S1	41 615 May
Two-Terminal Pair Network	50 IRE 4.S1	38 29 Jan
Two-Tone Keying	53 IRE 11.S1	41 615 May
U		
Ultrasonic Coagulation	51 IRE 6.S1	39 531 May
Ultrasonic Cross Grating	51 IRE 6.S1	39 531 May
Ultrasonic Delay Line	51 IRE 6.S1	39 531 May
Ultrasonic Detector	51 IRE 6.S1	39 531 May
Ultrasonic Frequency	51 IRE 6.S1	39 531 May
Ultrasonic Generator	51 IRE 6.S1	39 531 May
Ultrasonic Grating Constant	51 IRE 6.S1	39 531 May
Ultrasonic Light Diffraction	51 IRE 6.S1	39 531 May
Ultrasonic Material Dispersion	51 IRE 6.S1	39 531 May
Ultrasonic Space Grating	51 IRE 6.S1	39 531 May
Ultrasonic Stroboscope	51 IRE 6.S1	39 531 May
Ultrasonics	51 IRE 6.S1	39 531 May
Unconditional Jump	56 IRE 8.S1	44 1173 Sep
Unconditional Transfer of Control	56 IRE 8.S1	44 1173 Sep
Underbunching	57 IRE 7.S2	45 1009 Jul
Underlap	52 IRE 9.S1	Separate
Underlap X	56 IRE 9.S1	44 780 Jne
Underlap Y	56 IRE 9.S1	44 780 Jne
Underthrow Distortion	42 IRE 9.S1	Separate
Underwater Sound Projector	51 IRE 6.S1	39 531 May
Undirectional Microphone	51 IRE 6.S1	39 531 May
Undirectional Pulse	51 IRE 20.S1	39 626 Jne
Undirectional Pulse Train	52 IRE 20.S1	40 554 May
Unfired Tube	57 IRE 7.S2	45 1009 Jul
Uniconductor Waveguide	53 IRE 2.S1	41 1725 Dec
Unidirectional Antenna	48 IRE 2,11,15.S1	Separate
Unidirectional Pulses	48 IRE 2,11,15.S1	Separate
Uniform Plane Wave	50 IRE 24.S1	38 1268 Nov
Uniform Waveguide	53 IRE 2.S1	41 1725 Dec
Unilateral Area Track	51 IRE 6.S1	39 531 May
Unilateral Transducer	51 IRE 20.S2	39 898 Aug
Unipole	48 IRE 2,11,15.S1	Separate
Unipotential Cathode	57 IRE 7.S2	45 1009 Jul
Unit	56 IRE 8.S1	44 1173 Sep
Unloaded Applicator Impedance	55 IRE 10.S1	43 1072 Sep
Unloaded (Intrinsic) Q	57 IRE 7.S2	45 1009 Jul
Unmodulated Groove	51 IRE 6.S1	39 532 May
Useful Line	56 IRE 9.S1	44 781 Jne
V		
Vacuum Tube	57 IRE 7.S2	45 1009 Jul
Vacuum Tube	52 IRE 17.S1	40 1685 Dec
Vacuum-Tube Amplifier	48 IRE 2,11,15.S1	Separate
Vacuum-Tube Transmitter	48 IRE 2,11,15.S1	Separate
Valence Band	54 IRE 7.S2	42 1508 Oct
Value, Munsell	55 IRE 22.S1	43 748 Jne
V-Antenna	48 IRE 2,11,15.S1	Separate
VAR (VHF Aural-Visual Range)	54 IRE 12.S1	43 209 Feb
Variable Area Track	51 IRE 6.S1	39 532 May
Variable Density Track	51 IRE 6.S1	39 532 May
Variable-Induction Pickup	51 IRE 6.S1	39 532 May
Variable-u Tube	57 IRE 7.S2	45 1010 Jul
Variable-Reluctance Microphone	51 IRE 6.S1	39 532 May
Variable-Reluctance Pickup	51 IRE 6.S1	39 532 May
Variable-Resistance Pickup	51 IRE 6.S1	39 532 May
Variation	49 IRE 12.S1	37 1371 Dec
Varistor	54 IRE 7.S2 •	42 1508 Oct
V-Beam Radar	54 IRE 12.S1	43 207 Feb
Vehicle	54 IRE 12.S1	43 207 Feb
Velocity	51 IRE 6.S1	39 532 May
Velocity Level	51 IRE 6.S1	39 532 May
Velocity Microphone	51 IRE 6.S1	39 532 May
Velocity Modulation	57 IRE 7.S2	45 1010 Jul
Velocity-Modulated Oscillator	48 IRE 2,11,15.S1	Separate
Velocity Sorting	57 IRE 7.S2	45 1010 Jul
Verification	56 IRE 8.S1	44 1173 Sep
Vertex	50 IRE 4.S1	39 29 Jan
Vertical Recording	51 IRE 6.S1	39 532 May
Vertically Polarized Wave	50 IRE 24.S1	38 1268 Nov
Vestigial Sideband	56 IRE 9.S1	44 781 Jne
Vestigial Sideband Transmission	56 IRE 9.S1	44 781 Jne
Vestigial-Sideband Transmitter	48 IRE 2,11,15.S1	Separate
VHF Omnirange	54 IRE 12.S1	43 209 Dec
Vibration Meter	51 IRE 6.S1	39 532 May
Vibrato	51 IRE 6.S1	39 532 May
Video	55 IRE 23.S1	43 622 May
Video	52 IRE 17.S1	40 1685 Dec
Video-Frequency Amplifier	48 IRE 2,11,15.S1	Separate
Video Integration	54 IRE 12.S1	43 207 Feb
Video Mapping	54 IRE 12.S1	43 207 Feb
Video Stretching	54 IRE 12.S1	43 207 Feb
Vidicon	57 IRE 7.S2	45 1010 Jul
Virtual Cathode	57 IRE 7.S2	45 1010 Jul
Virtual Height	50 IRE 24.S1	38 1286 Nov
Visibility Factor (Display Loss)	54 IRE 12.S1	43 207 Feb
Visual-Aural Range	54 IRE 12.S1	43 207 Feb
Visual-Aural Radio Range	49 IRE 12.S1	37 1371 Dec
Visual Radio Range	49 IRE 12.S1	37 1371 Dec
Visual Transmitter	48 IRE 2,11,15.S1	Separate
Volatile	56 IRE 8.S1	44 1173 Sep
Voltage	57 IRE 7.S2	45 1010 Jul
Voltage Amplification	54 IRE 3.S1	42 1112 Jul
Voltage Amplification	51 IRE 20.S2	39 899 Aug
Voltage Amplification	48 IRE 2,11,15.S1	Separate
Voltage Attenuation	51 IRE 20.S2	39 899 Aug
Voltage Attenuation	54 IRE 3.S1	42 1112 Jul
Voltage Generator	57 IRE 7.S2	45 1010 Jul
Voltage Jump	57 IRE 7.S2	45 1010 Jul
Voltage Reference Tube	57 IRE 7.S2	45 1010 Jul
Voltage Regulator Tube	57 IRE 7.S2	45 1010 Jul
Volume	54 IRE 3.S1	42 1112 Jul
Volume Indicator	51 IRE 6.S1	39 532 May
Volume-Limiting Amplifier	48 IRE 2,11,15.S1	Separate
Volume Velocity	51 IRE 6.S1	39 532 May
Volumetric Radar	54 IRE 12.S1	43 207 Feb
VOR (VHF Omnirange)	54 IRE 12.S1	43 209 Feb
Vowel Articulation	51 IRE 6.S1	39 532 May
VSWR, High-Level	57 IRE 7.S2	45 1010 Jul
vu	54 IRE 3.S1	42 1112 Jul
W		
Wander	54 IRE 12.S1	43 207 Feb
Wave	48 IRE 2,11,15.S1	Separate
Wave	50 IRE 24.S1	38 1268 Nov
Wave	57 IRE 7.S2	45 1010 Jul
Wave Antenna	48 IRE 2,11,15.S1	Separate
Waveform-Amplitude Distortion	53 IRE 4.S1	42 555 Mar

	Standard	Proceedings Vol Page Mo
Wave Front	42 IRE 9.S1	Separate
Waveguide	50 IRE 24.S1	38 1268 Nov
Waveguide	53 IRE 2.S1	41 1725 Dec
Waveguide Wavelength	53 IRE 2.S1	41 1725 Dec
Wave Heating	55 IRE 10.S1	43 1072 Sep
Wave Interference	50 IRE 24.S1	38 1268 Nov
Wavelength	50 IRE 24.S1	38 1268 Nov
Wave Normal	53 IRE 2.S1	41 1725 Dec
Wave Normal	50 IRE 24.S1	38 1268 Nov
Wave Tail	42 IRE 9.S1	Separate
Wax	51 IRE 6.S1	39 532 May
Wax Original	51 IRE 6.S1	39 532 May
Way Point	54 IRE 12.S1	43 207 Feb
Weighting	48 IRE 2,11,15.S1	Separate
White	55 IRE 22.S1	43 748 Jne
White Compression (White Saturation)	55 IRE 23.S1	43 622 May
White Object	55 IRE 22.S1	43 748 Jne
White Peak	55 IRE 23.S1	43 622 May
White Recording	56 IRE 9.S1	44 781 Jne
White Signal	56 IRE 9.S1	44 781 Jne
White-to-Black Frequency Swing	42 IRE 9.S1	Separate
White-to-Black Amplitude Range	42 IRE 9.S1	Separate
White Transmission	56 IRE 9.S1	44 781 Jne
Whole Tone	51 IRE 6.S1	39 532 May
Wide-Band Axis	55 IRE 22.S1	43 748 Jne
Wide-Band Improvement	48 IRE 2,11,15.S1	Separate
Wide-Band Ratio	48 IRE 2,11,15.S1	Separate
Williams-Tube Storage	56 IRE 8.S1	44 1173 Sep
Word	56 IRE 8.S1	44 1173 Sep
Word Time	56 IRE 8.S1	44 1173 Sep
Work Coil	55 IRE 10.S1	43 1072 Sep
Work Function	57 IRE 7.S2	45 1010 Jul
Wow	52 IRE 17.S1	40 1685 Dec
Write	56 IRE 8.S1	44 1173 Sep
Write	57 IRE 7.S2	45 1010 Jul
Writing Speed	57 IRE 7.S2	45 1010 Jul
Wye Junction	55 IRE 2.S1	43 1074 Sep
X		
X Wave	50 IRE 24.S1	38 1268 Nov
Y		
Y Network	51 IRE 4.S1	39 29 Jan
Z		
Z (Zone) Marker	54 IRE 12.S1	43 209 Feb
Zero-Subcarrier Chromaticity	55 IRE 22.S1	43 748 Jne
Zero Time Reference	54 IRE 12.S1	43 207 Feb
Zone (Z) Marker	49 IRE 12.S1	37 1371 Dec
Zone Leveling	54 IRE 7.S2	42 1508 Oct
Zone Purification	54 IRE 7.S2	42 1508 Oct
Zoning	48 IRE 2,11,15.S1	Separate

Measurement of the Radar Cross Section of a Man*

F. V. SCHULTZ†, SENIOR MEMBER, IRE, R. C. BURGENER‡, ASSOCIATE MEMBER, IRE, AND S. KING§, SENIOR MEMBER, IRE

Summary—**Both the monostatic and the bistatic radar cross sections[1] of a man were measured at the five frequencies 410, 1120, 2890, 4800, and 9375 mc. The measurements were made using both horizontal and vertical polarizations, and for various directions of facing, or aspects, of the man being used as a target. The cw Doppler method[2] was used in making the measurements. The man whose cross section was measured weighed about 200 pounds and he was six feet tall.**

It was found that the man's cross section varied as follows, depending primarily upon polarization of the incident wave and aspect of the man:

410 mc	**0.033 to 2.33 square meters**
1120 mc	**0.098 to 0.997 square meters**
2890 mc	**0.140 to 1.05 square meters**
4800 mc	**0.368 to 1.88 square meters**
9375 mc	**0.495 to 1.22 square meters.**

A few measurements were made with men of different sizes, and these indicate that the cross section is approximately proportional to the weight of the man.

* Original manuscript received by the IRE, June 6, 1957; revised manuscript received, October 21, 1957. This work was conducted by Project Michigan under Department of the Army Contract, DA-36-039 SC-52654, administered by the U.S. Army Signal Corps, operating under a tri-service charter.

† School of Elec. Eng., Purdue Univ., Lafayette, Ind. Formerly with the Dept. of Elec. Eng., Univ. of Tennessee, Knoxville, Tenn.

‡ Battelle Memorial Inst., Columbus, Ohio. Formerly with the Dept. of Elec. Eng., Univ. of Tennessee, Knoxville, Tenn.

§ Hughes Aircraft Co., Fullerton, Calif. Formerly with the Dept. of Elec. Eng., Univ. of Tennessee, Knoxville, Tenn.

[1] The bistatic radar cross section is measured when the transmitter and receiver are not located on the same radial from the target. The monostatic cross section is a special case of the bistatic cross section. The monostatic value is obtained when the transmitter and receiver are at the same location, and thus on the same radial.

[2] D. D. King and H. Scharfman, "Antenna scattering measurements by modulation of the scatterer," PROC. IRE, vol. 42, pp. 854–858; May, 1954.

I. Introduction

OFTEN in making radar cross section measurements indicated above, it is desirable to utilize modeling techniques which make possible the use of indoor laboratory facilities for carrying out the measurements. Since a human being is neither a perfect conductor nor a perfect dielectric, it was considered unwise to attempt to use a modeling technique which would involve a modeling of the electrical properties of the target as well as of its size. Consequently full-scale measuring techniques were used.

II. Experimental Procedure

Since a cw Doppler system was used in making the measurements, it was necessary to impart radial motion (relative to the Doppler transmitter and receiver) to the target in order to obtain a Doppler signal. This was accomplished by constructing a test stand consisting of a wooden A frame that supported a swinging platform on which the man stood. A 16-inch sphere and one with a diameter of 10 inches served as standard targets for calibration purposes, and these were hung from the cross member of the test stand. Nylon cord, with a diameter of about 3/32 inch and a test strength of 190 pounds, supported the swinging platform as well as the standard spheres. No detectable Doppler signal was generated by the motion of these nylon supporting cords.

In order to reduce satisfactorily the Doppler return signal from the swinging platform on which the man stood, it was necessary to erect in front of the platform a barrier of microwave absorbing material. A block of Styrofoam was placed on top of the swinging wooden platform in order that a full view of the man standing thereon would be seen by the Doppler measuring system. The unwanted Doppler return was satisfactorily reduced by these techniques. The test stand was sufficiently rigid that no detectable Doppler return was generated by it. Multiple reflections involving various stationary objects and the swinging targets were believed to be of no consequence since cross checks on the measured cross sections obtained for the two different spheres, used as standards, were very satisfactory.

Each of the transmitters used consisted of a suitable cw generator coupled to an appropriate antenna, which could be rotated about a horizontal axis. This made possible the emission of either horizontally or vertically polarized waves. At the receiver an antenna identical to the transmitting antenna was coupled to a superheterodyne-type receiver. During operation the Doppler-shifted signal from the target and the leakage signal from the transmitter passed through the receiver and produced a Doppler beat signal at the output of the second detector of the receiver. This signal was fed through a variable band-pass audio filter to reduce the noise, and then finally used to drive the pen of a recording oscillograph. The pen deflections were proportional to the voltage of the Doppler signal returned by the target, the linearity of the system having been verified over the operating range. Typical tape records taken on the oscillograph are illustrated in Fig. 1(a) and 1(b).

A series of measurements commenced with setting the transmitter and receiver side by side at the correct distance from the test stand and directly in front of the test stand. Measurements were first made of the Doppler signals returned by each of the two spheres used as standards. After these calibration recordings the man was placed on the movable platform of the test stand and the Doppler signal returned by the swinging man was recorded with the man facing the Doppler transmitter and receiver. Further measurements were made of the signal returned by the man after he was rotated 45° about a vertical axis, then a 90° rotation (side view), next 135°, and finally 180° (rear view). Returns for five different aspects of the man were thus obtained. Following the recordings of the man's returns, calibration recordings of the two standards were made again. The entire process was then repeated, so that at least two series of records were obtained for each set of conditions. These measurements yielded the monostatic radar cross section of the man for one particular frequency and polarization.

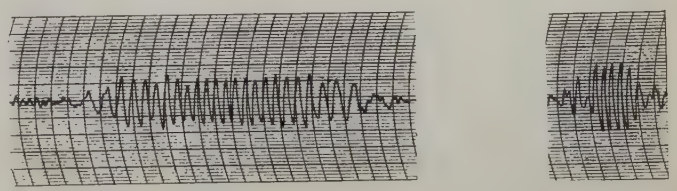

(a) (b)

Fig. 1—(a) Recording of the 16-inch standard sphere made at 9375 mc, a bistatic angle of 30°, and horizontal polarization. The voltage scale is 10 mv per mm, and the recording speed was 125 mm per second. (b) Recording of man's return at 45° front aspect with all conditions as above, except that the recording tape speed was 25 mm per second.

In order to measure the bistatic cross section, the transmitter was first moved 15° clockwise, considering the test stand and the line of motion of the swinging target platform as references, and the Doppler receiver was moved 15° counterclockwise. The measuring process described in the preceding paragraph was repeated and thus the 30° bistatic-angle radar cross section of the man was obtained. In the same way the 60° and 90° bistatic-angle cross sections were measured.

Since it was not feasible to elevate the Doppler system and the target sufficiently above the ground to eliminate the ground-reflected waves, it was necessary to take steps to reduce sufficiently the variation of field intensity over the surface of the man, this variation being caused by the interference between the direct wave from the transmitter and the ground-reflected wave. A similar phenomenon existed, of course, for the

propagation path from the target to the receiving antenna. The most satisfactory means of reducing this effect proved to be the use of diffracting screens[3,4] placed on the ground between the transmitter and target and between the target and receiver. By this method it was possible to reduce the measured field variation in the area occupied by the target to approximately plus or minus 1 db.

Since the cw Doppler system employed for the measurements detects all moving objects, noise caused by moving vegetation and insects entered the system along with the return from the desired target. The effect of this noise was satisfactorily reduced by taking three steps. First, a band-pass filter centered at the frequency of the target return was connected to the output of the second detector of the receiver to eliminate the portion of the clutter return that was not at the target frequency. Second, vegetation was removed as much as possible. Third, the transmitter and receiver were moved as close as allowable to the target so that a return of sufficient magnitude to override the clutter might be received from the target.

The third step mentioned above could not be carried to an extreme because of the requirement that the phase-front curvature of the rf wave over the target be satisfactorily small. A number of workers in the microwave measurements field have developed experimental and theoretical criteria for the minimum range necessary in radar cross section measurements in order to minimize the errors resulting from the curvature of the wave phase front at the target.[2-5] For the present measurements the criterion for allowable phase-front curvature was set at $\pi/16$ radian. The minimum range for the measurements as developed from this criterion is $R=4D^2/\lambda$, where R is the minimum permissible range, D is the major dimension of the target, and λ is the wavelength at which the measurements are being made. Computations from the above equation, with D equal to six feet, give the results shown in Table I. No allowance was made here for phase shifts introduced by the ground-reflected wave.

At 4800 mc and 9375 mc, it was not possible to obtain adequately large return signals from the target for target-transmitter separations of greater than 400 feet because of extraneous signal return from moving vegetation. The phase-front curvature over the target for this separation of 400 feet and for 4800 and 9375 mc is of course greater than $\pi/16$ radian, selected as the maximum allowable. Consequently it was necessary to determine as well as possible the results of this condition. In order to do this, an experiment was undertaken

[3] H. E. Bussey, "Reflected ray suppression," Proc. IRE, vol. 38, p. 1453; December, 1950.
[4] C. C. Cutler, A. P. King, and W. E. Kock, "Microwave antenna measurements," Proc. IRE, vol. 35, pp. 1469–1470; December, 1947.
[5] D. R. Rhodes, "On minimum range for radiation patterns," Proc. IRE, vol. 42, pp. 1408–1410; September, 1954.

TABLE I

Minimum Allowable Separation (R) Between Transmitter and Target for a Maximum Phase-Front Variation Over the Target of $\pi/16$ Radian. Target Height Is 6 Feet

Frequency	R
410 mc	60 feet
1120 mc	164 feet
2890 mc	422 feet
4800 mc	702 feet
9375 mc	1370 feet

to evaluate this effect of phase-front curvature on the measured cross section of a man. This experiment was conducted at a frequency of 1120 mc and consisted of identical measurements made at three different ranges. The first range used (71 feet) was chosen because it produced the same phase variation over the target as occurred during the 9375-mc measurements made at a range of 400 feet. The second range (104 feet) simulated the conditions of phase variation during the 4800-mc measurements, while the third range (200 feet) insured a phase variation of less than the $\pi/16$-radian criterion. In all three measurements the diffracting screens were used to make the signal strength over the target uniform. It was not possible to scale the target, so the measurements were not completely definitive, but the results did indicate that an error of probably not more than about 20 per cent was introduced in the 9375-mc measurements, and one of probably not more than about 5 per cent in the 4800-mc results.

III. Data Reduction

As mentioned previously, the Doppler beat signal generated by the moving target was traced on paper tape by a recording oscillograph. Sample tape recordings are shown in Fig. 1(a) and 1(b), and, as stated before, the deflections are proportional to the voltage of the Doppler beat signal. The measurement procedure has also been described earlier in the paper; this consisted of first obtaining calibration recordings of the two standard spheres, then recordings of the human target, and finally check recordings of the two spheres. The entire procedure was then repeated once or twice.

The first step in the data reduction consisted of reading the deflections recorded on the tapes. This was done by drawing straight lines through the average peak values and the average through values attained by the deflections, after the Doppler beat signal had settled down to a fairly steady tone. The averaging process was done visually. These total swings on the tapes were read and recorded for both the human target and the spheres. The two sets of values obtained on the spheres, one set at the beginning of an experiment and the other at the end, were averaged. In no case were these two sets of values sufficiently different to indicate a systematic drift in the characteristics of the complete measurement system.

TABLE II

CALCULATED RADAR CROSS SECTIONS IN SQUARE METERS OF THE STANDARD SPHERES

Sphere	Frequency	Horizontal Polarization				Vertical Polarization			
		Bistatic Angle in Degrees				Bistatic Angle in Degrees			
		0°	30°	60°	90°	0°	30°	60°	90°
10 inches	410 mc	0.17886	0.15720	0.10073	0.04017	0.17886	0.17915	0.17162	0.15300
16 inches	1120 mc	0.16911	0.09064	0.17965	0.11448	0.16911	0.14704	0.20315	0.23490
16 inches	2890 mc	0.12901	0.12901	0.12901	0.12901	0.12901	0.12901	0.12901	0.12901
16 inches	4800 mc	0.12888	0.12888	0.12888	0.12888	0.12888	0.12888	0.12888	0.12888
16 inches	9375 mc	0.12888	0.12888	0.12888	0.12888	0.12888	0.12888	0.12888	0.12888

Since the targets were swung through a distance of never less than about two wavelengths, the error due to changing target velocity, as discussed by Ruze,[6] should never exceed about 10 per cent.

After all the tape deflection readings for the signal return from the human target were recorded, they were smoothed by the use of a least-squares technique and these final regression values were used for calculating the radar cross sections.

The radar cross section of the human target, corresponding to each final regression value of tape deflection, was calculated by using the following:

$$\sigma_m = \left[\frac{R_m}{R_s}\right]^2 \sigma_s.$$

Here

σ_m = radar cross section, in square meters, of the man.

R_m = tape deflection, in millimeters, corresponding to Doppler signal generated by human target.

R_s = tape deflection, in millimeters, corresponding to Doppler signal generated by sphere used as standard for calibration.

σ_s = calculated radar cross section, in square meters, of the sphere used as a standard.

In all cases, except at 410 mc, the 16-inch sphere was used as a standard and the readings obtained on the 10-inch sphere were used as a check of the system accuracy. The calculated and the measured values of the cross section of this 10-inch sphere differed by an average of about 0.5 db, or about 12 per cent.

The radar cross sections of the spheres at the lower frequencies were calculated by using the exact electromagnetic solution.[7] At the higher frequencies the geometrical optics values were used. The calculated cross sections of the spheres are listed in Table II. It should be mentioned that the average diameter of the 16-inch sphere was 15.95 inches and that of the 10-inch sphere was 9.88 inches. The sphericity of both spheres was excellent, various diameters differing by only 3/32 inch, or less.

IV. Results Obtained

The values of the radar cross section of the man are listed in Tables III–VII, inclusive, for the various frequencies, polarizations, bistatic angles, and aspect angles used in the experiment. It is an easy matter to see from the tables how the radar cross section of the man varies with aspect angle and with bistatic angle for a given frequency and a given polarization, but the variations with frequency and with polarization are somewhat more difficult to observe. For this reason Fig. 2–Fig. 6 have been prepared. Values of the cross section, averaged over bistatic angle, are shown in Fig. 2 and in normalized form in Fig. 3. For Fig. 4 and Fig. 5 the values of cross section were averaged over target aspect for given values of polarization, frequency, and bistatic angle. The curves then give indications of how, for a given polarization and frequency, the man's cross section varies with bistatic angle. In order to obtain Fig. 6, the cross section values corresponding to a given polarization and frequency were averaged over bistatic angle and aspect of the target. Fig. 6 then indicates how these average values of cross section vary with frequency for each of the two polarizations.

V. Conclusion

As shown in the Summary, the measured radar cross section of the man used varies from 0.033 square meter to 2.33 square meters. These extreme values were obtained at 410 mc, the smaller for horizontal polarization and a side view of the man, the larger for vertical polarization and a rear view of the man. These results might be expected for a quasi-cylindrical target such as a man. As the frequency was increased the cross section differed less and less between the two polarizations.

Examination of Tables III–VII reveals that, in general, the cross section is least for a side view of the man and

[6] J. Ruze, "Errors in Radar Cross-Section Reflection Measurements," Air Force Cambridge Field Station, Cambridge, Mass., Rep. No. 4-24; July 30, 1947.

[7] D. E. Kerr, "Propagation of Short Radio Waves," McGraw-Hill Book Co., New York, N. Y., pp. 445–454; 1951.

TABLE III

RADAR CROSS SECTIONS IN SQUARE METERS FOR 410 MC

Target Aspect	Horizontal Polarization				Vertical Polarization			
	Bistatic Angle in Degrees				Bistatic Angle in Degrees			
	0°	30°	60°	90°	0°	30°	60°	90°
Front	0.897	0.641	0.795	0.464	1.127	0.939	1.628	2.163
45° Front	0.197	0.108	0.264	0.196	0.312	0.217	0.613	0.941
Side	0.083	0.033	0.157	0.136	0.161	0.095	0.397	0.681
45° Rear	0.321	0.197	0.367	0.251	0.464	0.346	0.816	1.174
Rear	1.091	0.796	0.931	0.529	1.343	1.138	1.880	2.327

TABLE IV

RADAR CROSS SECTIONS IN SQUARE METERS FOR 1120 MC

Target Aspect	Horizontal Polarization				Vertical Polarization			
	Bistatic Angle in Degrees				Bistatic Angle in Degrees			
	0°	30°	60°	90°	0°	30°	60°	90°
Front	0.718	0.359	0.410	0.388	0.879	0.718	0.608	0.997
45° Front	0.322	0.156	0.124	0.154	0.433	0.344	0.224	0.447
Side	0.281	0.135	0.098	0.131	0.386	0.305	0.187	0.391
45° Rear	0.518	0.256	0.259	0.268	0.656	0.531	0.410	0.719
Rear	0.718	0.359	0.410	0.388	0.879	0.718	0.608	0.997

TABLE V

RADAR CROSS SECTIONS IN SQUARE METERS FOR 2890 MC

Target Aspect	Horizontal Polarization				Vertical Polarization			
	Bistatic Angle in Degrees				Bistatic Angle in Degrees			
	0°	30°	60°	90°	0°	30°	60°	90°
Front	0.409	0.665	0.471	0.322	0.496	0.774	0.564	0.400
45° Front	0.228	0.427	0.275	0.165	0.294	0.516	0.347	0.221
Side	0.198	0.386	0.242	0.140	0.260	0.471	0.310	0.192
45° Rear	0.268	0.481	0.318	0.198	0.339	0.574	0.395	0.260
Rear	0.613	0.920	0.688	0.506	0.719	1.048	0.800	0.602

TABLE VI

RADAR CROSS SECTIONS IN SQUARE METERS FOR 4800 MC

Target Aspect	Horizontal Polarization				Vertical Polarization			
	Bistatic Angle in Degrees				Bistatic Angle in Degrees			
	0°	30°	60°	90°	0°	30°	60°	90°
Front	1.499	1.404	1.320	1.039	1.745	1.643	1.552	1.247
45° Front	0.858	0.786	0.724	0.521	1.047	0.968	0.898	0.670
Side	0.658	0.596	0.542	0.368	0.825	0.755	0.694	0.495
45° Rear	0.940	0.865	0.799	0.585	1.137	1.054	0.982	0.742
Rear	1.624	1.525	1.438	1.144	1.881	1.774	1.680	1.361

TABLE VII

RADAR CROSS SECTIONS IN SQUARE METERS FOR 9375 MC

Target Aspect	Horizontal Polarization				Vertical Polarization			
	Bistatic Angle in Degrees				Bistatic Angle in Degrees			
	0°	30°	60°	60°	0°	30°	60°	90°
Front	1.018	0.749	0.933	0.799	1.003	0.736	0.919	0.786
45° Front	0.858	0.612	0.780	0.658	0.845	0.601	0.767	0.647
Side	0.730	0.505	0.658	0.547	0.718	0.495	0.647	0.536
45° Rear	0.905	0.652	0.825	0.700	0.891	0.641	0.812	0.688
Rear	1.215	0.919	1.122	0.975	1.199	0.905	1.106	0.961

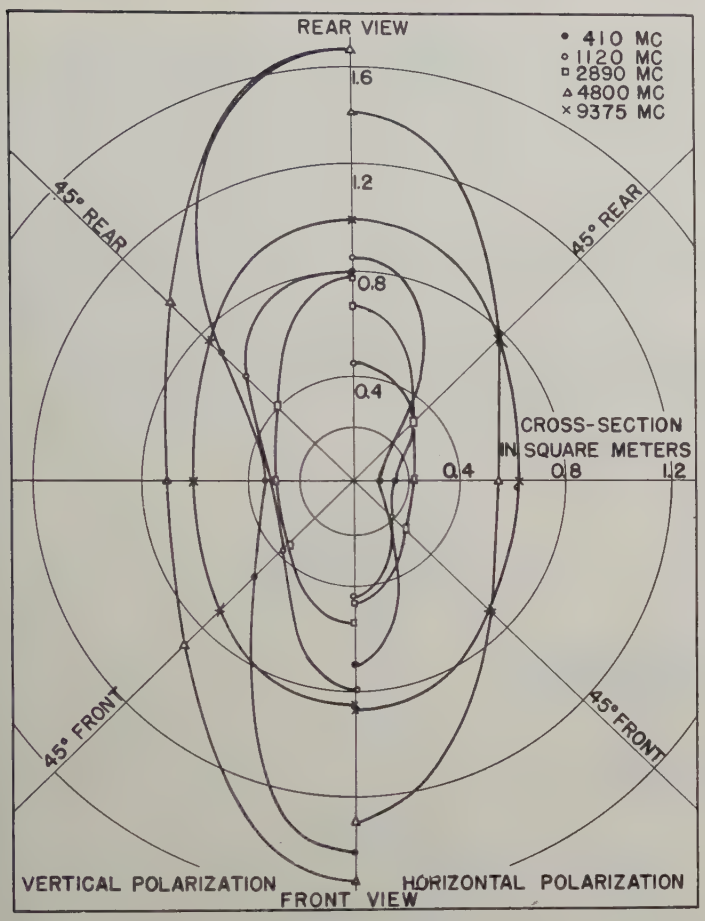

Fig. 2—Average bistatic radar cross section of a man as a function of target aspect angle, with frequency and polarization as parameters.

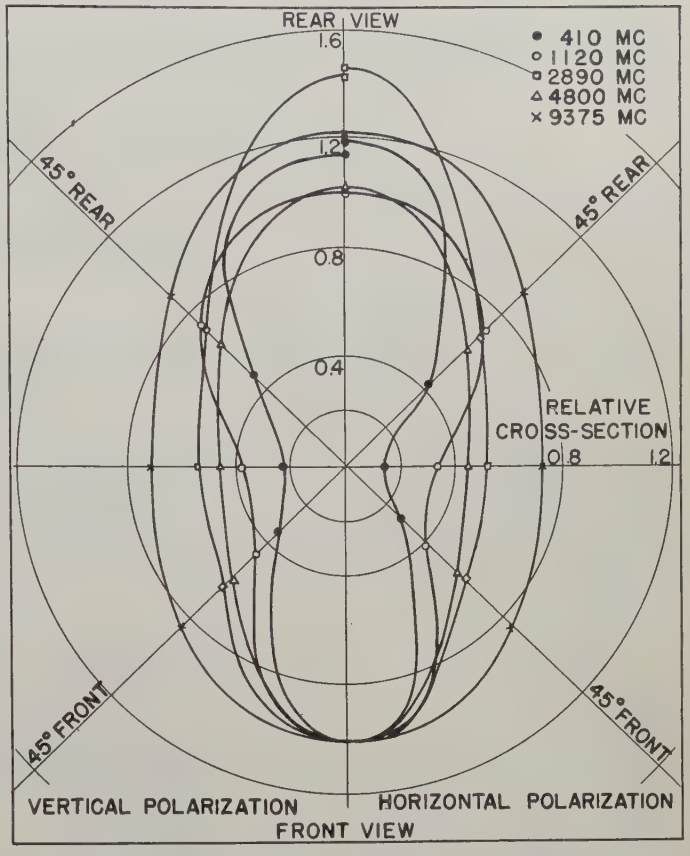

Fig. 3—Average relative bistatic radar cross section of a man as a function of target aspect angle, with frequency and polarization as parameters. (The curves are normalized with respect to the radar cross section of the front aspect.)

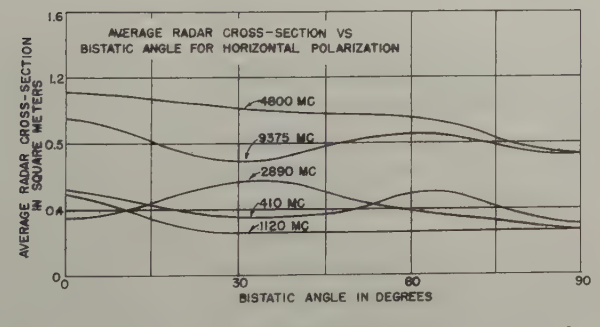

Fig. 4—Average bistatic radar cross section of a man as a function of bistatic angle, for horizontal polarization with frequency as a parameter.

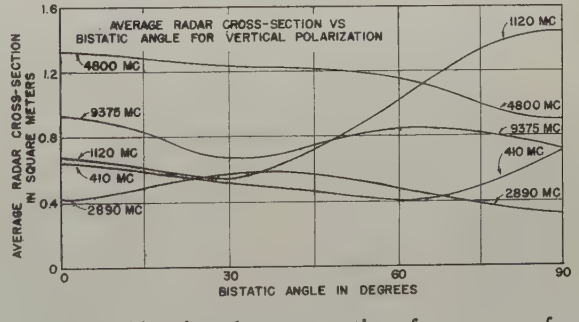

Fig. 5—Average bistatic radar cross section of a man as a function of bistatic angle, for vertical polarization with frequency as a parameter.

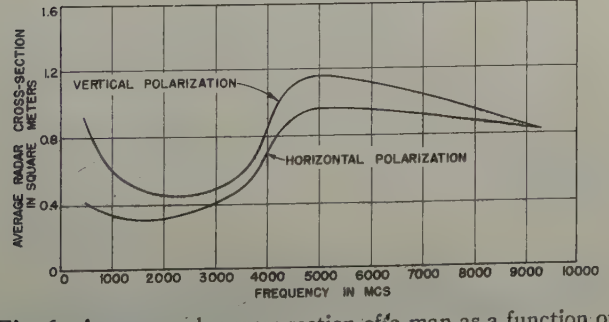

Fig. 6—Average radar cross section of a man as a function of frequency, with polarization as a parameter.

somewhat greater for a rear view than a front view. Fig. 4 and Fig. 5 show that the cross section varies but little with bistatic angle, except for vertical polarization at 410 mc, where the cross section increases about twice as the bistatic angle goes from 0° to 90°. These are not unexpected results.

Fig. 6 illustrates the over-all variation of the cross section with frequency. The general decrease in polarization dependence as the frequency is increased is, of course, to be anticipated. Because of the complex nature of the object being measured, however, no explanation is offered for the other characteristics of the two curves contained in this figure.

IRE Standards on Television: Measurement of Luminance Signal Levels, 1958*

(58 IRE 23. S1)

COMMITTEE PERSONNEL

Subcommittee on Video Signal Transmission Methods of Measurement
1957–1958

J. M. Barstow, *Chairman*

M. H. Diehl
A. B. Ettlinger
H. P. Kelly
H. Mate
R. M. Morris
J. R. Popkin-Clurman
E. B. Pores
E. H. Schreiber
L. Staschover
J. W. Wentworth
W. B. Whalley

Committee on Video Techniques
1957–1958

S. Doba, Jr., *Chairman*
G. L. Fredendall, *Vice-Chairman*

I. C. Abrahams
S. W. Athey
A. J. Baracket
J. M. Barstow
J. H. Battison
E. E. Benham
K. B. Benson
E. M. Coan
L. B. Davis
V. J. Duke
J. R. Hefele
J. L. Jones
R. T. Petruzzelli
W. J. Poch

Standards Committee
1957–1958

M. W. Baldwin, Jr., *Chairman*
C. H. Page, *Vice-Chairman*
R. F. Shea, *Vice-Chairman*
L. G. Cumming, *Vice-Chairman*

J. Avins
W. R. Bennett
J. G. Brainerd
D. R. Brown
T. J. Carroll
P. S. Carter
A. G. Clavier
G. A. Deschamps
S. Doba, Jr.
J. E. Eiselein
D. Frezzolini
E. A. Gerber
A. B. Glenn
H. Goldberg
V. M. Graham
R. A. Hackbusch
H. C. Hardy
D. E. Harnett
A. G. Jensen
I. M. Kerney
J. G. Kreer, Jr.
W. A. Lynch
A. A. Macdonald
Wayne Mason
D. E. Maxwell
H. R. Mimno
G. A. Morton
J. H. Mulligan, Jr.
W. Palmer
R. L. Pritchard
P. A. Redhead
R. Serrell
H. R. Terhune
W. E. Tolles
J. E. Ward
E. Weber
W. T. Wintringham

Measurements Coordinator

R. F. Shea

* Approved by IRE Standards Committee, September 12, 1957. Reprints of this Standard, 58 IRE 23. S1, may be purchased while available from the Institute of Radio Engineers, 1 East 79th Street, New York, N. Y., at $0.60 per copy. A 20 per cent discount will be allowed for 100 or more copies mailed to one address.

1.0 Introduction

This Standard is a revision of Part 1 of Standard 50 IRE 23. S1 and replaces in all respects this previously issued part of the Standard. The need for the revision stems from the standardization of color television signals in the USA, and the inadequacy of the earlier Standard in providing methods of measuring the luminance component of the color signal. The revision consists primarily of a change in the response characteristics of the oscilloscopes to insure adequate suppression of the color subcarrier. Other minor changes in wording and in the associated figures have been made to bring the standard into accord with present terminology and practice.

1.1 Description

This Standard describes methods of measuring the significant amplitude levels of a monochrome or color television signal, either composite or noncomposite. It is concerned with measurements at points in transmission systems where the signals are at video frequency. The methods described in this Standard are limited to those involving the use of oscilloscopes, and are primarily directed to specifying means of measuring television signal levels for operating purposes.

For the purposes of this Standard, the levels which are significant are the levels of monochrome signals or the levels of the luminance portion of color signals. The peak amplitude excursion of a color signal may exceed, by substantial amounts, the peak amplitude excursions of the luminance portion of the signal, but since subjective brightness is more nearly proportional to the luminance signal than to any other quantity, it is most desirable from the operating standpoint to control and adjust levels using the luminance signal as a gauge. When this is done, monochrome and color signals, interspersed in a given program sequence, will produce approximately the same brightness and contrast when viewed on color or monochrome monitors without supplementary adjustments.

In the succeeding paragraphs of this Standard, the words "luminance signal" will refer to either a monochrome signal or to the luminance portion of a color signal.

Six significant amplitude levels of a composite luminance signal have been defined as follows.[1] These are shown in the right-hand portion of Fig. 1.

Reference White Level. The picture signal level corresponding to a specified maximum limit for *White Peaks.*

White Peak. A peak excursion of the picture signal in the white direction.

Black Peak. A peak excursion of the picture signal in the black direction.

[1] Cf. "IRE standards on television: Definitions of television signal measurement terms, 1955 (55 IRE 23. S1)," Proc. IRE, vol. 43, pp. 619–622; May, 1955.

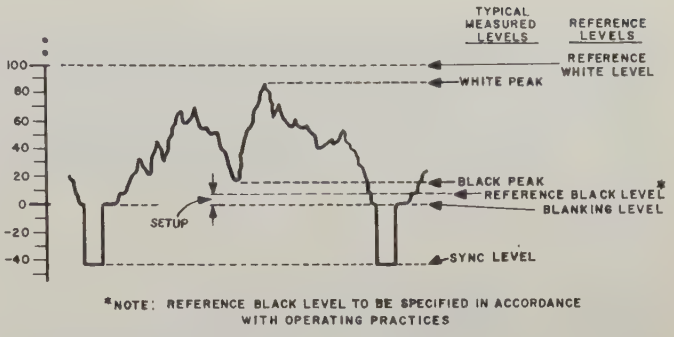

Fig. 1—Significant levels and details of IRE standard scale.

Reference Black Level. The picture signal level corresponding to a specified maximum limit for *Black Peaks.*

Blanking Level. That level of a composite picture signal which separates the range containing picture information from the range containing synchronizing information.

Note: The setup region is regarded as picture information.

Sync Level. The level of the peaks of the sync signal.

This Standard specifies a method of measuring the differences between these levels in a manner permitting ready correlation between the measurements at different parts of a system, regardless of the nominal voltages at the points of measurement.

1.2 Theory of Measurements

1.2.1 General: The method of level measurement prescribed in this Standard is based on the provision of oscilloscopes of standardized characteristics, with a linear scale for indicating the various levels. The scale is the same on all oscilloscopes, but each oscilloscope is calibrated with a voltage related to the nominal signal level at the point where the measurements are to be made. If the gains or losses between two measuring points on a system are normal, therefore, similar scale readings should be obtained for all the significant levels on oscilloscopes at both points regardless of differences in the voltages at the two points.

1.2.2 Scale: The standard scale is shown in the left-hand portion of Fig. 1, together with an illustrative luminance signal to show the relation between the scale and the oscilloscope presentation. It will be observed that the zero or reference point of the scale is placed at the blanking level. The upper part of this scale is marked from 0 to 100 with 100 corresponding to the reference white level. The scale is linear and two additional points (at 110 and 120) are provided to permit reading abnormally high *White Peaks.* The various levels of the picture signal are read on this scale above zero. The lower part of the scale is marked in linear steps from 0 to −50 and on it are read the levels of the sync signal.

Where other scales are used for specific purposes,

such as modulation monitoring at broadcast transmitters, the standard scale should be added to any existing scales to permit correlation with measurements at other points in the system. The standard level scale should be placed with the 0 and 100 markings corresponding to the normal *Blanking* and *Reference White Levels*, respectively, of the other scale.

2.0 Apparatus Required

2.1 List of Equipment

A suitable oscilloscope is required for these measurements. Its specifications are given below and form a part of this Standard.

2.2 Specifications of Standard Oscilloscope for Level Measurements

2.2.1 Measurement Accuracy: An oscilloscope which is suitable for this application should be capable of television level measurements with errors not exceeding 2.5 units on the scale. Factors which contribute to error include:

Spot size and brightness,
Deflection amplitude,
Amplifier linearity,
Readability of scales or markers, including a reasonable allowance for parallax,
Calibration accuracy, and stability of calibration.

2.2.2 Bandwidth: The oscilloscope response characteristic should be such as to introduce negligible measurement errors due to low-frequency distortion or overshoot. The response characteristics should be standardized so that uniform measurements are obtained with different oscilloscopes. The bandwidth should be great enough to yield satisfactory luminance signal level readings and narrow enough that the readings are negligibly affected by the subcarrier portion of a color signal. To meet these requirements, this Standard prescribes that the response shall be monotonic and within the limits indicated in Fig. 2. This provides 20-db attenuation (−3 db or +5 db) at 3.58 mc with respect to the low frequencies and a rise time on the order of 0.3 μsec.

The specified characteristic may be obtained by adding a suitable network to an oscilloscope of wider bandwidth. For example, Fig. 3 shows a one-stage four-terminal network that may be used for this purpose with an oscilloscope having a bandwidth much wider than the specified characteristic. By arranging to remove the network, the oscilloscope can be made available for other uses where its full bandwidth is needed, such as 1) to measure color burst amplitude in terms of IRE scale units or 2) to check the amplitude of chrominance signal peaks on a color test signal. Fig. 3 also shows the circuit constants of an idealized three-stage amplifier having the specified nominal characteristics. For oscilloscopes having intermediate bandwidth, the prescribed responses may be attained with a smaller number of interstage networks or with different constants in the three networks.

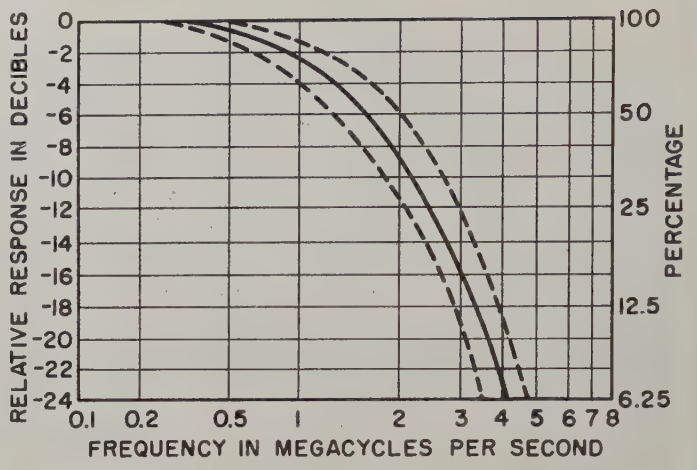

Fig. 2—Frequency response for standard oscilloscope (IRE roll-off).

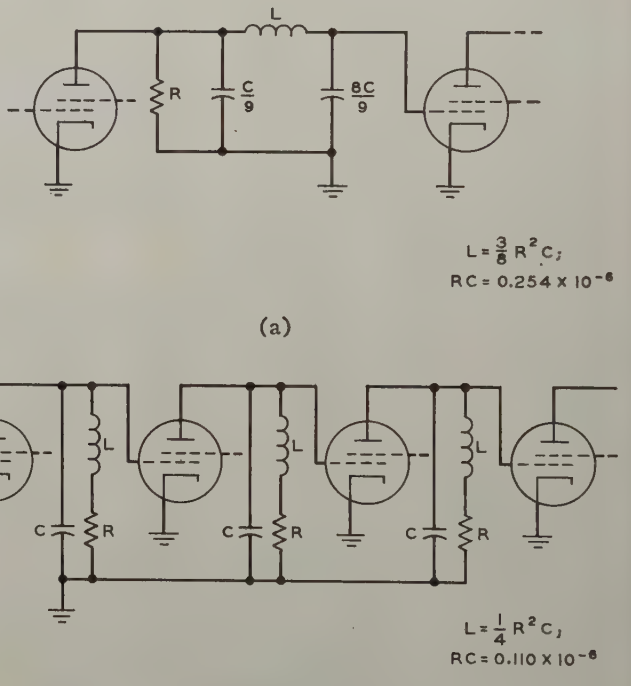

Fig. 3—Idealized networks for standard oscilloscope, R in ohms, L in henrys, and C in farads. (a) One-stage four-terminal network and (b) three-stage RCL network.

There should be no sudden break in the response curve above 3.58 mc and the maximum response above 5 mc should be at least 20 db down with respect to that of 100 kc. The oscilloscope should indicate less than 2 per cent tilt in a 60-cps symmetrical square wave.

2.2.3 Scale: The oscilloscope shall be provided with the standard scale shown in Fig. 1 and described in 1.2.2 of this Standard.

2.2.4 Calibration: A suitable voltage calibration means shall be provided.

2.2.5 DC Restoration: It is highly desirable that dc

restoration at the deflection plates of the oscilloscope be employed for operational measurements on signals having changing picture content in order to prevent shifts of the trace with variations in average value of the signal. It is desirable that the time constants of such dc restoration circuits be shorter than the equivalent time constants of the ac portions of the oscilloscope amplifier to avoid shift and bounce of the base line with picture changes. At the same time, it is desirable that the time constants of the restoration circuits be as long as the above limitation allows, in order that the true low-frequency content of the signal may be exhibited.

2.2.6 Vertical and Horizontal Centering: Means shall be provided for adjusting the relative position of the scale and the oscilloscope image. This may consist either of electrical centering controls on the oscilloscope or of a movable scale.

3.0 Method of Measurement

3.1 Application

Whether the oscilloscope is permanently connected to the circuit to be measured, as is the case in many operational systems, or is connected only periodically, care must be taken that the oscilloscope input circuit and the manner of connection have no adverse effect upon the signal circuit. It is essential that the circuit being measured operate with its normal source and the load impedances during the measurements.

In a transmission system the terminations may often be complex impedances, which cause the waveform to appear severely distorted when observed on an oscilloscope bridged across such a circuit. In measuring signal levels at such points, care must be exercised to properly interpret the indications. For example, where a constant-current source is used to drive a transmission system through a coupling transformer, the waveform measured directly across the transformer terminals may be so distorted as to be unusable for level measurements. It is usually preferable to connect the oscilloscope across a constant resistance point in the circuit, to which transmission from the signal origin is constant with frequency.

Low-frequency interference or distortion may seriously impair the accuracy of observation unless effective clamping means are employed. It is therefore recommended that such devices be employed wherever possible.

3.2 Adjustment

In using the oscilloscope the usual precautions must be taken to insure adequate brightness, sharp nonastigmatic beam focus, and gain-control settings which allow the necessary deflection without amplifier overload.

The oscilloscope time base should normally be synchronized at either the line rate or at one half of the line rate when making level measurements, providing a convenient display of the longer duration *Blanking* and *Sync Levels* which occur during the vertical blanking interval. The oscilloscope brightness and focus should be adjusted to make these portions of the signal wave form visible and well defined.

3.3 Calibration

Since, in general, the measurements will be made on a video bus or line in which the signal is to be maintained at a predetermined voltage chosen for that point in the system, it shall be standard practice to maintain an oscilloscope deflection within the appropriate calibrated boundaries of the standard scale.

In using the oscilloscope method of level measurement, accurate calibration of the oscilloscope amplifier gain is a very important aspect of the technique. Calibration is concerned with adjustment of the oscilloscope amplifier gain so that a normal signal will produce a standard oscilloscope deflection. This may conveniently be done by introducing a known calibrating voltage to the input of the oscilloscope in place of the normal input signal. The calibrating signal should be one whose principal frequency components lie within the band of uniform response of the oscilloscope. If such a calibrating signal has a peak-to-peak deflection equivalent to, for example, the *Blanking*-to-*Reference-White Level* of the standard signal, the oscilloscope gain would be adjusted so its calibrating voltage produces a deflection from 0 to 100 on the standard scale. Experience will indicate how often calibration checks should be made to maintain the desired accuracy of level measurement.

3.4 Interpretation

Standardizing the response characteristic of the oscilloscope serves to minimize possible differences in interpretation of signal levels. To further insure uniformity in interpreting the oscilloscope indication, the measurement of *Sync* and *Blanking Levels* should be observed at a point in the waveform where the voltages representing these levels are substantially at their steady-state value. The longer duration signals of both *Sync* and *Blanking Levels* which occur during the vertical sync interval are suitable. A representation of the appearance of these portions is shown in Fig. 4, the measurements being made as indicated to minimize errors due to transmission distortion. For noncomposite picture signals, *Blanking Level* may be observed similarly during the vertical blanking interval. In setting picture signal levels, important information-bearing signal peaks will be normally held within the 0 to 100 scale range. Certain highlight signals may occasionally exceed this range. Where comparison measurements are being made at different points in a transmission system, it is important to insure that identical peaks are being considered.

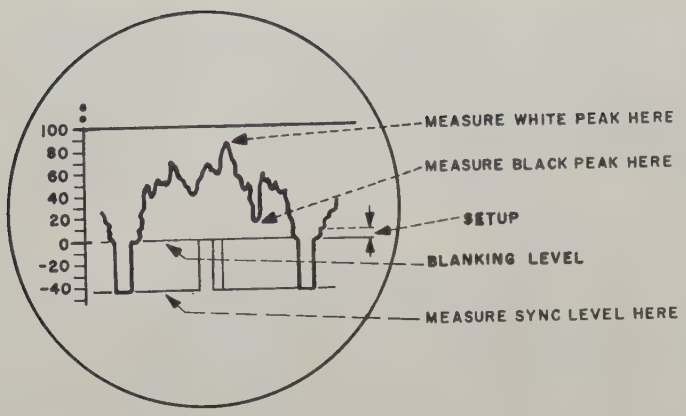

Fig. 4—Use and interpretation of IRE standard scale.

Measurements made with the IRE standard scale may be expressed as follows:

White Peak. 86 (meaning 86 IRE scale units or 86 per cent of the range between *Blanking* and *Reference-White Levels*).

Black Peak. 13 (meaning 13 IRE scale units or 13 per cent of the range between *Blanking* and *Reference-White Levels*).

Sync Level. −43 (meaning 43 IRE scale units or 43 per cent of the range between *Blanking* and *Reference-White Levels* but negative with respect to *Blanking Level*).

Theory of Networks of Linearly Variable Resistances*

HAROLD LEVENSTEIN†, MEMBER, IRE

Summary—**A network theory is derived for circuits constructed of linear rheostats driven from a common input shaft. A correspondence between these networks and *RL* networks is used to demonstrate that driving point impedances and transfer functions are real rational fractions in a real variable, the input shaft rotation. Requirements on the pole-zero characteristics of these functions are established. Methods for developing functions approximating a given input-output relation in physically realizable form are discussed. Modern methods of transfer-function realization can be applied to these fractions to synthesize the physical networks. Networks for sine and log transfer functions obtained by the technique are presented.**

Background

IN the design of analog computers, the engineer often makes use of potentiometers whose output voltage is required to vary in a prescribed manner as the shaft of the potentiometer is rotated. To meet these requirements a variety of ingenious techniques and special circuits have been advised. Special potentiometers may be employed whose variation in resistance is obtained by winding on nonlinear cards, by winding different wire sizes along the length of the card, or by varying the spacing between wires. Taps may be distributed along the winding and connected to appropriate voltages from a voltage divider. The potentiometer may be loaded by connecting resistances from the slider to some reference potential.[1,2]

These and more intricate circuits all have been employed widely. It is characteristic of loading methods that a wholly empirical approach is used most often. In such methods the designer "guesses" at an appropriate circuit, takes literal values for the circuit elements, and then, by more or less sophisticated mathematics, attempts to discover numbers for the literal quantities which cause the circuit to approximate best the original prescription.

Such a technique is inefficient. It provides no basis for establishing an economical design, nor does it provide any suggestion for the improvement of the design if this is required.

From a practical point of view, the use of linear potentiometers as the basis for generating prescribed nonlinear functions of shaft rotation has considerable importance. There are several reasons for this. Linear poteniometers are considerably less expensive than nonlinear components of the same precision. They are manufactured more easily. Finally, they can be obtained commercially with an extremely high degree of linearity; at present, they can be obtained with linearity tolerances of 0.015 per cent. In this paper we present derivations of some of the significant properties of networks constructed of linearly varying rheostats. Methods for reducing data to a form appropriate to such networks are described, and some of the aspects of network synthesis are considered.

Statement of the Problem

The problem will be formulated in the following way. Given a network with two input terminals and two out-

* Original manuscript received by the IRE, January 30, 1957; revised manuscript received, November 6, 1957.

† W. L. Maxson Corp., New York, N. Y.

[1] I. Greenwood, J. Holdam, and D. Mackae, "Electronic Instruments," McGraw-Hill Book Co., Inc., New York, N. Y.; 1946.

[2] H. Levenstein, "Generating Non-Linear Functions with Linear Potentiometers," *Trans. 1953 Natl. Conf. on Airborne Electronics.*

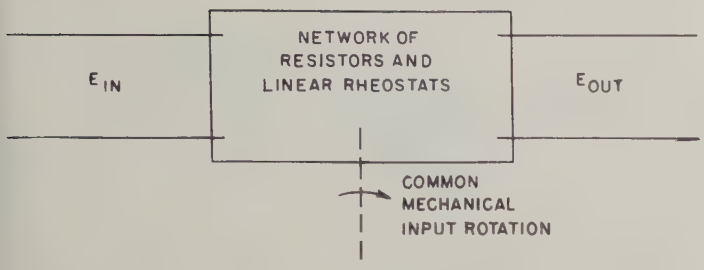

Fig. 1—The general problem.

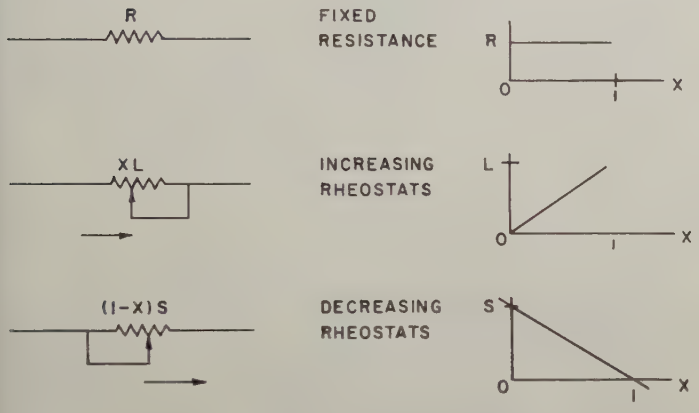

Fig. 2—The three types of elements.

put terminals and containing only fixed resistances and linear rheostats, the latter driven by a common shaft accessible from the outside, what is the relationship of the output voltage to the input voltage as a function of shaft rotation?

Note that rheostat has replaced potentiometer in this statement. Since any potentiometer can be replaced by a series connection of two rheostats, we may regard this as a more general statement of the problem.

When we have solved this problem we then can consider the problems of synthesizing networks and the problem of approximating prescribed functions. A graphic description of the problem is shown in Fig. 1.

Basic Descriptions of Network Elements

The three types of elements which must be considered are shown schematically in Fig. 2. R denotes a fixed resistance of value R. We take x, the shaft rotation, to be a variable running from zero to one, so that x represents fractional shaft rotation. There are two possible connections for rheostats: resistance increasing with x and resistance decreasing with x. If the rheostat resistance increases with x, its "instantaneous" resistance is xL, where L is the total resistance. If the start and end of the winding are reversed, the resistance decreases with x and can be denoted $(1-x)S$, where S is the total resistance. These three cases are schematically distinguished as Fig. 2(a), 2(b), and 2(c).

An Equivalent Circuit Theorem

So far we have described a network containing three types of elements. The present state of electric circuit

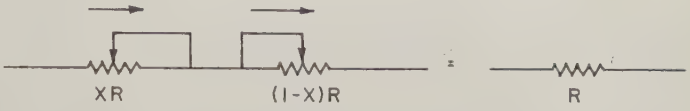

Fig. 3—Equivalent circuit for fixed resistor.

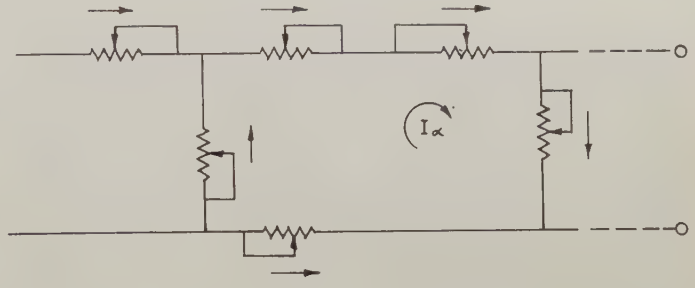

$$|Z_{\alpha\beta}| \cdot |I_\alpha| = |E_\beta|$$

WHERE

$$Z_{\alpha\beta} = XL_{\alpha\beta} + (1-X)S_{\alpha\beta}$$

Fig. 4—Circuit relationships.

theory does not permit the complete treatment of circuits of more than two mathematically independent elements. Accordingly, we shall make note of a superficially trivial relation which permits a complete treatment of this problem. We observe that every fixed resistance R can be replaced by a series connection of two rheostats of values xR and $(1-x)R$. (See Fig. 3.) Thus, if we replace each fixed resistance by its equivalent circuit of two series rheostats, the network is reduced to one containing only two types of elements.

We may now refer to the general theory of such networks for a solution.

Properties of Networks Containing Two Types of Elements

While it is not necessary to do so, we shall find it most convenient from the viewpoint of exposition to draw a close analogy between the networks we have hypothesized and networks consisting of resistors and inductors (with no mutual coupling), and to make use of the analogy to arrive at the properties of the networks.

To arrive at this analogy, we may begin by considering Fig. 4, which illustrates a typical network. Each element is either of the x type or $(1-x)$ type. If we assume mesh currents and write mesh equations, we find the customary matrix relation:

$$|Z_{\alpha\beta}| \times |I_\alpha| = |E_\beta|. \tag{1}$$

Each term of $Z_{\alpha\beta}$ is generally of the form:

$$Z_{\alpha\beta} = xL_{\alpha\beta} + (1-x)S_{\alpha\beta}. \tag{2}$$

Now, if we divide every term of $Z_{\alpha\beta}$ by x and multiply every current by x, we will have modified the elements of the matrices without modifying the matrix equation. Formally let us define

$$Z_{\alpha\beta}^* = Z_{\alpha\beta}/x \tag{3}$$

and

$$I_\alpha^* = xI_\alpha. \tag{4}$$

Then the matrix equation becomes:

$$|Z_{\alpha\beta}^*| \times |I_\alpha^*| = |E_\beta|. \tag{5}$$

The elements of the Z^* matrix will now have the form:

$$Z_{\alpha\beta}^* = L + \frac{1-x}{x} S. \tag{6}$$

If we introduce a new parameter p defined by (7)

$$p = \frac{1-x}{x}, \tag{7}$$

these elements become:

$$Z_{\alpha\beta}^* = L + pS. \tag{8}$$

Thus, the relations between the starred mesh currents and the voltages have the same mathematical structure as the relations which exist in a network constructed of resistances and inductances. Since the theory of these circuits has been highly developed, we may adopt it and use it to predict the properties of variable resistance networks.[3]

Accordingly, we may now make the following statements:

1) The driving-point impedance of the starred networks, the ratio of voltage to starred current, is a rational fraction in p. The degree of the numerator is equal to or one more than the degree of the denominator. The roots of the numerator and the denominator must be simple, real, negative, and must alternate with the least (magnitude) root of the numerator less than the least root of the denominator.

2) The transfer function of the starred network, the ratio of voltage across the load to input voltage, is a rational fraction in p. The order of the numerator is equal to or less than the order of the denominator. The roots of the numerator may lie anywhere in the complex p plane, with the restriction that complex roots must occur in conjugate pairs. The roots of the denominator must be simple, real, and negative.

When we introduce the inverse transformation from p to x we can restate 1) and 2) as follows:

3) The driving point impedance of the variable resistance networks is a rational fraction in x. The order of the numerator may be equal to, or one, or two more than the order of the denominator. The roots of the numerator and the denominator must be simple, real, and lie outside the range of $0<x<1$.

Within the ranges $-\infty<x<0$ and $1<x<\infty$ the alternation property of the poles and zeros still holds, with the zeros of the numerator closer to 0 and 1 than the corresponding zeros of the denominator. A picture of the zero-pole distribution in the p and x planes is shown in Fig. 5.

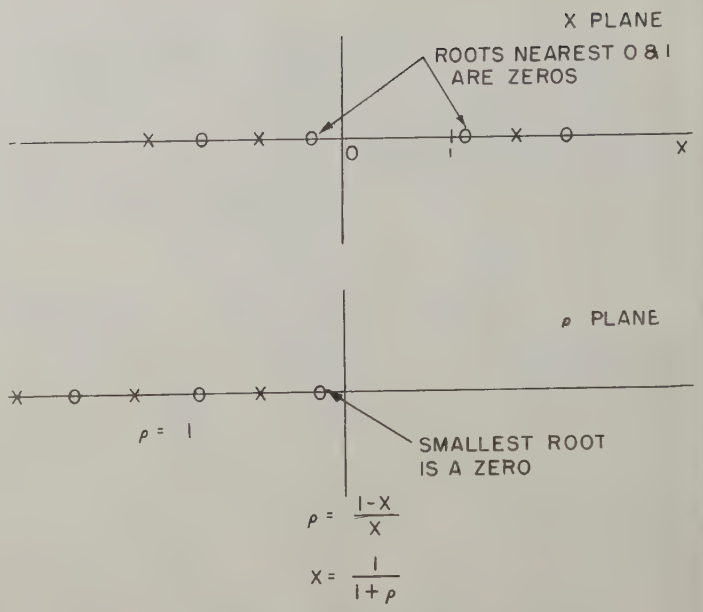

Fig. 5—Typical pole-zero distribution of driving-point impedance in p plane and x plane.

4) The transfer function of the variable resistance networks is a rational fraction in x. The order of the numerator may be equal to or less than the order of the denominator plus one. The roots of the numerator may lie anywhere in the complex plane. The roots of the denominator must be simple and real and may lie anywhere except in the range $0\leq x\leq 1$.

In all cases, complex roots appear in complex conjugate pairs.

The derivations of the above relations appear in Appendix I.

While it is possible to deduce other related properties, these are sufficient to characterize the next phase of the problem, the approximation problem. We shall derive additional information where we require it (for example, in the synthesis phase).

It may be informative to note that the transformation of p to x is a mapping of the p plane into the x plane. While we are most often concerned with the real axes, the general character of the mapping, a bilinear transformation, is of interest when we are dealing with the complex roots of the numerator of the transfer function. Fig. 6 shows the nature of the mapping performed.

The Approximation Problem

Since for the most part these networks are not used as impedances, we shall concern outselves primarily with methods of approximating prescribed data by functions characteristic of the transfer function. In any event, there is no serious difficulty in extending these methods to specification of impedance function.

[3] E. Guillemin, "A Summary of Modern Methods of Network Synthesis" in "Advances in Electronics," Academic Press, New York, N. Y., vol. 3, pp. 261–301; 1951.

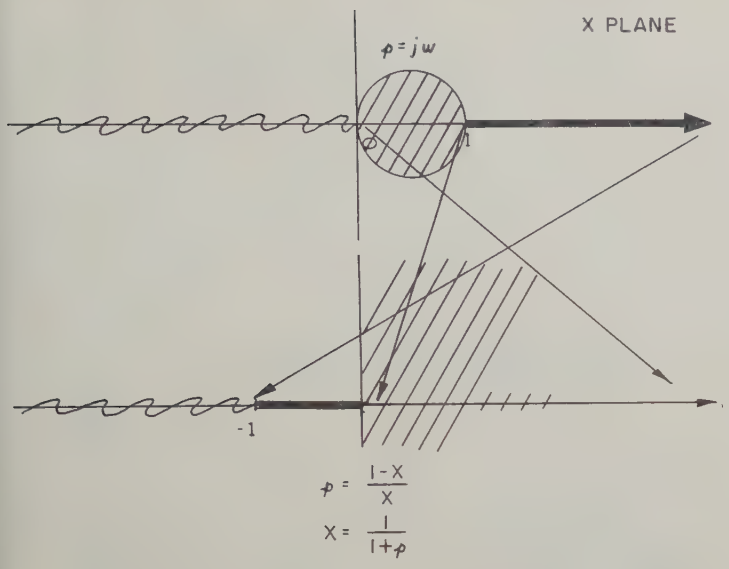

Fig. 6—Mapping between p and x planes.

GIVEN: $y = y_0, y_1, \cdots\cdots y_R \cdots\cdots y_N$ CORRESPONDING TO $X = X_0, X_1, \cdots\cdots X_R \cdots\cdots X_N$

FIND: $Z = N(X)/D(X)$ SUCH THAT $Z = y$ AT THE SELECTED POINTS

SOLUTION: FORM THE FOLLOWING DETERMINANT, SET EQUAL TO ZERO, AND SOLVE FOR Z.

$$\begin{vmatrix} 1 & y_0 & x_0 & x_0 y_0 & x_0^2 & x_0^2 y_0^2 & \cdots \\ 1 & y_1 & x_1 & x_1 y_1 & x_1^2 & x_1^2 y_1^2 & \cdots \\ \cdots & \cdots & \cdots & \cdots & \cdots & \cdots & \cdots \\ 1 & y_N & x_N & x_N y_N & x_N^2 & x_N^2 y_N^2 & \cdots \\ 1 & Z & x & xZ & x^2 & x^2 Z^2 & \cdots \end{vmatrix} = 0$$

Fig. 7—Milne's method for finding rational fraction approximation. (Milne, *op. cit.*, ch. VIII.)

The approximation problem usually is presented as follows: the desired output function y shall vary with an independent parameter z in a certain functional, graphical, or tabular manner. What rational fraction in x shall we select to best approximate this relation between z and y? This fraction must have the properties stated as 3).

Since the range of variation of x is zero to one, we must first establish a scale factor between z and x; sometimes, as in the case of the log function, we must shift the origin. While it is conceivable that we may select a nonlinear transformation from z to x (for example, in the case where the x shaft carries a calibrated dial displaying the inverse transformation), we ordinarily employ a linear transformation. In any event we must first establish a relation between y and x over the range $0 \leq x \leq 1$.

It is not necessary to modify the scale of y at this time, although it is likely that this will be necessary in synthesizing the network.

An answer to this approximation problem has been found in standard interpolation theory.[4,5] Formally, if we select n values of y: $y_0, y_1, \cdots, y_s, \cdots, y_{n-1}$ corresponding to $x_0, x, \cdots, x_i, \cdots$, values at which we wish to make our approximation exact, we merely need to substitute them in the determinant of Fig. 7 and solve for y to find an approximating rational fraction.

Unfortunately, there is no guarantee that the roots of the denominator will be of the proper nature. There is every likelihood that they will be complex.

One recourse we have is to manufacture a rational fraction with the proper denominator. An effective technique is the following:

1) Fit a polynomial in x to y by any suitable technique; for example, by least squares. Call it $Q(x)$.

2) Divide this by a polynomial in x, denoted $P(x)$, constructed of pairs of factors of the form $(x-a)(x+a-1)$. That is,

$$P(x) = \prod^{n} (x - a_i)(x + a_i - 1). \tag{9}$$

The order of $P(x)$ is $2n$ and is selected to be equal to or greater than one plus the order of $Q(x)$. The a_i are all different and chosen remote from the range of interpolation. Accordingly, $P(x)$ approximates a constant over $0 \leq x \leq 1$. It is often convenient to factor $Q(x)$ first since, if it possesses a root b_i which is real and outside the range of interpolation, we may make one of the a_i identical with b_i and thus reduce the order of $Q(x)$ and $P(x)$.

3) $Q(x)/P(x)$ is an acceptable transfer function which is physically realizable.

A further refinement of this process consists of forming the product $P(x)Y$ and fitting a polynomial $Q^*(x)$ to this modified datum. Generally, if $Q(x)$ and $Q^*(x)$ are of the same order, $Q^*(x)/P(x)$ more accurately fits the data than $Q(x)/P(x)$.

Another method for finding a rational fraction approximation which provides some control of the denominator is presented in Appendix II.

For the purposes of this paper, we may consider the approximation problem solved.

The Synthesis Problem

Since network synthesis is an ever changing art with the personal preference or experience of the engineer often the dominating factor in the solution, we shall merely show how the problem is reduced to a form suitable for synthesis by any acceptable technique. Some post-synthesis considerations will be introduced.

At the conclusion of the approximation stage we

[4] W. E. Milne, "Numerical Calculus," Princeton Univ. Press, Princeton, N. J., 1949.
[5] L. M. Milne-Thompson, "Calculus of Finite Differences," Macmillan & Co., Ltd., London, Eng., pp. 106–108; 1951.

$$\text{SINH}\,\theta \cong K\,\frac{X(X+4.3503)}{(X-3.1312)(X+1.5474)}$$

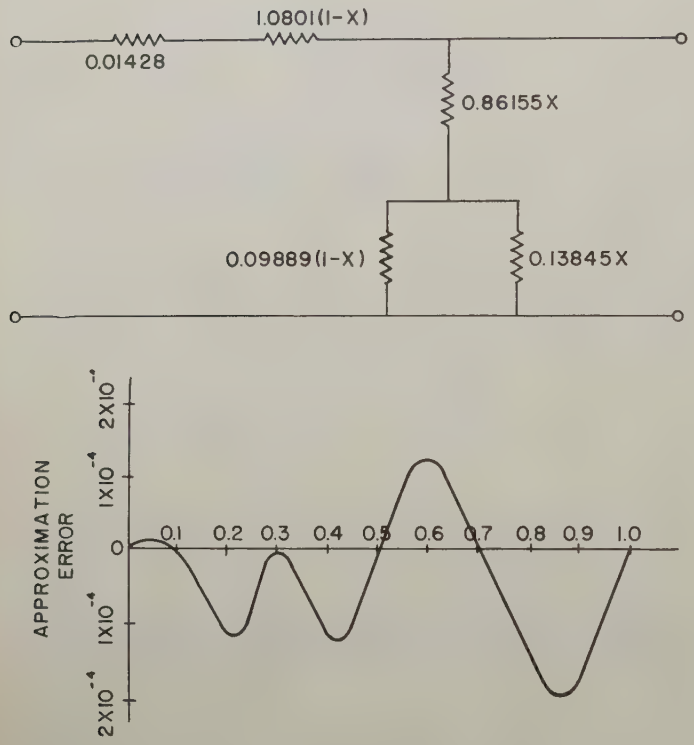

Fig. 8—Network for sinh θ.

possessed a function Y

$$Y = Q(x)/P(x) \qquad (10)$$

which approximates $y=y(x)$ in a satisfactory manner over the range of x.

The substitution of $x=1/(1+p)$ into (10) provides a relation between Y and p identical with the transfer function of an RL network. Accordingly, using the methods of Guillemin[3,6,7] or Bower and Ordung,[8] we can arrive at a network configuration and component values for this equivalent RL network.

We next replace p by $(1-x)/x$ in the circuit impedances. This, of course, leaves us with nothing recognizable. We must recall that the transformation into the RL network also included the scaling of every component value by division by x. Accordingly, we multiply every component by x and find that we can now interpret the network as a combination of x-type rheostats and $(1-x)$-type rheostats. By use of equivalent circuits we may be able to replace some of the rheostats by fixed resistors or potentiometers. Some of these equivalences are shown below (Figs. 10 and 11).

[6] J. G. Truxal, "Control System Synthesis," McGraw-Hill Book Co., Inc., New York, N. Y., ch. 3, pp. 161–220; 1955.
[7] P. M. Lewis, "The Synthesis of Voltage Transfer Functions," M.I.T., Res. Lab. of Electronics, Cambridge, Mass., Tech. Rep. 314; June, 1956.
[8] J. L. Bower and P. F. Ordung, "The synthesis of resistor capacitor networks," PROC. IRE, vol. 38, pp. 263–269; March, 1950.

$$\gamma = K\,\frac{X(X+0.64436)}{(X+1.5618)(X+0.28629)}$$

$$\sim \text{LOG}(10X+1) \qquad 0<X<1$$

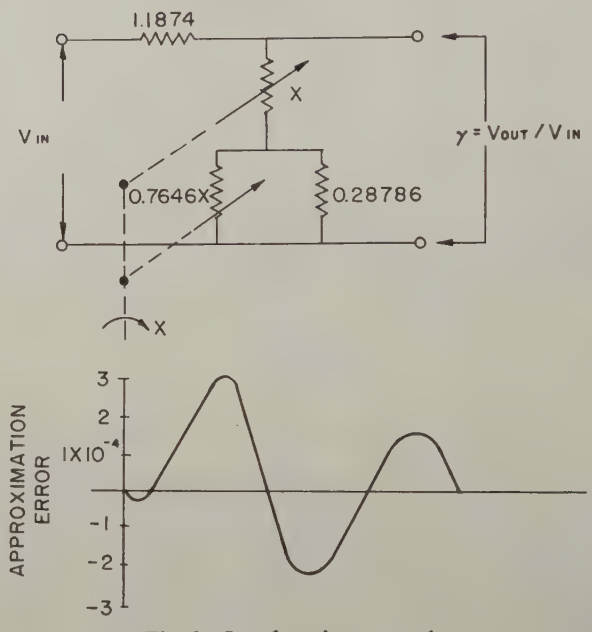

Fig. 9—Log function network.

Two Examples

Figs. 8 and 9 show two examples of the application of the theory. In both cases it happened that it was not necessary to force the approximating functions into appropriate form. Fig. 8 shows a network for generating the hyperbolic sine over the range zero to one. Fig. 9 is a circuit for generating log x; it is notable for its simplicity. In each figure the error is plotted as a function of shaft rotation. The extraordinary quality of the approximating function coupled with the simplicity of the circuits is indicative of what can be accomplished when the properties of these networks are properly used.

Some Equivalent Circuits

In Fig. 10 we have tabulated some equivalent circuits and their impedance representations in the x and p variables. They are intended primarily for use in recognizing standard configurations and in simplifications of the synthesized networks.

Fields for Extension of the Theory

Several questions can be raised which indicate possible directions for extension of the theory. One important question is: what are the properties of networks in which the rheostats are turned by several independent variables? Perhaps this can be answered partly by considering what the possibilities are for networks whose driving point impedances are substantially constant over a considerable range, while possessing prescribed transfer functions. Such networks could be cascaded to obtain products of functions of independent variables.

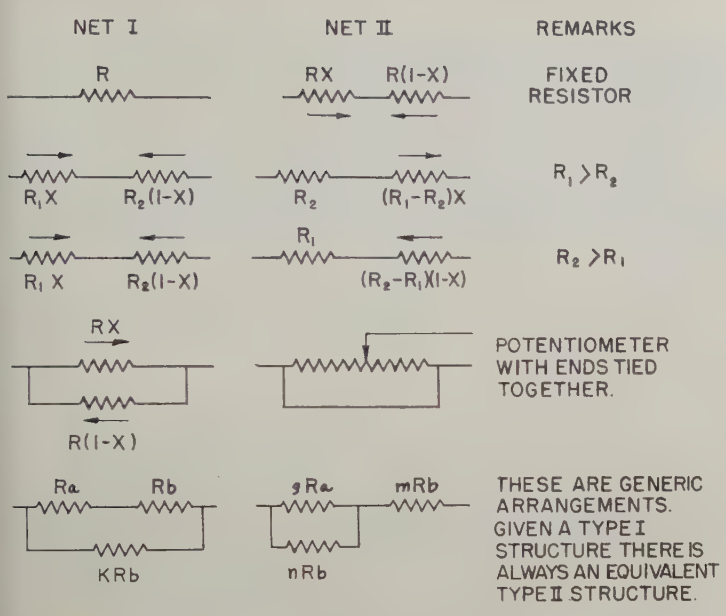

Fig. 10—Equivalent two-terminal nets.

While the discussion has been limited to linear rheostats, it is obvious that it is applicable to similar networks made up of adjustable capacitors or inductors. There may be special advantages to these circuits.

Finally, there may be some advantage in range of application to circuits constructed of some special functional rheostats which are not so readily obtained commercially. As an example, the use of sine-cosine elements may simplify some of the elaborate trigonometric relations associated with changes of coordinate reference systems in gimbal structures.

Appendix I

Derivation of Driving-Point Impedance and Transfer-Function Relations in the x Plane

Driving-Point Impedance

In the text it is shown that the driving-point impedance can be written by means of suitable transformations in the form

$$Z = xZ^*(p). \tag{11}$$

Where $Z^*(p)$ has the form of an RL network driving point impedance

$$Z^*(p) = K\frac{(p-p_1)(p-p_3)\cdots}{(p-p_2)(p-p_4)\cdots}. \tag{12}$$

In this form the p_i's are negative, real, and alternate and p_1 is closest to the origin. The degree of the numerator may be equal to or one greater than the degree of the denominator.

By definition

$$p = \frac{1-x}{x}. \tag{13}$$

Substituting in (12) and rationalizing we have

$$Z^* = \overline{K}x^{m-n}\frac{\left(x-\frac{1}{1+p_1}\right)\left(x-\frac{1}{1+p_3}\right)\cdots}{\left(x-\frac{1}{1+p_2}\right)\left(x-\frac{1}{1+p_4}\right)\cdots} \tag{14}$$

m = the degree of the denominator,
n = the degree of the numerator,
$\overline{K^*}$ = a new value of K appropriate to the rearranged form. Then

$$Z = xZ^* = \overline{K}x^{m-n+1}\frac{\left(x-\frac{1}{1+p_1}\right)\left(x-\frac{1}{1+p_3}\right)\cdots}{\left(x-\frac{1}{1+p_2}\right)\left(x-\frac{1}{1+p_4}\right)\cdots}. \tag{15}$$

We can now evaluate the polynomial relationships under the following possible conditions:

$$n = m$$

and

$$n = m+1$$

If $n=m$, there are the same number of roots in numerator and denominator and

$$Z = \overline{K}x\frac{N(x,n)}{D(x,n)}. \tag{16}$$

In this form the total numerator is one degree higher than the denominator.

If $n=m+1$, then

$$Z = \overline{K}\frac{N(x,n)}{D(x,n-1)}. \tag{17}$$

The numerator is again one degree higher than the denominator.

We must add to this the special case in which one of the p_i's is (-1). We handle all of the factors except this one as before. This factor disappears. To see this we evaluate the factor explicitly:

$$F = (p+1) = \left(\frac{1-x}{x}+1\right) = \frac{1}{x}. \tag{18}$$

Thus the contribution to x^{m-n+1} appears as before but the factor disappears from N or D, depending upon where it appeared.

Since the poles and zeros are simple, this situation can happen only once. But it can occur in either the numerator or the denominator.

In summary, the degree of the numerator may be equal to or one or two greater than the degree of the denominator.

Transfer Function

We may develop the transfer function relationship in

much the same manner that we have handled the driving point impedance.

We are concerned with the ratio here of an output voltage to the input voltage as a function of p first, and then x.

Starting with the RL equivalent of the resistance network we can describe the voltage transfer function as a ratio of polynomials in p

$$T = K \frac{N(p)}{D(p)} \cdot \tag{19}$$

The roots of $D(p)$ must be simple, negative, and real. The roots of $N(p)$ may be anywhere in the complex plane provided that for every complex root a conjugate root appears.

The degree of the numerator may be equal to or less than the degree of the denominator.

Note that x does not appear explicitly since we are dealing with a voltage ratio only, not an impedance.

Now rewrite (19) in the form

$$T = K \frac{(p - p_1)(p - p_3) \cdots}{(p - p_2)(p - p_4) \cdots} \cdot \tag{20}$$

No special ordering is implied here by the subscripts.

Letting $p = (1-x)/x$, and rationalizing

$$T = \overline{K} x^{m-n} \frac{\left(x - \frac{1}{1+p_1}\right)\left(x - \frac{1}{1+p_3}\right) \cdots}{\left(x - \frac{1}{1+p_2}\right)\left(x - \frac{1}{1+p_4}\right) \cdots} \cdot \tag{21}$$

We are interested in the cases, $m = n$ and $m > n$. We must also consider the effects of a root at $p = (-1)$ which may occur simply in the denominator or multiply in the numerator.

Let $m = n$. Then the leading terms in the numerator and the denominator are both x^m; their degree is the same.

Let $m > n$; the leading terms are x^m in both polynomials and the degree is the same, again.

Now let a simple root occur at $p = -1$ in the denominator. As before this factor will disappear from the denominator. The leading term in the numerator will be x^m, in the denominator x^{m-1}. The degree of the numerator is one higher than the degree of the denominator.

Let a multiple root of order k appear at $p = -1$ in the numerator. The leading term in the numerator will be x^{m-k}, in the denominator x^m, k higher than the numerator.

In summary, the degree of the numerator may be equal to or less than one plus the degree of the denominator.

Ordering Property of the Poles and Zeros of a Driving-Point Impedance

Poles and zeros of $Z^*(p)$ alternate on the real negative axis. A detailed examination of the way in which these roots map into the x axis shows the following:

1) The alternation property is preserved. However if these roots lie outside the range $(-1 < P < 0)$, the relationship occurs over two regions.

The poles and zeros lying between $(-1 < P < 0)$ map into the corresponding range $(0 < x < 1)$. The root closest to $x = 1$ is a zero and the poles and zeros alternate along the axis out to infinity. The ordering relationship then continues in along the negative real x axis from $-\infty$ to zero.

If $m = n$ in $Z^*(p)$ there will be a zero at the origin in the x plane due to the relationship

$$Z = xZ^*.$$

If $m = n-1$, the root closest to the origin in the x plane along the negative x axis will be a zero. Thus, in general, the alternation property holds, starting with a zero at or to the right of $x = 1$, continuing to infinity and returning along the negative axis, and concluding with a zero at or to the left of the x origin.

Appendix II

Construction of a Rational Fraction to Fit Assigned Data

Milne-Thompson[5] describes a method due to Thiele for constructing a continued fraction approximation to data. By terminating the fraction we obtain a rational fraction fitting the data at n specified points. A minor modification of this method gives additional freedom to adjust the roots of the denominator so that frequently they can be made to lie in the desired ranges without increasing the complexity of the network or changing the points of fit. Since the method is direct and reasonably simple it is usually worth trying.

The continued fraction proposed has the form

$$\bar{y} = a_0 + \cfrac{(x - x_0)}{a_1 + \cfrac{(x - x_2)}{a_2 + \cfrac{(x - x_2)}{a_3 + \cdots}}} \cdot \tag{22}$$

The x_i's are the points of fit, $\bar{y}$ is the approximation to y, the given data, and the a_i's are initially unknown.

Inspection of the above equation shows that the a's are readily determined in sequence.

If we set $x = x_0$, and $y = y_0$, we compute a_0. Then set $x = x_1$, $y = y_1$, and compute a_1. Setting $x = x_n$ makes the portion of the succeeding fraction identically zero, so that we can terminate the fraction at $x = x_n$ without changing the previous points of fit. The fraction can then be written in the form:

$$\bar{y} = a_0 + \cfrac{(x - x_0)}{a_1 + \cfrac{(x - x_1)}{a_2 + \cdots \cfrac{(x - x_{n-2})}{a_{n-1} + \cfrac{(x - x_{n-1})}{a_n}}}}. \tag{23}$$

As we noted $\bar{y}$ is identical with y at the points $x=x_0$, $x_1 \cdots x_{n-1}$. In addition, they are identical at $x=x_n$, since at that point the quantity $(x-x_n)$ is zero and would contribute nothing to the function in this form. Thus the $n+1$ coefficients characterize the function.

It is merely a matter of some algebra to rearrange this function as a rational fraction, which now approximates the data over the range $x_0 \leq x \leq x_n$.

$$\bar{y} = \frac{P(x)}{Q(x)} . \tag{24}$$

However, the roots of Q may not be properly placed for y to be a realizable function. So, instead of terminating the function with a_n we add the term $K(x-x_n)$ where K is an arbitrary parameter to be determined. Since when $x=x_n$ this term is zero, we have not changed the points of fitting.

Rearrangement of the function into a rational fraction now yields

$$\bar{y} = \frac{P(x) + K(x - x_n)P_1(x)}{Q(x) + K(x - x_n)Q_1(x)} . \tag{25}$$

This is a function which has the same points of fit as (24), but by adjustment of K we have some freedom to adjust the roots of the denominator. At the most this increases the complexity of the network by one degree.

It is clear that the functions P_1 and Q_1 must be proportional to P and Q at all points of fit except X_n, where this is unnecessary.

When $Q(x)$ is of reasonable degree, say 3 or 4, the numerical work associated with finding suitable values of K so that the roots of Q are real, simple, and do not lie inside the $0 \leq x \leq 1$ range is not usually prohibitive.

When a suitable selection has been made, it is necessary of course to check performance between the points of fit to determine the magnitude of errors; increasing the number of points of fit will, in general, permit reduction of errors.

Appendix III

Characteristics of Driving-Point Impedances

Shannon and Hargelbarger[9] show the driving-point impedance of a variable resistance network must always be a convex upward function of rotation. This is accomplished through investigation of hypothetical experimental connections of the network. In the following paragraphs, we wish to prove this relation using the network theory developed in the body of this paper.

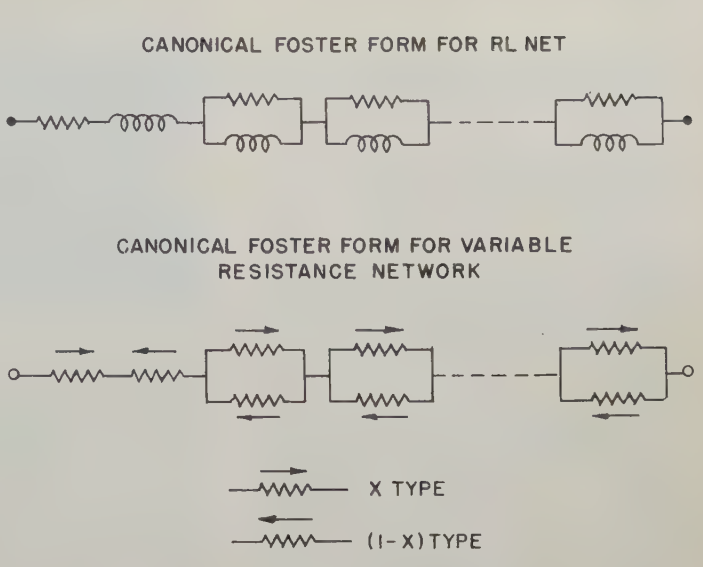

Fig. 11.

Every variable resistance network has an analog in the form of an *RL* network. Cauer's investigation of two terminal *RL* nets displays as one general canonical configuration a Foster form in which the network can be drawn as a series connection of parallel *RL* nets in series with a resistance and inductance. The series resistor and inductor may be identically zero.

The variable resistance analog of this is shown in Fig. 11.

The equation for the driving-point impedance can be written

$$Z(x) = R_{10}(x) + R_{20}(1 - x) + \sum \frac{R_{1i}R_{2i}(1 - x)x}{xR_{1i} + R_{2i}(1 - x)} .$$

Double differentiation of $Z(x)$ shows that

$$\frac{d^2Z(x)}{dx^2} \leq 0.$$

This can be verified very simply by sketching the $Z(x)$ curve of any of typical sections.

Acknowledgment

The author is indebted to Dr. H. Hochstadt for working out the two illustrative approximating functions and to Miss M. Whitfield and Mrs. R. Waldmann for the calculations associated with them.

[9] C. E. Shannon and D. W. Hargelbarger, "Concavity of resistance functions," *J. Appl. Phys.*, vol. 27, pp. 42–43; January, 1956.

Correspondence

A Parametric Electron Beam Amplifier*

A new type of solid state microwave amplifier has recently been proposed by Suhl.[1] Amplification of the signal occurs by transfer of power from a local rf source at a frequency higher than the signal and can be achieved by using certain properties of ferrites.

The purpose of this note is to show that a similar amplifier can be devised using an electron beam instead of the ferrite. Such an amplifier has the possibility of very-low-noise operation. The fundamental limitations[2] of the noise performance of conventional microwave amplifiers do not apply to it. An amplifier of this type has been built and some initial experimental results are given. The term "parametric amplifier" has been used because the device works by a variation in a circuit parameter.

In the simplest form of parametric amplifier the local source of power (usually called the pump) operates at exactly twice the signal frequency. The arrangement is shown in Fig. 1, where a parallel tuned circuit is resonant to the signal. The capacity (or inductance) is modulated at twice the signal frequency $\omega/2\pi$;

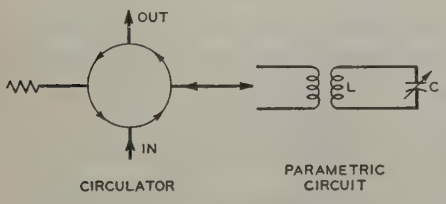

Fig. 1—Simple parametric circuit.

$$e.g.,\ C = C_0[1 + \epsilon \sin (2\omega t + \phi)]. \quad (1)$$

ϵ is a modulation coefficient with maximum value of 1.

If a signal at ω is applied to the circuit, then it can be shown that the capacity variation will inject, or extract power from the signal, depending on the value of the phase angle ϕ. The effect is equivalent to shunting a conductance G_p across the capacity where

$$G_p = -\frac{\omega C_0 \epsilon}{2} \cos \phi. \quad (2)$$

When $\phi = 0$, G_p has a maximum negative value and conditions are best for feeding power into the circuit.

If ϵ is then increased until $-G_p$ equals the loaded shunt conductance G_L of the circuit, oscillations will occur at frequency ω without the presence of the external signal. This condition is given by

$$G_L = -G_p = \frac{\omega C_0 \epsilon}{2}$$

or

$$\epsilon = \frac{2G_L}{\omega C_0} = \frac{2}{Q_L}, \quad (3)$$

where Q_L = loaded Q of circuit.

At a value of ϵ slightly less than that for oscillation, the circuit is stable and amplification can be obtained. The device acts as a regenerative amplifier like the maser and the regenerative reflex klystron amplifier. The operation of such an amplifier has been described by Gordon and White.[3] A single line is coupled to the circuit and the input and output signals are separated in a circulator. (See Fig. 1.) As well as preventing the loss of some of the output power into the input line, the circulator isolates the cavity from external load variations and enables stable operation much closer to the oscillation point with correspondingly higher gain.

Operating in this way the power gain is simply the square of the reflection coefficient (Γ) of the resonant circuit.

Power gain

$$= \Gamma^2 = \left[\frac{2}{1 + Q_E\left(\frac{1}{Q_0} - \frac{\epsilon}{2}\cos\phi\right)} - 1\right]^2, \quad (4)$$

where Q_E is the external Q of the loaded circuit and Q_0 is the unloaded Q of the circuit. It will be noticed that the gain cannot exceed 1 (assuming cos $\phi = 1$) unless $\epsilon/2 > 1/Q_0$; *i.e.*, unless the parametric variation is sufficient to make the unloaded circuit oscillate.

If the signal frequency differs slightly from half the pump frequency ($\omega_p/2\pi$), then the result can be described by a variation of the phase angle with time.

$$\phi = 2\left(\omega - \frac{\omega_p}{2}\right)t. \quad (5)$$

This causes a periodic amplification and attenuation of the signal at the frequency $(\omega - \omega_p/2)/\pi$. Essentially the output signal is modulated at twice the beat between the signal and half the pump frequency, giving rise to sidebands. The actual bandwidth of the amplifier is determined by the loaded Q.

An electron beam can be used to produce an electronic admittance in a microwave cavity, and one way of doing this is used in klystron oscillators. Take for example the "floating drift tube" klystron. There are two equal gaps in a single cavity separated by a field free drift space. A beam of electrons passes through the cavity and is arranged to have a drift angle beteen gaps given by

$$\alpha = (2n + 3/2)\pi \text{ radians},$$

where α = drift angle

$$n = 0, 1, 2, 3 \cdots.$$

An electronic admittance is produced across the cavity which is a pure negative conductance. This can overcome the positive conductance of the cavity and give rise to oscillation.

If, however, the drift angle is made a quarter cycle greater or smaller than this, the electronic admittance becomes a pure susceptance shunted across the cavity. This occurs when

$\alpha = (2n + 1)\pi$ for a positive susceptance,

$\alpha = (2n + 2)\pi$ for a negative susceptance.

This susceptance will change the resonant frequency of the cavity without altering the effective losses. As seen above, however, by modulating this susceptance at twice the signal frequency, a negative conductance will be produced which can overcome the cavity losses and give oscillation or amplification of the signal.

To modulate the susceptance, the beam must be modulated. This can be done by means of a preceding cavity resonant to the pumping frequency. If this is supplied with pumping power, any degree of beam modulation up to 100 per cent can be obtained at the signal cavity. The optimum spacing between cavities is a quarter of the effective plasma wavelength. The arrangement is shown in Fig. 2.

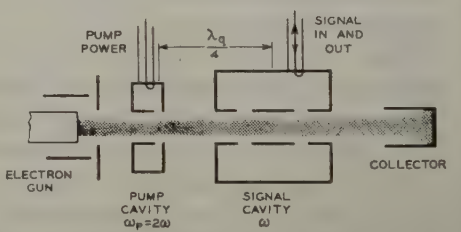

Fig. 2—Parametric beam amplifier.

The rf current (at the pump frequency) in the beam necessary to start parametric oscillations is given by

$$I_{rf} = \frac{4G_L V_0}{M^2 \alpha}, \quad (6)$$

where

V_0 = beam voltage;
M = signal cavity gap coupling factor;
I_{rf} = peak rf current on the beam.

If the beam is 100 per cent modulated,

$$I_{rf} = I_0,$$

where I_0 = dc beam current. It will be recognized that I_{rf} is just twice the start oscillation current of a floating drift tube klystron. A parametric beam amplifier should therefore operate with reasonable values of voltage and current.

Now, consider noise currents in the beam at the signal frequency. If the drift angle between gaps is $(2n+1)\pi$ radians (corresponding to a positive susceptance) and is short

* Received by the IRE, November 8, 1957.

[1] H. Suhl, "Proposal for a ferro-magnetic amplifier in the microwave range," *Phys. Rev.*, vol. 106, p. 384; April 15, 1957.

[2] H. A. Haus and F. N. H. Robinson, "The minimum noise figure of microwave beam amplifiers," PROC. IRE, vol. 43, pp. 981–991; August, 1955.

[3] J. P. Gordon and L. D. White, "Experimental determination of the noise figure of an ammonia maser," *Phys. Rev.*, vol. 107, pp. 1728–1729; September 15, 1957.

in terms of the plasma wavelength, the currents at the two gaps are essentially equal in amplitude and are in antiphase. No noise currents will be induced into the cavity. In other words, by choosing the drift cycle to be π, 3π, 5π, etc., it is possible to excite a cavity to produce amplification without coupling to the noise current in the beam, at least to a first order of approximation.

A demountable tube based on Fig. 2 has been built. This operated, as far as gain and oscillation, substantially as expected. No noise measurements have yet been made. Table I shows the measured characteristics

TABLE I

Signal Cavity	
Resonant Frequency	4150 mc
Drift Angle	3π radians
Pump frequency	8300 mc
Beam voltage	2450 v
Beam current	18 ma
Pump power	140 mw
Maximum observed gain	20 db

of the device. Fig. 3 demonstrates amplification obtained as a function of pumping power. In this figure cw power at constant frequency was used for the pump and the signal frequency was swept through the resonance of the signal cavity. In Fig. 3(a) the pumping power was zero, and the oscillation mode of the signal source klystron is seen with the resonance absorption of the signal cavity in the center (critically coupled). By increasing the pumping power to 35 mw and tuning in to twice the signal cavity frequency, some reduction in cavity loss was obtained [Fig. 3(b)]. Fig. 3(c)–3(e) shows gain with 56, 82, 140 mw of pumping power, respectively.

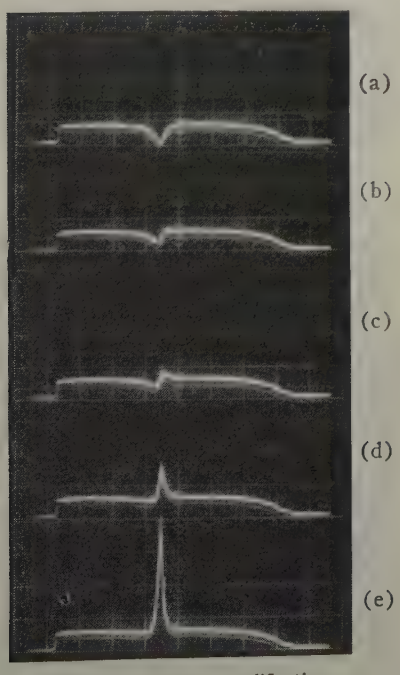

Fig. 3—Parametric amplification as function of pumping power.

Fig. 4 shows an enlarged section of the gain region. During the sweep, the phase changes periodically from that giving amplification to that giving attenuation, and this

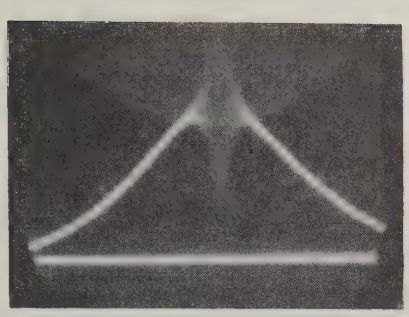

Fig. 4—Enlarged portion of Fig. 3(e).

accounts for the pattern seen in the center of the picture. The width of the pattern depends on the bandwidth of the video amplifiers used.

T. J. Bridges
Bell Telephone Labs., Inc.
Murray Hill, N. J.

On the Earth Geometry—A Theorem*

If one chooses an arbitrary point P inside of a circle other than its center, a normal s upon the diameter, both through P, intersects the circle with ψ, which is the angle between s and the tangent to the circle through the intersection point (Fig. 1). It can be shown analytically that ψ increases if s is rotated on P in either sense. For the conditions stated above ψ must be a minimum.

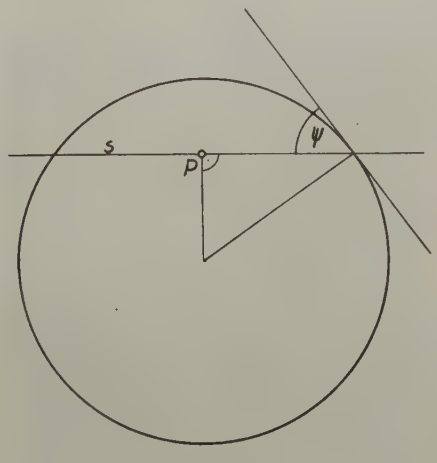

Fig. 1.

Applied to the earth geometry and to propagating radio waves which are reflected by the ionosphere, one arrives at the following conclusion: if the antenna height is zero and a radio beam is moved progressively from the zenith to the horizon, ψ, the angle of incidence at the reflecting layer, diminishes monotonously and reaches a minimum for zero elevation angle Δ of the beam, provided earth and ionosphere are concentric

* Received by the IRE, August 30, 1957.

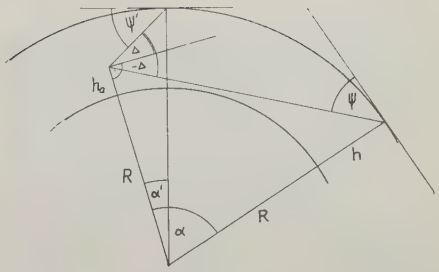

Fig. 2—The earth geometry.

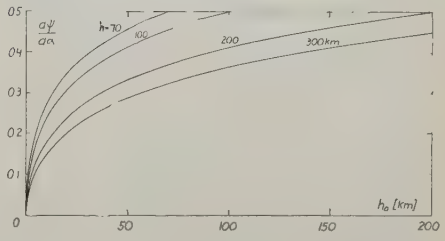

Fig. 3—$d\psi/d\alpha$ for negative elevation angles Δ as a function of antenna h_a and layer height h.

spheres (Fig. 2). Applying the same procedure to finite antenna heights, it can be shown that ψ passes through this minimum before the beam becomes tangent to the earth, *i.e.*, for a negative elevation angle Δ of the beam $d\psi/d\alpha$ is positive. For an earth whose radius is modified so as to include uniform refraction in the atmosphere $k=1.25$ and for negative values of Δ, $d\psi/d\alpha$ was calculated as a function of antenna elevation h_a for various heights of the reflecting layer h (Fig. 3). $d\psi/d\alpha$ is less than one half for all practical cases of $h_a < h$.[1]

Kurt Toman
Geophysics Res. Directorate
Boston, Mass.

[1] Negative values of Δ correspond to the beam grazing the earth.

Behavior of Noise Figure in Junction Transistors*

Nielsen[1] has presented a well-organized treatise on a timely subject. He has simplified van der Ziel's circuit by assuming the emitter and collector noise generators are uncorrelated. It may be of interest to see how the noise figure expressions may be modified to include the effect of partial correlation of the emitter and collector noise generators.

Van der Ziel[2,3] has determined the magnitudes of the noise generators to be

* Received by the IRE, September 13, 1957.

[1] E. G. Nielsen, Proc. IRE, vol. 45, pp. 957–963; July, 1957.

[2] A. van der Ziel, "Theory of shot noise in junction diodes and junction transistors," Proc. IRE, vol. 43, pp. 1639–1646; November, 1955.

[3] "Theory of shot noise in junction diodes and junction transistors," Proc. IRE, vol. 45, p. 1011; July, 1957.

$$\overline{e_s^2} = \frac{2kTdf(2g_e - g_0)}{g_s^2 + b_s^2} \quad (1)$$

$$\overline{i_p^2} = 4kTG_n df = 2kTdf\alpha_0 g_0\left(1 - \frac{|\alpha|^2}{\alpha_0}\right) + 2eI_{c_{sat}}df \quad (2)$$

or

$$G_n = \frac{\alpha_0 g_0}{2}\left(1 - \frac{|\alpha|^2}{\alpha_0}\right) + 20I_{c_{sat}}$$

$$e_s^* i_p = 2kTdf\alpha\left(1 - \frac{g_0}{Y_e^*}\right). \quad (3)$$

Van der Ziel sets $e_s = e_s'' + e_s'$ where e_s'' is uncorrelated with i_p, and e_s' is completely correlated with i_p.[4]

He also sets

$$\overline{e_s''^2} = 4kTR_{n}df, \quad (4)$$

where $R_n = r_e/2$ at low frequencies.

$$e_s' = \frac{Z_1 i_p}{\alpha} \text{ where } Z_1 = \pm R_1 \pm jX_1 \quad (5)$$

$$\therefore e_s^* i_p = \left(e_s''^* + \frac{Z_1^* i_p^*}{\alpha^*}\right) i_p = e_s''^* i_p + \frac{Z_1^* \overline{i_p^2}}{\alpha^*}. \quad (6)$$

Since $e_s''^* i_p = 0$ then, neglecting effects of collector saturated current, $I_{c_{sat}}$,

$$Z_1^* = \frac{e_s^* i_p \alpha^*}{\overline{i_p^2}} = \frac{2kTdf\alpha\left(1 - \frac{g_0}{Y_e^*}\right)\alpha^*}{2kTdf\alpha_0 g_0\left(1 - \frac{|\alpha|^2}{\alpha_0}\right)} \quad (7)$$

$$Z_1^* = \frac{|\alpha|^2\left(1 - \frac{g_0}{Y_e^*}\right)}{\alpha_0 g_0\left(1 - \frac{|\alpha|^2}{\alpha_0}\right)} = \frac{|\alpha|^2\left(\frac{1}{g_0} - \frac{1}{Y_e^*}\right)}{\alpha_0 - |\alpha|^2}. \quad (8)$$

Thus at very low frequencies $Y_e^* \to g_0$ and $Z_1 \to 0$ in the absence of If noise, and at very high frequencies $|\alpha| \to 0$ and $Z_1 \to 0$. At some intermediate frequency Z_1 will reach a maximum value. To find that approximate maximum value and the approximate frequency at which it occurs, the expressions for Y_e and α derived by Pritchard[5] may be substituted into (8). Y_e is the diffusion admittance of the emitter-base junction.

$$Y_e \approx \frac{qI_e}{kT}\frac{[(1 + 0.25x^2) + j0.8x]}{1 + 0.06x^2} \quad (9)$$

where

$$\frac{qI_e}{kT} = g_0, \quad x = \frac{f}{f_\alpha},$$

f_α = inherent alpha cutoff frequency.

$$\alpha \approx \alpha_0 \frac{[(1 - 0.25x^2) - j1.2x]}{(1 + x^2)}. \quad (10)$$

[4] G. N. Hanson and A. van der Ziel, "Noise in transistors," to be published.
[5] R. L. Pritchard, "Frequency response of theoretical models of junction transistors," IRE TRANS., vol. CT-2, pp. 183–191; June, 1955.

At this time (9) and (10) will be simplified to

$$Y_e \approx g_0(1 + jx) \quad (11)$$

$$\alpha \approx \frac{\alpha_0}{1 + jx}. \quad (12)$$

The magnitude of alpha in (12) should be within 10 per cent of the value in (10) up to twice f_α. The magnitude of Y_e in (11) is within 15 per cent of the value of (9) up to $f = 2f_\alpha$. However, there is an excess angle in (11) of 12° at f_α and 25° at $2f_\alpha$. With the emitter-base transition capacity assumed small compared to the diffusion capacity, then

$$Z_1 \approx \frac{\frac{\alpha_0}{g_0}\left(1 - \frac{1}{1 + jx}\right)}{(1 - \alpha_0 + x^2)}, \quad (13)$$

$$R_1 \approx \frac{\alpha_0}{g_0}\frac{x^2}{(1 + x^2)(1 - \alpha_0 + x^2)}, \quad (14)$$

$$X_1 \approx \frac{\alpha_0}{g_0}\frac{x}{(1 + x^2)(1 - \alpha_0 + x^2)}, \quad (15)$$

$$|Z_1| \approx \frac{\alpha_0}{g_0}\frac{x}{\sqrt{1 + x^2}(1 - \alpha_0 + x^2)}. \quad (16)$$

Using values of $\alpha_0 = 0.98$, $r_{e_0} = 1/g_0 = 26\Omega$ at $I_\xi = 1$ ma, (14), (15), and (16) reach maximum values at the indicated frequencies below:

$$R_{1_{max}} \approx 19.5\Omega\, f \approx 0.38 f_\alpha$$

$$X_{1_{max}} \approx 88.0\Omega\, f \approx 0.14 f_\alpha$$

$$|Z_1|_{max} \approx 90.0\Omega\, f \approx 0.14 f_\alpha.$$

Under those conditions of transistor amplifier operation where Z_L (the load impedance across which is obtained the output signal) contains a source of thermal noise $e_{nL}^2 = 4kTR_L df$, and provided $\alpha Z_c \gg Z_e$, $\alpha Z_c \gg Z_g + Z_b$, $\alpha Z_c \gg R_L$, the common-base and common-emitter noise figures then become

$$F_b = F_e = 1 + \frac{r_b'}{R_g} + \frac{R_n}{R_g} + \frac{G_n}{R_g|\alpha|^2}|(R_g + r_b' + r_e - R_1)^2 + (x_g - x_b' - x_e - X_1)^2|, \quad (17)$$

where the complex base impedance $Z_b' = r_b' - jx_b'$. In alloy transistors $Z_b' = r_b'$.

The common collector noise figure is

$$F_c = 1 + \frac{r_b'}{R_g} + \frac{R_n + R_L}{R_g} + \frac{G_n}{R_g}\left[\left(R_g + r_b' - R_e\left[\frac{Z_1}{\alpha}\right]\right)^2 + \left(x_g - x_b' - I_m\left[\frac{Z_1}{\alpha}\right]\right)^2\right]. \quad (18)$$

It is interesting to observe that the noise figures for the common-emitter and common-base configurations are independent of Z_L to the extent that the above conditions are satisfied. However, it should be noted that the common collector amplifier noise figure is degraded as R_L is increased. Decreasing R_L in this case to improve the noise figure will also decrease the dynamic input impedance to the stage, which may be undesirable.

Nielsen points out the noise figure of the common collector becomes fairly constant at high frequencies. However, lest one be tempted to use this configuration at frequencies above f_α, it should be pointed out that the available power gain must inevitably decrease to zero so that the device becomes useless as a signal amplifier in spite of its lower noise figure.

The contribution to the noise figure of the correlation impedance Z_1 is probably negligible in Nielsen's measurements in view of the moderate value of emitter current used (1–3 ma) and the magnitude of the source resistance (around 500Ω). However, under conditions of low emitter current and low source resistance the contribution may have to be included. Also, the contribution to the noise figure from the reactive term multiplying $G_n/R_g|\alpha|^2$ may also become important when R_g becomes smaller.

Finally, to those interested in the design of transistor amplifiers with the ultimate in sensitivity (hence minimum noise figure), it may be well to show how an unbypassed emitter resistance or a partially bypassed emitter resistance in the common-emitter configuration may degrade the noise figure. Let the net effective external emitter impedance be represented in the series impedance form of $Z_0 = R_0 - jx_0$. Then

$$F_e = 1 + \frac{r_b'}{R_g} + \frac{R_n + R_0}{R_g} + \frac{G_n}{|\alpha|^2 R_g}|(R_g + r_b' + r_e + R_0 - R_1) + (x_g + x_b' + x_e + x_0 - x_1)^2|. \quad (19)$$

At audio frequencies in the shot noise region $Z_1 \to 0$, $X_b' \to 0$, $x_e \to 0$. Let us assume the actual generator driving the stage is purely resistive, but let us lump the reactance of the input coupling capacitor x_{c_1} into x_g so that $x_g = x_{c_1}$. Then

$$F_e = 1 + \frac{r_b'}{R_g} + \frac{R_n + R_0}{R_g} + \frac{G_n}{|\alpha|^2 R_g} \cdot |(R_g + r_b' + r_e + R_0)^2 + (x_{c_1} + x_0)^2|. \quad (20)$$

Not only does R_0 degrade the noise figure but so does X_0 and x_{c_1} as well. If possible, one should ground the emitter directly. Otherwise, if an external resistance is employed, use a large capacitance to reduce R_0 and x_0 to a small value. Also, x_{c_1} should be made small compared to R_g for minimum noise figure.

This may be a new criterion for some who have been used to making x_{c_1} at some low frequency f_l small, compared to generator resistance plus the input resistance to the particular stage, to help insure adequate low-frequency response down to f_l.

The writer would like to acknowledge helpful discussions with R. L. Watters and K. E. Mortenson of this Laboratory and with Prof. A. van der Ziel, University of Minnesota.

W. N. COFFEY
General Electric Res. Lab.
Schenectady, N.Y.

Electrolytic Tank Design of Electron Guns with Curved Electron Trajectories*

The general problem in electron gun design is to find a set of electrode shapes which approximate along the beam edge a theoretically determined gradient and potential distribution. For guns employing rectilinear flow, the problem is relatively simple, for the equipotentials are normal to the electron trajectories and the beam edge may be simulated in an electrolytic tank by an insulating strip, a method due to Pierce.[1] Of increasing interest, however, are types of motion in which the equipotentials are not normal to the beam edge as, for example, the curved trajectory flows discussed by Meltzer[2] and Walker[3] and more recently reported on by Kirstein and Kino.[4] If an electrolytic tank is to be used for gun design in these more general cases, an alternative to the insulating strip method must be employed.

Since it is no longer practical to fix the direction of the gradient at the beam edge, the potential distribution is the logical function to specify. For the general case then, the beam edge is simulated in an electrolytic tank by a resistance card cut so that a current caused to flow from one end to the other will establish along the card a potential distribution which will match the potential distribution required along the edge electron trajectory. After cutting, the card is placed in the tank and curved so as to duplicate the electron path. With the proper voltage applied across the card, the electrode shapes and positions are adjusted until the correct angles are established between the resistance card and the equipotentials. This operation is facilitated by placing immediately adjacent to the resistance card a series of probe pairs oriented so that the direction each pair defines is appropriate to the correct equipotential at that point (see Fig. 1). Proper

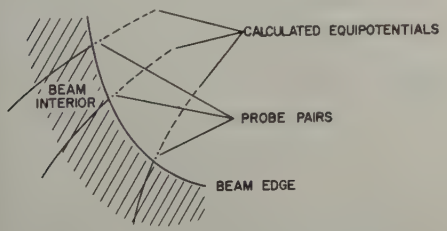

Fig. 1.

electrode design will then make the potential difference between the two probes of a given pair zero. In practice, it suffices to calculate for each pair the potential difference resulting from some allowable error in the angle of the equipotential and then settle for a design where the measured potential difference is less than or equal to this value.

To simplify the cutting of the resistance card, the potential distribution may be approximated by a series of chords and the resistance card cut, as in Fig. 2. The dotted lines indicate strands of fine wire which are

Fig. 2.

woven into the card at each discontinuity in order to keep the equipotentials on the card parallel. The conductivity of the card should be much greater than that of the electrolyte so that the current flowing into the tank from the card will not appreciably alter the potential distribution.

The device used to measure the probe pair potential differences must present identical high input impedances to each probe. In addition, each probe should be etched and coated with aqua-dag before use, in order to minimize surface effects.

The method of design just described generally is applicable to any flow which requires that a given potential and gradient be matched along a path. It has been used here quite successfully in connection with the design of electron guns which operate in the presence of a transverse magnetic field and should find additional application with the curved trajectory flows mentioned.

E. J. Cook
General Electric Research Laboratory
Schenectady, New York

Space-Charge-Balanced Hollow Beam with Uniform Charge Distribution*

In 1949, Samuel[1] proposed a convergent hollow-beam electron gun with an external conductor and a special shielding magnet, which is used to divide the magnetic flux at the mouth of a focusing solenoid in such a way that the flux threading through the hole in the cathode is the flux contained within the inner beam radius. In a subsequent investigation carried out by Harris,[2] this configuration was shown to be one of a class of electron beams utilizing what has since been called *space-charge-balanced flow*; *i.e.*, the type of beam focusing in which electrons are caused to rotate about the axis in an axial magnetic field in such a way that the outward space-charge-spreading plus centrifugal forces are just balanced by the inward Lorentz force. (The well-known *Brillouin-flow* focusing is a special case, in which the magnetic field drops off to zero at the cathode.) The hollow beam in space-charge-balanced flow requires a specific radial charge distribution, given by[1]

$$\rho = 2\epsilon_0\eta A_0^2\left[1+\left(\frac{r_a}{r}\right)^4\right] \qquad (1)$$

where A_0 is the normalized magnetic vector potential and r_a is the inner beam radius. If the radial charge distribution deviates from the form of (1), individual electrons follow stable oscillating trajectories; but as Harris has shown,[2] the angular frequency of oscillation is *not* independent of radius, so that adjacent electrons at different initial radial positions oscillate with different frequencies. Under this condition adjacent electron paths ultimately must cross, and the important laminar-flow assumption of space-charge-balanced flow analysis is violated.

The present note is a report on an analysis and experimental investigation of the case in which a deliberate deviation from the distribution of (1) is made by making ρ independent of radius. The uniform charge distribution is of obvious practical interest since it would be extremely difficult to obtain any other distribution from a conventional cathode without an elaborate design of the transition region between the gun and the interaction regions.

The equation of motion for this case can be derived quite simply if it is assumed that adjacent electrons do *not* cross radially—an assumption that will be shown below to be satisfied if beam lengths are restricted to a certain range (which is, nevertheless, of considerable practical interest).

$$\ddot{r} = r_0^2\frac{\omega_p^2}{2r}\left(1-\frac{r_a^2}{r_0^2}\right)-\omega_L^2 r\left(1-\frac{r_a^4}{r^4}\right) \qquad (2)$$

where $\omega_L \equiv \eta B/2$ is the Larmor frequency, $\omega_p^2 \equiv -\eta\rho_0/\epsilon_0$ is the plasma frequency, and ρ_0 is the charge density inside the radius r_0 of a given electron. Again, (2) can be readily solved if it is assumed that electron trajectories deviate only slightly from straight paths (an assumption that likewise is justified by the results of the analysis). Then $r=r_0+\Delta$, where $\Delta \ll r_0$; $\ddot{r}=\ddot{\Delta}$; and

$$\frac{1}{r}\approx\frac{1}{r_0}\left(1-\frac{\Delta}{r_0}\right);\quad \frac{1}{r^3}\approx\frac{1}{r_0^3}\left(1-3\frac{\Delta}{r_0}\right).$$

Thus

$$\ddot{\Delta} = \alpha - \beta^2\Delta \qquad (3)$$

where

$$\alpha \equiv r_0\left[\frac{\omega_p^2}{2}\left(1-\frac{r_a^2}{r_0^2}\right)-\omega_L^2\left(1-\frac{r_a^4}{r_0^4}\right)\right]$$
$$\beta^2 \equiv \frac{\omega_p^2}{2}\left(1-\frac{r_a^2}{r_0^2}\right)+\omega_L^2\left(1+3\frac{r_a^4}{r_0^4}\right). \qquad (4)$$

Eq. (3) has the solution

$$\Delta = \gamma\cos(\beta t-\delta)+\frac{\alpha}{\beta^2} \qquad (5)$$

and the constants γ and δ can be evaluated from the entrance conditions $\Delta=0$ and $\dot{\Delta}=\dot{r}_a$ at $t=0$, where $\dot{r}_a$ is the slope at entrance, so that finally

$$\Delta = \frac{\alpha}{\beta^2}(1-\cos\beta t)+\frac{\dot{r}_a}{\beta}\sin\beta t. \qquad (5a)$$

The value of α/β^2 may be adjusted in accordance with the boundary conditions that one chooses to impose on the configuration; *e.g.*, the specification of a nonoscillating outer beam boundary ($\ddot{r}=0$ at $r_0=r_b$, the equilibrium radius of the outermost electron) leads to a generalized form of the familiar Brillouin flow equilibrium condition

* Received by the IRE, September 23, 1957.
[1] J. R. Pierce, *J. Appl. Phys.*, vol. 11, pp. 548–554; August, 1940.
[2] B. Meltzer, *Proc. Phys. Soc.*, vol. B62, pp. 813–817; December, 1949.
[3] G. B. Walker, *Proc. Phys. Soc.*, vol. B63, pp. 1017–1027; December, 1950.
[4] Kirstein and Kino, paper presented at the IRE Tube Conference, Berkeley, Calif., June, 1957.

* Received by the IRE, July 29, 1957; revised manuscript received, September 26, 1957. Much of this work was carried out under the sponsorship of the U. S. Navy, Army, and Air Force under Contracts N6onr 25132 and DA36-039-sc-63189.
[1] A. L. Samuel, "On the theory of axially symmetric electron beams in an axial magnetic field," Proc. IRE, vol. 37, pp. 1252-1258; November, 1949.
[2] L. A. Harris, "Axially symmetric electron beam and magnetic-field systems," Proc. IRE, vol. 40, pp. 700–708; June, 1952.

$$\frac{\omega_p^2}{2} = \omega_L^2\left(1 + \frac{r_a^2}{r_b^2}\right). \tag{6}$$

It is obvious from (4) that the angular frequency of oscillation β is not independent of r_0, and hence adjacent trajectories must cross, as mentioned previously. However, in the first few oscillation wavelengths, the electrons merely begin to slip past one another, and relatively little crossing takes place. As an example, consider trajectories of a hollow beam for which $\dot{r}_a=0$ (beam parallel to the axis at entrance), and the outer boundary is held at constant radius. (The inner boundary is automatically parallel to the axis, since $\alpha=0$ at $r_0=r_a$.) Two adjacent paths at radii r_1 and $r_2(r_1<r_2)$ will not cross if at all times $r_2+\Delta_2 \geq r_1+\Delta_1$; *i.e.*, if $\Delta_2-\Delta_1 \geq -(r_2-r_1)$, which in the limit becomes

$$\frac{d\Delta}{dr_0} \geq -1. \tag{7}$$

But from (5a), for the case $\dot{r}_a=0$,

$$\frac{d\Delta}{dr_0} = (1-\cos\beta t)\frac{d}{dr_0}\left(\frac{\alpha}{\beta^2}\right) + t\frac{\alpha}{\beta^2}\sin\beta t\frac{d\beta}{dr_0}.$$

It can be shown (perhaps most readily by means of a plot, as described below) that the term α/β^2 has its maximum negative slope at $r_0=r_a$ (the equilibrium radius of the innermost electron), and that the first term of (8) consequently always is greater than -1, so that only the second term invalidates the inequality (7). Since this term is proportional to t, it is possible that the assumption of noncrossing trajectories may be satisfied if t remains small (*i.e.*, if the time necessary to pass through the interaction region is small). A graphical representation of the case $r_a=\frac{2}{3}r_b$ (Fig. 1) shows that such is indeed the case. The change in angular oscillation frequency β over the beam width is so small that virtually no crossing takes place within the first few oscillation cycles.

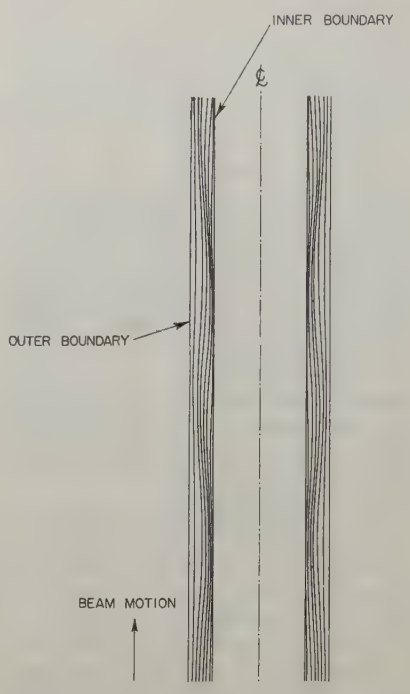

Fig. 1—Electron trajectories in a hollow beam initially parallel to the axis with uniform charge distribution under space-charge-balanced flow for $r_a=\frac{2}{3}r_b$.

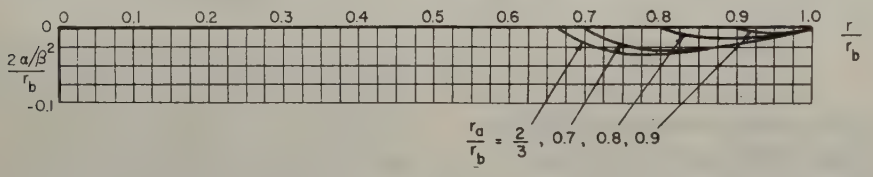

Fig. 2—Maximum deviation from initial radius (as a function of radius) for several beam thicknesses.

The amplitude of the oscillation for the present case varies with r_0 as α/β^2 (5a) and is zero at the inner and outer edges. The maximum amplitude $2\alpha/\beta^2$ is plotted as a function of radius r in Fig. 2, both normalized with regard to the outer beam radius r_b. The graphs show that the greatest deviation occurs near the middle between inner and outer boundary, and that the relative deviation becomes quite small for thin beams. The graphs also clearly illustrate the above statement that α/β^2 has its maximum negative slope at $r=r_a$.

The angular frequency of oscillation varies from $\beta_a=2\omega_L$ (*i.e.*, a "wavelength" of $2\pi v_0/2\omega_L$ where v_0 is the dc beam velocity and ω_L is the Larmor frequency) at the inner boundary to $\beta_b=\omega_L\sqrt{2}[1+(r_a/r_b)^4]^{1/2}$ (*i.e.*, a wavelength of just under $2\pi v_0/\sqrt{2}\omega_L$) at the outer boundary). These values can be readily related by means of (6) to the plasma wavelength $\lambda_p=2\pi v_0/\omega_p$, where ω_p is the plasma frequency. For the present example, for instance, the oscillation "wavelength" varies from $0.423\lambda_p$ at the inner boundary to $0.556\lambda_p$ at the outer boundary.

The oscillation wavelength is thus of the order of half a plasma wavelength, and we may conclude that, even though an analysis of a hollow beam (with a uniform charge distribution) based on (2), and assuming noncrossing trajectories cannot be rigorously said to hold for arbitrary beam lengths, in practice the assumption is likely to be satisfied in a large number of actual applications in which the length of the beam is of the order of a few plasma wavelengths (*e.g.*, klystrons and most high-power traveling-wave tubes). A previously described and executed design[3] of a hollow-beam electron gun appears to bear out this conclusion.

Marvin Chodorow
Stanford University
Stanford, Calif.
Charles Süsskind
University of California
Berkeley, Calif.

[3] C. Süsskind, "A Convergent Hollow-Beam Electron Gun for Microwave Tubes," Stanford Electronics Labs. and Microwave Lab., Stanford University, Stanford, Calif., Tech. Rep. No. 450–1; June 29, 1956.

Design of Three-Resonator Dissipative Band-Pass Filters Having Minimum Insertion Loss*

In the above paper[1] Taub and Bogner have presented a great deal of useful design information for uniformly dissipative three-resonator filters which are to be driven by a resistive generator and work into a resistive load. The desire is to maximize the ratio of the power delivered to the load to that available from the generator.

We recently have had need to design such a filter for the Butterworth response shape and took this opportunity to compare our design equations with the analytical solution developed by Dr. E. G. Fubini and given as (5) and (6) in the above paper. Unfortunately, we find the presented equations to be incorrect and, in fact, simple numerical substitution in them shows that (5d) calls for imaginary values for k_{23} for even such a low-normalized decrement as 0.1.

The correct equations, arrived at by B. Sellers of the Federal Telecommunication Laboratories, Nutley, N. J., are given below:

$$\delta_1 = \frac{U_2 - V_2}{2} + \delta_2 \tag{1a}$$

$$\delta_3 = \frac{U_2 + V_2}{2} + \delta_2 \tag{1b}$$

$$k_{12}^2 = \frac{U_0 + V_0}{U_2 + V_2} \tag{1c}$$

$$k_{23}^2 = \frac{U_0 - V_0}{U_2 - V_2} \tag{1d}$$

$$(P_1/P_a) = \frac{(U_0+V_0)(U_0-V_0)}{C_0^2} \tag{1e}$$

where

$$U_2 = (2 - 3\delta_2) \tag{2a}$$

$$U_0 = (1 - 2\delta_2 + 2\delta_2^2 - \delta_2^3) \tag{2b}$$

$$V_2 = \sqrt{2B - A} \tag{2c}$$

$$V_0 = (B + A)\sqrt{(2B - A)} \tag{2d}$$

where

$$A = 1/3(4\delta_2 - 3\delta_2^2) \tag{2e}$$

$$B = 1/3\sqrt{(6\delta_2 - 8\delta_2^2)} \tag{2f}$$

$$C_0 = 1.0.$$

These solutions were obtained by using the twelve synthesis steps detailed in a previous paper.[2] These steps are one way of expressing the Darlington procedure. When performing the steps all quantities were kept literal; *i.e.*, no numerical values were used, and the following two basic points were included:

1) It was realized that, for the specific case wherein the numeric 1.0 is used in step 6 (in order that minimum insertion loss result), the resulting cubic polynomial in $(\omega/\omega_{3db})^2$ must have a positive real *double* root. Thus when step 7 is performed, we may use

* Received by the IRE, August 26, 1957.

[1] J. J. Taub and B. F. Bogner, "Design of three-resonator dissipative band-pass filters having minimum insertion loss," Proc. IRE, vol. 45, pp. 681–687; May, 1957.

[2] M. Dishal, "Two new equations for the design of filters," *Elec. Commun.*, vol. 30, pp. 324–337; December, 1953. Addendum, vol. 32, p. 178; September, 1955.

the explicit (and quite simple) closed form expressions for the roots of a cubic which is known to have a double root. Having the roots of step 7 in closed literal form enables the following steps 8 through 12 also to be performed in a literal manner.

2) The continued fraction expansion of steps 9 and 10 produces the so-called ladder-network coefficients (a_1, a_2, and a_3) *in terms of the left-hand termination.* To obtain the left-hand end decrement and the coefficients of coupling, it is necessary to realize that the simple relationship between the above two forms of circuit constants is as follows:[3]

$$\delta_1 = \left(\frac{1}{a_1} + \delta_0\right), \quad k_{12}^2 = \frac{1}{a_1 a_2},$$

$$k_{23}^2 = \frac{1}{a_2 a_3}, \text{ etc.}$$

Similarly, the continued fraction expansion of steps 11 and 12 produces a different set of a's (a_{III}, a_{II}, a_I) *in terms of the right-hand termination.* This set then gives the right-hand end decrement and the coefficient of couplings as:

$$\delta_3 = \left(\frac{1}{a_{III}} + \delta_0\right), \quad k_{23}^2 = \frac{1}{a_{II} a_{III}},$$

$$k_{12}^2 = \frac{1}{a_I a_{II}}, \text{ etc.}$$

The simplest resulting expressions then were picked to provide the design equations (1a) through (1e) of this letter.

Incidentally, as pointed out in the Taub and Bogner paper, the important (Butterworth) design chart Fig. 4(a) was obtained by "graphical" methods and not by the analytical solutions, (5), presented by them. We do agree with the values called for in Fig. 4(a), except in the region to the left of 0.2 of the abscissa. In this region of low loss the graphical solution is rather inaccurate and the design equations presented in this letter show that even with such a low-normalized decrement as 0.05 the required network values have changed from their "lossless" values more rapidly than as given in Fig. 4(a); *e.g.*, at $(\delta_2/\delta_{2max}) = 0.05$, $\delta_1 = 0.765$, $k_{12} = 0.655$, $k_{23} = 0.780$, and $\delta_3 = 1.225$. This rapid change from the symmetrical values, called for with lossless resonators, stresses the fact that optimum filters (with respect to insertion loss) are markedly unsymmetrical—as can be seen, this is particularly true of the required end resonator decrements.

Incidentally, by comparing our solutions with those given in the Taub and Bogner paper, Sellers has found the error in the latter solutions; when corrected, they should read as follows:

$$k_{12}^2 = \delta_2^2\left[\frac{\gamma + (\beta - 2\rho)\sqrt{\alpha^2 - 4\rho}}{\alpha + \sqrt{\alpha^2 - 4\rho}}\right]$$

$$k_{23}^2 = \delta_2^2\left[\frac{\gamma - (\beta - 2\rho)\sqrt{\alpha^2 - 4\rho}}{\alpha - \sqrt{\alpha^2 - 4\rho}}\right].$$

[3] "Filters, Modern-Network-Theory Design," in "Reference Data for Radio Engineers," International Telephone and Telegraph Corp., 4th ed., pp. 187–235; 1956.

It is straightforward to obtain the closed form solutions for the end decrements and the coefficients of couplings required when uniformly lossy resonators are used and the general Tchebycheff response shape with minimum insertion loss is desired—(1) of this letter applies to this case also, but the U's and V's must be defined more generally as follows:

$$U_2 = (C_2 - 3d_0) \tag{3a}$$

$$U_1 = (C_1 - 2C_2 d_0 + 3d_0^2) \tag{3b}$$

$$U_0 = (C_0 - C_1 d_0 + C_2 d_0^2 - d_0^3 \tag{3c}$$

and again

$$V_2 = \sqrt{2B - A} \tag{3d}$$

$$V_0 = (B + A)\sqrt{2B - A} \tag{3e}$$

where now

$$A = 1/3(2U_1 - U_2^2) \tag{3f}$$

$$B = 1/3\sqrt{(2U_1 - U_2^2)^2 - 3(U_1^2 - 2U_2 U_0)} \tag{3g}$$

and

$$C_2 = \left(\frac{S_3}{C_3}\right)(2) \tag{3h}$$

$$C_1 = \left(\frac{S_3}{C_3}\right)^2\left(2 + \frac{0.75}{S_3^2}\right) \tag{3i}$$

$$C_0 = \left(\frac{S_3}{C_3}\right)^3\left(1 + \frac{0.75}{S_3^2}\right) \tag{3j}$$

where

$$S_3 = \sinh\left[1/3 \sinh^{-1}\left([V_\rho/V_v]^2 - 1\right)^{-1/2}\right] \tag{3k}$$

$$C_3 = \cosh\left[1/3 \cosh^{-1}\left([V_\rho/V_v]^2 - 1\right)^{-1/2}\right]. \tag{3l}$$

In the above equations, all decrements and coefficients of coupling are normalized to the 3-db down fractional bandwidth.

M. Dishal
B. Sellers
Federal Telecommun. Labs.
Nutley, N. J.

Authors' Comment[4]

We appreciate Dishal and Sellers pointing out an error in our paper. Upon rechecking the solution, it was found that an error was made in (5c) and (5d). The error was not in Dr. Fubini's solution. It came about in transcribing it from his notation to that used in our paper. The corrected expressions for (5c) and (5d) should read:

$$k_{12}^2 = \delta_2^2\left[\frac{-\frac{1}{2}(\alpha - \sqrt{\alpha^2 - 4\rho})(\beta - \rho) + \gamma}{\sqrt{\alpha^2 - 4\rho}}\right] \tag{5c}$$

$$k_{23}^2 = \delta_2^2\left[\frac{\frac{1}{2}(\beta - \rho)(\alpha + \sqrt{\alpha^2 - 4\rho}) - \gamma}{\sqrt{\alpha^2 - 4\rho}}\right]. \tag{5d}$$

Although not apparent, a check of these expressions and those given by Dishal and Sellers reveals that they are identical. This identity of the two solutions demonstrates that either the Darlington procedure or the direct minimization of the insertion loss, in conjunction with the three design equations, are equally valid approaches for obtaining the set of circuit constants which yield minimum midband insertion loss.

The nature of the numerical computations used in obtaining the graphical solution for the Butterworth response gave rise to errors (in the low-loss region—$\delta_2 < 0.1$) of 0.2-db maximum in the filter midband insertion loss. A recheck of the design chart, Fig. 4(a), showed agreement with the closed form solution. It therefore is recommended that the closed form solution be used in obtaining the correct deisgn parameters for $\delta_2 < 0.1$.

J. J. Taub
B. F. Bogner
Airborne Instruments Lab., Inc.
Mineola, N.Y.

[4] Received by the IRE, September 26, 1957.

Space-Frequency Equivalence*

Correlation systems comprising a pair of widely separated antennas have been suggested for the detection of signals encompassing a wide frequency band.[1-3] The purpose of this note is twofold: 1) to observe that such wide-band correlation systems will operate equally well if the source consists of a number of discrete frequencies, and 2) to discuss the correspondence which exists between the spatial complexity of the usual single-frequency antenna system and the frequency complexity of the antenna-pair multifrequency correlation system.

Directional patterns of the two-receiver cross-correlation system are easily calculated from a consideration of the power spectrum employed and the use of Wiener's theorem which states that the correlation function is the Fourier transform of the power spectrum of the original wave. A noise band extending from zero frequency has a Fourier transform represented by $\sin x/x$ and the output of a cross-correlator at the two receivers therefore will follow a $\sin x/x$ pattern as a noise source passes through the plane equidistant from the two receivers. The Fourier transform of a limited noise band (say an octave of noise) is a $\sin x/x$ function multiplied by a cosine term. Directional patterns for noise sources of other frequency extent can be similarly determined. For the discrete frequency case, the space-frequency plot shown in Fig. 1 is of interest. The conventional single-frequency space array of discrete elements is indicated as the horizontal line of circles. The directional pattern of any radiator pair is maintained if the product of frequency and spacing is kept constant; *i.e.*, if the pair is moved along the hyperbolas shown. In this way the horizontal row of radiators is converted to a radiator pair functioning at the frequencies indicated on the two vertical rows of circles. The process can, of course, be generalized to more than two elements. Because of squaring of the cosine terms which is inherent in the cor-

* Received by the IRE, October 7, 1957.

[1] M. Ryle, "A new radio interferometer audits application to the observation of weak radio stars," *Proc. Roy. Soc. A.*, vol. 211, pp. 351–375; March 6, 1952.

[2] R. Hanbury Brown, R. C. Jennison, and M. K. DasGupta, "Apparent angular sizes of discrete radio sources—observations at Jodrill Bank, Manchester," *Nature*, vol. 170, pp. 1061–1063; December 20, 1952.

[3] J. J. Faran, Jr. and R. Hills, Jr., Acoustics Res. Lab., Harvard Univ., Cambridge, Mass., Tech. Memo Nos. 27 and 28; 1952.

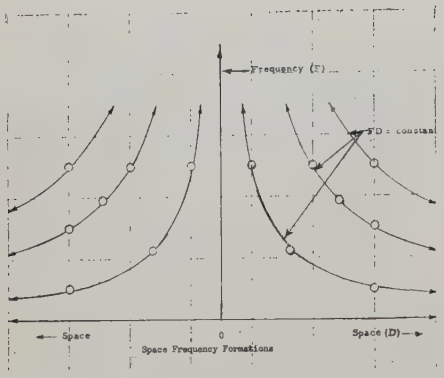

Fig. 1—The 6-element linear array operating at one frequency (top row of circles) has the same beam pattern as the correlation receiver pair detecting a source of three frequencies (two vertical rows of circles).

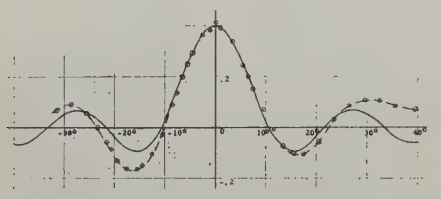

Fig. 2—Experimental test of the space-frequency equivalence indicated in Fig. 1. Dotted curve, an experimental beam pattern of the correlated outputs of two isotropic receivers spaced 21.5 inches apart against a source comprising frequencies 300, 900, and 1500 cps. Solid curve, the calculated pattern for a 6-element linear array 43 inches long against a 1500-cps source.

relation process, the pair spacing obtained by the method described must be divided by two.

Experimental verification of the concept was accomplished using sound waves. In Fig. 2 the solid curve is calculated for a 6-element array 5 wavelengths long; the dotted curve is a measured correlation pattern of a pair-array receiving three audio frequencies: 300, 900, and 1500 cps. The pair spacing was $2\frac{1}{2}$ wavelengths at 1500 cps. It is observed that the correlation array is half the length of the conventional array.

We conclude that in a detection system, the space complexity and size of an antenna could be reduced by increasing the frequency complexity of the system. Such a process requires that the antennas be effective at several frequencies; however, the saving in antenna size and extent may outweigh this difficulty in certain applications. Either continuous noise bands or multiple discrete frequencies can be used to produce narrow directional patterns having low side lobes. Extensions of the concept could include 1) tapering of the intensity of the higher frequency components to reduce side lobes, 2) manipulation of the phases of individual frequencies to create shaped beams (*e.g.*, cosecant-squared beams) from a receiver pair, 3) alternate reversing of the polarity of discrete frequencies to achieve a superdirective multifrequency detection system,[4] and 4) the use of three or four receivers located in a plane with double cross-correlation to form a pencil beam.

This note has discussed mostly receiving aspects, applications of which would include radio astronomy, microwave radiometry, passive acoustic detection, and beacon tracking of moving objects. Signal-to-noise considerations, power gain evaluation, and the use of the concept in active systems will be discussed in a later paper.

W. E. Kock
J. L. Stone
Bendix Systems Division
Ann Arbor, Mich.

[4] Comparable to the single-frequency technique discussed by R. L. Pritchard, "Optimum directivity patterns for linear point arrays," *J. Acoust. Soc. Amer.*, vol. 25, pp. 879–891; September, 1953.

Thermal Properties of Tungsten vs Copper for Electron Tube Delay Lines*

A calculational comparison has been made of the thermal load capacity of copper as against tungsten fingers in an interdigital delay line of particular, but not unrepresentative, dimensions for use in an electron tube. The finger was assumed to be a right circular cylinder of 0.050-inch diameter with a length of 10 diameters, or 0.500 inch, and was assumed to be heated uniformly along its length by electron bombardment, such as exists in tubes with a ribbon beam.

The choice of finger extremity temperatures can be made in several ways. A finger base temperature of 300°K was chosen for the problem as indicative of what can be obtained with the finger base in intimate contact with coolants at temperatures near 280°K. For the free end extremity temperature, three options are possible: 1) temperature adjusted so that the copper and tungsten delay lines have equal vapor pressures, 2) temperature adjusted so that rate of finger reduction due to evaporation is the same for the two metals, and 3) operation at the melting temperature of the metal involved. One can eliminate the third choice since the comparison ought to be made on a normal operation basis rather than on a condition tantamount to destruction of the delay line. The extremity temperatures were chosen according to option 2) based on a 1000-hour evaporation of 10 per cent of the finger mass. These values are 2680°K for tungsten and 1160°K for copper. In this case the calculated[1] vapor pressures are reasonable, $5.7 \cdot 10^{-7}$ mm Hg for copper and $1.1 \cdot 10^{-6}$ mm Hg for tungsten. Actually, options 1) and 2) give closely related extremity temperatures.

The differential equation governing the steady-state temperature distribution along the finger in the presence of radiation is,

$$Kc \frac{d^2T}{dz^2} = -[Pi - Kr(T^4 - C)] \quad (1)$$

where Kc and Kr are conduction and radiation "constants" (actually functions of temperature) and Pi is the incident power per unit length. For tungsten, the absolute value and variation of Kc have some spread in the literature, but what appeared to be the most reliable values were chosen.[2,3] Also, in the Kr for tungsten, the effective radiating area is approximately 0.80 of the actual area since there is some radiation exchange between adjacent hot fingers. For copper, radiation is ineffective at the temperature achieved.

A numerical solution of (1) then yielded a permissible power input of 73 w per finger for tungsten, while the value for copper was 61 w per finger. Without radiation the tungsten value would be about 48 w.

For fingers of other diameters and length/diameter ratios, estimates can be made of their relative thermal capabilities keeping in mind that the conduction/radiation ratio is proportional to diameter/length.[2] An additional point is that increased diameters permit increased temperatures for a 1000-hour evaporation life.

Because tungsten at the chosen finger terminal temperature is an excellent thermionic emitter, some extra heating could be expected due to finger-to-finger electronic currents caused where rf power is transmitted along the delay line. Also, the average resistance of the tungsten under the assumed conditions of the problem is about 8 times that of hot copper, causing a $\sqrt{8}$ ratio of attenuation for the two lines. For tubes working at the higher microwave frequencies, a particular case shows that due to this cause about 3 extra watts/finger must be subtracted from the permissible thermal load of tungsten as against copper for a basic finger thermal load of about 36 w. Plating of the tungsten fingers with copper or silver to increase their surface conductivity is ineffective against this latter effect because of the high temperatures attained.

Roy A. Paananen
Raytheon Manufacturing Co.
Waltham, Mass.

* Received by the IRE, September 30, 1957.

[1] L. B. Loeb, "Kinetic Theory of Gases," McGraw-Hill Book Co., Inc., New York, N. Y., 2nd ed., p. 106; 1934.

[2] Forsythe and Worthing, "The properties of tungsten and characteristics of tungsten lamps," *Astrophys. J.*, vol. 61, pp. 146–185; 1925.

[3] Langmuir and Taylor, "Heat conductivity of tungsten and cooling effect of leads upon filaments at low temperatures," *Phys. Rev.*, vol. 50, pp. 68–87; 1936.

Microwave Magnetic Field in Dielectric-Loaded Coaxial Line*

In a recent publication,[1] the authors described a probable mode configuration for a coaxial line one-half filled with a low-loss high dielectric constant material. This mode picture was based on the initial experimental results reported in that article. By additional experimental work and by subsequent theoretical considerations, it has been determined that this suggested picture should be rotated by 180° relative to the dielectric. The corrected picture is shown in Fig. 1, but this does not affect the previously re-

* Received by the IRE, April 26, 1957.

[1] B. J. Duncan, L. Swern, K. Tomiyasu, and J. Hannwacker, "Design considerations for broadband ferrite coaxial line isolators," Proc. IRE, vol. 45, pp. 483–490; April, 1957.

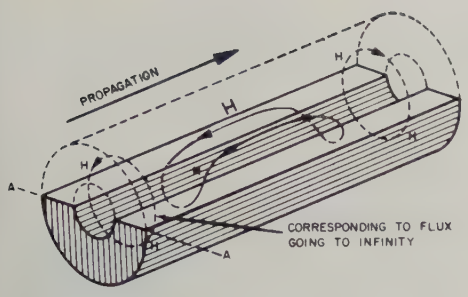

Fig. 1—Microwave H-field configuration in partially dielectric-loaded coaxial line.

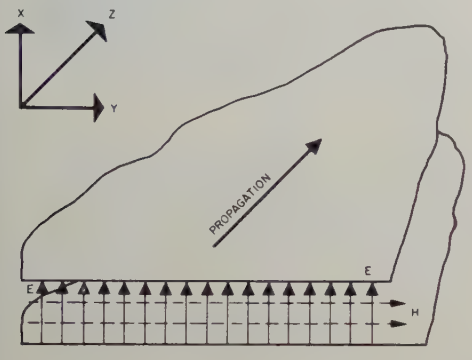

(a)

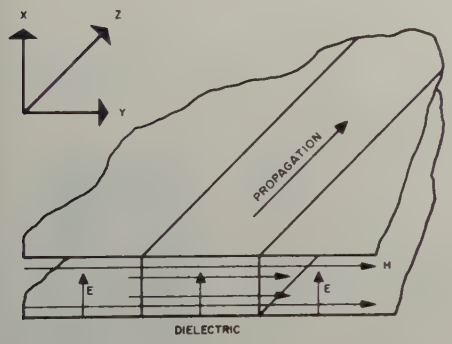

(b)

Fig. 2—(a) Microwave E and H fields in an air-filled plane parallel transmission line propagating the TEM mode. (b) Microwave E and H fields in a partially dielectric-loaded plane parallel transmission line—isometric view.

ported experimental data. That the latter picture is indeed the correct one will be demonstrated in this paper from a qualitative analysis using Maxwell's equations and by describing the additional experimental work.

An approach, to show that the strongest component of longitudinal magnetic field (Fig. 1) is in the air-filled one-half of the coax, starts with a parallel plane transmission line propagating the TEM mode [Fig. 2(a)]. As shown, only a transverse component of the microwave magnetic field H exists for the air filled transmission line. Next, consider a dielectric wedge ($\epsilon' > 1$) located in the parallel plane line as depicted in Fig. 2(b). Under these conditions it will be shown that the instantaneous microwave magnetic field is as depicted in Fig. 2(b) (cross-sectional view) and Fig. 3 (top view).

The reasoning leading to this mode picture is based on several considerations. The dielectric is transparent to the microwave magnetic field due to the permeability (μ) of the dielectric being unity. Also, in this region of the dielectric it can be assumed to a first-order approximation that the potential difference between the top and bottom plates [Fig. 2(b)] is a constant; *i.e.*,

$$\int E_x dx = \text{constant} \tag{1}$$

and is independent of y. In this equation, E_x represents the x component of the microwave electric field. This means that since the displacement vector (D) is defined by

$$D = \epsilon_0 \epsilon_m E, \tag{2}$$

where ϵ_0 is the dielectric constant of free space and ϵ_m is the dielectric constant of the medium and satisfies Maxwell's divergence equation,

$$\nabla \cdot D = \rho, \tag{3}$$

where ρ represents surface charge density, there must be more surface charge at the dielectric-conductor interface than at the air-conductor interface on either side. Because of the greater moving charge ρ_m under the dielectric, there is a greater longitudinal current here and, hence, greater transverse field (H_y) as shown in Fig. 2(b) and Fig. 3. That is

$$\frac{\partial H_y}{\partial y} \neq 0.$$

Now, since away from the dielectric the longitudinal current, and hence H_y, becomes smaller, and since $\nabla \cdot B$ or $\nabla \cdot H$ must equal zero, there must be a longitudinal component of B_z or H_z near the dielectric-air interfaces to cancel out the nonzero derivative of H_y.

It has been demonstrated previously[2] that the change in charge distribution is not abrupt at the interface and it is reasonable to expect this for the parallel-plane case as well. This would lead, at microwave frequencies, to the picture given in Fig. 4. The kink in E lines becomes essential to permit $\int E_x dx$ to remain constant, and to account for the increase in surface charge on the conductor in the region slightly removed in the transverse direction from the dielectric. This increase in surface charge and its consequent longitudinal current permits the change in H-flux lines shown in Fig. 3 to be gradual in the immediate vicinity of the dielectric. Since there is a kink in E, there is a curl of E. On the left side of the dielectric the curl is in the positive z direction and since

$$\nabla \times E = -\frac{1}{c} \dot{B}, \tag{4}$$

this means that B is increasing in the negative z direction with increasing time. This result is compatible with the mode configuration of Fig. 3. Curl E is oppositely oriented on opposite sides of the dielectric which also is consistent with the picture of Fig. 3.

A TEM mode coaxial line is, to a first approximation, a wrapped around version of the parallel-plane line of Fig. 2(a). Similarly, the structure of Fig. 2(b) and Fig. 3

[2] D. J. Angelakos, "A coaxial line filled with two nonconcentric dielectrics," IRE TRANS., vol. MTT-2, pp. 39–44; July, 1954.

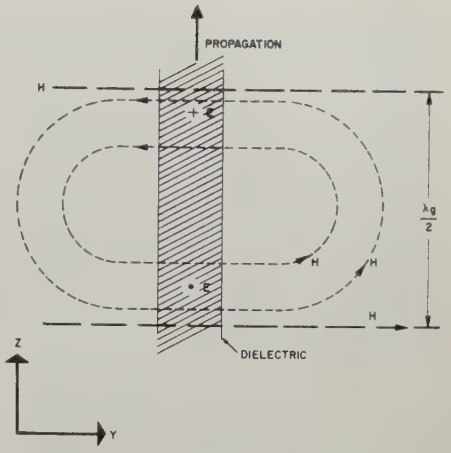

Fig. 3—Microwave E and H fields in a partially dielectric-loaded plane parallel transmission line—top view.

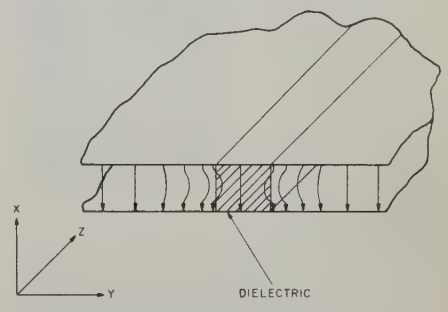

Fig. 4—Microwave E-field configuration in a partially dielectric-loaded plane parallel transmission line.

can be wrapped around to form the coax structure of Fig. 1, thus giving rise to the TE mode configuration depicted in this same figure.

A similar argument can be given to show that a TM mode can, if excited, be propagated in the dielectric loaded structure. However, if a TM mode were generated it would exhibit no appreciable H-vector circular polarization on the dielectric surfaces and, hence, would not give rise to appreciable nonreciprocity of ferrite characteristics for the field orientation and other conditions under consideration. Since a very large nonreciprocity has been experimentally observed, most of the TEM energy incident on the dielectric loaded structure must be converted into the desired TE mode with only negligible conversion to the TM mode.

An experimental verification of the correctness of the mode picture of Fig. 1 over that previously reported can be achieved quite simply by checking the sense of circular polarization which exists on the dielectric surface under a known set of conditions.[3] This is readily apparent if it is realized that for a given direction of propagation and of transversely applied dc magnetic field along the dielectric surfaces, a 180° rotation of the mode picture changes the sense of circular polarization which exists on these surfaces.

In line with these considerations, a small diameter ferrite rod was placed on one and

[3] R. Mangiaracina and B. J. Duncan, "Nonreciprocal Ferrite Devices in TEM Mode Transmission Lines," presented at the Annual PGMTT Meeting, New York, N. Y., May 9–10, 1957.

then on the remaining flat dielectric surface of Fig. 1. The direction of propagation is as shown in the figure and a dc magnetic field of sufficient strength to produce ferrite resonance is applied along the direction from A to A'. Under these conditions, no appreciable resonance attenuation is encountered with the ferrite located on either of the dielectric surfaces. However, when either the direction of applied magnetic field or propagation are reversed a large resonance absorption is encountered for location of the ferrite on either of the two surfaces. Therefore, it is apparent that these results are those which would be expected only for the mode configuration of Fig. 1.

B. J. Duncan
L. Swern
Sperry Gyroscope Co.
Great Neck, N. Y.
K. Tomiyasu
General Electric Microwave Lab.
Palo Alto, Calif.
(Formerly with Sperry Gyroscope Co.)

Carrier Mobilities at Low Injection Levels*

In a recent paper,[1] Sah, Noyce, and Shockley have derived expressions for the diffusion currents flowing across a p-n junction. They take into consideration the existence of an electric field, E, outside the transition layer, but they assume that the space charge due to the divergence of this field is negligible. The resulting mobility of minority carriers for any injection level is the ambipolar mobility, $\bar{\mu}=2\mu_n\mu_p/(\mu_n+\mu_p)$. The conclusion reached is that even at low injection levels the hole current injected in n-type material differs from the usual relation,[2] by a factor $\sqrt{\frac{1}{2}(\mu_n+\mu_p)/\mu_n}$, and implies that, under equal conditions, transit times across the bases of n-p-n and p-n-p transistors should be identical. We wish to point out here that the approximation used by Sah, Noyce, and Shockley is not justified.

Consider the steady-state equations:

$$J_p = q\mu_p pE - kT\mu_p \text{ grad } p, \quad (1)$$

$$J_n = q\mu_n nE + kT\mu_n \text{ grad } n, \quad (2)$$

$$\text{div } J_p = -\text{ div } J_n = -qU,$$

$$(J_p + J_n = J = \text{const}), \quad (3)$$

where the symbols have their usual meaning. Since space charge neutrality very nearly holds, $n\approx p+N$, and grad $n\approx$ grad p. We obtain the result of Sah, Noyce, and Shockley by adding the divergences of (1) and (2) (multiplied respectively by $-\mu_n$ and μ_p) and neglecting terms containing div E. We shall check the validity of this procedure by computing the terms appearing in div J_n in the case of low-level injection of holes in n-type material ($p\ll n\approx N$). From (1) and (2), using grad $n\approx$ grad p_n,

$$E = \frac{J - kT(\mu_n - \mu_p)\text{ grad } p}{q(\mu_p p + \mu_n n)} \approx \frac{J - kT(\mu_n - \mu_p)\text{ grad } p}{q\mu_n N}. \quad (4)$$

In the expression for div J_n, the terms $q\mu_n n$ div $E=-kT(\mu_n-\mu_p)\nabla^2 p$ and $kT\mu_n\nabla^2 p$ are comparable in magnitude, so that there is no justification in dropping the former term. This comes from the fact that the small factor div E is multiplied by the majority carrier density. We then have

$$-\mu_n \text{ div } J_p + \mu_p \text{ div } J_n = (\mu_n+\mu_p)U = kT(\mu_n+\mu_p)\mu_p\nabla^2 p, \quad (5)$$

which leads to the correct low-level approximation.

In the same way, it can be shown that the ambipolar mobility, $\bar{\mu}$, is involved at very high-injection levels only ($n\approx p\gg N$). At intermediate levels, the effective mobility is a complicated function of the carrier densities and their gradients, as shown by Rittner.[3]

The author is indebted to Dr. R. N. Noyce and Dr. C. T. Sah for helpful discussions on this subject.

J. A. Hoerni
Fairchild Semiconductor Corp.
Palo Alto, Calif.

* Received by the IRE, October 15, 1957.

[1] C. T. Sah, R. N. Noyce and W. Shockley, "Carrier generation and recombination in p-n junctions and p-n junction characteristics," Proc. IRE, vol. 45, pp. 1228–1243; September, 1957.

[2] W. Shockley, "Electrons and Holes in Semiconductors," D. Van Nostrand Co., Inc., New York, N. Y., sec. 12.5; 1950.

[3] E. S. Rittner, "Extension of the theory of the junction transistor," *Phys. Rev.*, vol. 94, pp. 1161–1171; June 1, 1954.

Hyperbolic Analogs*

To the extent to which the voltage (V), current (I), and reverse saturation current (I_s) of a semiconductor diode are related by the expression $I=I_s[\exp(qV/kT)-1]$, it is possible to construct circuits which provide hyperbolic relations between electrical quantities therein.

For example, if two identical semiconductor diodes are connected in series and poled to conduct in opposite directions, it is easily shown that the terminal voltage and current are related by $I=I_s\tanh(qV/2kT)$.

Two such diodes connected in parallel and oppositely poled will provide a dependence between terminal voltage and current given by $I=2I_s\sinh(qV/kT)$.

There are variations or extensions of these circuits which can be used to provide hyperbolic analog devices. For example, the diode pairs might be used as input or feedback elements in a standard operational amplifier (Fig. 1).

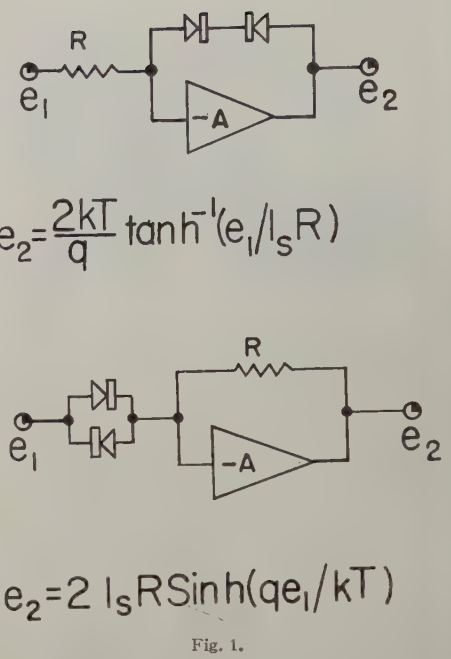

Fig. 1.

In another incorporation of these principles transistors provide both the necessary exponential characteristic and gain. A transfer characteristic measured for such a circuit is shown in Fig. 2, along with a fitted curve,

$$y=2.9\tanh^{-1}x.$$

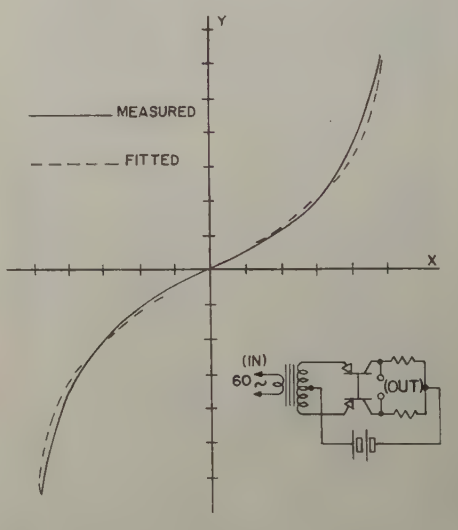

Fig. 2.

It is also possible, although somewhat more complicated, to obtain hyperbolic cosine analogs.

Melbourne J. Hellstrom
Westinghouse Electric Corp.
Metuchen, N. J.

* Received by the IRE, September 24, 1957.

Contributors

J. Robert Anderson (S'53–M'57) was born in New York, N. Y. on December 31, 1932. He received the B.S. degree in engineering physics from New York University in 1954. From 1954 to 1957, he was a member of the technical staff at the Electron Tube Laboratory of Hughes Aircraft Company. During part of this time, he received graduate training in physics at U.C.L.A. under a Howard Hughes Cooperative Fellowship.

J. R. Anderson

Mr. Anderson presently is continuing his graduate training in electrical engineering, while holding an appointment as a research engineer in the Electron Tube Laboratory at the University of California, Berkeley, Calif.

He is a member of Tau Beta Pi, Sigma Pi Sigma, and AAAS.

❖

Elie J. Baghdady (A'52–M'57) was born in Zahleh, Lebanon, on November 10, 1930. Between 1949 and 1951, he was a British Council Scholar and recipient of the university first prize scholarship at the American University of Beirut. He received the B.A. degree with high distinction in physics in 1951.

E. J. Baghdady

In the summer of 1951, he came to the United States on a Georgia Institute of Technology World Student Fund Fellowship and enrolled in the Institute's graduate division of electrical engineering. In June, 1952, he joined the electrical engineering staff of the Massachusetts Institute of Technology as a graduate student and research assistant in the Research Laboratory of Electronics. He became an instructor in electrical engineering in 1955 and assistant professor in 1956. He received the M.S. and D.Sc. degrees in electrical engineering from M.I.T. in 1954 and 1956, respectively.

Dr. Baghdady's research has been mainly concerned with frequency-modulation studies, including problems of improving reception in the presence of high-level noise and interference and the analysis of network response to fm waves. Since 1954, he has taught advanced courses in radio engineering and modulation theory, mathematical methods in electrical engineering, network analysis and synthesis, electronic circuits, and transient analysis of linear electromechanical systems. Presently, he is in charge of a graduate course on modulation theory and a research project on fm.

George R. Brewer (A'43–M'49–SM'54) was born in New Albany, Ind., on September 10, 1922. He received the B.E.E. degree from the University of Louisville in 1943, and the Ph.D. degree in electrical engineering from the University of Michigan in 1952.

G. R. Brewer

Dr. Brewer has been principally engaged in research and development of electron tubes from 1943 to 1944, at the Radiation Laboratory, Massachusetts Institute of Technology; from 1944 to 1947, at the Naval Research Laboratory; and from 1947 to 1951, at the Engineering Research Institute of the University of Michigan. He now is a member of the Electron Tube Laboratory of Hughes Research Laboratories.

He is a member of the American Physical Society, Sigma Xi, and Phi Kappa Phi.

❖

T. J. Bridges (M'57) was born at Gillingham, Kent, Eng., in December, 1923. He attended London University, London, Eng., where he received the Bachelor of Science degree in engineering in 1944.

T. J. Bridges

He joined the Admiralty in 1945 and is a member of the Royal Naval Scientific Service at the Services Electronics Research Laboratory, Baldock, Eng. Since November, 1956, he has been on leave of absence from the Admiralty and is engaged in microwave tube research at Bell Telephone Laboratories, Murray Hill, N. J.

❖

R. C. Burgener (A'54) was born October 10, 1921 in Galion, Ohio. He received the B.S.E.E. degree from Case Institute of Technology in 1950. After graduation he was engaged in relay development at the North Electric Mfg. Co., Galion, Ohio until September, 1951. At that time he joined the Department of Electrical Engineering of The University of Tennessee as research engineer, where he was primarily concerned with development in the field of radar. He received the M.S.E.E. degree from The University of Tennessee in June, 1956. He is presently employed at Battelle Memorial Institute as a research engineer and he also is attending Ohio State University as a candidate for the Ph.D. degree.

R. C. Burgener

He has a professional engineering license in Tennessee.

❖

Harold J. Curnow was born at Birmingham, Eng., in November, 1930. He was educated at Solihull School, Warwickshire, Eng. He also attended Birmingham University, Birmingham, Eng. He received the degree of Bachelor of Science with honors in mathematical physics from Birmingham University in 1951.

H. J. Curnow

Since then, he has been a member of the Royal Naval Scientific Service, and at the present time is employed at the Services Electronics Research Laboratory, Baldock, Hertfordshire, Eng.

❖

E. T. Jaynes (SM'54) was born in Waterloo, Iowa, on July 5, 1922. He attended Cornell College and Iowa State University, receiving the B.A. degree in physics from the latter in 1942. He studied in the graduate school of the University of California in Berkeley and at Princeton University from which he received the M.A. degree in 1948 and the Ph.D. degree in theoretical physics in 1950.

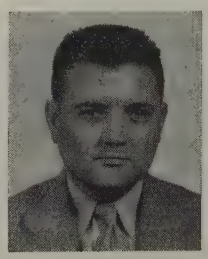

E. T. Jaynes

From 1942 to 1946, he was engaged in microwave research and development as a project engineer at the Sperry Gyroscope Co., Garden City, N. Y., and in the combined research group of the Naval Research Laboratory.

Since 1950, he has been on the faculty of Stanford University and at present holds the titles of associate professor in the microwave laboratory and lecturer in physics.

❖

Sherwood King (S'40–A'41–SM'53) was born in Schenectady, N. Y. on August 5, 1917. He received the B.S. degree in engineering sciences from Harvard University in 1938 and the M.S.E.E. degree from Lafayette College in 1940. From 1940 until

1947, he was a member of the technical staff of Bell Telephone Laboratories, engaged in the development of sonar and radar test equipment and of mobile radio telephone systems. In 1947, he joined the staff of the Department of Electrical Engineering of the University of Tennessee as assistant professor. He became associate professor of electrical engineering in 1955. At Tennessee he was in charge of the electronics laboratories and supervisor of a research group engaged in radar development. In 1956 Mr. King became a member of the technical staff in the Ground Systems Division, Hughes Aircraft Company, and at present is head of the Studies and Analysis Section of that Division's Radar Laboratory.

S. KING

Mr. King is a member of Sigma Xi and Eta Kappa Nu.

❖

David I. Kosowsky (S'50–A'53–M'57) was born in New York, N. Y., in 1930. He received the B.E.E. degree from the College of the City of New York in 1951 and the S.M. and Sc.D. degrees from Massachusetts Institute of Technology in 1952 and 1955. He was a staff member of the Research Laboratory of Electronics (M.I.T.) from 1951 to 1955 and was engaged in research on missile systems, applications of statistical communication theory, and filter theory. He was responsible for the development of techniques for the synthesis and realization of crystal filters.

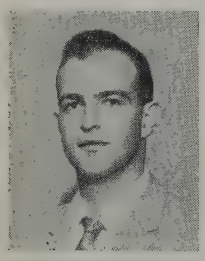

D. I. KOSOWSKY

He is presently employed by Hycon Eastern, Inc., as Director of the Crystal Filter Division. He is a member of Eta Kappa Nu, Tau Beta Pi, and Sigma Xi.

❖

Harold Levenstein (A'46–M'55) was born on June 28, 1923, in Philadelphia, Pa. He received the B.E.E. degree from Cooper Union, New York, N. Y., in 1943, and the M.E.E. degree from the Polytechnic Institute of Brooklyn in 1949. In addition to course work for the doctorate, he has been a special student in fire control systems and communications theory at Massachusetts Institute of Technology in 1949, 1953, and 1955.

H. LEVENSTEIN

Mr. Levenstein joined Western Electric in 1943 as a test planning engineer on radar systems. In 1946, he was a member of the Sight Laboratory, Fairchild Camera and Instrument Co., working in fire control systems. From 1947 to 1950, he was employed by Fairchild Guided Missiles Division as an electronics engineer on telemetering and guidance systems for the Lark Missile. In 1950, he joined the W. L. Maxson Corp. as a senior engineer, responsible for fire control and bombing and navigation systems. He has been manager of the analysis group and the systems engineering department. In 1955, he took a leave of absence to work as a member of the M.I.T. Instrumentation Laboratory on inertial navigation systems. Since June, 1956, he has been research assistant to the Vice-President of the R&D Division of the W. L. Maxson Corp., acting as consultant in systems and control engineering and is responsible for preliminary system planning.

Mr. Levenstein is a member of Tau Beta Pi, Sigma Xi, the American Physical Society, and the American Mathematical Society.

❖

O. Thomas Purl (S'50–A'54) was born on June 5, 1924 in East St. Louis, Ill. He received the B.S. degree in general engineering from the University of Illinois in 1948. Prior to that, he was a meteorologist with the Air Force from 1943 to 1946. He was engaged in microwave tube work at the Collins Radio Co. from 1948 to 1949. In 1949, he returned to the University of Illinois, where he received the B.S.E.E., M.S.E.E., and Ph.D. degrees in 1951, 1952, and 1955, respectively. During part of this time, he was a research associate in the Electrical Engineering Research Laboratory.

O. T. PURL

Since 1955, he has been a member of the technical staff at the Hughes Electron Tube Laboratory, where he has been engaged in research and development on microwave tubes.

Dr. Purl is a member of Sigma Xi, Eta Kappa Nu, Phi Kappa Phi, and Sigma Tau.

❖

J. F. Ramsay (A'56) was born at Milngavie, Dunbartonshire, Scotland, in 1908. He received the M.A. degree in mathematics and physics from the University of Glasgow in 1934. From 1933 to 1935, he was employed by the Cosmos Lamp Works, Enfield, Eng., as assistant engineer engaged on circuit applications of receiving tubes. In 1935, he was employed by the General Electric Co., Ltd., Coventry, Eng., as radio circuit engineer on broadcast receiver problems.

J. F. RAMSAY

In 1936, Mr. Ramsay joined the research staff of Marconi's Wireless Telegraph Co., Ltd., Chelmsford, Eng., as assistant engineer on broadcast receiver investigational work. From 1938 to 1940, he was attached to the Air Division on transmitter drive development. In 1941, he returned to research in the development of superregenerative radar: seconded to the Admiralty in the same year, Mr. Ramsay took part in war-time microwave antenna research both with Marconi's Wireless Telegraph Co., Ltd., and at Admiralty establishments. Among the antenna types with which he was associated were metal-plate lens, mirror-connected horn, squintless linear array, polyrod, channel-guide antenna, and circularly polarizing mirrors. Returning to Marconi's in 1946, he published papers on Fourier transform theory for antennas based on G. A. Campbell's memoir for circuit theory. In further antenna work, he was associated with antennas for marine radar, VOR, tv broadcasting, fm broadcasting, microwave relay, and millimetric techniques. The problems encountered in the millimeter field led to the discovery of the old microwave techniques of the 1890's. Since 1956, Mr. Ramsay has been employed by Canadian Marconi Company, Montreal, Canada.

He is a member of the IEE, London.

❖

F. V. Schultz (A'32–SM'45) was born on November 7, 1910 in Petersburg, Mich. He received the B.S.E.E. degree in 1932, the M.S.E.E. degree in 1939, and the Ph.D. degree in 1950, all from the University of Michigan. After five years in industry, primarily as a receiver development engineer, he joined the Department of Electrical Engineering of Michigan State University East Lansing. Mich., where he remained from 1937 until 1941.

F. V. SCHULTZ

During World War II, Dr. Schultz was a group leader in the Radar Laboratory of the Wright Air Development Center, where he was concerned with the development of antennas and radar beacons. From 1946 to 1950, he was research engineer in the Engineering Research Institute of the University of Michigan. During this time, Dr. Schultz was engaged in research studies on missile guidance systems and on electromagnetic wave scattering problems. From 1950 until 1956, he was professor of electrical engineering at the University of Tennessee, in charge of instruction and research in electronics. Since 1956, he has been professor of electrical engineering at Purdue University, Lafayette, Ind.

He is a member of Sigma Xi, Tau Beta Pi, Phi Kappa Phi, Eta Kappa Nu, the American Physical Society, and the American Society for Engineering Education.

IRE News and Radio Notes

Early Reservations Urged for IRE National Convention

Plans are all but completed for the forty-sixth annual national convention of the IRE, scheduled for the Waldorf-Astoria Hotel and the New York Coliseum, March 24–27. Fifty-five technical sessions are being set up by the Technical Program Committee with the aid of all IRE Professional Groups. Thirty-three sessions will be held at the Waldorf; the remainder, at the Coliseum. The program will feature two special symposia on the evening of March 25 in which the nation's leading experts will discuss "Electronics in Space" and "Electronics in Industry." Full program details will be published in the March issue of the PROCEEDINGS OF THE IRE.

The popular social events will open with a "get-together" cocktail party on the afternoon of March 24. The annual banquet, to be held in the Grand Ballroom of the Waldorf during the evening of March 26, will feature Robert C. Sprague, Chairman of the Board of Sprague Electric Co. and of the Federal Reserve Bank of Boston, who will speak on "The Federal Reserve and the Electronics Industry."

Since a convention attendance of 55,000 is anticipated, all members are urged to place their reservations for cocktail party tickets at $4.30 each, and banquet tickets at $15.00 with IRE Headquarters quickly.

The annual Single Sideband Dinner will be held March 25 at the Hotel New Yorker. Tickets can be obtained for $7.50 each at Single Sideband Amateur Radio Assn., 261 Madison Ave., N. Y. 16, N. Y.

I. J. Kaar is Recipient of IRE-EIA Fall Meeting Plaque

I. J. Kaar (J'22–M'29–F'41), Vice-President of Hoffman Electronics, received the Radio Fall Meeting Plaque at the 29th meeting in Toronto, Canada. He received the award for "his many contributions to the broadcast and television receiver industry."

I. J. KAAR

Mr. Kaar was former head of the General Electric Color System Technical Project. For the previous thirty years he had been closely associated with the organization of the General Electric radio and television engineering developments.

He also served as panel chairman on receiver-transmitter coordination for the first National Television System Committee and vice-chairman of the panel on coordination for the second NTSC.

Alois W. Graf
1901–1957

The following resolution was adopted by the IRE Board of Directors at a meeting on November 20, 1957.

Resolution

With profound sorrow the Directors of The Institute of Radio Engineers record the death of one of their friends and associates—Alois W. Graf. Mr. Graf was an IRE member for over thirty years, having joined as an Associate in 1926, advancing to Member grade in 1944, Senior Member in 1945, and Fellow in 1955. He served as a Director in 1952, 1953, and 1957.

Perhaps his most important contributions to IRE nationally were the time and effort taken from his personal law practice to devote to legal matters for IRE. A great deal of his time was spent on trade-mark applications to safeguard the IRE name, symbol, and publication titles.

Having served as the Chairman of the Constitution and Laws Committee since 1954, he believed that the Constitution and Bylaws were in need of modernization, and he undertook the tremendous task of drafting a proposal for a new Constitution and Bylaws.

Mr. Graf was very active in Professional Group administration, serving as Central Division Vice-Chairman since 1954.

He contributed vastly to the welfare of IRE on the Section level, serving as Chairman of the Chicago Section in 1946–47, and continuing thereafter, as an elder statesman, to guide the destinies of a large and flourishing Section.

The Board of Directors of The Institute of Radio Engineers desires to spread upon its records its keen sense of personal loss in Mr. Graf's death and its deep sympathy for the members of his family.

Calendar of Coming Events and Authors' Deadlines*

1958

Cleveland Elec. Conf. Masonic Audit., Cleveland, Ohio, Feb. 14–15

Transistor-Solid State Circuits Conf., Phil., Pa., Feb. 20–21

Nuclear Eng. and Science Congress, Palmer House, Chicago, Ill., Mar. 16–21

IRE Nat'l Convention, N. Y. Coliseum and Waldorf-Astoria Hotel, New York City, Mar. 24–27 (DL*: Nov. 1, G. L. Haller, IRE Headquarters, New York City)

Single Sideband Dinner, Hotel New Yorker, New York City, Mar. 25

Instruments & Regulators Conf., Univ. of Del., Newark, Del., March 31–Apr. 2

Conf. on Automatic Optimization, Univ. of Del., Apr. 2–4

Symp. on Electronic Waveguides, Eng. Soc. Bldg., New York City, Apr. 8–10

SW Regional Conf. & Show, Mun. Audit, San Antonio, Tex., Apr. 10–12

Conf. on Automatic Techniques, Statler Hotel, Detroit, Mich., Apr. 14–16

Spring Tech. Conf. on TV and Transistors, Eng. Soc. Bldg., Cincinnati, Ohio, Apr. 18–19

Elec. Components Symp., Ambassador Hotel, Los Angeles, Calif., Apr. 22–24 (DL*: Nov. 15, E. E. Brewer, Convair, Pomona, Calif.)

URSI Spring Mtg., Willard Hotel, Wash., D. C., Apr. 24–26

Semiconductor Symposium of Electrochemical Society, Statler Hotel, New York City, Apr. 27–May 1

Seventh Region Conf. & Show, Sacramento, Calif., Apr. 30–May 2

PGMTT Symp., Stanford Univ., Stanford, Calif., May 5–7 (DL*: Jan. 15, K. Tomiyasu, G. E. Microwave Lab., 601 California Ave., Palo Alto, Calif.)

Western Joint Computer Conf., Ambassador Hotel, Los Angeles, Calif., May 6–8 (DL*: Jan. 15, Tech. Program, Chairman, P. O. Box 213, Claremont, Calif.)

Nat'l Aero. & Nav. Elec. Conf., Dayton, Ohio, May 12–14

IEE Convention on Microwave Values Savoy Place, London, England, May, 10–23

PGME Mtg., Wash., D. C., May

*DL = Deadline for submitting abstracts.

(Continued on page 506)

Calendar of Coming Events and Authors' Deadlines*

(Continued)

PGPT Symp., Hotel New Yorker, New York City, June 5–6

PGMIL Convention, Sheraton-Park Hotel, Wash., D. C., June 16–18

Spec. Tech. Conf. on Nonlinear Mag. and Mag. Amplifiers, Los Angeles, Calif., Aug. 6–8

Elec. Radio & Standards Conf., Univ. of Colo. and NBS, Boulder, Colo., Aug. 13–15

WESCON, Ambassador Hotel and Pan-Pacific Audit., Los Angeles, Calif., Aug. 19–22 (DL*: May 1)

Nat'l Symp. on Telemetering Americana Hotel, Miami Beach, Fla., Sept. 22–24

Indus. Elec. Conf., Detroit, Mich., Sept. 24–25

Nat'l Electronics Conf., Hotel Sherman, Chicago, Ill., Oct. 13–15

IRE Canadian Convention, Toronto, Can., Oct. 15–17

PGCS Symp. on Aero. Communications, Hotel Utica, Utica, N. Y., Oct. 20–22

Nat'l Simulation Conf., Dallas, Tex., Oct. 23–25

EIA-IRE Radio Fall Meeting, Sheraton Hotel, Rochester, N. Y., Oct. 27–29

East Coast Aero. & Nav. Elec. Conf., Lord Baltimore Hotel and 7th Regiment Armory, Baltimore, Md., Oct. 27–29

PGED Meeting, Shoreham Hotel, Washington, D. C., Oct. 30–Nov. 1

Atlanta Section Conf., Atlanta-Biltmore Hotel, Atlanta, Ga., Nov. 17–19

Elect. Computer Exhibition, Olympia, London, Eng., Nov. 29–Dec. 4

Eastern Joint Computer Conf., Bellevue-Stratford Hotel, Philadelphia, Pa., Dec. 3–5

Nat'l Symp. on Global Comm., St. Petersburg, Fla., Dec. 3–5

PGVC Annual Mfg., Hotel Sherman, Chicago, Ill., Dec. 4–5

Mid-America Elec. Convention, Mun. Audit., Kan. City, Mo., Dec. 9–11 (DL*: Aug. 1, Wilbert O'Neal, Vendo Co., 7400 E. 12, Kan. City, Mo.)

1959

IRE Nat'l Convention, New York City, Mar. 23–26

SW Regional Conf., Dallas, Tex., Apr. 16–18

Nat'l Aero & Nav. Elec. Conf., Dayton, Ohio, May 11–13

WESCON, San Francisco, Calif., Aug. 18–21

Nat'l Electronics Conf., Chicago, Ill., Oct. 12–14

East Coast Aero. & Nav. Conf., Baltimore, Md., Oct. 26–28

PGED Meeting, Shoreham Hotel, Washington, D. C., Oct. 29–31

Radio Fall Meeting, Syracuse, N. Y., Nov. 9–11

Eastern Joint Computer Conf., Hotel Statler, Boston, Mass., Nov. 30–Dec. 3

* DL = Deadline for submitting abstracts.

L. S. McDowell Is the First Woman to Become Life Member

On January 1, 1958, Louise S. McDowell (M'23–SM'43) was the first woman to become a Life Member of the IRE. The IRE bylaws provide that the Board of Directors shall waive the dues of each and every member of the IRE who has attained the age of 65 years and been a member for 35 years. These members are then designated "Life Members," and at the present time there are 131 IRE Life Members.

L. S. McDowell

Dr. McDowell is professor emeritus of physics at Wellesley College. She has been associated with Wellesley since 1909, and from 1913 until retirement in 1945 head of the physics department. Beginning in 1917, she also taught a semester course in electromagnetic waves and radio communication which offered to undergraduates experimental lectures and laboratory work as well. During 1918 and 1919 on leave from Wellesley, Dr. McDowell did physical research on crystal detectors and vacuum tube oscillators in the Radio Section of the National Bureau of Standards. In 1921, she did further research at Cruft Laboratory of Harvard University.

Dr. McDowell obtained the Ph.D. degree from Cornell University in 1909 where she had received her master's degree in 1907; her bachelor's degree from Wellesley was awarded in 1898. She is a fellow of the American Physical Society, and has had several papers published in the *Physical Review* of the American Physical Society. In 1947 she retired from active life after serving as assistant editor of *Very High Frequency Techniques*.

MAECON Proves Successful

The IRE Mid-America Electronics Convention was held at the Municipal Auditorium in Kansas City, Mo., November 13–14, 1957, with headquarters at the Hotel Muehlebach. It was the ninth annual convention sponsored by the IRE Kansas City Section.

The convention drew approximately 1500 engineers and scientific-minded personnel, from more than 13 states.

There were 77 exhibit booths with displays of some of the latest electronic instruments, products and associated equipment. The featured exhibit was a complete technical model of America's earth satellite which was displayed by the Naval Research Laboratories.

There were ten technical sessions covered by 28 technical paper presentations. J. T. Henderson, IRE National President, gave the opening address, and also spoke on "The IRE Today" at the annual banquet. Dr. Simon Ramo, executive vice-president of the Ramo-Wooldridge Corp., was the guest banquet speaker and spoke on "The Increasing Role of Electronics in Missile Systems." The banquet was attended by nearly 300 persons.

Temporary Memberships for Research Now Available

For the second year, the Institute of Mathematical Sciences at New York University offers temporary memberships to mathematicians and other scientists holding the Ph.D. degree who intend to study and do research in the fields in which the Institute is active. These fields include functional analysis, ordinary and partial differential equations, mathematical physics, fluid dynamics, electromagnetic theory, numerical analysis and digital computing, and various specialized branches, such as linear programming, hydromagnetics, and reactor theory. Membership will be awarded for one year, but it may be renewed. Special arrangements can be made for applicants who expect to be on leave of absence from their institutions.

Temporary members may participate freely in the research projects, the advanced graduate courses and the research seminars of the Institute, and they will have the opportunity of using the computational facilities which include an IBM 704 computer and a Univac. They will receive a stipend commensurate with their status.

Requests for information and for application blanks should be addressed to the Membership Committee, Institute of Mathematical Sciences, 25 Waverly Place, New York 3, N. Y.

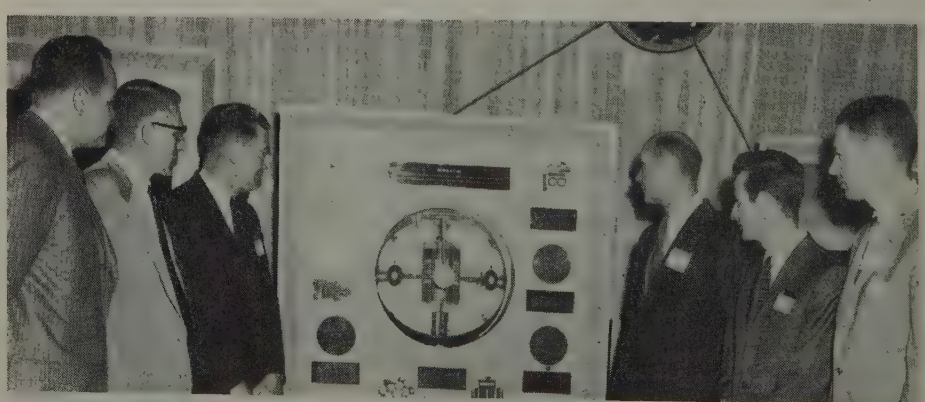

Shown at MAECON looking at a model of an earth satellite are (*left to right*): K. V. Newton, IRE Region Six Director; R. M. Somers, Bendix Aviation Corp.; L. H. Montgomery, Vanderbilt Univ.; J. T. Henderson, IRE President; P. C. Constant, Jr., IRE Kansas City Section chairman; and W. H. Ashley, Jr., convention chairman.

Ted Rynda of the IRE Dayton Section addresses a meeting of local science teachers. The Section's program for the past two years has provided its community with speakers for science clubs and secondary school teachers, and judges for the local science fairs.

MARS Names Radio Speakers

The Air Force MARS Eastern Technical Net, which broadcasts over the air every Sunday afternoon at 2 p.m. (EST) on 3295, 7540 and 7635 kc, announces the following program: February 23—"Telemetry," by R. Popkin-Clurman; March 2, 9 and 16—"Airways Electronics Symposium," by spokesmen for major domestic and international airlines with W. T. Carnes as moderator.

Obituaries

E. E. Freeman (A'23–M'26–SM'43) chief engineer for Freeman Radio Engineering Service, New York City, died recently.

After receiving a certificate in electrical engineering from the International Correspondence School in 1907, he worked as a radio operator on vessels and on shore in a high power radio station. From 1915 to 1917 he piloted his own business in the design and manufacture of radio transmission and receiving apparatus. In 1917 he was commissioned radio engineering officer in the U. S. Navy. He designed, constructed and taught at several naval radio schools. Eventually he became officer in charge and chief instructor of the U. S. Naval Radiophone School at New London, Conn. Returning to civilian life in 1922, Capt. Freeman became, first, radio officer on large vessels, and then assistant engineer for radio stations WJY and WJZ for RCA. In 1923, he became chief engineer of Freeman Radio Engineering Service and manufactured equipment under the "Resonator" trademark.

John J. Gilbert (A'16–SM'50)(L) died recently. A graduate of the University of Pennsylvania and a graduate student at Harvard and the University of Chicago, Mr. Gilbert's first employment was as an instructor at Illinois Institute of Technology. After serving in the First World War, he was employed by the Western Electric Co. and Bell Telephone Labs. He specialized in the development, manufacture and testing of permalloy loaded telegraph cable, submarine telephone cable, equipment for carrier frequency transmission underground and on submarines, and the laying of communication wires from airplanes. During the Second World War, he did confidential work for the armed services on submarine cable matters.

Professional Group News

The First National Symposium on **Engineering Writing and Speech** held on October 21–22, 1957, a two-day program attended by about 300 engineers, technical writers, and editors, featured speakers from industry, universities, and government.

The keynote address, prepared by J. R. Pierce of Bell Telephone Labs. and delivered in his absence by his associate, Dr. Harold S. Black, was entitled "The Challenging Field of Engineering Writing and Speech."

One of the most stimulating events of the symposium was a talk entitled "Formula for Platform Poise" by Rudy Norko, Administrator of Training for Radio Corp. of America.

Other features of the meeting included a description of editing techniques which the engineer-writer can use by Joseph Chapline of Philco Corp., a demonstration of the "flannel-board technique" of illustration by Charles Tiene of Sperry Gyroscope Co., some practical advice on how to write for the Air Force by Brig. Gen. H. A. Boushey, and a talk and exhibit on technical motion-picture films by Ronald Murray of Hughes Aircraft Co.

The Professional Group on Engineering Writing and Speech is one of the newest of the IRE Groups, having been established May, 1957. It currently has more than 300 members representing 27 states and 6 foreign countries. Chapters of the Group are being formed in Los Angeles, New York City, Long Island, and Washington, D. C. The Group is presently making plans for participation in the 1958 IRE National Convention, WESCON, and other national meetings. All IRE members wishing to present papers in the field of this Group are invited to submit abstracts to the Group Chairman, D. J. McNamara, Sperry Gyroscope. Co., Mail Station 1C30, Great Neck, L. I., N. Y.

The IRE Professional Group on **Military Electronics** will sponsor a second national convention, which will be held at the Sheraton-Park Hotel, Washington, D.C., June 16–18, 1958. The theme of the convention will be "Missiles and Electronics—1958: Ad Astra Per Aspera."

Gen. W. B. Larew, staff assistant to the vice-president for research and engineering of Melpar, has been chosen to preside over the convention. L. O. Whitelock of the Navy Department will supervise exhibit arrangements; R. Cranshaw of General Electric Co. will handle local arrangements; B. J. Goldfarb of Westinghouse will be responsible for the publication of papers in the TRANSACTIONS; and George Rappaport of Emerson Radio & Phonograph Co. is director of public relations.

The Third National Symposium on Aeronautical Communications, held at Utica, N. Y. recently, featured twenty technical papers, 44 exhibits, a Junior Science exhibit, an one-day classified symposium, women's activities, and a meeting of the PGCS administrative committee. *Above left*—Dignitaries at the symposium chat. Left to right, they are: J. H. Vogelman, guest speakers chairman; G. R. Wilson, editor-publisher of *Flying* magazine who was the banquet speaker; Brig. Gen. E. E. Mitchell, symposium chairman; and D. Tallman, guest speaker. *Above right*—Symposium committee chairmen listen to J. D. McLean, president of Hoffman Labs., luncheon speaker. Left to right, they are: Fred Priest, Arrangements; Charles Strom, Classified Sessions; Ray Homan, Secretary; R. C. Benoit, Jr., Public Relations; Robert Zachary, Technical Papers; H. J. Crowley, Vice-Chairman; and J. D. McLean. The next symposium will be at Utica, N. Y., October 20–22, 1958.

1958 Transistor & Solid State Circuits Conference

UNIVERSITY OF PENNSYLVANIA AND SHERATON HOTEL, PHILADELPHIA, PA.

FEBRUARY 20–21, 1958

FEBRUARY 20

9:30 a.m.–Noon

Irvine Auditorium

COMPUTER CIRCUITS

Chairman: T. R. Finch, Bell Tel. Labs.

The Advantages of Linear Selection in Transistor-Core Memories, R. E. McMahon, Lincoln Lab., M.I.T.

Transistor Resistor Logic Circuit Analysis, Q. W. Simkins, Bell Tel. Labs.

Ten Megapulse Transistorized Pulse Circuits for Computer Application, W. N. Carroll and R. A. Cooper, IBM.

High-Speed, Graded-Base Transistor, Digital Circuit Techniques, R. H. Baker, Lincoln Lab., M.I.T.

Higher-Speed Computer Circuits, A. K. Rapp and M. M. Fortini, Philco Corp.

University Museum

SURVEY

Chairman: J. A. Rajchman, RCA.

Noise in Semiconductors, W. H. Fonger, RCA.

Review of Some Novel State Devices and Their Applications, W. H. Katz, General Electric Co.

2:45–5:15 p.m.

Irvine Auditorium

SWITCHING

Chairman: P. M. Thompson, Defense Research Board, Ottawa, Canada.

New Configurations in Nonsaturating Complementary-Current Switching Circuits, C. M. Campbell, Jr., Burroughs Corp

The Application of Transistors Operated in the Avalanche Mode to the Generation of Millimicrosecond Pulses, G. B. B. Chaplin, United Kingdom Atomic Energy Authority, England.

The Use of Junction Transistors as a Three-Terminal Temporary Memory for Digital Circuits, G. H. Perry, Royal Radar Research Establishment, England.

Transistor Bilateral Switches, W. M. Cook and P. I. Bargellini, RCA.

A Two-Transistor Gate for Time-Division Switching, J. D. Johannesen and P. B. Myers, Bell Tel. Labs.

3:15–5:15 p.m.

University Museum

NEW TECHNIQUES

Chairman: H. E. Tompkins, Univ. of Pennsylvania.

Low-Level, High-Speed Voltage Comparator, J. W. Higginbotham and H. H. Douglass, Martin Co.

A High-Speed Analog Multiplier with a Linearity Better than +0.3 Per Cent, R. J. Bibby and P. M. Thompson, Defense Research Board, Ottawa, Canada.

A Semiconductor Voltage Regulator for Rotating Generators, J. L. Jensen, Minneapolis-Honeywell Regulator Co.

A Transistorized Overload-Proof Electronic Regulator—TOPER, P. A. Dodge, General Electric Co.

FEBRUARY 21

9:00 a.m.–Noon

Irvine Auditorium

LINEAR APPLICATION

Chairman: J. G. Linvill, Stanford Univ.

Methods of Cascading Unneutralized Tuned Transistor Amplifiers, R. M. Frazier, Jr., Westinghouse Electric.

Transistor 70-MC IF Amplifier, V. R. Saari, Bell Tel. Labs.

Optimum Noise Performance of Transistor Input Circuits, R. D. Middlebrook, Calif. Inst. of Technology.

Paper to be announced by J. T. Paupin and/or H. T. Mooers, Minneapolis-Honeywell Regulator Co.

Dielectric Modulators Using Space-Charge Capacitance of Junction Diodes, Carl Hurtig, M.I.T.

University Museum

SURVEY ON SWITCHING and POWER CONTROL

Chairman: J. J. Suran, General Electric Co.

Switching, Gary Clark, Burroughs Corp.

Power Control with Semiconductors, Louis Bright, Westinghouse.

2:00–4:30 p.m.

Irvine Auditorium

NEW DEVICES

Chairman: George Royer, IBM.

Operation of a Low-Temperature Memory Element, C. J. Kraus, IBM.

The Application of the Dynister Diode to Off-On Controllers, P. F. Pittman, Westinghouse Electric.

Diode Amplifiers, H. W. Abbott and L. D. Wechsler, General Electric Co.

Magnetoresistive Amplifiers and Second Harmonic Modulators, H. N. Putschi, General Electric Co.

Photoelectronic Circuit Applications, S. K. Ghandhi, General Electric Co.

Books

Microwave Measurements by E. L. Ginzton

Published (1957) by McGraw-Hill Book Co., 330 W. 42 St., N. Y. 36, N. Y. 476 pages+21 index pages +17 pages of appendix+xvii pages. Illus. 9¼×6¼. $12.00.

The author has successfully consolidated a multitude of basic microwave techniques into a book which can serve both as a basic text to a first year graduate course in microwave measurements and as a reference text to microwave engineers. Topics are carefully selected, clearly described, and very well integrated into a valuable unity. The impedance concept, transmission-line theory, and the equivalent-circuit approach are fully treated and utilized in the development of methods suitable for microwave measurements.

The first chapter delves into sources of microwave power, presents a practical discussion of klystrons, microwave triodes, and traveling-wave tubes, and includes the need and devices for isolating laboratory oscillators. Also considered are standard signal and harmonic generators. Chapters 2 and 3 contain a comprehensive evaluation of methods for detecting and measuring microwave power. Bolometers are extensively covered.

An excellent exposition of the impedance concept is developed in Chapter 4, with stress on graphical procedures. It is followed by a chapter on impedance measurements, which includes an elaborate treatment on the standing-wave detector and practices for achieving precision measurements. The behavior of microwave circuits and equivalent representations are discussed in Chapter 6.

Topics relating to the measurement of wavelength and frequency are dealt with in Chapters 7 and 8. The presentation is extended to wavemeter techniques and frequency standards. Chapters 9 and 10 concern resonant-cavity characteristics and the evaluation of the important parameters, Q and R. The final chapter investigates the measurement of attenuation and describes the power-ratio, substitution, cavity-resonance and scattering-coefficient methods.

There are many figures, footnotes and experimental data coherently introduced into the text. Perhaps the bibliography may be considered to be rather limited although a large number is not really required. All in all, the book reflects much credit on those concerned with it and will prove to be of great value for any one who desires to become thoroughly familiar with microwave measurements.

A. B. GIORDANO
Polytechnic Institute of Brooklyn
Brooklyn 1, N. Y.

Analytical Design of Linear Feedback Controls by G. C. Newton, Jr., L. A. Gould and J. F. Kaiser

Published (1957) by John Wiley & Sons, Inc., 440 Fourth Ave., N. Y. 16, N. Y. 282 pages+3 index pages+130 pages of appendix+3 pages of bibliography+xi pages. Illus. 9¼×6¼. $12.00.

This book covers the theory of the design of linear feedback control systems by the process of minimizing the integral of error squared for step and ramp inputs, or minimizing rms error for stochastic (random) in-

puts to linear mathematical models of the actual systems. Lagrangian multipliers are used to account for certain restraints, such as those placed on the amplitude of signals in order to maintain essentially linear operation.

The minimization procedure leads to a form of the Wiener-Hopf integral equation. The solution of this equation supplies the data for design of the compensating element, and for calculating the minimum possible rms error. This information is intended to be used as a guide in the trial and error design for the actual system.

The book is intended for readers who have had some graduate study in control systems, or are prepared to do collateral reading. It is assumed that the reader has already obtained an insight into the conventional frequency approach, and to the practical design of feedback control systems. There is a brief coverage of basic material in the appendices.

The book is terse. The basic thesis is developed in 286 pages. Of necessity the development is mathematical, and the description of the minimization procedure involves complicated integral expressions. Essentially there is no deviation from the basic thesis, and no exposition on practical aspects. Where examples are used, they are stripped to mathematical models in all cases except that of the example which makes up Chapter 9. However, the authors are careful to point out the assumptions they introduce and the restrictions on the methods they advocate.

There is little reference to somewhat similar work done by others, such as the work on minimization of the integral of time-weighted absolute value of error response to step inputs done by R. C. Lathrop and D. Graham.

It is felt that development of the minimization expressions in the frequency domain rather than the time domain would have resulted in expressions more readily interpreted by control people. The end results would have been the same, providing that key expressions were transformed back to the time domain.

The book is recommended for reading by every person wishing to be sophisticated in the area of feedback controls. The presentation is straightforward and clean cut. It provides a unified coverage of material not available elsewhere except in scattered journal reports.

A. M. Hopkin
Univ. of Calif.
Berkeley 4, Calif.

Nomograms of Complex Hyperbolic Functions, 2nd ed., by Jorgen Rybner

Published (1955) by Jul. Gjellerups Forlag, Copenhagen, Denmark. 99 pages. 12×8½. Dan. Kr. 44.00.

The second edition of this book incorporates a number of improvements over the first edition, as well as some additional nomograms. The notation of complex arguments has been changed to the common English usage. The ring binding has been changed from the top to the side, making the book more convenient to use.

Thirteen separate nomograms for cosh $(A+jB)=p+jq$ cover the range $0\leq A\leq 4$, $0\leq B\leq \pi/2$. With one exception, the scales for A are given in both nepers and decibels, while B is expressed in both radians and degrees. sinh $(A+jB)=p+jq$ is treated similarly in thirteen nomograms.

tanh $(A+jB)=r\angle\theta$ is treated in twenty separate nomograms covering the range $0\leq A\leq 3$, $0\leq B\leq \pi/2$, A in nepers and decibels, B in radians, and θ in degrees.

In addition, nomograms are given for conversion of complex numbers from rectangular to polar form, and vice versa, for reflection loss and reflection phase shift in networks, new nomograms for interaction loss and phase shift, and for resonance circuits and filters. An introductory section of 39 pages discusses the use of the nomograms, and gives a collection of formulas for circular and hyperbolic functions, and for four-terminal networks and transmission lines. The text is given in both Danish and English.

This book will be found of value in transmission line, wave propagation, filter and other problems which involve complex hyperbolic functions. Their accuracy in unusually high, insuring at least three-figure accuracy over much of the range. Some spot checks gave errors of only a few parts in 10^{-4}. The accuracy and convenience of these nomograms should make them a useful addition to the library of the electronics engineer.

Martin Katzin
Electromagnetic Research Corp.
Washington, D. C.

Solid State Physics, Vol. IV, ed. by F. Seitz and D. Turnbull

Published (1957) by Academic Press Inc., 111 Fifth Ave., N. Y. 3, N. Y. 521 pages+19 index pages +xiv pages. Illus. 9¼×6¼. $12.00.

This is Volume IV of the series of texts covering advances in research and applications in solid state physics edited by F. Seitz and D. Turnbull. The topics selected for this volume are "Ferroelectrics and Antiferroelectrics" by Werner Kanzig; "Theory of Mobility of Electrons in Solids" by F. J. Blatt; "The Orthogonalized Plane-Wave Method" by T. O. Woodruff; "Bibliography of Atomic Wave Functions" by R. S. Knox; and "Techniques of Zone Melting and Crystal Growing" by W. G. Pfann.

Kanzig has attempted to present a systematic review of the field of ferroelectricity as seen by the solid state physicist with principal emphasis on the behavior of single crystals. This monograph is quite long, containing nearly 200 pages and subdivided into 13 chapters. These chapters include the "Phenomenological Behavior of Ferroelectrics: Experimental," "Thermodynamic Theory of Ferroelectric Crystals," "Optical Properties of Ferroelectrics in the Visible Range," "Domain Structure and Hysteresis," "Thermodynamic Behavior of Antiferroelectrics," "Thermodynamic Theory of Antiferroelectrics," "Optical Properties of Antiferroelectrics," "Antiferroelectric Domains," "The Static and Dynamic Structure of Ferroelectric and Antiferroelectric Crystals," "Isotope Effects," "Ferroelectricity and Antiferroelectricity of Solid Solutions," and a chapter on "Molecular Models."

This review is comprehensive, systematic and authoritative. It refers to 378 articles in the literature. It is well organized, well illustrated and represents a valuable reference for workers in the field.

The monograph on the "Theory of Mobility of Electronics in Solids" by F. J. Blatt is also very long. It contains 167 pages and 328 references to original literature. The article is broken down into 6 chapters including an introductory chapter, a chapter each on "Statistics of Free Electrons," "Boltzmann Equation," "Solution of the Boltzmann Equation for Nonspherical Energy Surfaces and Anisotropic Relaxation Times," "Scattering Mechanisms," and "Effects Arising from Lack of Thermal Equilibrium."

The emphasis in this article is primarily on the theoretical approach but a certain amount of experimental work is cited in order to establish the validity of the theoretical deductions. It is concerned primarily with transport phenomena and the effects of electric and magnetic fields and of thermal gradients separately and simultaneously. The one electron approximation neglecting correlation and exchange effects is employed throughout. This review is unusually good and will serve as a valuable reference for workers in the field.

The article on "The Orthogonalized Plane-Wave Method" by T. O. Woodruff is primarily an elaboration of Part X of an article in the first volume of this series by Reitz. This article contains 44 pages and three chapters. The first chapter is devoted to a description of the method, the second to a survey of some applications of the method, and the third is a calculation of an example in which this method is applied to the silicon crystal. The principal merit of this article is in its detailed outline of the calculation of the specific solid state problem by a method of approximation which has shown promise of giving quantitative results with reasonably rapidly convergent solutions. This article will prove useful to those concerned with the calculations of wave functions and energy eigenvalues of an electron in an arbitrary crystal potential.

The article "Bibliography of Atomic Wave Functions" by R. S. Knox is a compilation of references to the literature on atomic wave functions which have been computed. This compilation makes use of five earlier compilations which have been corrected, expanded and brought up to date. The article includes an alphabetical list of atoms and ions with the literature references. 117 articles in the literature have been employed in this compilation.

The article on "Techniques of Zone Melting and Crystal Growing" by W. G. Pfann contains nearly 100 pages and 187 literature references. It is organized in eight chapters including "Distribution and Coefficient and Normal Freezing," "Principles of Zone Refining," "Practice of Zone Refining," "Zone Leveling," Methods of Perturbing the Concentration," "Temperature-Gradient Zone Melting," and "Crystal Growth and Dislocations."

This is an article describing techniques employed by research men in the preparation of crystalline materials for research purposes. It discusses the techniques in a manner rarely found in standard texts and highly desirable from the point of view of the research man. Pfann has done an outstanding job in compiling in a very readable form material which is difficult to obtain and organize from the literature.

Volume IV is a very welcome addition to this highly interesting series of monographs on special topics in solid state physics.

L. T DeVore
Stewart-Warner Electronics
Chicago, Ill

Scanning the Transactions

It has been suggested that the average IRE member, although he is not interested in reading highly specialized papers outside his own field, would nevertheless, welcome a report on some of the significant or unusual work that is going on in other fields which appears in IRE publications he does not normally see.

With this objective in mind we are hereby inaugurating a new monthly feature in which the Managing Editor, with the aid of TRANSACTIONS editors, will single out and interpret for the general reader, appropriate papers appearing in current issues of the TRANSACTIONS of the 28 IRE Professional Groups. Further information about the issues from which these papers are selected will be found in the "Abstracts of IRE TRANSACTIONS" section that immediately follows.

The title of this new section is actually incomplete. We plan to cover not only the TRANSACTIONS but the STUDENT QUARTERLY and the WESCON and NATIONAL CONVENTION RECORDS as well. As a case in point we refer readers to the first item below.

Comments from readers on the utility (or futility) of this endeavor will be welcomed by the IRE Editorial Board.—*The Editor*

Life in a laboratory was revealed to the surprised readers of the STUDENT QUARTERLY in the most unusual form yet to appear in an IRE publication. Twelve verses, ranging over the laboratory scene from Conferences to Applied Mathematics, indicate that the author, already distinguished as a leading engineer, as a past Editor of the IRE and as a prolific and articulate writer of science fiction and nonfiction, must now take a bow as a poet of no small talent. The verses were so delightful and stimulating that we feel compelled to offer a sample below. (J. R. Pierce, "Life in a laboratory," IRE STUDENT QUARTERLY, December, 1957.)

Bosses

Bosses are people up a fantastic tree
Which stretches rootlets into the fertile earth
And bears some fragrant blossoms at its top.
Well-digested achievement upward flows,
And what flows down? Dirty jobs from on high
Sediment themselves among the mucky roots
And interrupt the uneven course of thought.
But bosses have the dirty end as well:
The men who can't do better, God help them;
The unhappy ones (who isn't?) who blame the boss;
The happy ones, who need more things and men
To make their little millennium in a year,
The ones in a rut, who go on and on and on,
And who can stop what he has once set going?
And the bosses themselves, who wonder if they are right—
That is, good bosses do.
And then, the endless splicing of red tape
To see that all is done as is allowed,
And things are run to please yet higher bosses,
Or bosses dead, whose muddled thoughts are sacred,
Or The Machine, transcending all the bosses,
With meshed parts, plant men, accountants, et cetera, such
As grind along how no one understands
Nor dares to interrupt.

Credit

You can seek credit. Maybe you can get it.
Don't bother whether for your work or others';
Credit is credit; never mind the source.
Getting things done is a different kettle of fish.
If you want another to do it, he'll do it faster
With your ideas a part of his very substance,
Digested flesh of his brain, grown fruit of his labor.
If you want another to help you, he'll do it better
If he believes that his is the greater part.
Besides which, credit itself may be overrated;
Do reputations grow on credit alone?
Only when the seeker of credit is clever.
And why quibble about his reputation then?

Direction

Every one needs good advice; a few men want it,
But how can one get it? That is the troublesome question.
You can't go by quantity. I've met some great advisers
Whose advice was neither pertinent nor right.
Can the boss advise? He doesn't know the details,
And sometimes misses the problem quite as much,
And yet, he may have an inner feeling for things
Which can be translated hardly into sense;
If you are clever, there may be advice in the boss—
If he's a good boss; that is, if he's a good man.
And that is the point. Advice is where you find it.
Choose the good, I say, from any source.
But if you know the good when once you see it,
After all, do you really need advice?

Sending signals backwards offers intriguing possibilities as a means of self-correcting the delay distortion that occurs in transmission circuits. Suppose that a magnetic tape recorder is placed at the midpoint of a transmission system to record the signals that have traversed the first half of the route. Suppose further that the recorded signals are then played backwards into the second half of the system. The delay distortion of the two halves of the system would then cancel, since the components of the signal delayed the most in the first half of the circuit would get a head start when they are fed into the second half. If necessary, a second time-reversing recorder could be installed at the terminus of the system to revert the segments of the signal to their original sequence. This ingenious scheme is of particular interest in the use of standard telephone circuits for data transmission and slow-speed television, where delay distortion requirements are much more severe than for the voice transmissions for which the circuits were originally designed. Bell Laboratories has used this time-reversal technique in experimental transmissions of slow-speed pictures over a 5-kilocycle 16,000-mile loop between Murray Hill and Los Angeles with impressive results. Perhaps the network theorists will soon be adding time inverters to their bag of analytical tools, and the circuit designers, magnetic recorders to their supply of standard circuit elements. (B. P. Bogert, "Demonstration of delay distortion correction by time reversal techniques," IRE TRANS. ON COMMUNICATION SYSTEMS, December, 1957.)

Unionization of engineers has come up for discussion for the first time in any IRE publication. Two articles, one presenting the union viewpoint and the other written by a management representative in labor relations, point up the fact that approximately 11 per cent of the country's more than 500,000 engineers are represented in collective bargaining by unions and that their numbers will, in all likelihood, continue to increase. Both are agreed as to why there are engineering unions today. They trace it directly to the widespread growth

of vast engineering organizations within individual companies since World War II, coupled with the more recent scrambling for hard-to-find engineers at rapidly increasing salaries. In some instances this has led to salary inequities, a diminishing of the engineer's accustomed identity and treatment as an individual and a professional, and a hardening or impairment of the traditional communication arteries which held the engineer in close and direct contact with management. Missing from the discussion, though, were the views of those opposed to engineering unions. (J. Amann, "Unionization of engineers—I," IRE TRANS. ON ENGINEERING MANAGEMENT, December, 1957. H. H. Rains, "Unionization of engineers—II," *loc. cit.*)

Steinmetz, whose life is the subject of an absorbing article in the December STUDENT QUARTERLY, was one of the great mathematical wizards of his era. For those readers with a similar bent, we offer a problem posed to him by an associate who was trying to stump him: If you bore a hole two inches in diameter through the side of a circular solid rod two inches in diameter, how much material is removed? The answer, which Steinmetz gave without hesitation after jotting a few figures on a pad, is given below.[1] (C. D. Wagoner, "Steinmetz revisited: The myth and the man," IRE STUDENT QUARTERLY, December, 1957.)

Coded pictures have been proposed as a means of speeding up digital facsimile transmissions over telephone circuits. The coding scheme has its basis in the fact that most documents that are transmitted, whether they be pictures, drawings or printed matter, have substantial patches of all-white or all-black in them. Therefore, a run of all-white or all-black dots in part of a scanning line could be represented by a simple code which indicated the number of dots in the sequence and whether they were black or white. The number of binary digits required for this code would on the average be less than if each dot were transmitted individually in the customary fashion. Thus, simple documents could be automatically handled faster than the complex ones. The equipment required for this, although it has not been built, has been given enough thought to prove that it would be feasible, although more complex. This proposal represents an interesting engineering application of information theory which, in its ramifications, conceivably could find use in special types of television systems, as well. (W. S. Michel, W. C. Fleckenstein, and E. R. Kretzmer, "A coded facsimile system," 1957 IRE WESCON CONVENTION RECORD, Part 2.)

The impact of computers on network theory may well prove to be revolutionary. Not only can a computer solve problems faster, cheaper and more reliably than a man armed with a slide rule and desk calculator, but it promises to eliminate what has heretofore been the major restrictions in the application of network theory to practical design problems. No longer does the designer have to avoid using a difficult method he doesn't understand or that isn't "practical" to solve. The chances are good that the computer programming staff will be able to code it, making it immediately available to all. The result will be a virtual elimination of the frustrating 20-year lag between theory and application, and a flourishing of complex techniques that might otherwise be considered purely academic. Even more important, circuit theory as we know it today will in time disappear, to become part of a broader field which we might call system theory. The engineer of the future, instead of tinkering with this and that circuit or component and then trying to fit them all together somehow, will set out with yet unborn techniques to design the entire system as a whole with the aid of a computer. In a broader sense, the computer will require that engineering schooling and training place an increasingly greater emphasis on creativity and fundamental knowledge, as the standardized details and specialized techniques are relegated more and more to punch cards. The machine, rather than replacing man, will require that he be more of a man and less of a machine. (T. R. Bashkow and C. A. Desoer, "Digital computers and network theory," 1957 IRE WESCON CONVENTION RECORD, Part 2.)

Aluminum, which is being used these days in everything from house sidings to automobile brakes, is now being used to boost the power handling capabilities of very high power germanium transistors. A fabrication scheme has been devised for evaporating aluminum and condensing it on a hot germanium wafer to form an aluminum emitter or collector junction. The evaporated aluminum technique is superior for high power applications to the standard fused indium junctions because aluminum provides higher conductivities and emitter injection efficiencies. Moreover, it is possible to obtain more accurate control of certain important dimensional characteristics of the junction when it is formed by an evaporation process. Transistors with aluminum junctions are capable of switching currents of 10 amperes with a power handling capacity of 500 watts, which bodes well for the future of the transistor in the industrial control field. (H. W. Henkels and G. Strull, "Very high-power transistors with evaporated aluminum electrodes," IRE TRANS. ON ELECTRON DEVICES, October, 1957.)

The information-handling capacity of humans has been the subject of some novel tests to determine how fast a person can read aloud. Some details of the tests were reported here last year.[2] The tests showed that the highest capacity of a human as an information channel was about 43 bits per second, and that this figure represents a fundamental mental limitation of the human being and not a physical limitation connected with the speed of uttering words. These reading-rate tests are a first small step in efforts to measure the least information rate necessary in order to transmit a signal, such as a speech or picture signal, well enough so as to be perfectly satisfactory to a hearer or viewer. At present, a channel capacity of 50,000 bits per second is used in sending voice signals over a telephone circuit, and 50,000,000 bits per second in sending television signals. However, no one is suggesting that anything like 43 bits per second are all that is necessary, since innumerable other factors that cannot be determined by reading rates are also involved. As an interesting sidelight, the tests showed that reading rates were about the same for different languages. Also, some small comfort can be taken in the finding that engineers are faster readers than porters. (J. R. Pierce and J. E. Karlin, "Reading rates and information rates of a human channel," 1957 IRE WESCON CONVENTION RECORD, Part 2, p. 60.)

Transistor circuits. If anyone needs to be convinced of the important impact that transistors are having on network theorists, they need only to look at the 236-page September issue of the CIRCUIT THEORY TRANSACTIONS, the second largest issue ever produced by a Professional Group. In the opening editorial of the issue, PGCT Chairman, H. J. Carlin, quoted a statement by E. W. Herold that has appeared twice before in the PROCEEDINGS,[3,4] Nevertheless it bears repeating: "The chemical synthesis of an improved compound can do more to revolutionize the performance of an electronic system than years of painstaking circuit work." To which Carlin adds, "The circuit theorist recognizes this situation but is prepared to take the new elements given him by materials scientists and to modify his methods to exploit these elements in an optimum manner." That the network specialist is indeed modifying his methods because of the transistor, and to good

[1] The answer is 5.333 cubic inches.

[2] J. R. Pierce and J. E. Karlin, "Information rate of a human channel," PROC. IRE, vol. 45, p. 368; March, 1957.

[3] "Poles and Zeros," PROC. IRE, vol. 45, p. 1457; November, 1957.

[4] E. W. Herold, "Future circuit aspects of solid-state phenomena," PROC. IRE, vol. 45, p. 1463; November, 1957.

advantage, is attested to by this impressive group of 31 papers.

Ferrite mixers for microwave frequencies, which have been the subject of some theoretical speculation during the last two years, have now undergone experimental tests, with the best conversion efficiencies ranging from about −15 db for the sum frequency output to −47 db for the difference frequency. While this doesn't match the −6 db figure reported for ferrites when used as frequency doublers,[5] further improvements can be expected as the technique is refined. Indeed, the first ferrite frequency doublers showed only a −60 db efficiency. In any event, this experimental verification should give added stimulus to the use of ferrites for mixing and doubling, especially at high power levels where they promise to prove superior to crystals. (P. N. Vartanian and E. N. Skomal, "Mixing in ferrites at microwave frequencies," 1957 IRE WESCON Convention Record, Part 1.)

X-raying germanium wafers has been proposed as a simple and straightforward method to determine how thick they are. X-ray absorption measurements can reveal the thickness of a 2-mil (0.002-inch) wafer to within 0.1 mil. Conceivably, this method could be used to control an electrolytic etching operation so as to cut off the electrolysis automatically at the correct thickness. The scheme, while by no means revolutionary, is nevertheless an interesting example of the many ways in which the absorption of waves (whether they be electromagnetic or ultrasonic) can be used to determine important physical characteristics of materials. (A. R. Moore, "A method of accurate thickness determination of germanium wafers suitable for transistor production," IRE Trans. on Electron Devices, October, 1957.)

[5] J. L. Melchor, W. P. Ayres, P. H. Vartanian, "Microwave frequency doubling from 9 to 18 kmc in ferrites," Proc. IRE, vol. 45, pp. 643–646; May, 1957.

Abstracts of IRE Transactions

The following issues of "Transactions" have recently been published, and are now available from the Institute of Radio Engineers, Inc., 1 East 79th Street, New York 21, N. Y. at the following prices. The contents of each issue and, where available, abstracts of technical papers are given below.

Sponsoring Group	Publication	Group Members	IRE Members	Non-Members*
Circuit Theory	Vol. CT-4, No. 3	$2.50	$3.75	$7.50
Communications Systems	Vol. CS-5, No. 3	0.95	1.40	2.85
Electron Devices	Vol. ED-4, No. 4	0.80	1.20	2.40
Engineering Management	Vol. EM-4, No. 4	0.70	1.05	2.10

*** Public libraries and colleges may purchase copies at IRE Member rates.**

Circuit Theory

Vol. CT-4, No. 3, September, 1957

Pandora's Black Boxes—H. J. Carlin (p. 60)

Abstracts of Active-Network Papers (p. 62)

Foreword to Active-Network Papers—J. G. Truxal (p. 69)

Survey of Some Properties of Linear Networks—E. F. Bolinder (p. 70)

An attempt is made to give a brief exposé of some modern works on linear network properties. The concepts treated are the following: passivity, stability, efficiency, and nonreciprocity; n-terminal-pair networks and two-terminal-pair networks in particular are studied at a fixed frequency.

Active RC Networks—R. D. Thornton (p. 78)

If all available amplifying devices can be approximated by linear models with capacitive, terminal, energy storage, there are bounds on the allowed natural frequencies of circuits constructed from these devices. These bounds are readily determined from the eigenvalues of a frequency matrix and can be related to the maximum power that can be dissipated by the device per unit energy stored in the terminal capacity. Synthesis of unilateral and constant-k amplifiers is considered, and concepts such as the gain-bandwidth product and the maximum frequency of oscillation are related to the bounds on allowed natural frequencies.

About Such Things as Unistors, Flow Graphs, Probability, Partial Factoring, and Matrices—S. J. Mason (p. 90)

The purpose here is to point out three things. 1) Topological circuit analysis, in which we look for trees, and topological flow-graph analysis, in which we look for loops, are intimately related, since both have to do with simultaneous linear algebraic equations. The intimate relationship becomes an identity when we deal with Markoff probability diagrams, for which the circuit model of the problem and the flow-graph model of the problem are one and the same. 2) The expression for a flow-graph transmission in terms of the branch transmissions can often be made much more compact by a process called partial factoring. Fortunately, this process has a simple topological interpretation, so that the compact form is obtainable by inspection of the flow-graph. 3) Simultaneous linear matrix equations may be conveniently expressed in flow-graph form, whereupon the solution is obtainable by standard flow-graph reduction techniques.

Multipole Analysis of Active Networks—L. A. Zadeh (p. 97)

To replace the conceptual framework of network theory as based on the building blocks of two-terminal elements, a framework is suggested that is built on the premise that a network element is a black box with finitely many—but not necessarily two—accessible terminals. The greater generality and abstractness of the multipole method give it a considerably broader range of applicability than that possessed by the two-pole method.

Transformation Theory Applied to Linear Active and/or Nonbilateral Networks—E. A. Guillemin (p. 106)

A nonpassive and/or nonbilateral (linear) network can be represented analytically as a passive bilateral one in which the variables are subjected to an appropriate linear transformation. In contrast to the "dependent source" method of analysis, transformation theory offers not only a very general and elegant way of dealing with both the nonbilateral as well as the active character of devices, but through the existence of a considerable number of interpretive mechanisms such as geometric visualization in multidimensional spaces and the concept of normal coordinate transformations, it represents a relatively untapped storehouse of manipulative artifices that may ultimately provide a clearer understanding of this broader class of networks.

Separation Transformations for Square Matrices—H. E. Meadows, Jr. and B. J. Dasher (p. 111)

A class of transformations of square matrices which may be regarded as a generalization of matrix transposition and complex conjugation is defined by a set of five postulates. These transformations, termed "separation transformations," make evident certain characteristics of form for square matrices by resolving every square matrix into two additive component matrices called the "consonant" and "dissonant" parts. This property may be valuable in the study of active linear networks since the impedance matrices, for example, of these networks may display no obvious special characteristic of form.

Separation transformations and the related consonant and dissonant parts of square matrices have some interesting manipulative properties. These properties lead to an extension of the concept of orthogonality of matrices.

An example to illustrate the possible use of the relations derived for separation transformations shows a generalization of Mason's invariant for active linear networks subjected to lossless, linear, reciprocal coupling.

The A Matrix, New Network Description—T. R. Bashkow (p. 117)

Both the loop and node methods of network analysis produce a system of second-order differential equations. A method of analysis is proposed which produces a set of first-order differential equations. With this method, the network equations obtained can be expressed in the form $F+dy/dt=Ay$, where F and y are column matrices and A is a square matrix. The variables, y, are currents through inductances and voltages across capacitances; the forcing functions F are proportional to voltage and current sources. The elements of A are inductances, capacitances, and resistances, or combinations thereof. Characteristic roots (natural frequencies) of the network are identical with the eigenvalues of the A matrix.

Some Simplifications for Analysis of Linear Circuits—G. L. Matthaei (p. 120)

Any linear, passive, or active two-terminal pair network is describable in terms of six, interrelated "characteristic polynomials." A method for finding them is presented which requires less labor than is usually involved in finding a set of the conventional circuit param-

eters. Examples are given. Having found the characteristic polynomials, all of the conventional parameters, such as the open-circuit impedances, can be written down simply as ratios of the polynomials. Methods are discussed for finding the characteristic polynomials for interconnected networks from those of their component networks. Such calculations utilizing all six polynomials save labor over conventional methods by introducing additional information at the outset and by eliminating redundant factors.

Negative-Impedance Converters—A. I. Larky (p. 124)

The conditions under which an active device exhibits an input impedance at one terminal pair which is exactly the negative of the load impedance connected to the other terminal pair are discussed. There are an infinite number of ways by which such a device, which is called a negative-impedance converter (NIC), can be made. One of the limits of this set is represented by a transistor circuit which was discussed previously by Linvill; the other limit, by a new circuit introduced recently.

Practical negative-impedance converters are not exact; however, they may be made so by the addition of a pair of compensating impedances. The parameters of the NIC which most affect circuit performance are indicated as a guide to NIC design. Two typical transistor NIC circuits are compared on this basis. Experimental results are given.

Negative Impedance Circuits—Some Basic Relations and Limitations—W. R. Lundry (p. 132)

Much of the current interest in negative impedance circuits is directed toward potential applications as components of transmission networks—filters, equalizers, and similar structures. To permit maximum flexibility in the analysis and design of such structures, a complete specification of the characteristics of the negative impedance circuit is required. Four parameters are required for such a specification. The present discussion in terms of the *ABCD* matrix is particularly useful when a tandem connection of negative impedance circuits and passive networks is to be investigated.

The behavior of a practical circuit can be represented as the sum of a matrix stating the ideal behavior and an error matrix. In the cases studied, the elements of the error matrix are inversely proportional to the gain of the amplifier used.

Stability of an over-all circuit and sensitivity to component variations are expressed in terms of the elements of the scattering matrix.

RC Active Networks Using Current Inversion Type Negative Impedance Converters—Takesi Yanagisawa (p. 140)

The RC active filter, which has been established by J. G. Linvill, has a circuit configuration of a negative impedance converter sandwiched between two RC networks. This paper deals with a new circuit also using two RC networks and a converter, but its configuration is based on the parallel or series connection and the converter must be a current-inversion type.

The main results obtained here are as follows:

1) The filter characteristic function which has attenuation poles at finite frequency can be realized by the synthesis of only RC two-terminal impedances without using twin-T circuits.

2) The characteristic all-pass function is realized by the same method as a filter characteristic.

3) A current-inversion type converter, which uses a pair of unction transistors or vacuum tubes, is obtained.

4) Some design examples and experimental results are reported on filters and phase shifters.

Design Principles for Single Loop Transistor Feedback Amplifiers—F. H. Blecher (p. 145)

The design of single loop transistor feedback amplifiers is considered. A criterion of stability is introduced which is useful for either calculating or measuring the stability margins of transistor amplifiers, and in particular, single loop feedback amplifiers. Expressions are derived for relating sensitivity and impedance to feedback. Practical design techniques are discussed and are illustrated by the design of a one-megacycle carrier-frequency feedback amplifier. It is shown that a transistor feedback amplifier is an excellent wideband video amplifier.

Design of Conditionally Stable Feedback Systems—J. Oizumi and M. Kimura (p. 157)

Under equivalent circumstances, a conditionally stable feedback system may exhibit much more feedback than would be obtainable from an unconditionally stable feedback system. The theory of design and practical methods of stabilization of conditionally stable feedback systems are presented and some experimental results are shown.

Network Design by First-Order Predistortion Technique—C. A. Desoer (p. 167)

A new predistortion technique based on perturbation theory is applied to the synthesis of slightly dissipative networks. The basic idea is to predistort the design of the dissipationless network in such a way that when the slight loss of the reactive elements is taken into account, the resulting transmittance has the same zeros and poles as those of the prescribed transmittance (except for second-order terms). As a result, the difference between the resulting transmittance and the prescribed one is a flat loss. One feature of the method is that the elements need not have identical Q's. A numerical example is included.

Synthesis of Non-*PR* Driving Point Impedance Functions Using Analog Computer Units—W. J. Karplus (p. 170)

When the real part of a driving point impedance function is negative at some real frequency, or when the residues of any of its poles on the $j\omega$ axis are negative, the function is not positive real and cannot be synthesized without recourse to active elements. The negative resistors and reactors required under these circumstances fall into two categories: the open-circuit stable, current-controlled, and the short-circuit stable, voltage-controlled types. This paper demonstrates how linear negative resistors and capacitors of both types may be simulated conveniently on electronic analog computers. Two operational amplifiers with a combined gain of 2 are used for each negative element. Examples of the application of this method to the synthesis of nonpositive real impedances and admittances are included, and the dependence of the stability of these networks upon the external circuitry is considered.

Foreword to Transistor Papers—H. E. Tompkins (p. 173)

Abstracts of Transistor Conference Papers in this Issue (p. 63)

Series Tuned Methods in Transistor Radio Circuitry—W. F. Chow and D. A. Paynter (p. 174)

Series resonant LC networks can be effectively utilized in transistor-tuned amplifiers and oscillators to achieve simplicity of circuitry coupled with excellent performance. A new method for designing intermediate frequency transistor amplifiers is described. Series resonant LC elements are employed in the emitter circuits of the transistors along with direct coupling of the amplifier stages to achieve a relatively simple and stable amplifier.

A transistor oscillator which employs series resonant tank circuit elements is also described. A high degree of frequency stability is realized without the use of elaborate nonlinear compensation techniques. Tests made on an uncompensated circuit indicate a frequency stability of about six parts per million per 10 per cent variation in supply voltage. The circuit configuration of both the amplifier and oscillator permits the design of units in which the operating frequency is almost independent of transistor properties and supply voltage.

Analyses of circuit operation and experimental results are given for both the amplifier and oscillator applications.

Wide-Band Feedback Amplifiers—F. D. Waldhauer (p. 178)

An approach to the problem of the design of transistor wide-band feedback amplifiers is given. Choice of feedback circuit configurations for the stabilization of amplifier circuit transconductance, transresistance, voltage gain, and current gain are discussed in terms of an idealized phase-reversing amplifier. A composite stage including two transistors which may be made to approach this idealized amplifier is described, including considerations of biasing, asymptotic high-frequency cutoff characteristic, and composite hybrid parameters.

The design of a three-transistor amplifier for a bandwidth of 8 mc having a closed-loop gain of 36 db and over 30 db of feedback is discussed. Local feedback is made an integral part of the design to enable the amplifier to accommodate a wide range of transistor parameters without individual adjustment. Shaping of the open-loop frequency characteristic is accomplished largely by the transistors themselves. The circuit configuration permits the variation of return ratio with frequency to be controlled primarily in one stage, whereby the gain-phase characteristic may be readily tailored to provide a preassigned transient characteristic. The design procedure for the amplifier is discussed, including maximization of return ratio and shaping of the high-frequency characteristic. Signal-flow diagrams are used to derive the frequency dependence of the return ratio. Measurements of magnitude and phase of the return ratio and the closed-loop gain and transient response are shown.

Some Solutions to Problems of Operating Germanium Transistor Servo Amplifiers at High Ambient Temperatures—P. M. Thompson and J. Mitchell (p. 190)

Some solutions are outlined to the problem of using readily available types of germanium power transistor at ambient temperatures as high as 85°C, such as might be found in aircraft.

Germanium transistors can be used at ambients within 5°C of their maximum storage temperatures if the power dissipated in the transistor is kept low and there is provision to handle the high I_{c0}.

Both the mean power dissipation and the peak instantaneous dissipation must be considered, and the thermal and electrical circuits designed to insure that the junctions never, even instantaneously, exceed the maximum temperatures set by the transistor manufacturers.

A typical design for high-temperature operation is described, consisting of a three-stage direct-coupled amplifier to operate a standard 3-watt 400 cps servo motor. This amplifier, in which sound engineering practices are stressed, sacrifices some gain for stability, reliability, and efficiency. It is designed to tolerate wide variations in transistors and most other components with a minimum change in gain or available output. The maximum mean power dissipation is $\frac{1}{3}$ watt, and the maximum peak instantaneous dissipation is $1\frac{1}{2}$ watts.

The first of these amplifiers was built two years ago, and although several have been in operation, there have been no failures. The techniques are applicable to other circuits where transistors must operate close to their maximum storage temperature.

Bias Considerations in Transistor Circuit Design—S. K. Ghandhi (p. 194)

It is well known that the operating point of a transistor has a tendency to shift with temperature. An analysis is made of the factors contributing to this shift. It is found necessary to define two stability factors for an adequate formulation of the bias problem. These factors, together with the voltage and current defining the operating point, are used in the design of bias networks.

Various stabilization circuits are considered

in detail, and design procedures set up for these schemes. A comparison is made of the various schemes; in particular, direct and feedback stabilization are compared on the basis of battery drain, ac gain, and variation of operating point with battery voltage.

The stabilization of direct-coupled stages is also discussed, and the design of a bias circuit for a two-stage direct-coupled pair is taken up in detail.

Nonlinear techniques for temperature stabilization are also discussed. These are useful in special applications such as high-power output stages, where the temperature changes are extreme, or in low-level circuits where extremely stable operation is required, *e.g.*, in oscillators.

Thermal Stability of Junction Transistors and Its Effect on Maximum Power Dissipation—H. C. Lin (p. 202)

When the junction temperature of a transistor increases, the collector current increases, as a result of increases in 1) saturation currents and 2) dc conductances. Thermal instability occurs when junction temperature and collector current increase in regenerative and uncontrollable fashion. The limit depends on factors both within and external to the transistor. The internal factors are the thermal resistance, the current amplification factor, and the base lead resistance. The external factors are ambient temperature, collector voltage, circuit resistances, and the thermal coupling between the transistor and temperature compensation elements, if any. Circuits with greater temperature stability permit a higher maximum power dissipation. The factors are discussed which determine the thermal stability and consequently, the maximum dissipation of transistors. The criteria for stability are derived mathematically and some thermal compensation techniques are treated.

A Survey of Magnetic and Other Solid-State Devices for the Manipulation of Information—J. A. Rajchman (p. 210)

A review is made of the art of manipulating digital information by means of magnetic devices. Also included are some remarks on other solid-state devices. There is a brief introductory discussion of semiconductor diodes and of the unique properties of the transistor. The storage and switching capabilities of magnetic cores made of square hysteresis loop materials are discussed with some detail. This discussion includes: random access memories made of individual cores or ferrite apertured plates, various types of decoding and encoding switches, shift registers, current and voltage driven circuits, the principle of current steering, transistor coupled circuits, the principle of the transfluxor, the application of the transfluxor to nondestructive read-out memories and channel commutators, the principle of transfluxor current steering, and some examples of multiapertured transfluxors. The potentialities of some phenomena as yet not widely exploited are discussed: ferroelectric, electro-optical and magnetoresistive effects.

Counting Circuits Employing Ferroelectric Devices—R. M. Wolfe (p. 226)

A new type of counting circuit utilizing ferroelectric devices has been developed. This circuit, although similar to the older energy storage type of counter, overcomes most of the disadvantages of the older circuit. Whereas the older circuit required standardization of the input pulse to stabilize the counting ratio, *i.e.*, the number of input pulses per output pulse, the use of a ferroelectric device to meter charge removes the need for such standardization. A second ferroelectric device used to integrate the packets of charge developed by the first removes the lower bound on the repetition rate of pulses to be counted.

Circuits have been built with counting ratios up to 40 to 1. They have operated satisfactorily under conditions of changing voltage, temperature, and pulse spacing. Several counters may be connected in cascade to provide higher counting ratios.

A High-Speed Two-Winding Transistor-Magnetic-Core Oscillator—A. J. Meyerhoff and R. M. Tillman (p. 228)

Recent articles in the literature have described voltage-controlled square-wave oscillators using transistors and square-loop magnetic cores and generally incorporating four windings. These oscillators give output frequency directly proportional to applied voltage; hence they are useful as solid-state dc to dc converters, telemetering oscillators, and many other devices. Each application is based on the fact that the volt seconds applied to a core are proportional to the flux switched, which is essentially constant for the core.

This paper is primarily devoted to the fundamentals and applications of a novel two-winding transistor-core oscillator and derived circuits. The two-winding circuit is capable of true square-wave output at 700 kc, the upper frequency limit being determined by the present state of the art of transistor and core development.

A review is given first of the usual four-winding oscillator, tracing its operating cycle step by step and showing the circuit to be derivable directly from a fundamental transistor-core switching circuit.

Then the two-winding oscillator is discussed. With this circuit, the two separate base windings are eliminated through cross-coupling of each collector to the base of the opposite transistor. During switching time, the collector winding of the OFF transistor supplies the necessary regenerative voltage to the base of the ON transistor. A parallel RC in each base circuit speeds up the turn-off action by application of inverse current to the ON base. Direct electrical cross-connection from the ON base to the OFF collector means that at switch-over the inverse transient voltage, due to flyback, will momentarily place the OFF transistor into inverse saturated conduction, thereby presupplying it with holes so that it can take on its load in the forward direction extremely rapidly when the ON transistor shuts off. In this circuit, self-starting is inherent, due to the direct connections from base to negative supply.

The circuit operation is analyzed in detail and worst-case design equations are derived. A bibliography of the literature is included.

Millimicrosecond Transistor Current Switching Circuits—H. S. Yourke (p. 236)

If transistor switching circuits are to have response times limited by the bandwidths of the transistors operating as amplifiers and by diffusion or transit time delay, it becomes necessary to avoid operation in saturation. Since a low collector to base voltage, or operation near saturation, has a detrimental effect on transistor bandwidth, it is desirable to avoid this operating region as well.

Where nonsaturating circuits are used with transistors having cutoff frequencies of several hundred megacycles, transistor and circuit capacitances become the primary limitation on speed. To minimize the delays due to capacitance, it is desirable to operate with voltage swings as small as reliability consideration will permit.

A new mode of operation has been developed whereby well-specified currents can be switched reliably with small voltage swings. The complementary current switching technique described provides a means of constructing relatively simple logical circuits in which transistors are operated well out of saturation in a region of maximum bandwidth. This technique offers several advantages besides high-speed switching. The resulting logical circuits have complemented outputs, and reset their own levels. There is no requirement on the upper limit of α and dc stability factors are essentially unity. The circuits are simple and relatively noise free. A few basic circuits and working examples are presented in the paper. Application and extension of this current switching technique results in a large body of new and useful logical circuits.

Some New Transistor Bistable Elements for Heavy Duty Operation—N. F. Moody and C. D. Florida (p. 241)

Bistable elements of fast switching speed (0.2 μsec), capable of delivering load currents up to 100 ma and having a low-output impedance, are required in many electronic circuits. Such an element is particularly useful in digital computers employing passive routing.

The paper shows that circuits which use both p-n-p and n-p-n transistors are well suited for such duties. It also describes both nonsaturated and saturated forms.

Part I devotes itself to nonsaturated circuits, and the analysis is mathematical in approach. The general properties thus deduced are applicable to all members of the circuit family.

Part II turns to the problems introduced by saturation and is a general theoretical discussion of wide application. It leads to a concept denoted controlled saturation; this is applied to switching circuits in order to minimize the penalty of lost speed which saturation can cause.

Part III applies the theoretical work of the preceding parts to a fast trigger circuit in which saturation is permitted. It concludes by showing that this basic saturated circuit can be developed into a variety of forms.

A Decade Ring Counter Using Avalanche-Operated Junction Transistors—J. E. Lindsay (p. 262)

The avalanche mode of operation for junction transistors is encountered at higher-than-normal collector voltages. In this avalanche region of operation the electrical character of the junction transistor is profoundly altered because of a voltage sensitive current-multiplication occurring at the collector junction. Current controlled N-type negative resistance characteristics suitable for bistable operation are obtained. Important features of these characteristics can be treated analytically to obtain results suitable for design purposes.

Twelve experimental avalanche-operated junction transistors have been used in a decade ring counter and driver. This represents a saving of two-to-one in semiconductor devices, as contrasted to the use of conventionally operated junction transistors for the same function. A like saving of other components is obtained. The ring counter uses a new method of count transfer which provides improved reliability and higher counting speed capability. The driver and counter achieve operation to 500 kilocycles using transistors having a frequency of α_e cutoff in the range 30 to 40 kilocycles for conventional operation. The counter operates to 300 kilocycles over a temperature range from below $-50°$ to 50°C without compensation or optimized design.

Transient Response Characteristics of Unijunction Transistors—J. J. Suran and B. K. Eriksen (p. 267)

Carrier transport in unijunction transistors is due primarily to electric fields rather than diffusion gradients. Thus, the high-frequency and transient response characteristics of unijunction transistors are considerably different from the characteristics associated with diffusion type devices.

The high-frequency and transient response characteristics of silicon unijunction transistors are described. A previously published solution of the electrodynamic equations, taking into account field and recombination effects, is used to calculate theoretical frequency and transient response characteristics which are subsequently compared to experimental measurements.

It is shown that:

1) Electric field effects lead to resonance characteristics which are somewhat similar to those encountered in wave interference phenomena.

2) The frequency response characteristics of unijunction transistors are predominantly determined by the electric field gradient for high fields and by recombination effects for low fields.

3) The large-signal transient response of unijunction transistors is characterized by at least two time constants, one related to transit time and the other to minority carrier lifetime.

4) The maximum large-signal switching speeds and minimum trigger energy of regenerative unijunction transistor circuits depend upon both the electric field and lifetime characteristics of the device.

An Improved Square-Wave Oscillator Circuit—J. L. Jensen (p. 276)

Inductively coupled square-wave transistor oscillators using a saturating output transformer subject the transistor to rather severe transient conditions and require an expensive transformer. The improved circuit, however, uses a separate saturating feedback transformer and a conventional output transformer. The described circuit has improved performance with less severe duty on the transistors, permits the use of inexpensive transformers, and allows the adaption to a variety of operating requirements.

A Phase-Regulated Transistor Power Supply—D. E. Deuitch and H. J. Paz (p. 279)

Transistors have been utilized effectively for class A regulation of power supplies. However, the power-handling capacity and high-temperature performance of these power supplies are basically restricted because of the power-temperature limitation of transistors.

This paper describes a type of regulated transistor power supply in which the dissipation in the regulator transistors is extremely small. This enables low-power transistors to control large amounts of power and permits substantial improvement of power supply capabilities at high temperature over that of the Class A regulated supply.

The principle of operation of this supply is similar to that used in thyratron regulation. The regulator transistors are operated as rectifying switches whose conduction period is varied in phase with respect to the ac input. Regulation is obtained by controlling the conduction phase of the transistors in response to load and input voltage variation.

A transistor switch circuit for this power supply is described together with general design and operating considerations for its power supply application. The performance of a 12-volt, 0- to 1-ampere developmental phase regulated power supply is discussed.

Abstracts of Transistor Conference Papers Not in This Issue (p. 66)

Correction (p. 284)

Correspondence (p. 285)

Reviews of Current Literature—Finite Duration Signals With Maximum Filtered Energy—J. A. Ville and J. Bouzitat (in French) (p. 293)

Mode Conversion Phenomena in the Case of Multilayer Conductors and its Effect on the Transmission Through Individual or Through Connected Partial Sections—Horst-Edgar Martin (in German) (p. 293)

Experimental Study of Tapped Delay-Line Filters—D. W. Lytle (p. 294)

Piecewise-Linear Network Theory—T. E. Stern (p. 294)

Double Tuned Filter Circuits for Wide Relative Pass-Band—F. Carassa (in Italian) (p. 294)

Analysis of Electric Circuits Containing Nonlinear Resistance—L. A. Pipes (in English) (p. 294)

Wave Dispersion in Disk Transmission Lines—Gerhard Piefke (in German) (p. 294)

Concerning the Chain Connection of Two Multipoles—W. Ruppe (in German) (p. 294)

Calculation of Current Distribution in a Linear Network—Joannis Vratsanos (in German) (p. 294)

Communications Systems

Vol. CS-5, No. 3, December, 1957

20/20 Visualization—J. E. Schlaikjer (p. 1)

Demonstration of Delay Distortion Correction by Time-Reversal Techniques—B. P. Bogert (p. 2)

Experiments relating to methods of correcting delay distortion by time-reversal have been made utilizing a slow-speed picture transmission system. The improvements in picture quality by phase correction of a 3 kc telephone loop 30.4 miles long and a 5 kc loop from Murray Hill, N. J., to Los Angeles, Calif., and back are demonstrated. The total distance that the signal was transmitted over the 5 kc loop was 16,600 miles and there were 16 type L carrier links involved. By way of an introduction, the improvement in the impulse response of networks and transmission circuits is discussed.

Quadruple-Diversity Tropospheric Scatter Systems—W. G. Long and R. R. Weeks (p. 8)

Operations Research and Communications Systems Planning—R. V. Higdon (p. 20)

A discussion is presented outlining the general concept of operations research for those who are not familiar with it. A necessarily brief description is given of efforts to apply these concepts to specifying effective communications for complex organizations or weapons systems.

High-Speed Frequency-Shift Keying of LF and VLF Radio Circuits—H. G. Wolff (p. 29)

Present VLF transmitters are limited in transmission speed to approximately 20 words per minute because of the bandwidth limitations of the High-Q antenna circuit. To permit an increase in transmission speed, an unique method has been developed which makes use of the variation of reactance of the antenna circuit in synchronism with frequency shift modulation of the carrier. The method makes possible the transmission of teletype or high speed Morse signals at speeds of 100 words per minute or more. This increase by a significant factor in present traffic handling capabilities of VLF stations can be accomplished by increasing the cost of the station less than ten per cent.

An Electronic Multicoupler and Antenna Amplifier for the VHF-Range—K. Fischer (p. 43)

A single-stage distributed amplifier for the frequency range from 25 to 223 mc/s may be used as an antenna amplifier for compensation of cable-attenuation or, in connection with a divider network, as a multicoupler for feeding six receivers from a common antenna. Single-stage amplification results in not only low noise level due to the parallel tube circuitry employed but also in a low cross-modulation figure. Second order distortions are minimized by special push-pull operation without doubling the number of tubes. Another advantage of the distributed amplifier is its reliability, which is further improved by dividing the power supply into two independent sections.

Contributors to This Issue (p. 49)

Electron Devices

Vol. ED-4, No. 4, October, 1957

Very High-Power Transistors with Evaporated Aluminum Electrodes—H. W. Henkels and G. Strull (p. 291)

The principles involved in the design of high-power and very high-power transistors are considered in brief. The important factors in high-gain, high-current transistor design are the emitter-injection efficiency, the emitter and collector planarity, and the base-bias high-current falloff. The fabrication techniques involved in the production of transistors to maximize the injection efficiency and planarity (by evaporation of aluminum electrodes) and minimize base bias drop (by choice of optimum emitter geometry), are discussed. The characteristics of devices capable of handling currents in the range from 1 to 10 amperes at very high common-emitter current gains ranging from 50 to above 300 are described.

An Equivalent Circuit for Microwave Noise at the Potential Minimum—A. E. Siegman and S. Bloom (p. 295)

It has been suggested that an inductive element should be added to Watkins RC equivalent circuit for the microwave noise current fluctuations at the potential minimum of a diode, and that this added element gives closer agreement with more recent work which shows a pronounced peak in noise current near the plasma resonance, $\alpha = \frac{1}{2}$. This paper presents an approximate analytical argument for the inclusion of an inductive element, based on the density-function method of analysis, which predicts the proper value for the inductance and yields a curve of reduction factor vs frequency in agreement with more detailed theories. The value of the inductance is such as to resonate with the capacitance of the potential minimum at $\alpha = \frac{1}{2}$. A discussion of the linearity of the potential minimum and of the idealized potential-minimum model is also included.

A Novel Approach to Microwave Duplexer Tube Design—L. Gould, E. V. Edwards, and I. Reingold (p. 300)

An encapsulated input window with an independent gas fill has been incorporated in the design of a broad-band duplexer tube. This design has been effective in separating the interdependence of the high-power characteristics of the tr tube. Recovery time and arc loss are determined predominantly by the input window design, whereas spike leakage energy and flat leakage power are determined by the tube body design. The two portions of the tube are designed independently for optimum performance. The effects of gas pressure and nature of the gas on the behavior of the high-power characteristics have been investigated. The factors determining adequate tube operation are discussed, and experimental data are presented to verify the advantages of the encapsulated structure.

Multicolor Storage Tube—C. D. Beintema, S. T. Smith, and L. L. Vant-Hull (p. 303)

Multicolor storage tubes for applications with low frame rates have been built by modification of direct-viewing storage tubes. A perforated shadow mask is placed between the three writing guns and the storage surface. This shadow mask allows electrons from each writing gun to strike discrete storage areas, each containing a single aperture in register with a color dot on the view plate. In this way, it is possible to write and store electrical signals independently in adjacent color areas. Factors causing color impurity are described, together with the steps taken to minimize their effects. A tube has been built that shows good color purity in a 6-inch-diameter circle; it has 75 total color dots per inch resolution, 8 foot-lamberts brightness, and about 1-minute persistence. Other possible multicolor storage tube designs are discussed.

Experimental Notes and Techniques (p. 309)

Contributors (p. 311)

Index to IRE Transactions on Electron Devices—Volume ED-4, 1957 (follows p. 313)

Engineering Management

Vol. EM-4, No. 4, December, 1957

The Climate of Research in the University—C. W. Gartlein (p. 109)

Unionization of Engineers—I—Joseph Amann (p. 113)

Unionization of Engineers—II—H. H. Rains (p. 116)

The Nation's Need for Greater Scientific and Technical Strength—Means for its Attainment—M. J. Kelly (p. 122)

Dynamic Project-Orientated Industrial Organization—Henry Imus (p. 128)

The Establishment and Operation of a Semiautonomous Field Organization—J. D. Finley (p. 132)

Abstracts and References

Compiled by the Radio Research Organization of the Department of Scientific and Industrial Research, London, England, and Published by Arrangement with that Department and the *Electronic and Radio Engineer*, incorporating *Wireless Engineer*, London, England

NOTE: The Institute of Radio Engineers does not have available copies of the publications mentioned in these pages, nor does it have reprints of the articles abstracted. Correspondence regarding these articles and requests for their procurement should be addressed to the individual publications, not to the IRE.

Acoustics and Audio Frequencies..... 516
Antennas and Transmission Lines..... 516
Automatic Computers..... 517
Circuits and Circuit Elements..... 517
General Physics..... 519
Geophysical and Extraterrestrial Phenomena..... 520
Location and Aids to Navigation..... 521
Materials and Subsidiary Techniques.. 521
Mathematics..... 523
Measurements and Test Gear..... 523
Other Applications of Radio and Electronics..... 525
Propagation of Waves..... 525
Reception..... 525
Stations and Communication Systems.. 526
Subsidiary Apparatus..... 526
Television and Phototelegraphy..... 527
Transmission..... 527
Tubes and Thermionics..... 527
Miscellaneous..... 528

The number in heavy type at the upper left of each Abstract is its Universal Decimal Classification number and is not to be confused with the Decimal Classification used by the United States National Bureau of Standards. The number in heavy type at the top right is the serial number of the Abstract. DC numbers marked with a dagger (†) must be regarded as provisional.

U.D.C. NUMBERS

Extensions and changes in U.D.C. numbers published in P.E. Notes, up to and including P.E. Note 609, will be introduced in Abstracts and References where applicable, notably the subdivisions of 621.372.8 waveguides published in P.E. Note 594. U.D.C. publications are obtainable from The International Federation for Documentation, Willem Witsenplein 6, The Hague, Netherlands, or from The British Standards Institution, 2 Park Street, London, W.1, England.

JOURNAL REFERENCES

References to Russian publications will henceforth be based on the Russian title which will be abbreviated on the principles of The World List of Scientific Periodicals. The main changes are as follows:

Dokl. Ak. Nauk S.S.S.R. (formerly C.R. Acad. Sci. U.R.S.S.),

Izv. Ak. Nauk S.S.S.R. (formerly Bull. Acad. Sci. U.R.S.S.).

The Index to the Abstracts and References published in the PROC. IRE from February, 1956 through January, 1957 is published by the PROC. IRE, May, 1957, Part II. It is also published by *Electronics and Radio Engineer*, incorporating *Wireless Engineer*, and included in the March, 1957 issue of that journal. Included with the Index is a selected list of journals scanned for abstracting with publishers' addresses.

ACOUSTICS AND AUDIO FREQUENCIES

534.2–13:536.3 1

Effect of Heat Radiation on Sound Propagation in Gases—P. W. Smith, Jr. (*J. Acoust. Soc. Amer.*, vol. 29, pp. 693–698; June, 1957.)

534.21–8–14 2

Ultrasonic Propagation Measurement in Sea Water up to 400 kc/s—T. Hashimoto and Y. Kikuchi. (*J. Acoust. Soc. Amer.*, vol. 29, pp. 702–707; June, 1957.) Methods of measurement for horizontal and for vertical propagation are described. Measured values of absorption were 10–20 db/km at 28 kc increasing to 120 db/km at 400 kc.

534.23 3

Sound Transmission through Thin Cylindrical Shells—P. W. Smith, Jr. (*J. Acoust. Soc. Amer.*, vol. 29, pp. 721–729; June, 1957.) An analysis of the impedance presented by a thin cylindrical elastic shell to a pressure or normal stress as a function of the axial wavelength and the angular dependence of the forces.

534.23:537.227 4

Vibrations of Ferroelectric Cylindrical Shells with Transverse Isotropy: Part 1—Radially Polarized Case—J. F. Haskins and J. L. Walsh. (*J. Acoust. Soc. Amer.*, vol. 29, pp. 729–734; June, 1957.) Expressions for the coupled mechanical vibrations and electrical admittance of ferroelectric tubes having transverse isotropy are derived and the results supported by experimental data.

534.232 5

Experimental Investigation of Conical Horns Used with Underwater Sound Transducers—W. R. Owens and C. M. McKinney. (*J. Acoust. Soc. Amer.*, vol. 29, pp. 744–748; June, 1957.) A simple conical horn lined with pressure-release material is very effective in increasing the axial sensitivity of transducers and improving directivity. Design curves are given.

534.232:534.24 6

Effect of a Reflecting Plane on the Power Output of Sound Sources—U. Ingard and G. L. Lamb, Jr. (*J. Acoust. Soc. Amer.*, vol. 29, pp. 743–744; June, 1957.) The effect of a rigid reflecting plane on the output from a sound source above it is expressed as a "power amplification factor." This is calculated for a number of elementary sound sources and power output is determined as a function of source height.

534.414 7

Accoustic Impedance of a Helmholtz Resonator at Very High Amplitude—D. A. Bies and O. B. Wilson, Jr. (*J. Accoust. Soc. Amer.*, vol. 29, pp. 711–714; June, 1957.) A Helmholtz resonator terminating a 10-inch diameter tube has been investigated for sound pressure levels 100–170 db. With increasing sound pressure the same general rise in acoustic resistance and resonance frequency was observed for two different mountings.

534.612 8

Acoustical Radiation Pressure due to Incident Plane Progressive Waves on Spherical Objects—G. Maidanik. (*J. Acoust. Soc. Amer.* vol. 29, pp. 738–742; June, 1957.)

534.75 9

On the Fusion of Sounds Reaching Different Sense Organs—D. E. Broadbent and P. Ladefoged. (*J. Acoust. Soc. Amer.*, vol. 29, pp. 708–710; June, 1957.) Experiments with synthetically produced speech show that fusion occurs when the first formant is presented to one ear and the second formant to the other, but not if the formants are given different fundamental frequencies.

534.78 10

Constant-Ratio Rule for Confusion Matrices in Speech Communication—F. R. Clarke. (*J. Acoust. Soc. Amer.*, vol. 29, pp. 715–720; June, 1957.) "Three experiments are reported which give support to an empirical rule which may be used for predicting the entries in a closed confusion matrix for any subset of items drawn from a master set of items with a known confusion matrix."

534.78 11

The Intelligibility of Synthetic Speech—O. Warns. (*Frequenz*, vol. 11, pp. 169–175; June, 1957.) The results of subjective tests on the intelligibility of synthetic logatoms are analyzed. For the German language 700–1100 interchangeable speech elements would be adequate, requiring an information rate of 40 bits per second.

621.395.625.3:621.397.5 12

Video Tape Recorder Design—(See 294.)

ANTENNAS AND TRANSMISSION LINES

621.315.212 13

The Characteristic Impedance of Coaxial Cables—F. Raggi. (*Note Recensioni Notiz.*, vol. 6, pp. 174–188; March/April, 1957.) Note summarizing the factors which determine the characteristic impedance of coaxial cables.

621.315.212:621.397.24 14

A New 4-Mc/s Coaxial Line Equipment—C.E.L. No. 6A—M. E. Collier and W. G. Simpson. (*P.O. Elec. Eng. J.*, vol. 50, Pt. 1, pp. 24–34; April, 1957.) The equipment described is suitable for the transmission of either 16 telephony supergroups (960 circuits) or a 405-line television signal.

621.315.212:621.397.24 15

A 4-Mc/s Coaxial Line Equipment—C.E.L. No. 4A—E. Davis. (*P.O. Elec. Eng. J.*, vol. 50, Pt. 2, pp. 92–97; July, 1957.) A description of

equipment suitable for the transmission of either 17 telephony supergroups (1020 circuits) or a television signal of 3-mc video bandwidth. See also 14 above.

621.372.2 16
Return Loss: Part 1—T. Roddam. (*Wireless World*, vol. 63, pp. 521–524; November, 1957.) The use of the concept of return loss instead of standing wave ratios is recommended in dealing with reflections of short pulses on long loss-free incorrectly terminated lines.

621.372.8:621.372.5 17
Noisy and Noise-Free Two-Port Networks Treated by the Isometric Circle Method—E. F. Bolinder. (PROC. IRE, vol. 45, pp. 1412–1413; October, 1957.)

621.372.823 18
Circular Electric Wave Transmission through Serpentine Bends—H. G. Unger. (*Bell Sys. Tech. J.*, vol. 36, pp. 1279–1291; September, 1957.) An analysis of the propagation in a circular waveguide with equally spaced discrete supports and deformed elastically into a serpentine bend under its own weight.

621.372.831.4 19
Slots in an Imperfectly Conducting Waveguide—B. Chatterjee. (*Indian J. Phys.*, vol. 40, pp. 278–282; May, 1957.) The shunt conductance of a slot initially increases with departure from perfect conductivity of the guide wall but decreases rapidly in almost direct proportion to further decreases in conductivity.

621.372.852.21 20
Theory of Curved Circular Waveguide containing an Inhomogeneous Dielectric—S. P. Morgan. (*Bell Sys. Tech. J.*, vol. 36, pp. 1209–1251; September, 1957.) General equations are derived for all modes in a curved circular waveguide containing an inhomogeneous dielectric. The results are applied to the problem of preventing mode conversion from TE_{01} to TM_{11}. Design equations are given for various compensators with criteria for keeping the power level of spurious modes at a minimum.

621.372.853.1 21
Circular Electric Wave Transmission in a Dielectric-Coated Waveguide—H. G. Unger. (*Bell Sys. Tech. J.*, vol. 36, pp. 1253–1278; September, 1957.) The mode conversion from the TE_{01} wave to the TM_{11} wave in a curved circular waveguide may be reduced by applying a thin uniform dielectric coating to the inner wall. Design curves are given for both uniform bends of small radius and for large bending radii which may occur in a normally straight guide.

621.372.853.1 22
Normal Mode Bends for Circular Electric Waves—H. G. Unger. (*Bell Sys. Tech. J.*, vol. 36, pp. 1292–1307; September, 1957.) The TE_{01}-TM_{11} degeneracy is removed by a thin dielectric coating, and a further reduction in the mode conversion at a bend is obtained by tapering the curvature along the guide. Details are given of the bend loss for $\lambda = 5.4$ mm. See also 21 above.

621.396.674:621.396.93 23
A Versatile Multiport Biconical Antenna—R. C. Honey and E. M. T. Jones. (PROC. IRE, vol. 45, pp. 1374–1383; October, 1957.) This antenna can be used as a wide-band direction finder, as it excites in the feeding waveguide modes whose ratios are azimuth dependent. It also has uses as a multiplexer.

621.396.677 24
Bi-directional F.M. Antennas—H. B. Dent. (*Wireless World*, vol. 63, pp. 534–536; November, 1957.) Description of stacked horizontal half-wave dipoles which are simple to construct and erect.

621.396.677.43 25
Rhombic Antennas—F. J. Norman and J. F. Ward. (*Electronic Radio Eng.*, vol. 34, pp. 398–403; November, 1957.) "The design of aperiodic rhombic antennas is examined and a method derived whereby a set of charts of open scale yields all the antenna parameters of practical significance for high-frequency operation. The angle of fire and the gain with respect to a dipole in free space are displayed for an adequate range of antenna side lengths and included angles. Corrections are given for the height above ground and a simple method to find the shape of the main lobe is suggested."

621.396.677.8:523.16 26
The Mullard Radio Astronomy Observatory, Cambridge—Ryle. (See 107.)

621.396.677.833:523.16 27
World's Largest Radio Telescope—(See 108.)

621.396.677.85 28
Calculated Intensity and Phase Distribution in the Image Space of a Microwave Lens—G. W. Farnell. (*Can. J. Phys.*, vol. 35, pp. 777–783; June, 1957.) Intensity and constant-phase contours and an energy-flow diagram are shown for a 3.2-cm-λ lens with exit pupil of 25-cm radius distant 105 cm from the image point. Calculations are based on scalar diffraction theory. Results of measurements show close agreement.

621.396.677.85 29
Study of Optical Diffraction Images at Microwave Frequencies—M. P. Bachynski and G. Bekefi. (*J. Opt. Soc. Amer.*, vol. 47, pp. 428–438; May, 1957.) "Experimental investigations of the intensity distribution in the region of the focus of microwave lenses are described. The circularly symmetric lenses, made from polystyrene plastic, were illuminated by a linearly polarized beam of radiation of 1.25-cm wavelength. Most of the measurements are presented in the form of intensity contours in planes both containing the principal ray and lying perpendicular to it. Images formed by nearly perfect optical systems and by systems suffering from various third-order monochromatic aberrations were examined. In most cases the results are compared with calculations made from the scalar-diffraction theory of optical systems. In general, good agreement between theory and experiment is found."

AUTOMATIC COMPUTERS

681.142 30
Controlling the Digital Computer—R. W. Hamming. (*Sci. Mon.*, vol. 85, pp. 169-175; October, 1957.) A nonmathematical discussion of the programming and application of computers for scientific purposes.

681.142 31
An Experimental 50-Mc/s Arithmetic Unit—R. M. Walker, D. E. Rosenheim, P. A. Lewis, and A. G. Anderson. (*IBM J. Res. Devel.*, vol. 1, pp. 257–278; July, 1957.) Detailed description of a unit which performs a repetitive multiplication program and checks the results for errors.

681.142 32
The Design of the Ferranti Pegasus Computer: Part 2—G. Emery. (*Electronic Eng.*, vol. 29, pp. 420–425; September, 1957.) The detailed engineering aspects of the design problem are discussed. Part 1: 3753 of 1957 (Braunholtz).

681.142 33
A 32000-Word Magnetic-Core Memory—E. Foss and R. S. Partridge. (*IBM J. Res. Devel.*, vol. 1, pp. 102–109; April, 1957.) The storage matrix consists of $128 \times 256 \times 36$ ferrite cores and has a read-write cycle of 12 μsec. Its construction is described, together with the driver and sense amplifier circuits.

681.142 34
A Positive-Integer Arithmetic for Data Processing—R. W. Murphy. (*IBM J. Res. Devel.*, vol. 1, pp. 158–170; April, 1957.)

681.142 35
Irredundant Disjunctive and Conjunctive Forms of a Boolean Function—M. J. Ghazala (Gazale). (*IBM J. Res. Devel.*, vol. 1, pp. 171–176; April, 1857.) A thorough algebraic method is described for determining the complete set of irredundant normal and conjunctive forms. The procedure is mechanical and the method can be applied for programming computers.

681.142 36
Electronic Computers—W. Taeger. (*Frequenz*, vol. 11, pp. 185–191; June, 1957.) The application of analog computers to the solution of control-system problems is discussed.

681.142 37
Approximating Nonlinear Functions by Shunt-Loading Tapped Potentiometers in Analogue Computing Machines—D. W. C. Shen. (*Electronic Eng.*, vol. 29, pp. 434–439; September, 1957.)

681.142:621.314.7 38
The Multipurpose Bias Device: Part 1—The Commutator Transistor—B. Dunham. (*IBM J. Res. Devel.*, vol. 1, pp. 116–129; April, 1957.) A study of the application of the Rutz commutator transistor to three-input, one-output logical problems for handling by automatic computer systems. The Rutz commutator is a single-emitter amplitude-sensitive device with three separate input wires applied to the emitter. Its design will be detailed in a subsequent paper.

681.142:621.314.7 39
Two-Collector Transistor for Binary Full Addition—Rutz. (See 315.)

681.142:621.395.625.3 40
A Mathematical Model for Determining the Probabilities of Undetected Errors in Magnetic Tape Systems—M. Schatzoff and W. B. Harding. (*IBM J. Res. Devel.*, vol. 1, pp. 177–184; April, 1957.)

681.142:621.395.625.3 41
The Magnetic Tape Store for Pegasus—T. G. H. Braunholtz and D. Hogg. (*Electronic Eng.*, vol. 29, pp. 484–489; October, 1957.)

681.142:621.395.625.3 42
The Recording of Digital Information on Magnetic Drums—D. G. N. Hunter and D. S. Ridler. (*Electronic Eng.*, vol. 29, pp. 490–496; October, 1957.) "Methods of representing binary digital information on magnetic drums are discussed with regard to their reliability, cost, and technical merits."

CIRCUITS AND CIRCUIT ELEMENTS

621.3:061.3 43
International Components Symposium—(*Electronic Radio Eng.*, vol. 34, pp. 428–431; November, 1957.) Summary of papers read at the Royal Radar Establishment, Malvern, in September, 1957. Reliability, efficient use of space, liquid cooling techniques, and optimum component shapes for automatic assembly are discussed.

621.3.011.3 44
Calculation of Inductance of Toroids with Rectangular Cross Section and Few Turns—R. F. Schwartz. (PROC. IRE, vol. 45, pp. 1416–1417; October, 1957.)

621.3.049.7:621.39.03:061.3 45
"Solid Circuits"—(*Wireless World*, vol. 63, pp. 516–517; November, 1957.) Discussion of the International Symposium on Electronic Components held at Malvern, England. A "solid circuit" forming the equivalent of several transistors connected by resistors and capacitors is obtained by depositing films of conductive, resistive, and dielectric materials on a small block of semiconductor material. The solution of problems regarding the operation of components at high temperatures is mentioned.

621.3.049.75 46
Printed Circuits in Receiver Construction—W. I. Flack. (*J. Telev. Soc.*, vol. 8, pp. 176–185; January/March, 1957.) Outline of development of the printed circuit, and description of modern production techniques.

621.3.049.75 47
Pro and Con on Seven Different Methods of Printed Wiring—A. E. Stones. (*Electronic Inds. Tele-Tech.*, vol. 16, pp. 64–66, 158; March, 1957.) The basic techniques for each method are described and compared. A table of relevant U.S. patents is included.

621.314.6 48
A General Circuit Theorem on Rectification—J. W. Gewartowski. (PROC. IRE, vol. 45, p. 1410; October, 1957.) Nonlinear capacitors and inductors cannot effect rectification unless nonlinear resistance is present in the circuit.

621.318.424 49
New Method of Evaluating Ferro-inductors—W. J. Polydoroff. (*Electronic Inds. Tele-Tech.*, vol. 16, pp. 78–79, 150; April, 1957.) Formulas for calculating the insertion loss and the resistance increase due to the iron core are derived. The practical factors governing optimum coil design are investigated.

621.318.57:621.387 50
Cold-Cathode Voltage-Transfer Circuits—J. H. Beesley. (*GEC Telecommun.*, no. 23, pp. 6–19; February, 1957.) Practical techniques used in the application of cold-cathode triodes are given in detail. A number of circuit diagrams are included.

621.319.4:537.311.33 51
Charge and Discharge of a Non-linear Condenser through a Linear Nondissipative Inductance—A. Mozumder. (*Z. angew. Math. Phys.*, vol. 8, pp. 261–280; July 25, 1957.) Macdonald (*J. Chem. Phys.*, vol. 22, pp. 1317–1322; August, 1954) has shown that for a capacitor with a semiconductor as dielectric the capacitance is proportional to $\sinh \alpha V/\alpha V$ where V is the voltage across the capacitor and α is a constant. A circuit is analyzed in which such a capacitor is connected in series with a lossless inductance and a direct-voltage source, and a comparison is made with an exponential capacitor ($C\alpha \exp |\alpha V|$). Applications to the generation of rectangular and triangular waveforms are indicated. See also 958 of 1955 (Macdonald and Brackman).

621.319.42:621.3.049.75 52
Evaluating Base Materials for Printed Capacitors—J. J. Logan. (*Electronic Inds. Tele-Tech.*, vol. 16, pp. 72–73., 160; August, 1957.) Definition of terms specifying the losses of base materials used for printed circuits which affect the size and Q factor of printed capacitors.

621.372.412.002.2:549.514.51:621.793.14 53
A Vacuum Plant for the Frequency Calibration of Quartz Vibrators—J. Green, L. Holland, and B. D. Power. (*Electronic Eng.*, vol. 29, pp. 440–444; September, 1957.) See also 503 of 1956 (Awender, *et al*).

621.372.5 54
A Network Theorem—E. Green. (*Marconi Rev.*, vol. 20, pp. 35–38; 2nd Quart., 1957.) The impedance level of half a symmetrical network can be changed without altering the frequency response; the use of this theorem for the solution of network problems is discussed and illustrated by an example.

621.372.5:621.372.8 55
Noisy and Noise-Free Two-Port Networks Treated by the Isometric Circle Method—Bolinder. (PROC. IRE, vol. 45, pp. 1412–1413; October, 1957.)

621.372.5:621.375.2.018.75 56
On the Design of Four-Terminal Interstages for Pulse Applications—A. K. Choudhury and N. B. Chakrabarti. (*Indian J. Phys.*, vol. 40, pp. 193–210; April, 1957.) The limits set by the input and output capacitance on the time response and the conditions for no overshoot are determined. Methods for achieving the necessary pole distributions are described and circuit networks suggested.

621.372.52:621.314.7 57
The Mathematical Treatment of Transistor Feedback Circuits—W. Glaser. (*Nachr-Tech.*, vol. 7, pp. 159–162; April, 1957.) Formulas are tabulated giving in convenient form the parameters of transistor networks for four types of feedback circuit.

621.372.54.029.64 58
Design and Development of Strip-Line Filters—E. H. Bradley. (IRE TRANS., vol. MTT-4, pp. 86–93; April, 1956. Abstract, PROC. IRE, vol. 44, p. 956; July, 1956.)

621.372.543.2:538.652 59
Concentric-Shear-Mode 455-kc/s Electromechanical Filter—R. W. George. (*RCA Rev.*, vol. 18, pp. 186–194; June, 1957.) An experimental filter of simplified design is described which consists of four magnetostrictive ferrite disk resonators.

621.372.55:621.396.4:621.376.3 60
A Broad-Band Variable Group-Delay Equalizer—R. Hamer and R. C. Wilkinson. (*P.O. Elec. Eng. J.*, vol. 50, Pt. 2, pp. 120–123; July, 1957.) The equalizer has been developed for use in fm microwave systems. It is inserted in the 70-mc IF signal path in long radio-relay systems. The performance is adequate for the transmission of frequency-division-multiplex telephony of at least 600 channels, or subcarrier color-television transmission.

621.373.029.64:538.569.4 61
Comments on Frequency Pulling of Maser Oscillators—C. H. Townes. (*J. Appl. Phys.*, vol. 28, pp. 920–921; August, 1957.) The physical origin is illustrated of the theoretically predicted reduction in frequency pulling with increasing number of beam molecules, and reasons are given for its failure to occur in practice.

621.373.029.64:538.569.4:538.221 62
A Solid-State Microwave Amplifier and Oscillator using Ferrites—M. T. Weiss. (*Phys. Rev.*, vol. 107, p. 317; July 1, 1957.) Experimental results obtained with an oscillator based on the proposal by Suhl (3076 of 1957). The active element is a piece of magnetized ferrite at room temperature.

621.373.421 63
Sensitivity of a Self-Excited Oscillator—I. S. Shpigel', M. D. Raĭzer, and E. A. Myae. (*Zh. Tekh. Fiz.*, vol. 27, pp. 387–390; February, 1957.) Theoretical and experimental investigation of the characteristics of a tube feedback oscillator suitable for nuclear resonance detection.

621.373.5:621.396.621 64
Crystal Oscillators in Communication Receivers—A. G. Manke. (IRE TRANS., vol. PGVC-7, pp. 10–15; December, 1956. Abstract, PROC. IRE, vol. 45, p. 258; February, 1957.)

621.373.52:621.373.431.1 65
Unijunction Transistor forms Flip-Flop—E. Keonjian and J. J. Suran. (*Electronics*, vol. 30, pp. 165–167; September 1, 1957.) The construction and performance are described of a multivibrator circuit for a stable or monostable operation (see also 2878 of 1955). Its active element is the double-base diode, a 3-terminal p-n junction device [see 3562 of 1956 (Suran)].

621.373.52.018.756 66
Pulse Generator uses Junction Transistors—E. J. Fuller. (*Electronics*, vol. 30, pp. 176–179; September 1, 1957.) A transistor circuit is described giving pulses of 1 to 10-μsec. duration at repetition rates of 50–5000 pulses per second with internal delays of 1–100 μsec.

621.373.52.018.78 67
Distortion in Transistor Amplifiers—P. Tharma. (*Mullard tech. Commun.*, vol. 3, pp. 62–64; March, 1957.) An analysis of the distortion in low-level grounded-emitter stages are due to input-circuit nonlinearity and to variations of collector-to-base current gain.

621.373.52.029.4 68
Low-Frequency Transistor Oscillators—L. G. Gripps. (*Mullard tech. Commun.*, vol. 3, pp. 44–58; March, 1957. *Electronic Applic. Bull.*, vol. 17, pp. 113–128; May, 1957.) Theoretical treatment of a junction-transistor oscillator for frequencies of a few kc. Frequency and amplitude stability, conversion efficiency and the conditions governing starting, are considered. A practical circuit design is derived and experimental results are given.

621.374.32 69
Build-Up of Large Signals with Elimination of Reflections in Magnetostrictive Storage Lines—D. Maeder. (*Z. angew. Math. Phys.*, vol. 8, pp. 326–327; July 25, 1957.) Greater reliability and increased storage capacity are obtained by substituting twelve energizing coils for the usual one. With this arrangement, a steel-wire delay line can be used. See also 2385 of 1957.

621.374.33:621.314.7 70
A Transistor Gating Matrix for a Simulated Warfare Computer—W. H. MacWilliams, Jr. (*Bell Lab. Rec.*, vol. 35, pp. 94–99; March, 1957.) Brief description of a circuit, devised in 1949, which used a matrix of 4×10 point-contact transistors. Amplification of signals was also achieved.

621.374.5 71
Signal-Enhanced Delay Line—T. I. Humphreys. (*Electronic Inds. Tele-Tech.* vol. 16, pp. 70–71, 167; August, 1957.) To maintain pulse shape the high-frequency response of the delay line described is improved by selective amplification.

621.374.5:621.396.962.3 72
Pulse Compression—R. Krönert. (*Nachr-Tech.*, vol. 7, pp. 148–152, 162; April, 1957.) A method is described for compressing frequency-modulated rf pulses, *i.e.*, shortening them and increasing their amplitude by passing them

through a delay-distortion network consisting of a chain of lattice quadripoles. The theory outlined is based on work by Cauer, published posthumously. Its practical application in the field of radar should result in higher resolving power for a given snr.

621.375:621.372.51 73
Minimizing Mismatch Loss—H. E. Hollmann. (*Electronic Inds. Tele-Tech.* vol. 16, pp. 74–75, 165; August, 1957.) Simple formulas and curves are given.

621.375.2+621.375.4 74
Upper Limits of Output Power in Vacuum-Tube and Transistor A.C. Amplifiers—L. M. Vallese. (*Commun. and Electronics*, no. 29, pp. 87–92; March, 1957.) Simple analysis and comparison based on idealized characteristics.

621.375.2 75
Stacked Valve Circuits—J. B. Earnshaw. (*Electronic Radio Eng.*, vol. 34, pp. 404–406; November, 1957.) An analysis by means of feedback theorems and modified equivalent circuits. Application of the method to the cascade amplifier and the cathode-follower circuits is given in detail.

621.375.2.029.3 76
Single-Ended Push-Pull Output Stages—(*Electronic Applic. Bull.*, vol. 17, pp. 81–106; May, 1957.) The development of low-dc-resistance pentodes and high-resistance moving-coil loudspeakers has made possible the construction of transformerless output stages several types of which are described. The paper is based on the work of W. Aschermann and J. Rodrigues de Miranda (see 3727 of 1957).

621.375.2.029.4 77
A Low-Frequency Selective Amplifier—C. K. Battye. (*J. Sci. Instr.*, vol. 34, pp. 263–265; July, 1957.) The frequency is variable in steps from 1 to 1000 cps. The selectivity can be set up to $Q=100$. The amplifier is dc coupled; a twin-T network shunted by a capacitor acts as a selective network in the negative feedback line.

621.375.2.029.55 78
PT-15 P.A. Unit—J. N. Walker. (*Short Wave Mag.*, vol. 14, pp. 624–630; February, 1957.) Description of a band-switching rf amplifier for 80, 40, and 20 m, which uses a pair of tubes Type PT 15 in parallel.

621.375.221.029.62:621.396.4:621.376.3 79
A Broad-Band Intermediate-Frequency Amplifier for Use in Frequency-Modulation Microwave Radio-Relay Systems—R. Hamer and C. H. Gibbs. (*P.O. Elec. Eng. J.*, vol. 50, Pt. 2, pp. 124–126; July, 1957.) A 70-mc amplifier is described which is suitable for the transmission of 600-channel frequency-division-multiplex telephony or subcarrier color-television signals in fm microwave radio-relay systems. A test-tone/noise ratio of 70 db is not significantly degraded after transmission through five amplifiers in tandem.

621.375.227.029.3 80
400-Watt Audio Amplifier—G. R. Woodville. (*Wireless World*, vol. 63, pp. 543–546; November, 1957.) The circuit described includes small output tubes in parallel push-pull connection.

621.375.3 81
Self-Balancing Magnetic Amplifiers of the Differential-Feedback Type—W. A. Geyger. (*Commun. and Electronics*, no. 29, pp. 39–46; March, 1957.) A 60-cps magnetic amplifier for extending the range of a moving-coil ink recorder is described.

621.375.4.029.3:629.13 82
The Use of Transistors in Airborne Audio Equipment—V. P. Holec. IRE TRANS., vol. AU-4, pp. 90–93; July/August, 1956. Abstract, PROC. IRE, vol. 44, p. 1641; November, 1956.)

621.375.43.029.3:621.314.7 83
Negative-Feedback Transistor Amplifiers—H. R. Lowry. (*Radio Ü Telev. News*, vol. 57, pp. 55–58, 109; May, 1957.) Design data are given for high-fidelity af amplifiers.

621.375.9.029.64:538.569.4 84
Microwave Amplification by MASER Techniques—W. V. Smith. (*IBM J. Res. Devel.*, vol. 1, pp. 232–238; July, 1957.) Elementary analysis of maser operation, including its application to wide-band, short-transit-time amplification.

621.376:621.316.7.078 85
Demodulator-Limiter for Control System Signals—N. L. Johanson. (*Electronics*, vol. 30, p. 155; September 1, 1957.) Description of transistor circuit for automatic control systems which acts as limiter during modulation or demodulation.

621.376.239 86
Magnetically Keyed, Phase-Sensitive Demodulators—R. B. Mark, W. X. Johnson, and P. R. Johannessen. (*Commun. and Electronics*, no. 29, pp. 1–6; March, 1957.) The operation and performance of a pulse-shaping circuit using magnetic reactors is described. The properties of three types of phase-sensitive demodulator are compared. Diode demodulators have linear characteristics, magnetic amplifier demodulators have high input impedance, and transistor demodulators combine good linearity with low noise level.

621.376.4:621.314.7 87
Transistorized Phase Discriminators—A. N. De Sautels. (*Commun. and Electronics*, no. 29, pp. 19–26; March, 1957.) Half-wave and full-wave phase discriminators are described with two- or three-terminal dc outputs. An analysis of the operating characteristics of transistors in discriminator circuits is given; temperature stability and power limitations are discussed.

GENERAL PHYSICS

535.33–1 88
Interferometry for the Far Infrared—J. Strong. (*J. Opt. Soc. Amer.*, vol. 47, pp. 354–357; May, 1957.)

535.61–1 89
Infrared Radiation and its Detection—(*Electronic Radio Eng.*, vol. 34, pp. 412–415; November, 1957.) A comparison of the sensitivity and time constant of available detectors of infrared radiation. Thermal detectors of thermocouple, bolometer, and pneumatic type and photoelectric detectors are discussed.

537.311.1:536.21:537.311.33 90
The Lorenz Number—P. J. Price. (*IBM J. Res. Devel.*, vol. 1, pp. 147–157; April, 1957.) The theory of the Lorenz number of a conducting crystal is developed for the "band" and "one-electron" models of the electron assembly. With certain approximations, the Lorenz number is found to be equal to the mean square fluctuation of the thermoelectric power.

[537.311.1+536.212.2]:539.13 91
Some Scattering Problems in Conduction Theory—P. G. Klemens. (*Can. J. Phys.*, vol. 35, pp. 441–450; April, 1957.) An expression derived for the scattering of electrons by inhomogeneous slowly varying strain fields is applied to scattering by dislocations and stacking faults.

537.5 92
Free-Path Formulae for the Coefficient of Diffusion and Velocity of Drift of Electrons in Gases—L. G. H. Huxley. (*Aust. J. Phys.*, vol. 10, pp. 118–129; March, 1957. Correction, *ibid.*, vol. 10, p. 329; June, 1957.)

537.5:538.6 93
Type of Plasma Oscillations in a Magnetic Field—S. I. Braginski. (*Dokl. Ak. Nauk S.S.S.R.*, vol. 115, pp. 475–478; July 21, 1957.) Mathematical analysis based on a model of ideal electron and ion gases.

537.5:538.63 94
Free-Path Formulae for the Electronic Conductivity of a Weakly Ionized Gas in the Presence of a Uniform and Constant Magnetic Field and a Sinusoidal Electric Field—L. G. H. Huxley. (*Aust. J. Phys.*, vol. 10, pp. 240–245; June, 1957.) "A general free path formula is given for the drift velocity of electrons in a weakly ionized gas in a sinusoidal electric field. Most special cases of interest, including the magnetic deflection of an electron stream in a gas, are readily derivable from the general formula. The results find application in microwave and ionospheric studies of the motion of electrons in gases as well as in experiments on the magnetic deflection of an electron stream." See also 92 above.

537.525.8 95
Oscillations in Direct-Current Glow Discharges—A. M. Pilon. (*Phys. Rev.*, vol. 107, pp. 25–27; July 1, 1957.) Experimental results are given concerning the stable oscillations with the same period which occur in the current and in the light emitted by the positive column.

538.244.2 96
Magnetization in the Presence of Magnetic Viscosity—M. I. Rozovski. (*Zh. Tekh. Fiz.*, vol. 27, pp. 355–359; February, 1957.) A mathematical expression is derived for solving problems of magnetization of magnetically viscous samples, in particular those of cylindrical shape. See also 3697 of 1956 (Tikhonov and Samarski).

538.566:535.42 97
Diffraction of Electromagnetic Waves by Ribbon and Slit: Part 1—Y. Nomura and S. Katsura. (*J. phys. Soc. Japan*, vol. 12, pp. 190–200; February, 1957.) Rigorous solutions are presented for a wave incident on a plane normal to the edge of the ribbon or slit, but with arbitrary angles of incidence and polarization. For diffraction by circular plate and hole, see 3235 of 1955.

538.566:535.422]+534.26 98
Diffraction of a Spherical-Wave Pulse by a Half-Plane Screen—J. R. Wait. (*Can. J. Phys.*, vol. 35, pp. 693–696; May, 1957.) Fourier-integral treatment for a point source.

538.569.4 99
Distortions of Magnetic Resonances by Additional and Excessive Oscillatory Fields—H. R. Lewis, A. Pery, W. Quinn, and N. F. Ramsey. (*Phys. Rev.*, vol. 107, pp. 446–449; July 15, 1957.) A theoretical explanation is given of the shift of the resonance frequency which occurs as a result of the presence of an extraneous rf electric field. See also 1386 of 1956 (Ramsey).

538.569.4:539.15.098 100
The Dependence of the Amplitude of the First Harmonic of Nuclear-Magnetic-Resonance Absorption on the Amount of Detuning

—I. S. Shpigel', M. D. Raizer, and E. A. Myae. (*Zh. Tekh. Fiz.*, vol. 27, pp. 351–354; February, 1957.)

538.569.4:546.171.1 101
Equivalence between the Line Width and the Rate of Energy Relaxation in the Inversion Spectrum of Ammonia—K. Tomita. (*Progr. theoret. Phys.*, vol. 17, pp. 513–515; March, 1957.)

538.6 102
On the Equilibrium Configurations of Oblate Fluid Spheroids under the Influence of a Magnetic Field—S. P. Talwar. (*Proc. nat. Inst. Sci. India*, Pt. A, vol. 22, pp. 316–323; September 26, 1956.)

538.6 103
Toroidal Oscillations of a Spherical Mass of Viscous Conducting Fluid in a Uniform Magnetic Field—K. Stewartson. (*Z. angew. Math. Phys.*, vol. 8, pp. 290–297; July, 25 1957.) See also 3352 of 1956.

539.1:541.124 104
Theoretical Treatment of the Kinetics of Diffusion-Limited Reactions—T. R. Waite. (*Phys. Rev.*, vol. 107, pp. 463–470; July 15, 1957.) The diffusion-limited reaction $A+B \rightarrow AB$ has been solved for a random initial distribution of A and B particles.

GEOPHYSICAL AND EXTRATERRESTRIAL PHENOMENA

523.16:551.510.535 105
Radio-Star Ridges—M. Dagg. (*J. Atmos. Terr. Phys.*, vol. 11, no. 2, pp. 118–127; 1957.) The distinctive amplitude variations known as "ridges" can probably be explained in terms of divergent-lens effects in the E region. See also 2058 of 1956 (Wild and Roberts).

523.16:551.510.535 106
A Consideration of Radio-Star Scintillations as Caused by Interstellar Particles Entering the Ionosphere: Part 1—Daily and Seasonal Variations of the Scintillation of a Radio Star. Part 2—The Accretion of Interstellar Particles as a Cause of Radio-Star Scintillations—G. A. Harrower. (*Can. J. Phys.*, vol. 35, pp. 512–535; May, 1957.) An analysis is made of measurements of scintillations of the rf source in Cassiopeia recorded at Ottawa during 1954 at a frequency of 50 mc. The data show certain daily maxima occurring at solar times dependent on the date of the year and grouped unsymmetrically in a way which suggests that they are due to the infall of interstellar particles from outside the solar system. The velocities of certain of these particles are derived by simple applications of vector addition employing the known velocity of the earth. See 2116 of 1957.

523.16:621.396.677.8 107
The Mullard Radio Astronomy Observatory, Cambridge—M. Ryle. (*Nature, London*, vol. 180, pp. 110–112; July 20, 1957.) The observatory was formally opened in July, 1957. Two instruments then under construction were a radio-star interferometer for 1.7 mλ, and a pencil-beam system for investigating continuous galactic radiation at 7.9 mλ. The aperture synthesis technique applied in the two systems is described. See also 3749 of 1957.

523.16:621.396.677.833 108
World's Largest Radio Telescope—(*Overseas Eng.*, vol. 31, pp. 15–18; August, 1957.) An illustrated description of the design and construction of the 250-foot fully steerable paraboloid of the Jodrell Bank instrument with details of the driving system and drive control equipment.

523.5 109
The Distribution of the Orbits of Sporadic Meteors—A. A. Weiss. (*Aust. J. Phys.*, vol. 10, pp. 77–102; March, 1957.) Radio observations at Adelaide during 1952–1956, are analyzed. A distribution of orbits is derived which is consistent with radar and visual observations in the northern hemisphere.

523.5:621.396.11.029.62 110
Variations in the Intrinsic Strength of the 1956 Quadrantid Meteor Shower—C. O. Hines and E. L. Vogan. (*Can. J. Phys.*, vol. 35, pp. 703–711; June, 1957.) Analysis of the occurrence rate of meteoric signals detected on a vhf forward-scatter east-west path in Canada. See also 3392 of 1955 (Forsyth and Vogan).

523.5:621.396.11.029.62:551.510.535 111
A Theory of Long-Duration Meteor-Echoes based on Atmospheric Turbulence with Experimental Confirmation—L. A. Manning and V. R. Eshleman. (*J. Geophys. Res.*, vol. 62, pp. 367–371; September, 1957.) Comments on 1417 of 1957 (Booker and Cohen). The experimental evidence is examined with the conclusion that the theory does not accurately represent the properties of meteoric echoes.

523.5:621.396.96 112
Meteor Activity in the Southern Hemisphere—A. A. Weiss. (*Aust. J. Phys.*, vol. 10, pp. 299–309; June, 1957.) Activity and radiants of meteor showers are discussed and compared with similar data for the northern hemisphere. See also 109 above and 2938 of 1955.

523.74:551.510.535 113
Ionospheric Indices of Solar Activity—W. J. G. Beynon and G. M. Brown. (*J. Atmos. Terr. Phys.*, vol. 11, no. 2, pp. 128–131; 1957.) It is suggested that a simple index based on E-layer measurements at a single station is adequate, and that the additional effort required to provide the index I_F based on F_2-layer measurements at three stations is not justified. See also 1397 of 1956 (Minnis).

523.75 114
Observation of a New Type of Flare—R. J. Bray, R. E. Loughhead, V. R. Burgess, and M. K. McCabe. (*Aust. J. Phys.*, vol. 10, pp. 319–323; June, 1957.) A mass of very bright material was ejected from a flare about 28° from the sun's limb. Except for the velocity, the mass possessed all the properties of a small flare.

550.372 115
The Effective Electrical Constants of Soil at Low Frequencies—J. R. Wait. (PROC. IRE, vol. 45, pp. 1411–1412; October, 1957.) A possible explanation is presented for the large apparent dielectric constants ($\approx 10^3$) which occur at frequencies of the order of 15 kc.

550.389.2 116
I. G. Y. Rocket Program—N. W. Spencer. (*Sci. Mon.*, vol. 85, pp. 130–142; September, 1957.) An outline of the work of the IGY subcommittee of the U.S. Technical Panel for Rocketry. A table is given listing organizations participating and their objectives.

551.510.52:551.510.535 117
A Possible Troposphere-Ionosphere Relationship—S. J. Bauer. (*J. Geophys. Res.*, vol. 62, pp. 425–430; September, 1957.) A relation is suggested between F_2-layer characteristics and the passage of meteorological fronts through the troposphere. An hypothesis for dynamical coupling between the two regions is outlined.

551.510.53 118
Electric Field Measurements in the Stratosphere—C. G. Stergis, G. C. Rein, and T. Kangas. (*J. Atmos, Terr. Phys.*, vol. 11, no. 2, pp. 77–82; 1957.) Above the exchange layer the field decreases monotonically up to the limit (90,000 feet) of measurements made in 1955 and 1956. The measured and calculated values are in good agreement.

551.510.53:551.594.21 119
Electric Field Measurements above Thunderstorms—C. G. Stergis, G. C. Rein, and T. Kangas. (*J. Atmos. Terr. Phys.*, vol. 11, no. 2, pp. 83–90; 1957.) In measurements at heights of 70,000 to 90,000 feet above central Florida a positive upward-flowing current of about 1.3 a was found.

551.510.535 120
Models of the Lower Ionosphere as may be Inferred from Absorption Results—P. Bandyopadhyay. (*Indian J. Phys.*, vol. 31, pp. 297–308; June, 1957.) Values of deriative and nondeviative absorption and their variations with cos χ are calculated for the D-region models of Nertney (2306 of 1953), Piggott (unpublished), and Mitra (see 2087 of 1954) and for the E-region model of Jones (1661 of 1955). Satisfactory agreement with experimental results is found for Mitra's model of the D region but not for Jones's model of the E region.

551.510.535 121
A Study of "Spread-F" Ionospheric Echoes at Night at Brisbane: Part 3—Frequency Spreading—D. G. Singleton. (*Aust. J. Phys.*, vol. 10, pp. 60–76; March, 1957.) Diurnal and seasonal variations in spreading of the penetration frequency are compared with similar world-wide data. The observations are interpreted in terms of scattering from clouds of enhanced ionization near the F_2-layer maximum and a seasonal vertical movement of these clouds is suggested, the extent of which increases with latitude. Parts 1 and 2: 119 of 1957 (McNicol, *et al.*).

551.510.535 122
Severe Ionospheric Storm—(*Wireless World*, vol. 63, p. 553; November, 1957.) Notes on the disturbances of August 29–September 6, 1957.

551.510.535:523.75:621.396.11.029.62 123
Disturbances in the Lower Ionosphere Observed at V.H.F. following the Solar Flare of 23 February 1956 with Particular Reference to Auroral-Zone Absorption—D. K. Bailey. (*J. Geophys. Res.*, vol. 62, pp. 431–463; September, 1957.) The effects of the flare on ionospheric-scatter links in the band 30–40 mc at high latitudes are reported. An abrupt increase in oblique-incidence signal intensity, occurring almost simultaneously with the arrival of cosmic rays, was followed during the next three days by abnormally high levels at night and low levels during the day. Background cosmic noise measurements showed increased absorption at night and greatly increased absorption during daylight. The penetration into the D region of moderately heavy solar atomic ions is suggested as an explanation of the absorption phenomena.

551.510.535:523.78 124
Solar Eclipse of 30th June 1954 and its Effect upon the Ionosphere—S. N. Mitra. (*Indian J. Phys.*, vol. 31, pp. 309–323; June, 1957.) The investigations at Delhi reported include vertical-incidence ionospheric measurements, the recording of variations of sw and mf signals, and the recording of solar noise on 204 mc. Evidence of three distinct "corpuscular eclipses" was obtained both on the ionization density of the F layer and on the absorption in the nondeviating region. These were found to occur 2, 4, and $6\frac{1}{2}$ hours before the optical eclipse. Theoretical arguments and past observations indicate that these corpuscular

emissions may have originated from the so-called M region of the sun.

551.510.535:523.78:621.396.11 125
Ionospheric Research—A. P. Dale. (*RSGB Bull.*, vol. 32, pp. 499–501; May, 1957.) Note on signal-strength changes during the annular solar eclipse on December 25, 1954, and the control days for transmitters both in South Africa and in other countries.

551.510.535:550.385 126
Disturbances in the F_1 and E Regions of the Ionosphere Associated with Geomagnetic Storms—T. Sato. (*J. Geomag. Geoelect.*, vol. 9, pp. 57–60; March, 1957.) The E- and F_1-layer variations which occur during geomagnetic disturbances are examined for different phases of the solar cycle and for a number of latitudes. The data are discussed in relation to the electron drifts associated with geomagnetic disturbances. See also 127 below.

551.510.535:550.385 127
Disturbances in the Ionospheric F_2 Region associated with Geomagnetic Storms: Part 2—Middle Latitudes—T. Sato. (*J. Geomag. Geoelect.*, vol. 9, pp. 1–22; March, 1957.) Disturbances at middle latitudes are divided into negative and positive types, characteristic of high and low latitudes, respectively. These results are discussed in terms of vertical drift of electrons and the disturbance daily variations in the geomagnetic field. The bearing of the *Sq* dynamo current on seasonal and latitude variations of disturbances is discussed. Part 1: 3139 of 1957.

551.510.535:621.396.812.3 128
Ionospheric Irregularities Causing Random Fading of Very Low Frequencies—Bowhill. (See 251.)

551.510.535:621.396.9:523.3 129
Ionospheric Studies by the Lunar Technique—B. C. Blevis. (*Nature, London*, vol. 180, pp. 138–139; July 20, 1957.) Equipment operating near Ottawa comprises a 10-kw 488-mc transmitter, keyed "on" for 2 seconds and "off" for 4 seconds, feeding a 28-foot paraboloid via a horn, and orthogonal dipoles with a similar reflector feeding a dual-conversion receiver (IF 32 and 4 mc). Synchronous detection is used to give an af output signal equal in frequency to the Doppler shift of the signal reflected from the moon. Preliminary results indicate the presence of fading due to libration, long- and short-period Faraday rotation, and long-term fading without Faraday rotation.

551.594.21/.25 130
The Electrification of Precipitation and Thunderstorms—R. Gunn. (Proc. IRE, vol. 45, pp. 1331–1358; October, 1957.) A review article. Cosmic rays, radioactivity, and other agencies produce ion pairs which are transferred to cloud droplets or ice crystals and establish a droplet charge distribution greatly influenced by differences in conductivity for positive and negative ions. Rain formed from these droplets may be electrified, usually both positive and negative drops being present. Processes are considered which charge this rain and may eventually lead to a lightning stroke. The conditions necessary to establish gross free charge distributions by regeneration are specified and shown to be met under frequently occurring meteorological situations. Forty-seven references.

551.594.5 131
Rotational Temperatures Measured in Aurorae at Churchill, Manitoba—R. Montalbetti. (*Can. J. Phys.*, vol. 35, pp. 831–836; August, 1957.) The measurements indicate there is no latitude effect. A vertical temperature gradient of 6°K/km is deduced. See also 3871 of 1957 (Montalbetti and Jones).

551.594.6:523.745 132
A Study of the Audio-Frequency Radio Phenomenon Known as "Dawn Chorus"—G. McK. Allcock. (*Aust. J. Phys.*, vol. 10, pp. 286–298; June, 1957.) Experimental evidence supports the hypothesis that "dawn chorus" signals are generated by the entry into the ionosphere of clouds of positively charged particles of solar origin. Propagation appears to take place in the extraordinary magnetoionic mode along the earth's magnetic lines of force.

LOCATION AND AIDS TO NAVIGATION

621.396.932 133
Electronic Clock-Coder for Marine Radio Beacons—A. C. MacKellar and A. J. B. Baty. (*Brit. Commun. Electronics*, vol. 4, pp. 476–477; August, 1957.) Crystal control is used to give more reliable service.

621.396.932.2 134
The TALBE: a V.H.F. C.W. Radio Aid for Air/Sea Rescue—W. Kiryluk. (*J. Brit. IRE*, vol. 17, pp. 489–500; September, 1957.) Describes the development and construction of a "talk-and-listen beacon," together with prior work on an unmodulated dinghy transmitter.

621.396.932.2 135
An Introduction to Radio Aids to Air/Sea Rescue—G. W. Hosie. (*J. Brit. IRE*, vol. 17, pp. 481–488; September, 1957.) Developments since 1940, are surveyed, and the mf, cw, and vhf radar beacons in general use during the war are discussed, together with post-war equipment. A crystal-controlled vhf beacon of low duty cycle is suggested, and also a crash location beacon.

621.396.962.3:621.374.5 136
Pulse Compression—Krönert. (See 72.)

621.396.965.8 137
Optimizing the Dynamic Parameters of a Track-While-Scan System—J. Sklansky. (*RCA Rev.*, vol. 18, pp. 163–185; June, 1957.)

MATERIALS AND SUBSIDIARY TECHNIQUES

535.215:546.48.241.1 138
Preparation and Photoconductive Properties of Cadmium Telluride Films—G. G. Kretschmar and L. E. Schilberg. (*J. Appl. Phys.*, vol. 28, pp. 865–867; August, 1957.) A thin film gave a high dark resistance, falling by 10 to 200 times with 2-foot candle illumination. A film prepared in indium vapor gave a dark resistance of 1–10 mΩ falling to a few hundred kΩ.

535.37 139
Critical Comment on a Method for Determining Electron Trap Depths—C. H. Haake. (*J. Opt. Soc. Amer.*, vol. 47, pp. 649–652; July, 1957.) "A critical analysis of Garlick and Gibson's method (3421 of 1948) based on a mathematical determination of the applicable temperature range and on experimental evidence shows that the trap depths obtained are lower than those found by other methods. Especially the frequency-of-escape constants calculated subsequently contrast strongly to those determined by separate measurements."

535.37 140
Energy Transport by Cascade and Resonance Processes in Doubly Activated Phosphors—E. W. Claffy and C. C. Klick. (*J. Electrochem. Soc.*, vol. 104, pp. 445–447; July, 1957.)

535.376 141
Review of Articles on Luminescence for 1955–1956—G. R. Fonda. (*J. Electrochem. Soc.* vol. 104, pp. 524–530; August, 1957.) Review covering articles published in English, German, and French. One-hundred and fifty-six references.

535.376:546.472.21 142
Electroluminescence of ZnS Single Crystals—G. F. Neumark. (*Sylvania Technologist*, vol. 10, pp. 29–34; April, 1957.) Electroluminescence in ZnS depends on the number and type of traps in the crystal. Impact ionization appears to be the predominant mechanism for the excitation. Thirty-one references.

537.226/.228.1:546.431.824–31:534.232 143
An Investigation of some Barium Titanate Compositions for Transducer Applications—D. Schofield and R. F. Brown. (*Can. J. Phys.*, vol. 35, pp. 594–607; May, 1957.) The addition of Co to 5 per cent Ca, 95 per cent Ba titanate compositions, produces a large reduction in the dielectric loss in high electric fields without significant effect on the piezoelectric characteristics. Preliminary results were given earlier (3160 of 1957).

537.226/.227:534.1.087 144
The Use of Ferroelectric Ceramics for Vibration Analysis—R. C. Kell, G. A. Luck, and L. A. Thomas. (*J. Sci. Instr.*, vol. 34, pp. 271–274; July, 1957.)

537.227:546.431.824–31 145
Preparation of $BaTiO_3$ Single Crystals in Coal Gas Atmosphere—K. Kawabe and S. Sawada. (*J. phys. Soc. Japan*, vol. 12, p. 218; February, 1957.)

537.227:546.431.824–31 146
Heating Effects in Single Crystal Barium Titanate—D. S. Campbell. (*J. Electronics Control*, vol. 3, pp. 330–338; September, 1957.) The coercive field inccreases with frequency up to a certain limiting frequency above which it falls due to heating effects. This gives a criterion for the maximum frequency at which crystals can be expected to operate in a matrix storage system.

537.227:546.431.824–31 147
Quasi-static Hysteresis in Barium-Titanate Single Crystals—K. Zen'iti, K. Husimi, and K. Kataoka. (*J. phys. Soc. Japan*, vol. 12, p. 432; April, 1957.)

537.227:546.431.824–31 148
On the 180°-Type Domain Wall of $BaTiO_3$ Crystal—W. Kinase and H. Takahasi. (*J. phys. Soc. Japan*, vol. 12, pp. 464–476; May, 1957.) At room temperature the domain width is about 10^{-4} cm and its energy is 1.4 erg/cm² The structure of the domains and their reversing process are also discussed.

537.228.5:546.36 149
Stark Effect on Caesium-133 Hyperfine Structure—R. D. Haun, Jr and J. R. Zacharias. (*Phys. Rev.*, vol. 107, pp. 107–109; July 1, 1957.) The change of the hyperfine-structure separation energy caused by an electric field has been measured in ^{133}Cs by the atomic-beam magnetic-resonance method and is compared with other experimental and theoretical data.

537.311.33 150
Generation of an E.M.F. in Semiconductors with Nonequilibrium Current Carrier Concentrations—J. Tauc. (*Rev. mod. Phys.*, vol. 29, pp. 308–324; July, 1957.) A general formulation of the problem is presented. Solutions are obtained for two special cases for which the impurity-concentration change occurs over a distance either long or short

compared with the diffusion length of current carriers; these are bulk and barrier-layer photovoltaic effects, respectively. Practical implications are discussed. One-hundred and two references.

537.311.33 151
Statistics of the Charge Distribution for a Localized Flaw in a Semiconductor—W. Shockley and J. T. Last. (*Phys. Rev.*, vol. 107, pp. 392–396; July 15, 1957.) The charge situation is described by a set of energy levels which are independent of the Fermi level but are temperature-dependent. The charge of the flaw increases by one electron unit of negative charge as the Fermi level is raised successively above each level of the set and, conversely, as it is lowered.

537.311.33 152
Scattering of Current Carriers in Semiconductors with Ionic Type of Bond—T. A. Kontorova. (*Zh. Tekh. Fiz.*, vol. 27, pp. 269–274; February, 1957.) The scattering of carriers in the optical and acoustic modes is investigated and their free path is calculated. Approximate formulas for the carrier mobility are derived. The dependence of mobility on temperature is examined.

537.311.33 153
High-Frequency Relaxation Processes in the Field-Effect Experiment—C. G. B. Garrett. (*Phys. Rev.*, vol. 107, pp. 478–487; July 15, 1957.) A theoretical treatment is given of two dispersion phenomena in the semiconductor field-effect experiment [see, *e.g.*, 3532 of 1951 (Montgomery)]: 1) dispersion arising from the finite time required to generate minority carriers, and 2) relaxation of the fast surface states.

537.311.33:538.632 154
On the Electrical Properties of Degenerate Semiconductors—E. Haga. (*J. phys. Soc. Japan*, vol. 12, p. 217; February, 1957.) Theoretical derivation of quantitative data on resistivity and the Hall coefficient.

537.311.33:538.632 155
Resistivity and Hall Coefficient of Semiconductors—K. Shogenji and S. Uchiyama. (*J. phys. Soc. Japan*, vol. 12, p. 434; April, 1957.) Calculations assuming scattering of current carriers by acoustic and optical modes of lattice vibration, but neglecting scattering by impurity centers.

537.311.33:546.23:621.314.6 156
The Surface Potential of Selenium and its Relation to the Rectification and the Photovoltaic Effects—U. Yoshida and A. Suzuki. (*J. phys. Soc. Japan*, vol. 12, pp. 459–463; May, 1957.) The changes with time of the surface potential and the rectification ratio after heat treatment are reduced by coating with a thin film of synthetic resin.

537.311.33:546.24 157
Electrical Properties of Tellurium at the Melting Point and in the Liquid State—A. S. Epstein, H. Fritzsche, and K. Lark-Horovitz. (*Phys. Rev.*, vol. 107, pp. 412–419; July 15, 1957.) The experimental results show that semiconductor properties persist in the liquid state, but as the temperature is raised a gradual transition to metallic behavior occurs.

537.311.33:546.27 158
Electrical Properties of Boron Single Crystals—W. C. Shaw, D. E. Hudson, and G. C. Danielson. (*Phys. Rev.*, vol. 107, pp. 419–427; July 15, 1957.) The electrical resistivity, Hall coefficient, and thermoelectric power of microscopic crystals have been measured as functions of temperature. A value of 1.55 ± 0.05 ev is deduced for the energy gap.

537.311.33:[546.28+546.289 159
Expansions in Reactor Irradiated Germanium and Silicon—M. C. Wittels. (*J. Appl. Phys.*, vol. 28, p. 921; August, 1957.) The lattice expansions observed were greater in Ge than Si, as expected from theory. The retained damage in Ge was dependent on the irradiation temperature.

537.311.33:546.28 160
Donor Electron Spin Relaxation in Silicon—E. Abrahams. (*Phys. Rev.*, vol. 107, pp. 491–496; July 15, 1957.) The effects of spin-orbit coupling on the relaxation time for donor electron spins are considered.

537.311.33:546.28 161
Damage to Silicon Produced by Bombardment with Helium Ions—U. F. Gianola. (*J. Appl. Phys.*, vol. 28, pp. 868–873; August, 1957.) Helium ions at 3×10^4 ev were used. The surface layer was found to be converted to a quasi-stable amorphous form, which becomes partially crystalline on annealing. The amorphous material is soluble in aqueous hydrofluoric acid and has about 1/10th the thickness of the affected Si.

537.311.33:546.28 162
Oxygen Content of Silicon Single Crystals—W. Kaiser and P. H. Keck. (*J. Appl. Phys.*, vol. 28, pp. 882–887; August, 1957.) The oxygen content of pulled Si crystals is correlated with the infrared absorption at 9 microns. Methods of altering the oxygen concentration are discussed.

537.311.33:546.289 163
Study of the Minority-Carrier Mobility in Germanium—M. Shtenbek and P. I. Baranski. (*Zh. Tekh. Fiz.*, vol. 27, pp. 221–232; February, 1957.) Report of investigation on *n*-type single-crystal Ge. The transit time, the mobility, and the coefficients of longitudinal and transverse diffusion of minority carriers are calculated.

537.311.33:546.289 164
Experimental Investigation of the Correlation between Peltier Effect and Thermo-e.m.f. in Germanium—M. Shtenbek and P. I. Baranski. (*Zh. Tekh. Fiz.*, vol. 27, pp. 233–237; February, 1957.) This correlation is investigated in the impurity and intrinsic conduction bands for samples of *n*- and *p*-type Ge of differing specific resistance.

537.311.33:546.289 165
Nature of Recombination Centres in Germanium Originated by Low-Temperature Heat Treatment—T. V. Mashovets and S. M. Ryvkin. (*Zh. Tekh. Fiz.*, vol. 27, pp. 238–241; February, 1957.) See also 2794 of 1956.

537.311.33:546.289 166
Probability of Capture by Carrier Recombination at Frenkel-Type Defects in n-Type Germanium—L. S. Smirnov and V. S. Vasilov. (*Zh. Tekh. Fiz.*, vol. 27, pp. 427–429; February, 1957.) Bombardment of Ge crystals with electrons of energy over 500 kev produces at room temperature stable dislocations of crystal structure, called Frenkel defects, corresponding to several levels in the forbidden zone, which act as effective recombination centers of holes and electrons.

537.311.33:546.289 167
Electrical Properties of Nickel-Doped Germanium at Low Temperatures—Y. Kanai and R. Nii. (*J. phys. Soc. Japan*, vol. 12, pp. 125–133; February, 1957.) Anomalous behavior was found at temperatures in the range 120–170°K, the resistivity increasing as the temperature was reduced. The electrical properties could be explained by use of the model proposed by Hung (*Phys. Rev.*, vol. 79, pp. 727–728; August 15, 1950.)

537.311.33:546.289 168
Peripheral Inhomogeneities of the Alloyed Germanium *p-n* Junction—M. Kikuchi. (*J. phys. Soc. Japan*, vol. 12, pp. 133–139; February, 1957.) The local photocurrent exhibits peaks, the positions of which depend on the bias voltage. A model for the junction is proposed.

537.311.33:546.289 169
Observation of the Drift of Germanium Surface by Field-Effect Experiment—M. Kikuchi. (*J. phys. Soc. Japan*, vol. 12, p. 436; April, 1957.) The surface conductance and photoconductance were measured at various time intervals after the etching of *n*-type Ge.

537.311.33:546.289 170
Alloying Properties of Germanium Free of Edge Dislocations—C. W. Mueller. (*RCA Rev.*, vol. 18, pp. 205–212; June, 1957.) The main factors involved in alloying In on dislocation-free Ge are considered. The controlled alloying method described gives extremely flat and uniform junctions.

537.311.33:546.289 171
The Dissolution of Germanium by Molten Indium—B. Goldstein. (*RCA Rev.*, vol. 18, pp. 213–220; June, 1957.) Experimental results of an investigation of dissolution as a function of crystal axis orientation, temperature, and amount of Ge already contained in the molten In solvent.

537.311.33:546.289 172
Preferential Diffusion of Sb along Small-Angle Boundaries in Ge and the Dependence of this Effect on the Direction of the Dislocation Lines in the Boundary—F. Karstensen. (*J. Electronics Control*, vol. 3, pp. 305–307; September, 1957.) Experiment shows that preferential diffusion occurs if the grain boundary contains dislocation lines parallel to the direction of diffusion, but does not occur if these are perpendicular to it.

537.311.33:546.289 173
Diffusion of Antimony out of Germanium and some Properties of the Antimony-Germanium System—R. C. Miller and F. M. Smits. (*Phys. Rev.*, vol. 107, pp. 65–70; July 1, 1957.) Experimental Sb distributions are shown to be consistent with a rate limitation or potential barrier at the Ge/ambient interface. Introduced external rate limitations provide data for calculating partition and sticking coefficients for the system and estimating the binding energy of Sb in Ge. See also 1478 of 1957.

537.311.33:546.289 174
Distribution and Cross-Sections of Fast States on Germanium Surfaces in Different Gaseous Ambients—A. Many and D. Gerlich. (*Phys. Rev.*, vol. 107, pp. 404–411; July 15, 1957.) Simultaneous measurements of surface recombination velocity and trapped charge density in the fast states as a function of surface potential show that the energy distribution of the fast states consists of four discrete sets of levels. Only one of these sets is significant in the recombination process.

537.311.33:546.289 175
The Depth of Surface Damage Produced by Lapping Germanium Monocrystals—D. Baker and H. Yemm. (*Brit. J. Appl. Phys.*, vol. 8, pp. 302–303; July, 1957.) The depth of damage is estimated from the variation of the effective diffusion distance of minority carriers as the disturbed layer is removed by etching.

537.311.33:546.289:534.13-8 176
Ultrasonic Attenuation by Free Carriers in Germanium—G. Weinreich. (*Phys. Rev.*, vol. 107, pp. 317–318; July 1, 1957.) The close re-

lationship with the acoustoelectric effect is noted and the amount of attenuation is predicted from the observed magnitude of this effect. See also 2499 of 1957 (Blatt).

537.311.33:546.289:537.32 177
Magnetic Field Dependence of the Seebeck Effect in Germanium—M. C. Steele. (*Phys. Rev.*, vol. 107, pp. 81–83; July 1, 1957.) The thermoelectric power of n-type Ge single crystals increases with magnetic field at temperatures from 78° to 278°K. The thermal conductivity is constant for magnetic fields between zero and 11500 oersteds.

537.311.33:546.289:538.6 178
Investigation of Thermomagnetic Effects in p-Type Germanium—I. V. Mochan, Yu. N. Obraztsov, and T. V. Krylova. (*Zh. Tekh. Fiz.*, vol. 27, pp. 242–259; February, 1957.) The transverse and longitudinal Nernst-Ettingshausen and Hall effects are measured on samples of p-type Ge of specific resistance 69 Ω cm at room temperature, in the impurity conduction band. In the temperature range 80°–240°K and a field of 5000 G the transverse Nernst-Ettingshausen effect appears to be due to hole transfer by phonons.

537.311.33:546.289:538.63 179
On the Measurements of the Galvanomagnetic Effect in Semiconductors at Microwave Frequencies—T. Fukuroi and M. Date. (*Sci. Rep. Res. Inst. Tohoku Univ., Ser. A.*, vol. 9, pp. 190–195; June, 1957.) The resonant cavity method is used to make measurements at 9800 mc at temperatures down to 1.5°K. The results obtained for the magnetoresistance of pure Ge are compared with those of Fritzche (153 of 1956).

537.311.33:546.289:538.632 180
Galvanomagnetic Theory for n-Type Germanium and Silicon: Hall Theory and General Behaviour of Magnetoresistance—L. Gold and L. M. Roth. (*Phys. Rev.*, vol. 107, pp. 358–364; July 15, 1957.) The magnetoresistance $\Delta\rho/\rho$, and Hall coefficient R_H for n-type Ge and Si are calculated from the resistivity tensor. The angular dependence of $\Delta\rho/\rho$ is compared with experimental data. The field dependence of $\Delta\rho/\rho$ and of R_H are considered for various current and field orientations.

537.311.33:546.289:539.1 181
Diffusion-Limited Annealing of Radiation Damage in Germanium—T. R. Waite. (*Phys. Rev.*, vol. 107, pp. 471–478; July 15, 1957.) The theory given in 104 above has been applied to experimental data [see, *e.g.*, 1469 of 1954 (Brown, *et al.*)]; reasonable agreement was found.

537.311.33:546.682.19:535.215 182
Photoelectromagnetic Effect in Indium Arsenide—J. R. Dixon. (*Phys. Rev.*, vol. 107, pp. 374–378; July 15, 1957.) Experimental studies on n- and p-type single crystals at room temperature are described. The dependence of the photoelectromagnetic short-circuit current on magnetic induction is consistent with the theory of Kurnick and Zitter (2429 of 1956). Bulk lifetimes are found to be about 6×10^{-8} for n-type, and 5×10^{-10} for p-type material; estimates of surface recombination velocity for n-type material are 0–10^3 cm for an etched surface, and 10^5 cm for a ground surface.

537.311.33:621.3.049.7 183
Technique for Connecting Electrical Leads to Semiconductors—C. L. Anderson, H. Christensen, and P. Andreatch. (*J. Appl. Phys.*, vol. 28, p. 923; August, 1957.) Two techniques are described which give adhesion between certain soft metals and semiconductors at temperatures well below the eutectic point.

537.311.33:621.314.63 184
Minority Carrier Lifetime in p-n Junction Devices—M. Byczkowski and J. R. Madigan. (*J. Appl. Phys.*, vol. 28, pp. 878–881; August, 1957.) Minority-carrier lifetime is conveniently determined by studying the switching time in junction diodes. Some theoretical and experimental results are given.

537.533:546.883 185
Electrostatic Emission from Tantalum Single Crystals—N. A. Gorbatyĭ, L. V. Reshetnikova, E. P. Sytaya, and G. N. Shuppe. (*Zh. Tekh. Fiz.*, vol. 27, pp. 296–298; February, 1957.) Field emission patterns for Ta single crystals appear identical to those obtained for W and Mo.

538.22 186
Effective Gyromagnetic Ratio for Triangular Ferrimagnetic States—A. Eskowitz and R. K. Wangsness. (*Phys. Rev.*, vol. 107, pp. 379–380; July 15, 1957.)

538.22 187
Magnetic Properties of Perovskites Containing Strontium: Part 1—Strontium-Rich Ferrites and Cobaltites—H. Watanabe. (*J. phys. Soc. Japan*, vol. 12, pp. 515–522; May, 1957.) Magnetic susceptibilities and electrical conductivities for samples sintered in vacuo differ from those sintered in oxygen. An interpretation of experimental results is given.

538.22:538.569.4:546.763-31 188
Antiferromagnetic Resonance in Cr_2O_3—E. S. Dayhoff. (*Phys. Rev.*, vol. 107, pp. 84–91; July 1, 1957.) Theory and experimental data are given for the antiferromagnetic resonance spectrum of single-crystal Cr_2O_3 for 12-2.8 mmλ and magnetic field intensities from zero to 30,000 oersteds.

538.22:538.613 189
Magnetography—the Microscopy of Magnetism—F. G. Foster. (*Bell Lab. Rec.*, vol. 35, pp. 175–178; May, 1957.) The Kerr magneto-optical effect is applied to the microscopy of magnetic domain structure.

538.221 190
Transverse Impedance Transformation for Ferromagnetic Media—F. R. Morgenthaler. (PROC. IRE, vol. 45, p. 1407; October, 1957.) The transformation relates to media magnetized transversely, and is valid for TE_{m0} modes with the magnetization in the E-field direction.

538.221 191
Domain Wall Orientations in Silicon-Iron Crystals—C. D. Graham, Jr., and P. W. Neurath. (*J. Appl. Phys.*, vol. 28, pp. 888–891; August, 1957.) The stable orientation of a 180° ferromagnetic domain wall in a cubic crystal is calculated and the results are compared with experimentally determined orientations.

538.221:538.122 192
Experimental Investigation of the Magnetic Field Distribution due to Artificial Surface Defects in Ferromagnetic Substances—N. N. Zatsepin. (*Zh. Tekh. Fiz.*, vol. 27, pp. 368–373; February, 1957.)

538.221:539.23 193
Magnetization Reversal in Thin Films at Low Fields—R. L. Conger and F. C. Essig. (*J. Appl. Phys.*, vol. 28, pp. 855–858; August, 1957.) Statistical theory is presented for reversing fields less than the anisotropy field under the assumption that reversal takes place by domain wall motion; experimental data supporting the theory are given. See also 1513 of 1957.

538.221:[621.318.124+621.318.134 194
Dielectric Spectroscopy of Ferromagnetic Semiconductors—P. A. Miles, W. B. Westphal, and A. von Hippel. (*Rev. mod. Phys.*, vol. 29, pp. 279–307; July, 1957.) Methods of measuring the electric and magnetic spectra, within the range from dc to optical frequencies, are described and results discussed. In addition to a general review some new experimental data including the rf spectra of a single-crystal Ni ferrite are presented.

538.221:[621.318.124+621.318.134 195
On the Origin of the Magnetic Anisotropy Energy of Ferrites—K. Yosida and M. Tachiki. (*Progr. Theoret. Phys.*, vol. 17, pp. 331–359; March, 1957.) The anisotropy energy for Ni ferrites comes mainly from Fe^{3+} ions for magnetite from Fe^{2+} and Fe^{3+} ions and for Mn ferrites from Fe^{3+} and Mn^{2+} ions. The large anisotropy energy of Co ferrites arises from the pseudo-quadrupole and anisotropic exchange reactors among Co and Fe ions.

538.221:[621.318.124+621.318.134 196
A Theory of the Uniaxial Anisotropy Induced by Magnetic Annealing in Ferrites—S. Taniguchi. (*Sci. Rep. Res. Inst. Tohoku Univ., Ser. A*, vol. 9, pp. 196–214; June, 1957.)

538.221:621.318.134 197
Magnetic and Magnetostrictive Properties of Magnesium-Nickel Ferrites—P. O. Hoffmann. (*J. Amer. Ceram. Soc.*, vol. 40, pp. 250–252; July 1, 1957.) A study of mixed Ni-Mg ferrites of various compositions shows them to be inferior to Ni ferrite.

538.221:621.318.134 198
Magnetic Properties and Associated Microstructure of Zinc-Bearing Square-Loop Ferrites—G. G. Palmer, R. W. Johnston, and R. E. Schultz. (*J. Amer. Ceram. Soc.*, vol. 40, pp. 256–262; August 1, 1957.) A series of Mn-Mg ferrites in which Zn is substituted for Mg has been prepared and tested in a successful attempt to obtain a material having a lower coercive force and higher magnetic saturation than standard rectangular-loop ferrites used extensively in digital computers.

538.221:621.318.134:538.6 199
Rotation of the Plane of Polarization in a Longitudinal Magnetic Field (Faraday Effect) in the Millimetre Wavelength Range—D. I. Mash. (*Zh. Tekh. Fiz.*, vol. 27, pp. 360–363; February, 1957.) Results of tests on ferrites are summarized and discussed.

538.632 200
Temperature Dependence of the Hall Coefficients in some Silver Palladium Alloys—F. E. Allison and E. M. Pugh. (*Phys. Rev.*, vol. 107, pp. 103–105; July 1, 1957.)

666.1.037.5 201
Fundamentals of Glass-to-Metal Bonding: Part 3—Temperature and Pressure Dependence of Wettability of Metals by Glass—R. M. Fulrath, S. P. Mitoff, and J. A. Pask. (*J. Amer. Ceram. Soc.*, vol. 40, pp. 269–274; August 1, 1957.) Part 2: 3576 of 1957 (Mitoff).

MATHEMATICS

512.25 202
A Least-Squares Solution of Linear Equations with Coefficients Subject to a Special Type of Error—J. K. Mackenzie. (*Aust. J. Phys.*, vol. 10, pp. 103–109; March, 1957.)

MEASUREMENTS AND TEST GEAR

529.786+531.711 203
The Units of Time and Length—L. Essen. (*Nature, London*, vol. 180, pp. 137–138; July 20, 1957.) Difficulties in an ideal system using an atomic frequency standard to define the unit of time are discussed. A practical solution would be to define time in terms of the caesium

line and length in terms of the radiation of a suitable light source. A system in which time interval is based on an atomic unit and epoch on astronomical measurements has been satisfactory during two years of operation at the National Physical Laboratory.

529.786 204
The Caesium Resonator as a Standard of Frequency and Time—L. Essen and J. V. L. Parry. (*Phil. Trans. A.*, vol. 250, pp. 45–69; August 8, 1957.) The construction, operation, and testing of the standard are described. The present experimental model can be used to define frequency with a standard deviation of ± 1 part in 10^{10}. The design of a resonator with sharper reasonance less than 100 cps wide appears possible and should improve the definition. See also 2471 of 1956.

529.786:538.569.4 205
Recent Developments in Measurement of Time—C. H. Townes. (*Nuovo Cim.*, vol. 5, Supplement No. 1, pp. 222–229; 1957. In English.) The use of the molecular oscillator described in 100 of 1955 (Gordon, *et al.*) as a frequency standard is discussed.

621.3.018.41(083.74)+529.786]:538.569.4 206
Precise Frequency of the 3,3 Inversion Line of Ammonia—K. Shimoda. (*J. phys. Soc. Japan*, vol. 12, p. 558; May, 1957.)

621.3.018.41(083.74):621.385.029.6 207
A New Microwave Frequency Standard by Quenching Oscillator Control—N. Sawazaki and T. Honma. (IRE TRANS., vol. MTT-4, pp. 116–121; April, 1956. Abstract, PROC. IRE, vol. 44, pp. 956–957; July, 1957.)

621.317.1.087:519.24 208
The Automatic Classification and Storage of Measurement Results—H. J. Vogt and E. Zimmer. (*Elektronik*, vol. 6, pp. 191–197; July, 1957.) Description of methods and electronic equipment for use in the statistical analysis of manufacturing processes with particular reference to applications in the textile industry.

621.317.3:537.311.33 209
Direct-Reading Minority-Carrier-Lifetime Measuring Apparatus—A. R. Engler and C. J. Kevane. (*Rev. Sci. Instr.*, vol. 28, pp. 548–551; July, 1957.) The decay of optically injected excess minority carriers is compared with voltage decay in a *RC* circuit, and lifetimes (>10 μsec) are read directly from a calibrated dial.

621.317.3:538.63 210
Geometrical Effects in Transverse Magnetoresistance Measurements—J. R. Drabble and R. Wolfe. (*J. Electronics Control*, vol. 3, pp. 259–266; September, 1957.) "The effect of finite length-to-width ratio and of probe positions on measurements of resistivity in a transverse magnetic field is investigated for various Hall angles. Wick's method (3161 of 1954) is extended to include the case of measurements made between probes symmetrically placed at various distances from the ends. Graphs are included which give the fractional change of resistance for various probe positions and Hall angles for specimens of any length-to-width ratio greater than two."

621.317.3:538.632 211
Experimental Use of Hall-Effect Linear Detector for Measurements—V. N. Bogomolov and V. D. Vasil'ev. (*Zh. Tekh. Fiz.*, vol. 27, pp. 260–261; February, 1957.) The circuit described incorporates an *n*-type Ge plate as the Hall detector; an experimental application is briefly described.

621.317.3:621.314.63 212
Measurements of Crystal Impedances at Low Levels—H. N. Dawirs and E. K. Damon. (IRE TRANS., vol. MTT-4, pp. 94–96; April, 1956. Abstract, PROC. IRE, vol. 44, p. 956; July, 1956.)

621.317.3:621.314.7 213
Transistor Tests Predict High-Frequency Performance—R. L. Pritchard. (*Electronic Inds. Tele-Tech.*, vol. 16, pp. 62–63, 144; March, 1957.) Methods are described for measuring the alpha cutoff frequency, the ohmic base resistance and the collector-base capacitance from which parameters the high-frequency performance may be determined.

621.317.3:621.396.822:621.396.62.029.6 214
Absolute Measurement of Receiver Noise Figures at U.H.F.—E. Maxwell and B. J. Leon. (IRE TRANS., vol. MTT-4, pp. 81–85; April, 1956. Abstract, PROC. IRE, vol. 44, p. 956; July, 1956.)

621.317.331:621.316.993 215
Measuring Earth Conductivity—M. Strohfeldt. (*Electronic Radio Eng.*, vol. 34, pp. 425–427; November, 1957.) Measurements at an "ideal" site by radio methods gave a much lower value than those obtained by electrode methods. Some correlation exists between measurements by the two methods when applied to the variation of conductivity with distance.

621.317.335.3.029.64 216
A Rod Method of Measuring Dielectric Constants. Application to $(NH_4)_2H_3IO_2$ at 3-cm Wavelength—H. Gränicher and W. Schurter. (*Z. angew. Math. Phys.*, vol. 8, pp. 382–400; September 25, 1957.) A modified version of the method described by Le Bot and Le Montagner (2067 of 1953) was adopted to measure the complex permittivity of rod specimens. The experimental results are discussed.

621.317.34.029.63/.64 217
Automatic Microwave Transmission Measuring Equipment—J. B. Linker, Jr. and H. H. Grimm. (*Rev. Sci. Instr.*, vol. 28, pp. 559–563; July, 1957.) The phase of a 200-kc heterodyne is compared with that of a phase-coherent 200-kc reference source by a null-seeking servo phase discriminator, and loss is measured by a commercial ratio meter. A traveling-wave tube produces the phase-coherent 200-kc frequency offset which is passed through a waveguide containing the ferrite or other material to be measured.

621.317.343.029.6 218
V.H.F. Line Measurements—F. J. Charman. (*Electronic Eng.*, vol. 29, pp. 499–503; October, 1957.) A method is described of using a single loop directional coupler by which the impedance or admittance of an unknown load may be obtained graphically. The method is compared with that of the impedometer [155 of 1950 (Parzen)]; the parameters measured by the new device are not directly applicable to a Smith chart.

621.317.351:621.397 219
Equipment for the Oscillographic Display of the Phase and Amplitude Characteristics of Video and I.F. Networks—W. Kroebel and L. A. Wegner. (*Rundfunktech. Mitt.*, vol. 1, pp. 37–44; April, 1957.) In the equipment described parameters representing phase shift and amplitude distortion are displayed on two cr tubes as a function of modulation frequency in the range 0.1–6.0 mc, together with an electronically produced graticule. Special methods of phase measurements are described and some test results are reproduced.

621.317.353.1 220
A New Method of Measuring Nonlinear Distortion—O. Henkler. (*Nachr-Tech.*, vol. 7, pp. 145–147; April, 1957.) The "combination-factor" method outlined is more suitable, particularly for application to carrier-frequency systems, than the conventional distortion-factor and difference-tone methods. Two test signals of equal amplitude are used with a frequency difference depending on the application. The "combination factor" obtained is the ratio of the amplitude of a certain intermodulation product to that of one of the test signals.

621.317.382 221
A Wide-Band Level-Measuring Set—R. C. Bolt. (*A.T.E.J.*, vol. 13, pp. 151–156; April, 1957.) The instrument is suitable for power measurements at various input impedances, in the frequency range 200 cps–612 kc at levels from −50 to +40 db relative to 1 mw.

621.317.444:621.385 222
Rectilinearity of Electron-Beam Focusing Fields from Transverse Component Determinations—P. P. Cioffi. (*Commun. and Electronics*, no. 29, pp. 15–19; March, 1957.) An accurate method of measuring the transverse component of the magnetic focusing field using a small search coil is described. The longitudinal field component produced by errors in positioning of the coil is eliminated. For a description of the recording fluxmeter used, see 3174 of 1952.

621.317.733.025 223
Component Testing Bridge—C. D. Lindsay. (*Wireless World*, vol. 63, pp. 549–550; November, 1957.) Design of an ac comparator working at 50 cps.

621.317.755 224
Calibrated D.C. Oscilloscope—B. Pearce. (*Wireless World*, vol. 63, pp. 539–542; November, 1957.) Design details are given.

621.317.755:621.397.5 225
Oscillographs for Television Work—O. H. Davie. (*J. Telev. Soc.*, vol. 8, pp. 225–233; April/June, 1957.) A description of the design and application of ancillary equipment required when using a general-purpose oscilloscope for television measurements.

621.317.79.029.64 226
A Focused Spectrometer for Microwave Measurements—E. G. A. Goodall and J. A. C. Jackson. (*Marconi Rev.*, vol. 20, pp. 51–59; 2nd Quart., 1957.) Two variants of spectrometer are described for X-band frequencies. Measurements of transmission and reflection characteristics for incident angles of 15° to 70° on single sandwich-type radome samples are presented.

621.317.79.029.64:538.569.4 227
A Frequency-Modulated Microwave Spectrometer for Electron-Resonance Measurements—A. C. Rose-Innes. (*J. Sci. Instr.*, vol. 34, pp. 276–278; July, 1957.) The instrument is designed for use in the 3-cm band. Frequency modulation allows spectra to be recorded with simple equipment; details are given of a special technique for increasing the sensitivity. The instrument is especially suitable for measurements at low temperatures and for recording wide lines.

621.317.794 228
Comparison of Subtraction-Type and Multiplier-Type Radiometers—J. Galejs. (PROC. IRE, vol. 45, pp. 1420–1422; October, 1957.)

621.317.794.029.64 229
A Calibration Procedure for Microwave Radiometers—R. N. Whitehurst, F. H. Mitchell, and J. Copeland. (PROC. IRE, vol. 45, pp. 1410–1411; October, 1957.) A procedure allowing for the antenna side lobes in estimating radiation from a stellar source. Three measurements are made: one with the fixed antenna

pointing to the west of the source, one towards it, and one with the forward lobes absorbed. See also 2739 of 1957.

621.317.799:621.385.832 230
An Electrostatic Cathode-Ray Tube Tester—R. B. Hale. (*Brit. Commun. Electronics*, vol. 4, p. 496; August, 1957.)

OTHER APPLICATIONS OF RADIO AND ELECTRONICS

621.373.52:612 231
A Simple Physiological Stimulator, using a Transistor Oscillating Circuit—W. T. Catton, L. Molyneux, and B. Schofield. (*Electronic Eng.*, vol. 29, pp. 496–498; October, 1957.)

621.373.52.029.3:53.087.25:616 232
Monitoring of Low-Frequency Phenomena—C. F. Rothe and M. W. Street. (*Science*, vol. 126, pp. 77–78; July 12, 1957.) A transistor regenerative oscillator has been adapted to convert subaudio frequencies into af for monitoring phenomena such as the electrical activity of the heart in a way more convenient than visual observation of instruments.

621.387:654.924.56 233
The Ionization Fire-Alarm. Electronics in the Service of Fire Protection—H. P. Halm. (*Elektronik*, vol. 6, pp. 205–207; July, 1957.) The apparatus described uses an ionization chamber in which the presence of combustion gases causes a change in the normal ionization produced by a radioactive source. Some recent refinements are discussed.

621.387.4:621.374.3 234
Some Electronic Instruments used in Nuclear Spectroscopic Investigations—B. Åström. (*Ark. Fys.*, vol. 12, Pt. 3, pp. 215–236; 1957.) A description is given of two complete sets of equipment: 1) an automatic scintillation spectrometer comprising scintillation detector and single channel pulse height analyzer, 2) an α-particle spectrometer comprising ionization chamber and 50-channel pulse-height analyzer of stacked discriminator type. To facilitate maintenance and improve cooling, all tubes are mounted horizontally and concentrated in a ventilated space.

621.398:551.508.822 235
Telemetering System is Balloon Borne—E. K. Novak. (*Electronics*, vol. 30, pp. 158–164; September 1, 1957.) Description of fm/AM telemetry system for a weather radiosonde. It provides a 1680-mc carrier with three simultaneous channels one of which is time-multiplexed into 12 additional channels with sampling rate of one sample per minute; the maximum range is approximately 360 miles.

PROPAGATION OF WAVES

621.396.11 236
A New Solution of the Problem of Propagation over a Flat Earth—G. Boudouris. (*Nuovo Cim.*, vol. 5, Supplement No. 1, pp. 71–91; 1957. In French.) Simplifications of classical theory are introduced in fixing the boundary conditions for the problem. This "method of approximate boundary conditions" is more convenient for practical applications.

621.396.11 237
Electromagnetic Fields due to Current Flowing Parallel to Interface of Two Different Media—K. Horiuchi. (*J. phys. Soc. Japan*, vol. 12, pp. 170–176; February, 1957.) Integral equations are established for various configurations. The results have applications in problems of wave propagation over an inhomogeneous earth, or through a stratified atmosphere.

621.396.11 238
Fading of Radio Waves Scattered by Dielectric Turbulence—R. A. Silverman. (*J. Appl. Phys.*, vol. 28, p. 922; August, 1957.) Note of corrections to 3274 of 1957.

621.396.11 239
Short-Range Echoes Observed on Ionospheric Recorders—R. L. Dowden. (*J. Atmos. Terr. Phys.*, vol. 11, no. 2, pp. 111–117; 1957.) Echoes from the 20–100-km region observed at ionospheric stations near the sea are found to arrive at very low angles of elevation with vertical polarization. They are due to coherent back scatter from sea waves of length $\lambda/2$.

621.396.11:551.510.52 240
A New Technique for the Study of Scatter Propagation in the Troposphere—J. H. Chapman, W. S. Haikkila, and J. E. Hogarth. (*Can. J. Phys.*, vol. 35, pp. 823–830; August, 1957.) Fluctuations of received field strength may be considered to have the characteristics of noise. Measurements on 500-mc near-optical links show the "propagations noise" power varies as $1/f^2$ for 0.1 cps$<f<$10 cps, f being the difference between carrier and side-band frequencies.

621.396.11:551.510.535 241
Refractive Corrections to Scatter Propagation—A. D. Wheelon. (*J. Geophys. Res.*, vol. 62, pp. 343–349; September, 1957.) An examination of the role of the mean electron density of the ionosphere in scatter propagation. Correlations between the field strength of F-layer scattered signals and the maximum usable frequency for classical propagation along the path are studied.

621.396.11:551.510.535 242
A Method for Obtaining L.F. Oblique-Incidence Reflection Coefficients and its Application to 135.6-kc/s Data in the Alaskan Area—J. E. Bickel. (*J. Geophys. Res.*, vol. 62, pp. 373–381; September, 1957.)

621.396.11:551.510.535 243
The Relation of Forward Scattering of Very High Frequency Radio Waves to Partial Reflection of Medium Frequency Waves at Vertical incidence—J. B. Gregory. (*J. Geophys. Res.*, vol. 62, pp. 383–388; September, 1957.) Some characteristics of vhf forward scatter, such as temporal variations and the region of the ionosphere responsible, are shown to be similar to those of vertical-incidence reflection at 1.75 mc. It is considered that the two phenomena have a common origin.

621.396.11:551.510.535 244
Studies of Transequatorial Ionospheric Propagation by the Scatter-Sounding Method—O. G. Villard, Jr., S. Stein, and K. C. Yeh. (*J. Geophys. Res.*, vol. 62, pp. 399–412; September, 1957.) Long-delay echoes on a hf radar are interpreted as ground back scatter propagated by two or more successive reflections from the F region without intermediate ground reflection. Ionospheric tilts could lead to this type of propagation, which occurs regularly in equatorial regions.

621.396.11:551.510.535 245
Self-Distortion of Radio Waves in the Ionosphere, near the Gyro Frequency—F. H. Hibberd. (*J. Atmos. Terr. Phys.*, vol. 11, no. 2, pp. 102–110; 1957.) The theory described in 2198 of 1956 is extended to include the effect of the geomagnetic field near the gyro frequency. The reduction in modulation depth varies slowly with frequency and shows no resonance-like variation. The reduction is proportional to radiated power and decreases rapidly as the modulation frequency is increased.

621.396.11:551.510.535 246
Ionospheric Demodulation of Radio Waves at Vertical Incidence—G. J. Aitchison. (*Aust. J. Phys.*, vol. 10, pp. 204–207; March, 1957.) Agreement between observations and theory indicates that demodulation occurs in the E layer, affecting the wave on both upward and downward paths. The actual mechanism of the demodulation requires further investigation. See also 3070 of 1955 (Aitchison and Goodwin).

621.396.11:551.510.535:523.78 247
Ionospheric Research—Dale. (See 125.)

621.396.11.029.6 248
Radio Propagation above 40 Mc/s over Irregular Terrain—J. J. Egli. (Proc. IRE, vol. 45, pp. 1383–1391; October, 1957.) The available statistical wave-propagation data on terrain effects as a function of frequency, antenna height, polarization, and distance are analyzed and expressed by empirical formulas and in the form of nomographs and correction curves.

621.396.11.029.6:551.510.535 249
Delayed Signals in Ionospheric Forward-Scatter Communication—G. W. Luscombe. (*Nature, London*, vol. 180, p. 138; June 20, 1957.) Long-delay multipath effects observed at Slough in the reception of 37-mc pulsed transmissions from Gibraltar indicate that the signal with the largest delay was due to round-the-world propagation and that ground back scatter was not involved. See 1217 of 1957 (Crow, *et al*).

621.396.11.029.62:551.510.535:523.75 250
Disturbances in the Lower Ionosphere Observed at V.H.F. following the Solar Flare of 23 February 1956 with Particular Reference to Auroral-Zone Absorption—Bailey. (See 123.)

621.396.812.3:551.510.535 251
Ionospheric Irregularities Causing Random Fading of Very Low Frequencies—S. A. Bowhill. (*J. Atmos. Terr. Phys.*, vol. 11, no. 2, pp. 91–101; 1957.) An investigation, based on measurements at 75 and 150 kc, into the two component sources of random fading of signals reflected from the ionosphere: 1) scattering in the reflecting layer, 2) diffraction during propagation down to the ground.

RECEPTION

621.376 252
Intermodulation Products for ν-Law Biased Wave Rectifier for Multiple-Frequency Input—E. Feuerstein. (*Quart. appl. Math.*, vol. 15, pp. 183–192; July, 1957.) The intermodulation products obtained by passing the same of $N+1$ sinusoids of amplitudes $P_1, \ldots, P_N$ through a rectifier of characteristic

$$I=\begin{cases}10 & V<B\\ 1a(V-B)^{\nu} & V>B \quad \nu>0\end{cases}$$

have been expressed in terms of contour integrals involving products of Bessel functions [see, *e.g.*, 2169 of 1945 (Rice) and 3506 of 1947 (Bennett)]. These integrals are rewritten as improper integrals on the real line plus constant terms. These integrals converge fast enough in many cases to be useful in numerical integration.

621.376.23:621.396.822 253
Optimum vs. Correlation Methods in Tracking Random Signals in Background Noise—R. C. Davis. (*Quart. appl. Math.*, vol. 15, pp. 123–138; July, 1957.) A comparison of the use of statistical methods of analysis in estimating unknown parameters of probability distribution with the use of correlation methods previously applied to the problem of obtaining maximum snr.

621.376.332 254
An Improved F. M. Discriminator—V. B. Hulme. (*Electronic Eng.*, vol. 29, pp. 416–419; September, 1957.) Details are given of a constant-area type circuit which provides a relation to 0.1 per cent between input frequency and output voltage over the range 100 kc–1 mc.

621.396.62.029.6:621.396.822:621.317.3 255
Absolute Measurement of Receiver Noise Figures at U.H.F.—E. Maxwell and B. J. Leon. (IRE TRANS., vol. MTT-4, pp. 81–85; April, 1956. Abstract, PROC. IRE, vol. 44, p. 956; July, 1956.)

621.396.621 256
Receiver Selectivity—B. J. Rogers. (*RSGB Bull.*, vol. 32, pp. 444–448; April, 1957.) Some modern methods of improving the selectivity of communication receivers are described.

621.396.621 257
F.M./A.M. "Second Set"—G. D. Browne. (*Mullard tech. Commun.*, vol. 3, pp. 38–43; March, 1957.) Design suggestions for a simple and economical receiver in which all tubes are operative in both systems of reception.

621.396.621:621.314.7 258
Design Considerations in the First Stage of Transistor Receivers—L. A. Freedman. (*RCA Rev.*, vol. 18, pp. 145–162; June, 1957.) Noise performance of transistor rf stages using capacitive antennas and mixer stages with loop antennas is discussed with examples. Comparisons are made between transistor stages and corresponding tube stages.

621.396.621:621.314.7 259
Circuit Techniques associated with Transistor Broadcast Receivers—J. N. Barry. (*Electronic Eng.*, vol. 29, pp. 408–415 and 478–483; September and October, 1957.) A discussion of transistor circuit problems and their solution. The various stages of the receiver are considered and the economic aspects of using transistors are discussed with reference to the performance of 6 commercial-type portable and car receivers.

621.396.621:621.314.7 260
The Thunderbird—a New Transistorized Portable Radio—T. Vanacore. (*Sylvania Technologist*, vol. 10, pp. 35–37; April, 1597.)

621.396.621:621.376 261
A New Method of Demodulation for Phase, Frequency and Amplitude—P. Knudu. (*Indian J. Phys.* vol. 40, pp. 231–234; April, 1957.) Limiting and differentiating a modulated sinusoidal wave produces pulses with leading edges separated by an amount dependent upon the instantaneous phase of the modulated wave, and upon its amplitude if the limiting level is above the zero axis. The pulses are converted to variable-amplitude sawtooth waves and passed through a low-pass filter to reproduce the modulating signal. See also 551 of 1956.

621.396.621:621.396.822 262
Receiver Detects Signals below Noise Level—W. L. Blair. (*Electronics*, vol. 30, pp. 168–171; September 1, 1957.) The integrating receiver described uses a modified form of Dicke's technique (475 of 1947) with a comparison switching rate of 500 cps and a counter display.

621.396.621.029.63/.64 263
Design for a Broadband Microwave Receiver—B. Rosen and R. Saul. (*Electronic Inds. Tele-Tech.*, vol. 16, pp. 81–82, 170; March, 1957.) Brief description of a receiver covering the frequency range 950–11260 mc in four bands. It is suitable for AM, fm, and pm reception and for use as a microwave power meter.

621.396.8:621.3.018.41(083.74) 264
Doppler Shift of the Received Frequency from the Standard Station Reflected by the Ionosphere—I. Takahashi, T. Ogawa, M. Yamano, A. Hirai, and M. Takiuchi. (PROC. IRE, vol. 45, p. 1408; October, 1957.) Equipment for recording frequency continuously is described, and results of Doppler-shift measurements made on waves reflected from the E region on 4 mc over a 400-km path are given.

621.396.8:621.396.931.029.62/.63 265
Propagation Tests of Frequencies for V.H.F. Mobile Radio—E. Shimizu, T. Morinaga, T. Kawano, S. Sato, and M. Hirasaki. (*Rep. elect. Commun. Lab., Japan*, vol. 5, pp. 13–16; January, 1957.) Measurements are given of signal and noise received at a mobile station from fixed transmitters in Tokyo operating at 60, 200, and 470 mc. Less fluctuation was observed than in comparable U. S. measurements, and this is attributable to the wooden houses normal in Japan.

621.396.812.3:621.396.666.029.64 266
Some Results with Frequency Diversity in a Microwave Radio System—F. H. Willis. (*Commun. and Electronics*, no. 29, pp. 63–67; March, 1957.) The results of tests with 240-mc frequency separation and an appreciable switching differential are discussed.

STATIONS AND COMMUNICATION SYSTEMS

621.39.001.11:621.372.012 267
Signal-Flow Graphs and Random Signals—L. A. Zadeh and W. H. Huggins. (PROC. IRE, vol. 45, pp. 1413–1414; October, 1957.) Comments on 1227 of 1957 and author's reply.

621.394.3:621.394.828 268
Distortion Correction of Teleprinter Signals by Electronic Means—E. K. Aschmoneit. (*Elektronik*, vol. 6, pp. 199–203 and 244–245; July and August, 1957.) The principles and circuits of some electronic distortion-correcting and regenerative repeaters are described.

621.396.41:621.396.324:621.314.7 269
Transistorized Multiplex Radio-Teletypewriter—P. G. Wray. (*Electronics*, vol. 30, pp. 150–154; September 1, 1957.) Lightweight four-channel time-division multiplex equipment for use on board ship is described. Ring counter and digital synchronizer circuits using transistors give an operating speed of 100 words per minute.

621.396.41.029.63 270
Ultra-high-Frequency Radio Equipment for 60 Speech Circuits—(*GEC Telecommun.*, no. 22, pp. 34–49; August, 1956.) The Type-SPO 5500 equipment described uses fm and operates in the band 1700–2300 mc. Up to three rf channels each carrying 60 speech channels can be arranged in multiplex.

621.394.441 271
An Electronic Error-Correcting Multiplex Telegraph System—(*P.O. Elec. Eng. J.*, vol. 50, Pt. 1, p. 44; April, 1957.)

621.396.5.029.6:621.396.822 272
Noise Considerations on Toll Telephone Microwave Radio Systems—T. A. Combellick and M. E. Ferguson. (*Commun. and Electronics*, no. 29, pp. 67–70; March, 1957.) The noise level requirements for microwave radio equipment to be used in multichannel telephone systems are discussed. The magnitude of and relation between the noise generated in the transmitter, in the receiver, or by intermodulation, are examined.

621.396.71.029.55 273
The Rugby "B" High-Frequency Transmitting Station—A. Cook and L. L. Hall. (*P.O. Elec. Eng. J.*, vol. 50, Pt. 1, pp. 15–23; April, 1957.) The layout and technical facilities of the station are described. There are 28 hf transmitters of 30-kw power rating in operation and some 70 antennas on a site of 700 acres. See also 2538 of 1956 (Booth and MacLarty).

621.396.74:621.397.743 274
Frequency Transposers as Very-Low-Power Transmitters—A. Kolarz. (*Rundfunktech. Mitt.*, vol. 1, pp. 53–57; April, 1957.) A 50-mw relay transmitter for providing a local television service is described. The transposition from received to transmitted frequency is made without the use of an IF. See also 1927 of 1957.

621.396.74.029.62:621.376.3 275
Investigation of Coverage Facilities with Frequency-Offset U.S.W. F.M. Operation—E. Belger, E. Paulesn, and L. Dahrendorf. (*Rundfunktech. Mitt.*, vol. 1, pp. 58–64; April, 1957.) The limitations and advantages of this method of obtaining regional coverage are discussed with reference to experimental results. See also 1869 of 1956 (Belger and von Rautenfeld).

621.396.931 276
Radio Communication in Railroad Tunnels—H. S. Winbigler. (*Bell Lab. Rec.*, vol. 35, pp. 57–60; February, 1957.) Radiation from a continuous length of twin transmission line suspended from the tunnel wall is received satisfactorily up to 5000 feet from the transmitter, using frequencies in the 159–162-mc band.

621.396.932 277
Ships and Coast Stations—P. N. Spooner. (*Short Wave Mag.*, vol. 14, pp. 636–639; February, 1957.) Details of systems, procedure, operating frequencies, and general organization.

621.396.945 278
The Guided Radio Telephone—W. H. Hill. (*A.T.E.J.*, vol. 13, pp. 113–118; April, 1957.) This communication system uses currents induced in metallic conductors by the transmitter. A satisfactory portable transmitter/receiver is described for use in coal mines.

SUBSIDIARY APPARATUS

621.3–71 279
Removal of Heat from Sealed Miniature Equipment—E. P. Newell. (*Brit. Commun. Electronics*, vol. 4, pp. 468–475; August, 1957.) Experimental investigation has shown that the most satisfactory way of dissipating the heat generated internally is by providing thermal conduction paths from the heat sources to the front panel.

621.311.6:537.311.33:535.215 280
Utilizing the Sun's Energy—(*Elec. J.*, vol. 159, pp. 1256–1257; November 1, 1957.) Report on progress in the development of solar batteries of the Si *p-n*-junction type with description of experimental installations in England.

621.311.6:621.314.7 281
A Stabilized D.C. Power Supply using Transistors—T. H. Brown and W. L. Stephenson. (*Electronic Eng.*, vol. 29, pp. 425–428; September, 1957.) A mains-operated unit is described which provides an output voltage variable from 0 to 30 v at currents of up to 1 a.

621.314.63:546.289 282
Germanium Rectifiers as Electronic Components—J. T. Cataldo. (*Electronic Inds.*

Tele-Tech., vol. 16, pp. 61–63, 168; August, 1957.) Discussion of advantages and applications. Cooling methods and overload characteristics are considered.

621.316.722.1:621.314.7 283
A Low-Voltage Stabilizer employing Junction Transistors and a Silicon Junction Reference Diode—D. Aspinall. (*Electronic Eng.*, vol. 29, pp. 450–454; September, 1957.)

621.316.722.1:621.314.7 284
Voltage Regulator uses Multivibrators—W. A. Scism. (*Electronics*, vol. 30, pp. 184–186; September 1, 1957.) Voltage changes vary the frequency of an astable transistor multivibrator and the average value of the load voltage is thus kept constant.

621.396.662.029.5 285
Multichannel Drives for Transmitters and Receivers in the H.F. Band—D. J. Fewings. (*Marconi Rev.*, vol. 20, pp. 60–76; 2nd Quart., 1957.) Methods of tuning accurately to a prescribed frequency are described, as applied to 1) a diversity oscillator with manual tuning, 2) an automatically tuned airborne receiver /transmitter drive.

621.396.664:621.376 286
Monitoring the Modulator—P. M. Carment. (*Short Wave Mag.*, vol. 14, pp. 631–632; February, 1957.) A circuit for monitoring the output of a high-power modulator on a pair of headphones.

TELEVISION AND PHOTOTELEGRAPHY

621.397:628.93 287
Techniques of Television Lighting—D. Thayer. (*J. Soc. Mot. Pict. Telev. Eng.*, vol. 66, Pt. 1, pp. 212–216; April, 1957.)

621.397.2:621.372.55 288
Error-Predicting D.C.-Restoring Circuits for Television Signals—E. L. C. White. (*Electronic Eng.*, vol. 29, pp. 472–477; October, 1957.) The performance of direct and negative-feedback types of dc restoring circuit is analyzed. By a combination of slope equalization and error prediction the low-frequency cutoff of the circuit prior to dc restoration may be raised by a large factor. Some experimental results are given.

621.397.24 289
Performance of the A2A Video Transmission System—R. W. Edmonds. (*Bell Lab. Rec.*, vol. 35, pp. 85–88; March, 1957.) Design considerations and performance details of a broadband local wire transmission system for monochrome and color television.

621.397.24:621.315.212 290
A New 4-Mc/s Coaxial Line Equipment—C. E. L. No. 6A—Collier and Simpson. (See 14.)

621.397.24:621.315.212 291
A 4-Mc/s Coaxial Line Equipment—C.E.L. No. 4A—E. Davis. (See 15.)

621.397.242 292
Television Terminals for the L3 System—J. J. Jansen. (*Bell Lab. Rec.*, vol. 35, pp. 179–183; May, 1957.) 600 telephone channels and a 4.2-mc television channel may be transmitted by the coaxial cable system the terminal equipment of which is described.

621.397.5:535.623 293
Some Alternatives to the N.T.S.C. Colour Television System—E. L. C. White. (*J. Telev. Soc.*, vol. 8, pp. 191–206; January/March, 1957.) The NTSC system is compared with the two-subcarrier, the French L.E.P. "3 double-message," and the Valensi systems. For a three-gun picture tube, the first system seems most satisfactory. The signal requirements of single-gun tubes, such as the chromatron and "apple" tubes, are then discussed; here a symmetrical ratio system may be better.

621.397.5:621.395.625.3 294
Video Tape Recorder Design—(*J. Soc. Mot. Pict. Telev. Eng.*, vol. 66, Pt. 1, pp. 177–188; April, 1957.) Three papers, describing equipment incorporating a system of four magnetic recording heads on a revolving drum for recording transverse tracks on tape traveling at 15 inches per second. See also 4018 of 1957 (Snyder).

Comprehensive Description of the Ampex Video Tape Recorder—C. P. Ginsburg (pp. 177–182).

The Modulation System of the Ampex Video Tape Recorder—C. E. Anderson (pp. 182–184).

Rotary-Head Switching in the Ampex Video Tape Recorder—R. M. Dolby (pp. 184–188).

621.397.5(083.74) 295
Comparison of Four Television Standards—R. D. A. Maurice. (*Electronic Radio Eng.*, vol. 34, pp. 416–421; November, 1957.) "The resolutions of four CCIR standard television systems are compared, some account being taken of the effects of the asymmetric side-band reception. The extent to which some of the distortions may be due to nonlinearity of the phase-frequency characteristic is briefly mentioned."

621.397.611:778.5 296
The Limits of Optical Compensation by Polygonal Prisms in relation to Freedom from Flicker, Registration and Relative Aperture—H. Grabke. (*Rundfunktech. Mitt.*, vol 1, pp 65–72; April, 1957.) Theoretical treatment of the problem based on earlier experiments with film scanning equipment (1227 of 1956). The design of a "polygon-ring scanner" is discussed and data for calculating tolerances and color correction of the system are given. The manufacture of such a scanner with 40–60 faces appears feasible; it should produce satisfactory pictures comparable to those obtained by other flying-spot scanners.

621.397.621.2 297
Television Frame Pulse Separator—H. D. Kitchin. (*Wireless World*, vol. 63, pp. 554–559; November, 1957.) A single-pulse circuit for accurate interlacing is described.

621.397.621.2 298
The Return of Electrostatic Focusing—R. R. Pearce. (*J. Telev. Soc.*, vol. 8, pp. 237–248; April/June, 1957.) A survey of the developments in post-war television tubes and techniques with a detailed discussion of the characteristics and relative merits of modern electrostatic guns.

621.397.82 299
The Visibility of Sinusoidal Interference in Television Images—H. Grosskopf and R. Suhrmann. (*Rundfunktech. Mitt.*, vol. 1, pp. 45–52; April, 1957.) The nature of interference patterns is reviewed and the effects of interference due to frequencies which are specially related to line or frame frequency are examined. Curves for evaluating some of these effects are given and the requisite "safe" frequency spacing between adjacent transmitters is compared with that recommended by CCIR.

TRANSMISSION

621.396.61.029.6:621.396.662 300
Transmitter Tuned by Distortion Indicator—C. R. Ellis, K. Owen, and G. R. Weatherup. (*Electronics*, vol. 30, pp. 180–183; September 1, 1957.) The system described gives harmonic distortion of less than 3 per cent rms over the range 200 cps–20 kc when the transmitter is operated at 225–400 mc, with 80 per cent AM of a 1-kw carrier.

621.396.61.072.9 301
A New Device for the Automatic Radio-Frequency Synchronization of Common-Frequency Broadcasting in the Medium-Wave Band—A. Karaminkov. (*Nachr-Tech.*, vol. 7, pp. 163–166; April, 1957.) In the system proposed synchronization is carried out by radio transmission during breaks in the program. During these interruptions of about 12-seconds duration which are intentionally introduced at intervals of about 1 hour, the carrier of the local transmitter is stopped so that the distant master transmitter can be received for the automatic frequency correction of the local carrier. Using quartz oscillators with long-term stability 1 part in 10^8 an hourly stability within about 1 part in 10^8 can be achieved.

TUBES AND THERMIONICS

621.314.63:621.317.3 302
Measurements of Crystal Impedances at Low Levels—H. N. Dawirs and E. K. Damon. (IRE TRANS., vol. MTT-4, pp. 94–96; April, 1956. Abstract, PROC. IRE, vol. 44, p. 956; July, 1956.

621.314.63:621.372.632 303
The Frequency Dependence of Noise Temperature Ratio in Microwave Mixer Crystals—M. E. Sprinks, G. T. G. Robinson, and B. G. Bosch. (*Brit. J. Appl. Phys.*, vol. 8, pp. 275–277; July, 1957.) A discussion with experimental results of the contribution of the noise temperature ratio of the mixer to the over-all noise factor of the receiver. The latter has an intermediate frequency in the range 10–60 mc.

621.314.7 304
Some Aspects of Transistor Progress—H. W. Loeb. (*A.T.E.J.*, vol. 13, pp. 119–134; April, 1957.) Reprint. See 295 of 1957.

621.314.7 305
Heat Sinks for Power Transistors—O. J. Edwards. (*Mullard tech. Commun.*, vol. 3, pp. 59–61; March, 1957.) Sinks of mild steel and aluminum are examined and the effects of thickness, area, and surface treatment are discussed.

621.314.7 306
Design Theory for Depletion-Layer Transistors—W. W. Gärtner. (PROC. IRE, vol. 45, pp. 1392–1400; October, 1957.) This new type of high-frequency transistor uses maximum attainable carrier velocities in solids by injecting electrons or holes into the high electric fields prevailing in properly designed depletion layers of reverse-biased *p-n* junctions. Low- and high-frequency performance, small-signal behavior, power gain, and stability are discussed in a particular theoretical design. The short transit times should be important for solid-state microwave amplification.

621.314.7 307
Design for an Improved High-Frequency Transistor—C. Thornton, J. Roschen, and T. Miles. (*Electronic Inds. Tele-Tech.*, vol. 16, pp. 47–49, 124; July, 1957.) The construction and properties of the Type L-6100 silicon surface-alloy transistor are described. It has a base width of 7×10^{-5} inches and a maximum oscillation frequency of about 16 mc.

621.314.7 308
The Junction Transistor as a Charge-Controlled Device—R. Beaufoy and J. J. Sparkes. (*A.T.E.J.*, vol. 13, pp. 310–327; October, 1957.) Transistor operation is described in terms of the charge in the base region so that the transistor performance is defined in the form of time constants (pc/μa). The analysis was developed for large-signal opera-

tion but yields complete expressions for small-signal admittance parameters. Methods of measurement are outlined.

621.314.7 309
Flow Line Analysis—R. B. Hurley. (*Electronic Inds. Tele-Tech.*, vol. 16, pp. 52–54, 140; April, 1957.) A pictorial representation of the expressions derived by Ebers and Moll (884 of 1955) to analyze transistor behavior in various types of switching circuit.

621.314.7:546.289 310
Influence of Surface Oxidation on Alpha$_{cb}$ of Germanium *p-n-p* Transistors—J. T. Wallmark. (*RCA Rev.*, vol. 18, pp. 255–271; June, 1957.) Oxidation of the Ge surface is shown to be a major factor influencing surface recombination and thereby the slow decay of the current transfer ratio α_{cb} in *p-n-p* transistors. An outline of the underlying processes is given.

621.314.7:621.317.3 311
Transistor Tests Predict High-Frequency Performance—Pritchard. (See 213.)

621.314.7:621.318.57 312
Determination of Transient Response of a Drift Transistor using the Diffusion Equation—H. B. von Horn and W. Y. Stevens. (*IBM J. Res. Devel.*, vol. 1, pp. 189–191; April, 1957.) The one-dimensional diffusion equation is solved to give the time required for the collector current to reach a steady value in response to a step function of emitter current.

621.314.7:621.373.51 313
Unique Properties of the Four-Layer Diode—W. Shockley. (*Electronic Inds. Tele-Tech.*, vol. 16, pp. 58–60, 165; August, 1957.) Description of a new bistable two-terminal semiconductor device and details of some of its applications. See also 3899 of 1956 (Moll, *et al*).

621.314.7:681.142 314
The Multipurpose Bias Device: Part 1—The Commutator Transistor—Dunham. (See 38.)

621.314.7:681.142 315
Two-Collector Transistor for Binary Full Addition—R. F. Rutz. (*IBM J. Res. Devel.*, vol. 1, pp. 212–222; July, 1957.) Two versions of a two-collector transistor are described, one using point contacts, and the other using *p-n* "hook" junctions as collectors. The function of such a transistor as a binary adder and its circuit characteristics are discussed. See also 38 above.

621.314.7(083.7) 316
Semiconductor Symbols—P. M. Thompson and J. Bateson. (*Wireless World*, vol. 63, pp. 525–528; November, 1957.) A logical system for diodes, transistors, and other junction devices is proposed.

621.383.27 317
Photomultiplier Tubes—J. Sharpe. (*Brit. Commun. Electronics*, vol. 4, pp. 484–492; August, 1957.) The design and applications of the various types of photomultiplier tube are described. A table of representative tubes available in the U. K. is given.

621.383.27:621.387.464 318
Improved Performance of Photomultipliers in Scintillation Counters—A. Ashmore, B. Collinge, and S. K. Sen. (*Indian J. Phys.*, vol. 40, pp. 261–264; May, 1957.) A cathode follower reduces the effective capacitance to earth of the collecting electrode of a photomultiplier, enabling bigger voltage pulses to be obtained for the same degree of nonlinearity in the photomultiplier.

621.383.4:535.371.07 319
An Improved High-Gain Panel Light Amplifier—B. Kazan. (PROC. IRE, vol. 45, pp. 1358–1364; October, 1957.) A grooved photoconductor light-amplifying picture panel is described, whose gain is more than 10 times greater than any previous amplifier and whose threshold for input light is reduced. See also 933 of 1956 (Kazan and Nicoll).

621.385:621.317.321 320
A Survey of Methods Used to Determine Contact Potentials in Receiving Tubes—E. R. Schrader. (*RCA Rev.*, vol. 18, pp. 243–254; June, 1957.)

621.385:621.317.444 321
Rectilinearity of Electron-Beam Focusing Fields from Transverse Component Determinations—Cioffi. (See 222.)

621.385.029.6 322
Investigation of a Special Type of Reflex Klystron—W. N. Shevchik, S. A. Suslov, and Yu. D. Zharkov. (*Zh. Tekh. Fiz.*, vol. 27, pp. 377–386; February, 1957.) A theoretical and experimental investigation of a reflex klystron operating with a large transit angle ($>2\pi$) in the interaction space is described. Good agreement is found between the theoretical evaluation of the tube efficiency and the experimental results.

621.385.029.6 323
On the Nonlinear Behavior of Electron-Beam Devices—F. Paschke. (*RCA Rev.*, vol. 18, pp. 221–242; June, 1957.) The nonlinear space-charge-wave equation is derived and reduced by third-order successive approximation to three simultaneous linear differential equations which are solved for the case of a velocity-modulated electron beam. Nonlinear phenomena in traveling-wave tubes can be treated similarly.

621.385.029.6 324
Electron Beam Focusing in Three-Anode Guns for Travelling-Wave Tubes—T. S. Chen and L. Kovach. (*J. Electronics Control*, vol. 3, pp. 287–304; September, 1957.) The electron trajectory in the accelerating region is solved and beam rippling in the drift region discussed. The principle of compensated three-anode guns is developed in the form of design formulas and curves. Experiments confirm that compensated guns result in a reduction of the focusing magnetic field for parallel-flow beams.

621.385.029.6 325
The Large-Signal Behaviour of Crossed-Field Travelling-Wave Devices—J. Feinstein and G. S. Kino. (PROC. IRE, vol. 45, pp. 1364–1373; October, 1957.) The limits of validity of the conventional small-signal theory are obtained theoretically, and the analysis is extended to follow the interaction to power saturation. Forward-wave and backward-wave amplifiers and a backward-wave oscillator are considered. In the amplifier tubes the gain is inherently low, and suggestions for improving this deficiency are examined.

621.385.029.6 326
An Experimental High-Power Pulsed Travelling-Wave Tube—J. F. Gittins, N. H. Rock, and A. B. J. Sullivan. (*J. Electronics Control*, vol. 3, pp. 267–286; September, 1957.) A high-impedance slow-wave structure with good thermal dissipation and suitable for a 100-kv electron beam is used. A saturated efficiency of 34 per cent, power output of 3 mw, and a gain of 35 db are obtained.

621.385.029.6:621.372 327
Interdigital and other Slow-Wave Structures—J. C. Walling. (*J. Electronics Control*, vol. 3, pp. 239–258; September, 1957.) A method of calculating the properties of structures consisting of arrays of parallel conductors is developed and a table of numerical values is presented. This is applied to obtain dispersion characteristics, input and beam-coupling impedances for the Karp structure, interdigital line, and tape helix.

621.385.029.6:621.376 328
The Modulation of Travelling-Wave Tubes—G. F. Steele. (*Electronic Eng.*, vol. 29, pp. 429–433; September, 1957.) "The simple theory of traveling-wave tube modulation is discussed and some expressions derived for the cases of phase and amplitude modulation. Details are given of the experimental procedure used to measure phase shift and the side-band power resulting from a 60-mc modulation."

621.385.029.64 329
Velocity-Jump Amplification at 10000 Mc/s—B. V. Dore. (*Can. J. Phys.*, vol. 35, pp. 742–752; June, 1957.) Description of a vm tube based on an earlier design [2068 of 1951 (Field, *et al*)]. Theory previously developed for space-charge-wave amplifiers is applied to its operation and conclusions are drawn regarding the operation of coupling helices and the effect of small gaps in the amplifying section of the tube. See also 3721 of 1954 (Agdur).

621.385.832:621.317.799 330
An Electrostatic Cathode-Ray-Tube Tester—R. B. Hale. (*Brit. Commun. Electronics*, vol. 4, p. 496; August, 1957.)

MISCELLANEOUS

621.39(091) 331
Fifty Years of the Institution of Post Office Electrical Engineers—(*P.O. Elec. Eng. J.*, vol. 49, Pt. 3, pp. 147–274; October, 1956.) A number of papers surveying the history and activities of the Institution and detailing its achievements in all fields of telecommunications.

NEW!

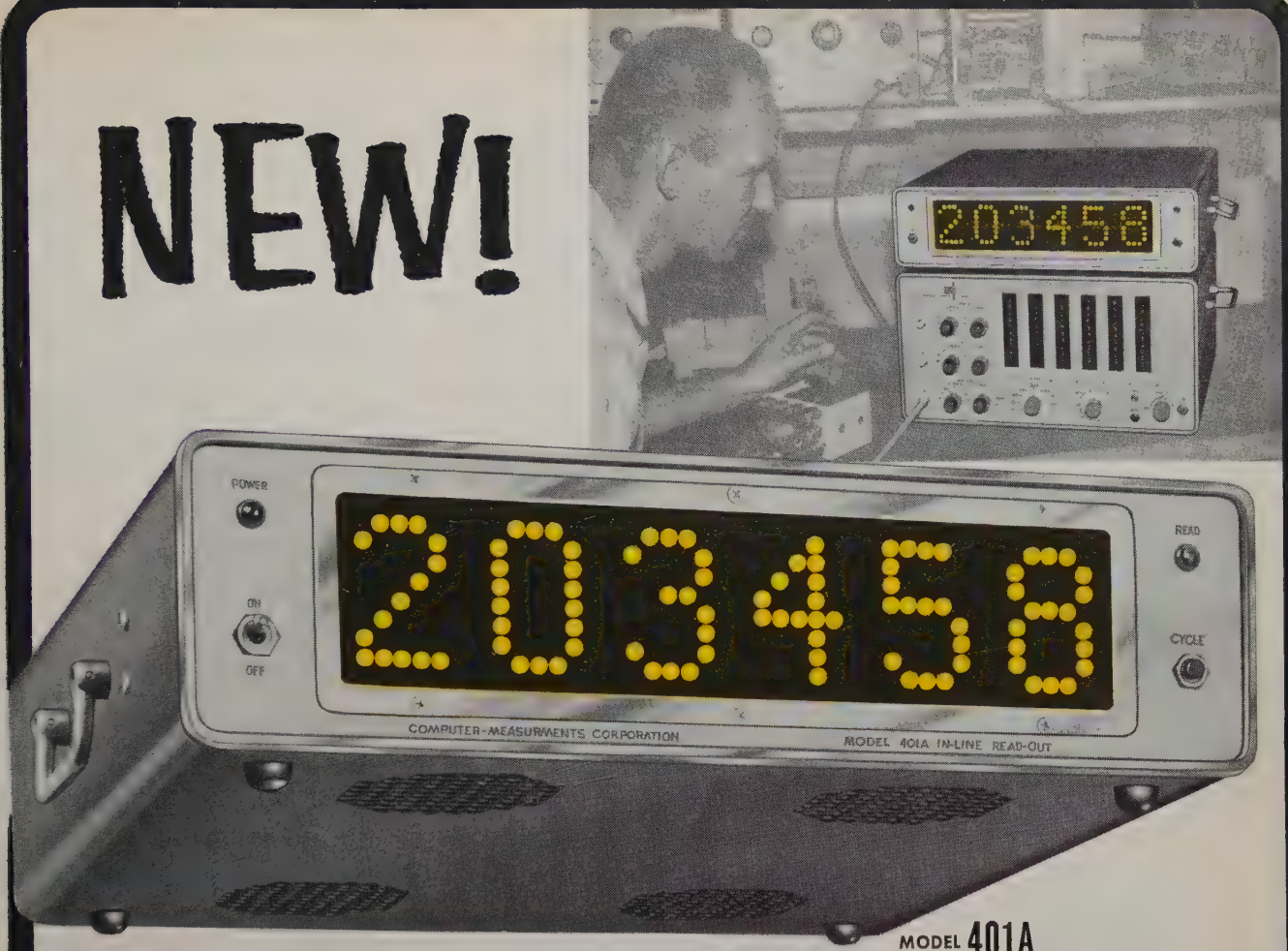

IN-LINE READ-OUT

All data is more accurate when taken from a straight-line read-out, as compared to reading the necessarily small numerals on a digital counter . . . especially when they are staggered on 10 rapidly changing decade levels. You can't always trust the eye, but you can always trust a CMC In-Line Read-Out.

The elimination of errors due to lamp filament failure is an important safeguard to accuracy. This feature is possible only with the new CMC IN-LINE READ-OUT designed for use with digital counting instruments. It is Fail-Safe!

Individual 2½" numerals with wide-angle readability, distinctly formed on a flat plane by many small high-intensity neon bulbs, are easily read even in strong ambient light. The memory circuit changes only on command, thus preventing loss of important data. Plug-in modular construction allows relay trees and lamp assemblies to be used separately as needed, or in other equipment.

For simultaneous multiple or remote use, two or more CMC In-Line Read-Out instruments may be connected to one Digital Computer.

Write today for full technical information, engineering data or assistance with your computing problems. Ask also for the new CMC Short-Form Computer Catalog.

SPECIFICATIONS

Indicating Capacity	6 Digits
Accuracy	Identical to counting instrument.
Signal Input Requirements	4-line 1-2-2-4 binary decimal code and read command from counting instrument for automatic operation.
Power Requirements	117 V ± 10%, or 230 V ±10%, 50-60 cps, 125 watts
Dimensions	17" W x 4½" H x 17½" D approximately.
Weight	33 pounds approximately.
Finish	Panel: Light grey baked enamel. Case: Dark grey baked enamel.
Accessories	One 48" signal cable.

MODEL 401A *Features*

- ★ LARGE NUMERALS — 2½" HIGH
- ★ FAIL-SAFE NUMERAL CONFIGURATION
- ★ FLAT PLANE PRESENTATION
- ★ BRILLIANT LONG-LIFE NEON BULBS
- ★ WIDE ANGLE READABILITY
- ★ PLUG-IN MODULAR CONSTRUCTION
- ★ MEMORY CIRCUIT
- ★ REMOTE READ-OUT FOR GROUP USE

CMC

9 8 7 6 5 4 3 2 1 0

Subsidiary of Hancock Manufacturing Company

Computer-Measurements Corporation

5528 Vineland Ave., Dept. 86B
No. Hollywood, Calif.

CC-101

NOW AVAILABLE in the SUBSONIC RANGE 0.5-2,250 cps

Panoramic's unique RESPONSE TRACING SYSTEM

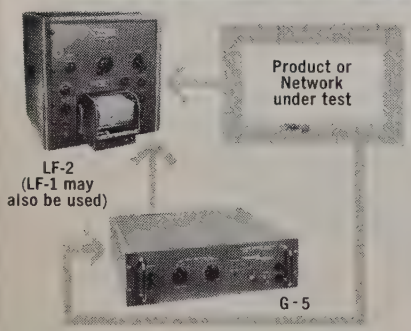

for

- **analyzing frequency response characteristics of**
  - **servo amplifiers • filters**
  - **acoustic reproducers**
  - **transformers • hearing aids**
  - **shaker tables**
- **locating resonant frequencies in mechanical structures**

Serving as a frequency sweep source and synchronous selective indicator, the G-5 and LF-2 or LF-1 form a frequency response tracing system in the SUBSONIC range . . . are invaluable in testing networks and devices which tend to produce distortion products, where hum and noise are present, or where measurements through large dynamic ranges are necessary.

Shows single line response to fundamental frequency only, discriminates against noise and hum, has virtually unlimited dynamic range. 3 sweep widths which may be centered at any point in the range from 0.5-2000 cps. Scan rate of 10 sec., 2 mins. or 16 mins. Analyzer I.F. bandwidth variable from 0.25 to 12 cps.

Write, wire, phone TODAY for more information or help on your specific problem.

the pioneer is the leader

PANORAMIC RADIO PRODUCTS, INC.

Send for our new CATALOG DIGEST and ask to be put on the mailing list for The PANORAMIC ANALYZER featuring application data.

PANORAMIC RADIO PRODUCTS, INC.
522 South Fulton Avenue, Mount Vernon, N.Y.
Phone: OWens 9-4600
Cables: Panoramic, Mount Vernon, N. Y. State

News-New Products

These manufacturers have invited PROCEEDINGS readers to write for literature and further technical information. Please mention your IRE affiliation.

(Continued from page 92A)

Rack Mounted Oscilloscopes

Two new Oscilloscopes, the 130BR dc to 300 kc High Sensitivity Oscilloscope, and the 150AR dc to 10 mc high frequency oscilloscope, designed for mounting in a standard 19 inch equipment rack, were announced recently by the **Hewlett-Packard Co.,** Dept. P. 395 Page Mill Rd., Palo Alto, Calif. According to the manufacturer the Model 130BR has electrically similar vertical and horizontal amplifiers which have less than 1° relative phase shift at 50 kc and a 1 millivolt/cm sensitivity. Balanced signals may be used on the most sensitive ranges, the manufacturer states, hence many transducers may be connected directly into its terminals.

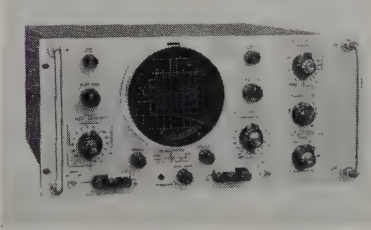

Model 150AR dc to 10 mc oscilloscope is mounted on slides for accessibility and features calibrated sweep magnifications of ×5, ×10, ×50, and ×100; any portion of the magnified trace may be viewed, and a single sweep provision permits unlimited sweep expansion. Model 150AR is used with plug-in vertical amplifiers—the Hewlett-Packard 151A which has 5 millivolt/cm sensitivity, and the 152A Dual Trace Amplifier, which has a 50 millivolt /cm sensitivity and presents two electrical phenomenom for simultaneous viewing. Both amplifiers pass dc to 10 mc, and sensitivity is accurate within ±5 per cent.

Both oscilloscopes have a universal synchronizing circuit; a single preset switch position establishes optimum triggering for nearly all conditions. Model 130BR (illustrated) is $650.00, Model 150AR is $1200.00, Model 151A is $200.00, and Model 152A is $250.00.

Precision Drive and Condenser

National Company, Inc., 61 Sherman St., Malden 48, Mass., has a new linear direct reading precision drive and condenser for use in precision direct-setting interpolation type oscillators. 2000:1 gear ratio permits precision setting of capacity to within ±5 parts in 10^4. Features smooth operating precision bearings for maximum resetability accuracy; silver ground brushes provide secure grounding of rotor assembly; $\frac{5}{8}$ inch diameter rotor shaft provides excellent stability and accuracy.

(Continued on page 104A)

FOR PUBLIC ADDRESS, RADIO, and kindred fields, JONES 400 SERIES PLUGS & SOCKETS of proven quality!

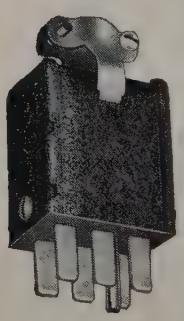
P-406-CCT

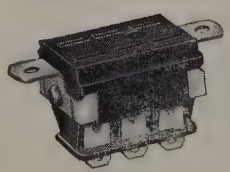
S-406-AB

Double Contact Area

Phosphor bronze knife-switch socket contacts engage both sides of flat plug contacts.

Socket contacts phosphor bronze, cadmium plated. Plug contacts hard brass, cadmium plated. Insulation molded bakelite. Plugs and sockets polarized. Steel caps with baked crackle enamel. 2, 4, 6, 8, 10, 12 contacts. Cap or panel mounting.

Information on complete line, in Jones Catalog 21. Electrical Connecting Devices, Plugs, Sockets, Terminal Strips. Write

Jones

HOWARD B. JONES DIVISION
CINCH MANUFACTURING CORPORATION
CHICAGO 24, ILLINOIS
SUBSIDIARY OF UNITED-CARR FASTENER CORP

miniaturization with reliability for UNIVERSAL ATOMICS®

Achieved by

GENERAL TRANSISTOR

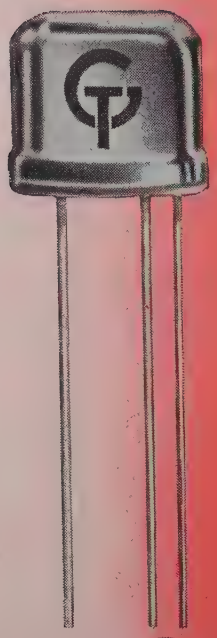

VERSATILE, TRANSISTORIZED UNIT ENABLES FASTER, MORE RELIABLE MEDICAL ANALYSIS

The design problem confronting Universal Atomics, for the UAC 522 Ratemeter, was to produce a completely miniaturized, compact portable unit using low-power consumption at a realistic price. The unit is intended for use in both clinical and medical radioisotope research and diagnosis. A reliable miniaturized circuit was essential . . . GT was called in.

General Transistor's engineering department recommended the GT-20 P-N-P type. This reliable audio transistor offered a current gain range of 35-50, maximum noise figure of 16 db., and a collector-base voltage of 25 volts. The equipment using these transistors continued to perform with extreme accuracy, even when exposed to severe environmental conditions.

All GT transistors must pass strict quality controls, production line testing plus a 100% final inspection . . . your assurance of a completely reliable product.

This is just one more example why *General Transistor is the fastest growing name in transistors.* Send today for Bulletin G-110.

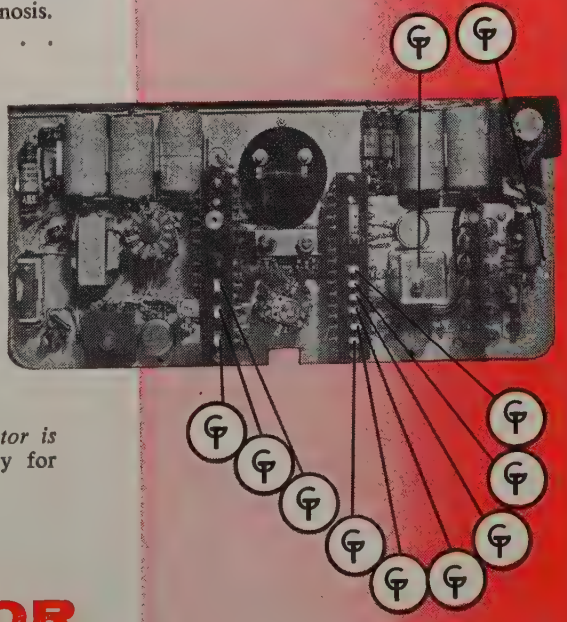

PHOTO COURTESY OF UNIVERSAL ATOMICS, A DIVISION OF UNIVERSAL TRANSISTOR PRODUCTS CORP.

FOR IMMEDIATE DELIVERY FROM STOCK, CONTACT YOUR NEAREST AUTHORIZED GENERAL TRANSISTOR DISTRIBUTOR OR GENERAL TRANSISTOR DISTRIBUTING CORP 95-27 SUTPHIN BLVD. JAMAICA 35, NEW YORK

FOR EXPORT: GENERAL TRANSISTOR INTERNATIONAL CORP., 91-27 138TH PLACE JAMAICA 35, NEW YORK

GENERAL TRANSISTOR
CORPORATION
91-27 138TH PLACE JAMAICA 35, NEW YORK

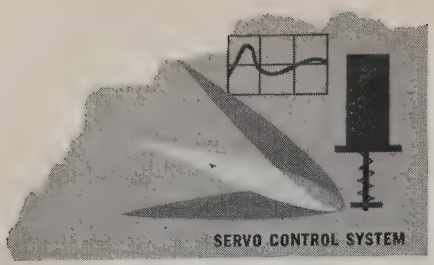

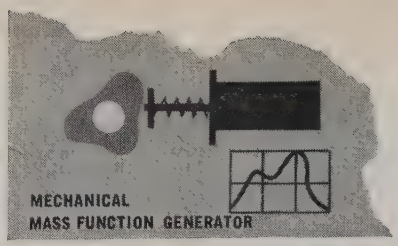

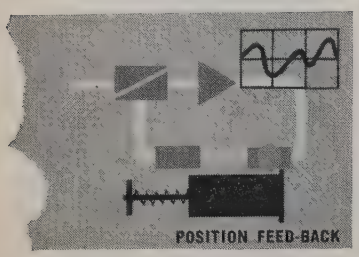

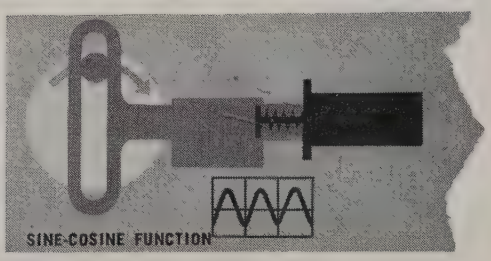

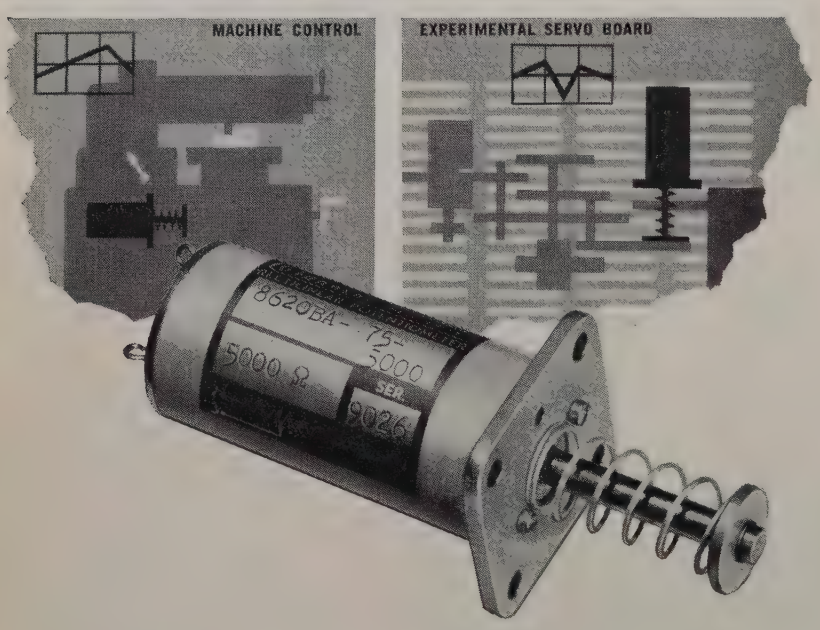

there are many ways you can use a

GIANNINI RECTIPOT

Reliable enough for the most severe airborne environments, sensitive enough for precision laboratory work! There is a RECTIPOT rectilinear potentiometer for any application where control or measurement of linear motion is required.

Standard RECTIPOTS are available with shaft displacements from 0.1" to 5.0". Resolution ranges from 0.001" to 0.003", and linearity of better than ±0.5% is typical for all models. The stainless steel shafts can be straight, threaded, keyed, or spring-loaded for automatic return to zero position.

specifications

SHAFT DISPLACEMENT: 0.1" to 5.0"
RESISTANCE: 80Ω /in. to 75,000Ω /in.
RESOLUTION: 0.001" to 0.003"
LINEARITY: ±0.5%
POWER RATING: 1.5 to 2 watts/inch
DIAMETER: 1.0 inch

See you at WESCON Booth 3204-3205

Giannini NEW JERSEY DIVISION
"Where reliability counts"

G. M. GIANNINI & CO. INC. • 918 E. GREEN STREET • PASADENA, CALIFORNIA

News-New Products

These manufacturers have invited PROCEEDINGS readers to write for literature and further technical information. Please mention your IRE affiliation.

(Continued from page 102A)

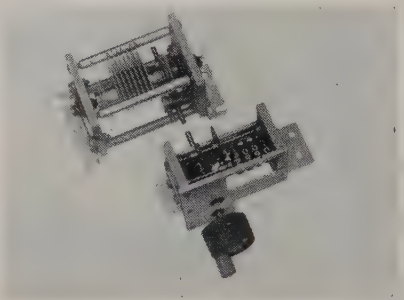

The design and materials result in a temperature stable unit. Temperature coefficient at 80 per cent of maximum capacity for 50°C rise from ambient room temperature is less than 3 parts in 10^6 per degree centrigrade.

National's components engineering staff is prepared to make specific recommendations for applications.

Broadband 10 DB Omnidirectional Antenna

Andrew Corp., 363 E. 75th St., Chicago 19, Ill., manufacturer of antenna systems, has produced a new fiberglas radome high gain antenna for the 450–470 mc. band. The Andrew type 212 antenna has a measured gain of 10 db across the entire band and can be used at any frequency in the band without troublesome tuning adjustments.

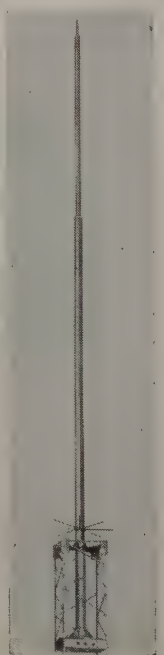

Newly developed suppressor elements incorporate the desirable features of a single feed point, while maintaining high aperture efficiency, eliminating wasted radiation and producing superior mast isolation.

This lightweight antenna is enclosed in a fiberglas radome which assures dependable systems performance under unfavorable weather conditions. Windload rating is 30 pounds per square inch, with ½ inch of radial ice.

To facilitate handling and installation, the antenna is supplied in three sections, the longest of which is 12 feet. Over-all length is 23 feet, with the lower 3 feet for mounting.

(Continued on page 106A)

Find facts faster in the IRE DIRECTORY

now, with basic modules build...

DIGITAL VOLTMETERS

DIGITAL OHMMETERS

DIGITAL RATIOMETERS

or a COMPLETE DIGITAL, MISSILE ELECTRICAL CHECKOUT SYSTEM

for measuring DC to 0.01%, AC to 0.1%, Ohms to 0.01%, DC ratios to 0.01% and AC ratios to 0.02%

Standard, off-the-shelf modules never become obsolete—provide maximum versatility. As needs change, simply regroup old modules or add new ones. Your system is always current at minimum cost and engineering. Internal construction is also modularized for ease of maintenance.

Fully transistorized circuits result in increased reliability, reduced power consumption, low heat dissipation, miniaturized packages, and eliminate radio noise and line transients.

Important new specifications—Wider, dynamic ranges cover all voltages from 100 microvolts to 1,000 volts; resistance from 10 milliohms to 10 megohms. Input power frequencies from 50 to 400 cycles. New balance logic speeds down ranging. Automatic AC ranging from 30 to 10,000 cycles. Use of transistors increases switch life by a factor of three.

Wide selection of input and output modules for operating printers, IBM punches, etc., can be accommodated without modifications. All contacts are accessible at rear panels with connectors. With plug-in modules, digitized data is provided in printed form, punched cards or tape without modification to basic measuring instruments.

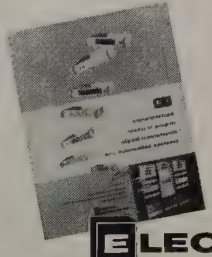

This Short Form Catalog gives complete specifications on both basic and auxiliary modules. ***Send for it . . . today.***

ELECTRO INSTRUMENTS INC.
3794 Rosecrans Street
San Diego, California

GET THE BACKGROUND YOU NEED FOR PRECISION WORK IN

NETWORK SYNTHESIS VOL. I

by DAVID F. TUTTLE, Jr.
Stanford University

A comprehensive, up-to-date, and highly readable treatment of the most important ideas used in the synthesis of networks. This first volume of a two-volume work covers the two-terminal (one-port) network or one-terminal pair. Combining new information with familiar material, the book features a three-step procedure to reach the final aim of *synthesis* or *design* of networks: —obtaining a working knowledge of the properties of networks; investigating ways of approximating desired behavior; and carrying out the actual synthesis of networks to achieve such attainable ends.

Note these chapter headings:

- Introduction
- Network Elements and How They Behave
- The Complex Frequency Variable
- A Consideration of Energy, with Some Remarkable Conclusions
- Properties of Driving-Point Immittance Functions—I
- The Nondissipative (L-C) One-Terminal Pair
- The R-C and R-L One Terminal Pairs
- Properties of Driving Point Immittance Functions—II
- The R-L-C One-Terminal Pair—I
- The R-L-C One-Terminal Pair—II
- Some Applications
- Some Practical Matters
- Approximation
- The Potential Analogy
- Illustrations

1958 **1176 pages** **Illus.** **$23.50**

Order your ON-APPROVAL copy TODAY!

JOHN WILEY & SONS, Inc. IRE-28
440 Fourth Ave., New York 16, N. Y.

Please send me a copy of NETWORK SYNTHESIS, Volume I, to read and examine ON APPROVAL. Within 10 days I will return the book and owe nothing, or remit $23.50, plus postage.

Name .....

Address .....

City ..... Zone .... State .....

( ) SAVE POSTAGE! Check here if you enclose payment in which case we pay postage. Same return privilege, of course.

News-New Products

These manufacturers have invited PROCEEDINGS readers to write for literature and further technical information. Please mention your IRE affiliation.

(Continued from page 104A)

Image Orthicon Tube Life Prolonged

First delivery of production units of Orth Saver, the device which is said to greatly extend the life of Image Orthicon tubes, was made last week with the installation of several of these devices in key TV broadcast centers by **Visual Electronic Corp.**, 342 W. 40 St., New York 18, N.Y.

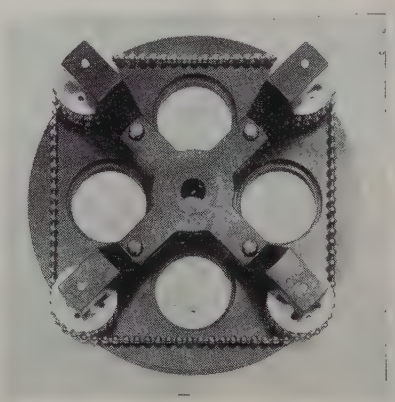

James B. Tharpe, the company's president stated that "Similar but less complete devices have been designed and patented by others who make TV broadcast equipment as well as Image Orthicon tubes. Although a patent was issued as long ago as 1953, the device was not available to TV broadcasters. The Orth Saver incorporates optical image movement to eliminate both target and photo cathode 'burn-in' with complete motion compensation so that the TV viewer sees no picture motion or picture degradation."

This statement was based on the fact that the unit incorporates optical image orbiting which permits a greater diameter of orbit and hence should provide longer life than electro-magnetic orbiting of the tube image section only. This optical method also eliminates the possible effect of image defocusing which may occur in devices requiring additional magnetic fields around the Image Orthicon tube.

Color Trinescope Cinerecorder

Telechrome Manufacturing Corp., 28 Ranick Drive, Amityville, L.I., N.Y., has developed the new Model 600M3DM color trinescope cinerecorder. It was shown that this equipment is capable of producing color TV pictures of such high intensity (brightness) that viewing with the naked eye is difficult. The resolution (clarity) of the pictures is of such high fidelity that kinescope recordings (motion pictures)

(Continued on page 108A)

Boesch

toroidal coil winding machines . . .

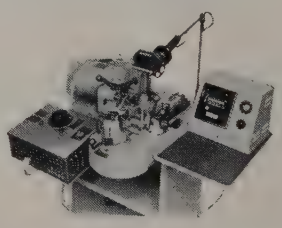

B BOESCH

feature one-piece shuttle, speed and easy operation . . . . . the world's most capable winders.

BOESCH MANUFACTURING CO., INC. • DANBURY, CONN.

CAPITOL RADIO ENGINEERING INSTITUTE

Pioneer in Radio Engineering Instruction Since 1927

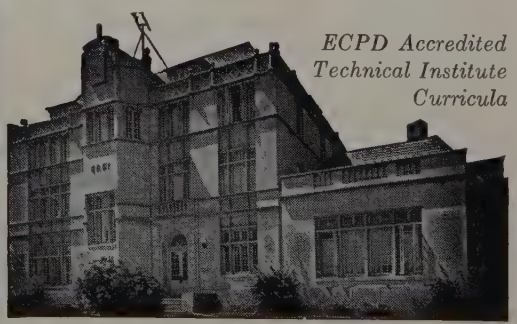

ECPD Accredited Technical Institute Curricula

Advanced Home Study and Residence Courses in Practical Radio-Electronics and Television Engineering Technology

Request your free Home Study or Resident School Catalog by writing to: Dept. 262E

3224 16th St., N. W. Washington 10, D. C.

Approved for Veteran Training

Introducing...

the world's most compact radiation-cooled high-power INDUSTRIAL TRIODE

...the new

Amperex® 7092

(Approx. ¾ actual size)

2 KW CONTINUOUS, 3 KW INTERMITTENT

INTO INDUSTRIAL LOADS – CLASS C – WITHOUT WATER COOLING

INDUSTRIAL OSCILLATOR, CLASS C
CONTINUOUS DUTY
SINGLE PHASE, RECTIFIED,
UNFILTERED PLATE SUPPLY

Typical Operation (Per Tube)

Frequency	50	50	50	Mc
D.C. Plate Voltage	2700	3600	4500	Volts
D.C. Grid Voltage	-270	-325	-360	Volts
Peak R.F. Grid Voltage	625	685	720	Volts
D.C. Plate Current (Full Load)	630	630	630	mA
D.C. Plate Current (No Load)	180	155	135	mA
D.C. Grid Current (Full Load)	180	160	145	mA
D.C. Grid Current (No Load)	305	270	250	mA
Grid Resistor	1500	2000	2500	Ohms
Driving Power (Approx.)	125	123	115	Watts
Plate Load Impedance	2250	3000	3800	Ohms
Plate Dissipation*	540	640	780	Watts
Plate Input	2100	2800	3500	Watts
Tube Plate Output	1560	2160	2720	Watts
Tube Efficiency	74	77	78	Percent

*For 50% duty cycle, averaging time 10 seconds, plate dissipation may be increased 50%.

- extra-thick hard-glass envelope for exceptional ruggedness and temperature resistance
- thoroughly dependable service in ultrasonics, induction and dielectric heating at a 40% saving in tube and accessory costs
- thoriated-tungsten filament–6.3 volts, 32.5 amps
- available from stock

ask ***Amperex***
...about new tubes for high-power industrial applications

Further details available from Industrial Tube Division
AMPEREX ELECTRONIC CORP., 230 DUFFY AVENUE, HICKSVILLE, L.I., N.Y.
In Canada: Rogers Electronic Tubes & Components, 11-19 Brentcliffe Road, Leaside, Toronto 17.

Krohn-Hite
VARIABLE
ELECTRONIC
FILTERS

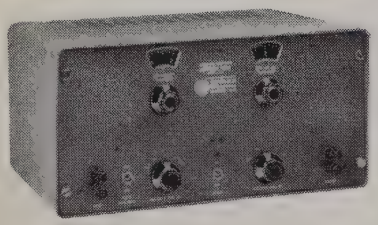

MODELS 330-A and 330-M

FEATURING
•ULTRA-LOW FREQUENCY COVERAGE
•100,000 to 1 FREQUENCY RANGE IN ONE INSTRUMENT
•DIRECT FREQUENCY CALIBRATION

The Krohn-Hite Filter Line

Model	Type	Frequency Range	Price
310-AB*	Band Pass	20 cps to 200 kc	$295.00
330-A*	Band Pass	.02 cps to 2 kc	$475.00
330-M*	Band Pass	0.2 cps to 20 kc	$475.00
340-A	Servo	.01 cps to 100 cps	$385.00
350-A*	Rejection	.02 cps to 2 kc	$475.00
360-A*	Rejection	20 cps to 200 kc	$295.00

*Available for rack mounting at $5.00 additional.

For further information on:
- Filters
- Power Supplies
- Oscillators
- Power Amplifiers

write for our free catalog D

Krohn-Hite
CORPORATION
580 MASSACHUSETTS AVENUE
CAMBRIDGE 39, MASS., U. S. A.

News-New Products

These manufacturers have invited PROCEEDINGS readers to write for literature and further technical information. Please mention your IRE affiliation.

(Continued from page 106A)

made by using an ordinary motion picture camera, are of such high quality that photographic engineers found it hard to believe that these films were made from electronic equipment and were not direct photographs of the subject.

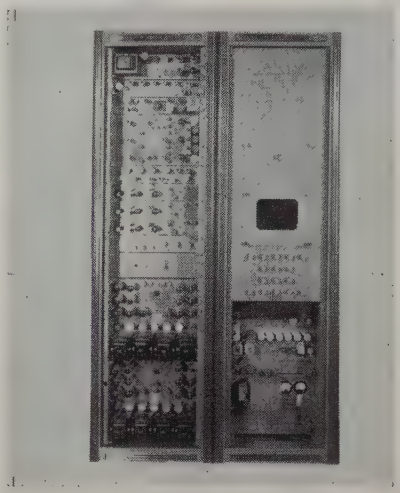

The Model 600M3DM is a high definition, high intensity, monochrome and color television display which provides a very brilliant television image, suitable for photographing on commercially available color film (such as that having an AFA speed rating of 12).

The entire system is contained in two steel rack width cabinets. Cabinet #1 contains the optical system with its control panel, deflection circuits and high voltage power supply. Cabinet #2 contains all the signal processing circuitry as well as the low voltage power supply.

The system consists of three (3) primary color phosphor high intensity cathode ray tubes having optically flat face plates. By the use of staggered dichroic mirrors, the tubes' images are made to superimpose. The effective image area measures seven (7) inches wide by five and one quarter inches high.

The equipment is switchable from monochrome, FCC-NTSC composite video signals or from separate red, green, blue, video inputs. Scanning synchronization may be selected internally (from composite video signal) or from an externally applied sync signal.

To utilize any commercial color film to its best advantage, a screen highlight brightness of 750 foot Lamberts for a 25 per cent white window is available. Resolution of the combined color signals within the "Quality Circle" is better than 500 lines. Tracking circuits are provided so that precise gray scale is maintained. After the warm-up period, stability is excellent and signal to noise ratio is subjectively negligible.

X-ray radiation has been measured and

(Continued on page 110A)

TELREX LABORATORIES

Designers and Manufacturers of

COMMERCIAL SERVICE
"BEAMED-POWER" ARRAYS

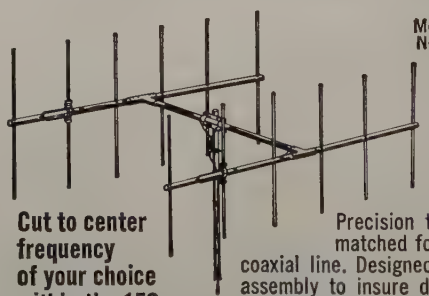

Model illustrated:
No. CY6S 150-175
Twin-Bay
(12 elements)

Cut to center frequency of your choice within the 150 to 175 mc. spectrum
(other models available)

Precision tuned and matched for 52 ohm coaxial line. Designed for easy assembly to insure duplication of our laboratory specifications at your site. Write for engineering prints and data.

Electrical specifications
Gain ..... 13 db
F/B ratio ..... 22 db
Mechanical specifications
Antenna net weight (approx.) ..... 27 lbs.
Shipping weight (approx.) ..... 33 lbs.
Shipping container size (approx.) ..... 6 feet long
Wind loading data
Wind surface area ..... 2.24 sq. ft.
Wind load at 100 mph ..... 66 lbs.
Transmission line ..... 52 ohm coaxial feed

2" OD aluminum boom; solid dural rod elements, Cycolac insulated driven dipole, stainless steel hardware, heavy-duty, heavily-plated steel mounting plate supplied. Telrex has many off-the-shelf models of hi-gain arrays or will build to order at moderate cost.

Telrex is equipped to design and supply to our specifications or yours, Broad-band or single frequency, fixed or rotary arrays for communications, FM, TV, scatter-propagation, etc.

Consultants and suppliers to communication firms, universities, propagation laboratories and the Armed Forces.

Telrex LABS.
COMMUNICATION & TV ANTENNAS SINCE 1921

ASBURY PARK 25
NEW JERSEY, U.S.A.
Tel. PRospect 5-7252

Professional Group on Audio

The IRE Professional Group on Audio is the oldest and one of the most active Groups in the IRE. Formed on June 2, 1948, the Audio Group now serves the specialized technical needs of over 4300 Group members who wish to keep abreast of progress in communication at audio frequencies, the audio portion of the radio frequency spectrum, and recording and reproducing.

Perhaps the most important activity of the Group is its technical publication, called TRANSACTIONS, which is sent bi-monthly to all Group members who have paid the $2 assessment. The TRANSACTIONS provides an invaluable source of authoritative information concerning the latest developments in the audio field. In addition to technical papers, the TRANSACTIONS contains informative technical editorials and news items pertaining to the audio field. To date, Group members have received 40 issues comprising 1270 pages of material devoted to their specific field of interest.

In addition to its publication activities, the Group sponsors technical sessions for the benefit of its members who attend national meetings, such as the IRE National Convention and the National Electronics Conference.

Supplementing its program of national meetings, the Audio Group has established 17 Chapters in cities throughout the country which, in cooperation with IRE Sections in those areas, hold frequent local meetings on subjects of timely interest to the audio engineer.

Thus the Audio Group, through its publications, national conferences, and Chapter meetings, renders a valuable service which no audio engineer can afford to be without.

W. R. G. Baker

Chairman, Professional Groups Committee

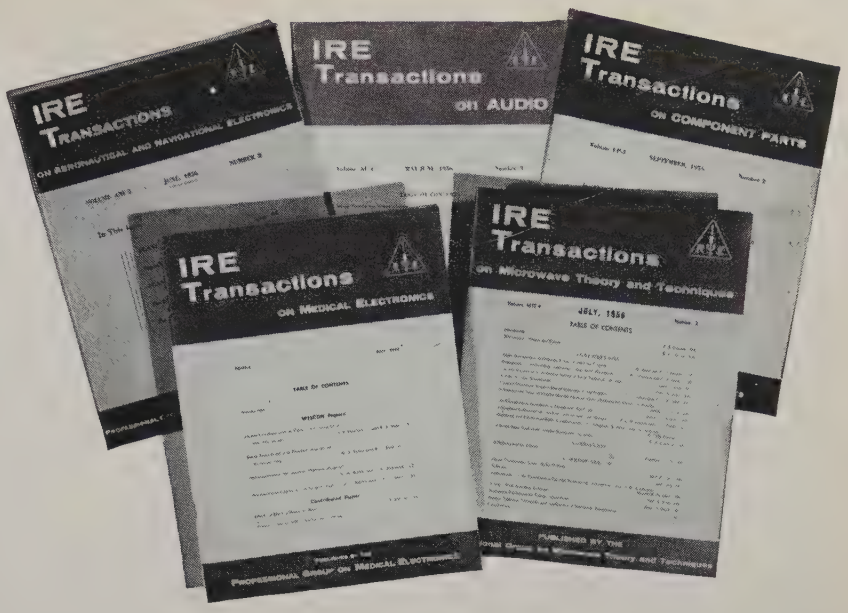

At least one of your interests is now served by one of IRE's 27 Professional Groups

Each group publishes its own specialized papers in its *Transactions*, some annually, and some bi-monthly. The larger groups have organized local Chapters, and they also sponsor technical sessions at IRE Conventions.

Aeronautical and Navigational Electronics (G 11)	Fee $2
Antennas and Propagation (G 3)	Fee $4
Audio (G 1)	Fee $2
Automatic Control (G 23)	Fee $2
Broadcast & Television Receivers (G 8)	Fee $2
Broadcast Transmission Systems (G 2)	Fee $2
Circuit Theory (G 4)	Fee $3
Communication Systems (G 19)	Fee $2
Component Parts (G 21)	Fee $3
Education (G 25)	Fee $3
Electron Devices (G 15)	Fee $3
Electronic Computers (G 16)	Fee $2
Engineering Management (G 14)	Fee $1
Engineering Writing and Speech (G 26)	Fee $2
Industrial Electronics (G 13)	Fee $2
Information Theory (G 12)	Fee $3
Instrumentation (G 9)	Fee $1
Medical Electronics (G 18)	Fee $3
Microwave Theory and Techniques (G 17)	Fee $3
Military Electronics (G 24)	Fee $2
Nuclear Science (G 5)	Fee $3
Production Techniques (G 22)	Fee $2
Radio Frequency Interference (G 27)	Fee $2
Reliability and Quality Control (G 7)	Fee $2
Telemetry and Remote Control (G 10)	Fee $1
Ultrasonics Engineering (G 20)	Fee $2
Vehicular Communications (G 6)	Fee $2

IRE Professional Groups are only open to those who are already members of the IRE. Copies of Professional Group Transactions are available to non-members at three times the cost-price to group members.

The Institute of Radio Engineers
1 East 79th Street, New York 21, N.Y.

USE THIS COUPON PG-2-58

Miss Emily Sirjane
IRE—1 East 79th St., New York 21, N.Y.

Please enroll me for these IRE Professional Groups

.....$ .....
.....$ .....
.....

Name .....
Address .....
Place .....

Please enclose remittance with this order.

E-I-R METER
MODEL 110

A portable battery-powered meter for the measurement of DC voltage, current and resistance. Combines a high input resistance, high sensitivity voltmeter, a wide range ammeter and an ohmmeter with the convenience and isolation capability of battery power to provide a versatile instrument for laboratory measurements including current measurements in high potential circuits.

Partial Specifications:

E... 100 mv. to 1000 v. full scale in 9 ranges. 111 megohms input resistance.

I... 1 mμa. to 300 ma. full scale in 18 ranges. 100 mv. voltage drop.

R... 10 ohms to 100 megohms center scale in 6 ranges.

Accuracy on center zero scale for voltage and current is better than ± 3%.

Zero drift is less than 2 mv. per hour.

Battery life is approximately 800 hours.

Price: $315 f.o.b. Los Gatos, California.

For complete specifications write,

The Belleville Hexem Corporation
638 University Avenue
Los Gatos, California

News-New Products

These manufacturers have invited PROCEEDINGS readers to write for literature and further technical information. Please mention your IRE affiliation.

(Continued from page 108A)

found to be negligible from the safety standpoint. Safety precautions such as warning labels, covers and guards are incorporated throughout the system. Pressurized blowers and an air filter located at the bottom of the cabinet containing the optical system, keep dust within the case and upon the face of the cathode ray tubes to a minimum.

Magnetic Core Transistor Counters

Mack Electronics, a div. of Mack Trucks, Inc., Dept. D., 40 Leon St., Boston 15, Mass., has released for sale a line of counters for industrial and military use, They require only one voltage supply, and use no standby power. An example of low power consumption is a counter with 100 million count capacity; at 100 kc count rate, this counter would use 0.2 watt average power. At 1 kc count rate, it would require 0.002 watt of average power. This line of counters will operate from −55 to +125°C. The counters are based on magnetic cores and transistors, and no auxiliary drivers are required.

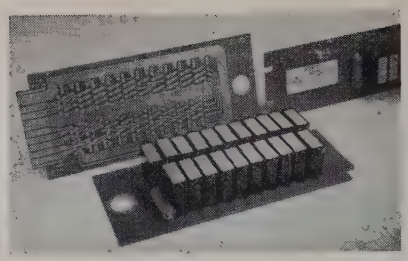

These units are available in many package forms down to as little as ½ cubic inch per binary counter stage or 1 cubic inch per decade stage. They are available as plug-in-units or with solder lugs, or printed board mounting.

Available in decade and binary stages. They are available to count to any base. The base to which the counter counts can be changed under high speed control.

Rack-Mounted Digital Multimeters

Featured in a new improved line of test instruments by **Hycon Electronics, Inc.,** 321 S. Arroyo Pkwy., Pasadena, Calif., are extremely rugged, rack-mounted, vacuum tube Voltohmmeters of high input impedance and a high degree of accuracy at moderate cost. These Hycon digital multimeters can be used by unskilled personnel to provide a wide range of ac and dc voltage and resistance readings at test points in production, incoming inspection, and quality control.

(Continued on page 112A)

NEW
improved
RECTANGULAR RECORDER

For Antenna Pattern Measurements Featuring New Plug-In Potentiometers

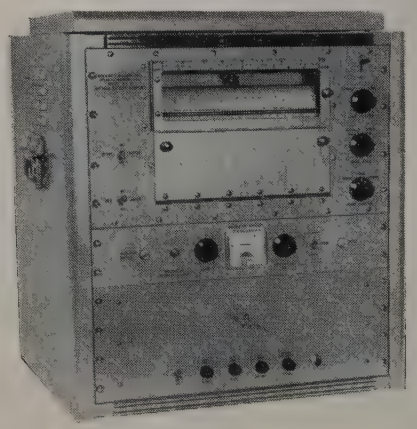

PEN SYSTEM

- writing speed: 40 inches per second (maximum);
- response: choice of linear, logarithmic and square-root or any combination;
- accuracy for linear response: ±0.3% of full scale over entire range;
- accuracy for logarithmic response: ±0.2 db over entire range of 40 db;*
- accuracy for square-root response: ±0.5% of full scale over first 20 db, ±1% over next 20 db range;*
- sensitivity: 1, 10 and 500 microvolts give full scale deflection for linear, square-root and logarithmic responses respectively.

* The accuracy and dynamic range of the recorder refer to the input of a square-law detector. The recorder actually has a dynamic range of 80 db.

CHART SYSTEM

- speed: 12 inches per second (maximum);
- scales: 0.5, 3 and 18 degrees of antenna rotation per inch of chart travel;
- chart accuracy: 0.02 inch static and 0.06 inch at chart speed of 4 inches per second.

PRICES:

The Series 121 Rectangular Recorders are available in the following models:

Model 121-A Logarithmic	$4,300
Model 121-A-1 Linear-Logarithmic	4,800
Model 121-A-2 Linear-Square Root	4,800
Model 121-A-3 Linear-Logarithmic-Square Root	5,600

SCIENTIFIC-ATLANTA, INC.
2162 Piedmont Road, N.E.
Atlanta 9, Georgia

(Left to Right) Frank Marshall, Assistant Engineer, Arthur H. Wulfsberg, an Assistant Director of Research & Development, and John Sprengeler, Project Engineer, discuss the use of a General Electric GL-6442 in a power amplifier assembly which is part of the AN/ARN-46 receiver-transmitter unit shown in center foreground.

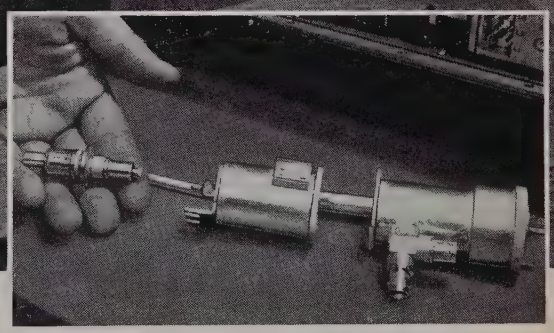

Disassembled power amplifier from AN/ARN-46. A G-E GL-6442 is used in each of 3 such amplifiers within the TACAN receiver-transmitter unit.

Collins Airborne TACAN Uses General Electric GL-6442 For Reliable Performance

EXCEPTIONAL performance characteristics of General Electric tube type GL-6442 are contributing significantly to the accurate and reliable performance of Collins TACAN equipment, which is capable of operation at altitudes over 70,000 feet.

TACAN provides the military or civil pilot with continuous, precise distance and bearing information for navigation at ranges up to about 200 miles.

The pressurized receiver-transmitter unit of the equipment employs five G-E GL-6442's—ceramic, disc-seal triodes of planar construction—in the frequency multiplier and power amplifier systems. Three of the tubes are used in the pulse-modulated final amplifier. These tubes are mounted in coaxial resonators, tunable over a 1025-1150 mc. range. More than 1 KW peak power output is obtained.

Designed primarily for use in grounded-grid cavity circuits as a plate pulsed oscillator or amplifier up to 4000 mcs., the tube is also useful as a continuous-wave RF power amplifier, oscillator, or frequency multiplier up to 2500 mcs. Typical operation in plate-pulsed oscillator service at 3500 mcs. produces 2 KW peak power output with an average power input of 7.5 watts and a duty cycle of 0.001.

Ratings for other classes of service available on request. For full information on Type GL-6442, call your regional G-E power tube representative. *Power Tube Dept., General Electric Co., Schenectady 5, N. Y.*

Progress Is Our Most Important Product

GENERAL ELECTRIC

9545-8481-6

GUDEBROD LACING TAPES ARE USED IN COMMUNICATION, UTILITIES & MILITARY AS WELL AS RESEARCH PROJECTS. CAN WE HELP YOU?

Gudebrod flat braided lacing tapes hold harness securely—no bite-through or slip, yet are easy on the hands. Some resist high temperature, some are color-coded . . . and they come wax-coated or wax-free . . . rubber-coated . . . or with special coating. Gudebrod makes many tapes for many purposes, including defense work. Send us your lacing problems or your specifications . . . we can supply the answer to both.

GUDELACE • GUDE-NYLACE
GUDELACE H • TEFLACE

GUDEBROD BROS. SILK CO., INC.
ELECTRONICS DIVISION
225 W. 34th St., New York 1, N. Y.
EXECUTIVE OFFICES
12 South 12th St., Philadelphia 7, Pa.

News-New Products

(Continued from page 110A)

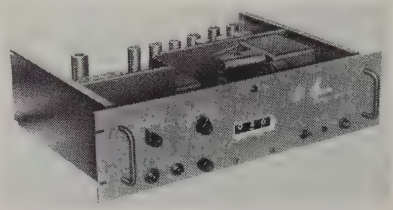

These multimeters, by slight modification, can be used in systems to accomplish a resultant readout or printout of temperature, pressure, velocity, or any other data that can be reduced to a form involving electrical resistance, current, or voltage.

With direct reading 3-digit display, the digital multimeters completely eliminate interpolation and parallax errors. An illuminated decimal point (which moves with the position of the range switch) eliminates multiple scale error, and a red illuminated signal indicates when the next higher scale should be selected.

Two models of Hycon rack-mounted VTVM's are available. Model 615 AR is a general-purpose volt-ohmmeter capable of measuring a wide range of voltages and resistances. Model 645 AR is a high precision instrument for use in applications where extreme accuracy is important.

Complete specifications and additional application information are available on request from Hycon.

(Continued on page 114A)

For Missile Testing
and general use
30 to 300 Amps
- Closely Regulated
- Fast Response
- Underwriters Approved
- Rigid Quality Control

CHRISTIE
SILICON
POWER RECTIFIERS

Available in Industrial and Military types. Military type meets specs MIL-E-4970 and MIL-I-6181. Other stationary and mobile styles available up to 1500 Amps.

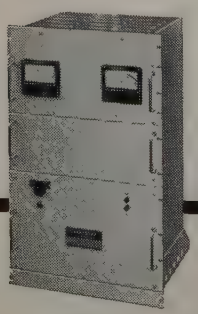

Write for Bulletin AC-58-A

CHRISTIE ELECTRIC CORP.
Dept. IR, 3410 W. 67th St., Los Angeles 43
Over a Quarter Century of Rectifier Manufacturing

Anywhere . . .
At sea, in the icy cold of the antarctic! S.S.WHITE Molded Resistors in values up to 50,000 megohms retain their characteristics.

in Any Weather
Airborne, in the steaming heat of the tropics! S.S.WHITE Molded Resistors are made of coated, non-hygroscopic material that resists moisture.

S.S.White
"ALL-WEATHER"
Molded Resistors Withstand Temperature and Humidity

FIXED RESISTANCE VALUES RANGE FROM 1000 OHMS TO 10,000,000 MEGOHMS!

65X Molded Resistor—1 watt
80X Molded Resistor—3 watts

While bargain buys in resistors are wearing out and being replaced, durable S.S. WHITE "All-Weather" Molded Resistors are still giving top performance in hundreds of commercial, industrial and scientific applications.

Our resistors are characterized by low noise level . . . precision . . . stability . . . have negative temperature and voltage coefficients. Compact . . . excellent stability and mechanical strength . . . values do not deteriorate due to age.

We'll be glad to cooperate with you in applying these high-quality resistors to your product. For our Bulletin 5409, just drop a line to Dept. PR.

S.S.White
INDUSTRIAL DIVISION
10 East 40th Street
New York 16, New York

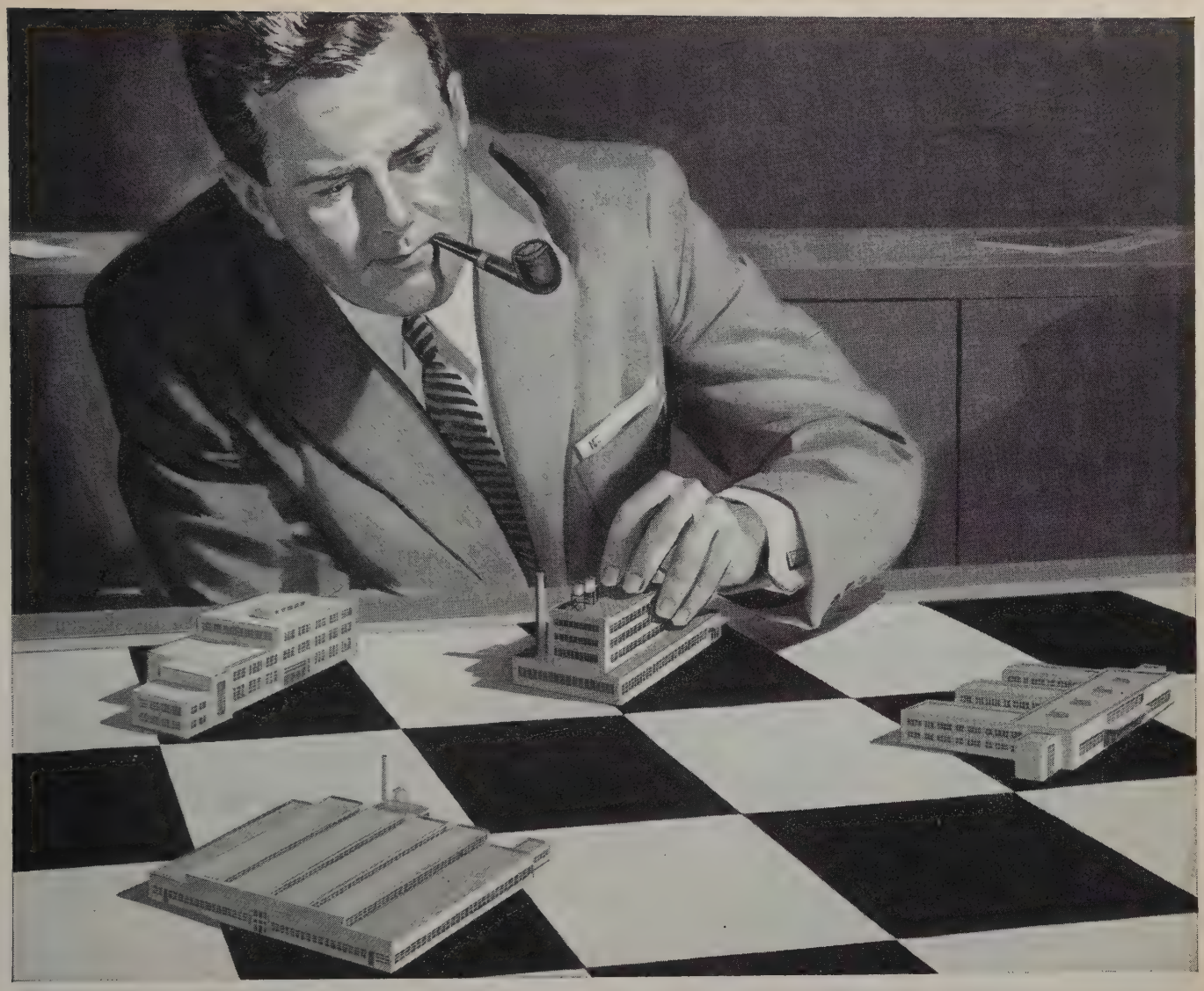

How to manage a system

For greater efficiency in carrying out the new weapons systems concept, military procurement officers work through central management contractors.

The Stromberg-Carlson Electronics Division is very proud to have been selected by the United States Air Force as a major systems management contractor.

These are some of our qualifications:

1. An established systems management group deep in managerial skill and experience;
2. An organizational setup under which the systems manager reports directly to the Vice President in charge of the Division;
3. An outstanding security record achieved in working with all the military services;
4. Strategic location close to major supply sources and convenient to all types of transportation.

Our manufacturing facilities and experience go hand in hand with systems management ability to qualify us as prime and sub-contractors, too.

The systems concept, which applies to military hardware *today*, can apply with equal force to civilian goods *tomorrow*. Stromberg-Carlson is ready . . . now, or any time.

"There is nothing finer than a Stromberg-Carlson"

STROMBERG-CARLSON
A DIVISION OF GENERAL DYNAMICS CORPORATION
1465 N. Goodman Street • Rochester 3, N. Y.

Electronic and communication products for home, industry and defense

Celco TRANSISTORIZED YOKES

⅞" ★ 1" ★ 1⅛" ★ 2" ★ 2½" CRT NECK DIA.

for MILITARY and COMMERCIAL PRECISION DISPLAYS

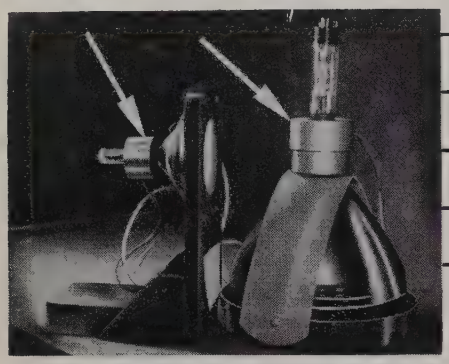

—HIGH RESOLUTION
—FAST RECOVERY
—HIGH SENSITIVITY
—LOW LI^2
—CONTROLLED MAGNETIC FIELDS

Write for CELCO DEFLECTION YOKE Catalogue & Design Sheets or for immediate engineering assistance Call your nearest CELCO Plant:

Mahwah, N. J. Davis 7-1123 | Miami, Fla. Plaza 1-9083 | Cucamonga, Calif. Yukon 2-2688

Celco Constantine Engineering Laboratories Co.

NEW CTS BOBBINLESS PRECISION WIRE FIXED RESISTORS

Featuring Unique CTS "Floating" Element
Small Space Factor • More Stable

New CTS patented winding process now permits resistance elements and contacts to be firmly embedded in epoxy resin, forming a monolithic mass. No bobbin or winding form—no wire strain. Exceptional Stability—permanent change in resistance less than 0.2% under most environmental conditions.

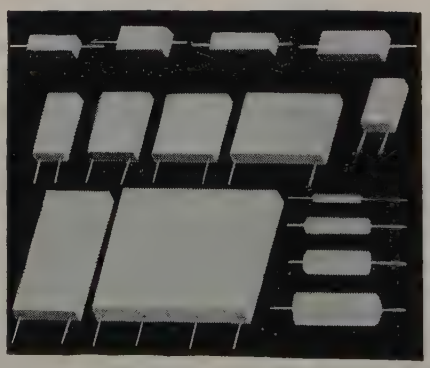

Guaranteed Close Tolerance—resistors guaranteed to be in tolerance under normal conditions of measurement. Tolerances down to ± 0.05% available in standard sizes depending upon resistance value. Closer tolerances or matched multiples available.

Low Inductance and Low Capacitance Characteristics with reproducible uniform frequency response made possible by new CTS patented winding technique. Less than 0.2% resistance change with humidity (MIL-R-93). Less than 0.2% resistance change with temperature cycling (MIL-R-93). Withstands extreme vibration and shock due to unique construction and encapsulation method. Extremely stable—resistance change with load life or 100% overload (MIL-R-93) less than 0.3%. Low temperature coefficient wire available. Offered in rectangular or tubular shapes in a wide variety of standard sizes with wattages ranging from 0.25 to 2.0 and resistances from 0.1 ohms. Special dimensions, tolerances, wattage ratings, etc. can be made to your exact specification.

CHICAGO TELEPHONE SUPPLY CORPORATION
Elkhart, Indiana • Founded 1896

News-New Products

These manufacturers have invited PROCEEDINGS readers to write for literature and further technical information. Please mention your IRE affiliation.

(Continued from page 112A)

5-mc Crystal

Manufactured to meet military and commercial standards for frequency measurement, the new 5-mc high-precision crystals manufactured by **Reeves-Hoffman Division of Dynamics Corp. of America,** Carlisle, Pa., offer exceptionally long-term frequency stability. Frequency tolerance is held at ±0.0001 per cent and aging is only one part per hundred million parts per week. These crystals are available in hermetically sealed glass T5 ½ enclosures with pigtail leads or 9-pin Bakelite base as specified.

Magazine-Processor Gives Immediate Oscillograph Records

A new direct-writing magazine which attaches to standard oscillographs and provides developed and dried photographic records as fast as the instrument records data is available from **Consolidated Electrodynamics,** 300 N. Sierra Madre Villa, Pasadena, Calif.

(Continued on page 116A)

PROBLEM:

Servicing the "heart" of a low, desk-mounted chassis.

SOLUTION:

Specification of Grant tilting slides to pivot the chassis over for "on-top" servicing.

The Soroban Engineering Company recently completed a repackaging program of their Perforated Tape Sequencer for Digital Control of Analogue Computers. This sequencer is a vital component of the Automatic Digital Input-Output Device (the ADIOD System) used at the White Sands Proving Grounds in New Mexico. Tape readers and their associated equipment are mounted within the desk, on Grant three-section tilt slides. These provide quick accessibility to every part of the chassis. Some of the equipment requiring servicing and adjustment is mounted underneath the chassis and Grant Slides are used to tilt the unit, bringing the bottom-mounted equipment into the view of the operator for easier servicing.

Grant No. 363-P2Y Slides
recommended for
loads up to 200 lbs./pair

Courtesy Soroban Engineering, Inc.

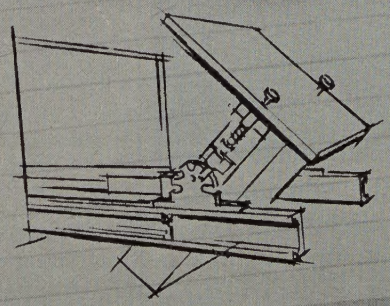

GRANT
INDUSTRIAL SLIDES

43 High Street, West Nyack, New York
944 Long Beach Avenue, Los Angeles, California

Write for complete technical data on the wide range of Grant Slides.

"INDIUM"

and High Purity Metals...

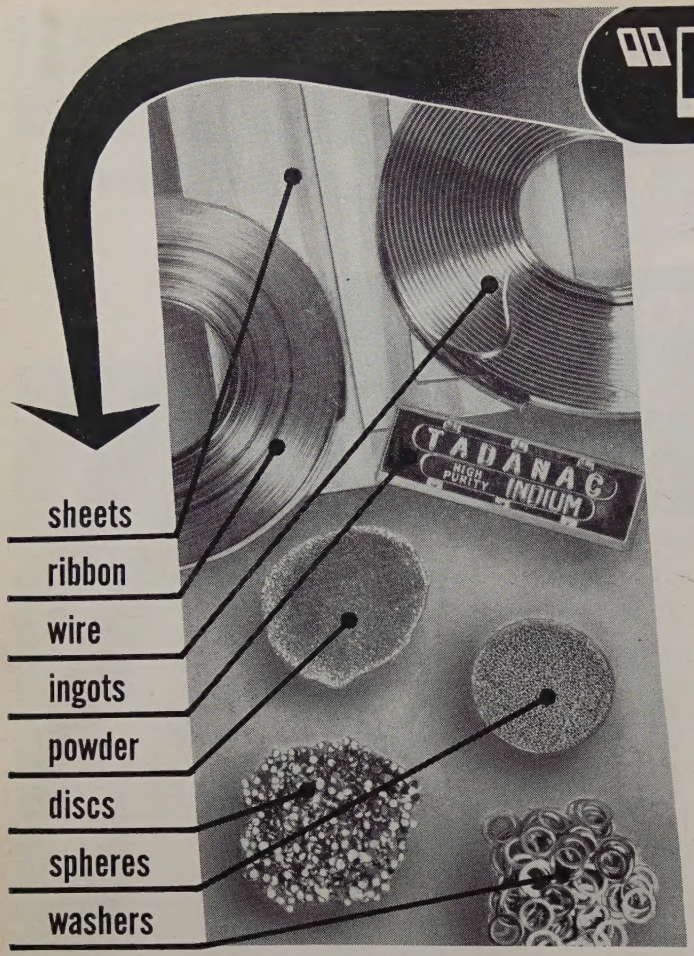

As one of the world's largest primary producers, we are supplying TADANAC Brand Indium and Indium Alloys to leading American, European and Canadian electronic firms. We are in quantity production of the forms shown and are prepared to preform and alloy to your specifications. Our prices include customs duties and we handle all customs procedures. Our Technical Service Department, backed by the full facilities of our Research Division, is ready to assist you in the use of this versatile metal, available as

TADANAC High Purity Indium—99.999% (by diff.)
TADANAC Standard Grade Indium—99.97+%
TADANAC Indium Alloys—a wide range to customer specifications

Other **TADANAC** High Purity Metals
We can supply **LEAD, CADMIUM, SILVER** or **BISMUTH** with a total impurity content of less than 1 p.p.m.* or **ZINC** with a total impurity content of less than 2 p.p.m.*
*Total impurity content determined by spectrographic analysis

For further information and a new booklet on Indium Properties and Uses write:

COMINCO

The Consolidated Mining and Smelting Company of Canada Limited
METAL SALES DIVISION
215 St. James Street. W. Montreal 1, Quebec, Canada

57164 ME

SOLDER WITH SAFETY AND SPEED

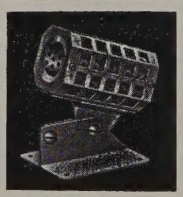

USE FIRST WILDER IN QUALITY

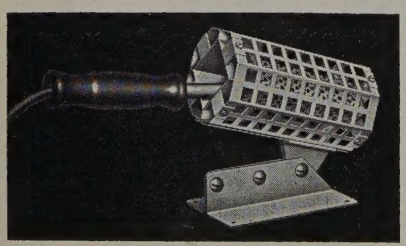

ADJUSTABLE SOLDERING IRON HOLDERS

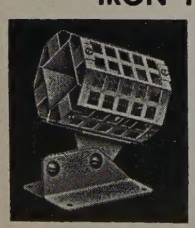

Three sizes for large and small irons. Can be placed on top of bench, fastened under bench or clamped to bench top or shelf. Available with wiping pad attachment, also slide for fastening small holder to large.

Write for further information.

WILDER MFG. CO., INC.
DEP'T E
MECHANIC ST. & ERIE R.R. PORT JERVIS, N. Y.

News-New Products

These manufacturers have invited PROCEEDINGS readers to write for literature and further technical information. Please mention your IRE affiliation.

(Continued from page 114A)

Called the 5-036 Datarite Magazine it represents the first "systems" approach to oscillographic instrumentation. Using an exclusive high-speed system of "flash-processing," the 5-036 chemically develops an oscillogram at rates up to 25 inches per second. The new unit features continuous and practically instant access to the record and furnishes a completely dried oscillogram which can be examined in full daylight while the test may be still going on.

The 5-036 is designed for direct attachment to Consolidated's widely used Type 5-119 Recording Oscillograph. The new unit is completely interchangeable with the 5-119's standard magazine without modification and can be installed in a few seconds.

Imparting new versatility to the use of conventional silver-halide emulsion recording papers, the Datarite allows the use of a wide range of materials and yields excellent record contrast. With a nominal capacity of 400 feet of 12-inch paper, the 5-036 provides high information-capacity for long recording runs.

Silicon Rectifier Data Sheets

Audio Devices, Inc., Rectifier Div., 620 East Dyer Rd., Santa Ana, Calif., have released 4 data sheets #1 to 4, describing their silicon rectifiers. These Engineering Data Sheets show details about these radio-television type rectifiers, and give curve tables and various applications.

Double-Ended Crystal Diodes

Double-ended microwave crystal diodes in S and X bands have been developed by **Sylvania Electric Products Inc., Special Tube Operations,** 1740 Broadway, New York 19, N. Y.

The new diodes are equipped with a detachable spring grip base which may be placed on either end, permitting their use as forward or reverse types.

The devices are said to eliminate the need to specify reverse diodes, thus providing substantial simplification in ordering and stocking.

Designations for the double-ended diodes are 1N416B, C, D and E for 1N21 types, and 1N415B, C, D and E for the 1N23 series. Of particular importance for both military and industrial use will be the premium E types.

Sylvania's 1N21 and 1N23 series are mixers designed for S and X band microwave superhetrodyne receiver application. The 1N23 series can also be used as video detectors in the 9,000 Mc region.

(Continued on page 136A)

ENGINEERS

NEW FLORIDA ELECTRONIC TUBE PLANT OF

SPERRY

Electronic Tube Division

offers unusual professional opportunities!

Here you will find a unique perfect combination for maximum professional development, expression and recognition . . . a new division, just starting production, offering the possibilities available in a rapidly growing organization. Our plant is located in the University City of Gainesville, Florida, noted for excellent all year round climate, unexcelled fishing, boating and swimming at nearby lake and gulf beaches, uncrowded living conditions with excellent housing available.

ENGINEERS

experienced in microwave tube development or production, microwave theory, electro mechanical assembly techniques to work

in

MAGNETRONS
KLYSTRONS
TRAVELING WAVE TUBES

•

Full Employee Benefits

•

Please submit Resume to Employment Dept.

SPERRY

Electronic Tube Division of Sperry Rand Corp.

GAINESVILLE, FLORIDA

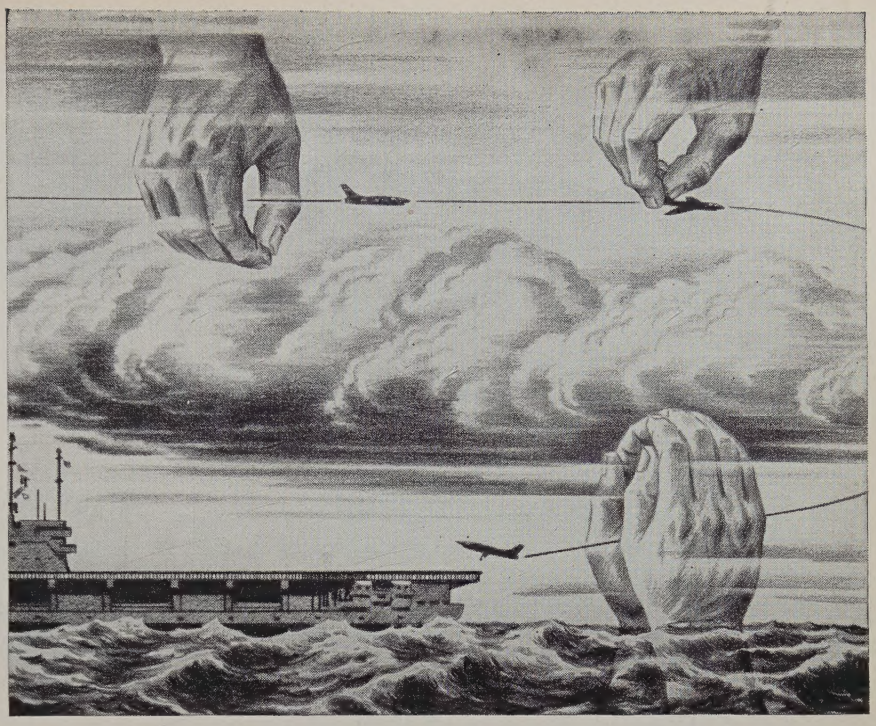

Cornell Aeronautical Laboratory and . . .

ALL-WEATHER RETURN-TO-CARRIER FLIGHT

A hundred jet aircraft scream toward their distant carrier. Some are disabled; others, critically low on fuel. Their landing must be swift; timed to the second. This systems problem was assigned to Cornell Aeronautical Laboratory scientists and engineers by the Bureau of Ships seven years ago. Project name: PACO—Problems of All-Weather Carrier Operations.

In order to link the carrier to the flight group beyond the horizon . . . establish mutually compatible flight paths . . . control an efficient landing sequence (with provision for emergency landings and wave-offs) . . . and to land the planes automatically on an unstable deck, electronics in every conceivable form has been focused on the problem.

Systems engineering, traffic control philosophy and the inter-relation of aerodynamics and electronics all play a part in the systems design and experimental support work of C.A.L.'s project team. Their efforts have resulted in significant contributions to equipment development including TACAN, Data Link and Traffic Control Computer, Transition and Wave-Off Computer, and Automatic Landing System with Deck Motion Predictor.

PACO typifies the broad scope and professional maturity of research projects at C.A.L. If you are interested in becoming a member of one of our small, closely-knit research teams, write today for the factual, well illustrated, 68-page report entitled, "A Decade of Research." Mail the coupon now for your free copy.

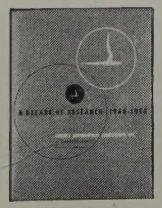

FREE REPORT

CORNELL AERONAUTICAL LABORATORY, INC.
OF CORNELL UNIVERSITY

J. P. RUCH RTC
CORNELL AERONAUTICAL LABORATORY, INC.
Buffalo 21, New York

Please send me a copy of "A Decade of Research."

Name _____

Street _____

City _____ Zone _____ State _____

→ ☐ Please include employment information

An Invitation To Join ORO...Pioneer In Operations Research

Operations Research is a young science, earning recognition rapidly as a significant aid to decision-making. It employs the services of mathematicians, physicists, economists, engineers, political scientists, psychologists, and others working on teams to synthesize all phases of a problem.

At ORO, a civilian and non-governmental organization, you will become one of a team assigned to vital military problems in the area of tactics, strategy, logistics, weapons systems analysis and communications.

No other Operations Research organization has the broad experience of ORO. Founded in 1948 by Dr. Ellis A. Johnson, pioneer of U. S. Opsearch, ORO's research findings have influenced decision-making on the highest military levels.

ORO's professional atmosphere encourages those with initiative and imagination to broaden their scientific capabilities. For example, staff members are taught to "program" their own material for the Univac computer so that they can use its services at any time they so desire.

ORO starting salaries are competitive with those of industry and other private research organizations. Promotions are based solely on merit. The "fringe" benefits offered are ahead of those given by many companies.

The cultural and historical features which attract visitors to Washington, D. C. are but a short drive from the pleasant Chevy Chase suburb in which ORO is located. Attractive homes and apartments are within walking distance and readily available in all price ranges. Schools are excellent.

For further information write:
Professional Appointments

OPERATIONS RESEARCH OFFICE
ORO The Johns Hopkins University
7100 CONNECTICUT AVENUE
CHEVY CHASE 15, MARYLAND

News-New Products

These manufacturers have invited PROCEEDINGS readers to write for literature and further technical information. Please mention your IRE affiliation.

(Continued from page 136A)

Thermester-L magnet wire is a recent development. It has a maximum operating temperature of 155°C., and has excellent electrical and mechanical properties. Also available in gauges as fine as 50 AWG is Temprite (Teflon) magnet wire. Temprite has a temperature range as high as 250°C. Along with excellent dielectric strength and chemical resistance, the Temprite magnet wire exhibits extremely low dielectric constant and power factor.

The space factor for both of these film insulated magnet wires makes them ideal for delicate and sensitive instruments, which have to meet commercial and military standards.

Shielding Data Sheet

Data Sheet 134 illustrates and describes the new seamless non-shock sensitive non-retentive Netic magnetic shields designed for greater effectiveness in attenuating both high and low frequencies of substantially increased transformer radiation in transistorized power supplies. Available without cost from **Magnetic Shield Div., Perfection Mica Co.,** 1322 No. Elston Ave., Chicago 22, Ill.

ELECTRONIC ENGINEERS
$7,500 - $20,000

Clients Pay Fees

A nationwide service working with 300 firms in the electronic industry.

Send 3 copies of your resume to:

Harry L. Brisk
Member I.R.E.

ACCREDITED PERSONNEL
12 South 12th Street
Philadelphia 7, Pa.
Established 1937